MECHANICAL VIBRATIONS AND STRUCTURAL DYNAMICS (R15A0368)

COURSE FILE

IV B. Tech I Semester

(2018-2019)

Prepared By

Mr. G Dheeraj Asst. Prof

Department of Aeronautical Engineering

MALLA REDDY COLLEGE OF ENGINEERING & TECHNOLOGY

(Autonomous Institution – UGC, Govt. of India)

Affiliated to JNTU, Hyderabad, Approved by AICTE - Accredited by NBA & NAAC – 'A' Grade - ISO 9001:2015 Certified)

Maisammaguda, Dhulapally (Post Via. Kompally), Secunderabad – 500100, Telangana State, India.

MRCET VISION

- To become a model institution in the fields of Engineering, Technology and Management.
- To have a perfect synchronization of the ideologies of MRCET with challenging demands of International Pioneering Organizations.

MRCET MISSION

To establish a pedestal for the integral innovation, team spirit, originality and competence in the students, expose them to face the global challenges and become pioneers of Indian vision of modern society.

MRCET QUALITY POLICY.

- To pursue continual improvement of teaching learning process of Undergraduate and Post Graduate programs in Engineering & Management vigorously.
- To provide state of art infrastructure and expertise to impart the quality education.

PROGRAM OUTCOMES
(PO's)

Engineering Graduates will be able to:

1. **Engineering knowledge**: Apply the knowledge of mathematics, science, engineering fundamentals, and an engineering specialization to the solution of complex engineering problems.
2. **Problem analysis**: Identify, formulate, review research literature, and analyze complex engineering problems reaching substantiated conclusions using first principles of mathematics, natural sciences, and engineering sciences.
3. **Design / development of solutions**: Design solutions for complex engineering problems and design system components or processes that meet the specified needs with appropriate consideration for the public health and safety, and the cultural, societal, and environmental considerations.
4. **Conduct investigations of complex problems**: Use research-based knowledge and research methods including design of experiments, analysis and interpretation of data, and synthesis of the information to provide valid conclusions.
5. **Modern tool usage**: Create, select, and apply appropriate techniques, resources, and modern engineering and IT tools including prediction and modeling to complex engineering activities with an understanding of the limitations.
6. **The engineer and society**: Apply reasoning informed by the contextual knowledge to assess societal, health, safety, legal and cultural issues and the consequent responsibilities relevant to the professional engineering practice.
7. **Environment and sustainability**: Understand the impact of the professional engineering solutions in societal and environmental contexts, and demonstrate the knowledge of, and need for sustainable development.
8. **Ethics**: Apply ethical principles and commit to professional ethics and responsibilities and norms of the engineering practice.
9. **Individual and team work**: Function effectively as an individual, and as a member or leader in diverse teams, and in multidisciplinary settings.
10. **Communication**: Communicate effectively on complex engineering activities with the engineering community and with society at large, such as, being able to comprehend and write effective reports and design documentation, make effective presentations, and give and receive clear instructions.
11. **Project management and finance**: Demonstrate knowledge and understanding of the engineering and management principles and apply these to one's own work, as a member and leader in a team, to manage projects and in multi disciplinary environments.
12. **Life- long learning**: Recognize the need for, and have the preparation and ability to engage in independent and life-long learning in the broadest context of technological change.

DEPARTMENT OF AERONAUTICAL ENGINEERING

VISION

Department of Aeronautical Engineering aims to be indispensable source in Aeronautical Engineering which has a zeal to provide the value driven platform for the students to acquire knowledge and empower themselves to shoulder higher responsibility in building a strong nation.

MISSION

The primary mission of the department is to promote engineering education and research. To strive consistently to provide quality education, keeping in pace with time and technology. Department passions to integrate the intellectual, spiritual, ethical and social development of the students for shaping them into dynamic engineers.

QUALITY POLICY STATEMENT

Impart up-to-date knowledge to the students in Aeronautical area to make them quality engineers. Make the students experience the applications on quality equipment and tools. Provide systems, resources and training opportunities to achieve continuous improvement. Maintain global standards in education, training and services.

PROGRAM EDUCATIONAL OBJECTIVES – Aeronautical Engineering

1. **PEO1 (PROFESSIONALISM & CITIZENSHIP):** To create and sustain a community of learning in which students acquire knowledge and learn to apply it professionally with due consideration for ethical, ecological and economic issues.
2. **PEO2 (TECHNICAL ACCOMPLISHMENTS):** To provide knowledge based services to satisfy the needs of society and the industry by providing hands on experience in various technologies in core field.
3. **PEO3 (INVENTION, INNOVATION AND CREATIVITY):** To make the students to design, experiment, analyze, and interpret in the core field with the help of other multi disciplinary concepts wherever applicable.
4. **PEO4 (PROFESSIONAL DEVELOPMENT):** To educate the students to disseminate research findings with good soft skills and become a successful entrepreneur.
5. **PEO5 (HUMAN RESOURCE DEVELOPMENT):** To graduate the students in building national capabilities in technology, education and research

PROGRAM SPECIFIC OUTCOMES – Aeronautical Engineering

1. To mould students to become a professional with all necessary skills, personality and sound knowledge in basic and advance technological areas.
2. To promote understanding of concepts and develop ability in design manufacture and maintenance of aircraft, aerospace vehicles and associated equipment and develop application capability of the concepts sciences to engineering design and processes.
3. Understanding the current scenario in the field of aeronautics and acquire ability to apply knowledge of engineering, science and mathematics to design and conduct experiments in the field of Aeronautical Engineering.
4. To develop leadership skills in our students necessary to shape the social, intellectual, business and technical worlds.

MALLA REDDY COLLEGE OF ENGINEERING & TECHNOLOGY

IV Year B. Tech, ANE-I Sem

L	T/P/D	C
5	1/-/-	4

(R15A0368) MECHANICAL VIBRATIONS AND STRUCTURAL DYNAMICS

Objectives:

- To gain fundamental knowledge on vibration and related systems in the context of Aircraft Structures
- To give Exposure on damped and undamped vibratory systems.
- Basic knowledge on dynamic balancing of rotor system

UNIT-I

FUNDAMENTALS OF VIBRATION: Brief history of vibration, Importance of the study of vibration, basic concepts of vibration, classification of vibrations, vibration analysis procedure, spring elements, mass or inertia elements, damping elements, harmonic analysis. FREE VIBRATION OF SINGLE DEGREE OF FREEDOM SYSTEMS: Introduction, Free vibration of an undamped translational system, free vibration of an undamped torsional system, stability conditions, Raleigh's energy method, free vibration with viscous damping, free vibration with coulomb damping, free vibration with hysteretic damping.

UNIT-II

HARMONICALLY EXITED VIBRATIONS: Introduction, Equation of motion, response of an undamped system under harmonic force, Response of a damped system under harmonic force, Response of a damped system under harmonic motion of the base, Response of a damped system under rotating unbalance, forced vibration with coulomb damping, forced vibration with hysteresis damping.

UNIT-III

VIBRATION UNDER GENERAL FORCING CONDITIONS: Introduction, Response under a general periodic force, Response under a periodic force of irregular form, Response under a non periodic force, convolution integral. Two Degree of Freedom Systems: Introduction, Equation of motion for forced vibration, free vibration analysis of an undamped system, Torsional system, Coordinate coupling and principal coordinates, forced vibration analysis.

UNIT-IV

MULTIDEGREE OF FREEDOM SYSTEMS: Introduction, Modeling of Continuous systems as multi degree of freedom systems, Using Newtons second law to derive equations of motion, Influence coefficients, Free and Forced vibration of undamped systems, Forced vibration of viscously damped systems. Determination Of Natural Frequencies and Mode Shapes: Introduction, Dunkerleys formula, Rayleighs method, Holzers method, Matrix iteration method, Jacobi;s method.

UNIT-V

CONTINUOUS SYSTEMS: Transverse vibration of a spring or a cable, longitudinal vibration of bar or rod, Torsional vibration of a bar or rod, Lateral vibration of beams, critical speed of rotors.

Text Books:

1. Mechanical Vibrations by S.S.Rao.
2. Mechanical Vibrations by V.P.Singh

Reference Books:

1. Mechanical Vibrations by G.K. Grover
2. Mechanical Vibrations by W.T. Thomson
3. Mechanical vibrations: theory and application to structural dynamics, Michel Géradin, Daniel Rixen, John Wiley, 1997

Outcomes:

- Fundamental frequency of Multi- DOF systems can estimate by various methods.
- Effect of unbalance in rotating masses has been studied.
- How to determine eigenvalues and eigenvectors for a vibratory system has analysed

AEROSPACE VEHICLE STRUCTURES -II

Model Question Paper – I

PART A

ANSWER ALL QUESTIONS

1. Write about resolution of bending moments with neat sketches.
2. Explain the energy method for bending of thin plates?
3. What are the factors that determine the angle of diagonal tension? If the flanges and stiffness are rigid what will be the angle of diagonal tension?
4. Write short notes on the following: i. Symmetrical bending ii. Unsymmetrical bending.
5. Explain the following terms. i. Shear center ii. Shear flow iii. Centre of twist.
6. Find the section properties of the following idealized panel.

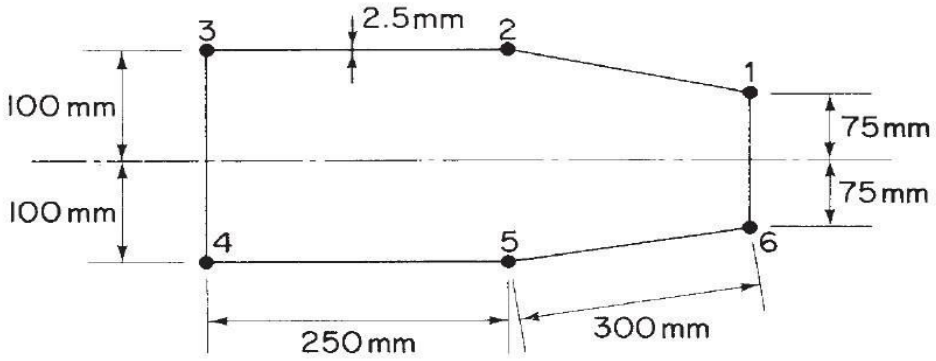

7. Find the sectional properties of given section

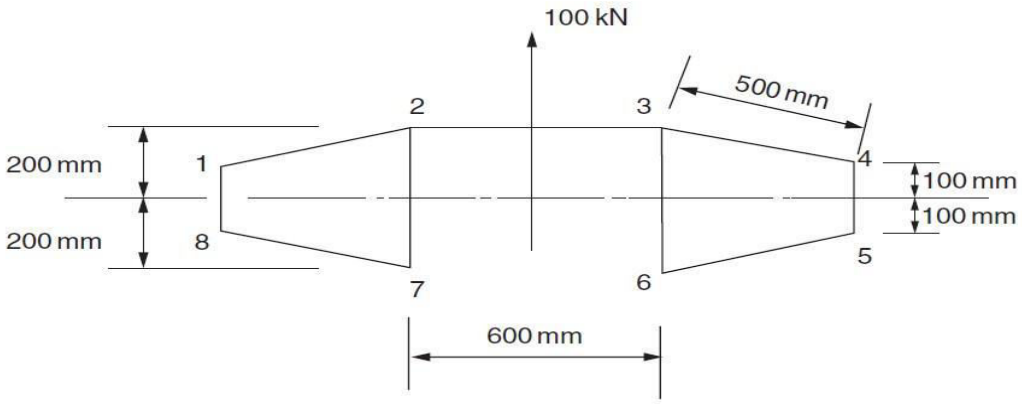

8. Write a short note on loading discontinuities in beams?
9. Write short onte on fuselage frames and wing ribs?
10. Explain about determinate and indeterminate structure of wing and fuselages?

1. Determine the deflected form of the thin rectangular plate a × b is simply supported along its edges and carrying a uniformly distributed load of intensity q_0. In addition to that it supports an in-plane tensile force Nx per unit length. Here 'a' is length and 'b' is width of the plate.

(OR)

2. A simply supported beam has a span of 2.4m and carries a central concentrated load of 10 kN. The flanges of the beam each have a cross-sectional area of$300mm^2$ while that of the vertical web stiffeners is $280mm^2$. If the depth of the beam, measured between the centroids of area of the flanges, is 350mm and the stiffeners are symmetrically arranged about the web and spaced at 300mm intervals, determine the maximum axial load in a flange and the compressive load in a stiffener. It may be assumed that the beam web, of thickness 1.5 mm, is capable of resisting diagonal tension only.
3. Determine the direct stress distribution in the thin-walled Z-section shown in Fig. produced by a positive bending moment *Mx*.

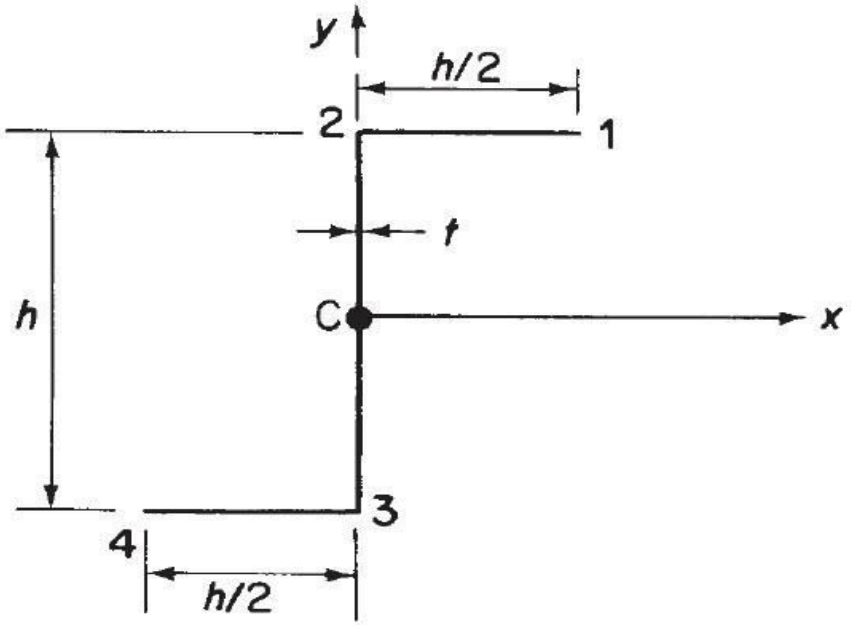

(OR)

4. A thin-walled closed section beam has the singly symmetrical cross-section shown in Fig. Each wall of the section is flat and has the same thickness *t* and shear modulus *G*. Calculate the distance of the shear centre from point 4
5. Idealize the box section shown in Fig. into an arrangement of direct stress carrying booms positioned at the four corners and panels which are assumed to carry only shear

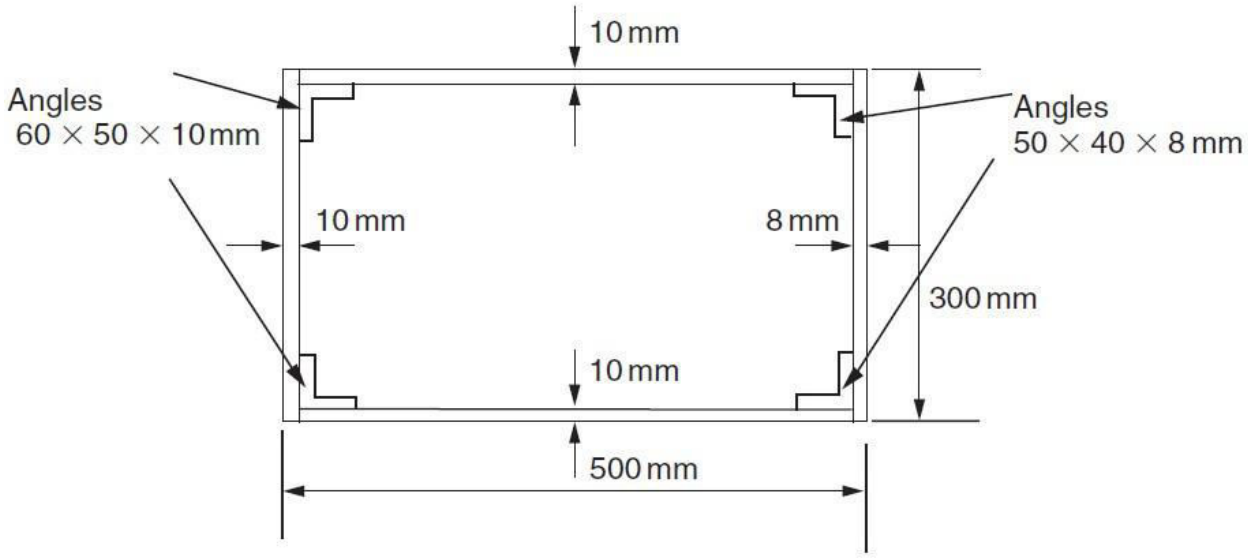

6. Figure shows the cross-section of a single cell, thin-walled beam with a horizontal axis of symmetry. The direct stresses are carried by the booms $B1$ to $B4$, while the walls are effective only in carrying shear stresses. Assuming that the basic theory of bending is applicable, calculate the position of the shear centre S. The shear modulus G is the same for all walls. Cell area=135000mm^2. Boom areas: $B1$ =$B4$ =450mm^2, $B2$ =$B3$ =550mm^2.

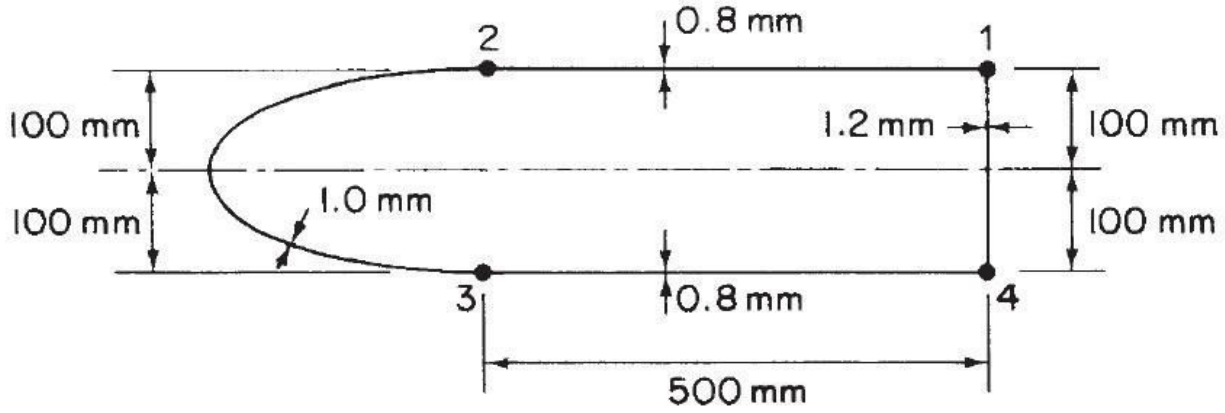

7. Determine the shear flow distribution at the built-in end of a beam whose cross-section is shown in Fig. All walls have the same thickness t and shear modulus G; R=200 mm.

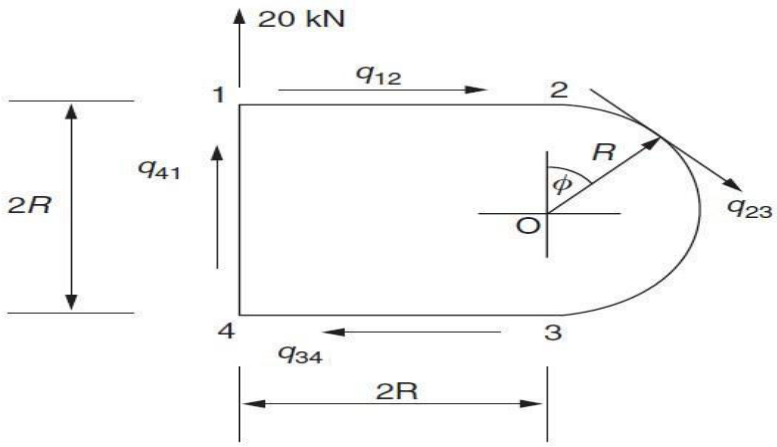

(OR)

8. An axially symmetric beam has the thin-walled cross-section shown in Fig. If the thickness *t* is constant throughout and making the usual assumptions for a thin-walled cross-section, show that the torsion bending constant Γ_R calculated about the shear centre S is

$$\Gamma_R = \frac{13}{12} d^5 t$$

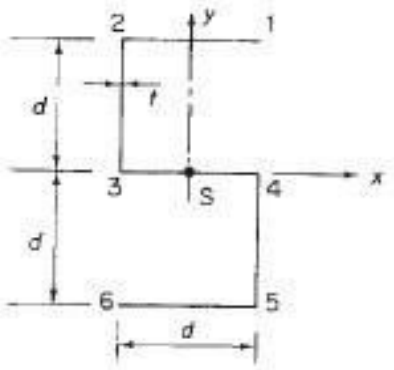

9. The fuselage of a light passenger carrying aircraft has the circular cross-section shown in Fig. The cross-sectional area of each stringer is 100mm^2 and the vertical distances given in Fig. are to the mid-line of the sectionwall at the corresponding stringer position.

(a) If the fuselage is subjected to a bending moment of 200 kNm applied in the vertical plane of symmetry, at this section, calculate the direct stress distribution.

(b) The fuselage is subjected to a vertical shear load of 100 kN applied at a distance of 150mm from the vertical axis of symmetry as shown, for the idealized section, in Fig. 22.2. Calculate the distribution of shear flow in the section.

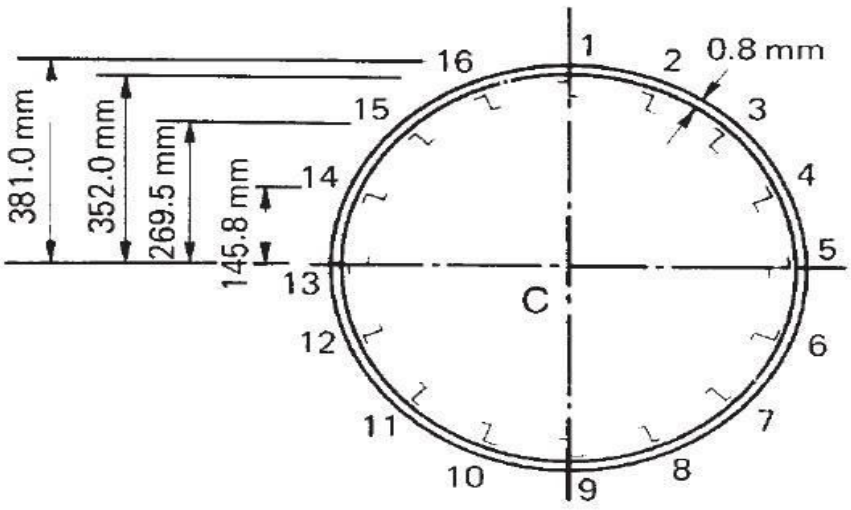

(OR)

10. The central cell of a wing has the idealized section shown in Fig. If the lift and drag loads on the wing produce bending moments of −120 000Nm and −30 000Nm, respectively at the section shown, calculate the direct stresses in the booms. Neglect axial constraint effects and assume that the lift and drag vectors are in vertical and horizontal planes.
Boom areas: $B1 = B4 = B5 = B8 = 1000\text{mm}^2$ $B2 = B3 = B6 = B7 = 600\text{mm}^2$

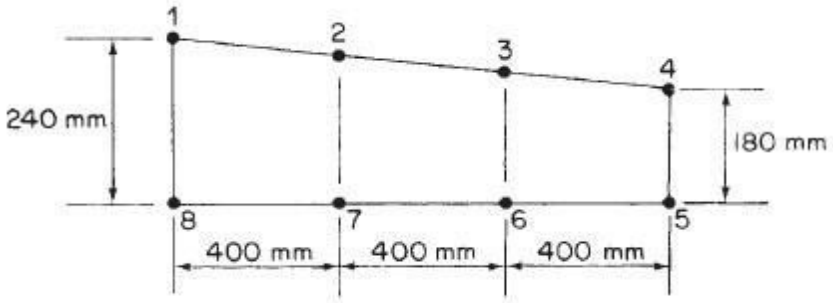

AEROSPACE VEHICLE STRUCTURES -II

Model Question Paper - II

PART A

ANSWER ALL QUESTIONS

1. Explain the basic theory of thin plates?
2. What is the term flexural rigidity called in bending of thin plates and explain?
3. How to determine the shear flow distribution of combined section beams subjected to shear loads.
4. If the cross section of a beam is 10mmx5mm and torque is 100Nmm. Calculate shear flow with neat sketch.
5. Explain how to idealization the panel.
6. What is the boom area?
7. Discuss shear stress distributions of a closed section beam built in one end and subjected to bending.
8. Explain shear lag that poses problems in the analysis of wide, shallow, thin walled beams.
9. How to find the shear flow distribution of variable string area wing.
10. Write about the cutouts in fuselage and wing with neat sketches.

PART – B ANSWER

ANY FIVE

1. A thin rectangular plate a × b is simply supported along its edges and carries a uniformly distributed load of intensity q_0. Determine the deflected form of the plate and the distribution of bending moment. Here 'a' is length and 'b' is width of the plate.

(OR)

2. Derive the equation to find out the shear center of figure shown

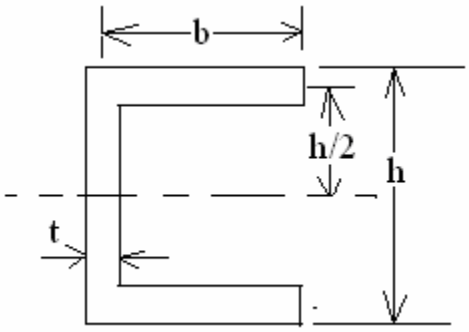

3. Derive Bredt-Batho formula and also explain displacements associated with the Bredt-Batho shear flow.

(OR)

4. Derive the equation

$$q_s = -\left(\frac{S_x I_{xx} - S_y I_{xy}}{I_{xx} I_{yy} - I_{xy}^2}\right)\left(\int_0^s t_D x\,ds + \sum_{r=1}^{n} B_r x_r\right) - \left(\frac{S_y I_{yy} - S_x I_{xy}}{I_{xx} I_{yy} - I_{xy}^2}\right)\left(\int_0^s t_D y\,ds + \sum_{r=1}^{n} B_r y_r\right)$$

5. Determine the shear flow distribution in the thin-walled Z-section shown in Figure due to a shear load *Sy* applied through the shear center of the section.

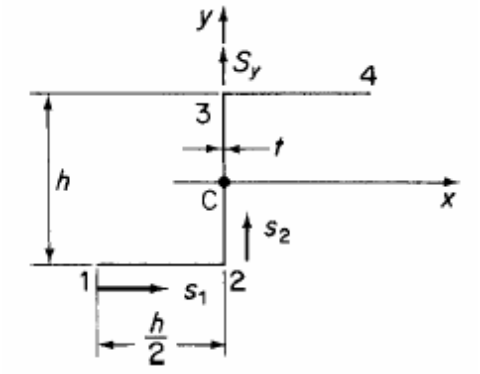

(OR)

6. The wing section shown in Figure has been idealized such that the booms carry all the direct stresses. If the wing section is subjected to a bending moment of 300 kN m applied in a vertical plane, calculate the direct stresses in the booms. Boom areas: $B1 = B6 = 2580$ mm^2 $B2 = B5 = 3880$ mm^2 $B3 = B4 = 3230$ mm^2

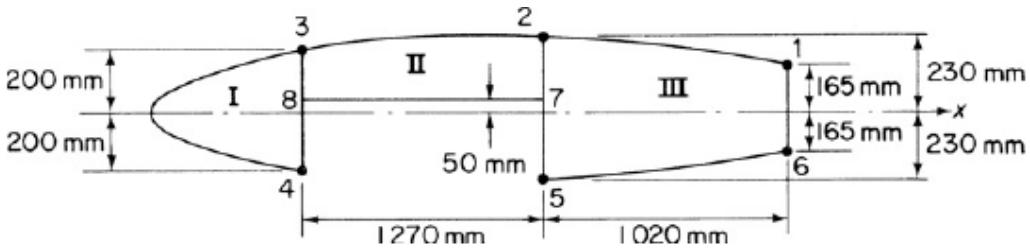

(OR)

7. The unsymmetrical panel shown in Fig. comprises three direct stress carrying booms and two shear stress carrying panels. If the panel supports a load P at its free end and is pinned to supports at the ends of its outer booms determine the distribution of direct load in the central boom. Determine also the load in the central boom when $A=B=C$ and shear lag effects are absent.

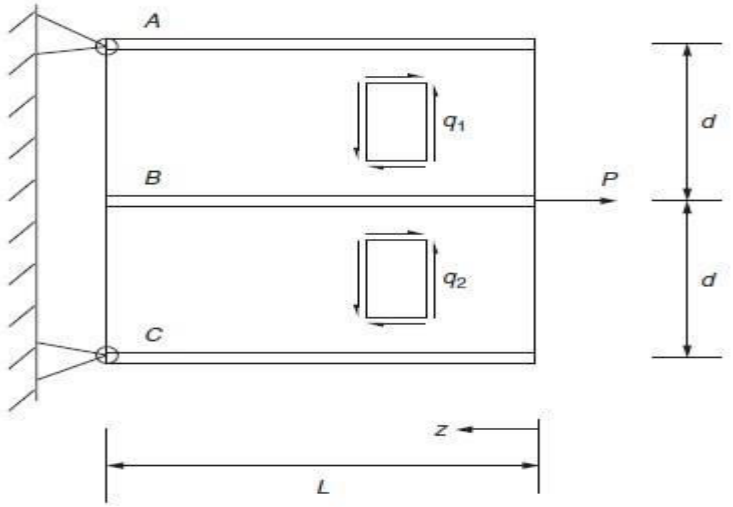

8. An open section beam of length L has the section shown in Figure. The beam is firmly built-in at one end and carries a pure torque T. Derive expressions for the direct stress and shear flow distributions produced by the axial constraint (the σ Γ and q Γ systems) and the rate of twist of the beam

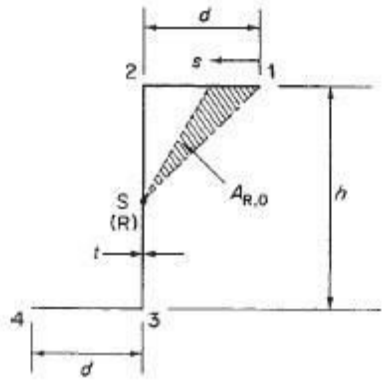

9. Calculate the shear flows in the web panels and direct load in the flanges and stiffeners of the beam shown in Figure if the web panels resist shear stresses only.

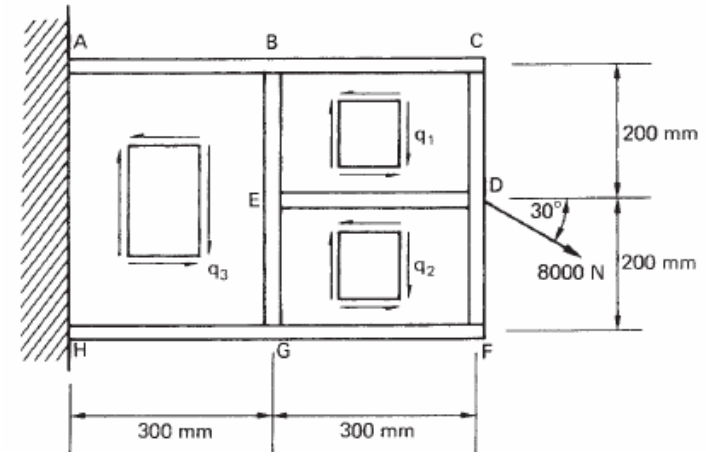

(OR)

10. Calculate the shear flows in the web panels and the axial loads in the flanges of the wing rib shown in Figure. Assume that the web of the rib is effective only in shear while the resistance of the wing to bending moments is provided entirely by the three flanges 1, 2 and 3.

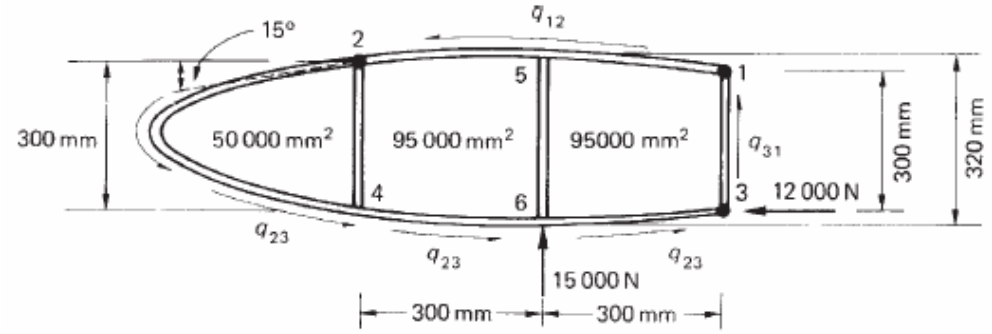

AEROSPACE VEHICLE STRUCTURES -II
Model Question Paper – III

PART A
ANSWER ALL QUESTIONS

1. Clearly explain the difference between synclastic and anticlastic surface of thin plates?
2. Clearly draw the figure for plate element subjected to bending, twisting and transverse loads?
3. Write the conditions for a plate which simply supported all edges? And write the assumed deflected form of the plate which satisfies the boundary conditions for this plate?
4. Explain warping distribution with neat sketch.
5. Discuss about primary and secondary warping of thin-walled beams.
6. Derive the equation to find out boom areas with neat sketches.
7. Explain the effect of idealization on the analysis of open and closed section beams.
8. Derive the equation to find out shear flow in a tapered wing.
9. How to find the shear flow of a fuselage with cutout.
10. What is the function of wing ribs with neat sketches.

PART B

ANSWER ALL QUESTIONS

1. Derive the equation $(1/\rho) = [\ D\ (1+\ \upsilon\ )]$of thin plate subjected to pure bending.

(OR)

2. Figure shows the section of an angle purlin. A bending moment of 3000 Nm is applied to the purlin in a plane at an angle of 30^{o} to the vertical *y* axis. If the sense of the bending moment is such that its components *Mx* and *My* both produce tension in the positive *xy* quadrant, calculate the maximum direct stress in the purlin, stating clearly the point at which i t acts.

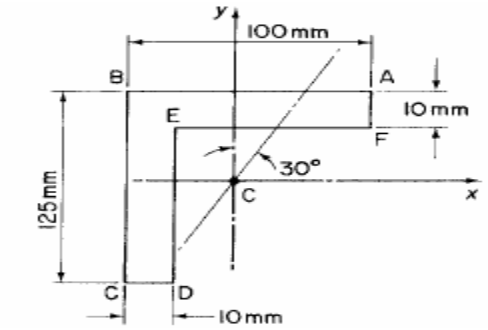

3. Determine the maximum shear stress and the warping distribution in the channel section shown in Figure when it is subjected to an anticlockwise torque of 10 Nm. *G*=25000 N/mm^2.

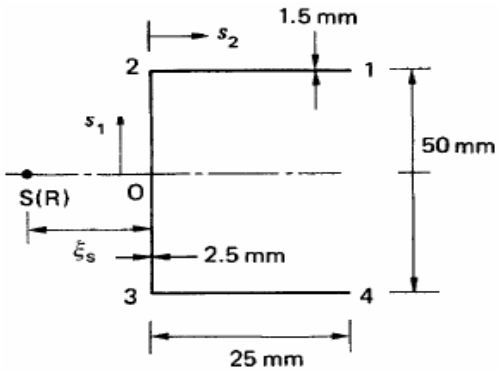

(OR)

4. A single cell, thin-walled beam with the double trapezoidal cross-section shown in Fig is subjected to a constant torque T =90 500Nmand is constrained to twist about an axis through the point R. Assuming that the shear stresses are distributed according to the Bredt–Batho theory of torsion, calculate the distribution of warping around the cross-section. Illustrate your answer clearly by means of a sketch and insert the principal values of the warping displacements. The shear modulus G=27 500N/mm2 and is constant throughout.

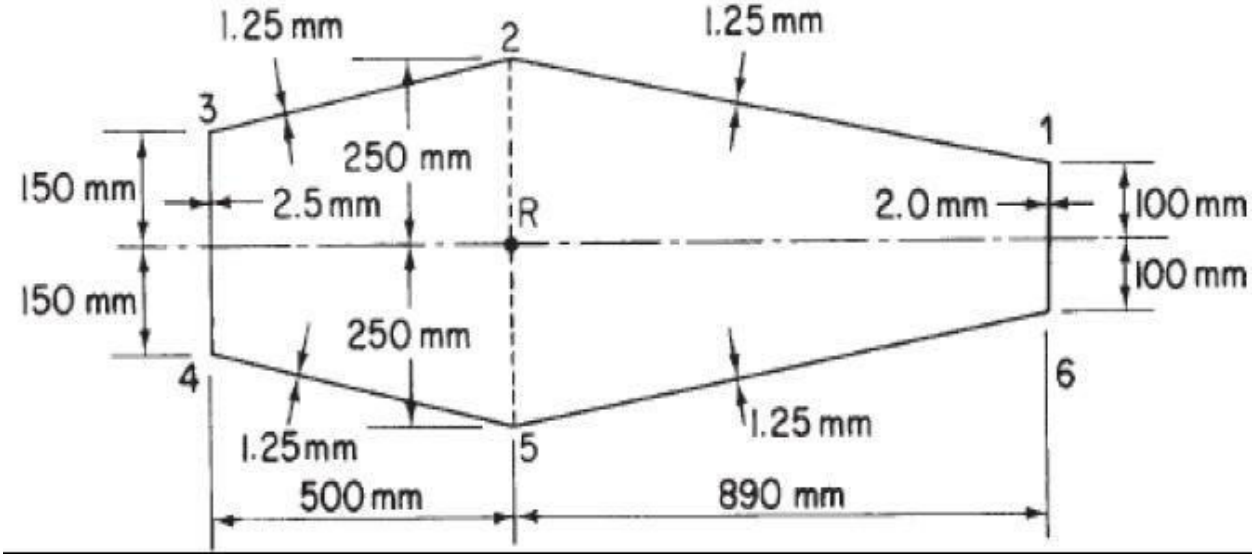

5. Part of a wing section is in the form of the two-cell box shown in Figure in which the vertical spars are connected to the wing skin through angle sections, all having a cross-sectional area of 300 mm^2. Idealize the section into an arrangement of direct stress-carrying booms and shear-stress-only-carrying panels suitable for resisting bending moments in a vertical plane. Position the booms at the spar/skin junctions.

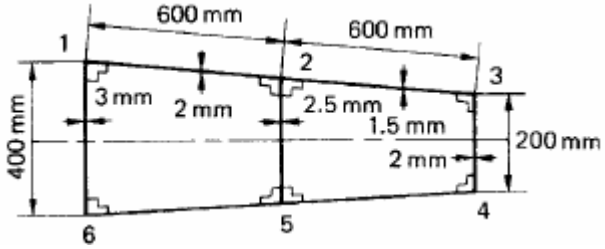

(OR)

6. Derive Torsion – Bending constant for an arbitrary section beam subjected to Torsion.
7. A shallow box section beam whose cross-section is shown in Fig. is simply supported over a span of 2m and carries a vertically downward load of 20 kN at midspan. Idealise the section into one suitable for shear lag analysis, comprising eight booms, and hence determine the distribution of direct stress along the top right-hand corner of the beam. Take G/E =0.36.

(OR)

8. Derive the expression for total torque of an I section beam.
9. The cantilever beam shown in Figure is uniformly tapered along its length in both x and y directions and carries a load of 100 kN at its free end. Calculate the forces in the booms and the shear flow distribution in the walls at a section 2 m from the built-in end if the booms resist all the direct stresses while the walls are effective only in shear. Each corner boom has a cross-sectional area of 900 mm^2 while both central booms have cross-sectional areas of 1200 mm^2.

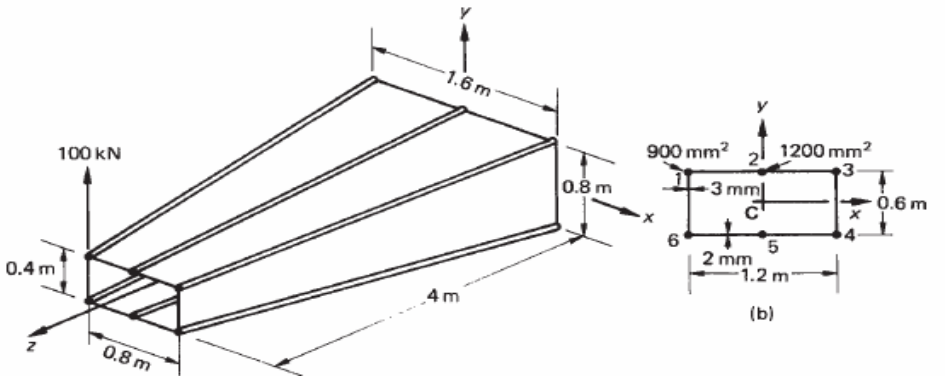

(OR)

10. A two-cell beam has singly symmetrical cross-sections 1.2m apart and tapers symmetrically in the y direction about a longitudinal axis. The beam supports loads which produce a shear force Sy =10 kN and a bending moment Mx =1.65 kNm at the larger cross-section; the shear load is applied in the plane of the internal spar web. If booms 1 and 6 lie in a plane which is parallel to the yz plane calculate the forces in the booms and the shear flow distribution in the walls at the larger cross-section. The booms are assumed to resist all the direct stresses while the walls are effective only in shear. The shear modulus is constant throughout, the vertical webs are all 1.0mm thick while the remaining walls are all 0.8mm thick: Boom areas: $B1 = B3 = B4 = B6 = 600mm^2$ $B2 = B5 = 900mm^2$

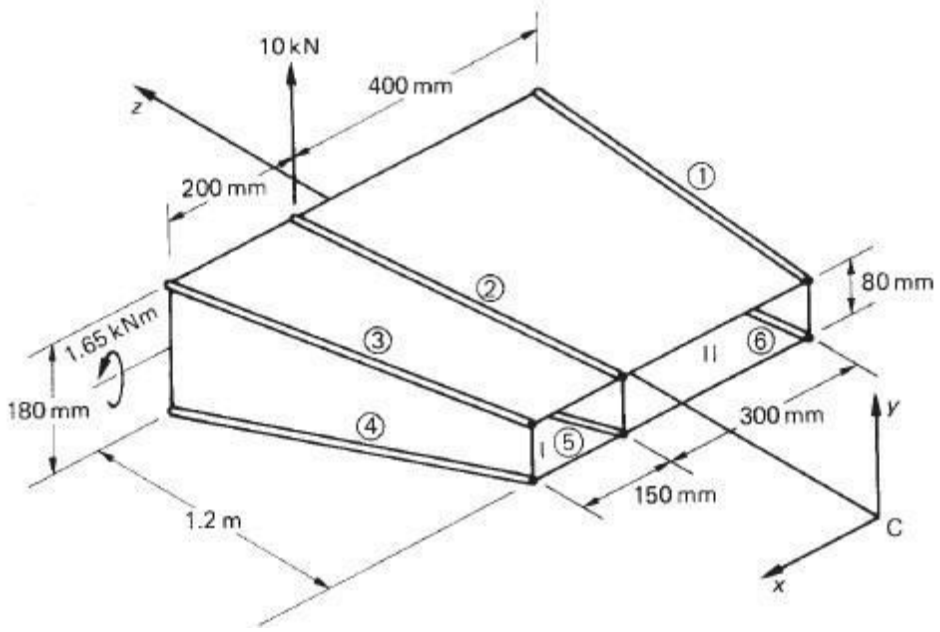
10 kN
400 mm
z
200 mm
①
②
80 mm
1.65 kNm
③
II
⑥
180 mm
④
300 mm
y
I
⑤
150 mm
1.2 m
C
x

AEROSPACE VEHICLE STRUCTURES -II

Model Question Paper – IV

PART A

ANSWER ALL QUESTIONS

1. Explain Instability of Stiffened panels.
2. A plate 10mmthick is subjected to bending moments Mx equal to 10 Nm/mm and My equal to 5 Nm/mm. Calculate the maximum direct stresses in the plate.
3. Explain about Bredt–Batho theory and formula.
4. Explain the condition for Zero warping at a section, and derive the warping of cross section.
5. What is the alternative method to find the shear flow distribution of idealized section.
6. Explain unitload method to find the deflection of beams.
7. Write the expressions for the bending and shear displacements of unsymmetrical thin-walled Beam using unitload method.
8. Write about general aspects of structural constraints.
9. What are the different methods of analysis for open section beams of wing structure?
10. Explain the effect of taper on shearflow distribution of wings.

PART A

ANSWER ALL QUESTIONS

1. Derive the equation $M_{xy} = D(1-\upsilon)\,\partial^2 w/\partial x \partial y$ for a thin plate subjected to bending and twisting.

(OR)

2. What are complete and incomplete diagonal tensions in Tension field beams? Also derive the equation to find out the uniform direct compressive stresses induced by the diagonal tension in the flanges and stiffeners.
3. A beam having the cross section shown in Figure is subjected to a bending moment of 1500 Nm in a vertical plane. Calculate the maximum direct stress due to bending stating the point at which it acts.

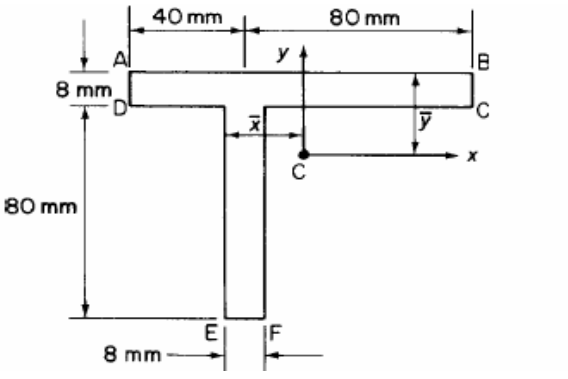

(OR)

4. Derive the equations to find out the primary and secondary warping of an open cross section subjected to Torsion.
5. The thin-walled single cell beam shown in Figure has been idealized into a combination

of direct stress-carrying booms and shear-stress-only-carrying walls. If the section supports a vertical shear load of 10 kN acting in a vertical plane through booms 3 and 6, calculate the distribution of shear flow around the section. Boom areas: $B1=B8=200$ mm^2, $B2=B7=250$ mm^2 $B3=B6=400$ mm^2, $B4=B5=100$ mm^2.

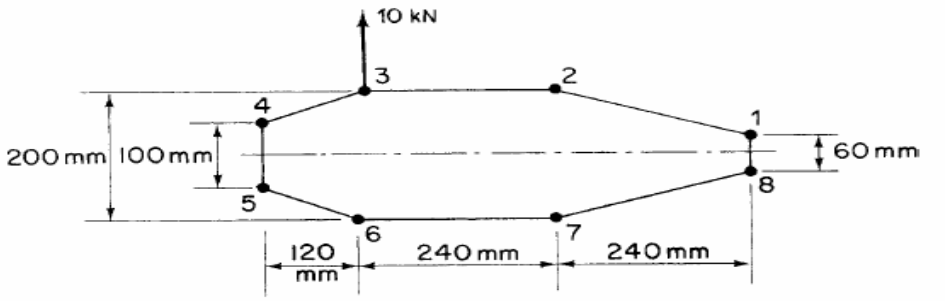

(OR)

6. Derive total Torque equation of an arbitrary section beam subjected to Torsion.

7. Calculate the shear stress distribution at the built-in end of the beam shown in Fig. when, at this section, it carries a shear load of 22 000N acting at a distance of 100mm from and parallel to side 12. The modulus of rigidity G is constant throughout the section:

Wall	12	34	23
Length (mm)	375	125	500

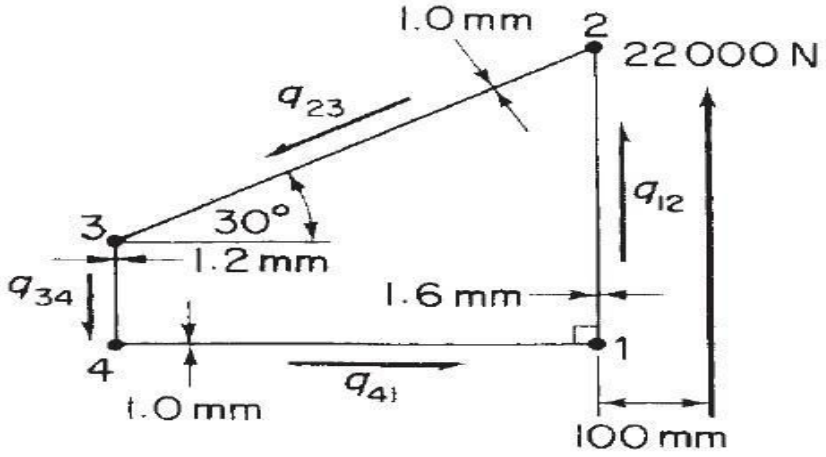

(OR)

8. Write short note on distributed torque loading and boundary conditions of cantilever beam.
9. A cantilever beam shown in Figure carries concentrated loads as shown. Calculate the distribution of stiffener loads and the shear flow distribution in the web panels assuming that the latter are effective only in shear.

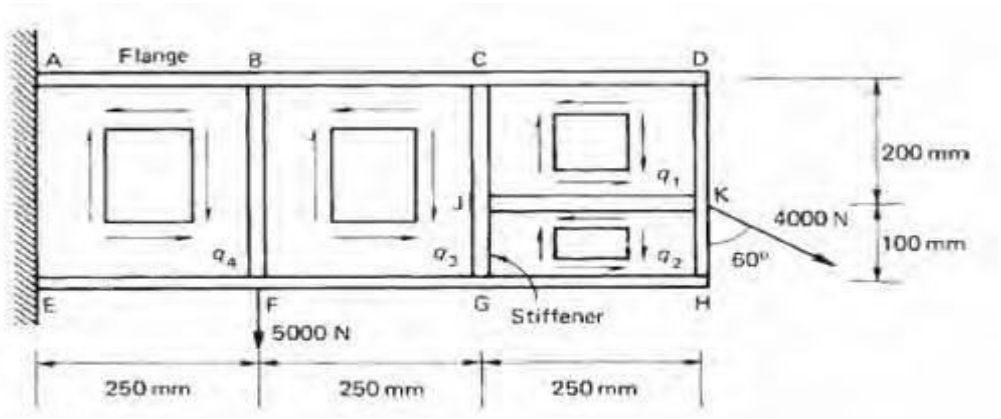

(OR)

10. Calculate the deflection at the free end of the two-cell beam shownin Fig. allowing for both bending and shear effects. The booms carry all the direct stresses while the skin panels, of constant thickness throughout, are effective only in shear. Take E = 69 000N/mm^2 and G = 25 900N/mm^2
Boom areas: $B1 = B3 = B4 = B6 = 650\text{mm}^2$ $B2 = B5 = 1300\text{mm}^2$

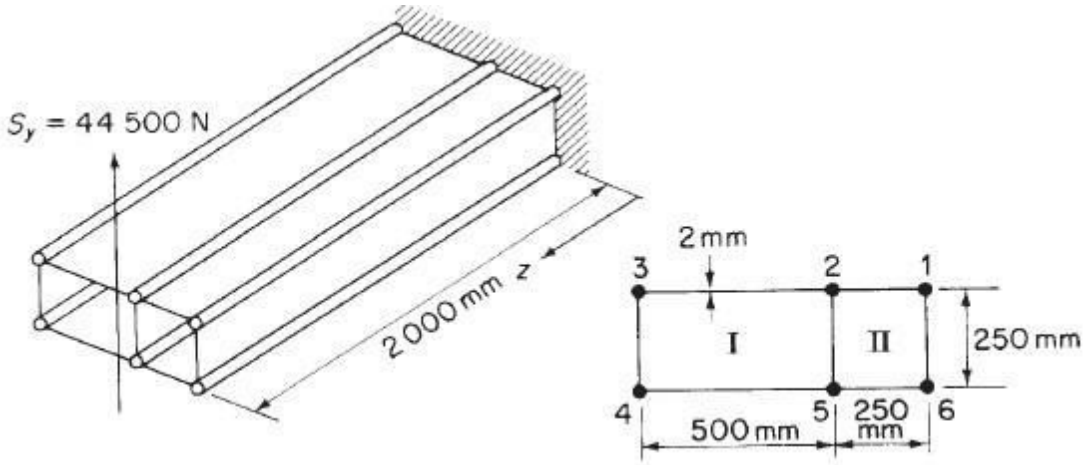

7

Bending of thin plates

Generally, we define a thin plate as a sheet of material whose thickness is small compared with its other dimensions but which is capable of resisting bending in addition to membrane forces. Such a plate forms a basic part of an aircraft structure, being, for example, the area of stressed skin bounded by adjacent stringers and ribs in a wing structure or by adjacent stringers and frames in a fuselage.

In this chapter we shall investigate the effect of a variety of loading and support conditions on the small deflection of rectangular plates. Two approaches are presented: an 'exact' theory based on the solution of a differential equation and an energy method relying on the principle of the stationary value of the total potential energy of the plate and its applied loading. The latter theory will subsequently be used in Chapter 9 to determine buckling loads for unstiffened and stiffened panels.

7.1 Pure bending of thin plates

The thin rectangular plate of Fig. 7.1 is subjected to pure bending moments of intensity M_x and M_y per unit length uniformly distributed along its edges. The former bending moment is applied along the edges parallel to the y axis, the latter along the edges

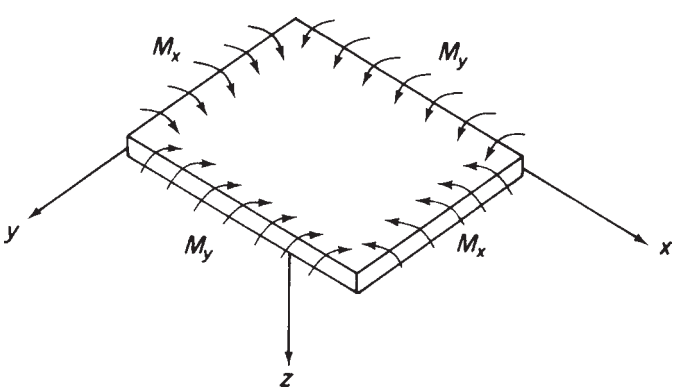

Fig. 7.1 Plate subjected to pure bending.

parallel to the x axis. We shall assume that these bending moments are positive when they produce compression at the upper surface of the plate and tension at the lower.

If we further assume that the displacement of the plate in a direction parallel to the z axis is small compared with its thickness t and that sections which are plane before bending remain plane after bending, then, as in the case of simple beam theory, the middle plane of the plate does not deform during the bending and is therefore a *neutral plane*. We take the neutral plane as the reference plane for our system of axes.

Let us consider an element of the plate of side $\delta x \delta y$ and having a depth equal to the thickness t of the plate as shown in Fig. 7.2(a). Suppose that the radii of curvature of the neutral plane n are ρ_x and ρ_y in the xz and yz planes respectively (Fig. 7.2(b)). Positive curvature of the plate corresponds to the positive bending moments which produce displacements in the positive direction of the z or downward axis. Again, as in simple beam theory, the direct strains ε_x and ε_y corresponding to direct stresses σ_x and σ_y of an elemental lamina of thickness δz a distance z below the neutral plane are given by

$$\varepsilon_x = \frac{z}{\rho_x} \quad \varepsilon_y = \frac{z}{\rho_y} \tag{7.1}$$

Referring to Eqs (1.52) we have

$$\varepsilon_x = \frac{1}{E}(\sigma_x - \nu\sigma_y) \quad \varepsilon_y = \frac{1}{E}(\sigma_y - \nu\sigma_x) \tag{7.2}$$

Substituting for ε_x and ε_y from Eqs (7.1) into (7.2) and rearranging gives

$$\left.\begin{aligned} \sigma_x &= \frac{Ez}{1-\nu^2}\left(\frac{1}{\rho_x} + \frac{\nu}{\rho_y}\right) \\ \sigma_y &= \frac{Ez}{1-\nu^2}\left(\frac{1}{\rho_y} + \frac{\nu}{\rho_x}\right) \end{aligned}\right\} \tag{7.3}$$

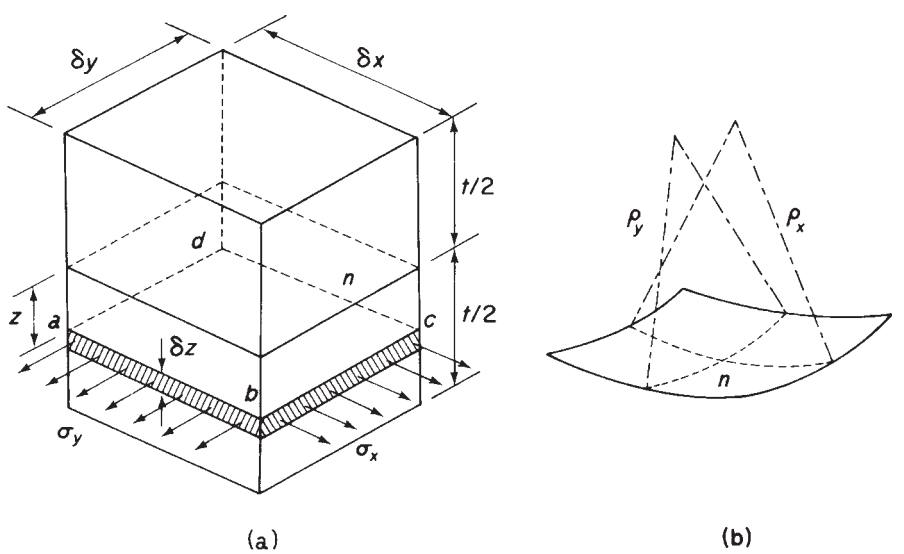

Fig. 7.2 (a) Direct stress on lamina of plate element; (b) radii of curvature of neutral plane.

As would be expected from our assumption of plane sections remaining plane the direct stresses vary linearly across the thickness of the plate, their magnitudes depending on the curvatures (i.e. bending moments) of the plate. The internal direct stress distribution on each vertical surface of the element must be in equilibrium with the applied bending moments. Thus

$$M_x \delta y = \int_{-t/2}^{t/2} \sigma_x z \delta y \, \mathrm{d}z$$

and

$$M_y \delta x = \int_{-t/2}^{t/2} \sigma_y z \delta x \, \mathrm{d}z$$

Substituting for σ_x and σ_y from Eqs (7.3) gives

$$M_x = \int_{-t/2}^{t/2} \frac{Ez^2}{1-\nu^2} \left(\frac{1}{\rho_x} + \frac{\nu}{\rho_y} \right) \mathrm{d}z$$

$$M_y = \int_{-t/2}^{t/2} \frac{Ez^2}{1-\nu^2} \left(\frac{1}{\rho_y} + \frac{\nu}{\rho_x} \right) \mathrm{d}z$$

Let

$$D = \int_{-t/2}^{t/2} \frac{Ez^2}{1-\nu^2} \mathrm{d}z = \frac{Et^3}{12(1-\nu^2)} \tag{7.4}$$

Then

$$M_x = D \left(\frac{1}{\rho_x} + \frac{\nu}{\rho_y} \right) \tag{7.5}$$

$$M_y = D \left(\frac{1}{\rho_y} + \frac{\nu}{\rho_x} \right) \tag{7.6}$$

in which D is known as the *flexural rigidity* of the plate.

If w is the deflection of any point on the plate in the z direction, then we may relate w to the curvature of the plate in the same manner as the well-known expression for beam curvature. Hence

$$\frac{1}{\rho_x} = -\frac{\partial^2 w}{\partial x^2} \quad \frac{1}{\rho_y} = -\frac{\partial^2 w}{\partial y^2}$$

the negative signs resulting from the fact that the centres of curvature occur above the plate in which region z is negative. Equations (7.5) and (7.6) then become

$$M_x = -D \left(\frac{\partial^2 w}{\partial x^2} + \nu \frac{\partial^2 w}{\partial y^2} \right) \tag{7.7}$$

$$M_y = -D \left(\frac{\partial^2 w}{\partial y^2} + \nu \frac{\partial^2 w}{\partial x^2} \right) \tag{7.8}$$

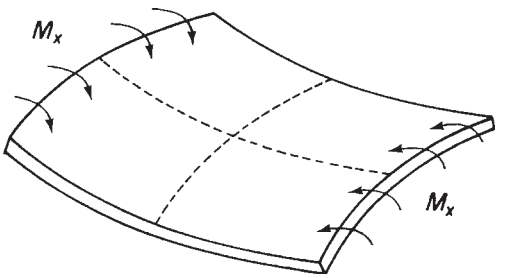

Fig. 7.3 Anticlastic bending.

Equations (7.7) and (7.8) define the deflected shape of the plate provided that M_x and M_y are known. If either M_x or M_y is zero then

$$\frac{\partial^2 w}{\partial x^2} = -\nu \frac{\partial^2 w}{\partial y^2} \quad \text{or} \quad \frac{\partial^2 w}{\partial y^2} = -\nu \frac{\partial^2 w}{\partial x^2}$$

and the plate has curvatures of opposite signs. The case of $M_y = 0$ is illustrated in Fig. 7.3. A surface possessing two curvatures of opposite sign is known as an *anticlastic surface*, as opposed to a *synclastic surface* which has curvatures of the same sign. Further, if $M_x = M_y = M$ then from Eqs (7.5) and (7.6)

$$\frac{1}{\rho_x} = \frac{1}{\rho_y} = \frac{1}{\rho}$$

Therefore, the deformed shape of the plate is spherical and of curvature

$$\frac{1}{\rho} = \frac{M}{D(1+\nu)} \tag{7.9}$$

7.2 Plates subjected to bending and twisting

In general, the bending moments applied to the plate will not be in planes perpendicular to its edges. Such bending moments, however, may be resolved in the normal manner into tangential and perpendicular components, as shown in Fig. 7.4. The perpendicular components are seen to be M_x and M_y as before, while the tangential components M_{xy} and M_{yx} (again these are moments per unit length) produce twisting of the plate about axes parallel to the x and y axes. The system of suffixes and the sign convention for these twisting moments must be clearly understood to avoid confusion. M_{xy} is a twisting moment intensity in a vertical x plane parallel to the y axis, while M_{yx} is a twisting moment intensity in a vertical y plane parallel to the x axis. Note that the first suffix gives the direction of the axis of the twisting moment. We also define positive twisting moments as being clockwise when viewed along their axes in directions parallel to the positive directions of the corresponding x or y axis. In Fig. 7.4, therefore, all moment intensities are positive.

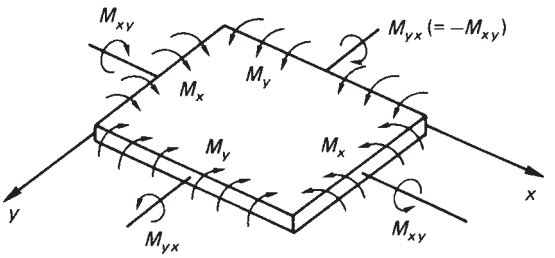

Fig. 7.4 Plate subjected to bending and twisting.

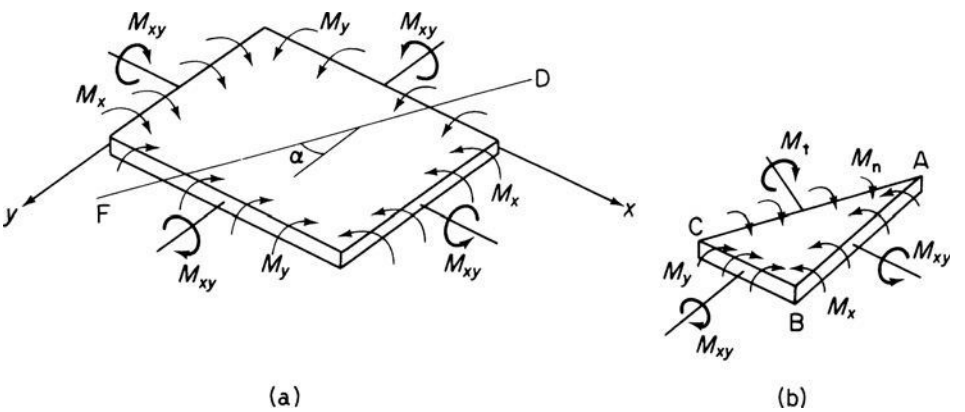

Fig. 7.5 (a) Plate subjected to bending and twisting; (b) tangential and normal moments on an arbitrary plane.

Since the twisting moments are tangential moments or torques they are resisted by a system of horizontal shear stresses τ_{xy}, as shown in Fig. 7.6. From a consideration of complementary shear stresses (see Fig. 7.6) $M_{xy} = -M_{yx}$, so that we may represent a general moment application to the plate in terms of M_x, M_y and M_{xy} as shown in Fig. 7.5(a). These moments produce tangential and normal moments, M_t and M_n, on an arbitrarily chosen diagonal plane FD. We may express these moment intensities (in an analogous fashion to the complex stress systems of Section 1.6) in terms of M_x, M_y and M_{xy}. Thus, for equilibrium of the triangular element ABC of Fig. 7.5(b) in a plane perpendicular to AC

$$M_\mathrm{n}\mathrm{AC} = M_x\mathrm{AB}\cos\alpha + M_y\mathrm{BC}\sin\alpha - M_{xy}\mathrm{AB}\sin\alpha - M_{xy}\mathrm{BC}\cos\alpha$$

giving

$$M_\mathrm{n} = M_x\cos^2\alpha + M_y\sin^2\alpha - M_{xy}\sin 2\alpha \tag{7.10}$$

Similarly for equilibrium in a plane parallel to CA

$$M_\mathrm{t}\mathrm{AC} = M_x\mathrm{AB}\sin\alpha - M_y\mathrm{BC}\cos\alpha + M_{xy}\mathrm{AB}\cos\alpha - M_{xy}\mathrm{BC}\sin\alpha$$

or

$$M_\mathrm{t} = \frac{(M_x - M_y)}{2}\sin 2\alpha + M_{xy}\cos 2\alpha \tag{7.11}$$

(compare Eqs (7.10) and (7.11) with Eqs (1.8) and (1.9)). We observe from Eq. (7.11) that there are two values of α, differing by 90° and given by

$$\tan 2\alpha = -\frac{2M_{xy}}{M_x - M_y}$$

for which $M_t = 0$, leaving normal moments of intensity M_n on two mutually perpendicular planes. These moments are termed *principal moments* and their corresponding curvatures *principal curvatures*. For a plate subjected to pure bending and twisting in which M_x, M_y and M_{xy} are invariable throughout the plate, the principal moments are the algebraically greatest and least moments in the plate. It follows that there are no shear stresses on these planes and that the corresponding direct stresses, for a given value of z and moment intensity, are the algebraically greatest and least values of direct stress in the plate.

Let us now return to the loaded plate of Fig. 7.5(a). We have established, in Eqs (7.7) and (7.8), the relationships between the bending moment intensities M_x and M_y and the deflection w of the plate. The next step is to relate the twisting moment M_{xy} to w. From the principle of superposition we may consider M_{xy} acting separately from M_x and M_y. As stated previously M_{xy} is resisted by a system of horizontal complementary shear stresses on the vertical faces of sections taken throughout the thickness of the plate parallel to the x and y axes. Consider an element of the plate formed by such sections, as shown in Fig. 7.6. The complementary shear stresses on a lamina of the element a distance z below the neutral plane are, in accordance with the sign convention of Section 1.2, τ_{xy}. Therefore, on the face ABCD

$$M_{xy}\delta y = -\int_{-t/2}^{t/2} \tau_{xy}\delta y z \, \mathrm{d}z$$

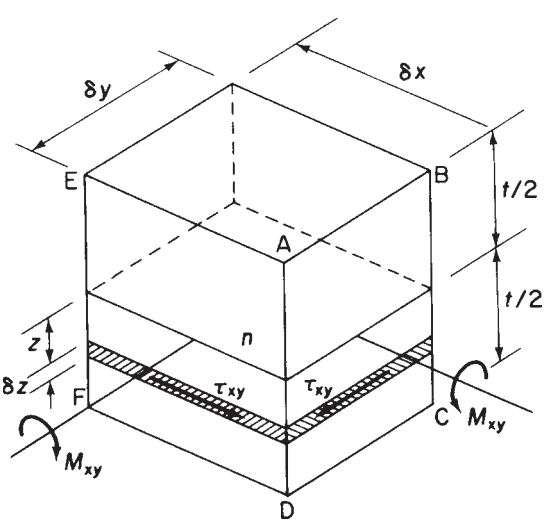

Fig. 7.6 Complementary shear stresses due to twisting moments M_{xy}.

and on the face ADFE

$$M_{xy}\delta x = -\int_{-t/2}^{t/2} \tau_{xy}\delta x z \, \mathrm{d}z$$

giving

$$M_{xy} = -\int_{-t/2}^{t/2} \tau_{xy} z \, \mathrm{d}z$$

or in terms of the shear strain γ_{xy} and modulus of rigidity G

$$M_{xy} = -G\int_{-t/2}^{t/2} \gamma_{xy} z \, \mathrm{d}z \tag{7.12}$$

Referring to Eqs (1.20), the shear strain γ_{xy} is given by

$$\gamma_{xy} = \frac{\partial v}{\partial x} + \frac{\partial u}{\partial y}$$

We require, of course, to express γ_{xy} in terms of the deflection w of the plate; this may be accomplished as follows. An element taken through the thickness of the plate will suffer rotations equal to $\partial w/\partial x$ and $\partial w/\partial y$ in the xz and yz planes respectively. Considering the rotation of such an element in the xz plane, as shown in Fig. 7.7, we see that the displacement u in the x direction of a point a distance z below the neutral plane is

$$u = -\frac{\partial w}{\partial x} z$$

Similarly, the displacement v in the y direction is

$$v = -\frac{\partial w}{\partial y} z$$

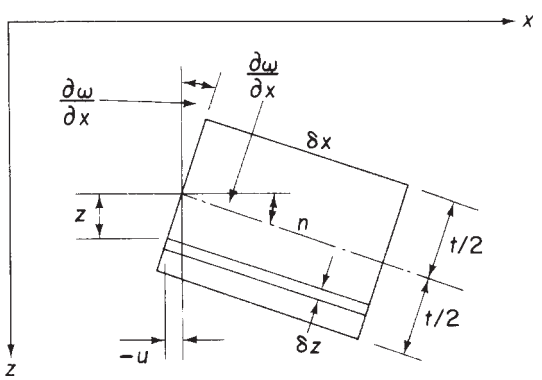

Fig. 7.7 Determination of shear strain γ_{xy}.

Hence, substituting for u and v in the expression for γ_{xy} we have

$$\gamma_{xy} = -2z\frac{\partial^2 w}{\partial x \partial y} \tag{7.13}$$

whence from Eq. (7.12)

$$M_{xy} = G\int_{-t/2}^{t/2} 2z^2 \frac{\partial^2 w}{\partial x \partial y} \mathrm{d}z$$

or

$$M_{xy} = \frac{Gt^3}{6}\frac{\partial^2 w}{\partial x \partial y}$$

Replacing G by the expression $E/2(1+\nu)$ established in Eq. (1.50) gives

$$M_{xy} = \frac{Et^3}{12(1+\nu)}\frac{\partial^2 w}{\partial x \partial y}$$

Multiplying the numerator and denominator of this equation by the factor $(1-\nu)$ yields

$$M_{xy} = D(1-\nu)\frac{\partial^2 w}{\partial x \partial y} \tag{7.14}$$

Equations (7.7), (7.8) and (7.14) relate the bending and twisting moments to the plate deflection and are analogous to the bending moment-curvature relationship for a simple beam.

7.3 Plates subjected to a distributed transverse load

The relationships between bending and twisting moments and plate deflection are now employed in establishing the general differential equation for the solution of a thin rectangular plate, supporting a distributed transverse load of intensity q per unit area (see Fig. 7.8). The distributed load may, in general, vary over the surface of the plate and is therefore a function of x and y. We assume, as in the preceding analysis, that the middle plane of the plate is the neutral plane and that the plate deforms such that plane sections remain plane after bending. This latter assumption introduces an apparent inconsistency in the theory. For plane sections to remain plane the shear strains γ_{xz} and γ_{yz} must be zero. However, the transverse load produces transverse shear forces (and therefore stresses) as shown in Fig. 7.9. We therefore assume that although $\gamma_{xz} = \tau_{xz}/G$ and $\gamma_{yz} = \tau_{yz}/G$ are negligible the corresponding shear forces are of the same order of magnitude as the applied load q and the moments M_x, M_y and M_{xy}. This assumption is analogous to that made in a slender beam theory in which shear strains are ignored.

The element of plate shown in Fig. 7.9 supports bending and twisting moments as previously described and, in addition, vertical shear forces Q_x and Q_y per unit length on faces perpendicular to the x and y axes, respectively. The variation of shear stresses τ_{xz} and τ_{yz} along the small edges δx, δy of the element is neglected and the resultant

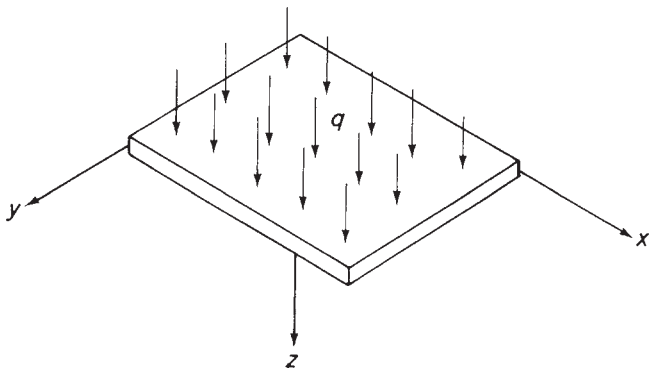

Fig. 7.8 Plate supporting a distributed transverse load.

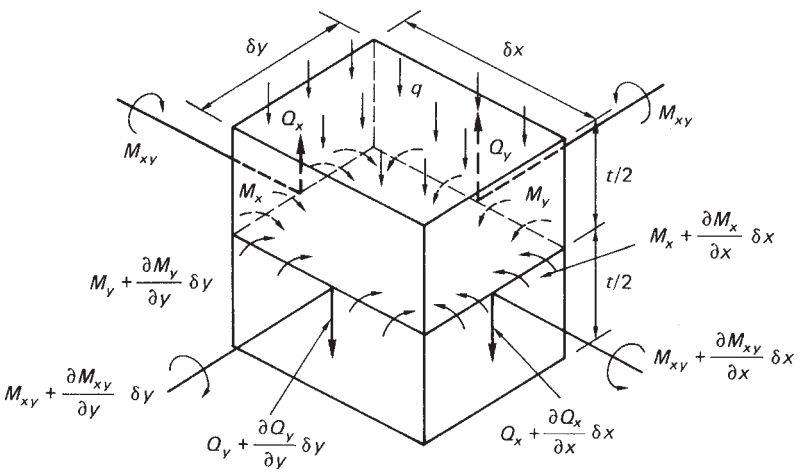

Fig. 7.9 Plate element subjected to bending, twisting and transverse loads.

shear forces $Q_x\delta y$ and $Q_y\delta x$ are assumed to act through the centroid of the faces of the element. From the previous sections

$$M_x = \int_{-t/2}^{t/2} \sigma_x z \, \mathrm{d}z \quad M_y = \int_{-t/2}^{t/2} \sigma_y z \, \mathrm{d}z \quad M_{xy} = (-M_{yx}) = -\int_{-t/2}^{t/2} \tau_{xy} z \, \mathrm{d}z$$

In a similar fashion

$$Q_x = \int_{-t/2}^{t/2} \tau_{xz} \, \mathrm{d}z \quad Q_y = \int_{-t/2}^{t/2} \tau_{yz} \, \mathrm{d}z \tag{7.15}$$

For equilibrium of the element parallel to Oz and assuming that the weight of the plate is included in q

$$\left(Q_x + \frac{\partial Q_x}{\partial x}\delta x\right)\delta y - Q_x\delta y + \left(Q_y + \frac{\partial Q_y}{\partial y}\delta y\right)\delta x - Q_y\delta x + q\delta x\delta y = 0$$

or, after simplification

$$\frac{\partial Q_x}{\partial x} + \frac{\partial Q_y}{\partial y} + q = 0 \tag{7.16}$$

Taking moments about the x axis

$$M_{xy}\delta y - \left(M_{xy} + \frac{\partial M_{xy}}{\partial x}\delta x\right)\delta y - M_y \delta x + \left(M_y + \frac{\partial M_y}{\partial y}\delta y\right)\delta x$$
$$- \left(Q_y + \frac{\partial Q_y}{\partial y}\delta y\right)\delta x \delta y + Q_x \frac{\delta y^2}{2} - \left(Q_x + \frac{\partial Q_x}{\partial x}\delta x\right)\frac{\delta y^2}{2} - q\delta x \frac{\delta y^2}{2} = 0$$

Simplifying this equation and neglecting small quantities of a higher order than those retained gives

$$\frac{\partial M_{xy}}{\partial x} - \frac{\partial M_y}{\partial y} + Q_y = 0 \tag{7.17}$$

Similarly taking moments about the y axis we have

$$\frac{\partial M_{xy}}{\partial y} - \frac{\partial M_x}{\partial x} + Q_x = 0 \tag{7.18}$$

Substituting in Eq. (7.16) for Q_x and Q_y from Eqs (7.18) and (7.17) we obtain

$$\frac{\partial^2 M_x}{\partial x^2} - \frac{\partial^2 M_{xy}}{\partial x \partial y} + \frac{\partial^2 M_y}{\partial y^2} - \frac{\partial^2 M_{xy}}{\partial x \partial y} = -q$$

or

$$\frac{\partial^2 M_x}{\partial x^2} - 2\frac{\partial^2 M_{xy}}{\partial x \partial y} + \frac{\partial^2 M_y}{\partial y^2} = -q \tag{7.19}$$

Replacing M_x, M_{xy} and M_y in Eq. (7.19) from Eqs (7.7), (7.14) and (7.8) gives

$$\frac{\partial^4 w}{\partial x^4} + 2\frac{\partial^4 w}{\partial x^2 \partial y^2} + \frac{\partial^4 w}{\partial y^4} = \frac{q}{D} \tag{7.20}$$

This equation may also be written

$$\left(\frac{\partial^2}{\partial x^2} + \frac{\partial^2}{\partial y^2}\right)\left(\frac{\partial^2 w}{\partial x^2} + \frac{\partial^2 w}{\partial y^2}\right) = \frac{q}{D}$$

or

$$\left(\frac{\partial^2}{\partial x^2} + \frac{\partial^2}{\partial y^2}\right)^2 w = \frac{q}{D}$$

The operator $(\partial^2/\partial x^2 + \partial^2/\partial y^2)$ is the well-known Laplace operator in two dimensions and is sometimes written as ∇^2. Thus

$$(\nabla^2)^2 w = \frac{q}{D}$$

Generally, the transverse distributed load q is a function of x and y so that the determination of the deflected form of the plate reduces to obtaining a solution of Eq. (7.20), which satisfies the known boundary conditions of the problem. The bending and twisting moments follow from Eqs (7.7), (7.8) and (7.14), and the shear forces per unit length Q_x and Q_y are found from Eqs (7.17) and (7.18) by substitution for M_x, M_y and M_{xy} in terms of the deflection w of the plate; thus

$$Q_x = \frac{\partial M_x}{\partial x} - \frac{\partial M_{xy}}{\partial y} = -D\frac{\partial}{\partial x}\left(\frac{\partial^2 w}{\partial x^2} + \frac{\partial^2 w}{\partial y^2}\right) \tag{7.21}$$

$$Q_y = \frac{\partial M_y}{\partial y} - \frac{\partial M_{xy}}{\partial x} = -D\frac{\partial}{\partial y}\left(\frac{\partial^2 w}{\partial x^2} + \frac{\partial^2 w}{\partial y^2}\right) \tag{7.22}$$

Direct and shear stresses are then calculated from the relevant expressions relating them to M_x, M_y, M_{xy}, Q_x and Q_y.

Before discussing the solution of Eq. (7.20) for particular cases we shall establish boundary conditions for various types of edge support.

7.3.1 The simply supported edge

Let us suppose that the edge $x = 0$ of the thin plate shown in Fig. 7.10 is free to rotate but not to deflect. The edge is then said to be simply supported. The bending moment along this edge must be zero and also the deflection $w = 0$. Thus

$$(w)_{x=0} = 0 \quad \text{and} \quad (M_x)_{x=0} = -D\left(\frac{\partial^2 w}{\partial x^2} + \nu\frac{\partial^2 w}{\partial y^2}\right)_{x=0} = 0$$

The condition that $w = 0$ along the edge $x = 0$ also means that

$$\frac{\partial w}{\partial y} = \frac{\partial^2 w}{\partial y^2} = 0$$

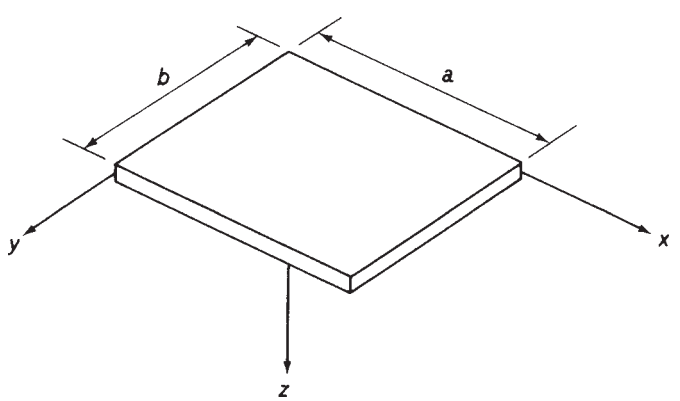

Fig. 7.10 Plate of dimensions $a \times b$.

along this edge. The above boundary conditions therefore reduce to

$$(w)_{x=0} = 0 \quad \left(\frac{\partial^2 w}{\partial x^2}\right)_{x=0} = 0 \tag{7.23}$$

7.3.2 The built-in edge

If the edge $x = 0$ is built-in or firmly clamped so that it can neither rotate nor deflect, then, in addition to w, the slope of the middle plane of the plate normal to this edge must be zero. That is

$$(w)_{x=0} = 0 \quad \left(\frac{\partial w}{\partial x}\right)_{x=0} = 0 \tag{7.24}$$

7.3.3 The free edge

Along a free edge there are no bending moments, twisting moments or vertical shearing forces, so that if $x = 0$ is the free edge then

$$(M_x)_{x=0} = 0 \quad (M_{xy})_{x=0} = 0 \quad (Q_x)_{x=0} = 0$$

giving, in this instance, three boundary conditions. However, Kirchhoff (1850) showed that only two boundary conditions are necessary to obtain a solution of Eq. (7.20), and that the reduction is obtained by replacing the two requirements of zero twisting moment and zero shear force by a single equivalent condition. Thomson and Tait (1883) gave a physical explanation of how this reduction may be effected. They pointed out that the horizontal force system equilibrating the twisting moment M_{xy} may be replaced along the edge of the plate by a vertical force system.

Consider two adjacent elements δy_1 and δy_2 along the edge of the thin plate of Fig. 7.11. The twisting moment $M_{xy}\delta y_1$ on the element δy_1 may be replaced by *forces* M_{xy} a distance δy_1 apart. Note that M_{xy}, being a twisting moment per unit length, has the dimensions of force. The twisting moment on the adjacent element δy_2 is $[M_{xy} + (\partial M_{xy}/\partial y)\delta y]\delta y_2$. Again this may be replaced by forces $M_{xy} + (\partial M_{xy}/\partial y)\delta y$. At the common surface of the two adjacent elements there is now a resultant force $(\partial M_{xy}/\partial y)\delta y$ or a vertical force per unit length of $\partial M_{xy}/\partial y$. For the sign convention for Q_x shown in Fig. 7.9 we have a statically equivalent vertical force per unit length of $(Q_x - \partial M_{xy}/\partial y)$. The separate conditions for a free edge of $(M_{xy})_{x=0} = 0$ and $(Q_x)_{x=0} = 0$ are therefore replaced by the equivalent condition

$$\left(Q_x - \frac{\partial M_{xy}}{\partial y}\right)_{x=0} = 0$$

or in terms of deflection

$$\left[\frac{\partial^3 w}{\partial x^3} + (2 - \nu)\frac{\partial^3 w}{\partial x \partial y^2}\right]_{x=0} = 0 \tag{7.25}$$

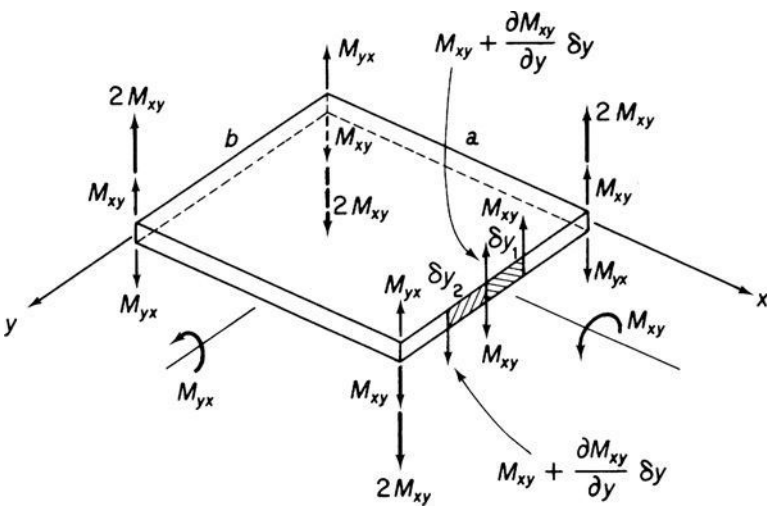

Fig. 7.11 Equivalent vertical force system.

Also, for the bending moment along the free edge to be zero

$$(M_x)_{x=0} = \left(\frac{\partial^2 w}{\partial x^2} + \nu\frac{\partial^2 w}{\partial y^2}\right)_{x=0} = 0 \tag{7.26}$$

The replacement of the twisting moment M_{xy} along the edges $x = 0$ and $x = a$ of a thin plate by a vertical force distribution results in leftover concentrated forces at the corners of M_{xy} as shown in Fig. 7.11. By the same argument there are concentrated forces M_{yx} produced by the replacement of the twisting moment M_{yx}. Since $M_{xy} = -M_{yx}$, then resultant forces $2M_{xy}$ act at each corner as shown and must be provided by external supports if the corners of the plate are not to move. The directions of these forces are easily obtained if the deflected shape of the plate is known. For example, a thin plate simply supported along all four edges and uniformly loaded has $\partial w/\partial x$ positive and numerically increasing, with increasing y near the corner $x = 0$, $y = 0$. Hence $\partial^2 w/\partial x \partial y$ is positive at this point and from Eq. (7.14) we see that M_{xy} is positive and M_{yx} negative; the resultant force $2M_{xy}$ is therefore downwards. From symmetry the force at each remaining corner is also $2M_{xy}$ downwards so that the tendency is for the corners of the plate to rise.

Having discussed various types of boundary conditions we shall proceed to obtain the solution for the relatively simple case of a thin rectangular plate of dimensions $a \times b$, simply supported along each of its four edges and carrying a distributed load $q(x, y)$.We have shown that the deflected form of the plate must satisfy the differential equation

$$\frac{\partial^4 w}{\partial x^4} + 2\frac{\partial^4 w}{\partial x^2 \partial y^2} + \frac{\partial^4 w}{\partial y^4} = \frac{q(x, y)}{D}$$

with the boundary conditions

$$(w)_{x=0,a} = 0 \quad \left(\frac{\partial^2 w}{\partial x^2}\right)_{x=0,a} = 0$$

$$(w)_{y=0,b} = 0 \quad \left(\frac{\partial^2 w}{\partial y^2}\right)_{x=0,b} = 0$$

Navier (1820) showed that these conditions are satisfied by representing the deflection w as an infinite trigonometrical or Fourier series

$$w = \sum_{m=1}^{\infty}\sum_{n=1}^{\infty} A_{mn} \sin\frac{m\pi x}{a} \sin\frac{n\pi y}{b} \tag{7.27}$$

in which m represents the number of half waves in the x direction and n the corresponding number in the y direction. Further, A_{mn} are unknown coefficients which must satisfy the above differential equation and may be determined as follows.

We may also represent the load $q(x, y)$ by a Fourier series, thus

$$q(x, y) = \sum_{m=1}^{\infty}\sum_{n=1}^{\infty} a_{mn} \sin\frac{m\pi x}{a} \sin\frac{n\pi y}{b} \tag{7.28}$$

A particular coefficient $a_{m'n'}$ is calculated by first multiplying both sides of Eq. (7.28) by $\sin(m'\pi x/a)\sin(n'\pi y/b)$ and integrating with respect to x from 0 to a and with respect to y from 0 to b. Thus

$$\begin{aligned}
&\int_0^a \int_0^b q(x, y) \sin\frac{m'\pi x}{a} \sin\frac{n'\pi y}{b}\, \mathrm{d}x\, \mathrm{d}y \\
&\quad = \sum_{m=1}^{\infty}\sum_{n=1}^{\infty} \int_0^a \int_0^b a_{mn} \sin\frac{m\pi x}{a} \sin\frac{m'\pi x}{a} \sin\frac{n\pi y}{b} \sin\frac{n'\pi y}{b}\, \mathrm{d}x\, \mathrm{d}y \\
&\quad = \frac{ab}{4} a_{m'n'}
\end{aligned}$$

since

$$\begin{aligned}
\int_0^a \sin\frac{m\pi x}{a} \sin\frac{m'\pi x}{a}\, \mathrm{d}x &= 0 \quad \text{when} \quad m \neq m' \\
&= \frac{a}{2} \quad \text{when} \quad m = m'
\end{aligned}$$

and

$$\begin{aligned}
\int_0^b \sin\frac{n\pi y}{b} \sin\frac{n'\pi y}{b}\, \mathrm{d}y &= 0 \quad \text{when} \quad n \neq n' \\
&= \frac{b}{2} \quad \text{when} \quad n = n'
\end{aligned}$$

It follows that

$$a_{m'n'} = \frac{4}{ab}\int_0^a \int_0^b q(x,y)\sin\frac{m'\pi x}{a}\sin\frac{n'\pi y}{b}\,\mathrm{d}x\,\mathrm{d}y \tag{7.29}$$

Substituting now for w and $q(x, y)$ from Eqs (7.27) and (7.28) into the differential equation for w we have

$$\sum_{m=1}^{\infty}\sum_{n=1}^{\infty}\left\{A_{mn}\left[\left(\frac{m\pi}{a}\right)^4 + 2\left(\frac{m\pi}{a}\right)^2\left(\frac{n\pi}{b}\right)^2 + \left(\frac{n\pi}{b}\right)^4\right] - \frac{a_{mn}}{D}\right\}\sin\frac{m\pi x}{a}\sin\frac{n\pi y}{b} = 0$$

This equation is valid for all values of x and y so that

$$A_{mn}\left[\left(\frac{m\pi}{a}\right)^4 + 2\left(\frac{m\pi}{a}\right)^2\left(\frac{n\pi}{b}\right)^2 + \left(\frac{n\pi}{b}\right)^4\right] - \frac{a_{mn}}{D} = 0$$

or in alternative form

$$A_{mn}\pi^4\left(\frac{m^2}{a^2} + \frac{n^2}{b^2}\right)^2 - \frac{a_{mn}}{D} = 0$$

giving

$$A_{mn} = \frac{1}{\pi^4 D}\frac{a_{mn}}{[(m^2/a^2) + (n^2/b^2)]^2}$$

Hence

$$w = \frac{1}{\pi^4 D}\sum_{m=1}^{\infty}\sum_{n=1}^{\infty}\frac{a_{mn}}{[(m^2/a^2) + (n^2/b^2)]^2}\sin\frac{m\pi x}{a}\sin\frac{n\pi y}{b} \tag{7.30}$$

in which a_{mn} is obtained from Eq. (7.29). Equation (7.30) is the general solution for a thin rectangular plate under a transverse load $q(x, y)$.

Example 7.1

A thin rectangular plate $a \times b$ is simply supported along its edges and carries a uniformly distributed load of intensity q_0. Determine the deflected form of the plate and the distribution of bending moment.

Since $q(x, y) = q_0$ we find from Eq. (7.29) that

$$a_{mn} = \frac{4q_0}{ab}\int_0^a \int_0^b \sin\frac{m\pi x}{a}\sin\frac{n\pi y}{b}\,\mathrm{d}x\,\mathrm{d}y = \frac{16q_0}{\pi^2 mn}$$

where m and n are odd integers. For m or n even, $a_{mn} = 0$. Hence from Eq. (7.30)

$$w = \frac{16q_0}{\pi^6 D}\sum_{m=1,3,5}^{\infty}\sum_{n=1,3,5}^{\infty}\frac{\sin(m\pi x/a)\sin(n\pi y/b)}{mn[(m^2/a^2) + (n^2/b^2)]^2} \tag{i}$$

The maximum deflection occurs at the centre of the plate where $x = a/2$, $y = b/2$. Thus

$$w_{\max} = \frac{16q_0}{\pi^6 D} \sum_{m=1,3,5}^{\infty} \sum_{n=1,3,5}^{\infty} \frac{\sin(m\pi/2)\sin(n\pi/2)}{mn[(m^2/a^2)+(n^2/b^2)]^2} \tag{ii}$$

This series is found to converge rapidly, the first few terms giving a satisfactory answer. For a square plate, taking $\nu = 0.3$, summation of the first four terms of the series gives

$$w_{\max} = 0.0443 q_0 \frac{a^4}{Et^3}$$

Substitution for w from Eq. (i) into the expressions for bending moment, Eqs (7.7) and (7.8), yields

$$M_x = \frac{16q_0}{\pi^4} \sum_{m=1,3,5}^{\infty} \sum_{n=1,3,5}^{\infty} \frac{[(m^2/a^2)+\nu(n^2/b^2)]}{mn[(m^2/a^2)+(n^2/b^2)]^2} \sin\frac{m\pi x}{a} \sin\frac{n\pi y}{b} \tag{iii}$$

$$M_y = \frac{16q_0}{\pi^4} \sum_{m=1,3,5}^{\infty} \sum_{n=1,3,5}^{\infty} \frac{[\nu(m^2/a^2)+(n^2/b^2)]}{mn[(m^2/a^2)+(n^2/b^2)]^2} \sin\frac{m\pi x}{a} \sin\frac{n\pi y}{b} \tag{iv}$$

Maximum values occur at the centre of the plate. For a square plate $a = b$ and the first five terms give

$$M_{x,\max} = M_{y,\max} = 0.0479 q_0 a^2$$

Comparing Eqs (7.3) with Eqs (7.5) and (7.6) we observe that

$$\sigma_x = \frac{12M_x z}{t^3} \quad \sigma_y = \frac{12M_y z}{t^3}$$

Again the maximum values of these stresses occur at the centre of the plate at $z = \pm t/2$ so that

$$\sigma_{x,\max} = \frac{6M_x}{t^2} \quad \sigma_{y,\max} = \frac{6M_y}{t^2}$$

For the square plate

$$\sigma_{x,\max} = \sigma_{y,\max} = 0.287 q_0 \frac{a^2}{t^2}$$

The twisting moment and shear stress distributions follow in a similar manner.

The infinite series (Eq. (7.27)) assumed for the deflected shape of a plate gives an exact solution for displacements and stresses. However, a more rapid, but approximate, solution may be obtained by assuming a displacement function in the form of a polynomial. The polynomial must, of course, satisfy the governing differential equation (Eq. (7.20)) and the boundary conditions of the specific problem. The "guessed" form of the deflected shape of a plate is the basis for the energy method of solution described in Section 7.6.

Example 7.2

Show that the deflection function

$$w = A(x^2y^2 - bx^2y - axy^2 + abxy)$$

is valid for a rectangular plate of sides a and b, built in on all four edges and subjected to a uniformly distributed load of intensity q. If the material of the plate has a Young's modulus E and is of thickness t determine the distributions of bending moment along the edges of the plate.

Differentiating the deflection function gives

$$\frac{\partial^4 w}{\partial x^4} = 0 \quad \frac{\partial^4 w}{\partial y^4} = 0 \quad \frac{\partial^4 w}{\partial x^2 \partial y^2} = 4A$$

Substituting in Eq. (7.20) we have

$$0 + 2 \times 4A + 0 = \text{constant} = \frac{q}{D}$$

The deflection function is therefore valid and

$$A = \frac{q}{8D}$$

The bending moment distributions are given by Eqs (7.7) and (7.8), i.e.

$$M_x = -\frac{q}{4}[y^2 - by + \nu(x^2 - ax)] \tag{i}$$

$$M_y = -\frac{q}{4}[x^2 - ax + \nu(y^2 - by)] \tag{ii}$$

For the edges $x = 0$ and $x = a$

$$M_x = -\frac{q}{4}(y^2 - by) \quad M_y = -\frac{\nu q}{4}(y^2 - by)$$

For the edges $y = 0$ and $y = b$

$$M_x = -\frac{\nu q}{4}(x^2 - ax) \quad M_y = -\frac{q}{4}(x^2 - ax)$$

7.4 Combined bending and in-plane loading of a thin rectangular plate

So far our discussion has been limited to small deflections of thin plates produced by different forms of transverse loading. In these cases we assumed that the middle or neutral plane of the plate remained unstressed. Additional in-plane tensile, compressive or shear loads will produce stresses in the middle plane, and these, if of sufficient magnitude, will affect the bending of the plate. Where the in-plane stresses are small

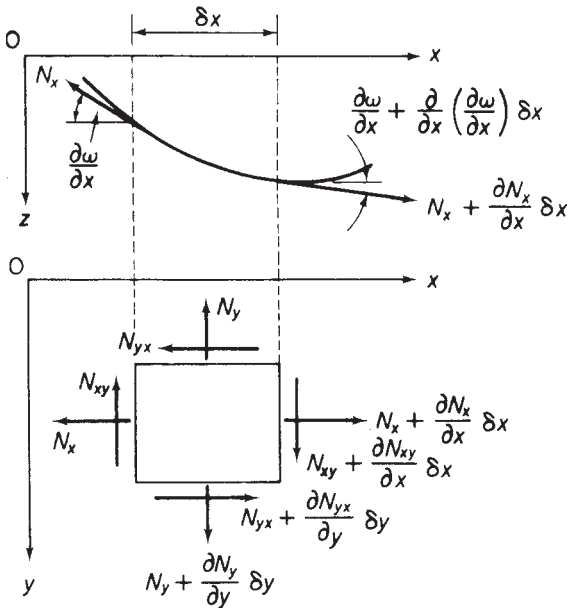

Fig. 7.12 In-plane forces on plate element.

compared with the critical buckling stresses it is sufficient to consider the two systems separately; the total stresses are then obtained by superposition. On the other hand, if the in-plane stresses are not small then their effect on the bending of the plate must be considered.

The elevation and plan of a small element $\delta x \delta y$ of the middle plane of a thin deflected plate are shown in Fig. 7.12. Direct and shear forces per unit length produced by the in-plane loads are given the notation N_x, N_y and N_{xy} and are assumed to be acting in positive senses in the directions shown. Since there are no resultant forces in the x or y directions from the transverse loads (see Fig. 7.9) we need only include the in-plane loads shown in Fig. 7.12 when considering the equilibrium of the element in these directions. For equilibrium parallel to Ox

$$\left(N_x + \frac{\partial N_x}{\partial x}\delta x\right)\delta y \cos\left(\frac{\partial w}{\partial x} + \frac{\partial^2 w}{\partial x^2}\delta x\right) - N_x \delta y \cos\frac{\partial w}{\partial x} + \left(N_{yx} + \frac{\partial N_{yx}}{\partial y}\delta y\right)\delta x - N_{yx}\delta x = 0$$

For small deflections $\partial w/\partial x$ and $(\partial w/\partial x) + (\partial^2 w/\partial x^2)\delta x$ are small and the cosines of these angles are therefore approximately equal to one. The equilibrium equation thus simplifies to

$$\frac{\partial N_x}{\partial x} + \frac{\partial N_{yx}}{\partial y} = 0 \tag{7.31}$$

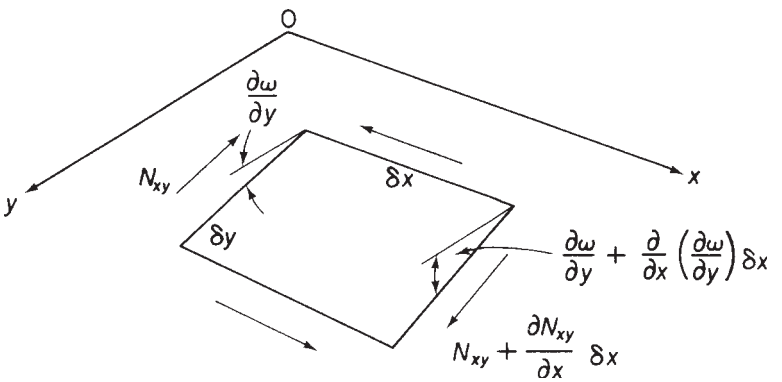

Fig. 7.13 Component of shear loads in the z direction.

Similarly for equilibrium in the y direction we have

$$\frac{\partial N_y}{\partial y} + \frac{\partial N_{xy}}{\partial x} = 0 \tag{7.32}$$

Note that the components of the in-plane shear loads per unit length are, to a first order of approximation, the value of the shear load multiplied by the projection of the element on the relevant axis.

The determination of the contribution of the shear loads to the equilibrium of the element in the z direction is complicated by the fact that the element possesses curvature in both xz and yz planes. Therefore, from Fig. 7.13 the component in the z direction due to the N_{xy} shear loads only is

$$\left(N_{xy} + \frac{\partial N_{xy}}{\partial x}\delta x\right)\delta y\left(\frac{\partial w}{\partial y} + \frac{\partial^2 w}{\partial x\,\partial y}\delta x\right) - N_{xy}\delta y\frac{\partial w}{\partial y}$$

or

$$N_{xy}\frac{\partial^2 w}{\partial x\,\partial y}\delta x\,\delta y + \frac{\partial N_{xy}}{\partial x}\frac{\partial w}{\partial y}\delta x\,\delta y$$

neglecting terms of a lower order. Similarly, the contribution of N_{yx} is

$$N_{yx}\frac{\partial^2 w}{\partial x\,\partial y}\delta x\,\delta y + \frac{\partial N_{yx}}{\partial y}\frac{\partial w}{\partial x}\delta x\,\delta y$$

The components arising from the direct forces per unit length are readily obtained from Fig. 7.12, namely

$$\left(N_x + \frac{\partial N_x}{\partial x}\delta x\right)\delta y\left(\frac{\partial w}{\partial x} + \frac{\partial^2 w}{\partial x^2}\delta x\right) - N_x\delta y\frac{\partial w}{\partial x}$$

or

$$N_x\frac{\partial^2 w}{\partial x^2}\delta x\,\delta y + \frac{\partial N_x}{\partial x}\frac{\partial w}{\partial x}\delta x\,\delta y$$

and similarly

$$N_y \frac{\partial^2 w}{\partial y^2}\delta x\,\delta y + \frac{\partial N_y}{\partial y}\frac{\partial w}{\partial y}\delta x\,\delta y$$

The total force in the z direction is found from the summation of these expressions and is

$$N_x \frac{\partial^2 w}{\partial x^2}\delta x\,\delta y + \frac{\partial N_x}{\partial x}\frac{\partial w}{\partial x}\delta x\,\delta y + N_y \frac{\partial^2 w}{\partial y^2}\delta x\,\delta y + \frac{\partial N_y}{\partial y}\frac{\partial w}{\partial y}\delta x\,\delta y$$
$$+ \frac{\partial N_{xy}}{\partial x}\frac{\partial w}{\partial y}\delta x\,\delta y + 2N_{xy}\frac{\partial^2 w}{\partial x\,\partial y}\delta x\,\delta y + \frac{\partial N_{xy}}{\partial y}\frac{\partial w}{\partial x}\delta x\,\delta y$$

in which N_{yx} is equal to and is replaced by N_{xy}. Using Eqs (7.31) and (7.32) we reduce this expression to

$$\left(N_x \frac{\partial^2 w}{\partial x^2} + N_y \frac{\partial^2 w}{\partial y^2} + 2N_{xy}\frac{\partial^2 w}{\partial x\,\partial y}\right)\delta x\,\delta y$$

Since the in-plane forces do not produce moments along the edges of the element then Eqs (7.17) and (7.18) remain unaffected. Further, Eq. (7.16) may be modified simply by the addition of the above vertical component of the in-plane loads to $q\delta x\delta y$. Therefore, the governing differential equation for a thin plate supporting transverse and in-plane loads is, from Eq. (7.20)

$$\frac{\partial^4 w}{\partial x^4} + 2\frac{\partial^4 w}{\partial x^2\,\partial y^2} + \frac{\partial^4 w}{\partial y^4} = \frac{1}{D}\left(q + N_x \frac{\partial^2 w}{\partial x^2} + N_y \frac{\partial^2 w}{\partial y^2} + 2N_{xy}\frac{\partial^2 w}{\partial x\,\partial y}\right) \qquad (7.33)$$

Example 7.3

Determine the deflected form of the thin rectangular plate of Example 7.1 if, in addition to a uniformly distributed transverse load of intensity q_0, it supports an in-plane tensile force N_x per unit length.

The uniform transverse load may be expressed as a Fourier series (see Eq. (7.28) and Example 7.1), i.e.

$$q = \frac{16q_0}{\pi^2}\sum_{m=1,3,5}^{\infty}\sum_{n=1,3,5}^{\infty}\frac{1}{mn}\sin\frac{m\pi x}{a}\sin\frac{n\pi y}{b}$$

Equation (7.33) then becomes, on substituting for q

$$\frac{\partial^4 w}{\partial x^4} + 2\frac{\partial^4 w}{\partial x^2\,\partial y^2} + \frac{\partial^4 w}{\partial y^4} - \frac{N_x}{D}\frac{\partial^2 w}{\partial x^2} = \frac{16q_0}{\pi^2 D}\sum_{m=1,3,5}^{\infty}\sum_{n=1,3,5}^{\infty}\frac{1}{mn}\sin\frac{m\pi x}{a}\sin\frac{n\pi y}{b} \quad \text{(i)}$$

The appropriate boundary conditions are

$$w = \frac{\partial^2 w}{\partial x^2} = 0 \quad \text{at} \quad x = 0 \quad \text{and} \quad a$$

$$w = \frac{\partial^2 w}{\partial y^2} = 0 \quad \text{at} \quad y = 0 \quad \text{and} \quad b$$

These conditions may be satisfied by the assumption of a deflected form of the plate given by

$$w = \sum_{m=1}^{\infty} \sum_{n=1}^{\infty} A_{mn} \sin \frac{m\pi x}{a} \sin \frac{n\pi y}{b}$$

Substituting this expression into Eq. (i) gives

$$A_{mn} = \frac{16q_0}{\pi^6 Dmn \left[\left(\frac{m^2}{a^2} + \frac{n^2}{b^2} \right)^2 + \frac{N_x m^2}{\pi^2 D a^2} \right]} \quad \text{for odd } m \text{ and } n$$

$$A_{mn} = 0 \quad \text{for even } m \text{ and } n$$

Therefore

$$w = \frac{16q_0}{\pi^6 D} \sum_{m=1,3,5}^{\infty} \sum_{n=1,3,5}^{\infty} \frac{1}{mn \left[\left(\frac{m^2}{a^2} + \frac{n^2}{b^2} \right)^2 + \frac{N_x m^2}{\pi^2 D a^2} \right]} \sin \frac{m\pi x}{a} \sin \frac{n\pi y}{b} \qquad \text{(ii)}$$

Comparing Eq. (ii) with Eq. (i) of Example 7.1 we see that, as a physical inspection would indicate, the presence of a tensile in-plane force decreases deflection. Conversely a compressive in-plane force would increase the deflection.

7.5 Bending of thin plates having a small initial curvature

Suppose that a thin plate has an initial curvature so that the deflection of any point in its middle plane is w_0. We assume that w_0 is small compared with the thickness of the plate. The application of transverse and in-plane loads will cause the plate to deflect a further amount w_1 so that the total deflection is then $w = w_0 + w_1$. However, in the derivation of Eq. (7.33) we note that the left-hand side was obtained from expressions for bending moments which themselves depend on the change of curvature. We therefore use the deflection w_1 on the left-hand side, not w. The effect on bending of the in-plane forces depends on the total deflection w so that we write Eq. (7.33)

$$\frac{\partial^4 w_1}{\partial x^4} + 2\frac{\partial^4 w_1}{\partial x^2 \partial y^2} + \frac{\partial^4 w_1}{\partial y^4} = \frac{1}{D}\left[q + N_x \frac{\partial^2 (w_0 + w_1)}{\partial x^2} + N_y \frac{\partial^2 (w_0 + w_1)}{\partial y^2} + 2N_{xy} \frac{\partial^2 (w_0 + w_1)}{\partial x\, \partial y} \right] \qquad (7.34)$$

The effect of an initial curvature on deflection is therefore equivalent to the application of a transverse load of intensity

$$N_x \frac{\partial^2 w_0}{\partial x^2} + N_y \frac{\partial^2 w_0}{\partial y^2} + 2N_{xy} \frac{\partial^2 w_0}{\partial x\, \partial y}$$

Thus, in-plane loads alone produce bending provided there is an initial curvature.

Assuming that the initial form of the deflected plate is

$$w_0 = \sum_{m=1}^{\infty} \sum_{n=1}^{\infty} A_{mn} \sin \frac{m\pi x}{a} \sin \frac{n\pi y}{b} \tag{7.35}$$

then by substitution in Eq. (7.34) we find that if N_x is compressive and $N_y = N_{xy} = 0$

$$w_1 = \sum_{m=1}^{\infty} \sum_{n=1}^{\infty} B_{mn} \sin \frac{m\pi x}{a} \sin \frac{n\pi y}{b} \tag{7.36}$$

where

$$B_{mn} = \frac{A_{mn} N_x}{(\pi^2 D/a^2)[m + (n^2 a^2/mb^2)]^2 - N_x}$$

We shall return to the consideration of initially curved plates in the discussion of the experimental determination of buckling loads of flat plates in Chapter 9.

7.6 Energy method for the bending of thin plates

Two types of solution are obtainable for thin plate bending problems by the application of the principle of the stationary value of the total potential energy of the plate and its external loading. The first, in which the form of the deflected shape of the plate is known, produces an exact solution; the second, the *Rayleigh–Ritz* method, assumes an approximate deflected shape in the form of a series having a finite number of terms chosen to satisfy the boundary conditions of the problem and also to give the kind of deflection pattern expected.

In Chapter 5 we saw that the total potential energy of a structural system comprised the internal or strain energy of the structural member, plus the potential energy of the applied loading. We now proceed to derive expressions for these quantities for the loading cases considered in the preceding sections.

7.6.1 Strain energy produced by bending and twisting

In thin plate analysis we are concerned with deflections normal to the loaded surface of the plate. These, as in the case of slender beams, are assumed to be primarily due to bending action so that the effects of shear strain and shortening or stretching of the middle plane of the plate are ignored. Therefore, it is sufficient for us to calculate the strain energy produced by bending and twisting only as this will be applicable, for the reason of the above assumption, to all loading cases. It must be remembered that we are only neglecting the contributions of shear and direct *strains* on the deflection of the plate; the stresses producing them must not be ignored.

Consider the element $\delta x \times \delta y$ of a thin plate $a \times b$ shown in elevation in the xz plane in Fig. 7.14(a). Bending moments M_x per unit length applied to its δy edge produce

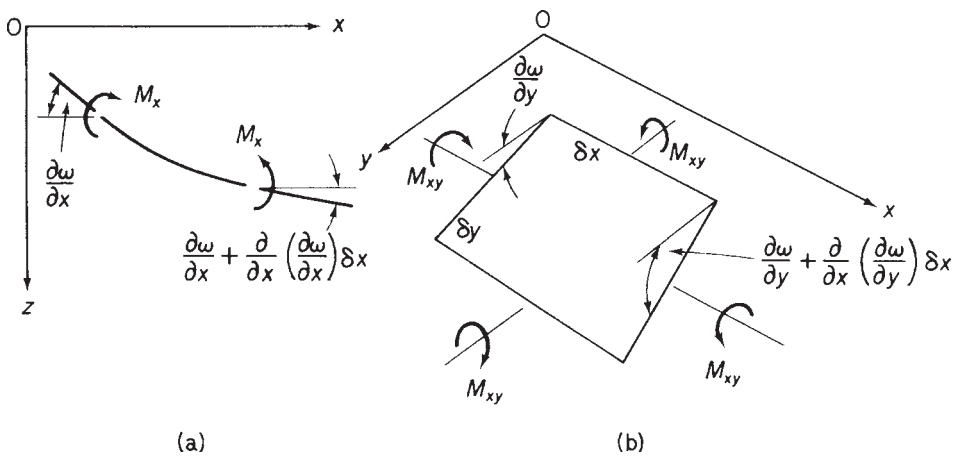

Fig. 7.14 (a) Strain energy of element due to bending; (b) strain energy due to twisting.

a change in slope between its ends equal to $(\partial^2 w/\partial x^2)\delta x$. However, since we regard the moments M_x as positive in the sense shown, then this change in slope, or relative rotation, of the ends of the element is negative as the slope decreases with increasing x. The bending strain energy due to M_x is then

$$\frac{1}{2}M_x \delta y \left(-\frac{\partial^2 w}{\partial x^2}\delta x\right)$$

Similarly, in the yz plane the contribution of M_y to the bending strain energy is

$$\frac{1}{2}M_y \delta x \left(-\frac{\partial^2 w}{\partial y^2}\delta y\right)$$

The strain energy due to the twisting moment per unit length, M_{xy}, applied to the δy edges of the element, is obtained from Fig. 7.14(b). The relative rotation of the δy edges is $(\partial^2 w/\partial x \partial y)\delta x$ so that the corresponding strain energy is

$$\frac{1}{2}M_{xy}\delta y \frac{\partial^2 w}{\partial x\, \partial y}\delta x$$

Finally, the contribution of the twisting moment M_{xy} on the δx edges is, in a similar fashion

$$\frac{1}{2}M_{xy}\delta x \frac{\partial^2 w}{\partial x\, \partial y}\delta y$$

The total strain energy of the element from bending and twisting is thus

$$\frac{1}{2}\left(-M_x \frac{\partial^2 w}{\partial x^2} - M_y \frac{\partial^2 w}{\partial y^2} + 2M_{xy}\frac{\partial^2 w}{\partial x\, \partial y}\right)\delta x \delta y$$

Substitution for M_x, M_y and M_{xy} from Eqs (7.7), (7.8) and (7.14) gives the total strain energy of the element as

$$\frac{D}{2}\left[\left(\frac{\partial^2 w}{\partial x^2}\right)^2+\left(\frac{\partial^2 w}{\partial y^2}\right)^2+2\nu\frac{\partial^2 w}{\partial x^2}\frac{\partial^2 w}{\partial y^2}+2(1-\nu)\left(\frac{\partial^2 w}{\partial x\,\partial y}\right)^2\right]\delta x\,\delta y$$

which on rearranging becomes

$$\frac{D}{2}\left\{\left(\frac{\partial^2 w}{\partial x^2}+\frac{\partial^2 w}{\partial y^2}\right)^2-2(1-\nu)\left[\frac{\partial^2 w}{\partial x^2}\frac{\partial^2 w}{\partial y^2}-\left(\frac{\partial^2 w}{\partial x\,\partial y}\right)^2\right]\right\}\delta x\,\delta y$$

Hence the total strain energy U of the rectangular plate $a \times b$ is

$$U=\frac{D}{2}\int_0^a\int_0^b\left\{\left(\frac{\partial^2 w}{\partial x^2}+\frac{\partial^2 w}{\partial y^2}\right)^2-2(1-\nu)\left[\frac{\partial^2 w}{\partial x^2}\frac{\partial^2 w}{\partial y^2}-\left(\frac{\partial^2 w}{\partial x\,\partial y}\right)^2\right]\right\}\mathrm{d}x\,\mathrm{d}y \tag{7.37}$$

Note that if the plate is subject to pure bending only, then $M_{xy}=0$ and from Eq. (7.14) $\partial^2 w/\partial x\partial y=0$, so that Eq. (7.37) simplifies to

$$U=\frac{D}{2}\int_0^a\int_0^b\left[\left(\frac{\partial^2 w}{\partial x^2}\right)^2+\left(\frac{\partial^2 w}{\partial y^2}\right)^2+2\nu\frac{\partial^2 w}{\partial x^2}\frac{\partial^2 w}{\partial y^2}\right]\mathrm{d}x\,\mathrm{d}y \tag{7.38}$$

7.6.2 Potential energy of a transverse load

An element $\delta x \times \delta y$ of the transversely loaded plate of Fig. 7.8 supports a load $q\delta x\delta y$. If the displacement of the element normal to the plate is w then the potential energy δV of the load on the element referred to the undeflected plate position is

$$\delta V=-wq\delta x\,\delta y \qquad \text{(See Section 5.7)}$$

Therefore, the potential energy V of the total load on the plate is given by

$$V=-\int_0^a\int_0^b wq\,\mathrm{d}x\,\mathrm{d}y \tag{7.39}$$

7.6.3 Potential energy of in-plane loads

We may consider each load N_x, N_y and N_{xy} in turn, then use the principle of superposition to determine the potential energy of the loading system when they act simultaneously. Consider an elemental strip of width δy along the length a of the plate in Fig. 7.15(a). The compressive load on this strip is $N_x\delta y$ and due to the bending of the plate the horizontal length of the strip decreases by an amount λ, as shown in

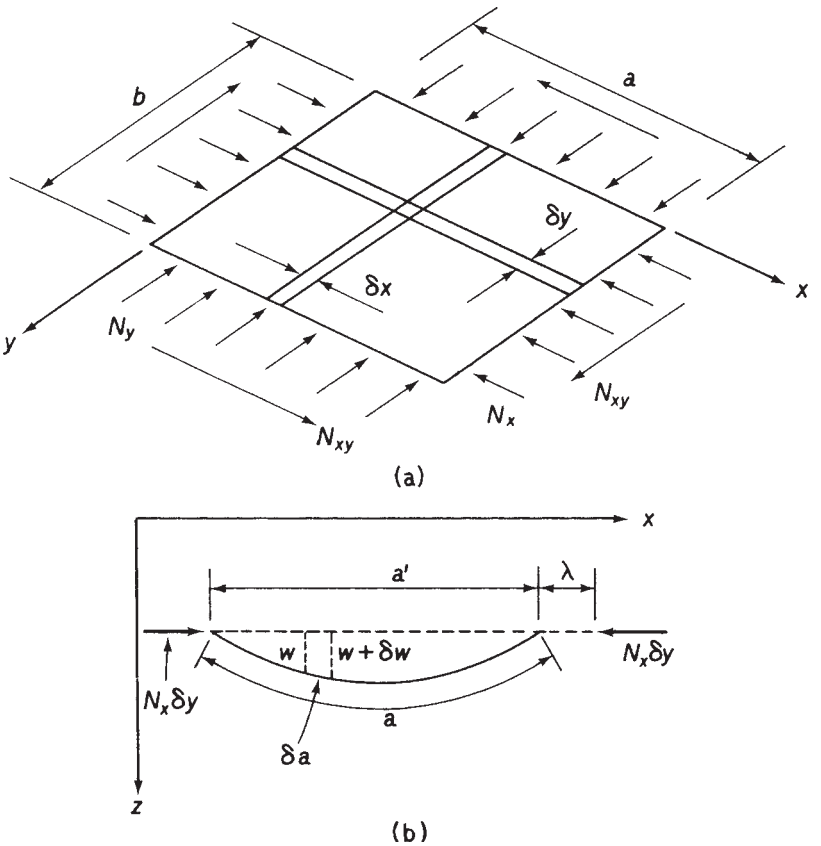

Fig. 7.15 (a) In-plane loads on plate; (b) shortening of element due to bending.

Fig. 7.15(b). The potential energy δV_x of the load $N_x\delta y$, referred to the undeflected position of the plate as the datum, is then

$$\delta V_x = -N_x\lambda\delta y \tag{7.40}$$

From Fig. 7.15(b) the length of a small element δa of the strip is

$$\delta a = (\delta x^2 + \delta w^2)^{\frac{1}{2}}$$

and since $\partial w/\partial x$ is small then

$$\delta a \approx \delta x\left[1 + \frac{1}{2}\left(\frac{\partial w}{\partial x}\right)^2\right]$$

Hence

$$a = \int_0^{a'}\left[1 + \frac{1}{2}\left(\frac{\partial w}{\partial x}\right)^2\right]\mathrm{d}x$$

giving

$$a = a' + \int_0^{a'} \frac{1}{2}\left(\frac{\partial w}{\partial x}\right)^2 \mathrm{d}x$$

and

$$\lambda = a - a' = \int_0^{a'} \frac{1}{2}\left(\frac{\partial w}{\partial x}\right)^2 \mathrm{d}x$$

Since

$$\int_0^{a'} \frac{1}{2}\left(\frac{\partial w}{\partial x}\right)^2 \mathrm{d}x \quad \text{only differs from} \quad \int_0^{a} \frac{1}{2}\left(\frac{\partial w}{\partial x}\right)^2 \mathrm{d}x$$

by a term of negligible order we write

$$\lambda = \int_0^{a} \frac{1}{2}\left(\frac{\partial w}{\partial x}\right)^2 \mathrm{d}x \tag{7.41}$$

The potential energy V_x of the N_x loading follows from Eqs (7.40) and (7.41), thus

$$V_x = -\frac{1}{2}\int_0^{a}\int_0^{b} N_x \left(\frac{\partial w}{\partial x}\right)^2 \mathrm{d}x\,\mathrm{d}y \tag{7.42}$$

Similarly

$$V_y = -\frac{1}{2}\int_0^{a}\int_0^{b} N_y \left(\frac{\partial w}{\partial y}\right)^2 \mathrm{d}x\,\mathrm{d}y \tag{7.43}$$

The potential energy of the in-plane shear load N_{xy} may be found by considering the work done by N_{xy} during the shear distortion corresponding to the deflection w of an element. This shear strain is the reduction in the right angle C_2AB_1 to the angle C_1AB_1 of the element in Fig. 7.16 or, rotating C_2A with respect to AB_1 to AD in the plane C_1AB_1, the angle DAC_1. The displacement C_2D is equal to $(\partial w/\partial y)\delta y$ and the angle DC_2C_1 is $\partial w/\partial x$. Thus C_1D is equal to

$$\frac{\partial w}{\partial x}\frac{\partial w}{\partial y}\delta y$$

and the angle DAC_1 representing the shear strain corresponding to the bending displacement w is

$$\frac{\partial w}{\partial x}\frac{\partial w}{\partial y}$$

so that the work done on the element by the shear force $N_{xy}\delta x$ is

$$\frac{1}{2}N_{xy}\delta x\frac{\partial w}{\partial x}\frac{\partial w}{\partial y}$$

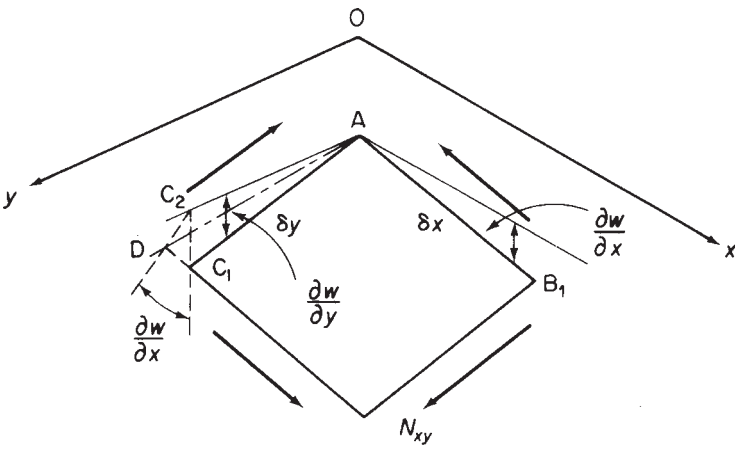

Fig. 7.16 Calculation of shear strain corresponding to bending deflection.

Similarly, the work done by the shear force $N_{xy}\delta y$ is

$$\frac{1}{2}N_{xy}\delta y\frac{\partial w}{\partial x}\frac{\partial w}{\partial y}$$

and the total work done taken over the complete plate is

$$\frac{1}{2}\int_0^a\int_0^b 2N_{xy}\frac{\partial w}{\partial x}\frac{\partial w}{\partial y}\mathrm{d}x\,\mathrm{d}y$$

It follows immediately that the potential energy of the N_{xy} loads is

$$V_{xy} = -\frac{1}{2}\int_0^a\int_0^b 2N_{xy}\frac{\partial w}{\partial x}\frac{\partial w}{\partial y}\mathrm{d}x\,\mathrm{d}y \tag{7.44}$$

and for the complete in-plane loading system we have, from Eqs (7.42), (7.43) and (7.44), a potential energy of

$$V = -\frac{1}{2}\int_0^a\int_0^b\left[N_x\left(\frac{\partial w}{\partial x}\right)^2 + N_y\left(\frac{\partial w}{\partial y}\right)^2 + 2N_{xy}\frac{\partial w}{\partial x}\frac{\partial w}{\partial y}\right]\mathrm{d}x\,\mathrm{d}y \tag{7.45}$$

We are now in a position to solve a wide range of thin plate problems provided that the deflections are small, obtaining exact solutions if the deflected form is known or approximate solutions if the deflected shape has to be 'guessed'.

Considering the rectangular plate of Section 7.3, simply supported along all four edges and subjected to a uniformly distributed transverse load of intensity q_0, we know that its deflected shape is given by Eq. (7.27), namely

$$w = \sum_{m=1}^{\infty}\sum_{n=1}^{\infty}A_{mn}\sin\frac{m\pi x}{a}\sin\frac{n\pi y}{b}$$

The total potential energy of the plate is, from Eqs (7.37) and (7.39)

$$U+V=\int_0^a\int_0^b\left\{\frac{D}{2}\left[\left(\frac{\partial^2 w}{\partial x^2}+\frac{\partial^2 w}{\partial y^2}\right)^2 -2(1-\nu)\left\{\frac{\partial^2 w}{\partial x^2}\frac{\partial^2 w}{\partial y^2}-\left(\frac{\partial^2 w}{\partial x\,\partial y}\right)^2\right\}\right]-wq_0\right\}\mathrm{d}x\,\mathrm{d}y \tag{7.46}$$

Substituting in Eq. (7.46) for w and realizing that 'cross-product' terms integrate to zero, we have

$$\begin{aligned}U+V=\int_0^a\int_0^b\Bigg\{&\frac{D}{2}\sum_{m=1}^{\infty}\sum_{n=1}^{\infty}A_{mn}^2\Bigg[\pi^4\left(\frac{m^2}{a^2}+\frac{n^2}{b^2}\right)^2\sin^2\frac{m\pi x}{a}\sin^2\frac{n\pi y}{b}\\&-2(1-\nu)\frac{m^2n^2\pi^4}{a^2b^2}\left(\sin^2\frac{m\pi x}{a}\sin^2\frac{n\pi y}{b}-\cos^2\frac{m\pi x}{a}\cos^2\frac{n\pi y}{b}\right)\Bigg]\\&-q_0\sum_{m=1}^{\infty}\sum_{n=1}^{\infty}A_{mn}\sin\frac{m\pi x}{a}\sin\frac{n\pi y}{b}\Bigg\}\mathrm{d}x\,\mathrm{d}y\end{aligned}$$

The term multiplied by $2(1-\nu)$ integrates to zero and the mean value of $\sin^2$ or $\cos^2$ over a complete number of half waves is $\frac{1}{2}$, thus integration of the above expression yields

$$U+V=\frac{D}{2}\sum_{m=1,3,5}^{\infty}\sum_{n=1,3,5}^{\infty}A_{mn}^2\frac{\pi^4 ab}{4}\left(\frac{m^2}{a^2}+\frac{n^2}{b^2}\right)^2-q_0\sum_{m=1,3,5}^{\infty}\sum_{n=1,3,5}^{\infty}A_{mn}\frac{4ab}{\pi^2 mn} \tag{7.47}$$

From the principle of the stationary value of the total potential energy we have

$$\frac{\partial(U+V)}{\partial A_{mn}}=\frac{D}{2}2A_{mn}\frac{\pi^4 ab}{4}\left(\frac{m^2}{a^2}+\frac{n^2}{b^2}\right)^2-q_0\frac{4ab}{\pi^2 mn}=0$$

so that

$$A_{mn}=\frac{16q_0}{\pi^6 Dmn[(m^2/a^2)+(n^2/b^2)]^2}$$

giving a deflected form

$$w=\frac{16q_0}{\pi^6 D}\sum_{m=1,3,5}^{\infty}\sum_{n=1,3,5}^{\infty}\frac{\sin(m\pi x/a)\sin(n\pi y/b)}{mn[(m^2/a^2)+(n^2/b^2)]^2}$$

which is the result obtained in Eq. (i) of Example 7.1.

The above solution is exact since we know the true deflected shape of the plate in the form of an infinite series for w. Frequently, the appropriate infinite series is not known so that only an approximate solution may be obtained. The method of solution, known

as the *Rayleigh–Ritz* method, involves the selection of a series for w containing a finite number of functions of x and y. These functions are chosen to satisfy the boundary conditions of the problem as far as possible and also to give the type of deflection pattern expected. Naturally, the more representative the 'guessed' functions are the more accurate the solution becomes.

Suppose that the 'guessed' series for w in a particular problem contains three different functions of x and y. Thus

$$w = A_1 f_1(x, y) + A_2 f_2(x, y) + A_3 f_3(x, y)$$

where A_1, A_2 and A_3 are unknown coefficients. We now substitute for w in the appropriate expression for the total potential energy of the system and assign stationary values with respect to A_1, A_2 and A_3 in turn. Thus

$$\frac{\partial(U+V)}{\partial A_1} = 0 \quad \frac{\partial(U+V)}{\partial A_2} = 0 \quad \frac{\partial(U+V)}{\partial A_3} = 0$$

giving three equations which are solved for A_1, A_2 and A_3.

Example 7.4

A rectangular plate $a \times b$, is simply supported along each edge and carries a uniformly distributed load of intensity q_0. Assuming a deflected shape given by

$$w = A_{11} \sin\frac{\pi x}{a} \sin\frac{\pi y}{b}$$

determine the value of the coefficient A_{11} and hence find the maximum value of deflection.

The expression satisfies the boundary conditions of zero deflection and zero curvature (i.e. zero bending moment) along each edge of the plate. Substituting for w in Eq. (7.46) we have

$$\begin{aligned} U+V = \int_0^a \int_0^b \Bigg[\frac{DA_{11}^2}{2} \Bigg\{ \frac{\pi^4}{(a^2b^2)^2}(a^2+b^2)^2 \sin^2\frac{\pi x}{a} \sin^2\frac{\pi y}{b} - 2(1-\nu) \\ \times \left[\frac{\pi^4}{a^2b^2} \sin^2\frac{\pi x}{a} \sin^2\frac{\pi y}{b} - \frac{\pi^4}{a^2b^2} \cos^2\frac{\pi x}{a} \cos^2\frac{\pi y}{b} \right] \Bigg\} \\ - q_0 A_{11} \sin\frac{\pi x}{a} \sin\frac{\pi y}{b} \Bigg] \mathrm{d}x\,\mathrm{d}y \end{aligned}$$

whence

$$U+V = \frac{DA_{11}^2}{2} \frac{\pi^4}{4a^3b^3}(a^2+b^2)^2 - q_0 A_{11} \frac{4ab}{\pi^2}$$

so that

$$\frac{\partial(U+V)}{\partial A_{11}} = \frac{DA_{11}\pi^4}{4a^3b^3}(a^2+b^2)^2 - q_0 \frac{4ab}{\pi^2} = 0$$

and

$$A_{11} = \frac{16q_0a^4b^4}{\pi^6 D(a^2+b^2)^2}$$

giving

$$w = \frac{16q_0a^4b^4}{\pi^6 D(a^2+b^2)^2} \sin\frac{\pi x}{a} \sin\frac{\pi y}{b}$$

At the centre of the plate w is a maximum and

$$w_{\max} = \frac{16q_0a^4b^4}{\pi^6 D(a^2+b^2)^2}$$

For a square plate and assuming $\nu = 0.3$

$$w_{\max} = 0.0455q_0\frac{a^4}{Et^3}$$

which compares favourably with the result of Example 7.1.

In this chapter we have dealt exclusively with small deflections of thin plates. For a plate subjected to large deflections the middle plane will be stretched due to *bending* so that Eq. (7.33) requires modification. The relevant theory is outside the scope of this book but may be found in a variety of references.

References

1 Jaeger, J. C., *Elementary Theory of Elastic Plates*, Pergamon Press, New York, 1964.

2 Timoshenko, S. P. and Woinowsky-Krieger, S., *Theory of Plates and Shells*, 2nd edition, McGraw-Hill Book Company, New York, 1959.

3 Timoshenko, S. P. and Gere, J. M., *Theory of Elastic Stability*, 2nd edition, McGraw-Hill Book Company, New York, 1961.

4 Wang, Chi-Teh, *Applied Elasticity*, McGraw-Hill Book Company, New York, 1953.

Problems

P.7.1 A plate 10 mm thick is subjected to bending moments M_x equal to 10 Nm/mm and M_y equal to 5 Nm/mm. Calculate the maximum direct stresses in the plate.

Ans. $\sigma_{x,\max} = \pm 600\,\text{N/mm}^2$, $\sigma_{y,\max} = \pm 300\,\text{N/mm}^2$.

P.7.2 For the plate and loading of problem P.7.1 find the maximum twisting moment per unit length in the plate and the direction of the planes on which this occurs.

Ans. 2.5 N m/mm at 45° to the x and y axes.

P.7.3 The plate of the previous two problems is subjected to a twisting moment of 5 Nm/mm along each edge, in addition to the bending moments of $M_x = 10$ N m/mm

and $M_y = 5$ N m/mm. Determine the principal moments in the plate, the planes on which they act and the corresponding principal stresses.

Ans. 13.1 N m/mm, 1.9 N m/mm, $\alpha = -31.7°$, $\alpha = +58.3°$, ± 786 N/mm^2, ± 114 N/mm^2.

P.7.4 A thin rectangular plate of length a and width $2a$ is simply supported along the edges $x = 0$, $x = a$, $y = -a$ and $y = +a$. The plate has a flexural rigidity D, a Poisson's ratio of 0.3 and carries a load distribution given by $q(x, y) = q_0 \sin(\pi x/a)$. If the deflection of the plate may be represented by the expression

$$w = \frac{qa^4}{D\pi^4}\left(1 + A\cosh\frac{\pi y}{a} + B\frac{\pi y}{a}\sinh\frac{\pi y}{a}\right)\sin\frac{\pi x}{a}$$

determine the values of the constants A and B.

Ans. $A = -0.2213$, $B = 0.0431$.

P.7.5 A thin, elastic square plate of side a is simply supported on all four sides and supports a uniformly distributed load q. If the origin of axes coincides with the centre of the plate show that the deflection of the plate can be represented by the expression

$$w = \frac{q}{96(1-\nu)D}[2(x^4 + y^4) - 3a^2(1-\nu)(x^2 + y^2) - 12\nu x^2y^2 + A]$$

where D is the flexural rigidity, ν is Poisson's ratio and A is a constant. Calculate the value of A and hence the central deflection of the plate.

Ans. $A = a^4(5 - 3\nu)/4$, Cen. def. $= qa^4(5 - 3\nu)/384D(1 - \nu)$

P.7.6 The deflection of a square plate of side a which supports a lateral load represented by the function $q(x, y)$ is given by

$$w(x, y) = w_0 \cos\frac{\pi x}{a}\cos\frac{3\pi y}{a}$$

where x and y are referred to axes whose origin coincides with the centre of the plate and w_0 is the deflection at the centre.

If the flexural rigidity of the plate is D and Poisson's ratio is ν determine the loading function q, the support conditions of the plate, the reactions at the plate corners and the bending moments at the centre of the plate.

Ans. $q(x, y) = w_0 D 100\frac{\pi^4}{a^4}\cos\frac{\pi x}{a}\cos\frac{3\pi y}{a}$

The plate is simply supported on all edges.

Reactions: $-6w_0D\left(\frac{\pi}{a}\right)^2(1 - \nu)$

$M_x = w_0D\left(\frac{\pi}{a}\right)^2(1 + 9\nu)$, $M_y = w_0D\left(\frac{\pi}{a}\right)^2(9 + \nu)$.

P.7.7 A simply supported square plate $a \times a$ carries a distributed load according to the formula

$$q(x, y) = q_0\frac{x}{a}$$

where q_0 is its intensity at the edge $x = a$. Determine the deflected shape of the plate.

$$Ans. \quad w = \frac{8q_0a^4}{\pi^6 D} \sum_{m=1,2,3}^{\infty} \sum_{n=1,3,5}^{\infty} \frac{(-1)^{m+1}}{mn(m^2+n^2)^2} \sin\frac{m\pi x}{a} \sin\frac{n\pi y}{a}$$

P.7.8 An elliptic plate of major and minor axes $2a$ and $2b$ and of small thickness t is clamped along its boundary and is subjected to a uniform pressure difference p between the two faces. Show that the usual differential equation for normal displacements of a thin flat plate subject to lateral loading is satisfied by the solution

$$w = w_0 \left(1 - \frac{x^2}{a^2} - \frac{y^2}{b^2}\right)^2$$

where w_0 is the deflection at the centre which is taken as the origin.

Determine w_0 in terms of p and the relevant material properties of the plate and hence expressions for the greatest stresses due to bending at the centre and at the ends of the minor axis.

$$Ans. \quad w_0 = \frac{3p(1-\nu^2)}{2Et^3\left(\frac{3}{a^4} + \frac{2}{a^2b^2} + \frac{3}{b^4}\right)}$$

Centre, $\quad \sigma_{x,\max} = \dfrac{\pm 3pa^2b^2(b^2+\nu a^2)}{t^2(3b^4+2a^2b^2+3a^4)}$, $\sigma_{y,\max} = \dfrac{\pm 3pa^2b^2(a^2+\nu b^2)}{t^2(3b^4+2a^2b^2+3a^4)}$

Ends of minor axis

$$\sigma_{x,\max} = \frac{\pm 6pa^4b^2}{t^2(3b^4+2a^2b^2+3a^4)}, \ \sigma_{y,\max} = \frac{\pm 6pb^4a^2}{t^2(3b^4+2a^2b^2+3a^4)}$$

P.7.9 Use the energy method to determine the deflected shape of a rectangular plate $a \times b$, simply supported along each edge and carrying a concentrated load W at a position (ξ, η) referred to axes through a corner of the plate. The deflected shape of the plate can be represented by the series

$$w = \sum_{m=1}^{\infty} \sum_{n=1}^{\infty} A_{mn} \sin\frac{m\pi x}{a} \sin\frac{n\pi y}{b}$$

$$Ans. \quad A_{mn} = \frac{4W \sin\frac{m\pi\xi}{a} \sin\frac{n\pi\eta}{b}}{\pi^4 Dab[(m^2/a^2)+(n^2/b^2)]^2}$$

P.7.10 If, in addition to the point load W, the plate of problem P.7.9 supports an in-plane compressive load of N_x per unit length on the edges $x = 0$ and $x = a$, calculate the resulting deflected shape.

$$Ans. \quad A_{mn} = \frac{4W \sin \dfrac{m\pi\xi}{a} \sin \dfrac{n\pi\eta}{b}}{abD\pi^4 \left[\left(\dfrac{m^2}{a^2} + \dfrac{n^2}{b^2} \right)^2 - \dfrac{m^2 N_x}{\pi^2 a^2 D} \right]}$$

P.7.11 A square plate of side a is simply supported along all four sides and is subjected to a transverse uniformly distributed load of intensity q_0. It is proposed to determine the deflected shape of the plate by the Rayleigh–Ritz method employing a 'guessed' form for the deflection of

$$w = A_{11} \left(1 - \frac{4x^2}{a^2} \right) \left(1 - \frac{4y^2}{a^2} \right)$$

in which the origin is taken at the centre of the plate.

Comment on the degree to which the boundary conditions are satisfied and find the central deflection assuming $\nu = 0.3$.

$$Ans. \quad \frac{0.0389 q_0 a^4}{Et^3}$$

P.7.12 A rectangular plate $a \times b$, simply supported along each edge, possesses a small initial curvature in its unloaded state given by

$$w_0 = A_{11} \sin \frac{\pi x}{a} \sin \frac{\pi y}{b}$$

Determine, using the energy method, its final deflected shape when it is subjected to a compressive load N_x per unit length along the edges $x = 0, x = a$.

$$Ans. \quad w = \frac{A_{11}}{\left[1 - \dfrac{N_x a^2}{\pi^2 D} \Big/ \left(1 + \dfrac{a^2}{b^2} \right)^2 \right]} \sin \frac{\pi x}{a} \sin \frac{\pi y}{b}$$

This page intentionally left blank

SECTION A4 STRUCTURAL INSTABILITY

Chapter 8 Columns 255
Chapter 9 Thin Plates 294

This page intentionally left blank

8

Columns

A large proportion of an aircraft's structure comprises thin webs stiffened by slender longerons or stringers. Both are susceptible to failure by buckling at a buckling stress or critical stress, which is frequently below the limit of proportionality and seldom appreciably above the yield stress of the material. Clearly, for this type of structure, buckling is the most critical mode of failure so that the prediction of buckling loads of columns, thin plates and stiffened panels is extremely important in aircraft design. In this chapter we consider the buckling failure of all these structural elements and also the flexural–torsional failure of thin-walled open tubes of low torsional rigidity.

Two types of structural instability arise: *primary* and *secondary*. The former involves the complete element, there being no change in cross-sectional area while the wavelength of the buckle is of the same order as the length of the element. Generally, solid and thick-walled columns experience this type of failure. In the latter mode, changes in cross-sectional area occur and the wavelength of the buckle is of the order of the cross-sectional dimensions of the element. Thin-walled columns and stiffened plates may fail in this manner.

8.1 Euler buckling of columns

The first significant contribution to the theory of the buckling of columns was made as early as 1744 by Euler. His classical approach is still valid, and likely to remain so, for slender columns possessing a variety of end restraints. Our initial discussion is therefore a presentation of the Euler theory for the small elastic deflection of perfect columns. However, we investigate first the nature of buckling and the difference between theory and practice.

It is common experience that if an increasing axial compressive load is applied to a slender column there is a value of the load at which the column will suddenly bow or buckle in some unpredetermined direction. This load is patently the buckling load of the column or something very close to the buckling load. Clearly this displacement implies a degree of asymmetry in the plane of the buckle caused by geometrical and/or material imperfections of the column and its load. However, in our theoretical stipulation of a perfect column in which the load is applied precisely along the perfectly straight centroidal axis, there is perfect symmetry so that, theoretically, there can be no sudden bowing or buckling. We therefore require a precise definition of buckling load which may be used in our analysis of the perfect column.

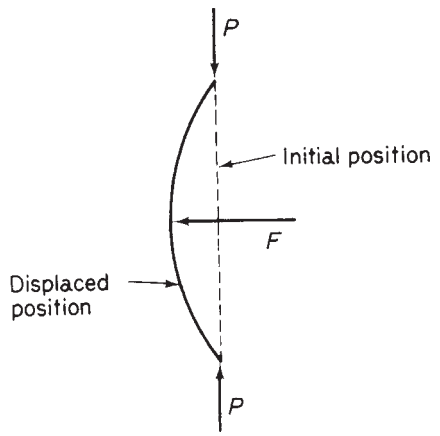

Fig. 8.1 Definition of buckling load for a perfect column.

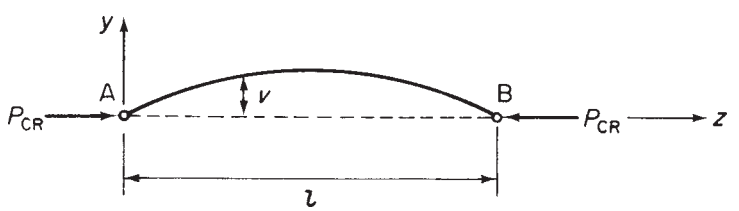

Fig. 8.2 Determination of buckling load for a pin-ended column.

If the perfect column of Fig. 8.1 is subjected to a compressive load P, only shortening of the column occurs no matter what the value of P. However, if the column is displaced a small amount by a lateral load F then, at values of P below the critical or buckling load, P_{CR}, removal of F results in a return of the column to its undisturbed position, indicating a state of stable equilibrium. At the critical load the displacement does not disappear and, in fact, the column will remain in *any* displaced position as long as the displacement is small. Thus, the buckling load P_{CR} is associated with a state of *neutral equilibrium.* For $P > P_{CR}$ enforced lateral displacements increase and the column is unstable.

Consider the pin-ended column AB of Fig. 8.2. We assume that it is in the displaced state of neutral equilibrium associated with buckling so that the compressive load P has attained the critical value P_{CR}. Simple bending theory (see Chapter 16) gives

$$EI\frac{\mathrm{d}^2v}{\mathrm{d}z^2} = -M$$

or

$$EI\frac{\mathrm{d}^2v}{\mathrm{d}z^2} = -P_{CR}v \tag{8.1}$$

so that the differential equation of bending of the column is

$$\frac{\mathrm{d}^2 v}{\mathrm{d}z^2} + \frac{P_{\mathrm{CR}}}{EI} v = 0 \tag{8.2}$$

The well-known solution of Eq. (8.2) is

$$v = A \cos \mu z + B \sin \mu z \tag{8.3}$$

where $\mu^2 = P_{\mathrm{CR}}/EI$ and A and B are unknown constants. The boundary conditions for this particular case are $v = 0$ at $z = 0$ and l. Thus $A = 0$ and

$$B \sin \mu l = 0$$

For a non-trivial solution (i.e. $v \neq 0$) then

$$\sin \mu l = 0 \quad \text{or} \quad \mu l = n\pi \quad \text{where } n = 1, 2, 3, \ldots$$

giving

$$\frac{P_{\mathrm{CR}} l^2}{EI} = n^2 \pi^2$$

or

$$P_{\mathrm{CR}} = \frac{n^2 \pi^2 EI}{l^2} \tag{8.4}$$

Note that Eq. (8.3) cannot be solved for v no matter how many of the available boundary conditions are inserted. This is to be expected since the neutral state of equilibrium means that v is indeterminate.

The smallest value of buckling load, in other words the smallest value of P which can maintain the column in a neutral equilibrium state, is obtained by substituting $n = 1$ in Eq. (8.4). Hence

$$P_{\mathrm{CR}} = \frac{\pi^2 EI}{l^2} \tag{8.5}$$

Other values of P_{CR} corresponding to $n = 2, 3, \ldots$, are

$$P_{\mathrm{CR}} = \frac{4\pi^2 EI}{l^2}, \frac{9\pi^2 EI}{l^2}, \ldots$$

These higher values of buckling load cause more complex modes of buckling such as those shown in Fig. 8.3. The different shapes may be produced by applying external restraints to a very slender column at the points of contraflexure to prevent lateral movement. If no restraints are provided then these forms of buckling are unstable and have little practical meaning.

The critical stress, σ_{CR}, corresponding to P_{CR}, is, from Eq. (8.5)

$$\sigma_{\mathrm{CR}} = \frac{\pi^2 E}{(l/r)^2} \tag{8.6}$$

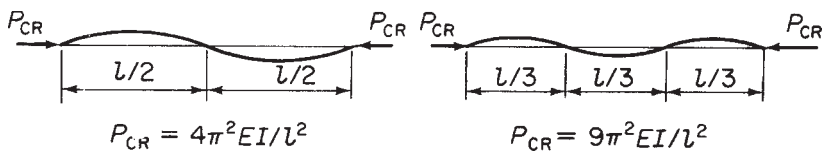

Fig. 8.3 Buckling loads for different buckling modes of a pin-ended column.

Table 8.1

Ends	l_e/l	Boundary conditions
Both pinned	1.0	$v = 0$ at $z = 0$ and l
Both fixed	0.5	$v = 0$ at $z = 0$ and $z = l$, $\mathrm{d}v/\mathrm{d}z = 0$ at $z = l$
One fixed, the other free	2.0	$v = 0$ and $\mathrm{d}v/\mathrm{d}z = 0$ at $z = 0$
One fixed, the other pinned	0.6998	$\mathrm{d}v/\mathrm{d}z = 0$ at $z = 0$, $v = 0$ at $z = l$ and $z = 0$

where r is the radius of gyration of the cross-sectional area of the column. The term l/r is known as the *slenderness ratio* of the column. For a column that is not doubly symmetrical, r is the least radius of gyration of the cross-section since the column will bend about an axis about which the flexural rigidity EI is least. Alternatively, if buckling is prevented in all but one plane then EI is the flexural rigidity in that plane.

Equations (8.5) and (8.6) may be written in the form

$$P_{\mathrm{CR}} = \frac{\pi^2 EI}{l_{\mathrm{e}}^2} \tag{8.7}$$

and

$$\sigma_{\mathrm{CR}} = \frac{\pi^2 E}{(l_{\mathrm{e}}/r)^2} \tag{8.8}$$

where l_{e} is the *effective length* of the column. This is the length of a *pin-ended column* that would have the same critical load as that of a column of length l, but with different end conditions. The determination of critical load and stress is carried out in an identical manner to that for the pin-ended column except that the boundary conditions are different in each case. Table 8.1 gives the solution in terms of effective length for columns having a variety of end conditions. In addition, the boundary conditions referred to the coordinate axes of Fig. 8.2 are quoted. The last case in Table 8.1 involves the solution of a transcendental equation; this is most readily accomplished by a graphical method.

Let us now examine the buckling of the perfect pin-ended column of Fig. 8.2 in greater detail. We have shown, in Eq. (8.4), that the column will buckle at *discrete* values of axial load and that associated with each value of buckling load there is a particular buckling mode (Fig. 8.3). These discrete values of buckling load are called *eigenvalues*, their associated functions (in this case $v = B \sin n\pi z/l$) are called *eigenfunctions* and the problem itself is called an *eigenvalue problem.*

Further, suppose that the lateral load F in Fig. 8.1 is removed. Since the column is perfectly straight, homogeneous and loaded exactly along its axis, it will suffer only axial compression as P is increased. This situation, theoretically, would continue until yielding of the material of the column occurred. However, as we have seen,

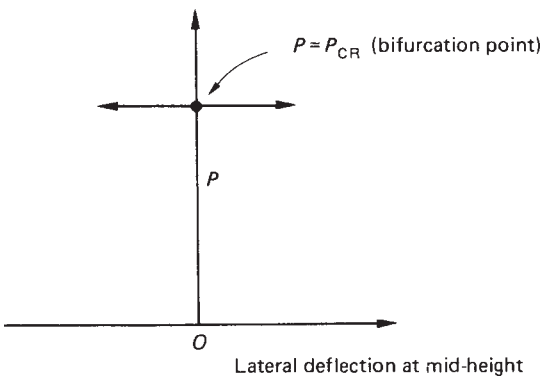

Fig. 8.4 Behaviour of a perfect pin-ended column.

for values of P below P_{CR} the column is in stable equilibrium whereas for $P > P_{CR}$ the column is unstable. A plot of load against lateral deflection at mid-height would therefore have the form shown in Fig. 8.4 where, at the point $P = P_{CR}$, it is theoretically possible for the column to take one of three deflection paths. Thus, if the column remains undisturbed the deflection at mid-height would continue to be zero but unstable (i.e. the trivial solution of Eq. (8.3), $v = 0$) or, if disturbed, the column would buckle in either of two lateral directions; the point at which this possible branching occurs is called a *bifurcation point*; further bifurcation points occur at the higher values of $P_{CR}(4\pi^2 EI/l^2, 9\pi^2 EI/l^2, \ldots)$.

Example 8.1

A uniform column of length L and flexural stiffness EI is simply supported at its ends and has an additional elastic support at midspan. This support is such that if a lateral displacement v_c occurs at this point a restoring force kv_c is generated at the point. Derive an equation giving the buckling load of the column. If the buckling load is $4\pi^2 EI/L^2$ find the value of k. Also if the elastic support is infinitely stiff show that the buckling load is given by the equation $\tan \lambda L/2 = \lambda L/2$ where $\lambda = \sqrt{P/EI}$.

The column is shown in its displaced position in Fig. 8.5.The bending moment at any section of the column is given by

$$M = Pv - \frac{kv_c}{2}z$$

so that, by comparison with Eq. (8.1)

$$EI\frac{d^2v}{dz^2} = -Pv + \frac{kv_c}{2}z$$

giving

$$\frac{d^2v}{dz^2} + \lambda^2 v = \frac{kv_c}{2EI}z \qquad \text{(i)}$$

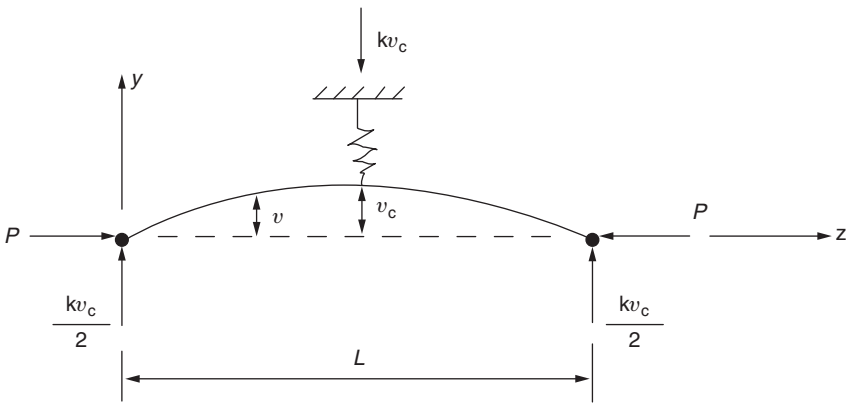

Fig. 8.5 Column of Example 8.1.

The solution of Eq. (i) is of standard form and is

$$v = A\cos\lambda z + B\sin\lambda z + \frac{kv_c}{2P}z$$

The constants A and B are found using the boundary conditions of the column which are: $v = 0$ when $z = 0$, $v = v_c$, when $z = L/2$ and $(dv/dz) = 0$ when $z = L/2$.

From the first of these, $A = 0$ while from the second

$$B = \frac{v_c}{\sin(\lambda L/2)}\left(1 - \frac{k\lambda}{4P}\right)$$

The third boundary condition gives, since $v_c \neq 0$, the required equation, i.e.

$$\left(1 - \frac{kL}{4P}\right)\cos\frac{\lambda L}{2} + \frac{k}{2P\lambda}\sin\frac{\lambda L}{2} = 0$$

Rearranging

$$P = \frac{kL}{4}\left(1 - \frac{\tan(\lambda L/2)}{\lambda L/2}\right)$$

If P (buckling load) $= 4\pi^2 EI/L^2$ then $\lambda L/2 = \pi$ so that $k = 4P/L$.
Finally, if $k \to \infty$

$$\tan\frac{\lambda L}{2} = \frac{\lambda L}{2} \qquad \text{(ii)}$$

Note that Eq. (ii) is the transcendental equation which would be derived when determining the buckling load of a column of length $L/2$, built in at one end and pinned at the other.

8.2 Inelastic buckling

We have shown that the critical stress, Eq. (8.8), depends only on the elastic modulus of the material of the column and the slenderness ratio l/r. For a given material the critical stress increases as the slenderness ratio decreases; i.e. as the column becomes shorter and thicker. A point is then reached when the critical stress is greater than the yield stress of the material so that Eq. (8.8) is no longer applicable. For mild steel this point occurs at a slenderness ratio of approximately 100, as shown in Fig. 8.6. We therefore require some alternative means of predicting column behaviour at low values of slenderness ratio.

It was assumed in the derivation of Eq. (8.8) that the stresses in the column remained within the elastic range of the material so that the modulus of elasticity $E(=\mathrm{d}\sigma/\mathrm{d}\varepsilon)$ was constant. Above the elastic limit $\mathrm{d}\sigma/\mathrm{d}\varepsilon$ depends upon the value of stress and whether the stress is increasing or decreasing. Thus, in Fig. 8.7 the elastic modulus at the point A is the *tangent modulus* E_t if the stress is increasing but E if the stress is decreasing.

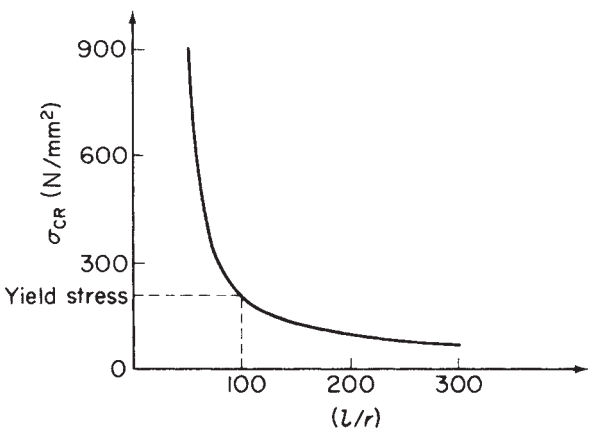

Fig. 8.6 Critical stress–slenderness ratio for a column.

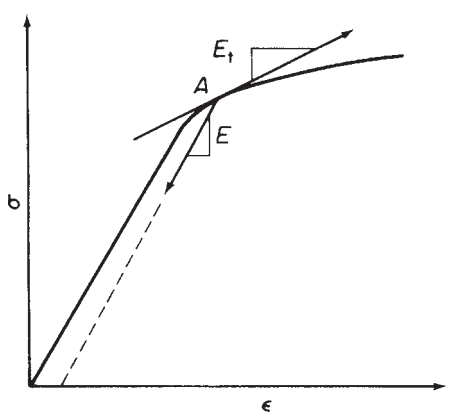

Fig. 8.7 Elastic moduli for a material stressed above the elastic limit.

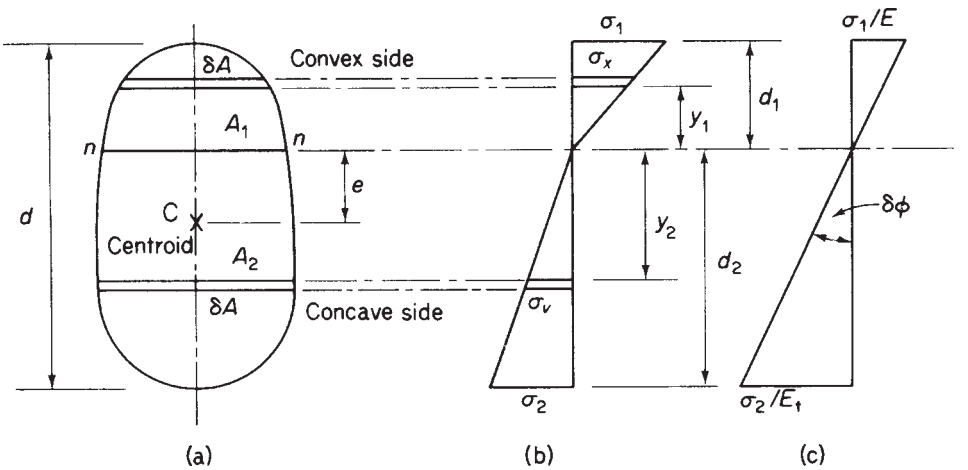

Fig. 8.8 Determination of reduced elastic modulus.

Consider a column having a plane of symmetry and subjected to a compressive load P such that the direct stress in the column P/A is above the elastic limit. If the column is given a small deflection, v, in its plane of symmetry, then the stress on the concave side increases while the stress on the convex side decreases. Thus, in the cross-section of the column shown in Fig. 8.8(a) the compressive stress decreases in the area A_1 and increases in the area A_2, while the stress on the line nn is unchanged. Since these changes take place outside the elastic limit of the material, we see, from our remarks in the previous paragraph, that the modulus of elasticity of the material in the area A_1 is E while that in A_2 is E_t. The homogeneous column now behaves as if it were non-homogeneous, with the result that the stress distribution is changed to the form shown in Fig. 8.8(b); the linearity of the distribution follows from an assumption that plane sections remain plane.

As the axial load is unchanged by the disturbance

$$\int_0^{d_1} \sigma_x \, \mathrm{d}A = \int_0^{d_2} \sigma_v \, \mathrm{d}A \tag{8.9}$$

Also, P is applied through the centroid of each end section a distance e from nn so that

$$\int_0^{d_1} \sigma_x (y_1 + e) \, \mathrm{d}A + \int_0^{d_2} \sigma_v (y_2 - e) \, \mathrm{d}A = -Pv \tag{8.10}$$

From Fig. 8.8(b)

$$\sigma_x = \frac{\sigma_1}{\mathrm{d}_1} y_1 \quad \sigma_v = \frac{\sigma_2}{\mathrm{d}_2} y_2 \tag{8.11}$$

The angle between two close, initially parallel, sections of the column is equal to the change in slope $\mathrm{d}^2 v/\mathrm{d}z^2$ of the column between the two sections. This, in turn, must be

equal to the angle $\delta\phi$ in the strain diagram of Fig. 8.8(c). Hence

$$\frac{\mathrm{d}^2 v}{\mathrm{d}z^2} = \frac{\sigma_1}{Ed_1} = \frac{\sigma_2}{E_\mathrm{t} d_2} \tag{8.12}$$

and Eq. (8.9) becomes, from Eqs (8.11) and (8.12)

$$E\frac{\mathrm{d}^2 v}{\mathrm{d}z^2}\int_0^{d_1} y_1 \mathrm{d}A - E_t\frac{\mathrm{d}^2 v}{\mathrm{d}z^2}\int_0^{d_2} y_2\,\mathrm{d}A = 0 \tag{8.13}$$

Further, in a similar manner, from Eq. (8.10)

$$\frac{\mathrm{d}^2 v}{\mathrm{d}z^2}\left(E\int_0^{d_1} y_1^2\,\mathrm{d}A + E_\mathrm{t}\int_0^{\mathrm{d}_2} y_2^2\,\mathrm{d}A\right) + e\frac{\mathrm{d}^2 v}{\mathrm{d}z^2}\left(E\int_0^{d_1} y_1\,\mathrm{d}A - E_\mathrm{t}\int_0^{d_2} y_2\,\mathrm{d}A\right) = -Pv \tag{8.14}$$

The second term on the left-hand side of Eq. (8.14) is zero from Eq. (8.13). Therefore we have

$$\frac{\mathrm{d}^2 v}{\mathrm{d}z^2}(EI_1 + E_\mathrm{t} I_2) = -Pv \tag{8.15}$$

in which

$$I_1 = \int_0^{d_1} y_1^2\,\mathrm{d}A \quad \text{and} \quad I_2 = \int_0^{d_2} y_2^2\,\mathrm{d}A$$

the second moments of area about *nn* of the convex and concave sides of the column respectively. Putting

$$E_\mathrm{r} I = EI_1 + E_\mathrm{t} I_2$$

or

$$E_\mathrm{r} = E\frac{I_1}{I} + E_\mathrm{t}\frac{I_2}{I} \tag{8.16}$$

where E_r is known as the *reduced modulus*, gives

$$E_\mathrm{r} I\frac{\mathrm{d}^2 v}{\mathrm{d}z^2} + Pv = 0$$

Comparing this with Eq. (8.2) we see that if P is the critical load P_CR then

$$P_\mathrm{CR} = \frac{\pi^2 E_\mathrm{r} I}{l_\mathrm{e}^2} \tag{8.17}$$

and

$$\sigma_\mathrm{CR} = \frac{\pi^2 E_\mathrm{r}}{(l_\mathrm{e}/r)^2} \tag{8.18}$$

The above method for predicting critical loads and stresses outside the elastic range is known as the *reduced modulus theory*. From Eq. (8.13) we have

$$E\int_0^{d_1} y_1\,\mathrm{d}A - E_\mathrm{t}\int_0^{d_2} y_2\,\mathrm{d}A = 0 \tag{8.19}$$

which, together with the relationship $d = d_1 + d_2$, enables the position of *nn* to be found.

It is possible that the axial load P is increased at the time of the lateral disturbance of the column such that there is no strain reversal on its convex side. The compressive stress therefore increases over the complete section so that the tangent modulus applies over the whole cross-section. The analysis is then the same as that for column buckling within the elastic limit except that E_t is substituted for E. Hence the *tangent modulus theory* gives

$$P_\mathrm{CR} = \frac{\pi^2 E_\mathrm{t} I}{l_\mathrm{e}^2} \tag{8.20}$$

and

$$\sigma_\mathrm{CR} = \frac{\pi^2 E_\mathrm{t}}{(l_\mathrm{e}/r^2)} \tag{8.21}$$

By a similar argument, a reduction in P could result in a decrease in stress over the whole cross-section. The elastic modulus applies in this case and the critical load and stress are given by the standard Euler theory; namely, Eqs (8.7) and (8.8).

In Eq. (8.16), I_1 and I_2 are together greater than I while E is greater than E_t. It follows that the reduced modulus E_r is greater than the tangent modulus E_t. Consequently, buckling loads predicted by the reduced modulus theory are greater than buckling loads derived from the tangent modulus theory, so that although we have specified theoretical loading situations where the different theories would apply there still remains the difficulty of deciding which should be used for design purposes.

Extensive experiments carried out on aluminium alloy columns by the aircraft industry in the 1940s showed that the actual buckling load was approximately equal to the tangent modulus load. Shanley (1947) explained that for columns with small imperfections, an increase of axial load and bending occur simultaneously. He then showed analytically that after the tangent modulus load is reached, the strain on the concave side of the column increases rapidly while that on the convex side decreases slowly. The large deflection corresponding to the rapid strain increase on the concave side, which occurs soon after the tangent modulus load is passed, means that it is only possible to exceed the tangent modulus load by a small amount. It follows that the buckling load of columns is given most accurately for practical purposes by the tangent modulus theory.

Empirical formulae have been used extensively to predict buckling loads, although in view of the close agreement between experiment and the tangent modulus theory they would appear unnecessary. Several formulae are in use; for example, the *Rankine, Straight-line* and *Johnson's parabolic* formulae are given in many books on elastic stability.[1]

8.3 Effect of initial imperfections

Obviously it is impossible in practice to obtain a perfectly straight homogeneous column and to ensure that it is exactly axially loaded. An actual column may be bent with some eccentricity of load. Such imperfections influence to a large degree the behaviour of the column which, unlike the perfect column, begins to bend immediately the axial load is applied.

Let us suppose that a column, initially bent, is subjected to an increasing axial load P as shown in Fig. 8.9. In this case the bending moment at any point is proportional to the change in curvature of the column from its initial bent position. Thus

$$EI\frac{\mathrm{d}^2v}{\mathrm{d}z^2} - EI\frac{\mathrm{d}^2v_0}{\mathrm{d}z^2} - Pv \tag{8.22}$$

which, on rearranging, becomes

$$\frac{\mathrm{d}^2v}{\mathrm{d}z^2} + \lambda^2 v = \frac{\mathrm{d}^2v_0}{\mathrm{d}z^2} \tag{8.23}$$

where $\lambda^2 = P/EI$. The final deflected shape, v, of the column depends upon the form of its unloaded shape, v_0. Assuming that

$$v_0 = \sum_{n=1}^{\infty} A_n \sin\frac{n\pi z}{l} \tag{8.24}$$

and substituting in Eq. (8.23) we have

$$\frac{\mathrm{d}^2v}{\mathrm{d}z^2} + \lambda^2 v = -\frac{\pi^2}{l^2}\sum_{n=1}^{\infty} n^2 A_n \sin\frac{n\pi z}{l}$$

The general solution of this equation is

$$v = B\cos\lambda z + D\sin\lambda z + \sum_{n=1}^{\infty}\frac{n^2 A_n}{n^2-\alpha}\sin\frac{n\pi z}{l}$$

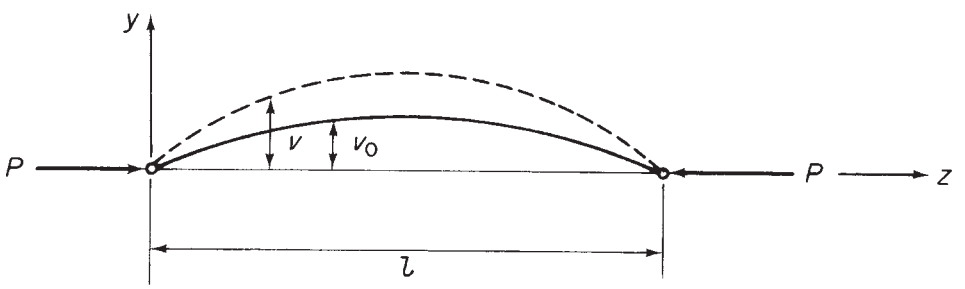

Fig. 8.9 Initially bent column.

where B and D are constants of integration and $\alpha = \lambda^2 l^2/\pi^2$. The boundary conditions are $v = 0$ at $z = 0$ and l, giving $B = D = 0$ whence

$$v = \sum_{n=1}^{\infty} \frac{n^2 A_n}{n^2 - \alpha} \sin \frac{n\pi z}{l} \tag{8.25}$$

Note that in contrast to the perfect column we are able to obtain a non-trivial solution for deflection. This is to be expected since the column is in stable equilibrium in its bent position at all values of P.

An alternative form for α is

$$\alpha = \frac{Pl^2}{\pi^2 EI} = \frac{P}{P_{\mathrm{CR}}} \qquad \text{(see Eq. (8.5))}$$

Thus α is always less than one and approaches unity when P approaches P_{CR} so that the first term in Eq. (8.25) usually dominates the series. A good approximation, therefore, for deflection when the axial load is in the region of the critical load is

$$v = \frac{A_1}{1 - \alpha} \sin \frac{\pi z}{l} \tag{8.26}$$

or at the centre of the column where $z = l/2$

$$v = \frac{A_1}{1 - P/P_{\mathrm{CR}}} \tag{8.27}$$

in which A_1 is seen to be the initial central deflection. If central deflections $\delta (= v - A_1)$ are measured from the initially bowed position of the column then from Eq. (8.27) we obtain

$$\frac{A_1}{1 - P/P_{\mathrm{CR}}} - A_1 = \delta$$

which gives on rearranging

$$\delta = P_{\mathrm{CR}} \frac{\delta}{P} - A_1 \tag{8.28}$$

and we see that a graph of δ plotted against δ/P has a slope, in the region of the critical load, equal to P_{CR} and an intercept equal to the initial central deflection. This is the well known *Southwell plot* for the experimental determination of the elastic buckling load of an imperfect column.

Timoshenko[1] also showed that Eq. (8.27) may be used for a perfectly straight column with small eccentricities of column load.

Example 8.2

The pin-jointed column shown in Fig. 8.10 carries a compressive load P applied eccentrically at a distance e from the axis of the column. Determine the maximum bending moment in the column.

The bending moment at any section of the column is given by

$$M = P(e + v)$$

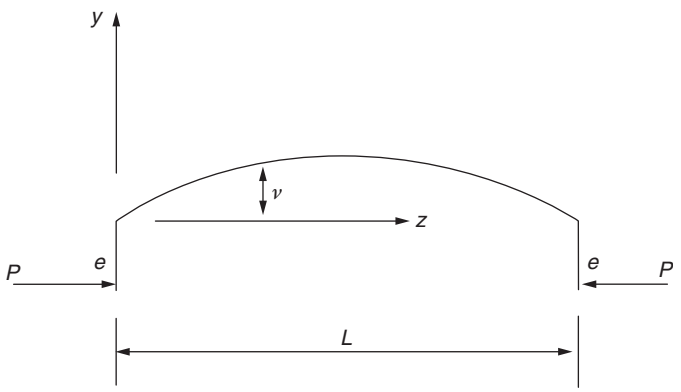

Fig. 8.10 Eccentrically loaded column of Example 8.2

Then, by comparison with Eq. (8.1)

$$EI\frac{\mathrm{d}^2v}{\mathrm{d}z^2} = -P(e+v)$$

giving

$$\frac{\mathrm{d}^2v}{\mathrm{d}z^2} + \mu^2 v = -\frac{Pe}{EI} \quad (\mu^2 = P/EI) \tag{i}$$

The solution of Eq. (i) is of standard form and is

$$v = A\cos\mu z + B\sin\mu z - e$$

The boundary conditions are: $v = 0$ when $z = 0$ and $(\mathrm{d}v/\mathrm{d}z) = 0$ when $z = L/2$.
From the first of these $A = e$ while from the second

$$B = e\tan\frac{\mu L}{2}$$

The equation for the deflected shape of the column is then

$$v = e\left[\frac{\cos\mu(z - L/2)}{\cos\mu L/2} - 1\right]$$

The maximum value of v occurs at midspan where $z = L/2$, i.e.

$$v_{\max} = e\left(\sec\frac{\mu L}{2} - 1\right)$$

The maximum bending moment is given by

$$M(\max) = Pe + Pv_{\max}$$

so that

$$M(\max) = Pe\sec\frac{\mu L}{2}$$

8.4 Stability of beams under transverse and axial loads

Stresses and deflections in a linearly elastic beam subjected to transverse loads as predicted by simple beam theory, are directly proportional to the applied loads. This relationship is valid if the deflections are small such that the slight change in geometry produced in the loaded beam has an insignificant effect on the loads themselves. This situation changes drastically when axial loads act simultaneously with the transverse loads. The internal moments, shear forces, stresses and deflections then become dependent upon the magnitude of the deflections as well as the magnitude of the external loads. They are also sensitive, as we observed in the previous section, to beam imperfections such as initial curvature and eccentricity of axial load. Beams supporting both axial and transverse loads are sometimes known as *beam-columns* or simply as *transversely loaded columns.*

We consider first the case of a pin-ended beam carrying a uniformly distributed load of intensity w per unit length and an axial load P as shown in Fig. 8.11. The bending moment at any section of the beam is

$$M = Pv + \frac{wlz}{2} - \frac{wz^2}{2} = -EI\frac{\mathrm{d}^2 v}{\mathrm{d}z^2}$$

giving

$$\frac{\mathrm{d}^2 v}{\mathrm{d}z^2} + \frac{P}{EI}v = \frac{w}{2EI}(z^2 - lz) \tag{8.29}$$

The standard solution of Eq. (8.29) is

$$v = A\cos\lambda z + B\sin\lambda z + \frac{w}{2P}\left(z^2 - lz - \frac{2}{\lambda^2}\right)$$

where A and B are unknown constants and $\lambda^2 = P/EI$. Substituting the boundary conditions $v = 0$ at $z = 0$ and l gives

$$A = \frac{w}{\lambda^2 P} \quad B = \frac{w}{\lambda^2 P \sin\lambda l}(l - \cos\lambda l)$$

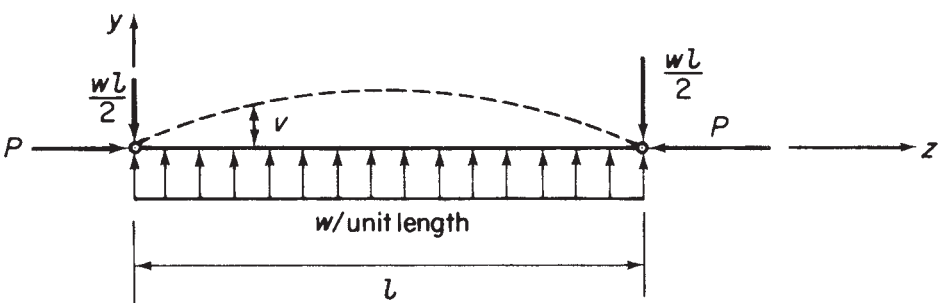

Fig. 8.11 Bending of a uniformly loaded beam-column.

so that the deflection is determinate for any value of w and P and is given by

$$v = \frac{w}{\lambda^2 P}\left[\cos\lambda z + \left(\frac{1-\cos\lambda l}{\sin\lambda l}\right)\sin\lambda z\right] + \frac{w}{2P}\left(z^2 - lz - \frac{2}{\lambda^2}\right) \tag{8.30}$$

In beam-columns, as in beams, we are primarily interested in maximum values of stress and deflection. For this particular case the maximum deflection occurs at the centre of the beam and is, after some transformation of Eq. (8.30)

$$v_{\max} = \frac{w}{\lambda^2 P}\left(\sec\frac{\lambda l}{2} - 1\right) - \frac{wl^2}{8P} \tag{8.31}$$

The corresponding maximum bending moment is

$$M_{\max} = -Pv_{\max} - \frac{wl^2}{8}$$

or, from Eq. (8.31)

$$M_{\max} = \frac{w}{\lambda^2}\left(1 - \sec\frac{\lambda l}{2}\right) \tag{8.32}$$

We may rewrite Eq. (8.32) in terms of the Euler buckling load $P_{CR} = \pi^2 EI/l^2$ for a pin-ended column. Hence

$$M_{\max} = \frac{wl^2}{\pi^2}\frac{P_{CR}}{P}\left(1 - \sec\frac{\pi}{2}\sqrt{\frac{P}{P_{CR}}}\right) \tag{8.33}$$

As P approaches P_{CR} the bending moment (and deflection) becomes infinite. However, the above theory is based on the assumption of small deflections (otherwise $\mathrm{d}^2v/\mathrm{d}z^2$ would not be a close approximation for curvature) so that such a deduction is invalid. The indication is, though, that large deflections will be produced by the presence of a compressive axial load no matter how small the transverse load might be.

Let us consider now the beam-column of Fig. 8.12 with hinged ends carrying a concentrated load W at a distance a from the right-hand support. For

$$z \le l - a \quad EI\frac{\mathrm{d}^2v}{\mathrm{d}z^2} = -M = -Pv - \frac{Waz}{l} \tag{8.34}$$

and for

$$z \ge l - a \quad EI\frac{\mathrm{d}^2v}{\mathrm{d}z^2} = -M = -Pv - \frac{W}{l}(l-a)(l-z) \tag{8.35}$$

Writing

$$\lambda^2 = \frac{P}{EI}$$

Eq. (8.34) becomes

$$\frac{\mathrm{d}^2v}{\mathrm{d}z^2} + \lambda^2 v = -\frac{Wa}{EIl}z$$

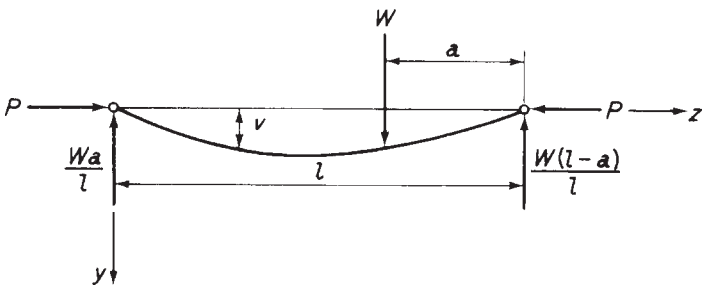

Fig. 8.12 Beam-column supporting a point load.

the general solution of which is

$$v = A\cos\lambda z + B\sin\lambda z - \frac{Wa}{Pl}z \tag{8.36}$$

Similarly, the general solution of Eq. (8.35) is

$$v = C\cos\lambda z + D\sin\lambda z - \frac{W}{Pl}(l-a)(l-z) \tag{8.37}$$

where A, B, C and D are constants which are found from the boundary conditions as follows.

When $z=0$, $v=0$, therefore from Eq. (8.36) $A=0$. *At* $z=l$, $v=0$ giving, from Eq. (8.37), $C=-D\tan\lambda l$. At the point of application of the load the deflection and slope of the beam given by Eqs (8.36) and (8.37) must be the same. Hence, equating deflections

$$B\sin\lambda(l-a) - \frac{Wa}{Pl}(l-a) = D[\sin\lambda(l-a) - \tan\lambda l\cos\lambda(l-a)] - \frac{Wa}{Pl}(l-a)$$

and equating slopes

$$B\lambda\cos\lambda(l-a) - \frac{Wa}{Pl} = D\lambda[\cos\lambda(l-a) - \tan\lambda l\sin\lambda(l-a)] + \frac{W}{Pl}(l-a)$$

Solving the above equations for B and D and substituting for A, B, C and D in Eqs (8.36) and (8.37) we have

$$v = \frac{W\sin\lambda a}{P\lambda\sin\lambda l}\sin\lambda z - \frac{Wa}{Pl}z \quad \text{for} \quad z \le l-a \tag{8.38}$$

$$v = \frac{W\sin\lambda(l-a)}{P\lambda\sin\lambda l}\sin\lambda(l-z) - \frac{W}{Pl}(l-a)(l-z) \quad \text{for } z \ge l-a \tag{8.39}$$

These equations for the beam-column deflection enable the bending moment and resulting bending stresses to be found at all sections.

A particular case arises when the load is applied at the centre of the span. The deflection curve is then symmetrical with a maximum deflection under the load of

$$v_{\max} = \frac{W}{2P\lambda}\tan\frac{\lambda l}{2} - \frac{Wl}{4p}$$

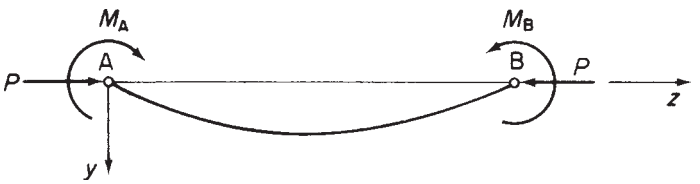

Fig. 8.13 Beam-column supporting end moments.

Finally, we consider a beam-column subjected to end moments M_A and M_B in addition to an axial load P (Fig. 8.13). The deflected form of the beam-column may be found by using the principle of superposition and the results of the previous case. First, we imagine that M_B acts alone with the axial load P. If we assume that the point load W moves towards B and simultaneously increases so that the product $Wa = \text{constant} = M_B$ then, in the limit as a tends to zero, we have the moment M_B applied at B. The deflection curve is then obtained from Eq. (8.38) by substituting λa for $\sin \lambda a$ (since λa is now very small) and M_B for Wa. Thus

$$v = \frac{M_B}{P}\left(\frac{\sin \lambda z}{\sin \lambda l} - \frac{z}{l}\right) \tag{8.40}$$

In a similar way, we find the deflection curve corresponding to M_A acting alone. Suppose that W moves towards A such that the product $W(l-a) = \text{constant} = M_A$. Then as $(l-a)$ tends to zero we have $\sin \lambda(l-a) = \lambda(l-a)$ and Eq. (8.39) becomes

$$v = \frac{M_A}{P}\left[\frac{\sin \lambda(l-z)}{\sin \lambda l} - \frac{(l-z)}{l}\right] \tag{8.41}$$

The effect of the two moments acting simultaneously is obtained by superposition of the results of Eqs (8.40) and (8.41). Hence for the beam-column of Fig. 8.13

$$v = \frac{M_B}{P}\left(\frac{\sin \lambda z}{\sin \lambda l} - \frac{z}{l}\right) + \frac{M_A}{P}\left[\frac{\sin \lambda(l-z)}{\sin \lambda l} - \frac{(l-z)}{l}\right] \tag{8.42}$$

Equation (8.42) is also the deflected form of a beam-column supporting eccentrically applied end loads at A and B. For example, if e_A and e_B are the eccentricities of P at the ends A and B, respectively, then $M_A = Pe_A, M_B = Pe_B$, giving a deflected form of

$$v = e_B\left(\frac{\sin \lambda z}{\sin \lambda l} - \frac{z}{l}\right) + e_A\left[\frac{\sin \lambda(l-z)}{\sin \lambda l} - \frac{(l-z)}{l}\right] \tag{8.43}$$

Other beam-column configurations featuring a variety of end conditions and loading regimes may be analysed by a similar procedure.

8.5 Energy method for the calculation of buckling loads in columns

The fact that the total potential energy of an elastic body possesses a stationary value in an equilibrium state may be used to investigate the neutral equilibrium of a buckled

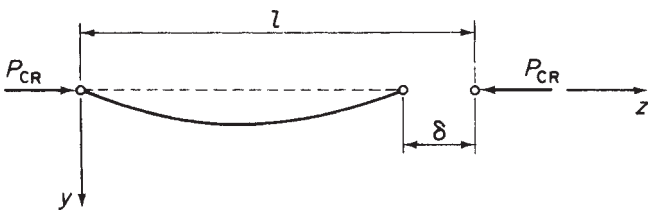

Fig. 8.14 Shortening of a column due to buckling.

column. In particular, the energy method is extremely useful when the deflected form of the buckled column is unknown and has to be 'guessed'.

First, we shall consider the pin-ended column shown in its buckled position in Fig. 8.14. The internal or strain energy U of the column is assumed to be produced by bending action alone and is given by the well known expression

$$U = \int_0^l \frac{M^2}{2EI}\,\mathrm{d}z \tag{8.44}$$

or alternatively, since $EI\,\mathrm{d}^2v/\mathrm{d}z^2 = -M$

$$U = \frac{EI}{2}\int_0^l \left(\frac{d^2v}{dz^2}\right)^2 \mathrm{d}z \tag{8.45}$$

The potential energy V of the buckling load P_{CR}, referred to the straight position of the column as the datum, is then

$$V = -P_{\mathrm{CR}}\delta$$

where δ is the axial movement of P_{CR} caused by the bending of the column from its initially straight position. By reference to Fig. 7.15(b) and Eq. (7.41) we see that

$$\delta = \frac{1}{2}\int_0^l \left(\frac{\mathrm{d}v}{\mathrm{d}z}\right)^2 \mathrm{d}z$$

giving

$$V = -\frac{P_{\mathrm{CR}}}{2}\int_0^l \left(\frac{\mathrm{d}v}{\mathrm{d}z}\right)^2 \mathrm{d}z \tag{8.46}$$

The total potential energy of the column in the neutral equilibrium of its buckled state is therefore

$$U + V = \int_0^l \frac{M^2}{2EI}\,\mathrm{d}z - \frac{P_{\mathrm{CR}}}{2}\int_0^l \left(\frac{\mathrm{d}v}{\mathrm{d}z}\right)^2 \mathrm{d}z \tag{8.47}$$

or, using the alternative form of U from Eq. (8.45)

$$U + V = \frac{EI}{2}\int_0^l \left(\frac{\mathrm{d}^2v}{\mathrm{d}z^2}\right)^2 \mathrm{d}z - \frac{P_{\mathrm{CR}}}{2}\int_0^l \left(\frac{\mathrm{d}v}{\mathrm{d}z}\right)^2 \mathrm{d}z \tag{8.48}$$

We have seen in Chapter 7 that exact solutions of plate bending problems are obtainable by energy methods when the deflected shape of the plate is known. An identical situation exists in the determination of critical loads for column and thin plate buckling modes. For the pin-ended column under discussion a deflected form of

$$v = \sum_{n=1}^{\infty} A_n \sin \frac{n\pi z}{l} \tag{8.49}$$

satisfies the boundary conditions of

$$(v)_{z=0} = (v)_{z=l} = 0 \quad \left(\frac{\mathrm{d}^2 v}{\mathrm{d}z^2}\right)_{z=0} = \left(\frac{\mathrm{d}^2 v}{\mathrm{d}z^2}\right)_{z=l} = 0$$

and is capable, within the limits for which it is valid and if suitable values for the constant coefficients A_n are chosen, of representing any continuous curve. We are therefore in a position to find P_{CR} exactly. Substituting Eq. (8.49) into Eq. (8.48) gives

$$U + V = \frac{EI}{2} \int_0^l \left(\frac{\pi}{l}\right)^4 \left(\sum_{n=1}^{\infty} n^2 A_n \sin \frac{n\pi z}{l}\right)^2 \mathrm{d}z - \frac{P_{\mathrm{CR}}}{2} \int_0^l \left(\frac{\pi}{l}\right)^2 \left(\sum_{n=1}^{\infty} n A_n \cos \frac{n\pi z}{l}\right)^2 \mathrm{d}z \tag{8.50}$$

The product terms in both integrals of Eq. (8.50) disappear on integration, leaving only integrated values of the squared terms. Thus

$$U + V = \frac{\pi^4 EI}{4l^3} \sum_{n=1}^{\infty} n^4 A_n^2 - \frac{\pi^2 P_{\mathrm{CR}}}{4l} \sum_{n=1}^{\infty} n^2 A_n^2 \tag{8.51}$$

Assigning a stationary value to the total potential energy of Eq. (8.51) with respect to each coefficient A_n in turn, then taking A_n as being typical, we have

$$\frac{\partial (U + V)}{\partial A_n} = \frac{\pi^4 EI n^4 A_n}{2l^3} - \frac{\pi^2 P_{\mathrm{CR}} n^2 A_n}{2l} = 0$$

from which

$$P_{\mathrm{CR}} = \frac{\pi^2 EI n^2}{l^2} \quad \text{as before.}$$

We see that each term in Eq. (8.49) represents a particular deflected shape with a corresponding critical load. Hence the first term represents the deflection of the column shown in Fig. 8.14, with $P_{\mathrm{CR}} = \pi^2 EI/l^2$. The second and third terms correspond to the shapes shown in Fig. 8.3, having critical loads of $4\pi^2 EI/l^2$ and $9\pi^2 EI/l^2$ and so on. Clearly the column must be constrained to buckle into these more complex forms. In other words the column is being forced into an unnatural shape, is consequently stiffer and offers greater resistance to buckling as we observe from the higher values of critical

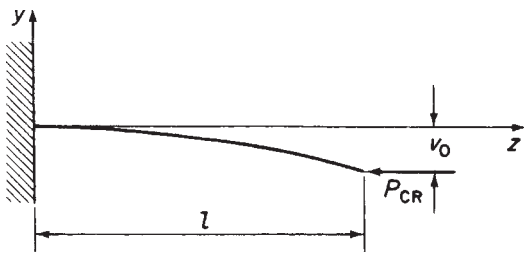

Fig. 8.15 Buckling load for a built-in column by the energy method.

load. Such buckling modes, as stated in Section 8.1, are unstable and are generally of academic interest only.

If the deflected shape of the column is known it is immaterial which of Eqs (8.47) or (8.48) is used for the total potential energy. However, when only an approximate solution is possible Eq. (8.47) is preferable since the integral involving bending moment depends upon the accuracy of the assumed form of v, whereas the corresponding term in Eq. (8.48) depends upon the accuracy of $\mathrm{d}^2v/\mathrm{d}z^2$. Generally, for an assumed deflection curve v is obtained much more accurately than $\mathrm{d}^2v/\mathrm{d}z^2$.

Suppose that the deflection curve of a particular column is unknown or extremely complicated. We then assume a reasonable shape which satisfies, as far as possible, the end conditions of the column and the pattern of the deflected shape (Rayleigh–Ritz method). Generally, the assumed shape is in the form of a finite series involving a series of unknown constants and assumed functions of z. Let us suppose that v is given by

$$v = A_1 f_1(z) + A_2 f_2(z) + A_3 f_3(z)$$

Substitution in Eq. (8.47) results in an expression for total potential energy in terms of the critical load and the coefficients A_1, A_2 and A_3 as the unknowns. Assigning stationary values to the total potential energy with respect to A_1, A_2 and A_3 in turn produces three simultaneous equations from which the ratios A_1/A_2, A_1/A_3 and the critical load are determined. Absolute values of the coefficients are unobtainable since the deflections of the column in its buckled state of neutral equilibrium are indeterminate.

As a simple illustration consider the column shown in its buckled state in Fig. 8.15. An approximate shape may be deduced from the deflected shape of a tip-loaded cantilever. Thus

$$v = \frac{v_0 z^2}{2l^3}(3l - z)$$

This expression satisfies the end-conditions of deflection, viz. $v = 0$ at $z = 0$ and $v = v_0$ at $z = l$. In addition, it satisfies the conditions that the slope of the column is zero at the built-in end and that the bending moment, i.e. $\mathrm{d}^2v/\mathrm{d}z^2$, is zero at the free end. The bending moment at any section is $M = P_{\mathrm{CR}}(v_0 - v)$ so that substitution for M and v in Eq. (8.47) gives

$$U + V = \frac{P_{\mathrm{CR}}^2 v_0^2}{2EI} \int_0^l \left(1 - \frac{3z^2}{2l^2} + \frac{z^3}{2l^3}\right)^2 \mathrm{d}z - \frac{P_{\mathrm{CR}}}{2} \int_0^l \left(\frac{3v_0}{2l^3}\right)^3 z^2(2l - z)^2 \,\mathrm{d}z$$

Integrating and substituting the limits we have

$$U + V = \frac{17}{35}\frac{P_{CR}^2 v_0^2 l}{2EI} - \frac{3}{5}P_{CR}\frac{v_0^2}{l}$$

Hence

$$\frac{\partial(U+V)}{\partial v_0} = \frac{17}{35}\frac{P_{CR}^2 v_0 l}{EI} - \frac{6P_{CR}v_0}{5l} = 0$$

from which

$$P_{CR} = \frac{42EI}{17l^2} = 2.471\frac{EI}{l^2}$$

This value of critical load compares with the exact value (see Table 8.1) of $\pi^2 EI/4l^2 = 2.467EI/l^2$; the error, in this case, is seen to be extremely small. Approximate values of critical load obtained by the energy method are always greater than the correct values. The explanation lies in the fact that an assumed deflected shape implies the application of constraints in order to force the column to take up an artificial shape. This, as we have seen, has the effect of stiffening the column with a consequent increase in critical load.

It will be observed that the solution for the above example may be obtained by simply equating the increase in internal energy (U) to the work done by the external critical load ($-V$). This is always the case when the assumed deflected shape contains a single unknown coefficient, such as v_0 in the above example.

8.6 Flexural–torsional buckling of thin-walled columns

It is recommended that the reading of this section be delayed until after Chapter 27 has been studied.

In some instances thin-walled columns of open cross-section do not buckle in bending as predicted by the Euler theory but twist without bending, or bend and twist simultaneously, producing flexural–torsional buckling. The solution of this type of problem relies on the theory presented in Chapter 27 for the torsion of open section beams subjected to warping (axial) restraint. Initially, however, we shall establish a useful analogy between the bending of a beam and the behaviour of a pin-ended column.

The bending equation for a simply supported beam carrying a uniformly distributed load of intensity w_y and having Cx and Cy as principal centroidal axes is

$$EI_{xx}\frac{\mathrm{d}^4 v}{\mathrm{d}z^4} = w_y \quad \text{(see Chapter 16)} \tag{8.52}$$

Also, the equation for the buckling of a pin-ended column about the Cx axis is (see Eq. (8.1))

$$EI_{xx}\frac{\mathrm{d}^2 v}{\mathrm{d}z^2} = -P_{CR}v \tag{8.53}$$

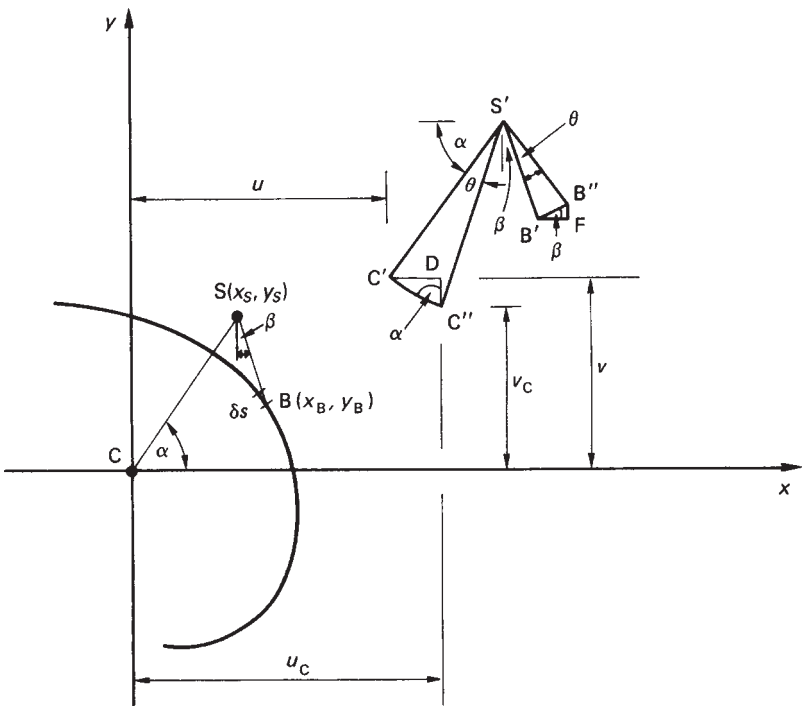

Fig. 8.16 Flexural–torsional buckling of a thin-walled column.

Differentiating Eq. (8.53) twice with respect to z gives

$$EI_{xx}\frac{\mathrm{d}^4 v}{\mathrm{d}z^4} = -P_{\mathrm{CR}}\frac{\mathrm{d}^2 v}{\mathrm{d}z^2} \tag{8.54}$$

Comparing Eqs (8.52) and (8.54) we see that the behaviour of the column may be obtained by considering it as a simply supported beam carrying a uniformly distributed load of intensity w_y given by

$$w_y = -P_{\mathrm{CR}}\frac{\mathrm{d}^2 v}{\mathrm{d}z^2} \tag{8.55}$$

Similarly, for buckling about the Cy axis

$$w_x = -P_{\mathrm{CR}}\frac{\mathrm{d}^2 u}{\mathrm{d}z^2} \tag{8.56}$$

Consider now a thin-walled column having the cross-section shown in Fig. 8.16 and suppose that the centroidal axes Cxy are principal axes (see Chapter 16); S(x_{S}, y_{S}) is the shear centre of the column (see Chapter 17) and its cross-sectional area is A. Due to the flexural–torsional buckling produced, say, by a compressive axial load P the cross-section will suffer translations u and v parallel to Cx and Cy, respectively and a rotation θ, positive anticlockwise, about the shear centre S. Thus, due to translation,

C and S move to C′ and S′ and then, due to rotation about S′, C′ moves to C″. The total movement of C, u_C, in the x direction is given by

$$u_c = u + \mathrm{C'D} = u + \mathrm{C'C''}\sin\alpha \quad (\mathrm{S'\hat{C}'C''} \simeq 90^\circ)$$

But

$$\mathrm{C'C''} = \mathrm{C'S'}\theta = \mathrm{CS}\theta$$

Hence

$$u_\mathrm{C} = u + \theta\mathrm{CS}\sin\alpha = u + y_\mathrm{S}\theta \tag{8.57}$$

Also the total movement of C in the y direction is

$$v_\mathrm{C} = v - \mathrm{DC''} = v - \mathrm{C'C''}\cos\alpha = v - \theta\mathrm{CS}\cos\alpha$$

so that

$$v_\mathrm{C} = v - x_\mathrm{s}\theta \tag{8.58}$$

Since at this particular cross-section of the column the centroidal axis has been displaced, the axial load P produces bending moments about the displaced x and y axes given, respectively, by

$$M_x = Pv_\mathrm{C} = P(v - x_\mathrm{S}\theta) \tag{8.59}$$

and

$$M_y = Pu_\mathrm{C} = P(u + y_\mathrm{S}\theta) \tag{8.60}$$

From simple beam theory (Chapter 16)

$$EI_{xx}\frac{\mathrm{d}^2v}{\mathrm{d}z^2} = -M_x = -P(v - x_\mathrm{S}\theta) \tag{8.61}$$

and

$$EI_{yy}\frac{\mathrm{d}^2u}{\mathrm{d}z^2} = -M_y = -P(u + y_\mathrm{S}\theta) \tag{8.62}$$

where I_{xx} and I_{yy} are the second moments of area of the cross-section of the column about the principal centroidal axes, E is Young's modulus for the material of the column and z is measured along the centroidal longitudinal axis.

The axial load P on the column will, at any cross-section, be distributed as a uniform direct stress σ. Thus, the direct load on any element of length δs at a point $\mathrm{B}(x_\mathrm{B}, y_\mathrm{B})$ is $\sigma t\,\mathrm{d}s$ acting in a direction parallel to the longitudinal axis of the column. In a similar manner to the movement of C to C″ the point B will be displaced to B″. The horizontal movement of B in the x direction is then

$$u_\mathrm{B} = u + \mathrm{B'F} = u + \mathrm{B'B''}\cos\beta$$

But

$$\mathrm{B'B''} = \mathrm{S'B'}\theta = \mathrm{SB}\theta$$

Hence

$$u_{\mathrm{B}} = u + \theta \mathrm{SB} \cos \beta$$

or

$$u_{\mathrm{B}} = u + (y_{\mathrm{S}} - y_{\mathrm{B}})\theta \tag{8.63}$$

Similarly the movement of B in the y direction is

$$v_{\mathrm{B}} = v - (x_{\mathrm{S}} - x_{\mathrm{B}})\theta \tag{8.64}$$

Therefore, from Eqs (8.63) and (8.64) and referring to Eqs (8.55) and (8.56), we see that the compressive load on the element δs at B, $\sigma t \delta s$, is equivalent to lateral loads

$$-\sigma t \delta s \frac{\mathrm{d}^2}{\mathrm{d}z^2}[u + (y_{\mathrm{S}} - y_{\mathrm{B}})\theta] \quad \text{in the } x \text{ direction}$$

and

$$-\sigma t \delta s \frac{\mathrm{d}^2}{\mathrm{d}z^2}[v - (x_{\mathrm{S}} - x_{\mathrm{B}})\theta] \quad \text{in the } y \text{ direction}$$

The lines of action of these equivalent lateral loads do not pass through the displaced position S′ of the shear centre and therefore produce a torque about S′ leading to the rotation θ. Suppose that the element δs at B is of unit length in the longitudinal z direction. The torque per unit length of the column $\delta T(z)$ acting on the element at B is then given by

$$\begin{aligned} \delta T(z) = &-\sigma t \delta s \frac{\mathrm{d}^2}{\mathrm{d}z^2}[u + (y_{\mathrm{S}} - y_{\mathrm{B}})\theta](y_{\mathrm{S}} - y_{\mathrm{B}}) \\ &+ \sigma t \delta s \frac{\mathrm{d}^2}{\mathrm{d}z^2}[v - (x_{\mathrm{S}} - x_{\mathrm{B}})\theta](x_{\mathrm{S}} - x_{\mathrm{B}}) \end{aligned} \tag{8.65}$$

Integrating Eq. (8.65) over the complete cross-section of the column gives the torque per unit length acting on the column, i.e.

$$\begin{aligned} T(z) = &-\int_{\mathrm{Sect}} \sigma t \frac{\mathrm{d}^2 u}{\mathrm{d}z^2}(y_{\mathrm{S}} - y_{\mathrm{B}})\mathrm{d}s - \int_{\mathrm{Sect}} \sigma t (y_{\mathrm{S}} - y_{\mathrm{B}})^2 \frac{\mathrm{d}^2\theta}{\mathrm{d}z^2}\mathrm{d}s \\ &+ \int_{\mathrm{Sect}} \sigma t \frac{\mathrm{d}^2 v}{\mathrm{d}z^2}(x_{\mathrm{S}} - x_{\mathrm{B}})\mathrm{d}s - \int_{\mathrm{Sect}} \sigma t (x_{\mathrm{S}} - x_{\mathrm{B}})^2 \frac{\mathrm{d}^2\theta}{\mathrm{d}z^2}\mathrm{d}s \end{aligned} \tag{8.66}$$

Expanding Eq. (8.66) and noting that σ is constant over the cross-section, we obtain

$$\begin{aligned} T(z) = &-\sigma\frac{\mathrm{d}^2u}{\mathrm{d}z^2}y_\mathrm{S}\int_\mathrm{Sect} t\,\mathrm{d}s + \sigma\frac{\mathrm{d}^2u}{\mathrm{d}z^2}\int_\mathrm{Sect} ty_\mathrm{B}\,\mathrm{d}s - \sigma\frac{\mathrm{d}^2\theta}{\mathrm{d}z^2}y_\mathrm{S}^2\int_\mathrm{Sect} t\,\mathrm{d}s \\ &+ \sigma\frac{\mathrm{d}^2\theta}{\mathrm{d}z^2}2y_\mathrm{S}\int_\mathrm{Sect} ty_\mathrm{B}\,\mathrm{d}s - \sigma\frac{\mathrm{d}^2\theta}{\mathrm{d}z^2}\int_\mathrm{Sect} ty_\mathrm{B}^2\,\mathrm{d}s + \sigma\frac{\mathrm{d}^2v}{\mathrm{d}z^2}x_\mathrm{S}\int_\mathrm{Sect} t\,\mathrm{d}s \\ &- \sigma\frac{\mathrm{d}^2v}{\mathrm{d}z^2}\int_\mathrm{Sect} tx_\mathrm{B}\,\mathrm{d}s - \sigma\frac{\mathrm{d}^2\theta}{\mathrm{d}z^2}x_\mathrm{S}^2\int_\mathrm{Sect} t\,\mathrm{d}s + \sigma\frac{\mathrm{d}^2\theta}{\mathrm{d}z^2}2x_\mathrm{S}\int_\mathrm{Sect} tx_\mathrm{B}\,\mathrm{d}s \\ &- \sigma\frac{\mathrm{d}^2\theta}{\mathrm{d}z^2}\int_\mathrm{Sect} tx_\mathrm{B}^2\,\mathrm{d}s \end{aligned} \tag{8.67}$$

Equation (8.67) may be rewritten

$$T(z) = P\left(x_\mathrm{S}\frac{\mathrm{d}^2v}{\mathrm{d}z^2} - y_\mathrm{S}\frac{\mathrm{d}^2u}{\mathrm{d}z^2}\right) - \frac{P}{A}\frac{\mathrm{d}^2\theta}{\mathrm{d}z^2}(Ay_\mathrm{S}^2 + I_{xx} + Ax_\mathrm{S}^2 + I_{yy}) \tag{8.68}$$

In Eq. (8.68) the term $I_{xx} + I_{yy} + A(x_\mathrm{S}^2 + y_\mathrm{S}^2)$ is the polar second moment of area I_0 of the column about the shear centre S. Thus Eq. (8.68) becomes

$$T(z) = P\left(x_\mathrm{S}\frac{\mathrm{d}^2v}{\mathrm{d}z^2} - y_\mathrm{S}\frac{\mathrm{d}^2u}{\mathrm{d}z^2}\right) - I_0\frac{P}{A}\frac{\mathrm{d}^2\theta}{\mathrm{d}z^2} \tag{8.69}$$

Substituting for $T(z)$ from Eq. (8.69) in Eq. (27.11), the general equation for the torsion of a thin-walled beam, we have

$$E\Gamma\frac{\mathrm{d}^4\theta}{\mathrm{d}z^4} - \left(GJ - I_0\frac{P}{A}\right)\frac{\mathrm{d}^2\theta}{\mathrm{d}z^2} - Px_\mathrm{S}\frac{\mathrm{d}^2v}{\mathrm{d}z^2} + Py_\mathrm{S}\frac{\mathrm{d}^2u}{\mathrm{d}z^2} = 0 \tag{8.70}$$

Equations (8.61), (8.62) and (8.70) form three simultaneous equations which may be solved to determine the flexural–torsional buckling loads.

As an example, consider the case of a column of length L in which the ends are restrained against rotation about the z axis and against deflection in the x and y directions; the ends are also free to rotate about the x and y axes and are free to warp. Thus $u = v = \theta = 0$ at $z = 0$ and $z = L$. Also, since the column is free to rotate about the x and y axes at its ends, $M_x = M_y = 0$ at $z = 0$ and $z = L$, and from Eqs (8.61) and (8.62)

$$\frac{\mathrm{d}^2v}{\mathrm{d}z^2} = \frac{\mathrm{d}^2u}{\mathrm{d}z^2} = 0 \text{ at } z = 0 \text{ and } z = L$$

Further, the ends of the column are free to warp so that

$$\frac{\mathrm{d}^2\theta}{\mathrm{d}z^2} = 0 \text{ at } z = 0 \text{ and } z = L \text{ (see Eq. (27.1))}$$

An assumed buckled shape given by

$$u = A_1\sin\frac{\pi z}{L} \quad v = A_2\sin\frac{\pi z}{L} \quad \theta = A_3\sin\frac{\pi z}{L} \tag{8.71}$$

in which A_1, A_2 and A_3 are unknown constants, satisfies the above boundary conditions. Substituting for u, v and θ from Eqs (8.71) into Eqs (8.61), (8.62) and (8.70), we have

$$\left.\begin{aligned}
&\left(P - \frac{\pi^2 EI_{xx}}{L^2}\right) A_2 - Px_S A_3 = 0 \\
&\left(P - \frac{\pi^2 EI_{yy}}{L^2}\right) A_1 + Py_S A_3 = 0 \\
&Py_S A_1 - Px_S A_2 - \left(\frac{\pi^2 E\Gamma}{L^2} + GJ - \frac{I_0}{A}P\right) A_3 = 0
\end{aligned}\right\} \tag{8.72}$$

For non-zero values of A_1, A_2 and A_3 the determinant of Eqs (8.72) must equal zero, i.e.

$$\begin{vmatrix} 0 & P - \pi^2 EI_{xx}/L^2 & -Px_S \\ P - \pi^2 EI_{yy}/L^2 & 0 & Py_S \\ Py_S & -Px_S & I_0 P/A - \pi^2 E\Gamma/L^2 - GJ \end{vmatrix} = 0 \tag{8.73}$$

The roots of the cubic equation formed by the expansion of the determinant give the critical loads for the flexural–torsional buckling of the column; clearly the lowest value is significant.

In the case where the shear centre of the column and the centroid of area coincide, i.e. the column has a doubly symmetrical cross-section, $x_S = y_S = 0$ and Eqs (8.61), (8.62) and (8.70) reduce, respectively, to

$$EI_{xx}\frac{\mathrm{d}^2 v}{\mathrm{d}z^2} = -Pv \tag{8.74}$$

$$EI_{yy}\frac{\mathrm{d}^2 u}{\mathrm{d}z^2} = -Pu \tag{8.75}$$

$$E\Gamma\frac{\mathrm{d}^4\theta}{\mathrm{d}z^4} - \left(GJ - I_0\frac{P}{A}\right)\frac{\mathrm{d}^2\theta}{\mathrm{d}z^2} = 0 \tag{8.76}$$

Equations (8.74), (8.75) and (8.76), unlike Eqs (8.61), (8.62) and (8.70), are uncoupled and provide three separate values of buckling load. Thus, Eqs (8.74) and (8.75) give values for the Euler buckling loads about the x and y axes respectively, while Eq. (8.76) gives the axial load which would produce pure torsional buckling; clearly the buckling load of the column is the lowest of these values. For the column whose buckled shape is defined by Eqs (8.71), substitution for v, u and θ in Eqs (8.74), (8.75) and (8.76), respectively gives

$$P_{\mathrm{CR}(xx)} = \frac{\pi^2 EI_{xx}}{L_2} \quad P_{\mathrm{CR}(yy)} = \frac{\pi^2 EI_{yy}}{L^2} \quad P_{\mathrm{CR}(\theta)} = \frac{A}{I_0}\left(GJ + \frac{\pi^2 E\Gamma}{L^2}\right) \tag{8.77}$$

Example 8.3

A thin-walled pin-ended column is 2 m long and has the cross-section shown in Fig. 8.17. If the ends of the column are free to warp determine the lowest value of axial

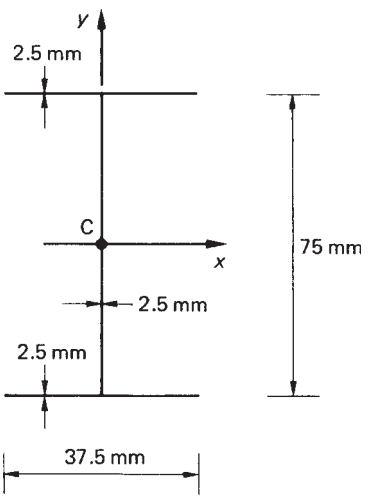

Fig. 8.17 Column section of Example 8.3.

load which will cause buckling and specify the buckling mode. Take $E = 75\,000\,\text{N/mm}^2$ and $G = 21\,000\,\text{N/mm}^2$.

Since the cross-section of the column is doubly-symmetrical, the shear centre coincides with the centroid of area and $x_S = y_S = 0$; Eq. (8.74), (8.75) and (8.76) therefore apply. Further, the boundary conditions are those of the column whose buckled shape is defined by Eqs (8.71) so that the buckling load of the column is the lowest of the three values given by Eqs (8.77).

The cross-sectional area A of the column is

$$A = 2.5(2 \times 37.5 + 75) = 375\,\text{mm}^2$$

The second moments of area of the cross-section about the centroidal axes Cxy are (see Chapter 16), respectively

$$I_{xx} = 2 \times 37.5 \times 2.5 \times 37.5^2 + 2.5 \times 75^3/12 = 3.52 \times 10^5\,\text{mm}^4$$

$$I_{yy} = 2 \times 2.5 \times 37.5^3/12 = 0.22 \times 10^5\,\text{mm}^4$$

The polar second moment of area I_0 is

$$I_0 = I_{xx} + I_{yy} + A(x_S^2 + y_S^2) \quad \text{(see derivation of Eq. (8.69))}$$

i.e.

$$I_0 = 3.52 \times 10^5 + 0.22 \times 10^5 = 3.74 \times 10^5\,\text{mm}^4$$

The torsion constant J is obtained using Eq. (18.11) which gives

$$J = 2 \times 37.5 \times 2.5^3/3 + 75 \times 2.5^3/3 = 781.3\,\text{mm}^4$$

Finally, Γ is found using the method of Section 27.2 and is

$$\Gamma = 2.5 \times 37.5^3 \times 75^2/24 = 30.9 \times 10^6\,\text{mm}^6$$

Substituting the above values in Eqs (8.77) we obtain

$$P_{CR(xx)} = 6.5 \times 10^4\,\text{N} \quad P_{CR(yy)} = 0.41 \times 10^4\,\text{N} \quad P_{CR(\theta)} = 2.22 \times 10^4\,\text{N}$$

The column will therefore buckle in bending about the Cy axis when subjected to an axial load of 0.41×10^4 N.

Equation (8.73) for the column whose buckled shape is defined by Eqs (8.71) may be rewritten in terms of the three separate buckling loads given by Eqs (8.77). Thus

$$\begin{vmatrix} 0 & P - P_{CR(xx)} & -Px_S \\ P - P_{CR(yy)} & 0 & Py_S \\ Py_S & -Px_S & I_0(P - P_{CR(\theta)})/A \end{vmatrix} = 0 \tag{8.78}$$

If the column has, say, Cx as an axis of symmetry, then the shear centre lies on this axis and $y_S = 0$. Equation (8.78) thereby reduces to

$$\begin{vmatrix} P - P_{CR(xx)} & -Px_S \\ -Px_S & I_0(P - P_{CR(\theta)})/A \end{vmatrix} = 0 \tag{8.79}$$

The roots of the quadratic equation formed by expanding Eq. (8.79) are the values of axial load which will produce flexural–torsional buckling about the longitudinal and x axes. If $P_{CR(yy)}$ is less than the smallest of these roots the column will buckle in pure bending about the y axis.

Example 8.4

A column of length 1 m has the cross-section shown in Fig. 8.18. If the ends of the column are pinned and free to warp, calculate its buckling load; $E = 70\,000\,\text{N/mm}^2$, $G = 30\,000\,\text{N/mm}^2$.

In this case the shear centre S is positioned on the Cx axis so that $y_S = 0$ and Eq. (8.79) applies. The distance $\bar{x}$ of the centroid of area C from the web of the section is found

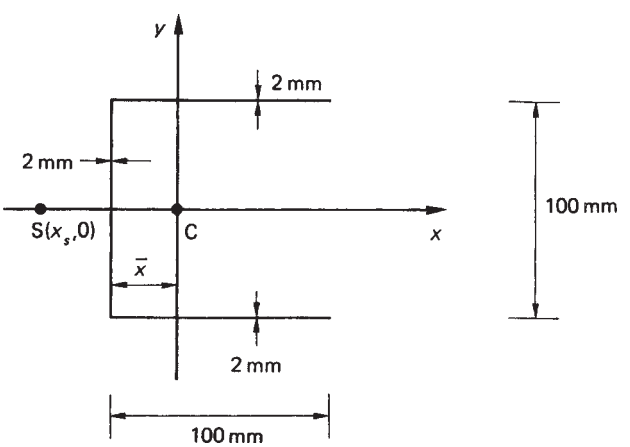

Fig. 8.18 Column section of Example 8.4.

by taking first moments of area about the web. Thus

$$2(100 + 100 + 100)\bar{x} = 2 \times 2 \times 100 \times 50$$

which gives

$$\bar{x} = 33.3\,\text{mm}$$

The position of the shear centre S is found using the method of Example 17.1; this gives $x_S = -76.2$ mm. The remaining section properties are found by the methods specified in Example 8.3 and are listed below

$$A = 600\,\text{mm}^2 \qquad I_{xx} = 1.17 \times 10^6\,\text{mm}^4 \qquad I_{yy} = 0.67 \times 10^6\,\text{mm}^4$$
$$I_0 = 5.32 \times 10^6\text{mm}^4 \qquad J = 800\,\text{mm}^4 \qquad \Gamma = 2488 \times 10^6\,\text{mm}^6$$

From Eq. (8.77)

$$P_{\text{CR}(yy)} = 4.63 \times 10^5\,\text{N} \quad P_{\text{CR}(xx)} = 8.08 \times 10^5\,\text{N} \quad P_{\text{CR}(\theta)} = 1.97 \times 10^5\,\text{N}$$

Expanding Eq. (8.79)

$$(P - P_{\text{CR}(xx)})(P - P_{\text{CR}(\theta)})I_0/A - P^2 x_S^2 = 0 \tag{i}$$

Rearranging Eq. (i)

$$P^2(1 - Ax_S^2/I_0) - P(P_{\text{CR}(xx)} + P_{\text{CR}(\theta)}) + P_{\text{CR}(xx)}P_{\text{CR}(\theta)} = 0 \tag{ii}$$

Substituting the values of the constant terms in Eq. (ii) we obtain

$$P^2 - 29.13 \times 10^5 P + 46.14 \times 10^{10} = 0 \tag{iii}$$

The roots of Eq. (iii) give two values of critical load, the lowest of which is

$$P = 1.68 \times 10^5\,\text{N}$$

It can be seen that this value of flexural–torsional buckling load is lower than any of the uncoupled buckling loads $P_{\text{CR}(xx)}$, $P_{\text{CR}(yy)}$ or $P_{\text{CR}(\theta)}$; the reduction is due to the interaction of the bending and torsional buckling modes.

Example 8.5

A thin walled column has the cross-section shown in Fig. 8.19, is of length L and is subjected to an axial load through its shear centre S. If the ends of the column are prevented from warping and twisting determine the value of direct stress when failure occurs due to torsional buckling.

The torsion bending constant Γ is found using the method described in Section 27.2. The position of the shear centre is given but is obvious by inspection. The swept area $2\lambda A_{R,0}$ is determined as a function of s and its distribution is shown in Fig. 8.20. The centre of gravity of the 'wire' is found by taking moments about the s axis.

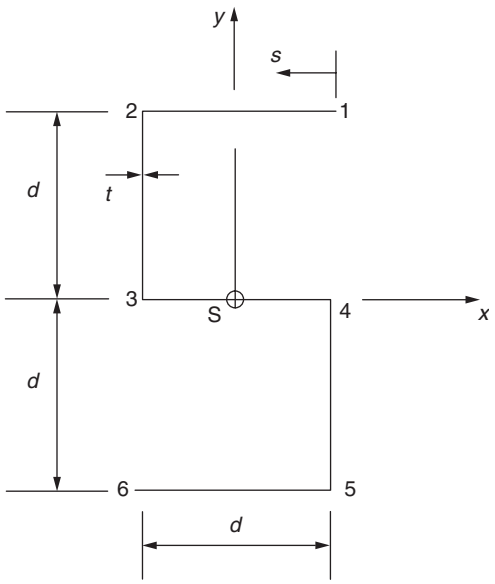

Fig. 8.19 Section of column of Example 8.5.

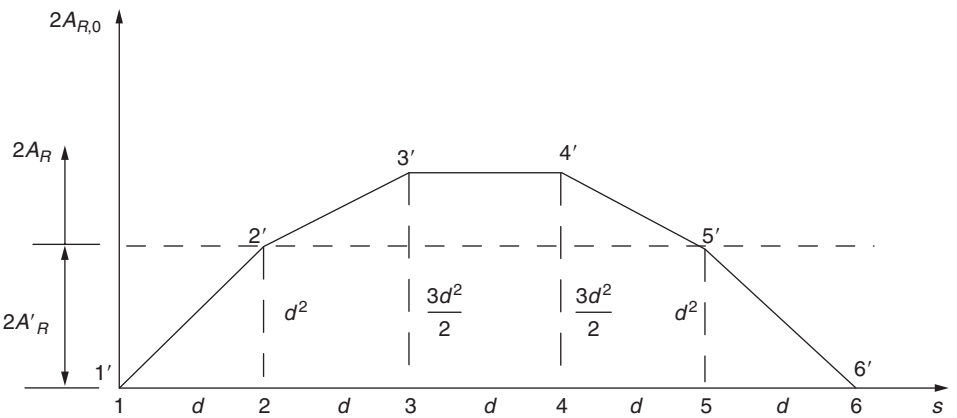

Fig. 8.20 Determination of torsion bending constant for column section of Example 8.5.

Then

$$2A'_R 5td = td\left(\frac{d^2}{2} + \frac{5d^2}{4} + \frac{3d^2}{2} + \frac{5d^2}{4} + \frac{d^2}{2}\right)$$

which gives

$$2A'_R = d^2$$

The torsion bending constant is then the 'moment of inertia' of the 'wire' and is

$$\Gamma = 2td\frac{1}{3}(d^2)^2 + \frac{td}{3}\left(\frac{d^2}{2}\right)^2 \times 2 + td\left(\frac{d^2}{2}\right)^2$$

from which

$$\Gamma = \frac{13}{12} t d^5$$

Also the torsion constant J is given by (see Section 3.4)

$$J = \sum \frac{st^3}{3} = \frac{5dt^3}{3}$$

The shear centre of the section and the centroid of area coincide so that the torsional buckling load is given by Eq. (8.76). Rewriting this equation

$$\frac{\mathrm{d}^4\theta}{\mathrm{d}z^4} + \mu^2 \frac{\mathrm{d}^2\theta}{\mathrm{d}z^2} = 0 \qquad \text{(i)}$$

where

$$\mu^2 = (\sigma I_0 - GJ)/E\Gamma \quad (\sigma = P/A)$$

The solution of Eq. (i) is

$$\theta = A\cos\mu z + B\sin\mu z + Cz + D \qquad \text{(ii)}$$

The boundary conditions are $\theta = 0$ when $z = 0$ and $z = L$ and since the warping is suppressed at the ends of the beam

$$\frac{\mathrm{d}\theta}{\mathrm{d}z} = 0 \quad \text{when } z = 0 \text{ and } z = L \qquad \text{(see Eq. (18.19))}$$

Putting $\theta = 0$ at $z = 0$ in Eq. (ii)

$$0 = A + D$$

or

$$A = -D$$

Also

$$\frac{\mathrm{d}\theta}{\mathrm{d}z} = -\mu A\sin\mu z + \mu B\cos\mu z + C$$

and since $(\mathrm{d}\theta/\mathrm{d}z) = 0$ at $z = 0$

$$C = -\mu B$$

When $z = L$, $\theta = 0$ so that, from Eq. (ii)

$$0 = A\cos\mu L + B\sin\mu L + CL + D$$

which may be rewritten

$$0 = B(\sin\mu L - \mu L) + A(\cos\mu L - 1) \qquad \text{(iii)}$$

Then for $(\mathrm{d}\theta/\mathrm{d}z) = 0$ at $z = L$

$$0 = \mu B\cos\mu L - \mu A\sin\mu L - \mu B$$

or

$$0 = B(\cos \mu L - 1) - A \sin \mu L \tag{iv}$$

Eliminating A from Eqs (iii) and (iv)

$$0 = B[2(1 - \cos \mu L) - \mu L \sin \mu L] \tag{v}$$

Similarly, in terms of the constant C

$$0 = -C[2(1 - \cos \mu L) - \mu L \sin \mu L] \tag{vi}$$

or

$$B = -C$$

But $B = -C/\mu$ so that to satisfy both equations $B = C = 0$ and

$$\theta = A \cos \mu z - A = A(\cos \mu z - 1) \tag{vii}$$

Since $\theta = 0$ at $z = l$

$$\cos \mu L = 1$$

or

$$\mu L = 2n\pi$$

Therefore

$$\mu^2 L^2 = 4n^2\pi^2$$

or

$$\frac{\sigma I_0 - GJ}{E\Gamma} = \frac{4n^2\pi^2}{L^2}$$

The lowest value of torsional buckling load corresponds to $n = 1$ so that, rearranging the above

$$\sigma = \frac{1}{I_0}\left(GJ + \frac{4\pi^2 E\Gamma}{L^2}\right) \tag{viii}$$

The polar second moment of area I_0 is given by

$$I_0 = I_{xx} + I_{yy} \qquad \text{(see Ref. 2)}$$

ie

$$I_0 = 2\left(td\,d^2 + \frac{td^3}{3}\right) + \frac{3td^3}{12} + 2td\frac{d^2}{4}$$

which gives

$$I_0 = \frac{4ltd^3}{12}$$

Substituting for I_0, J and Γ in Eq. (viii)

$$\sigma = \frac{4}{4ld^3}\left(sgt^2 + \frac{13\pi^2 Ed^4}{L^2}\right)$$

References

1 Timoshenko, S. P. and Gere, J. M., *Theory of Elastic Stability*, 2nd edition, McGraw-Hill Book Company, New York, 1961.

2 Megson, T. H. G., *Structural and Stress Analysis*, 2nd edition, Elsevier, Oxford, 2005.

Problems

P.8.1 The system shown in Fig. P.8.1 consists of two bars AB and BC, each of bending stiffness EI elastically hinged together at B by a spring of stiffness K (i.e. bending moment applied by spring $= K \times$ change in slope across B).

Regarding A and C as simple pin-joints, obtain an equation for the first buckling load of the system. What are the lowest buckling loads when (a) $K \to \infty$, (b) $EI \to \infty$. Note that B is free to move vertically.

Ans. $\mu K / \tan \mu l$.

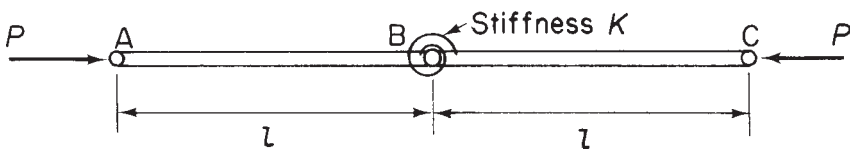

Fig. P.8.1

P.8.2 A pin-ended column of length l and constant flexural stiffness EI is reinforced to give a flexural stiffness $4EI$ over its central half (see Fig. P.8.2).

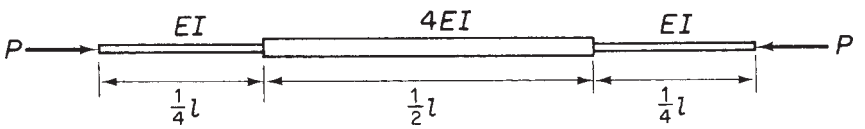

Fig. P.8.2

Considering symmetric modes of buckling only, obtain the equation whose roots yield the flexural buckling loads and solve for the lowest buckling load.

Ans. $\tan \mu l/8 = 1/\sqrt{2}, P = 24.2EI/l^2$

P.8.3 A uniform column of length l and bending stiffness EI is built-in at one end and free at the other and has been designed so that its lowest flexural buckling load is P (see Fig. P.8.3).

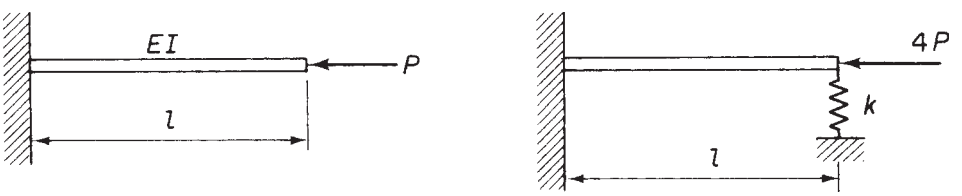

Fig. P.8.3

Subsequently it has to carry an increased load, and for this it is provided with a lateral spring at the free end. Determine the necessary spring stiffness k so that the buckling load becomes $4P$.

Ans. $k = 4P\mu/(\mu l - \tan \mu l)$.

P.8.4 A uniform, pin-ended column of length l and bending stiffness EI has an initial curvature such that the lateral displacement at any point between the column and the straight line joining its ends is given by

$$v_0 = a\frac{4z}{l^2}(l - z) \qquad \text{(see Fig. P.8.4)}$$

Show that the maximum bending moment due to a compressive end load P is given by

$$M_{\max} = -\frac{8aP}{(\lambda l)^2}\left(\sec\frac{\lambda l}{2} - 1\right)$$

where

$$\lambda^2 = P/EI$$

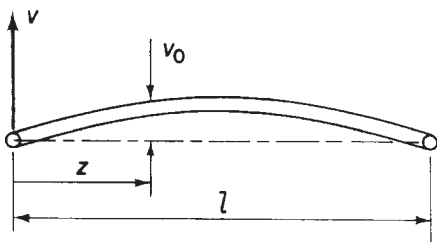

Fig. P.8.4

P.8.5 The uniform pin-ended column shown in Fig. P.8.5 is bent at the centre so that its eccentricity there is δ. If the two halves of the column are otherwise straight and have a flexural stiffness EI, find the value of the maximum bending moment when the column carries a compression load P.

Ans. $-P\dfrac{2\delta}{l}\sqrt{\dfrac{EI}{P}}\tan\sqrt{\dfrac{P}{EI}}\dfrac{l}{2}$.

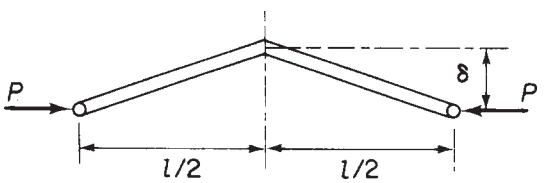

Fig. P.8.5

P.8.6 A straight uniform column of length l and bending stiffness EI is subjected to uniform lateral loading w/unit length. The end attachments do not restrict rotation

of the column ends. The longitudinal compressive force P has eccentricity e from the centroids of the end sections and is placed so as to oppose the bending effect of the lateral loading, as shown in Fig. P.8.6. The eccentricity e can be varied and is to be adjusted to the value which, for given values of P and w, will result in the least maximum bending moment on the column. Show that

$$e = (w/P\mu^2)\tan^2 \mu l/4$$

where

$$\mu^2 = P/EI$$

Deduce the end moment which will give the optimum condition when P tends to zero.

Ans. $wl^2/16$.

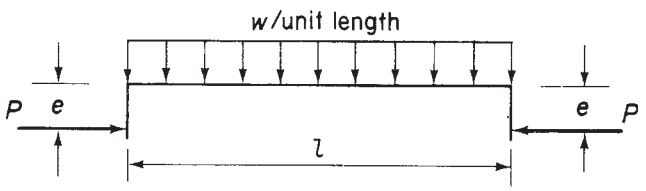

Fig. P.8.6

P.8.7 The relation between stress σ and strain ε in compression for a certain material is

$$10.5 \times 10^6 \varepsilon = \sigma + 21\,000 \left(\frac{\sigma}{49\,000}\right)^{16}$$

Assuming the tangent modulus equation to be valid for a uniform strut of this material, plot the graph of σ_b against l/r where σ_b is the flexural buckling stress, l the equivalent pin-ended length and r the least radius of gyration of the cross-section.

Estimate the flexural buckling load for a tubular strut of this material, of 1.5 units outside diameter and 0.08 units wall thickness with effective length 20 units.

Ans. 14 454 force units.

P.8.8 A rectangular portal frame ABCD is rigidly fixed to a foundation at A and D and is subjected to a compression load P applied at each end of the horizontal member BC (see Fig. P.8.8). If the members all have the same bending stiffness EI show that the buckling loads for modes which are symmetrical about the vertical centre line are given by the transcendental equation

$$\frac{\lambda a}{2} = -\frac{1}{2}\left(\frac{a}{b}\right)\tan\left(\frac{\lambda a}{2}\right)$$

where

$$\lambda^2 = P/EI$$

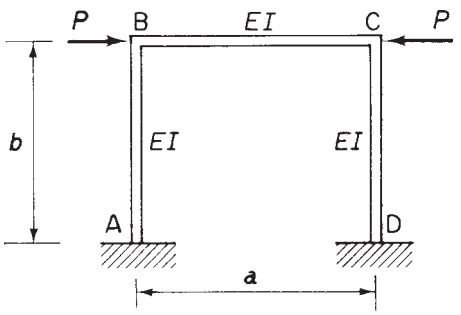

Fig. P.8.8

P.8.9 A compression member (Fig. P.8.9) is made of circular section tube, diameter d, thickness t. The member is not perfectly straight when unloaded, having a slightly bowed shape which may be represented by the expression

$$v = \delta \sin\left(\frac{\pi z}{l}\right)$$

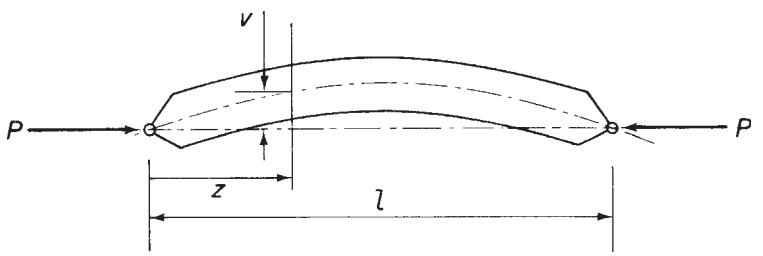

Fig. P.8.9

Show that when the load P is applied, the maximum stress in the member can be expressed as

$$\sigma_{\max} = \frac{P}{\pi dt}\left[1 + \frac{1}{1-\alpha}\frac{4\delta}{d}\right]$$

where

$$\alpha = P/P_{\mathrm{e}}, \quad P_{\mathrm{e}} = \pi^2 EI/l^2$$

Assume t is small compared with d so that the following relationships are applicable:

Cross-sectional area of tube $= \pi dt$.

Second moment of area of tube $= \pi d^3 t/8$.

P.8.10 Figure P.8.10 illustrates an idealized representation of part of an aircraft control circuit. A uniform, straight bar of length a and flexural stiffness EI is built-in at the end A and hinged at B to a link BC, of length b, whose other end C is pinned so that it is free to slide along the line ABC between smooth, rigid guides. A, B and C are initially in a straight line and the system carries a compression force P, as shown.

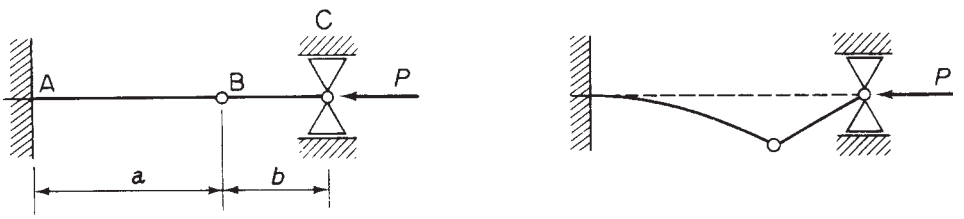

Fig. P.8.10

Assuming that the link BC has a sufficiently high flexural stiffness to prevent its buckling as a pin-ended strut, show, by setting up and solving the differential equation for flexure of AB, that buckling of the system, of the type illustrated in Fig. P.8.10, occurs when P has such a value that

$$\tan \lambda a = \lambda(a + b)$$

where

$$\lambda^2 = P/EI$$

P.8.11 A pin-ended column of length l has its central portion reinforced, the second moment of its area being I_2 while that of the end portions, each of length a, is I_1. Use the energy method to determine the critical load of the column, assuming that its centre-line deflects into the parabola $v = kz(l - z)$ and taking the more accurate of the two expressions for the bending moment.

In the case where $I_2 = 1.6I_1$ and $a = 0.2l$ find the percentage increase in strength due to the reinforcement, and compare it with the percentage increase in weight on the basis that the radius of gyration of the section is not altered.

Ans. $P_{CR} = 14.96EI_1/l^2, 52\%, 36\%$.

P.8.12 A tubular column of length l is tapered in wall-thickness so that the area and the second moment of area of its cross-section decrease uniformly from A_1 and I_1 at its centre to $0.2A_1$ and $0.2I_1$ at its ends.

Assuming a deflected centre-line of parabolic form, and taking the more correct form for the bending moment, use the energy method to estimate its critical load when tested between pin-centres, in terms of the above data and Young's modulus E. Hence show that the saving in weight by using such a column instead of one having the same radius of gyration and constant thickness is about 15%.

Ans. $7.01EI_1/l^2$.

P.8.13 A uniform column (Fig. P.8.13), of length l and bending stiffness EI, is rigidly built-in at the end $z = 0$ and simply supported at the end $z = l$. The column is also attached to an elastic foundation of constant stiffness k/unit length.

Representing the deflected shape of the column by a polynomial

$$v = \sum_{n=0}^{p} a_n \eta^n, \quad \text{where } \eta = z/l$$

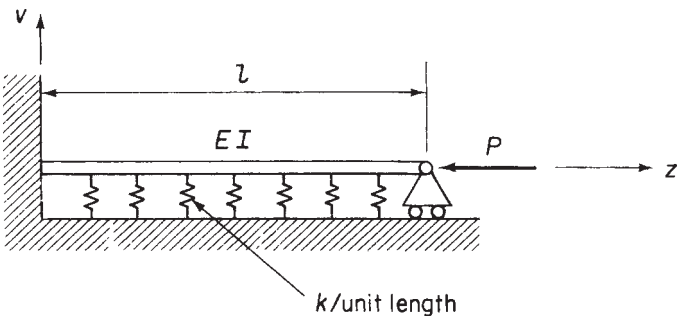

Fig. P.8.13

determine the form of this function by choosing a minimum number of terms p such that all the kinematic (geometric) and static boundary conditions are satisfied, allowing for one arbitrary constant only.

Using the result thus obtained, find an approximation to the lowest flexural buckling load P_{CR} by the Rayleigh–Ritz method.

Ans. $P_{CR} = 21.05EI/l^2 + 0.09kl^2$.

P.8.14 Figure P.8.14 shows the doubly symmetrical cross-section of a thin-walled column with rigidly fixed ends. Find an expression, in terms of the section dimensions and Poisson's ratio, for the column length for which the purely flexural and the purely torsional modes of instability would occur at the same axial load.

In which mode would failure occur if the length were less than the value found? The possibility of local instability is to be ignored.

Ans. $l = (2\pi b^2/t)\sqrt{(1+\nu)/255}$. Torsion.

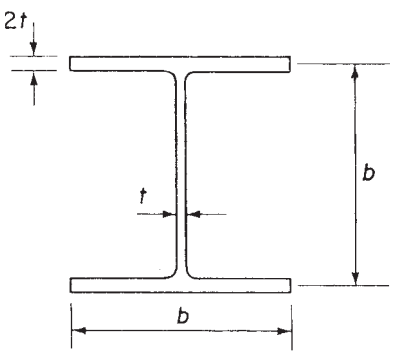

Fig. P.8.14

P.8.15 A column of length $2l$ with the doubly symmetric cross-section shown in Fig. P.8.15 is compressed between the parallel platens of a testing machine which fully prevents twisting and warping of the ends.

Using the data given below, determine the average compressive stress at which the column first buckles in torsion

$$l = 500\,\text{mm},\ b = 25.0\,\text{mm},\ t = 2.5\,\text{mm},\ E = 70\,000\,\text{N/mm}^2,\ E/G = 2.6$$

Ans. $\sigma_{CR} = 282\,\text{N/mm}^2$.

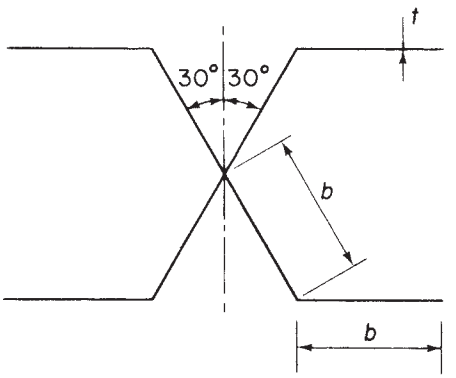

Fig. P.8.15

P.8.16 A pin-ended column of length 1.0 m has the cross-section shown in Fig. P.8.16. If the ends of the column are free to warp determine the lowest value of axial load which will cause the column to buckle, and specify the mode. Take $E = 70\,000\ \text{N/mm}^2$ and $G = 25\,000\ \text{N/mm}^2$.

Ans. 5527 N. Column buckles in bending about an axis in the plane of its web.

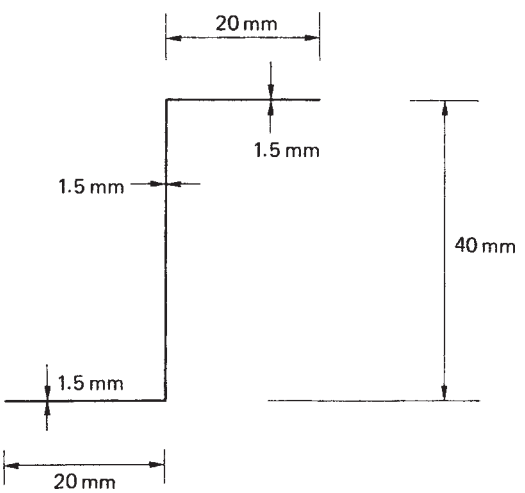

Fig. P.8.16

P.8.17 A pin-ended column of height 3.0 m has a circular cross-section of diameter 80 mm, wall thickness 2.0 mm and is converted to an open section by a narrow longitudinal slit; the ends of the column are free to warp. Determine the values of axial load which would cause the column to buckle in (a) pure bending and (b) pure torsion. Hence determine the value of the flexural–torsional buckling load. Take $E = 70\,000\ \text{N/mm}^2$ and $G = 22\,000\ \text{N/mm}^2$.

Note: the position of the shear centre of the column section may be found using the method described in Chapter 17.

Ans. (a) 3.09×10^4 N, (b) 1.78×10^4 N, 1.19×10^4 N.

9

Thin plates

We shall see in Chapter 12 when we examine the structural components of aircraft that they consist mainly of thin plates stiffened by arrangements of ribs and stringers. Thin plates under relatively small compressive loads are prone to buckle and so must be stiffened to prevent this. The determination of buckling loads for thin plates in isolation is relatively straightforward but when stiffened by ribs and stringers, the problem becomes complex and frequently relies on an empirical solution. In fact it may be the stiffeners which buckle before the plate and these, depending on their geometry, may buckle as a column or suffer local buckling of, say, a flange.

In this chapter we shall present the theory for the determination of buckling loads of flat plates and then examine some of the different empirical approaches which various researchers have suggested. In addition we shall investigate the particular case of flat plates which, when reinforced by horizontal flanges and vertical stiffeners, form the spars of aircraft wing structures; these are known as *tension field beams*.

9.1 Buckling of thin plates

A thin plate may buckle in a variety of modes depending upon its dimensions, the loading and the method of support. Usually, however, buckling loads are much lower than those likely to cause failure in the material of the plate. The simplest form of buckling arises when compressive loads are applied to simply supported opposite edges and the unloaded edges are free, as shown in Fig. 9.1. A thin plate in this configuration

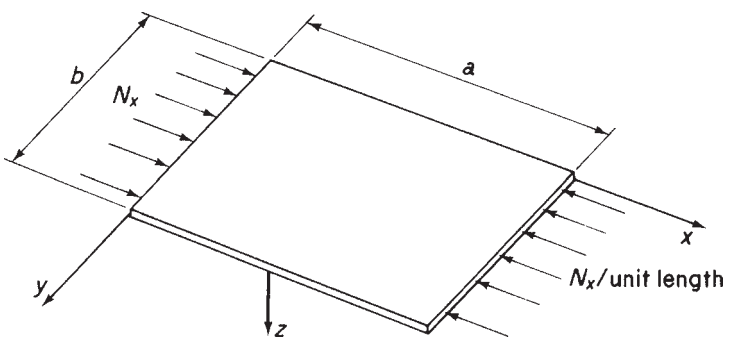

Fig. 9.1 Buckling of a thin flat plate.

behaves in exactly the same way as a pin-ended column so that the critical load is that predicted by the Euler theory. Once this critical load is reached the plate is incapable of supporting any further load. This is not the case, however, when the unloaded edges are supported against displacement out of the *xy* plane. Buckling, for such plates, takes the form of a bulging displacement of the central region of the plate while the parts adjacent to the supported edges remain straight. These parts enable the plate to resist higher loads; an important factor in aircraft design.

At this stage we are not concerned with this post-buckling behaviour, but rather with the prediction of the critical load which causes the initial bulging of the central area of the plate. For the analysis we may conveniently employ the method of total potential energy since we have already, in Chapter 7, derived expressions for strain and potential energy corresponding to various load and support configurations. In these expressions we assumed that the displacement of the plate comprises bending deflections only and that these are small in comparison with the thickness of the plate. These restrictions therefore apply in the subsequent theory.

First we consider the relatively simple case of the thin plate of Fig. 9.1, loaded as shown, but simply supported along all four edges. We have seen in Chapter 7 that its true deflected shape may be represented by the infinite double trigonometrical series

$$w = \sum_{m=1}^{\infty}\sum_{n=1}^{\infty} A_{mn} \sin\frac{m\pi x}{a} \sin\frac{n\pi y}{b}$$

Also, the total potential energy of the plate is, from Eqs (7.37) and (7.45)

$$\begin{aligned} U + V \quad = \quad & \frac{1}{2}\int_0^a \int_0^b \left[D \left\{ \left(\frac{\partial^2 w}{\partial x^2} + \frac{\partial^2 w}{\partial y^2} \right)^2 \right.\right. \\ & \left.\left. -2(1-\nu) \left[\frac{\partial^2 w}{\partial x^2}\frac{\partial^2 w}{\partial y^2} - \left(\frac{\partial^2 w}{\partial x\, \partial y} \right)^2 \right] \right\} - N_x \left(\frac{\partial w}{\partial x} \right)^2 \right] \mathrm{d}x\, \mathrm{d}y \end{aligned} \quad (9.1)$$

The integration of Eq. (9.1) on substituting for *w* is similar to those integrations carried out in Chapter 7. Thus, by comparison with Eq. (7.47)

$$U + V = \frac{\pi^4 abD}{8} \sum_{m=1}^{\infty}\sum_{n=1}^{\infty} A_{mn}^2 \left(\frac{m^2}{a^2} + \frac{n^2}{b^2} \right) - \frac{\pi^2 b}{8a} N_x \sum_{m=1}^{\infty}\sum_{n=1}^{\infty} m^2 A_{mn}^2 \quad (9.2)$$

The total potential energy of the plate has a stationary value in the neutral equilibrium of its buckled state (i.e. $N_x = N_{x,\mathrm{CR}}$). Therefore, differentiating Eq. (9.2) with respect to each unknown coefficient A_{mn} we have

$$\frac{\partial(U+V)}{\partial A_{mn}} = \frac{\pi^4 abD}{4} A_{mn} \left(\frac{m^2}{a^2} + \frac{n^2}{b^2} \right)^2 - \frac{\pi^2 b}{4a} N_{x,\mathrm{CR}} m^2 A_{mn} = 0$$

and for a non-trivial solution

$$N_{x,\mathrm{CR}} = \pi^2 a^2 D \frac{1}{m^2} \left(\frac{m^2}{a^2} + \frac{n^2}{b^2} \right)^2 \quad (9.3)$$

Exactly the same result may have been deduced from Eq. (ii) of Example 7.3, where the displacement w would become infinite for a negative (compressive) value of N_x equal to that of Eq. (9.3).

We observe from Eq. (9.3) that each term in the infinite series for displacement corresponds, as in the case of a column, to a different value of critical load (note, the problem is an eigenvalue problem). The lowest value of critical load evolves from some critical combination of integers m and n, i.e. the number of half-waves in the x and y directions, and the plate dimensions. Clearly $n = 1$ gives a minimum value so that no matter what the values of m, a and b the plate buckles into a half sine wave in the y direction. Thus we may write Eq. (9.3) as

$$N_{x,\mathrm{CR}} = \pi^2 a^2 D \frac{1}{m^2}\left(\frac{m^2}{a^2} + \frac{1}{b^2}\right)^2$$

or

$$N_{x,\mathrm{CR}} = \frac{k\pi^2 D}{b^2} \tag{9.4}$$

where the plate *buckling coefficient* k is given by the minimum value of

$$k = \left(\frac{mb}{a} + \frac{a}{mb}\right)^2 \tag{9.5}$$

for a given value of a/b. To determine the minimum value of k for a given value of a/b we plot k as a function of a/b for different values of m as shown by the dotted curves in Fig. 9.2. The minimum value of k is obtained from the lower envelope of the curves shown solid in the figure.

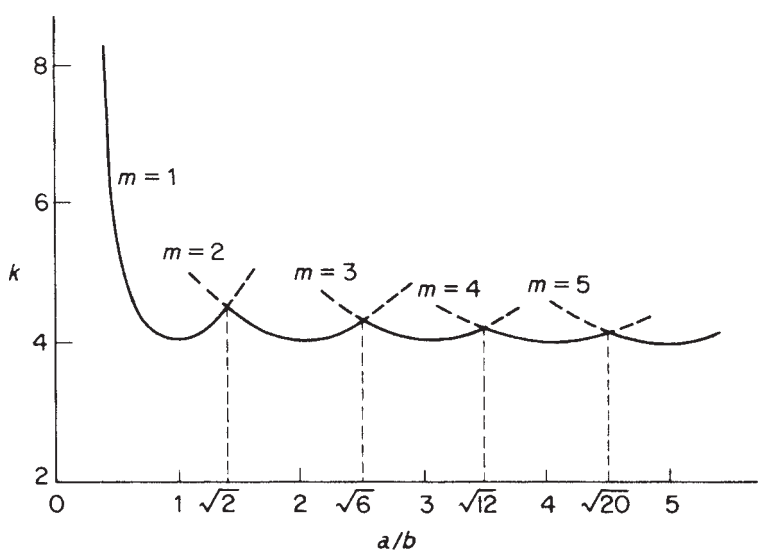

Fig. 9.2 Buckling coefficient k for simply supported plates.

It can be seen that m varies with the ratio a/b and that k and the buckling load are a minimum when $k = 4$ at values of $a/b = 1, 2, 3, \ldots$. As a/b becomes large k approaches 4 so that long narrow plates tend to buckle into a series of squares.

The transition from one buckling mode to the next may be found by equating values of k for the m and $m + 1$ curves. Hence

$$\frac{mb}{a} + \frac{a}{mb} = \frac{(m+1)b}{a} + \frac{a}{(m+1)b}$$

giving

$$\frac{a}{b} = \sqrt{m(m+1)}$$

Substituting $m = 1$, we have $a/b = \sqrt{2} = 1.414$, and for $m = 2$, $a/b = \sqrt{6} = 2.45$ and so on.

For a given value of a/b the critical stress, $\sigma_{CR} = N_{x,CR}/t$, is found from Eqs (9.4) and (7.4), i.e.

$$\sigma_{CR} = \frac{k\pi^2 E}{12(1-\nu^2)}\left(\frac{t}{b}\right)^2 \tag{9.6}$$

In general, the critical stress for a uniform rectangular plate, with various edge supports and loaded by constant or linearly varying in-plane direct forces (N_x, N_y) or constant shear forces (N_{xy}) along its edges, is given by Eq. (9.6). The value of k remains a function of a/b but depends also upon the type of loading and edge support. Solutions for such problems have been obtained by solving the appropriate differential equation or by using the approximate (Rayleigh–Ritz) energy method. Values of k for a variety of loading and support conditions are shown in Fig. 9.3. In Fig. 9.3(c), where k becomes the *shear buckling coefficient*, b is always the smaller dimension of the plate.

We see from Fig. 9.3 that k is very nearly constant for $a/b > 3$. This fact is particularly useful in aircraft structures where longitudinal stiffeners are used to divide the skin into narrow panels (having small values of b), thereby increasing the buckling stress of the skin.

9.2 Inelastic buckling of plates

For plates having small values of b/t the critical stress may exceed the elastic limit of the material of the plate. In such a situation, Eq. (9.6) is no longer applicable since, as we saw in the case of columns, E becomes dependent on stress as does Poisson's ratio ν. These effects are usually included in a plasticity correction factor η so that Eq. (9.6) becomes

$$\sigma_{CR} = \frac{\eta k\pi^2 E}{12(1-\nu^2)}\left(\frac{t}{b}\right)^2 \tag{9.7}$$

where E and ν are elastic values of Young's modulus and Poisson's ratio. In the linearly elastic region $\eta = 1$, which means that Eq. (9.7) may be applied at all stress levels. The

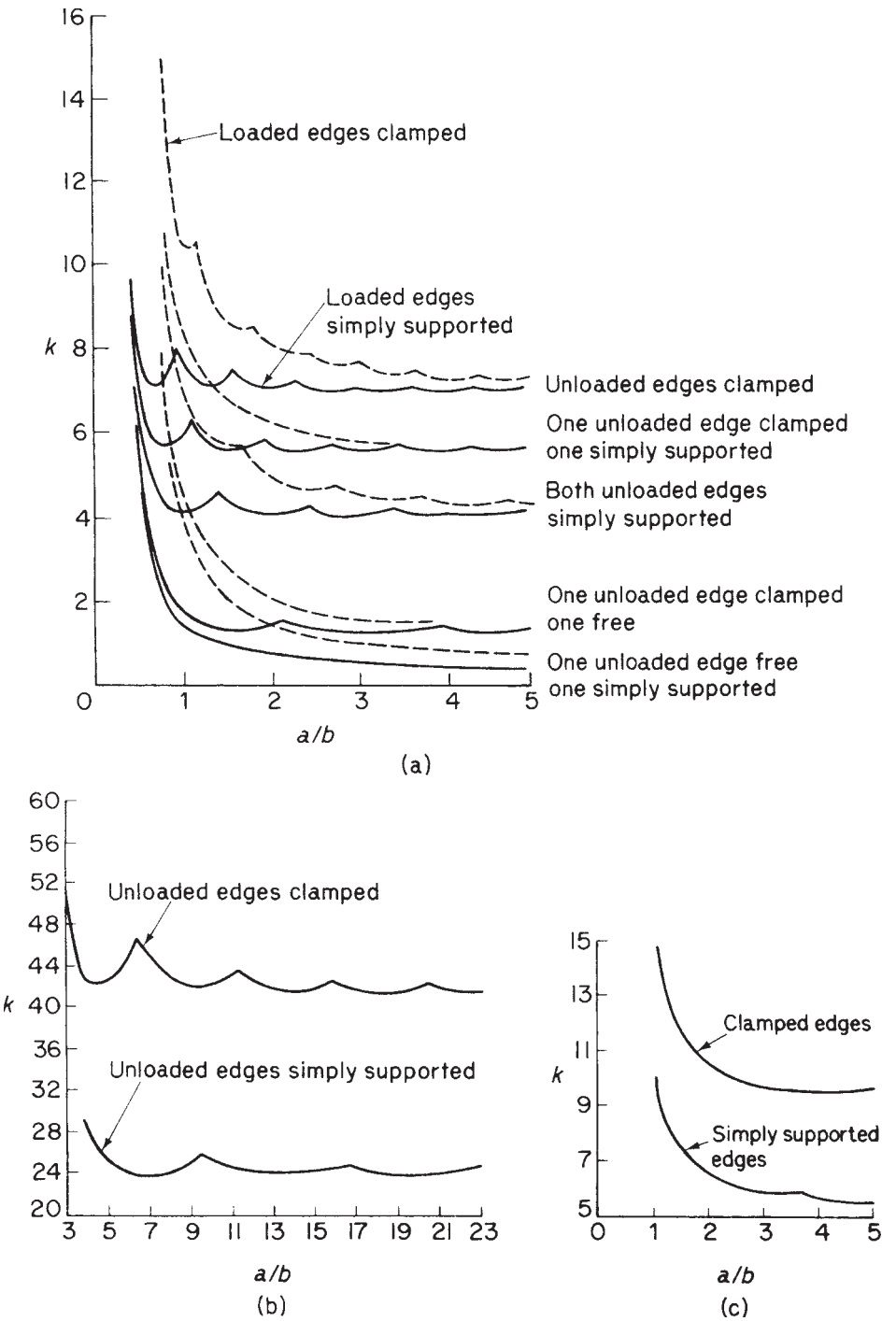

Fig. 9.3 (a) Buckling coefficients for flat plates in compression; (b) buckling coefficients for flat plates in bending; (c) shear buckling coefficients for flat plates.

derivation of a general expression for η is outside the scope of this book but one[1] giving good agreement with experiment is

$$\eta = \frac{1-\nu_e^2}{1-\nu_p^2}\frac{E_s}{E}\left[\frac{1}{2}+\frac{1}{2}\left(\frac{1}{4}+\frac{3}{4}\frac{E_t}{E_s}\right)^{\frac{1}{2}}\right]$$

where E_t and E_s are the tangent modulus and secant modulus (stress/strain) of the plate in the inelastic region and ν_e and ν_p are Poisson's ratio in the elastic and inelastic ranges.

9.3 Experimental determination of critical load for a flat plate

In Section 8.3 we saw that the critical load for a column may be determined experimentally, without actually causing the column to buckle, by means of the Southwell plot. The critical load for an actual, rectangular, thin plate is found in a similar manner.

The displacement of an initially curved plate from the zero load position was found in Section 7.5, to be

$$w_1 = \sum_{m=1}^{\infty}\sum_{n=1}^{\infty} B_{mn}\sin\frac{m\pi x}{a}\sin\frac{n\pi y}{b}$$

where

$$B_{mn} = \frac{A_{mn}N_x}{\frac{\pi^2 D}{a^2}\left(m+\frac{n^2a^2}{mb^2}\right)^2 - N_x}$$

We see that the coefficients B_{mn} increase with an increase of compressive load intensity N_x. It follows that when N_x approaches the critical value, $N_{x,\mathrm{CR}}$, the term in the series corresponding to the buckled shape of the plate becomes the most significant. For a square plate $n=1$ and $m=1$ give a minimum value of critical load so that at the centre of the plate

$$w_1 = \frac{A_{11}N_x}{N_{x,\mathrm{CR}} - N_x}$$

or, rearranging

$$w_1 = N_{x,\mathrm{CR}}\frac{w_1}{N_x} - A_{11}$$

Thus, a graph of w_1 plotted against w_1/N_x will have a slope, in the region of the critical load, equal to $N_{x,\mathrm{CR}}$.

9.4 Local instability

We distinguished in the introductory remarks to Chapter 8 between primary and secondary (or local) instability. The latter form of buckling usually occurs in the flanges

and webs of thin-walled columns having an effective slenderness ratio, $l_e/r < 20$. For $l_e/r > 80$ this type of column is susceptible to primary instability. In the intermediate range of l_e/r between 20 and 80, buckling occurs by a combination of both primary and secondary modes.

Thin-walled columns are encountered in aircraft structures in the shape of longitudinal stiffeners, which are normally fabricated by extrusion processes or by forming from a flat sheet. A variety of cross-sections are employed although each is usually composed of flat plate elements arranged to form angle, channel, Z- or 'top hat' sections, as shown in Fig. 9.4. We see that the plate elements fall into two distinct categories: flanges which have a free unloaded edge and webs which are supported by the adjacent plate elements on both unloaded edges.

In local instability the flanges and webs buckle like plates with a resulting change in the cross-section of the column. The wavelength of the buckle is of the order of the widths of the plate elements and the corresponding critical stress is generally independent of the length of the column when the length is equal to or greater than three times the width of the largest plate element in the column cross-section.

Buckling occurs when the weakest plate element, usually a flange, reaches its critical stress, although in some cases all the elements reach their critical stresses simultaneously. When this occurs the rotational restraint provided by adjacent elements to each other disappears and the elements behave as though they are simply supported along their common edges. These cases are the simplest to analyse and are found where the cross-section of the column is an equal-legged angle, T-, cruciform or a square tube of constant thickness. Values of local critical stress for columns possessing these types of section may be found using Eq. (9.7) and an appropriate value of k. For example, k for a cruciform section column is obtained from Fig. 9.3(a) for a plate which is simply supported on three sides with one edge free and has $a/b > 3$. Hence $k = 0.43$ and if the section buckles elastically then $\eta = 1$ and

$$\sigma_{CR} = 0.388E\left(\frac{t}{b}\right)^2 \quad (\nu = 0.3)$$

It must be appreciated that the calculation of local buckling stresses is generally complicated with no particular method gaining universal acceptance, much of the information available being experimental. A detailed investigation of the topic is therefore beyond the scope of this book. Further information may be obtained from all the references listed at the end of this chapter.

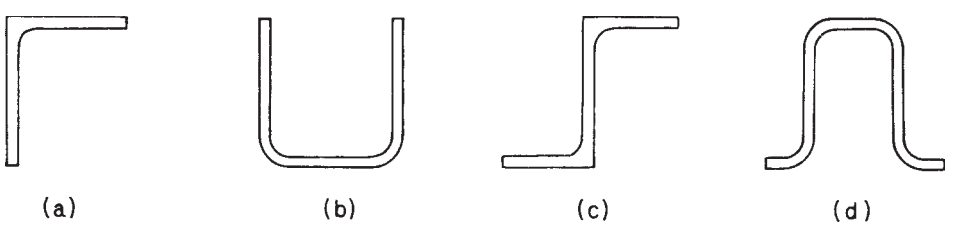

Fig. 9.4 (a) Extruded angle; (b) formed channel; (c) extruded Z; (d) formed 'top hat'.

9.5 Instability of stiffened panels

It is clear from Eq. (9.7) that plates having large values of b/t buckle at low values of critical stress. An effective method of reducing this parameter is to introduce stiffeners along the length of the plate thereby dividing a wide sheet into a number of smaller and more stable plates. Alternatively, the sheet may be divided into a series of wide short columns by stiffeners attached across its width. In the former type of structure the longitudinal stiffeners carry part of the compressive load, while in the latter all the load is supported by the plate. Frequently, both methods of stiffening are combined to form a grid-stiffened structure.

Stiffeners in earlier types of stiffened panel possessed a relatively high degree of strength compared with the thin skin resulting in the skin buckling at a much lower stress level than the stiffeners. Such panels may be analysed by assuming that the stiffeners provide simply supported edge conditions to a series of flat plates.

A more efficient structure is obtained by adjusting the stiffener sections so that buckling occurs in both stiffeners and skin at about the same stress. This is achieved by a construction involving closely spaced stiffeners of comparable thickness to the skin. Since their critical stresses are nearly the same there is an appreciable interaction at buckling between skin and stiffeners so that the complete panel must be considered as a unit. However, caution must be exercised since it is possible for the two simultaneous critical loads to interact and reduce the actual critical load of the structure[2] (see Example 8.4). Various modes of buckling are possible, including primary buckling where the wavelength is of the order of the panel length and local buckling with wavelengths of the order of the width of the plate elements of the skin or stiffeners. A discussion of the various buckling modes of panels having Z-section stiffeners has been given by Argyris and Dunne.[3]

The prediction of critical stresses for panels with a large number of longitudinal stiffeners is difficult and relies heavily on approximate (energy) and semi-empirical methods. Bleich[4] and Timoshenko (see Ref. 1, Chapter 8) give energy solutions for plates with one and two longitudinal stiffeners and also consider plates having a large number of stiffeners. Gerard and Becker[5] have summarized much of the work on stiffened plates and a large amount of theoretical and empirical data is presented by Argyris and Dunne in the *Handbook of Aeronautics*.[3]

For detailed work on stiffened panels, reference should be made to as much as possible of the above work. The literature is, however, extensive so that here we present a relatively simple approach suggested by Gerard[1]. Figure 9.5 represents a panel of width w stiffened by longitudinal members which may be flats (as shown), Z-, I-, channel or

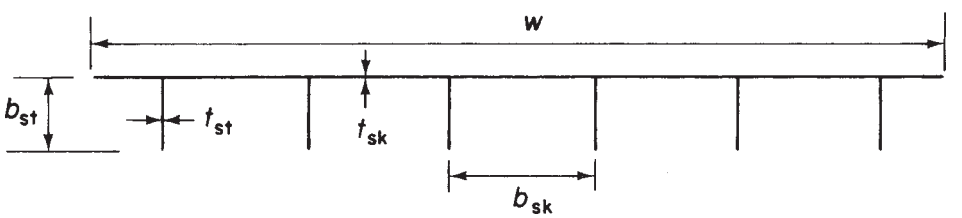

Fig. 9.5 Stiffened panel.

'top hat' sections. It is possible for the panel to behave as an Euler column, its cross-section being that shown in Fig. 9.5. If the equivalent length of the panel acting as a column is l_e then the Euler critical stress is

$$\sigma_{CR,E} = \frac{\pi^2 E}{(l_e/r)^2}$$

as in Eq. (8.8). In addition to the column buckling mode, individual plate elements comprising the panel cross-section may buckle as long plates. The buckling stress is then given by Eq. (9.7), i.e.

$$\sigma_{CR} = \frac{\eta k \pi^2 E}{12(1-\nu^2)} \left(\frac{t}{b}\right)^2$$

where the values of k, t and b depend upon the particular portion of the panel being investigated. For example, the portion of skin between stiffeners may buckle as a plate simply supported on all four sides. Thus, for $a/b > 3$, $k = 4$ from Fig. 9.3(a) and, assuming that buckling takes place in the elastic range

$$\sigma_{CR} = \frac{4\pi^2 E}{12(1-\nu^2)} \left(\frac{t_{sk}}{b_{sk}}\right)^2$$

A further possibility is that the stiffeners may buckle as long plates simply supported on three sides with one edge free. Thus

$$\sigma_{CR} = \frac{0.43\pi^2 E}{12(1-\nu^2)} \left(\frac{t_{st}}{b_{st}}\right)^2$$

Clearly, the minimum value of the above critical stresses is the critical stress for the panel taken as a whole.

The compressive load is applied to the panel over its complete cross-section. To relate this load to an applied compressive stress σ_A acting on each element of the cross-section we divide the load per unit width, say N_x, by an equivalent skin thickness $\bar{t}$, hence

$$\sigma_A = \frac{N_x}{\bar{t}}$$

where

$$\bar{t} = \frac{A_{st}}{b_{sk}} + t_{sk}$$

and A_{st} is the stiffener area.

The above remarks are concerned with the primary instability of stiffened panels. Values of local buckling stress have been determined by Boughan, Baab and Gallaher for idealized web, Z- and T- stiffened panels. The results are reproduced in Rivello[6] together with the assumed geometries.

Further types of instability found in stiffened panels occur where the stiffeners are riveted or spot welded to the skin. Such structures may be susceptible to *interrivet*

buckling in which the skin buckles between rivets with a wavelength equal to the rivet pitch, or *wrinkling* where the stiffener forms an elastic line support for the skin. In the latter mode the wavelength of the buckle is greater than the rivet pitch and separation of skin and stiffener does not occur. Methods of estimating the appropriate critical stresses are given in Rivello[6] and the *Handbook of Aeronautics*.[3]

9.6 Failure stress in plates and stiffened panels

The previous discussion on plates and stiffened panels investigated the prediction of buckling stresses. However, as we have seen, plates retain some of their capacity to carry load even though a portion of the plate has buckled. In fact, the ultimate load is not reached until the stress in the majority of the plate exceeds the elastic limit. The theoretical calculation of the ultimate stress is difficult since non-linearity results from both large deflections and the inelastic stress–strain relationship.

Gerard[1] proposes a semi-empirical solution for flat plates supported on all four edges. After elastic buckling occurs theory and experiment indicate that the average compressive stress, $\bar{\sigma}_a$, in the plate and the unloaded edge stress, σ_e, are related by the following expression

$$\frac{\bar{\sigma}_a}{\sigma_{CR}} = \alpha_1 \left(\frac{\sigma_e}{\sigma_{CR}} \right)^n \tag{9.8}$$

where

$$\sigma_{CR} = \frac{k\pi^2 E}{12(1-\nu^2)} \left(\frac{t}{b} \right)^2$$

and α_1 is some unknown constant. Theoretical work by Stowell[7] and Mayers and Budiansky[8] shows that failure occurs when the stress along the unloaded edge is approximately equal to the compressive yield strength, σ_{cy}, of the material. Hence substituting σ_{cy} for σ_e in Eq. (9.8) and rearranging gives

$$\frac{\bar{\sigma}_f}{\sigma_{cy}} = \alpha_1 \left(\frac{\sigma_{CR}}{\sigma_{cy}} \right)^{1-n} \tag{9.9}$$

where the average compressive stress in the plate has become the average stress at failure $\bar{\sigma}_f$. Substituting for σ_{CR} in Eq. (9.9) and putting

$$\frac{\alpha_1 \pi^{2(1-n)}}{[12(1-\nu^2)]^{1-n}} = \alpha$$

yields

$$\frac{\bar{\sigma}_f}{\sigma_{cy}} = \alpha k^{1-n} \left[\frac{t}{b} \left(\frac{E}{\sigma_{cy}} \right)^{\frac{1}{2}} \right]^{2(1-n)} \tag{9.10}$$

or, in a simplified form

$$\frac{\bar{\sigma}_f}{\sigma_{cy}} = \beta \left[\frac{t}{b} \left(\frac{E}{\sigma_{cy}} \right)^{\frac{1}{2}} \right]^m \tag{9.11}$$

where $\beta = \alpha k^{m/2}$. The constants β and m are determined by the best fit of Eq. (9.11) to test data.

Experiments on simply supported flat plates and square tubes of various aluminium and magnesium alloys and steel show that $\beta = 1.42$ and $m = 0.85$ fit the results within ± 10 per cent up to the yield strength. Corresponding values for long clamped flat plates are $\beta = 1.80$, $m = 0.85$.

Gerard[9–12] extended the above method to the prediction of local failure stresses for the plate elements of thin-walled columns. Equation (9.11) becomes

$$\frac{\bar{\sigma}_f}{\sigma_{cy}} = \beta_g \left[\left(\frac{gt^2}{A} \right) \left(\frac{E}{\sigma_{cy}} \right)^{\frac{1}{2}} \right]^m \tag{9.12}$$

where A is the cross-sectional area of the column, β_g and m are empirical constants and g is the number of cuts required to reduce the cross-section to a series of flanged sections plus the number of flanges that would exist after the cuts are made. Examples of the determination of g are shown in Fig. 9.6.

The local failure stress in longitudinally stiffened panels was determined by Gerard[10,12] using a slightly modified form of Eqs (9.11) and (9.12). Thus, for a section of the panel consisting of a stiffener and a width of skin equal to the stiffener spacing

$$\frac{\bar{\sigma}_f}{\sigma_{cy}} = \beta_g \left[\frac{g t_{sk} t_{st}}{A} \left(\frac{E}{\bar{\sigma}_{cy}} \right)^{\frac{1}{2}} \right]^m \tag{9.13}$$

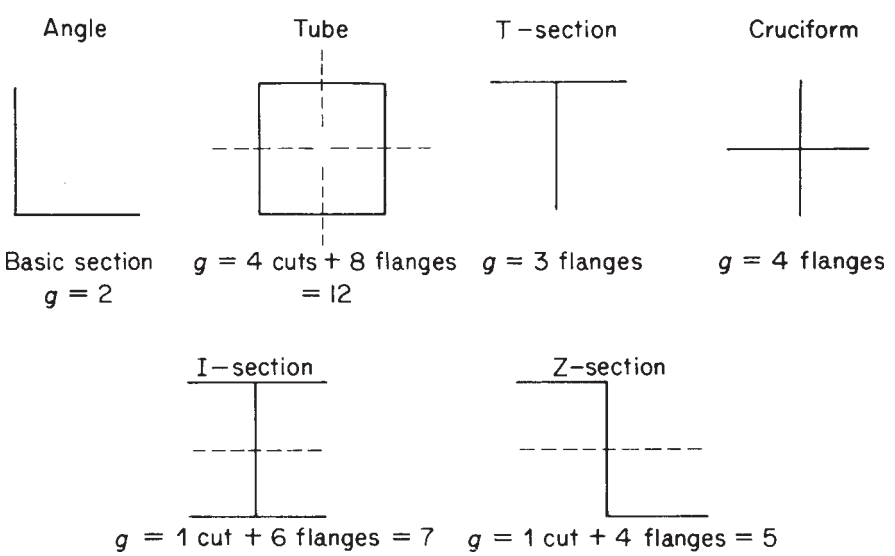

Fig. 9.6 Determination of empirical constant g.

where t_{sk} and t_{st} are the skin and stiffener thicknesses, respectively. A weighted yield stress $\bar{\sigma}_{cy}$ is used for a panel in which the material of the skin and stiffener have different yield stresses, thus

$$\bar{\sigma}_{cy} = \frac{\sigma_{cy} + \sigma_{cy,sk}[(\bar{t}/t_{st}) - 1]}{\bar{t}/t_{st}}$$

where $\bar{t}$ is the average or equivalent skin thickness previously defined. The parameter g is obtained in a similar manner to that for a thin-walled column, except that the number of cuts in the skin and the number of equivalent flanges of the skin are included. A cut to the left of a stiffener is not counted since it is regarded as belonging to the stiffener to the left of that cut. The calculation of g for two types of skin/stiffener combination is illustrated in Fig. 9.7. Equation (9.13) is applicable to either monolithic or built up panels when, in the latter case, interrivet buckling and wrinkling stresses are greater than the local failure stress.

The values of failure stress given by Eqs (9.11), (9.12) and (9.13) are associated with local or secondary instability modes. Consequently, they apply when $l_e/r \leq 20$. In the intermediate range between the local and primary modes, failure occurs through a combination of both. At the moment there is no theory that predicts satisfactorily failure in this range and we rely on test data and empirical methods. The NACA (now NASA) have produced direct reading charts for the failure of 'top hat', Z- and Y-section stiffened panels; a bibliography of the results is given by Gerard.[10]

It must be remembered that research into methods of predicting the instability and post-buckling strength of the thin-walled types of structure associated with aircraft construction is a continuous process. Modern developments include the use of the computer-based finite element technique (see Chapter 6) and the study of the sensitivity of thin-walled structures to imperfections produced during fabrication; much useful information and an extensive bibliography is contained in Murray.[2]

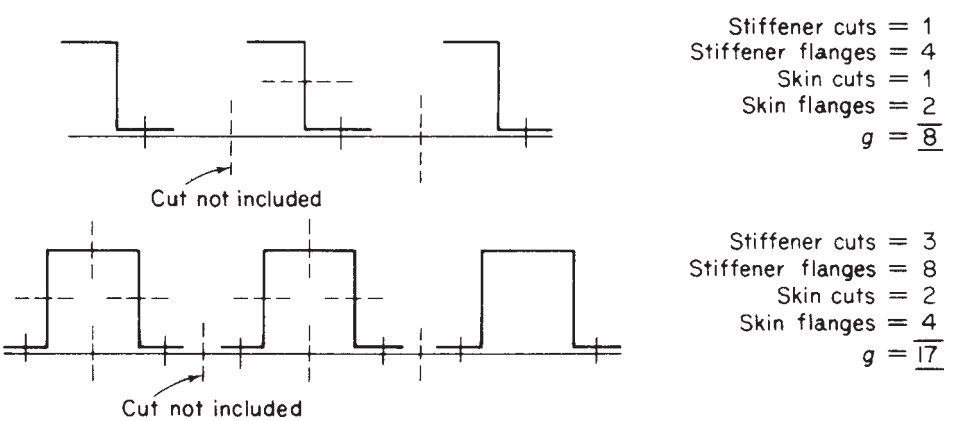

Fig. 9.7 Determination of g for two types of stiffener/skin combination.

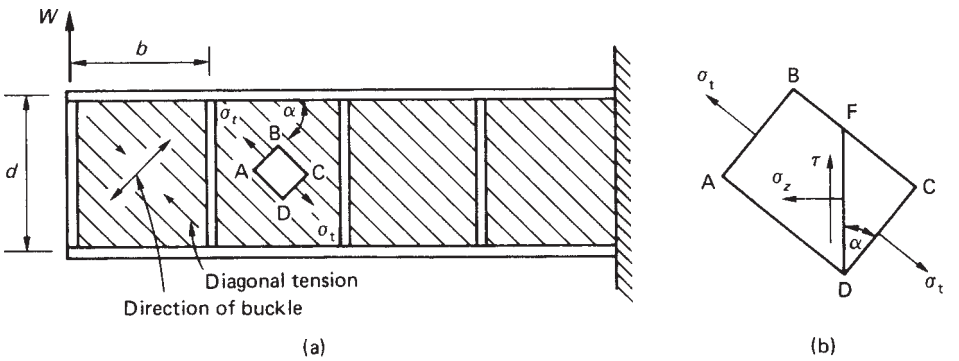

Fig. 9.8 Diagonal tension field beam.

9.7 Tension field beams

The spars of aircraft wings usually comprise an upper and a lower flange connected by thin stiffened webs. These webs are often of such a thickness that they buckle under shear stresses at a fraction of their ultimate load. The form of the buckle is shown in Fig. 9.8(a), where the web of the beam buckles under the action of internal diagonal compressive stresses produced by shear, leaving a wrinkled web capable of supporting diagonal tension only in a direction perpendicular to that of the buckle; the beam is then said to be a *complete tension field beam*.

9.7.1 Complete diagonal tension

The theory presented here is due to H. Wagner.[13]

The beam shown in Fig. 9.8(a) has concentrated flange areas having a depth d between their centroids and vertical stiffeners which are spaced uniformly along the length of the beam. It is assumed that the flanges resist the internal bending moment at any section of the beam while the web, of thickness t, resists the vertical shear force. The effect of this assumption is to produce a uniform shear stress distribution through the depth of the web (see Section 20.3) at any section. Therefore, at a section of the beam where the shear force is S, the shear stress τ is given by

$$\tau = \frac{S}{td} \tag{9.14}$$

Consider now an element ABCD of the web in a panel of the beam, as shown in Fig. 9.8(a). The element is subjected to tensile stresses, σ_t, produced by the diagonal tension on the planes AB and CD; the angle of the diagonal tension is α. On a vertical plane FD in the element the shear stress is τ and the direct stress σ_z. Now considering the equilibrium of the element FCD (Fig. 9.8(b)) and resolving forces vertically, we have (see Section 1.6)

$$\sigma_t \mathrm{CD}t \sin\alpha = \tau \mathrm{FD}t$$

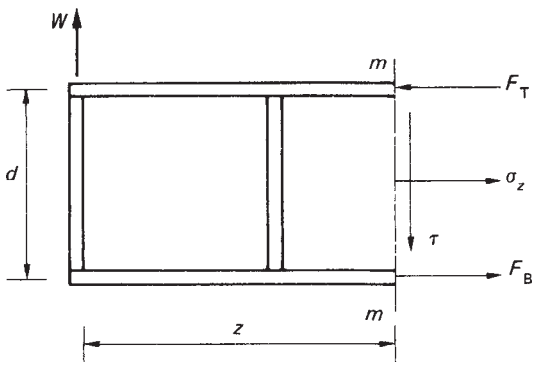

Fig. 9.9 Determination of flange forces.

which gives

$$\sigma_t = \frac{\tau}{\sin\alpha\cos\alpha} = \frac{2\tau}{\sin 2\alpha} \tag{9.15}$$

or, substituting for τ from Eq. (9.14) and noting that in this case $S = W$ at all sections of the beam

$$\sigma_t = \frac{2W}{td\sin 2\alpha} \tag{9.16}$$

Further, resolving forces horizontally for the element FCD

$$\sigma_z \mathrm{FD}t = \sigma_t \mathrm{CD}t\cos\alpha$$

which gives

$$\sigma_z = \sigma_t \cos^2\alpha$$

or, substituting for σ_t from Eq. (9.15)

$$\sigma_z = \frac{\tau}{\tan\alpha} \tag{9.17}$$

or, for this particular beam, from Eq. (9.14)

$$\sigma_z = \frac{W}{td\tan\alpha} \tag{9.18}$$

Since τ and σ_t are constant through the depth of the beam it follows that σ_z is constant through the depth of the beam.

The direct loads in the flanges are found by considering a length z of the beam as shown in Fig. 9.9. On the plane *mm* there are direct and shear stresses σ_z and τ acting in the web, together with direct loads F_T and F_B in the top and bottom flanges respectively. F_T and F_B are produced by a combination of the bending moment Wz at the section plus the compressive action (σ_z) of the diagonal tension. Taking moments about the bottom flange

$$Wz = F_T d - \frac{\sigma_z t d^2}{2}$$

Hence, substituting for σ_z from Eq. (9.18) and rearranging

$$F_{\mathrm{T}} = \frac{Wz}{d} + \frac{W}{2\tan\alpha} \tag{9.19}$$

Now resolving forces horizontally

$$F_{\mathrm{B}} - F_{\mathrm{T}} + \sigma_z td = 0$$

which gives, on substituting for σ_z and F_{T} from Eqs (9.18) and (9.19)

$$F_{\mathrm{B}} = \frac{Wz}{d} - \frac{W}{2\tan\alpha} \tag{9.20}$$

The diagonal tension stress σ_{t} induces a direct stress σ_y on horizontal planes at any point in the web. Then, on a horizontal plane HC in the element ABCD of Fig. 9.8 there is a direct stress σ_y and a complementary shear stress τ, as shown in Fig. 9.10.

From a consideration of the vertical equilibrium of the element HDC we have

$$\sigma_y \mathrm{HC}t = \sigma_{\mathrm{t}} \mathrm{CD}t \sin\alpha$$

which gives

$$\sigma_y = \sigma_{\mathrm{t}} \sin^2\alpha$$

Substituting for σ_{t} from Eq. (9.15)

$$\sigma_y = \tau \tan\alpha \tag{9.21}$$

or, from Eq. (9.14) in which $S = W$

$$\sigma_y = \frac{W}{td}\tan\alpha \tag{9.22}$$

The tensile stresses σ_y on horizontal planes in the web of the beam cause compression in the vertical stiffeners. Each stiffener may be assumed to support half of each adjacent panel in the beam so that the compressive load P in a stiffener is given by

$$P = \sigma_y tb$$

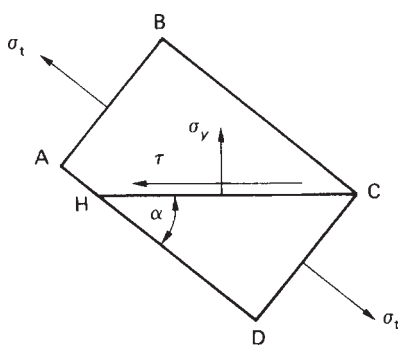

Fig. 9.10 Stress system on a horizontal plane in the beam web.

which becomes, from Eq. (9.22)

$$P = \frac{Wb}{d} \tan \alpha \tag{9.23}$$

If the load P is sufficiently high the stiffeners will buckle. Tests indicate that they buckle as columns of equivalent length

$$\text{or} \qquad \left.\begin{array}{ll} l_e = d/\sqrt{4 - 2b/d} & \text{for } b < 1.5d \\ l_e = d & \text{for } b > 1.5d \end{array}\right\} \tag{9.24}$$

In addition to causing compression in the stiffeners the direct stress σ_y produces bending of the beam flanges between the stiffeners as shown in Fig. 9.11. Each flange acts as a continuous beam carrying a uniformly distributed load of intensity $\sigma_y t$. The maximum bending moment in a continuous beam with ends fixed against rotation occurs at a support and is $wL^2/12$ in which w is the load intensity and L the beam span. In this case, therefore, the maximum bending moment M_{max} occurs at a stiffener and is given by

$$M_{max} = \frac{\sigma_y t b^2}{12}$$

or, substituting for σ_y from Eq. (9.22)

$$M_{max} = \frac{Wb^2 \tan \alpha}{12d} \tag{9.25}$$

Midway between the stiffeners this bending moment reduces to $Wb^2 \tan \alpha/24d$.

The angle α adjusts itself such that the total strain energy of the beam is a minimum. If it is assumed that the flanges and stiffeners are rigid then the strain energy comprises the shear strain energy of the web only and $\alpha = 45°$. In practice, both flanges and stiffeners deform so that α is somewhat less than 45°, usually of the order of 40° and, in the type of beam common to aircraft structures, rarely below 38°. For beams having all components made of the same material the condition of minimum strain energy leads to various equivalent expressions for α, one of which is

$$\tan^2 \alpha = \frac{\sigma_t + \sigma_F}{\sigma_t + \sigma_S} \tag{9.26}$$

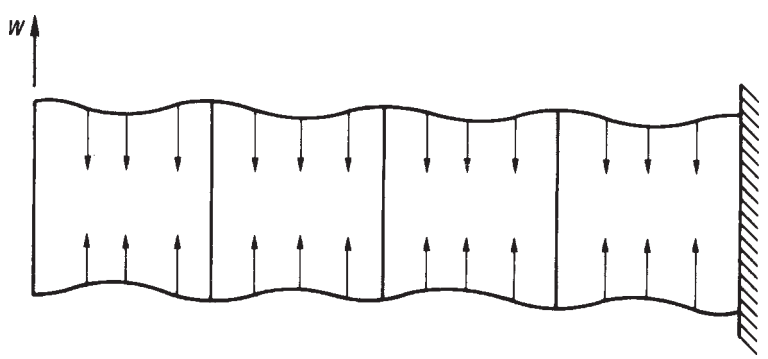

Fig. 9.11 Bending of flanges due to web stress.

in which σ_F and σ_S are the uniform direct *compressive* stresses induced by the diagonal tension in the flanges and stiffeners, respectively. Thus, from the second term on the right-hand side of either of Eqs (9.19) or (9.20)

$$\sigma_F = \frac{W}{2A_F \tan\alpha} \tag{9.27}$$

in which A_F is the cross-sectional area of each flange. Also, from Eq. (9.23)

$$\sigma_S = \frac{Wb}{A_S d} \tan\alpha \tag{9.28}$$

where A_S is the cross-sectional area of a stiffener. Substitution of σ_t from Eq. (9.16) and σ_F and σ_S from Eqs (9.27) and (9.28) into Eq. (9.26), produces an equation which may be solved for α. An alternative expression for α, again derived from a consideration of the total strain energy of the beam, is

$$\tan^4\alpha = \frac{1 + td/2A_F}{1 + tb/A_S} \tag{9.29}$$

Example 9.1

The beam shown in Fig. 9.12 is assumed to have a complete tension field web. If the cross-sectional areas of the flanges and stiffeners are, respectively, 350 mm^2 and 300 mm^2 and the elastic section modulus of each flange is 750 mm^3, determine the maximum stress in a flange and also whether or not the stiffeners will buckle. The thickness of the web is 2 mm and the second moment of area of a stiffener about an axis in the plane of the web is 2000 mm^4; $E = 70\,000$ N/mm^2.

From Eq. (9.29)

$$\tan^4\alpha = \frac{1 + 2 \times 400/(2 \times 350)}{1 + 2 \times 300/300} = 0.7143$$

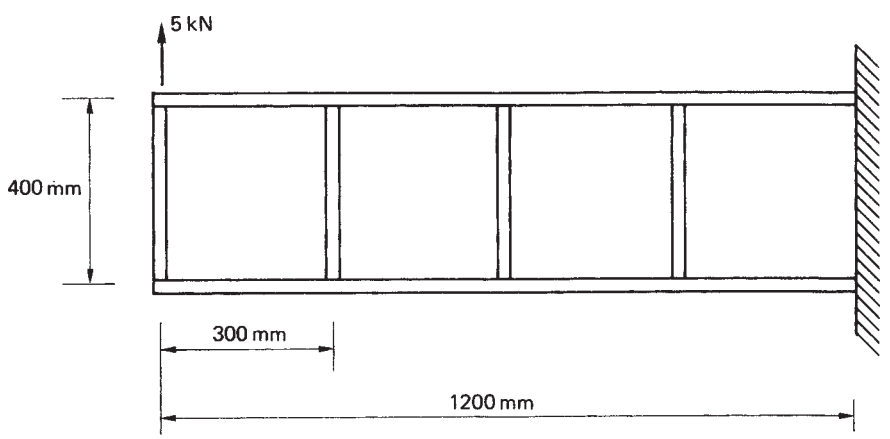

Fig. 9.12 Beam of Example 9.1.

so that

$$\alpha = 42.6^\circ$$

The maximum flange stress will occur in the top flange at the built-in end where the bending moment on the beam is greatest and the stresses due to bending and diagonal tension are additive. Therefore, from Eq. (9.19)

$$F_T = \frac{5 \times 1200}{400} + \frac{5}{2 \tan 42.6^\circ}$$

i.e.

$$F_T = 17.7\,\text{kN}$$

Hence the direct stress in the top flange produced by the externally applied bending moment and the diagonal tension is $17.7 \times 10^3/350 = 50.7\,\text{N/mm}^2$. In addition to this uniform compressive stress, local bending of the type shown in Fig. 9.11 occurs. The local bending moment in the top flange at the built-in end is found using Eq. (9.25), i.e.

$$M_{\max} = \frac{5 \times 10^3 \times 300^2 \tan 42.6^\circ}{12 \times 400} = 8.6 \times 10^4\,\text{N mm}$$

The maximum compressive stress corresponding to this bending moment occurs at the lower extremity of the flange and is $8.6 \times 10^4/750 = 114.9\,\text{N/mm}^2$. Thus the maximum stress in a flange occurs on the inside of the top flange at the built-in end of the beam, is compressive and equal to $114.9 + 50.7 = 165.6\,\text{N/mm}^2$.

The compressive load in a stiffener is obtained using Eq. (9.23), i.e.

$$P = \frac{5 \times 300 \tan 42.6^\circ}{400} = 3.4\,\text{kN}$$

Since, in this case, $b < 1.5d$, the equivalent length of a stiffener as a column is given by the first of Eqs (9.24), i.e.

$$l_e = 400/\sqrt{4 - 2 \times 300/400} = 253\,\text{mm}$$

From Eq. (8.7) the buckling load of a stiffener is then

$$P_{CR} = \frac{\pi^2 \times 70\,000 \times 2000}{253^2} = 22.0\,\text{kN}$$

Clearly the stiffener will not buckle.

In Eqs (9.28) and (9.29) it is implicitly assumed that a stiffener is fully effective in resisting axial load. This will be the case if the centroid of area of the stiffener lies in the plane of the beam web. Such a situation arises when the stiffener consists of two members symmetrically arranged on opposite sides of the web. In the case where the web is stiffened by a single member attached to one side, the compressive load P is offset from the stiffener axis thereby producing bending in addition to axial load. For

a stiffener having its centroid a distance e from the centre of the web the combined bending and axial compressive stress, σ_c, at a distance e from the stiffener centroid is

$$\sigma_c = \frac{P}{A_S} + \frac{Pe^2}{A_S r^2}$$

in which r is the radius of gyration of the stiffener cross-section about its neutral axis (note: second moment of area $I = Ar^2$). Then

$$\sigma_c = \frac{P}{A_S}\left[1 + \left(\frac{e}{r}\right)^2\right]$$

or

$$\sigma_c = \frac{P}{A_{S_e}}$$

where

$$A_{S_e} = \frac{A_S}{1 + (e/r)^2} \tag{9.30}$$

and is termed the effective stiffener area.

9.7.2 Incomplete diagonal tension

In modern aircraft structures, beams having extremely thin webs are rare. They retain, after buckling, some of their ability to support loads so that even near failure they are in a state of stress somewhere between that of pure diagonal tension and the pre-buckling stress. Such a beam is described as an *incomplete diagonal tension field beam* and may be analysed by semi-empirical theory as follows.

It is assumed that the nominal web shear τ (=S/td) may be divided into a 'true shear' component τ_S and a diagonal tension component τ_{DT} by writing

$$\tau_{DT} = k\tau, \quad \tau_S = (1 - k)\tau \tag{9.31}$$

where k, the *diagonal tension factor*, is a measure of the degree to which the diagonal tension is developed. A completely unbuckled web has $k = 0$ whereas $k = 1$ for a web in complete diagonal tension. The value of k corresponding to a web having a critical shear stress τ_{CR} is given by the empirical expression

$$k = \tanh\left(0.5 \log \frac{\tau}{\tau_{CR}}\right) \tag{9.32}$$

The ratio τ/τ_{CR} is known as the *loading ratio* or *buckling stress ratio*. The buckling stress τ_{CR} may be calculated from the formula

$$\tau_{CR,elastic} = k_{ss} E \left(\frac{t}{b}\right)^2 \left[R_d + \frac{1}{2}(R_b - R_d)\left(\frac{b}{d}\right)^3\right] \tag{9.33}$$

where k_{ss} is the coefficient for a plate with simply supported edges and R_d and R_b are empirical restraint coefficients for the vertical and horizontal edges of the web panel respectively. Graphs giving k_{ss}, R_d and R_b are reproduced in Kuhn.[13]

The stress equations (9.27) and (9.28) are modified in the light of these assumptions and may be rewritten in terms of the applied shear stress τ as

$$\sigma_F = \frac{k\tau \cot \alpha}{(2A_F/td) + 0.5(1-k)} \tag{9.34}$$

$$\sigma_S = \frac{k\tau \tan \alpha}{(A_S/tb) + 0.5(1-k)} \tag{9.35}$$

Further, the web stress σ_t given by Eq. (9.15) becomes two direct stresses: σ_1 along the direction of α given by

$$\sigma_1 = \frac{2k\tau}{\sin 2\alpha} + \tau(1-k)\sin 2\alpha \tag{9.36}$$

and σ_2 perpendicular to this direction given by

$$\sigma_2 = -\tau(1-k)\sin 2\alpha \tag{9.37}$$

The secondary bending moment of Eq. (9.25) is multiplied by the factor k, while the effective lengths for the calculation of stiffener buckling loads become (see Eqs (9.24))

or

$$\begin{aligned} l_e &= d_s/\sqrt{1 + k^2(3 - 2b/d_s)} && \text{for } b < 1.5d \\ l_e &= d_s && \text{for } b > 1.5d \end{aligned}$$

where d_s is the actual stiffener depth, as opposed to the effective depth d of the web, taken between the web/flange connections as shown in Fig. 9.13. We observe that Eqs (9.34)–(9.37) are applicable to either incomplete or complete diagonal tension field beams since, for the latter case, $k = 1$ giving the results of Eqs (9.27), (9.28) and (9.15).

In some cases beams taper along their lengths, in which case the flange loads are no longer horizontal but have vertical components which reduce the shear load carried by the web. Thus, in Fig. 9.14 where d is the depth of the beam at the section considered, we have, resolving forces vertically

$$W - (F_T + F_B)\sin\beta - \sigma_t(d\cos\alpha)\sin\alpha = 0 \tag{9.38}$$

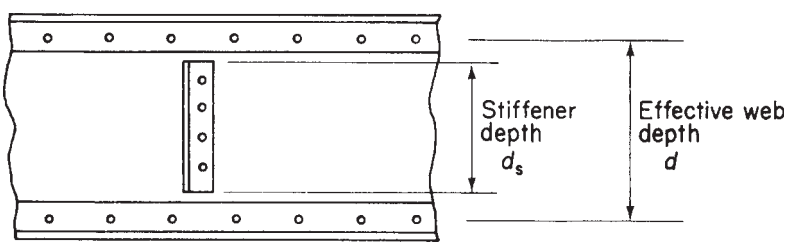

Fig. 9.13 Calculation of stiffener buckling load.

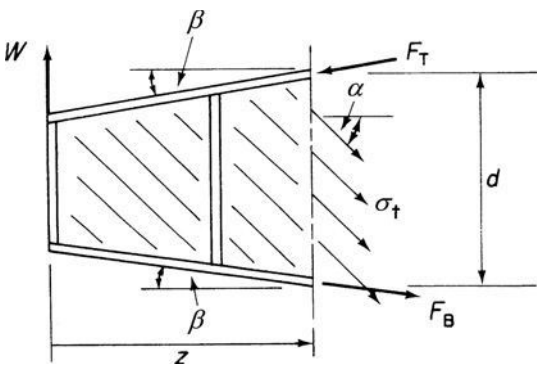

Fig. 9.14 Effect of taper on diagonal tension field beam calculations.

For horizontal equilibrium

$$(F_{\mathrm{T}} - F_{\mathrm{B}})\cos\beta - \sigma_{\mathrm{t}} t d \cos^2\alpha = 0 \tag{9.39}$$

Taking moments about B

$$Wz - F_{\mathrm{T}} d\cos\beta + \tfrac{1}{2}\sigma_{\mathrm{t}} t d^2 \cos^2\alpha = 0 \tag{9.40}$$

Solving Eqs (9.38), (9.39) and (9.40) for σ_{t}, F_{T} and F_{B}

$$\sigma_{\mathrm{t}} = \frac{2W}{td\sin 2\alpha}\left(1 - \frac{2z}{d}\tan\beta\right) \tag{9.41}$$

$$F_{\mathrm{T}} = \frac{W}{d\cos\beta}\left[z + \frac{d\cot\alpha}{2}\left(1 - \frac{2z}{d}\tan\beta\right)\right] \tag{9.42}$$

$$F_{\mathrm{B}} = \frac{W}{d\cos\beta}\left[z - \frac{d\cot\alpha}{2}\left(1 - \frac{2z}{d}\tan\beta\right)\right] \tag{9.43}$$

Equation (9.23) becomes

$$P = \frac{Wb}{d}\tan\alpha\left(1 - \frac{2z}{d}\tan\beta\right) \tag{9.44}$$

Also the shear force S at any section of the beam is, from Fig. 9.14

$$S = W - (F_{\mathrm{T}} + F_{\mathrm{B}})\sin\beta$$

or, substituting for F_{T} and F_{B} from Eqs (9.42) and (9.43)

$$S = W\left(1 - \frac{2z}{d}\tan\beta\right) \tag{9.45}$$

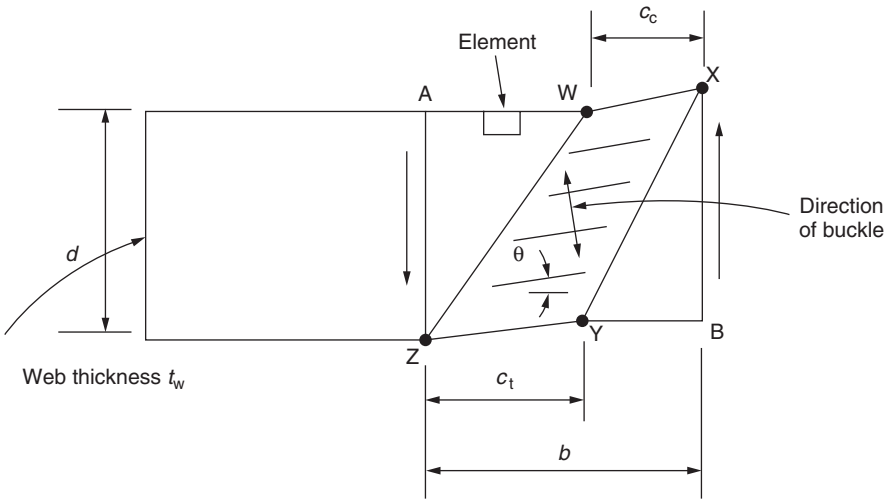

Fig. 9.15 Collapse mechanism of a panel of a tension field beam.

9.7.3 Post buckling behaviour

Sections 9.7.1 and 9.7.2 are concerned with beams in which the thin webs buckle to form tension fields; the beam flanges are then regarded as being subjected to bending action as in Fig. 9.11. It is possible, if the beam flanges are relatively light, for failure due to yielding to occur in the beam flanges after the web has buckled so that plastic hinges form and a failure mechanism of the type shown in Fig. 9.15 exists. This post buckling behaviour was investigated by Evans, Porter and Rockey[15] who developed a design method for beams subjected to bending and shear. It is their method of analysis which is presented here.

Suppose that the panel AXBZ in Fig. 9.15 has collapsed due to a shear load S and a bending moment M; plastic hinges have formed at W, X, Y and Z. In the initial stages of loading the web remains perfectly flat until it reaches its critical stresses i.e., τ_{cr} in shear and σ_{crb} in bending. The values of these stresses may be found approximately from

$$\left(\frac{\sigma_{mb}}{\sigma_{crb}}\right)^2 + \left(\frac{\tau_m}{\tau_{cr}}\right)^2 = 1 \tag{9.46}$$

where σ_{crb} is the critical value of bending stress with $S = 0, M \neq 0$ and τ_{cr} is the critical value of shear stress when $S \neq 0$ and $M = 0$. Once the critical stress is reached the web starts to buckle and cannot carry any increase in compressive stress so that, as we have seen in Section 9.7.1, any additional load is carried by tension field action. It is assumed that the shear and bending stresses remain at their critical values τ_m and σ_{mb} and that there are *additional* stresses σ_t which are inclined at an angle θ to the horizontal and which carry any increases in the applied load. At collapse, i.e. at ultimate load conditions, the additional stress σ_t reaches its maximum value $\sigma_{t(max)}$ and the panel is in the collapsed state shown in Fig. 9.15.

Consider now the small rectangular element on the edge AW of the panel before collapse. The stresses acting on the element are shown in Fig. 9.16(a). The stresses on planes parallel to and perpendicular to the direction of the buckle may be found by considering the equilibrium of triangular elements within this rectangular element. Initially we shall consider the triangular element CDE which is subjected to the stress system shown in Fig. 9.16(b) and is in equilibrium under the action of the forces corresponding to these stresses. Note that the edge CE of the element is parallel to the direction of the buckle in the web.

For equilibrium of the element in a direction perpendicular to CE (see Section 1.6)

$$\sigma_\xi \mathrm{CE} + \sigma_{\mathrm{mb}} \mathrm{ED} \cos\theta - \tau_{\mathrm{m}} \mathrm{ED} \sin\theta - \tau_{\mathrm{m}} \mathrm{DC} \cos\theta = 0$$

Dividing through by CE and rearranging we have

$$\sigma_\xi = -\sigma_{\mathrm{mb}} \cos^2\theta + \tau_{\mathrm{m}} \sin 2\theta \tag{9.47}$$

Similarly, by considering the equilibrium of the element in the direction EC we have

$$\tau_{\eta\xi} = -\frac{\sigma_{\mathrm{mb}}}{2} \sin 2\theta - \tau_{\mathrm{m}} \cos 2\theta \tag{9.48}$$

Further the direct stress σ_η on the plane FD (Fig. 9.16(c)) which is perpendicular to the plane of the buckle is found from the equilibrium of the element FED. Then,

$$\sigma_\eta \mathrm{FD} + \sigma_{\mathrm{mb}} \mathrm{ED} \sin\theta + \tau_{\mathrm{m}} \mathrm{EF} \sin\theta + \tau_{\mathrm{m}} \mathrm{DE} \cos\theta = 0$$

Dividing through by FD and rearranging gives

$$\sigma_\eta = -\sigma_{\mathrm{mb}} \sin^2\theta - \tau_{\mathrm{m}} \sin 2\theta \tag{9.49}$$

Note that the shear stress on this plane forms a complementary shear stress system with $\tau_{\eta\xi}$.

The failure condition is reached by adding $\sigma_{\mathrm{t(max)}}$ to σ_ξ and using the von Mises theory of elastic failure (see Ref. [14]) i.e.

$$\sigma_{\mathrm{y}}^2 = \sigma_1^2 + \sigma_2^2 - \sigma_1\sigma_2 + 3\tau^2 \tag{9.50}$$

where σ_{y} is the yield stress of the material, σ_1 and σ_2 are the direct stresses acting on two mutually perpendicular planes and τ is the shear stress acting on the same two planes. Hence, when the yield stress in the web is σ_{yw} failure occurs when

$$\sigma_{\mathrm{yw}}^2 = (\sigma_\xi + \sigma_{\mathrm{t(max)}})^2 + \sigma_\eta^2 - \sigma_\eta(\sigma_\xi + \sigma_{\mathrm{t(max)}}) + 3\tau_{\eta\xi}^2 \tag{9.51}$$

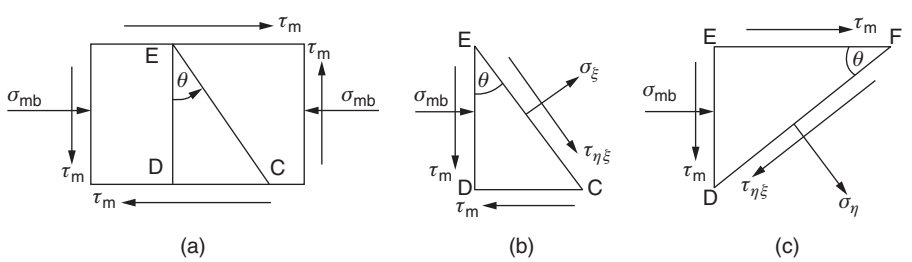

Fig. 9.16 Determination of stresses on planes parallel and perpendicular to the plane of the buckle.

Eqs (9.47), (9.48), (9.49) and (9.51) may be solved for $\sigma_{t(max)}$ which is then given by

$$\sigma_{t(max)} = -\frac{1}{2}A + \frac{1}{2}[A^2 - 4(\sigma_{mb}^2 + 3\tau_m^2 - \sigma_{yw}^2)]^{\frac{1}{2}} \tag{9.52}$$

where

$$A = 3\tau_m \sin 2\theta + \sigma_{mb} \sin^2 \theta - 2\sigma_{mb} \cos^2 \theta \tag{9.53}$$

These equations have been derived for a point on the edge of the panel but are applicable to any point within its boundary. Therefore the resultant force F_w corresponding to the tension field in the web may be calculated and its line of action determined.

If the average stresses in the compression and tension flanges are σ_{cf} and σ_{tf} and the yield stress of the flanges is σ_{yf} the reduced plastic moments in the flanges are (see Ref. [14])

$$M'_{pc} = M_{pc}\left[1 - \left(\frac{\sigma_{cf}}{\sigma_{yf}}\right)^2\right] \qquad \text{(compression flange)} \tag{9.54}$$

$$M'_{pt} = M_{pt}\left[1 - \left(\frac{\sigma_{tf}}{\sigma_{yf}}\right)\right] \qquad \text{(tension flange)} \tag{9.55}$$

The position of each plastic hinge may be found by considering the equilibrium of a length of flange and employing the principle of virtual work. In Fig. 9.17 the length WX of the upper flange of the beam is given a virtual displacement ϕ. The work done by the shear force at X is equal to the energy absorbed by the plastic hinges at X and W and the work done *against* the tension field stress $\sigma_{t(max)}$. Suppose the average value of the tension field stress is σ_{tc}, i.e. the stress at the midpoint of WX.

Then

$$S_x c_c \phi = 2M'_{pc}\phi + \sigma_{tc}\, t_w \sin^2 \theta \frac{c_c^2}{2}\phi$$

The minimum value of S_x is obtained by differentiating with respect to c_c, i.e.

$$\frac{dS_x}{dc_c} = -2\frac{M'_{pc}}{c_c^2} + \sigma_{tc}\, t_w \frac{\sin^2 \theta}{2} = 0$$

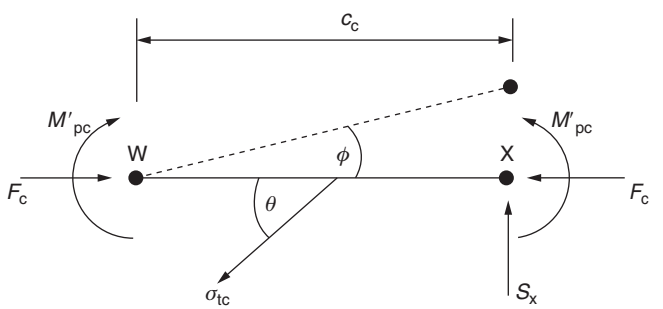

Fig. 9.17 Determination of plastic hinge position.

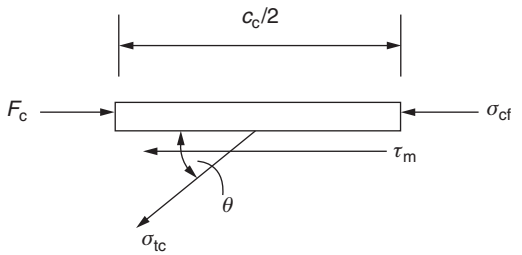

Fig. 9.18 Determination of flange stress.

which gives

$$c_c^2 = \frac{4M'_{pc}}{\sigma_{tc}\, t_w \sin^2\theta} \tag{9.56}$$

Similarly in the tension flange

$$c_t^2 = \frac{4M'_{pt}}{\sigma_{tt}\, t_w \sin^2\theta} \tag{9.57}$$

Clearly for the plastic hinges to occur within a flange both c_c and c_t must be less than b. Therefore from Eq. (9.56)

$$M'_{pc} < \frac{t_w b^2 \sin^2\theta}{4}\sigma_{tc} \tag{9.58}$$

where σ_{tc} is found from Eqs (9.52) and (9.53) at the midpoint of WX.

The average axial stress in the compression flange between W and X is obtained by considering the equilibrium of half of the length of WX (Fig. 9.18).

Then

$$F_c = \sigma_{cf}A_{cf} + \sigma_{tc}t_w\frac{c_c}{2}\sin\theta\cos\theta + \tau_m t_w\frac{c_c}{2}$$

from which

$$\sigma_{cf} = \frac{F_c - \frac{1}{2}(\sigma_{tc}\sin\theta\cos\theta + \tau_m)t_w c_c}{A_{cf}} \tag{9.59}$$

where F_c is the force in the compression flange at W and A_{cf} is the cross-sectional area of the compression flange.

Similarly for the tension flange

$$\sigma_{tf} = \frac{F_t + \frac{1}{2}(\sigma_{tt}\sin\theta\cos\theta + \tau_m)t_w c_t}{A_{tf}} \tag{9.60}$$

The forces F_c and F_t are found by considering the equilibrium of the beam to the right of WY (Fig. 9.19). Then, resolving vertically and noting that $S_{cr} = \tau_m t_w d$

$$S_{ult} = F_w\sin\theta + \tau_m t_w d + \sum W_n \tag{9.61}$$

Resolving horizontally and noting that $H_{cr} = \tau_m t_w\,(b - c_c - c_t)$

$$F_c - F_t = F_w\cos\theta - \tau_m t_w(b - c_c - c_t) \tag{9.62}$$

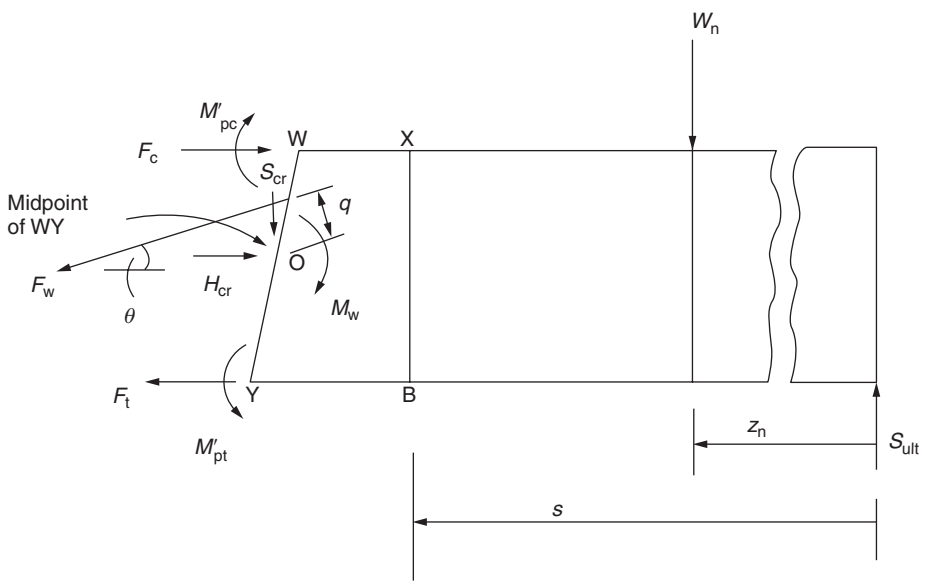

Fig. 9.19 Determination of flange forces.

Taking moments about O we have

$$F_c + F_t = \frac{2}{d}\left[S_{ult}\left(s + \frac{b + c_c - c_t}{2}\right) + M'_{pt} - M'_{pc} + F_w q - M_w - \sum_n W_n z_n\right] \tag{9.63}$$

where W_1 to W_n are external loads applied to the beam to the right of WY and M_w is the bending moment in the web when it has buckled and become a tension field, i.e.

$$M_w = \frac{\sigma_{mb} b d^2}{b}$$

The flange forces are then

$$F_c = \frac{S_{ult}}{2d}(d\cot\theta + 2s + b + c_c - c_t) + \frac{1}{d}\left(M'_{pt} - M'_{pc} + F_w q - M_w - \sum_n W_n z_n\right) - \frac{1}{2}\tau_m t_w (d\cot\theta + b - c_c - c_t) \tag{9.64}$$

$$F_t = \frac{S_{ult}}{2d}(d\cot\theta + 2s + b + c_c - c_t) + \frac{1}{d}\left(M'_{pt} - M'_{pc} - F_w q - M_w - \sum_n W_n z_n\right) + \frac{1}{2}\tau_m t_w (d\cot\theta + b - c_c - c_t) \tag{9.65}$$

Evans, Porter and Rockey adopted an iterative procedure for solving Eqs (9.61)–(9.65) in which an initial value of θ was assumed and σ_{cf} and σ_{tf} were taken to be zero. Then c_c and c_t were calculated and approximate values of F_c and F_t found giving better estimates for σ_{cf} and σ_{tf}. The procedure was then repeated until the required accuracy was obtained.

References

1 Gerard, G., *Introduction to Structural Stability Theory*, McGraw-Hill Book Company, New York, 1962.

2 Murray, N. W., *Introduction to the Theory of Thin-walled Structures*, Oxford Engineering Science Series, Oxford, 1984.

3 *Handbook of Aeronautics No. 1: Structural Principles and Data*, 4th edition, The Royal Aeronautical Society, 1952.

4 Bleich, F., *Buckling Strength of Metal Structures*, McGraw-Hill Book Company, New York, 1952.

5 Gerard, G. and Becker, H., *Handbook of Structural Stability, Pt. I, Buckling of Flat Plates*, NACA Tech. Note 3781, 1957.

6 Rivello, R. M., *Theory and Analysis of Flight Structures*, McGraw-Hill Book Company, New York, 1969.

7 Stowell, E. Z., *Compressive Strength of Flanges*, NACA Tech. Note 1323, 1947.

8 Mayers, J. and Budiansky, B., *Analysis of Behaviour of Simply Supported Flat Plates Compressed Beyond the Buckling Load in the Plastic Range*, NACA Tech. Note 3368, 1955.

9 Gerard, G. and Becker, H., *Handbook of Structural Stability, Pt. IV, Failure of Plates and Composite Elements*, NACA Tech. Note 3784, 1957.

10 Gerard, G., *Handbook of Structural Stability, Pt. V, Compressive Strength of Flat Stiffened Panels*, NACA Tech. Note 3785, 1957.

11 Gerard, G. and Becker, H., *Handbook of Structural Stability, Pt. VII, Strength of Thin Wing Construction*, NACA Tech. Note D-162, 1959.

12 Gerard, G., The crippling strength of compression elements, *J. Aeron. Sci.*, 25(1), 37–52, January 1958.

13 Kuhn, P., *Stresses in Aircraft and Shell Structures, McGraw-Hill Book Company*, New York, 1956.

14 Megson, T. H. G., *Structural and Stress Analysis*, 2nd edition, Elsevier, Oxford, 2005.

15 Evans, H. R., Porter, D. M. and Rockey, K. C. The collapse behaviour of plate girders subjected to shear and bending, Proc. Int. Assn. Bridge and Struct. Eng. P-18/78, 1–20.

Problems

P.9.1 A thin square plate of side a and thickness t is simply supported along each edge, and has a slight initial curvature giving an initial deflected shape.

$$w_0 = \delta \sin \frac{\pi x}{a} \sin \frac{\pi y}{a}$$

If the plate is subjected to a uniform compressive stress σ in the x-direction (see Fig. P.9.1), find an expression for the *elastic* deflection w normal to the plate. Show also that the deflection at the mid-point of the plate can be presented in the form of a Southwell plot and illustrate your answer with a suitable sketch.

Ans. $w = [\sigma t\delta/(4\pi^2 D/a^2 - \sigma t)] \sin \frac{\pi x}{a} \sin \frac{\pi y}{a}$

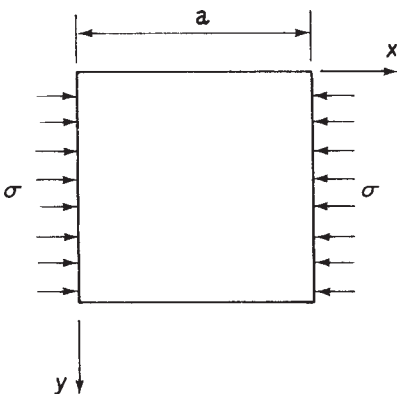

Fig. P.9.1

P.9.2 A uniform flat plate of thickness t has a width b in the y direction and length l in the x direction (see Fig. P.9.2). The edges parallel to the x axis are clamped and those parallel to the y axis are simply supported. A uniform compressive stress σ is applied in the x direction along the edges parallel to the y axis. Using an energy method, find an approximate expression for the magnitude of the stress σ which causes the plate to buckle, assuming that the deflected shape of the plate is given by

$$w = a_{11} \sin \frac{m\pi x}{l} \sin^2 \frac{\pi y}{b}$$

For the particular case $l = 2b$, find the number of half waves m corresponding to the lowest critical stress, expressing the result to the nearest integer. Determine also the lowest critical stress.

Ans. $m = 3,\ \sigma_{CR} = [6E/(1-\nu^2)](t/b)^2$

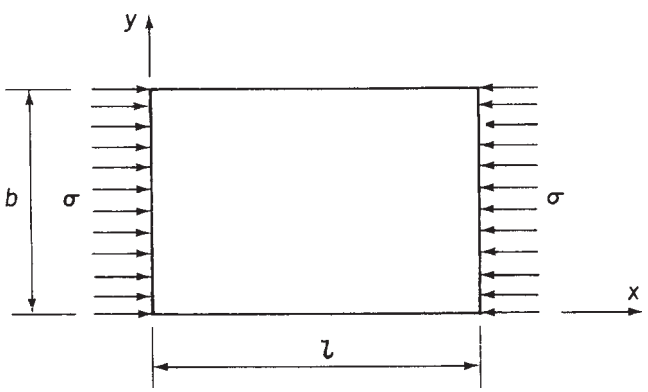

Fig. P.9.2

P.9.3 A panel, comprising flat sheet and uniformly spaced Z-section stringers, a part of whose cross-section is shown in Fig. P.9.3, is to be investigated for strength under uniform compressive loads in a structure in which it is to be stabilized by frames a distance l apart, l being appreciably greater than the spacing b.

(a) State the modes of failure which you would consider and how you would determine appropriate limiting stresses.

(b) Describe a suitable test to verify your calculations, giving particulars of the specimen, the manner of support and the measurements you would take. The latter should enable you to verify the assumptions made, as well as to obtain the load supported.

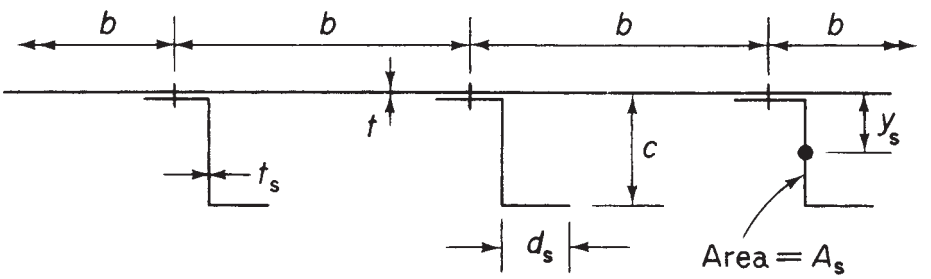

Fig. P.9.3

P.9.4 Part of a compression panel of internal construction is shown in Fig. P.9.4. The equivalent pin-centre length of the panel is 500 mm. The material has a Young's modulus of 70 000 N/mm^2 and its elasticity may be taken as falling catastrophically when a compressive stress of 300 N/mm^2 is reached. Taking coefficients of 3.62 for buckling of a plate with simply supported sides and of 0.385 with one side simply supported and one free, determine (a) the load per mm width of panel when initial buckling may be expected and (b) the load per mm for ultimate failure. Treat the material as thin for calculating section constants and assume that after initial buckling the stress in the plate increases parabolically from its critical value in the centre of sections.

Ans. 613.8 N/mm, 844.7 N/mm.

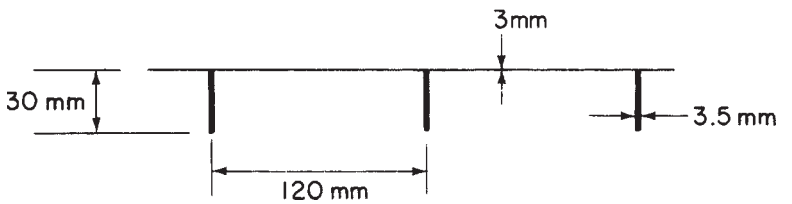

Fig. P.9.4

P.9.5 A simply supported beam has a span of 2.4 m and carries a central concentrated load of 10 kN. The flanges of the beam each have a cross-sectional area of

300 mm^2 while that of the vertical web stiffeners is 280 mm^2. If the depth of the beam, measured between the centroids of area of the flanges, is 350 mm and the stiffeners are symmetrically arranged about the web and spaced at 300 mm intervals, determine the maximum axial load in a flange and the compressive load in a stiffener.

It may be assumed that the beam web, of thickness 1.5 mm, is capable of resisting diagonal tension only.

Ans. 19.9 kN, 3.9 kN.

P.9.6 The spar of an aircraft is to be designed as an incomplete diagonal tension beam, the flanges being parallel. The stiffener spacing will be 250 mm, the effective depth of web will be 750 mm, and the depth between web-to-flange attachments is 725 mm.

The spar is to carry an ultimate shear force of 100 000 N. The maximum permissible shear stress is 165 N/mm^2, but it is also required that the shear stress should not exceed 15 times the critical shear stress for the web panel.

Assuming α to be 40° and using the relationships below:

(i) Select the smallest suitable web thickness from the following range of standard thicknesses. (Take Young's Modulus E as 70 000 N/mm^2.)

0.7 mm, 0.9 mm, 1.2 mm, 1.6 mm

(ii) Calculate the stiffener end load and the secondary bending moment in the flanges (assume stiffeners to be symmetrical about the web).

The shear stress buckling coefficient for the web may be calculated from the expression

$$K = 7.70[1 + 0.75(b/d)^2]$$

b and d having their usual significance.

The relationship between the diagonal tension factor and buckling stress ratio is

τ/τ_{CR}	5	7	9	11	13	15
k	0.37	0.40	0.42	0.48	0.51	0.53

Note that α is the angle of diagonal tension measured from the spanwise axis of the beam, as in the usual notation.

Ans. 1.2 mm, $130A_S/(1 + 0.0113A_S)$, 238 910 N mm.

P. 9.7 The main compressive wing structure of an aircraft consists of stringers, having the section shown in Fig. P.9.7(b), bonded to a thin skin (Fig. P.9.7(a)). Find suitable values for the stringer spacing b and rib spacing L if local instability, skin buckling and panel strut instability all occur at the same stress. Note that in Fig. P.9.7(a) only two of several stringers are shown for diagrammatic clarity. Also the thin skin should

be treated as a flat plate since the curvature is small. For a flat plate simply supported along two edges assume a buckling coefficient of 3.62. Take $E = 69\,000\ \text{N/mm}^2$.

Ans. $b = 56.5$ mm, $L = 700$ mm.

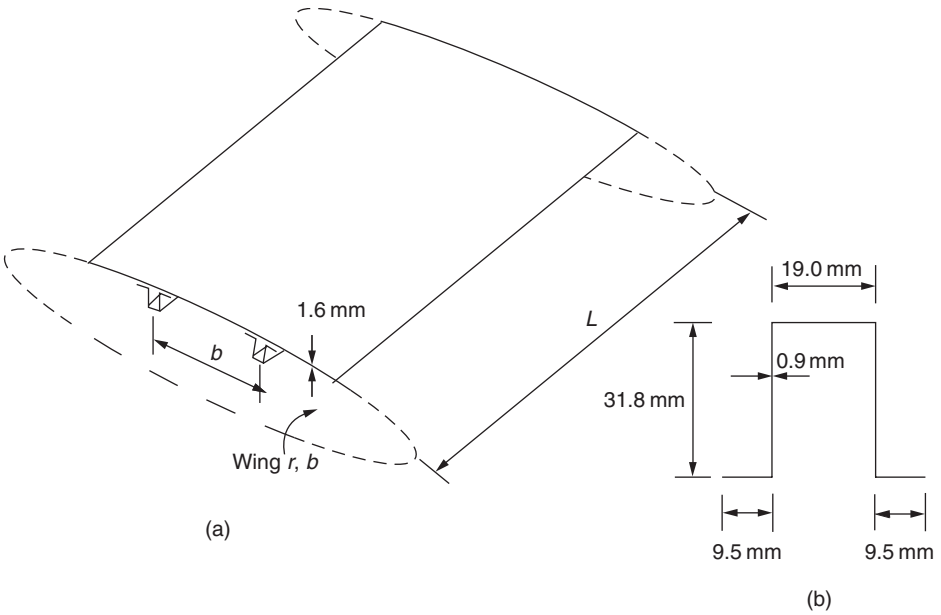

Fig. P.9.7

16

Bending of open and closed, thin-walled beams

In Chapter 12 we discussed the various types of structural component found in aircraft construction and the various loads they support. We saw that an aircraft is basically an assembly of stiffened shell structures ranging from the single cell closed section fuselage to multicellular wings and tail surfaces each subjected to bending, shear, torsional and axial loads. Other, smaller portions of the structure consist of thin-walled channel, T-, Z-, 'top-hat'-or I-sections, which are used to stiffen the thin skins of the cellular components and provide support for internal loads from floors, engine mountings, etc. Structural members such as these are known as *open section* beams, while the cellular components are termed *closed section* beams; clearly, both types of beam are subjected to axial, bending, shear and torsional loads.

In this chapter we shall investigate the stresses and displacements in thin-walled open and single cell closed section beams produced by bending loads.

In Chapter 1 we saw that an axial load applied to a member produces a uniform direct stress across the cross-section of the member. A different situation arises when the applied loads cause a beam to bend which, if the loads are vertical, will take up a sagging '$(\smile)$' or hogging shape '$(\frown)$'. This means that for loads which cause a beam to sag the upper surface of the beam must be shorter than the lower surface as the upper surface becomes concave and the lower one convex; the reverse is true for loads which cause hogging. The strains in the upper regions of the beam will, therefore, be different to those in the lower regions and since we have established that stress is directly proportional to strain (Eq. (1.40)) it follows that the stress will vary through the depth of the beam.

The truth of this can be demonstrated by a simple experiment. Take a reasonably long rectangular rubber eraser and draw three or four lines on its longer faces as shown in Fig. 16.1(a); the reason for this will become clear a little later. Now hold the eraser between the thumb and forefinger at each end and apply pressure as shown by the direction of the arrows in Fig. 16.1(b). The eraser bends into the shape shown and the lines on the side of the eraser *remain straight* but are now further apart at the top than at the bottom.

Since, in Fig. 16.1(b), the upper fibres have been stretched and the lower fibres compressed there will be fibres somewhere in between which are neither stretched nor compressed; the plane containing these fibres is called the *neutral plane*.

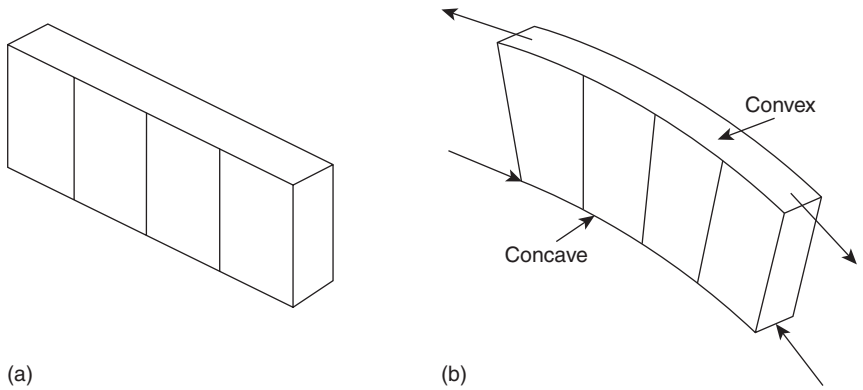

Fig. 16.1 Bending of a rubber eraser.

Now rotate the eraser so that its shorter sides are vertical and apply the same pressure with your fingers. The eraser again bends but now requires much less effort. It follows that the geometry and orientation of a beam section must affect its *bending stiffness*. This is more readily demonstrated with a plastic ruler. When flat it requires hardly any effort to bend it but when held with its width vertical it becomes almost impossible to bend.

16.1 Symmetrical bending

Although symmetrical bending is a special case of the bending of beams of arbitrary cross-section, we shall investigate the former first, so that the more complex general case may be more easily understood.

Symmetrical bending arises in beams which have either singly or doubly symmetrical cross-sections; examples of both types are shown in Fig. 16.2.

Suppose that a length of beam, of rectangular cross-section, say, is subjected to a pure, sagging bending moment, M, applied in a vertical plane. We shall define this later as a negative bending moment. The length of beam will bend into the shape shown in Fig. 16.3(a) in which the upper surface is concave and the lower convex. It can be seen that the upper longitudinal fibres of the beam are compressed while the lower fibres are stretched. It follows that, as in the case of the eraser, between these two extremes there are fibres that remain unchanged in length.

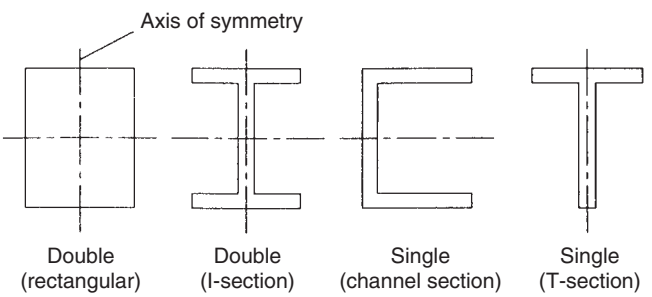

Fig. 16.2 Symmetrical section beams.

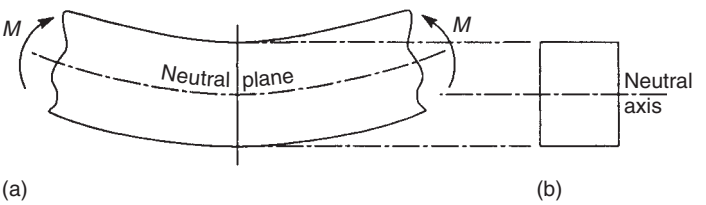

Fig. 16.3 Beam subjected to a pure sagging bending moment.

The direct stress therefore varies through the depth of the beam from compression in the upper fibres to tension in the lower. Clearly the direct stress is zero for the fibres that do not change in length; we have called the plane containing these fibres the *neutral plane*. The line of intersection of the neutral plane and any cross-section of the beam is termed the *neutral axis* (Fig. 16.3(b)).

The problem, therefore, is to determine the variation of direct stress through the depth of the beam, the values of the stresses and subsequently to find the corresponding beam deflection.

16.1.1 Assumptions

The primary assumption made in determining the direct stress distribution produced by pure bending is that plane cross-sections of the beam remain plane and normal to the longitudinal fibres of the beam after bending. Again, we saw this from the lines on the side of the eraser. We shall also assume that the material of the beam is linearly elastic, i.e. it obeys Hooke's law, and that the material of the beam is homogeneous.

16.1.2 Direct stress distribution

Consider a length of beam (Fig. 16.4(a)) that is subjected to a pure, sagging bending moment, M, applied in a vertical plane; the beam cross-section has a vertical axis of symmetry as shown in Fig. 16.4(b). The bending moment will cause the length of beam

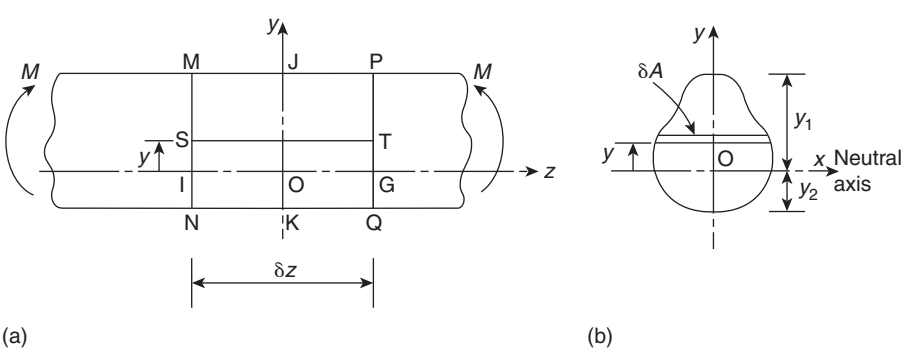

Fig. 16.4 Bending of a symmetrical section beam.

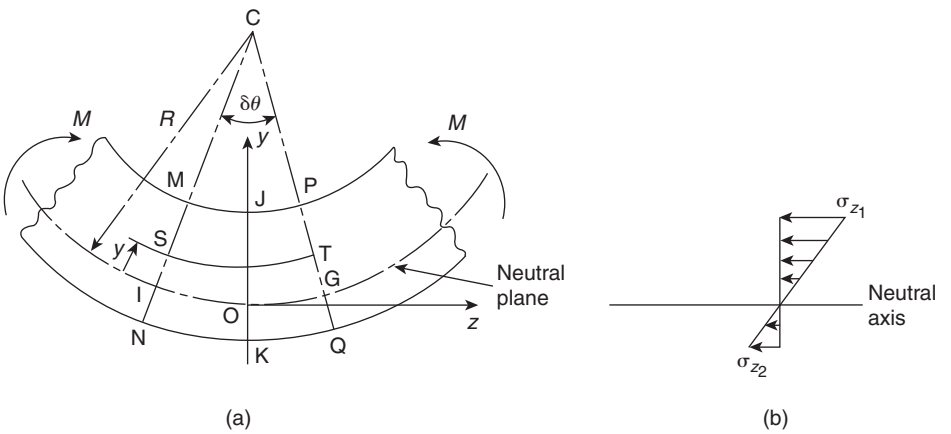

Fig. 16.5 Length of beam subjected to a pure bending moment.

to bend in a similar manner to that shown in Fig. 16.3(a) so that a neutral plane will exist which is, as yet, unknown distances y_1 and y_2 from the top and bottom of the beam, respectively. Coordinates of all points in the beam are referred to axes Oxyz in which the origin O lies in the neutral plane of the beam. We shall now investigate the behaviour of an elemental length, δz, of the beam formed by parallel sections MIN and PGQ (Fig. 16.4(a)) and also the fibre ST of cross-sectional area δA a distance y above the neutral plane. Clearly, before bending takes place MP = IG = ST = NQ = δz.

The bending moment M causes the length of beam to bend about a *centre of curvature* C as shown in Fig. 16.5(a). Since the element is small in length and a pure moment is applied we can take the curved shape of the beam to be circular with a *radius of curvature R* measured to the neutral plane. This is a useful reference point since, as we have seen, strains and stresses are zero in the neutral plane.

The previously parallel plane sections MIN and PGQ remain plane as we have demonstrated but are now inclined at an angle $\delta\theta$ to each other. The length MP is now shorter than δz as is ST while NQ is longer; IG, being in the neutral plane, is still of length δz. Since the fibre ST has changed in length it has suffered a strain ε_z which is given by

$$\varepsilon_z = \frac{\text{change in length}}{\text{original length}}$$

Then

$$\varepsilon_z = \frac{(R - y)\delta\theta - \delta z}{\delta z}$$

i.e.

$$\varepsilon_z = \frac{(R - y)\delta\theta - R\delta\theta}{R\delta\theta}$$

so that

$$\varepsilon_z = -\frac{y}{R} \tag{16.1}$$

The negative sign in Eq. (16.1) indicates that fibres in the region where y is positive will shorten when the bending moment is negative. Then, from Eq. (1.40), the direct stress σ_z in the fibre ST is given by

$$\sigma_z = -E\frac{y}{R} \tag{16.2}$$

The direct or normal force on the cross-section of the fibre ST is $\sigma_z \delta A$. However, since the direct stress in the beam section is due to a pure bending moment, in other words there is no axial load, the resultant normal force on the complete cross-section of the beam must be zero. Then

$$\int_A \sigma_z \, \mathrm{d}A = 0 \tag{16.3}$$

where A is the area of the beam cross-section.

Substituting for σ_z in Eq. (16.3) from (16.2) gives

$$-\frac{E}{R}\int_A y \, \mathrm{d}A = 0 \tag{16.4}$$

in which both E and R are constants for a beam of a given material subjected to a given bending moment. Therefore

$$\int_A y \, \mathrm{d}A = 0 \tag{16.5}$$

Equation (16.5) states that the first moment of the area of the cross-section of the beam with respect to the neutral axis, i.e. the x axis, is equal to zero. Thus we see that *the neutral axis passes through the centroid of area of the cross-section*. Since the y axis in this case is also an axis of symmetry, it must also pass through the centroid of the cross-section. Hence the origin, O, of the coordinate axes, coincides with the centroid of area of the cross-section.

Equation (16.2) shows that for a sagging (i.e. negative) bending moment the direct stress in the beam section is negative (i.e. compressive) when y is positive and positive (i.e. tensile) when y is negative.

Consider now the elemental strip δA in Fig. 16.4(b); this is, in fact, the cross-section of the fibre ST. The strip is above the neutral axis so that there will be a *compressive* force acting on its cross-section of $\sigma_z \delta A$ which is *numerically* equal to $(Ey/R)\delta A$ from Eq. (16.2). Note that this force will act at all sections along the length of ST. At S this force will exert a clockwise moment $(Ey/R)y\delta A$ about the neutral axis while at T the force will exert an identical anticlockwise moment about the neutral axis. Considering either end of ST we see that the moment resultant about the neutral axis of the stresses on all such fibres must be *equivalent* to the applied negative moment M, i.e.

$$M = -\int_A E\frac{y^2}{R}\mathrm{d}A$$

or

$$M = -\frac{E}{R}\int_A y^2 \mathrm{d}A \tag{16.6}$$

The term $\int_A y^2 \, dA$ is known as the *second moment of area* of the cross-section of the beam about the neutral axis and is given the symbol I. Rewriting Eq. (16.6) we have

$$M = -\frac{EI}{R} \tag{16.7}$$

or, combining this expression with Eq. (16.2)

$$\frac{M}{I} = -\frac{E}{R} = \frac{\sigma_z}{y} \tag{16.8}$$

From Eq. (16.8) we see that

$$\sigma_z = \frac{My}{I} \tag{16.9}$$

The direct stress, σ_z, at any point in the cross-section of a beam is therefore directly proportional to the distance of the point from the neutral axis and so varies linearly through the depth of the beam as shown, for the section JK, in Fig. 16.5(b). Clearly, for a positive bending moment σ_z is positive, i.e. tensile, when y is positive and compressive (i.e. negative) when y is negative. Thus in Fig. 16.5(b)

$$\sigma_{z,1} = \frac{My_1}{I} \text{ (compression)} \quad \sigma_{z,2} = \frac{My_2}{I} \text{ (tension)} \tag{16.10}$$

Furthermore, we see from Eq. (16.7) that the curvature, $1/R$, of the beam is given by

$$\frac{1}{R} = \frac{M}{EI} \tag{16.11}$$

and is therefore directly proportional to the applied bending moment and inversely proportional to the product EI which is known as the *flexural rigidity* of the beam.

Example 16.1

The cross-section of a beam has the dimensions shown in Fig. 16.6(a). If the beam is subjected to a negative bending moment of 100 kN m applied in a vertical plane, determine the distribution of direct stress through the depth of the section.

The cross-section of the beam is doubly symmetrical so that the centroid, C, of the section, and therefore the origin of axes, coincides with the mid-point of the web. Furthermore, the bending moment is applied to the beam section in a vertical plane so that the x axis becomes the neutral axis of the beam section; we therefore need to calculate the second moment of area, I_{xx}, about this axis.

$$I_{xx} = \frac{200 \times 300^3}{12} - \frac{175 \times 260^3}{12} = 193.7 \times 10^6 \text{ mm}^4 \text{ (see Section 16.4)}$$

From Eq. (16.9) the distribution of direct stress, σ_z, is given by

$$\sigma_z = -\frac{100 \times 10^6}{193.7 \times 10^6} y = -0.52y \tag{i}$$

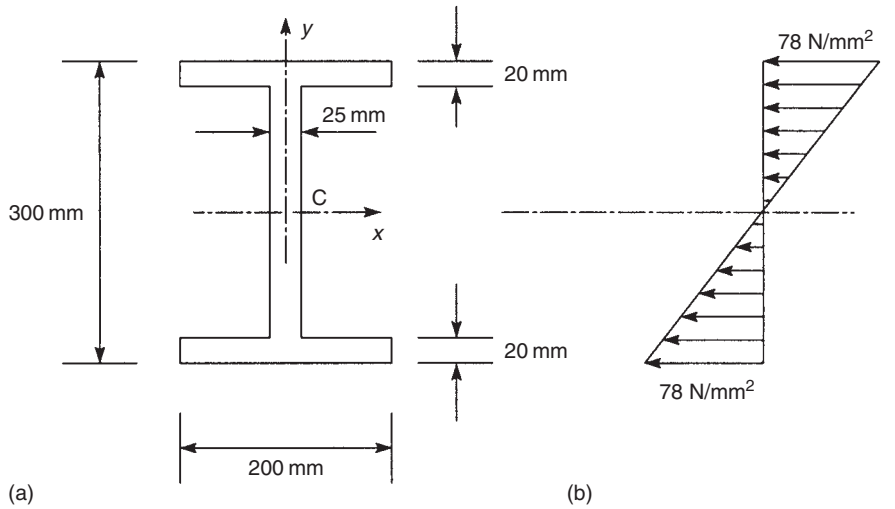

Fig. 16.6 Direct stress distribution in beam of Example 16.1.

The direct stress, therefore, varies linearly through the depth of the section from a value

$$-0.52 \times (+150) = -78\,\mathrm{N/mm^2}\ \text{(compression)}$$

at the top of the beam to

$$-0.52 \times (-150) = +78\,\mathrm{N/mm^2}\ \text{(tension)}$$

at the bottom as shown in Fig. 16.6(b).

Example 16.2

Now determine the distribution of direct stress in the beam of Example 16.1 if the bending moment is applied in a horizontal plane and in a clockwise sense about Cy when viewed in the direction yC.

In this case the beam will bend about the vertical y axis which therefore becomes the neutral axis of the section. Thus Eq. (16.9) becomes

$$\sigma_z = \frac{M}{I_{yy}}x \tag{i}$$

where I_{yy} is the second moment of area of the beam section about the y axis. Again from Section 16.4

$$I_{yy} = 2 \times \frac{20 \times 200^3}{12} + \frac{260 \times 25^3}{12} = 27.0 \times 10^6\,\mathrm{mm^4}$$

Hence, substituting for M and I_{yy} in Eq. (i)

$$\sigma_z = \frac{100 \times 10^6}{27.0 \times 10^6}x = 3.7x$$

We have not specified a sign convention for bending moments applied in a horizontal plane. However, a physical appreciation of the problem shows that the left-hand edges of the beam are in compression while the right-hand edges are in tension. Again the distribution is linear and varies from $3.7 \times (-100) = -370\,\text{N/mm}^2$ (compression) at the left-hand edges of each flange to $3.7 \times (+100) = +370\,\text{N/mm}^2$ (tension) at the right-hand edges.

We note that the maximum stresses in this example are very much greater than those in Example 16.1. This is due to the fact that the bulk of the material in the beam section is concentrated in the region of the neutral axis where the stresses are low. The use of an I-section in this manner would therefore be structurally inefficient.

Example 16.3

The beam section of Example 16.1 is subjected to a bending moment of 100 kN m applied in a plane parallel to the longitudinal axis of the beam but inclined at 30° to the left of vertical. The sense of the bending moment is clockwise when viewed from the left-hand edge of the beam section. Determine the distribution of direct stress.

The bending moment is first resolved into two components, M_x in a vertical plane and M_y in a horizontal plane. Equation (16.9) may then be written in two forms

$$\sigma_z = \frac{M_x}{I_{xx}} y \qquad \sigma_z = \frac{M_y}{I_{yy}} x \tag{i}$$

The separate distributions can then be determined and superimposed. A more direct method is to combine the two equations (i) to give the total direct stress at any point (x, y) in the section. Thus

$$\sigma_z = \frac{M_x}{I_{xx}} y + \frac{M_y}{I_{yy}} x \tag{ii}$$

Now

$$\left.\begin{aligned} M_x &= 100 \cos 30^\circ = 86.6\,\text{kN m} \\ M_y &= 100 \sin 30^\circ = 50.0\,\text{kN m} \end{aligned}\right\} \tag{iii}$$

M_x is, in this case, a positive bending moment producing tension in the upper half of the beam where y is positive. Also M_y produces tension in the left-hand half of the beam where x is negative; we shall therefore call M_y a negative bending moment. Substituting the values of M_x and M_y from Eq. (iii) but with the appropriate sign in Eq. (ii) together with the values of I_{xx} and I_{yy} from Examples 16.1 and 16.2 we obtain

$$\sigma_z = \frac{86.6 \times 10^6}{193.7 \times 10^6} y - \frac{50.0 \times 10^6}{27.0 \times 10^6} x \tag{iv}$$

or

$$\sigma_z = 0.45y - 1.85x \tag{v}$$

Equation (v) gives the value of direct stress at any point in the cross-section of the beam and may also be used to determine the distribution over any desired portion. Thus on

the upper edge of the top flange $y = +150\,\text{mm}$, $100\,\text{mm} \geq x \geq -100\,\text{mm}$, so that the direct stress varies linearly with x. At the top left-hand corner of the top flange

$$\sigma_z = 0.45 \times (+150) - 1.85 \times (-100) = +252.5\,\text{N/mm}^2 \text{ (tension)}$$

At the top right-hand corner

$$\sigma_z = 0.45 \times (+150) - 1.85 \times (+100) = -117.5\,\text{N/mm}^2 \text{ (compression)}$$

The distributions of direct stress over the outer edge of each flange and along the vertical axis of symmetry are shown in Fig. 16.7. Note that the neutral axis of the beam section does not in this case coincide with either the x or y axis, although it still passes through the centroid of the section. Its inclination, α, to the x axis, say, can be found by setting $\sigma_z = 0$ in Eq. (v). Then

$$0 = 0.45y - 1.85x$$

or

$$\frac{y}{x} = \frac{1.85}{0.45} = 4.11 = \tan\alpha$$

which gives

$$\alpha = 76.3^\circ$$

Note that α may be found in general terms from Eq. (ii) by again setting $\sigma_z = 0$. Hence

$$\frac{y}{x} = -\frac{M_y I_{xx}}{M_x I_{yy}} = \tan\alpha \tag{16.12}$$

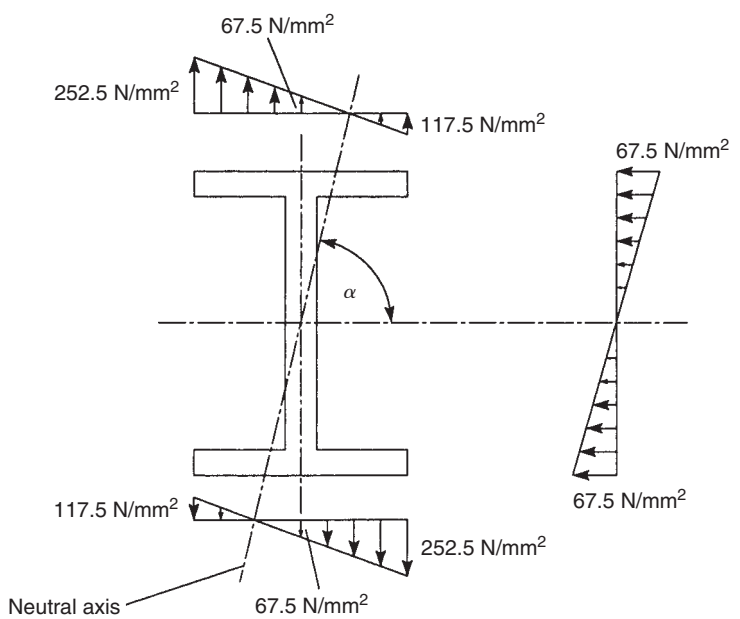

Fig. 16.7 Direct stress distribution in beam of Example 16.3.

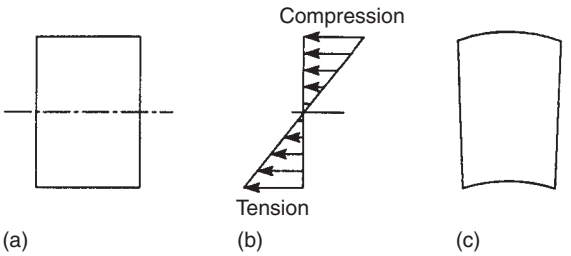

Fig. 16.8 Anticlastic bending of a beam section.

or

$$\tan\alpha = \frac{M_y I_{xx}}{M_x I_{yy}}$$

since y is positive and x is positive for a positive value of α. We shall define in a slightly different way in Section 16.2.4 for beams of unsymmetrical section.

16.1.3 Anticlastic bending

In the rectangular beam section shown in Fig. 16.8(a) the direct stress distribution due to a negative bending moment applied in a vertical plane varies from compression in the upper half of the beam to tension in the lower half (Fig. 16.8(b)). However, due to the Poisson effect the compressive stress produces a lateral elongation of the upper fibres of the beam section while the tensile stress produces a lateral contraction of the lower. The section does not therefore remain rectangular but distorts as shown in Fig. 16.8(c); the effect is known as *anticlastic bending*.

Anticlastic bending is of interest in the analysis of thin-walled box beams in which the cross-sections are maintained by stiffening ribs. The prevention of anticlastic distortion induces local variations in stress distributions in the webs and covers of the box beam and also in the stiffening ribs.

16.2 Unsymmetrical bending

We have shown that the value of direct stress at a point in the cross-section of a beam subjected to bending depends on the position of the point, the applied loading and the geometric properties of the cross-section. It follows that it is of no consequence whether or not the cross-section is open or closed. We therefore derive the theory for a beam of arbitrary cross-section and then discuss its application to thin-walled open and closed section beams subjected to bending moments.

The assumptions are identical to those made for symmetrical bending and are listed in Section 16.1.1. However, before we derive an expression for the direct stress distribution in a beam subjected to bending we shall establish sign conventions for moments, forces and displacements, investigate the effect of choice of section on the positive directions of these parameters and discuss the determination of the components of a bending moment applied in any longitudinal plane.

16.2.1 Sign conventions and notation

Forces, moments and displacements are referred to an arbitrary system of axes Oxyz, of which Oz is parallel to the longitudinal axis of the beam and Oxy are axes in the plane of the cross-section. We assign the symbols M, S, P, T and w to bending moment, shear force, axial or direct load, torque and distributed load intensity, respectively, with suffixes where appropriate to indicate sense or direction. Thus, M_x is a bending moment about the x axis, S_x is a shear force in the x direction and so on. Figure 16.9 shows positive directions and senses for the above loads and moments applied externally to a beam and also the positive directions of the components of displacement u, v and w of any point in the beam cross-section parallel to the x, y and z axes, respectively. A further condition defining the signs of the bending moments M_x and M_y is that they are positive when they induce tension in the positive xy quadrant of the beam cross-section.

If we refer internal forces and moments to that face of a section which is seen when viewed in the direction zO then, as shown in Fig. 16.10, positive internal forces and moments are in the same direction and sense as the externally applied loads whereas on the opposite face they form an opposing system. The former system, which we shall use, has the advantage that direct and shear loads are always positive in the positive directions of the appropriate axes whether they are internal loads or not. It must be realized, though, that internal stress resultants then become equivalent to externally applied forces and moments and are not in equilibrium with them.

16.2.2 Resolution of bending moments

A bending moment M applied in any longitudinal plane parallel to the z axis may be resolved into components M_x and M_y by the normal rules of vectors. However, a visual appreciation of the situation is often helpful. Referring to Fig. 16.11 we see that a bending moment M in a plane at an angle θ to Ox may have components of differing

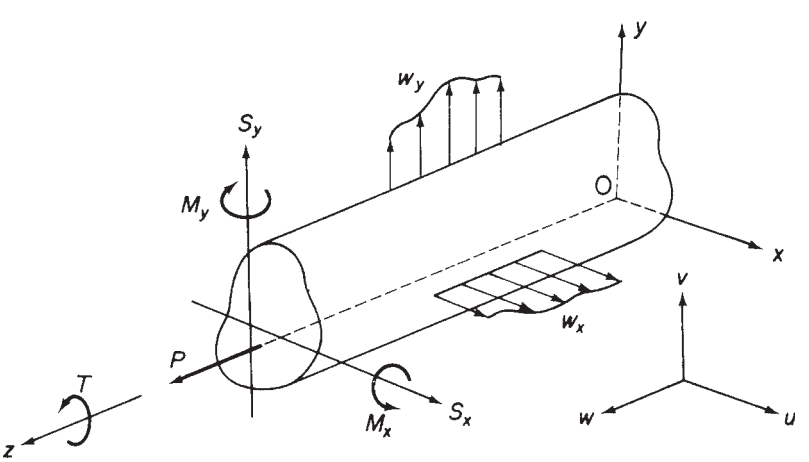

Fig. 16.9 Notation and sign convention for forces, moments and displacements.

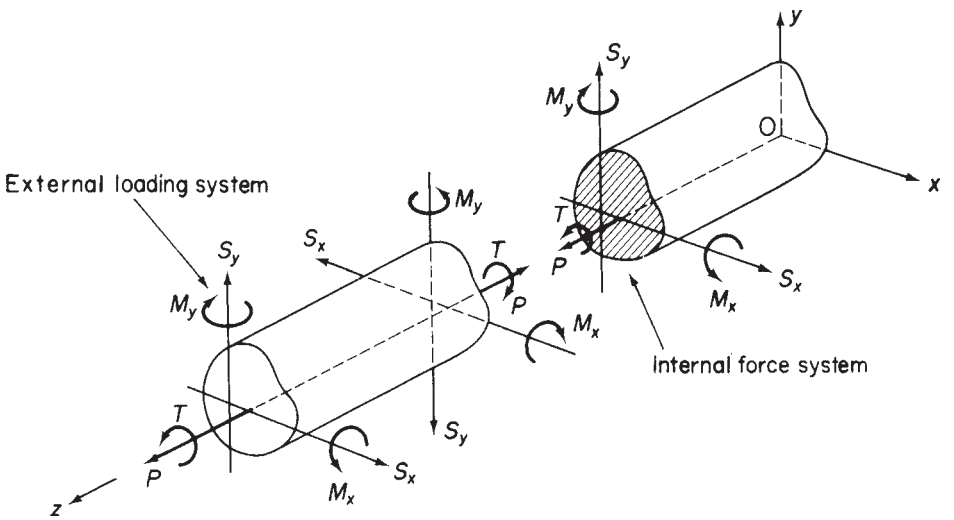

Fig. 16.10 Internal force system.

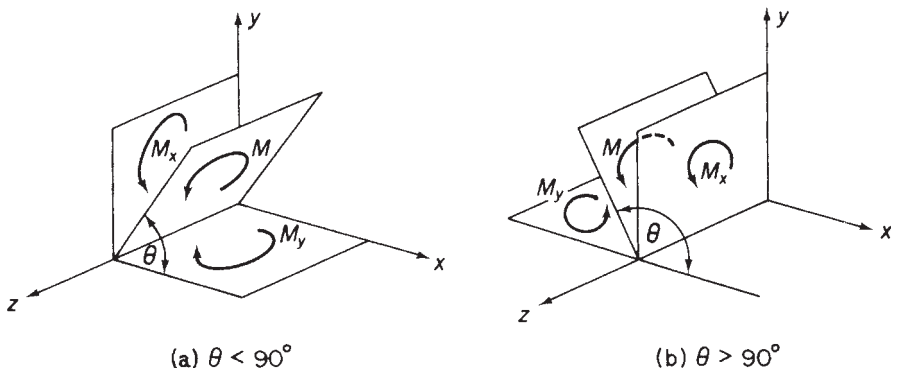

Fig. 16.11 Resolution of bending moments.

sign depending on the size of θ. In both cases, for the sense of M shown

$$M_x = M \sin\theta$$
$$M_y = M \cos\theta$$

which give, for $\theta < \pi/2$, M_x and M_y positive (Fig. 16.11(a)) and for $\theta > \pi/2$, M_x positive and M_y negative (Fig. 16.11(b)).

16.2.3 Direct stress distribution due to bending

Consider a beam having the arbitrary cross-section shown in Fig. 16.12(a). The beam supports bending moments M_x and M_y and bends about some axis in its cross-section which is therefore an axis of zero stress or a *neutral axis* (NA). Let us suppose that the

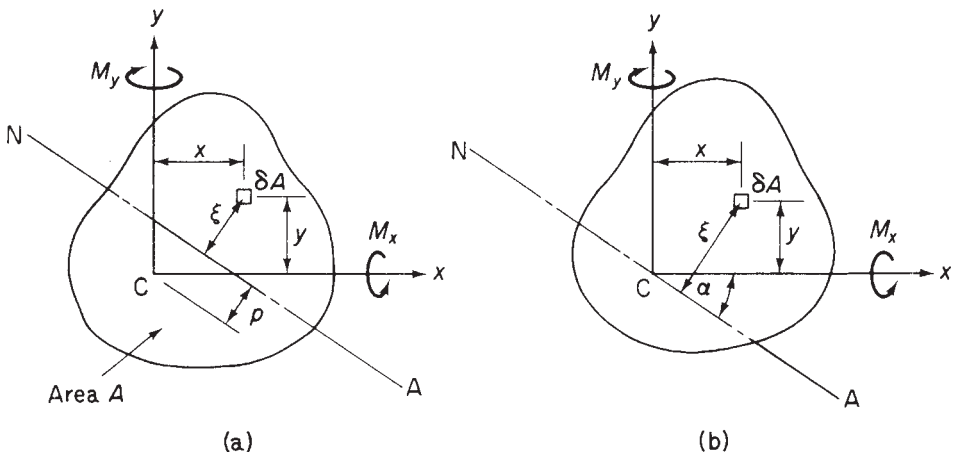

Fig. 16.12 Determination of neutral axis position and direct stress due to bending.

origin of axes coincides with the centroid C of the cross-section and that the neutral axis is a distance p from C. The direct stress σ_z on an element of area δA at a point (x, y) and a distance ξ from the neutral axis is, from the third of Eq. (1.42)

$$\sigma_z = E\varepsilon_z \tag{16.13}$$

If the beam is bent to a radius of curvature ρ about the neutral axis at this particular section then, since plane sections are assumed to remain plane after bending, and by a comparison with symmetrical bending theory

$$\varepsilon_z = \frac{\xi}{\rho}$$

Substituting for ε_z in Eq. (16.13) we have

$$\sigma_z = \frac{E\xi}{\rho} \tag{16.14}$$

The beam supports pure bending moments so that the resultant normal load on any section must be zero. Hence

$$\int_A \sigma_z \, \mathrm{d}A = 0$$

Therefore, replacing σ_z in this equation from Eq. (16.14) and cancelling the constant E/ρ gives

$$\int_A \xi \, \mathrm{d}A = 0$$

i.e. the first moment of area of the cross-section of the beam about the neutral axis is zero. It follows that the neutral axis passes through the centroid of the cross-section as shown in Fig. 16.12(b) which is the result we obtained for the case of symmetrical bending.

Suppose that the inclination of the neutral axis to Cx is α (measured clockwise from Cx), then

$$\xi = x\sin\alpha + y\cos\alpha \tag{16.15}$$

and from Eq. (16.14)

$$\sigma_z = \frac{E}{\rho}(x\sin\alpha + y\cos\alpha) \tag{16.16}$$

The moment resultants of the internal direct stress distribution have the same sense as the applied moments M_x and M_y. Therefore

$$M_x = \int_A \sigma_z y\,\mathrm{d}A, \quad M_y = \int_A \sigma_z x\,\mathrm{d}A \tag{16.17}$$

Substituting for σ_z from Eq. (16.16) in (16.17) and defining the second moments of area of the section about the axes Cx, Cy as

$$I_{xx} = \int_A y^2\,\mathrm{d}A, \quad I_{yy} = \int_A x^2\,\mathrm{d}A, \quad I_{xy} = \int_A xy\,\mathrm{d}A$$

gives

$$M_x = \frac{E\sin\alpha}{\rho}I_{xy} + \frac{E\cos\alpha}{\rho}I_{xx}, \quad M_y = \frac{E\sin\alpha}{\rho}I_{yy} + \frac{E\cos\alpha}{\rho}I_{xy}$$

or, in matrix form

$$\begin{Bmatrix} M_x \\ M_y \end{Bmatrix} = \frac{E}{\rho}\begin{bmatrix} I_{xy} & I_{xx} \\ I_{yy} & I_{xy} \end{bmatrix}\begin{Bmatrix} \sin\alpha \\ \cos\alpha \end{Bmatrix}$$

from which

$$\frac{E}{\rho}\begin{Bmatrix} \sin\alpha \\ \cos\alpha \end{Bmatrix} = \begin{bmatrix} I_{xy} & I_{xx} \\ I_{yy} & I_{xy} \end{bmatrix}^{-1}\begin{Bmatrix} M_x \\ M_y \end{Bmatrix}$$

i.e.

$$\frac{E}{\rho}\begin{Bmatrix} \sin\alpha \\ \cos\alpha \end{Bmatrix} = \frac{1}{I_{xx}I_{yy} - I_{xy}^2}\begin{bmatrix} -I_{xy} & I_{xx} \\ I_{yy} & -I_{xy} \end{bmatrix}\begin{Bmatrix} M_x \\ M_y \end{Bmatrix}$$

so that, from Eq. (16.16)

$$\sigma_z = \left(\frac{M_y I_{xx} - M_x I_{xy}}{I_{xx}I_{yy} - I_{xy}^2}\right)x + \left(\frac{M_x I_{yy} - M_y I_{xy}}{I_{xx}I_{yy} - I_{xy}^2}\right)y \tag{16.18}$$

Alternatively, Eq. (16.18) may be rearranged in the form

$$\sigma_z = \frac{M_x(I_{yy}y - I_{xy}x)}{I_{xx}I_{yy} - I_{xy}^2} + \frac{M_y(I_{xx}x - I_{xy}y)}{I_{xx}I_{yy} - I_{xy}^2} \tag{16.19}$$

From Eq. (16.19) it can be seen that if, say, $M_y = 0$ the moment M_x produces a stress which varies with both x and y; similarly for M_y if $M_x = 0$.

In the case where the beam cross-section has *either* (or both) Cx or Cy as an axis of symmetry the product second moment of area I_{xy} is zero and Cxy are *principal axes*. Equation (16.19) then reduces to

$$\sigma_z = \frac{M_x}{I_{xx}}y + \frac{M_y}{I_{yy}}x \tag{16.20}$$

Further, if either M_y or M_x is zero then

$$\sigma_z = \frac{M_x}{I_{xx}}y \quad \text{or} \quad \sigma_z = \frac{M_y}{I_{yy}}x \tag{16.21}$$

Equations (16.20) and (16.21) are those derived for the bending of beams having at least a singly symmetrical cross-section (see Section 16.1). It may also be noted that in Eq. (16.21) $\sigma_z = 0$ when, for the first equation, $y = 0$ and for the second equation when $x = 0$. Therefore, in symmetrical bending theory the x axis becomes the neutral axis when $M_y = 0$ and the y axis becomes the neutral axis when $M_x = 0$. Thus we see that the position of the neutral axis depends on the form of the applied loading as well as the geometrical properties of the cross-section.

There exists, in any unsymmetrical cross-section, a centroidal set of axes for which the product second moment of area is zero (see Ref. [1]). These axes are then principal axes and the direct stress distribution referred to these axes takes the simplified form of Eqs (16.20) or (16.21). It would therefore appear that the amount of computation can be reduced if these axes are used. This is not the case, however, unless the principal axes are obvious from inspection since the calculation of the position of the principal axes, the principal sectional properties and the coordinates of points at which the stresses are to be determined consumes a greater amount of time than direct use of Eqs (16.18) or (16.19) for an arbitrary, but convenient set of centroidal axes.

16.2.4 Position of the neutral axis

The neutral axis always passes through the centroid of area of a beam's cross-section but its inclination α (see Fig. 16.12(b)) to the x axis depends on the form of the applied loading and the geometrical properties of the beam's cross-section.

At all points on the neutral axis the direct stress is zero. Therefore, from Eq. (16.18)

$$0 = \left(\frac{M_y I_{xx} - M_x I_{xy}}{I_{xx}I_{yy} - I_{xy}^2}\right) x_{\mathrm{NA}} + \left(\frac{M_x I_{yy} - M_y I_{xy}}{I_{xx}I_{yy} - I_{xy}^2}\right) y_{\mathrm{NA}}$$

where x_{NA} and y_{NA} are the coordinates of any point on the neutral axis. Hence

$$\frac{y_{\mathrm{NA}}}{x_{\mathrm{NA}}} = -\frac{M_y I_{xx} - M_x I_{xy}}{M_x I_{yy} - M_y I_{xy}}$$

or, referring to Fig. 16.12(b) and noting that when α is positive x_{NA} and y_{NA} are of opposite sign

$$\tan\alpha = \frac{M_y I_{xx} - M_x I_{xy}}{M_x I_{yy} - M_y I_{xy}} \tag{16.22}$$

Example 16.4

A beam having the cross-section shown in Fig. 16.13 is subjected to a bending moment of 1500 N m in a vertical plane. Calculate the maximum direct stress due to bending stating the point at which it acts.

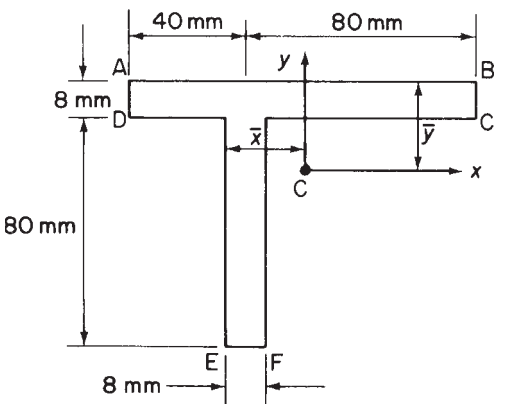

Fig. 16.13 Cross-section of beam in Example 16.4.

The position of the centroid of the section may be found by taking moments of areas about some convenient point. Thus

$$(120 \times 8 + 80 \times 8)\bar{y} = 120 \times 8 \times 4 + 80 \times 8 \times 48$$

giving

$$\bar{y} = 21.6\,\text{mm}$$

and

$$(120 \times 8 + 80 \times 8)\bar{x} = 80 \times 8 \times 4 + 120 \times 8 \times 24$$

giving

$$\bar{x} = 16\,\text{mm}$$

The next step is to calculate the section properties referred to axes Cxy (see Section 16.4)

$$I_{xx} = \frac{120 \times (8)^3}{12} + 120 \times 8 \times (17.6)^2 + \frac{8 \times (80)^3}{12} + 80 \times 8 \times (26.4)^2$$
$$= 1.09 \times 10^6\,\text{mm}^4$$
$$I_{yy} = \frac{8 \times (120)^3}{12} + 120 \times 8 \times (8)^2 + \frac{80 \times (8)^3}{12} + 80 \times 8 \times (12)^2$$
$$= 1.31 \times 10^6\,\text{mm}^4$$
$$I_{xy} = 120 \times 8 \times 8 \times 17.6 + 80 \times 8 \times (-12) \times (-26.4)$$
$$= 0.34 \times 10^6\,\text{mm}^4$$

Since $M_x = 1500\,\text{N m}$ and $M_y = 0$ we have, from Eq. (16.19)

$$\sigma_z = 1.5y - 0.39x \tag{i}$$

in which the units are N and mm.

By inspection of Eq. (i) we see that σ_x will be a maximum at F where $x = -8\,\text{mm}$, $y = -66.4\,\text{mm}$. Thus

$$\sigma_{z,\max} = -96\,\text{N/mm}^2 \text{ (compressive)}$$

In some cases the maximum value cannot be obtained by inspection so that values of σ_z at several points must be calculated.

16.2.5 Load intensity, shear force and bending moment relationships, general case

Consider an element of length δz of a beam of unsymmetrical cross-section subjected to shear forces, bending moments and a distributed load of varying intensity, all in the yz plane as shown in Fig. 16.14. The forces and moments are positive in accordance with the sign convention previously adopted. Over the length of the element we may assume that the intensity of the distributed load is constant. Therefore, for equilibrium of the element in the y direction

$$\left(S_y + \frac{\partial S_y}{\partial z}\delta z\right) + w_y \delta z - S_y = 0$$

from which

$$w_y = -\frac{\partial S_y}{\partial z}$$

Taking moments about A we have

$$\left(M_x + \frac{\partial M_x}{\partial z}\delta z\right) - \left(S_y + \frac{\partial S_y}{\partial z}\delta z\right)\delta z - w_y \frac{(\delta z)^2}{2} - M_x = 0$$

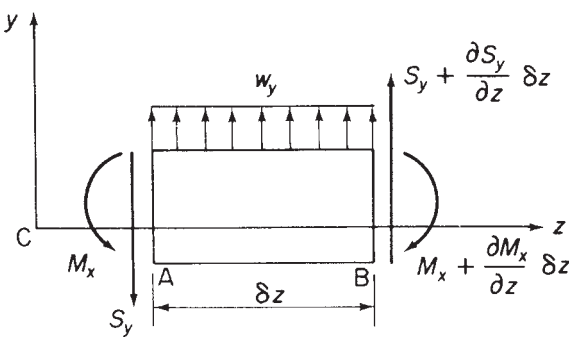

Fig. 16.14 Equilibrium of beam element supporting a general force system in the *yz* plane.

or, when second-order terms are neglected

$$S_y = \frac{\partial M_x}{\partial z}$$

We may combine these results into a single expression

$$-w_y = \frac{\partial S_y}{\partial z} = \frac{\partial^2 M_x}{\partial z^2} \tag{16.23}$$

Similarly for loads in the xz plane

$$-w_x = \frac{\partial S_x}{\partial z} = \frac{\partial^2 M_y}{\partial z^2} \tag{16.24}$$

16.3 Deflections due to bending

We have noted that a beam bends about its neutral axis whose inclination relative to arbitrary centroidal axes is determined from Eq. (16.22). Suppose that at some section of an unsymmetrical beam the deflection normal to the neutral axis (and therefore an absolute deflection) is ζ, as shown in Fig. 16.15. In other words the centroid C is displaced from its initial position C_I through an amount ζ to its final position C_F. Suppose also that the centre of curvature R of the beam at this particular section is on the opposite side of the neutral axis to the direction of the displacement ζ and that the radius of curvature is ρ. For this position of the centre of curvature and from the usual approximate expression for curvature we have

$$\frac{1}{\rho} = \frac{\mathrm{d}^2 \zeta}{\mathrm{d}z^2} \tag{16.25}$$

The components u and v of ζ are in the negative directions of the x and y axes, respectively, so that

$$u = -\zeta \sin\alpha \quad v = -\zeta \cos\alpha \tag{16.26}$$

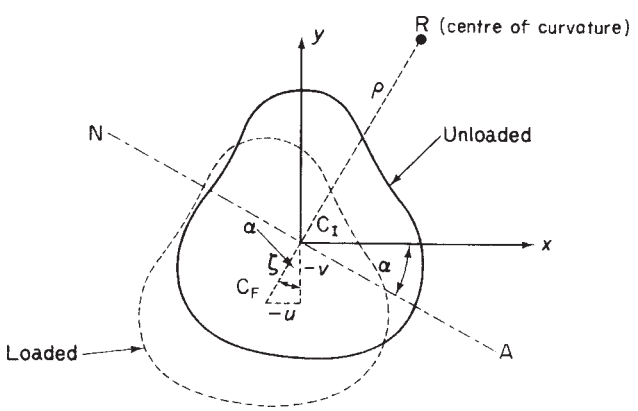

Fig. 16.15 Determination of beam deflection due to bending.

Differentiating Eqs (16.26) twice with respect to z and then substituting for ζ from Eq. (16.25) we obtain

$$\frac{\sin\alpha}{\rho} = -\frac{\mathrm{d}^2u}{\mathrm{d}z^2}, \quad \frac{\cos\alpha}{\rho} = -\frac{\mathrm{d}^2v}{\mathrm{d}z^2} \tag{16.27}$$

In the derivation of Eq. (16.18) we see that

$$\frac{1}{\rho}\begin{Bmatrix}\sin\alpha\\ \cos\alpha\end{Bmatrix} = \frac{1}{E(I_{xx}I_{yy} - I_{xy}^2)}\begin{bmatrix}-I_{xy} & I_{xx}\\ I_{yy} & -I_{xy}\end{bmatrix}\begin{Bmatrix}M_x\\ M_y\end{Bmatrix} \tag{16.28}$$

Substituting in Eqs (16.28) for $\sin\alpha/\rho$ and $\cos\alpha/\rho$ from Eqs (16.27) and writing $u'' = \mathrm{d}^2u/\mathrm{d}z^2$, $v'' = \mathrm{d}^2v/\mathrm{d}z^2$ we have

$$\begin{Bmatrix}u''\\ v''\end{Bmatrix} = \frac{-1}{E(I_{xx}I_{yy} - I_{xy}^2)}\begin{bmatrix}-I_{xy} & I_{xx}\\ I_{yy} & -I_{xy}\end{bmatrix}\begin{Bmatrix}M_x\\ M_y\end{Bmatrix} \tag{16.29}$$

It is instructive to rearrange Eq. (16.29) as follows

$$\begin{Bmatrix}M_x\\ M_y\end{Bmatrix} = -E\begin{bmatrix}I_{xy} & I_{xx}\\ I_{yy} & I_{xy}\end{bmatrix}\begin{Bmatrix}u''\\ v''\end{Bmatrix} \quad \text{(see derivation of Eq. (16.18))} \tag{16.30}$$

i.e.

$$\left.\begin{aligned}M_x &= -EI_{xy}u'' - EI_{xx}v''\\ M_y &= -EI_{yy}u'' - EI_{xy}v''\end{aligned}\right\} \tag{16.31}$$

The first of Eqs (16.31) shows that M_x produces curvatures, i.e. deflections, in both the xz and yz planes even though $M_y = 0$; similarly for M_y when $M_x = 0$. Thus, for example, an unsymmetrical beam will deflect both vertically and horizontally even though the loading is entirely in a vertical plane. Similarly, vertical and horizontal components of deflection in an unsymmetrical beam are produced by horizontal loads.

For a beam having either Cx or Cy (or both) as an axis of symmetry, $I_{xy} = 0$ and Eqs (16.29) reduce to

$$u'' = -\frac{M_y}{EI_{yy}}, \quad v'' = -\frac{M_x}{EI_{xx}} \tag{16.32}$$

Example 16.5

Determine the deflection curve and the deflection of the free end of the cantilever shown in Fig. 16.16(a); the flexural rigidity of the cantilever is EI and its section is doubly symmetrical.

The load W causes the cantilever to deflect such that its neutral plane takes up the curved shape shown Fig. 16.16(b); the deflection at any section Z is then v while that at its free end is v_{tip}. The axis system is chosen so that the origin coincides with the built-in end where the deflection is clearly zero.

The bending moment, M, at the section Z is, from Fig. 16.16(a)

$$M = W(L - z) \tag{i}$$

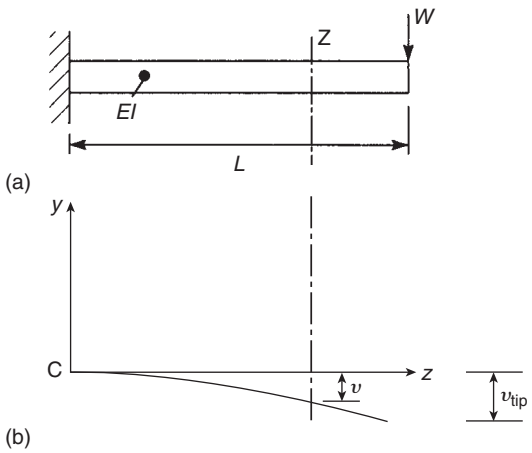

Fig. 16.16 Deflection of a cantilever beam carrying a concentrated load at its free end (Example 16.5).

Substituting for M in the second of Eq. (16.32)

$$v'' = -\frac{W}{EI}(L - z)$$

or in more convenient form

$$EIv'' = -W(L - z) \tag{ii}$$

Integrating Eq. (ii) with respect to z gives

$$EIv'' = -W\left(Lz - \frac{z^2}{2}\right) + C_1$$

where C_1 is a constant of integration which is obtained from the boundary condition that $v' = 0$ at the built-in end where $z = 0$. Hence $C_1 = 0$ and

$$EIv' = -W\left(Lz - \frac{z^2}{2}\right) \tag{iii}$$

Integrating Eq. (iii) we obtain

$$EIv = -W\left(\frac{Lz^2}{2} - \frac{z^3}{6}\right) + C_2$$

in which C_2 is again a constant of integration. At the built-in end $v = 0$ when $z = 0$ so that $C_2 = 0$. Hence the equation of the deflection curve of the cantilever is

$$v = -\frac{W}{6EI}(3Lz^2 - z^3) \tag{iv}$$

The deflection, v_{tip}, at the free end is obtained by setting $z = L$ in Eq. (iv). Then

$$v_{tip} = -\frac{WL^3}{3EI} \tag{v}$$

and is clearly negative and downwards.

Example 16.6

Determine the deflection curve and the deflection of the free end of the cantilever shown in Fig. 16.17(a). The cantilever has a doubly symmetrical cross-section.

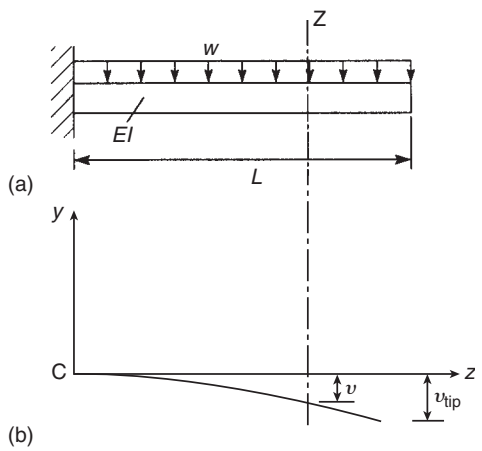

Fig. 16.17 Deflection of a cantilever beam carrying a uniformly distributed load.

The bending moment, M, at any section Z is given by

$$M = \frac{w}{2}(L - z)^2 \tag{i}$$

Substituting for M in the second of Eq. (16.32) and rearranging we have

$$EIv'' = -\frac{w}{2}(L - z)^2 = -\frac{w}{2}(L^2 - 2Lz + z^2) \tag{ii}$$

Integration of Eq. (ii) yields

$$EIv' = -\frac{w}{2}\left(L^2 z - Lz^2 + \frac{z^3}{3}\right) + C_1$$

When $z = 0$ at the built-in end, $v' = 0$ so that $C_1 = 0$ and

$$EIv' = -\frac{w}{2}\left(L^2 z - Lz^2 + \frac{z^3}{3}\right) \tag{iii}$$

Integrating Eq. (iii) we have

$$EIv = -\frac{w}{2}\left(L^2\frac{z^2}{2} - \frac{Lz^3}{3} + \frac{z^4}{12}\right) + C_2$$

and since $v = 0$ when $x = 0$, $C_2 = 0$. The deflection curve of the beam therefore has the equation

$$v = -\frac{w}{24EI}(6L^2z^2 - 4Lz^3 + z^4) \tag{iv}$$

and the deflection at the free end where $x = L$ is

$$v_{\text{tip}} = -\frac{wL^4}{8EI} \tag{v}$$

which is again negative and downwards.

Example 16.7

Determine the deflection curve and the mid-span deflection of the simply supported beam shown in Fig. 16.18(a); the beam has a doubly symmetrical cross-section.

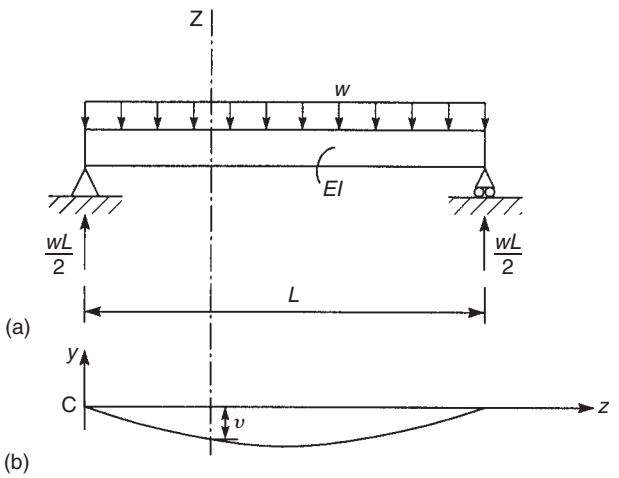

Fig. 16.18 Deflection of a simply supported beam carrying a uniformly distributed load (Example 16.7).

The support reactions are each $wL/2$ and the bending moment, M, at any section Z, a distance z from the left-hand support is

$$M = -\frac{wL}{2}z + \frac{wz^2}{2} \tag{i}$$

Substituting for M in the second of Eq. (16.32) we obtain

$$EIv'' = \frac{w}{2}(Lz - z^2) \tag{ii}$$

Integrating we have

$$EIv' = \frac{w}{2}\left(\frac{Lz^2}{2} - \frac{z^3}{3}\right) + C_1$$

From symmetry it is clear that at the mid-span section the gradient $v' = 0$.
Hence

$$0 = \frac{w}{2}\left(\frac{L^3}{8} - \frac{L^3}{24}\right) + C_1$$

which gives

$$C_1 = -\frac{wL^3}{24}$$

Therefore

$$EIv' = \frac{w}{24}(6Lz^2 - 4z^3 - L^3) \tag{iii}$$

Integrating again gives

$$EIv = \frac{w}{24}(2Lz^3 - z^4 - L^3z) + C_2$$

Since $v = 0$ when $z = 0$ (or since $v = 0$ when $z = L$) it follows that $C_2 = 0$ and the deflected shape of the beam has the equation

$$v = \frac{w}{24EI}(2Lz^3 - z^4 - L^3z) \tag{iv}$$

The maximum deflection occurs at mid-span where $z = L/2$ and is

$$v_{\text{mid-span}} = -\frac{5wL^4}{384EI} \tag{v}$$

So far the constants of integration were determined immediately they arose. However, in some cases a relevant boundary condition, say a value of gradient, is not obtainable. The method is then to carry the unknown constant through the succeeding integration and use known values of deflection at two sections of the beam. Thus in the previous example Eq. (ii) is integrated twice to obtain

$$EIv = \frac{w}{2}\left(\frac{Lz^3}{6} - \frac{z^4}{12}\right) + C_1z + C_2$$

The relevant boundary conditions are $v = 0$ at $z = 0$ and $z = L$. The first of these gives $C_2 = 0$ while from the second we have $C_1 = -wL^3/24$. Thus, the equation of the deflected shape of the beam is

$$v = \frac{w}{24EI}(2Lz^3 - z^4 - L^3z)$$

as before.

Example 16.8

Figure 16.19(a) shows a simply supported beam carrying a concentrated load W at mid-span. Determine the deflection curve of the beam and the maximum deflection if the beam section is doubly symmetrical.

The support reactions are each $W/2$ and the bending moment M at a section Z a distance $z(\leq L/2)$ from the left-hand support is

$$M = -\frac{W}{2}z \tag{i}$$

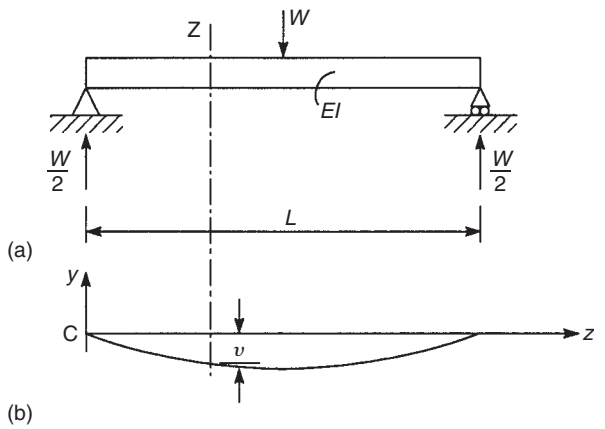

Fig. 16.19 Deflection of a simply supported beam carrying a concentrated load at mid-span (Example 16.8).

From the second of Eq. (16.32) we have

$$EIv'' = \frac{W}{2}z \tag{ii}$$

Integrating we obtain

$$EIv' = \frac{W}{2}\frac{z^2}{2} + C_1$$

From symmetry the slope of the beam is zero at mid-span where $z = L/2$. Thus $C_1 = -WL^2/16$ and

$$EIv' = \frac{W}{16}(4z^2 - L^2) \tag{iii}$$

Integrating Eq. (iii) we have

$$EIv = \frac{W}{16}\left(\frac{4z^3}{3} - L^2 z\right) + C_2$$

and when $z = 0$, $v = 0$ so that $C_2 = 0$. The equation of the deflection curve is, therefore

$$v = \frac{W}{48EI}(4z^3 - 3L^2 z) \tag{iv}$$

The maximum deflection occurs at mid-span and is

$$v_{\text{mid-span}} = -\frac{WL^3}{48EI} \tag{v}$$

Note that in this problem we could not use the boundary condition that $v = 0$ at $z = L$ to determine C_2 since Eq. (i) applies only for $0 \le z \le L/2$; it follows that Eqs (iii) and (iv) for slope and deflection apply only for $0 \le z \le L/2$ although the deflection curve is clearly symmetrical about mid-span.

Examples 16.5–16.8 are frequently regarded as 'standard' cases of beam deflection.

16.3.1 Singularity functions

The double integration method used in Examples 16.5–16.8 becomes extremely lengthy when even relatively small complications such as the lack of symmetry due to an offset load are introduced. For example, the addition of a second concentrated load on a simply supported beam would result in a total of six equations for slope and deflection producing six arbitrary constants. Clearly the computation involved in determining these constants would be tedious, even though a simply supported beam carrying two concentrated loads is a comparatively simple practical case. An alternative approach is to introduce so-called *singularity* or *half-range* functions. Such functions were first applied to beam deflection problems by Macauley in 1919 and hence the method is frequently known as *Macauley's method*.

We now introduce a quantity $[z-a]$ and define it to be zero if $(z-a)<0$, i.e. $z<a$, and to be simply $(z-a)$ if $z>a$. The quantity $[z-a]$ is known as a singularity or half-range function and is defined to have a value only when the argument is positive in which case the square brackets behave in an identical manner to ordinary parentheses.

Example 16.9

Determine the position and magnitude of the maximum upward and downward deflections of the beam shown in Fig. 16.20.

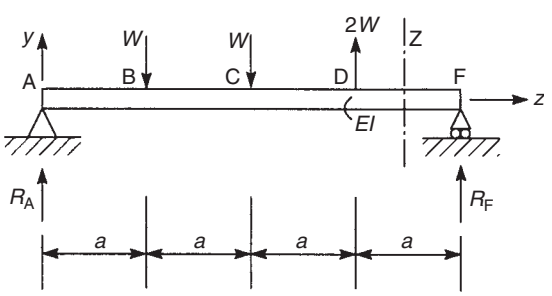

Fig. 16.20 Macauley's method for the deflection of a simply supported beam (Example 16.9).

A consideration of the overall equilibrium of the beam gives the support reactions; thus

$$R_A = \frac{3}{4}W \text{ (upward)} \quad R_F = \frac{3}{4}W \text{ (downward)}$$

Using the method of singularity functions and taking the origin of axes at the left-hand support, we write down an expression for the bending moment, M, at any section Z between D and F, *the region of the beam furthest from the origin*. Thus

$$M = -R_A z + W[z-a] + W[z-2a] - 2W[z-3a] \tag{i}$$

Substituting for M in the second of Eq. (16.32) we have

$$EIv'' = \frac{3}{4}Wz - W[z-a] - W[z-2a] + 2W[z-3a] \tag{ii}$$

Integrating Eq. (ii) and retaining the square brackets we obtain

$$EIv' = \frac{3}{8}Wz^2 - \frac{W}{2}[z-a]^2 - \frac{W}{2}[z-2a]^2 + W[z-3a]^2 + C_1 \qquad \text{(iii)}$$

and

$$EIv = \frac{1}{8}Wz^3 - \frac{W}{6}[z-a]^3 - \frac{W}{6}[z-2a]^3 + \frac{W}{3}[z-3a]^3 + C_1z + C_2 \qquad \text{(iv)}$$

in which C_1 and C_2 are arbitrary constants. When $z = 0$ (at A), $v = 0$ and hence $C_2 = 0$. Note that the second, third and fourth terms on the right-hand side of Eq. (iv) disappear for $z < a$. Also $v = 0$ at $z = 4a$ (F) so that, from Eq. (iv), we have

$$0 = \frac{W}{8}64a^3 - \frac{W}{6}27a^3 - \frac{W}{6}8a^3 + \frac{W}{3}a^3 + 4aC_1$$

which gives

$$C_1 = -\frac{5}{8}Wa^2$$

Equations (iii) and (iv) now become

$$EIv' = \frac{3}{8}Wz^2 - \frac{W}{2}[z-a]^2 - \frac{W}{2}[z-2a]^2 + W[z-3a]^2 - \frac{5}{8}Wa^2 \qquad \text{(v)}$$

and

$$EIv = \frac{1}{8}Wz^3 - \frac{W}{6}[z-a]^3 - \frac{W}{6}[z-2a]^3 + \frac{W}{3}[z-3a]^3 - \frac{5}{8}Wa^2z \qquad \text{(vi)}$$

respectively.

To determine the maximum upward and downward deflections we need to know in which bays $v' = 0$ and thereby which terms in Eq. (v) disappear when the exact positions are being located. One method is to select a bay and determine the sign of the slope of the beam at the extremities of the bay. A change of sign will indicate that the slope is zero within the bay.

By inspection of Fig. 16.20 it seems likely that the maximum downward deflection will occur in BC. At B, using Eq. (v)

$$EIv' = \frac{3}{8}Wa^2 - \frac{5}{8}Wa^2$$

which is clearly negative. At C

$$EIv' = \frac{3}{8}W4a^2 - \frac{W}{2}a^2 - \frac{5}{8}Wa^2$$

which is positive. Therefore, the maximum downward deflection does occur in BC and its exact position is located by equating v' to zero for any section in BC. Thus, from Eq. (v)

$$0 = \frac{3}{8}Wz^2 - \frac{W}{2}[z-a]^2 - \frac{5}{8}Wa^2$$

or, simplifying,

$$0 = z^2 - 8az + 9a^2 \qquad \text{(vii)}$$

Solution of Eq. (vii) gives

$$z = 1.35a$$

so that the maximum downward deflection is, from Eq. (vi)

$$EIv = \frac{1}{8}W(1.35a)^3 - \frac{W}{6}(0.35a)^3 - \frac{5}{8}Wa^2(1.35a)$$

i.e.

$$v_{\max}(\text{downward}) = -\frac{0.54Wa^3}{EI}$$

In a similar manner it can be shown that the maximum upward deflection lies between D and F at $z = 3.42a$ and that its magnitude is

$$v_{\max}(\text{upward}) = \frac{0.04Wa^3}{EI}$$

An alternative method of determining the position of maximum deflection is to select a possible bay, set $v' = 0$ for that bay and solve the resulting equation in z. If the solution gives a value of z that lies within the bay, then the selection is correct, otherwise the procedure must be repeated for a second and possibly a third and a fourth bay. This method is quicker than the former if the correct bay is selected initially; if not, the equation corresponding to each selected bay must be completely solved, a procedure clearly longer than determining the sign of the slope at the extremities of the bay.

Example 16.10

Determine the position and magnitude of the maximum deflection in the beam of Fig. 16.21.

Following the method of Example 16.9 we determine the support reactions and find the bending moment, M, at any section Z in the bay furthest from the origin of the axes.

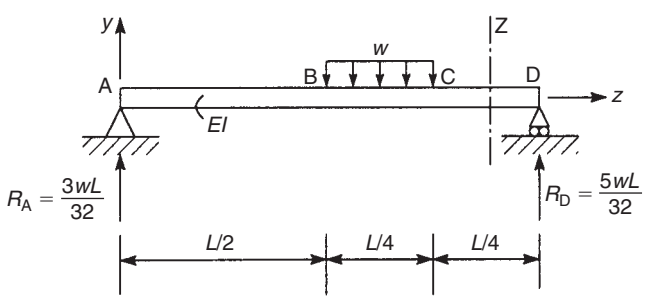

Fig. 16.21 Deflection of a beam carrying a part span uniformly distributed load (Example 16.10).

Then

$$M = -R_A z + w\frac{L}{4}\left[z - \frac{5L}{8}\right] \tag{i}$$

Examining Eq. (i) we see that the singularity function $[z - 5L/8]$ does not become zero until $z \leq 5L/8$ although Eq. (i) is only valid for $z \geq 3L/4$. To obviate this difficulty we extend the distributed load to the support D while simultaneously restoring the *status quo* by applying an upward distributed load of the same intensity and length as the additional load (Fig. 16.22).

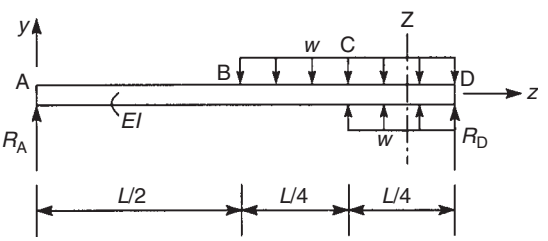

Fig. 16.22 Method of solution for a part span uniformly distributed load.

At the section Z, a distance z from A, the bending moment is now given by

$$M = -R_A z + \frac{w}{2}\left[z - \frac{L}{2}\right]^2 - \frac{w}{2}\left[z - \frac{3L}{4}\right]^2 \tag{ii}$$

Equation (ii) is now valid for all sections of the beam if the singularity functions are discarded as they become zero. Substituting Eq. (ii) into the second of Eqs (16.32) we obtain

$$EIv'' = \frac{3}{32}wLz - \frac{w}{2}\left[z - \frac{L}{2}\right]^2 + \frac{w}{2}\left[z - \frac{3L}{4}\right]^2 \tag{iii}$$

Integrating Eq. (iii) gives

$$EIv' = \frac{3}{64}wLz^2 - \frac{w}{6}\left[z - \frac{L}{2}\right]^3 + \frac{w}{6}\left[z - \frac{3L}{4}\right]^3 + C_1 \tag{iv}$$

$$EIv = \frac{wLz^3}{64} - \frac{w}{24}\left[z - \frac{L}{2}\right]^4 + \frac{w}{24}\left[z - \frac{3L}{4}\right]^4 + C_1 z + C_2 \tag{v}$$

where C_1 and C_2 are arbitrary constants. The required boundary conditions are $v = 0$ when $z = 0$ and $z = L$. From the first of these we obtain $C_2 = 0$ while the second gives

$$0 = \frac{wL^4}{64} - \frac{w}{24}\left(\frac{L}{2}\right)^4 + \frac{w}{24}\left(\frac{L}{4}\right)^4 + C_1 L$$

from which

$$C_1 = -\frac{27wL^3}{2048}$$

Equations (iv) and (v) then become

$$EIv' = \frac{3}{64}wLz^2 - \frac{w}{6}\left[z - \frac{L}{2}\right]^3 + \frac{w}{6}\left[z - \frac{3L}{4}\right]^3 - \frac{27wL^3}{2048} \qquad \text{(vi)}$$

and

$$EIv = \frac{wLz^3}{64} - \frac{w}{24}\left[z - \frac{L}{2}\right]^4 + \frac{w}{24}\left[z - \frac{3L}{4}\right]^4 - \frac{27wL^3}{2048}z \qquad \text{(vii)}$$

In this problem, the maximum deflection clearly occurs in the region BC of the beam. Thus equating the slope to zero for BC we have

$$0 = \frac{3}{64}wLz^2 - \frac{w}{6}\left[z - \frac{L}{2}\right]^3 - \frac{27wL^3}{2048}$$

which simplifies to

$$z^3 - 1.78Lz^2 + 0.75zL^2 - 0.046L^3 = 0 \qquad \text{(viii)}$$

Solving Eq. (viii) by trial and error, we see that the slope is zero at $z \simeq 0.6L$. Hence from Eq. (vii) the maximum deflection is

$$v_{\max} = -\frac{4.53 \times 10^{-3}wL^4}{EI}$$

Example 16.11

Determine the deflected shape of the beam shown in Fig. 16.23.

In this problem an external moment M_0 is applied to the beam at B. The support reactions are found in the normal way and are

$$R_A = -\frac{M_0}{L}(\text{downwards}) \quad R_C = \frac{M_0}{L}(\text{upwards})$$

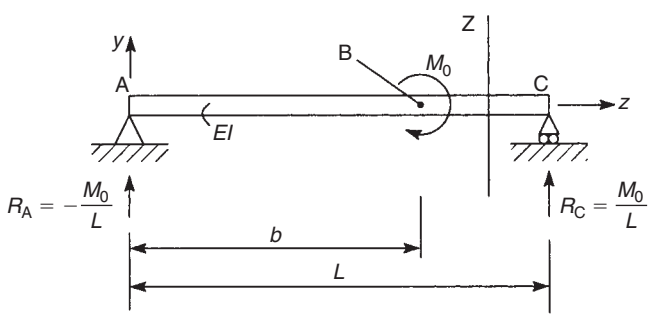

Fig. 16.23 Deflection of a simply supported beam carrying a point moment (Example 16.11).

The bending moment at any section Z between B and C is then given by

$$M = -R_A z - M_0 \tag{i}$$

Equation (i) is valid only for the region BC and clearly does not contain a singularity function which would cause M_0 to vanish for $z \leq b$. We overcome this difficulty by writing

$$M = -R_A z - M_0[z-b]^0 \quad \text{(Note: } [z-b]^0 = 1\text{)} \tag{ii}$$

Equation (ii) has the same value as Eq. (i) but is now applicable to all sections of the beam since $[z-b]^0$ disappears when $z \leq b$. Substituting for M from Eq. (ii) in the second of Eq. (16.32) we obtain

$$EIv'' = R_A z + M_0[z-b]^0 \tag{iii}$$

Integration of Eq. (iii) yields

$$EIv' = R_A \frac{z^2}{2} + M_0[z-b] + C_1 \tag{vi}$$

and

$$EIv = R_A \frac{z^3}{6} + \frac{M_0}{2}[z-b]^2 + C_1 z + C_2 \tag{v}$$

where C_1 and C_2 are arbitrary constants. The boundary conditions are $v = 0$ when $z = 0$ and $z = L$. From the first of these we have $C_2 = 0$ while the second gives

$$0 = -\frac{M_0}{L}\frac{L^3}{6} + \frac{M_0}{2}[L-b]^2 + C_1 L$$

from which

$$C_1 = -\frac{M_0}{6L}(2L^2 - 6Lb + 3b^2)$$

The equation of the deflection curve of the beam is then

$$v = \frac{M_0}{6EIL}\{z^3 + 3L[z-b]^2 - (2L^2 - 6Lb + 3b^2)z\} \tag{vi}$$

Example 16.12

Determine the horizontal and vertical components of the tip deflection of the cantilever shown in Fig. 16.24. The second moments of area of its unsymmetrical section are I_{xx}, I_{yy} and I_{xy}.

From Eqs (16.29)

$$u'' = \frac{M_x I_{xy} - M_y I_{xx}}{E(I_{xx}I_{yy} - I_{xy}^2)} \tag{i}$$

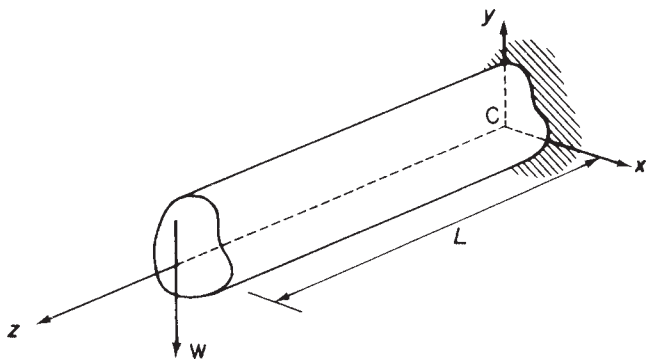

Fig. 16.24 Determination of the deflection of a cantilever.

In this case $M_x = W(L - z)$, $M_y = 0$ so that Eq. (i) simplifies to

$$u'' = \frac{WI_{xy}}{E(I_{xx}I_{yy} - I_{xy}^2)}(L - z) \tag{ii}$$

Integrating Eq. (ii) with respect to z

$$u' = \frac{WI_{xy}}{E(I_{xx}I_{yy} - I_{xy}^2)}\left(Lz - \frac{z^2}{2} + A\right) \tag{iii}$$

and

$$u = \frac{WI_{xy}}{E(I_{xx}I_{yy} - I_{xy}^2)}\left(L\frac{z^2}{2} - \frac{z^3}{6} + Az + B\right) \tag{iv}$$

in which u' denotes du/dz and the constants of integration A and B are found from the boundary conditions, viz. $u' = 0$ and $u = 0$ when $z = 0$. From the first of these and Eq. (iii), $A = 0$, while from the second and Eq. (iv), $B = 0$. Hence the deflected shape of the beam in the xz plane is given by

$$u = \frac{WI_{xy}}{E(I_{xx}I_{yy} - I_{xy}^2)}\left(L\frac{z^2}{2} - \frac{z^3}{6}\right) \tag{v}$$

At the free end of the cantilever ($z = L$) the horizontal component of deflection is

$$u_{\text{f.e.}} = \frac{WI_{xy}L^3}{3E(I_{xx}I_{yy} - I_{xy}^2)} \tag{vi}$$

Similarly, the vertical component of the deflection at the free end of the cantilever is

$$v_{\text{f.e.}} = \frac{-WI_{yy}L^3}{3E(I_{xx}I_{yy} - I_{xy}^2)} \tag{vii}$$

The actual deflection $\delta_{\text{f.e.}}$ at the free end is then given by

$$\delta_{\text{f.e.}} = (u_{\text{f.e.}}^2 + v_{\text{f.e.}}^2)^{\frac{1}{2}}$$

at an angle of $\tan^{-1} u_{\text{f.e.}}/v_{\text{f.e.}}$ to the vertical.

Note that if either Cx or Cy were an axis of symmetry, $I_{xy} = 0$ and Eqs (vi) and (vii) reduce to

$$u_{\text{f.e.}} = 0 \quad v_{\text{f.e.}} = \frac{-WL^3}{3EI_{xx}}$$

the well-known results for the bending of a cantilever having a symmetrical cross-section and carrying a concentrated vertical load at its free end (see Example 16.5).

16.4 Calculation of section properties

It will be helpful at this stage to discuss the calculation of the various section properties required in the analysis of beams subjected to bending. Initially, however, two useful theorems are quoted.

16.4.1 Parallel axes theorem

Consider the beam section shown in Fig. 16.25 and suppose that the second moment of area, I_C, about an axis through its centroid C is known. The second moment of area, I_N, about a parallel axis, NN, a distance b from the centroidal axis is then given by

$$I_N = I_C + Ab^2 \tag{16.33}$$

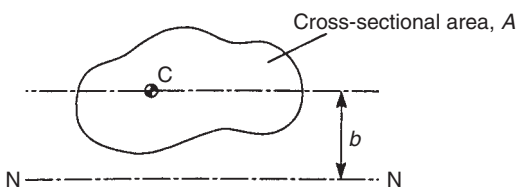

Fig. 16.25 Parallel axes theorem.

16.4.2 Theorem of perpendicular axes

In Fig. 16.26 the second moments of area, I_{xx} and I_{yy}, of the section about Ox and Oy are known. The second moment of area about an axis through O perpendicular to the

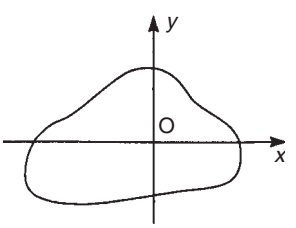

Fig. 16.26 Theorem of perpendicular axes.

plane of the section (i.e. a *polar second moment of area*) is then

$$I_o = I_{xx} + I_{yy} \tag{16.34}$$

16.4.3 Second moments of area of standard sections

Many sections may be regarded as comprising a number of rectangular shapes. The problem of determining the properties of such sections is simplified if the second moments of area of the rectangular components are known and use is made of the parallel axes theorem. Thus, for the rectangular section of Fig. 16.27.

$$I_{xx} = \int_A y^2 \mathrm{d}A = \int_{-d/2}^{d/2} by^2 \mathrm{d}y = b\left[\frac{y^3}{3}\right]_{-d/2}^{d/2}$$

which gives

$$I_{xx} = \frac{bd^3}{12} \tag{16.35}$$

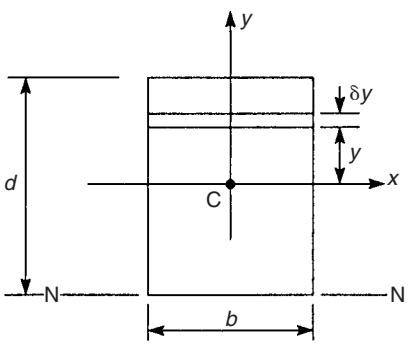

Fig. 16.27 Second moments of area of a rectangular section.

Similarly

$$I_{yy} = \frac{db^3}{12} \tag{16.36}$$

Frequently it is useful to know the second moment of area of a rectangular section about an axis which coincides with one of its edges. Thus in Fig. 16.27, and using the parallel axes theorem

$$I_N = \frac{bd^3}{12} + bd\left(-\frac{d}{2}\right)^2 = \frac{bd^3}{3} \tag{16.37}$$

Example 16.13

Determine the second moments of area I_{xx} and I_{yy} of the I-section shown in Fig. 16.28.

Using Eq. (16.35)

$$I_{xx} = \frac{bd^3}{12} - \frac{(b - t_w)d_w^3}{12}$$

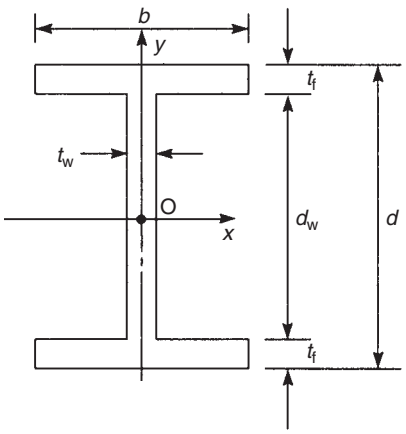

Fig. 16.28 Second moments of area of an I-Section.

Alternatively, using the parallel axes theorem in conjunction with Eq. (16.35)

$$I_{xx} = 2\left[\frac{bt_f^3}{12} + bt_f\left(\frac{d_{w+t_f}}{2}\right)^2\right] + \frac{t_w d_w^3}{12}$$

The equivalence of these two expressions for I_{xx} is most easily demonstrated by a numerical example.

Also, from Eq. (16.36)

$$I_{yy} = 2\frac{t_f b^3}{12} + \frac{d_w t_w^3}{12}$$

It is also useful to determine the second moment of area, about a diameter, of a circular section. In Fig. 16.29 where the x and y axes pass through the centroid of the section

$$I_{xx} = \int_A y^2 \mathrm{d}A = \int_{-d/2}^{d/2} 2\left(\frac{d}{2}\cos\theta\right) y^2 \mathrm{d}y \tag{16.38}$$

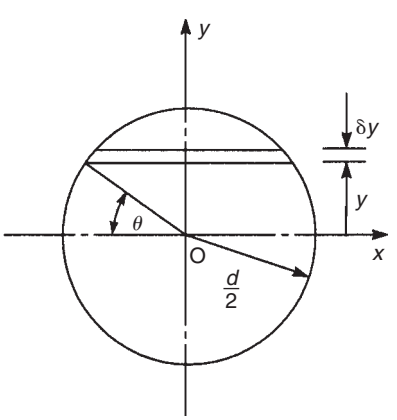

Fig. 16.29 Second moments of area of a circular section.

Integration of Eq. (16.38) is simplified if an angular variable, θ, is used. Thus

$$I_{xx} = \int_{-\pi/2}^{\pi/2} d\cos\theta \left(\frac{d}{2}\sin\theta\right)^2 \frac{d}{2}\cos\theta\,\mathrm{d}\theta$$

i.e.

$$I_{xx} = \frac{d^4}{8}\int_{-\pi/2}^{\pi/2} \cos^2\theta\,\sin^2\theta\,\mathrm{d}\theta$$

which gives

$$I_{xx} = \frac{\pi d^4}{64} \tag{16.39}$$

Clearly from symmetry

$$I_{yy} = \frac{\pi d^4}{64} \tag{16.40}$$

Using the theorem of perpendicular axes, the polar second moment of area, I_o, is given by

$$I_o = I_{xx} + I_{yy} = \frac{\pi d^4}{32} \tag{16.41}$$

16.4.4 Product second moment of area

The product second moment of area, I_{xy}, of a beam section with respect to x and y axes is defined by

$$I_{xy} = \int_A xy\,\mathrm{d}A \tag{16.42}$$

Thus each element of area in the cross-section is multiplied by the product of its coordinates and the integration is taken over the complete area. Although second moments of area are always positive since elements of area are multiplied by the square of one of their coordinates, it is possible for I_{xy} to be negative if the section lies predominantly in the second and fourth quadrants of the axes system. Such a situation would arise in the case of the Z-section of Fig. 16.30(a) where the product second moment of area of each flange is clearly negative.

A special case arises when one (or both) of the coordinate axes is an axis of symmetry so that for any element of area, δA, having the product of its coordinates positive, there is an identical element for which the product of its coordinates is negative (Fig. 16.30 (b)). Summation (i.e. integration) over the entire section of the product second moment of area of all such pairs of elements results in a zero value for I_{xy}.

We have shown previously that the parallel axes theorem may be used to calculate second moments of area of beam sections comprising geometrically simple components. The theorem can be extended to the calculation of product second moments of area. Let us suppose that we wish to calculate the product second moment of area,

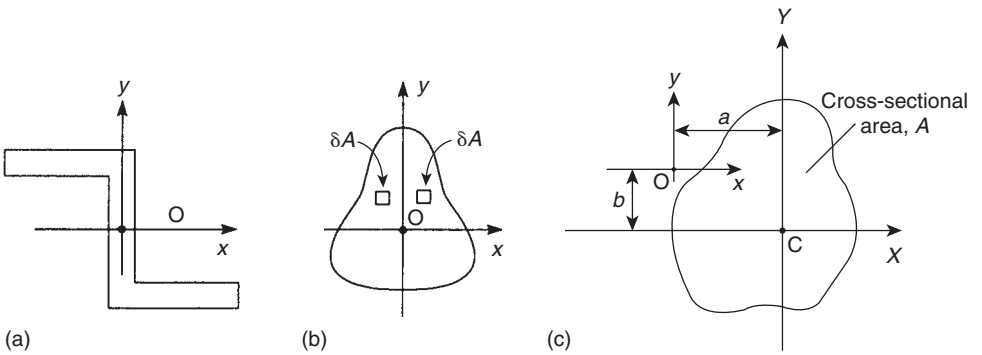

Fig. 16.30 Product second moment of area.

I_{xy}, of the section shown in Fig. 16.30(c) about axes xy when I_{XY} about its own, say centroidal, axes system CXY is known. From Eq. (16.42)

$$I_{xy} = \int_A xy \, \mathrm{d}A$$

or

$$I_{xy} = \int_A (X - a)(Y - b)\mathrm{d}A$$

which, on expanding, gives

$$I_{xy} = \int_A XY \, \mathrm{d}A - b\int_A X\mathrm{d}A - a\int_A Y \, \mathrm{d}A + ab\int_A \mathrm{d}A$$

If X and Y are centroidal axes then $\int_A X \, \mathrm{d}A = \int_A Y \, \mathrm{d}A = 0$. Hence

$$I_{xy} = I_{XY} + abA \tag{16.43}$$

It can be seen from Eq. (16.43) that if either CX or CY is an axis of symmetry, i.e. $I_{XY} = 0$, then

$$I_{xy} = abA \tag{16.44}$$

Therefore for a section component having an axis of symmetry that is parallel to either of the section reference axes the product second moment of area is the product of the coordinates of its centroid multiplied by its area.

16.4.5 Approximations for thin-walled sections

We may exploit the thin-walled nature of aircraft structures to make simplifying assumptions in the determination of stresses and deflections produced by bending. Thus, the thickness t of thin-walled sections is assumed to be small compared with their cross-sectional dimensions so that stresses may be regarded as being constant across the thickness. Furthermore, we neglect squares and higher powers of t in the computation

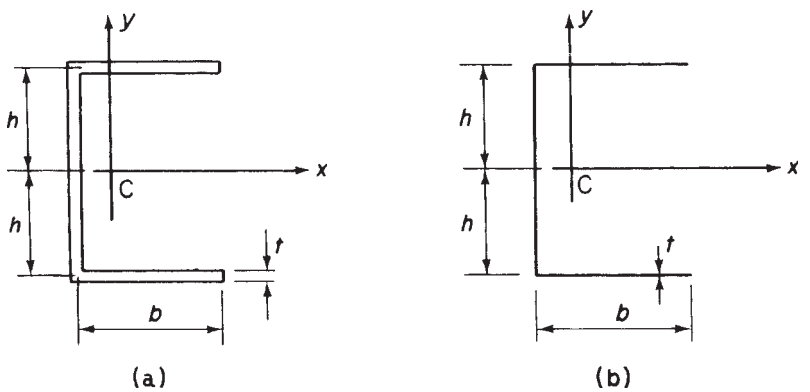

Fig. 16.31 (a) Actual thin-walled channel section; (b) approximate representation of section.

of sectional properties and take the section to be represented by the mid-line of its wall. As an illustration of the procedure we shall consider the channel section of Fig. 16.31(a). The section is singly symmetric about the x axis so that $I_{xy} = 0$. The second moment of area I_{xx} is then given by

$$I_{xx} = 2\left[\frac{(b + t/2)t^3}{12} + \left(b + \frac{t}{2}\right)th^2\right] + t\frac{[2(h - t/2)]^3}{12}$$

Expanding the cubed term we have

$$I_{xx} = 2\left[\frac{(b + t/2)t^3}{12} + \left(b + \frac{t}{2}\right)th^2\right] + \frac{t}{12}\left[(2)^3\left(h^3 - 3h^2\frac{t}{2} + 3h\frac{t^2}{4} - \frac{t^3}{8}\right)\right]$$

which reduces, after powers of t^2 and upwards are ignored, to

$$I_{xx} = 2bth^2 + t\frac{(2h)^3}{12}$$

The second moment of area of the section about Cy is obtained in a similar manner.

We see, therefore, that for the purpose of calculating section properties we may regard the section as being represented by a single line, as shown in Fig. 16.31(b).

Thin-walled sections frequently have inclined or curved walls which complicate the calculation of section properties. Consider the inclined thin section of Fig. 16.32. Its second moment of area about a horizontal axis through its centroid is given by

$$I_{xx} = 2\int_0^{a/2} ty^2\,\mathrm{d}s = 2\int_0^{a/2} t(s\sin\beta)^2\,\mathrm{d}s$$

from which

$$I_{xx} = \frac{a^3 t\sin^2\beta}{12}$$

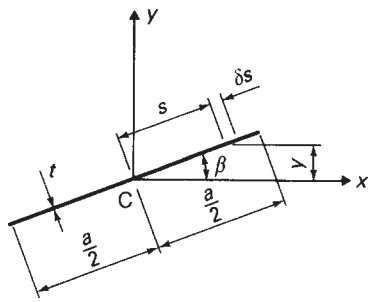

Fig. 16.32 Second moments of area of an inclined thin section.

Similarly

$$I_{yy} = \frac{a^3 t \cos^2 \beta}{12}$$

The product second moment of area is

$$\begin{aligned} I_{xy} &= 2\int_0^{a/2} txy \, \mathrm{d}s \\ &= 2\int_0^{a/2} t(s\cos\beta)(s\sin\beta)\, \mathrm{d}s \end{aligned}$$

which gives

$$I_{xy} = \frac{a^3 t \sin 2\beta}{24}$$

We note here that these expressions are approximate in that their derivation neglects powers of t^2 and upwards by ignoring the second moments of area of the element δs about axes through its own centroid.

Properties of thin-walled curved sections are found in a similar manner. Thus, I_{xx} for the semicircular section of Fig. 16.33 is

$$I_{xx} = \int_0^{\pi r} ty^2 \, \mathrm{d}s$$

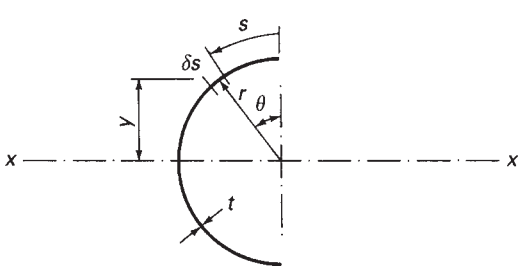

Fig. 16.33 Second moment of area of a semicircular section.

Expressing y and s in terms of a single variable θ simplifies the integration, hence

$$I_{xx} = \int_0^{\pi} t(r\cos\theta)^2 r\,\mathrm{d}\theta$$

from which

$$I_{xx} = \frac{\pi r^3 t}{2}$$

Example 16.14

Determine the direct stress distribution in the thin-walled Z-section shown in Fig. 16.34, produced by a positive bending moment M_x.

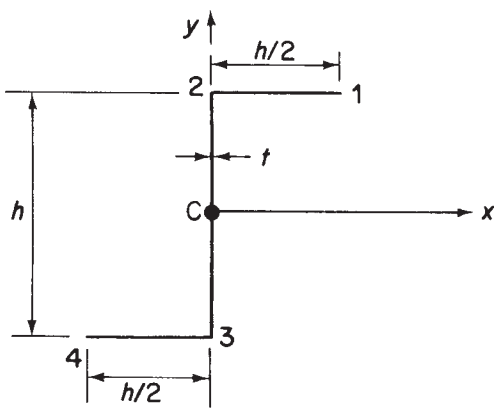

Fig. 16.34 *Z*-section beam of Example 16.14.

The section is antisymmetrical with its centroid at the mid-point of the vertical web. Therefore, the direct stress distribution is given by either of Eq. (16.18) or (16.19) in which $M_y = 0$. From Eq. (16.19)

$$\sigma_z = \frac{M_x(I_{yy}y - I_{xy}x)}{I_{xx}I_{yy} - I_{xy}^2} \tag{i}$$

The section properties are calculated as follows

$$I_{xx} = 2\frac{ht}{2}\left(\frac{h}{2}\right)^2 + \frac{th^3}{12} = \frac{h^3 t}{3}$$

$$I_{yy} = 2\frac{t}{3}\left(\frac{h}{2}\right)^3 = \frac{h^3 t}{12}$$

$$I_{xy} = \frac{ht}{2}\left(\frac{h}{4}\right)\left(\frac{h}{2}\right) + \frac{ht}{2}\left(-\frac{h}{4}\right)\left(-\frac{h}{2}\right) = \frac{h^3 t}{8}$$

Substituting these values in Eq. (i)

$$\sigma_z = \frac{M_x}{h^3 t}(6.86y - 10.30x) \tag{ii}$$

On the top flange $y = h/2$, $0 \leq x \leq h/2$ and the distribution of direct stress is given by

$$\sigma_z = \frac{M_x}{h^3 t}(3.43h - 10.30x)$$

which is linear. Hence

$$\sigma_{z,1} = -\frac{1.72M_x}{h^3 t} \quad \text{(compressive)}$$

$$\sigma_{z,2} = +\frac{3.43M_x}{h^3 t} \quad \text{(tensile)}$$

In the web $h/2 \leq y \leq -h/2$ and $x = 0$. Again the distribution is of linear form and is given by the equation

$$\sigma_z = \frac{M_x}{h^3 t}6.86y$$

whence

$$\sigma_{z,2} = +\frac{3.43M_x}{h^3 t} \quad \text{(tensile)}$$

and

$$\sigma_{z,3} = -\frac{3.43M_x}{h^3 t} \quad \text{(compressive)}$$

The distribution in the lower flange may be deduced from antisymmetry; the complete distribution is then as shown in Fig. 16.35.

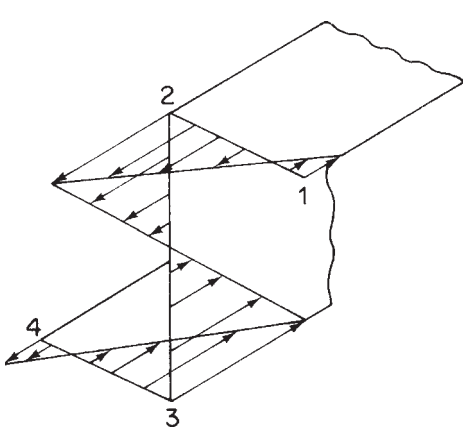

Fig. 16.35 Distribution of direct stress in *Z*-section beam of Example 16.14.

16.5 Applicability of bending theory

The expressions for direct stress and displacement derived in the above theory are based on the assumptions that the beam is of uniform, homogeneous cross-section and that plane sections remain plane after bending. The latter assumption is strictly true only if the bending moments M_x and M_y are constant along the beam. Variation of bending moment implies the presence of shear loads and the effect of these is to deform the beam section into a shallow, inverted 's' (see Section 2.6). However, shear stresses in beams whose cross-sectional dimensions are small in relation to their lengths are comparatively low so that the basic theory of bending may be used with reasonable accuracy.

In thin-walled sections shear stresses produced by shear loads are not small and must be calculated, although the direct stresses may still be obtained from the basic theory of bending so long as axial constraint stresses are absent; this effect is discussed in Chapters 26 and 27. Deflections in thin-walled structures are assumed to result primarily from bending strains; the contribution of shear strains may be calculated separately if required.

16.6 Temperature effects

In Section 1.15.1 we considered the effect of temperature change on stress–strain relationships while in Section 5.11 we examined the effect of a simple temperature gradient on a cantilever beam of rectangular cross-section using an energy approach. However, as we have seen, beam sections in aircraft structures are generally thin walled and do not necessarily have axes of symmetry. We shall now investigate how the effects of temperature on such sections may be determined.

We have seen that the strain produced by a temperature change ΔT is given by

$$\varepsilon = \alpha\,\Delta T \qquad \text{(see Eq. (1.55))}$$

It follows from Eq. (1.40) that the direct stress on an element of cross-sectional area δA is

$$\sigma = E\alpha\,\Delta T\,\delta A \tag{16.45}$$

Consider now the beam section shown in Fig. 16.36 and suppose that a temperature variation ΔT is applied to the complete cross-section, i.e. ΔT is a function of both x and y.

The total normal force due to the temperature change on the beam cross-section is then given by

$$N_T = \int\int_A E\alpha\,\Delta T\,\mathrm{d}A \tag{16.46}$$

Further, the moments about the x and y axes are

$$M_{xT} = \int\int_A E\alpha\,\Delta T y\,\mathrm{d}A \tag{16.47}$$

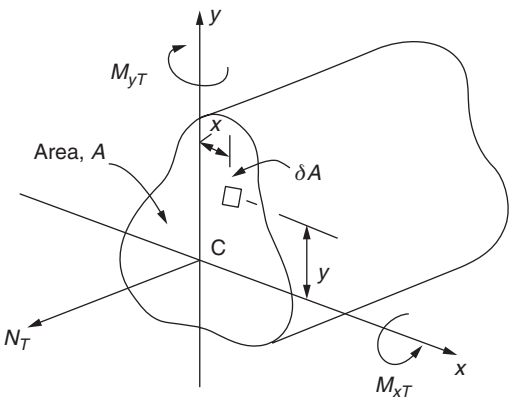

Fig. 16.36 Beam section subjected to a temperature rise.

and

$$M_{yT} = \int\int_A E\alpha\,\Delta T x\,\mathrm{d}A \tag{16.48}$$

respectively.

We have noted that beam sections in aircraft structures are generally thin walled so that Eqs (16.46)–(16.48) may be more easily integrated for such sections by dividing them into thin rectangular components as we did when calculating section properties. We then use the Riemann integration technique in which we calculate the contribution of each component to the normal force and moments and sum them to determine each resultant. Equations (16.46)–(16.48) then become

$$N_T = \Sigma E\alpha\,\Delta T\,A_i \tag{16.49}$$

$$M_{xT} = \Sigma E\alpha\,\Delta T\bar{y}_i\,A_i \tag{16.50}$$

$$M_{yT} = \Sigma E\alpha\,\Delta T\bar{x}_i\,A_i \tag{16.51}$$

in which A_i is the cross-sectional area of a component and $\bar{x}_i$ and $\bar{y}_i$ are the coordinates of its centroid.

Example 16.15

The beam section shown in Fig. 16.37 is subjected to a temperature rise of $2T_0$ in its upper flange, a temperature rise of T_0 in its web and zero temperature change in its lower flange. Determine the normal force on the beam section and the moments about the centroidal x and y axes. The beam section has a Young's modulus E and the coefficient of linear expansion of the material of the beam is α.

From Eq. (16.49)

$$N_T = E\alpha(2T_0\,at + T_0\,2at) = 4E\alpha\,at\,T_0$$

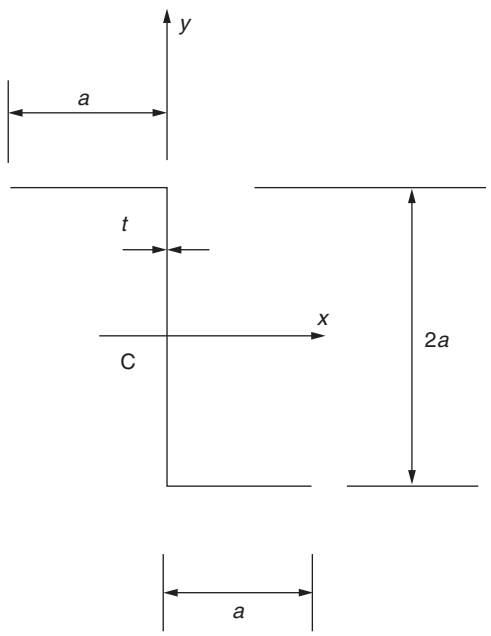

Fig. 16.37 Beam section of Example 16.15.

From Eq. (16.50)

$$M_{xT} = E\alpha[2T_0\, at(a) + T_0\, 2at(0)] = 2E\alpha\, a^2 t\, T_0$$

and from Eq. (16.51)

$$M_{yT} = E\alpha[2T_0\, at(-a/2) + T_0\, 2at(0)] = -E\alpha\, a^2 t\, T_0$$

Note that M_{yT} is negative which means that the upper flange would tend to rotate out of the paper about the web which agrees with a temperature rise for this part of the section. The stresses corresponding to the above stress resultants are calculated in the normal way and are added to those produced by any applied loads.

In some cases the temperature change is not conveniently constant in the components of a beam section and must then be expressed as a function of x and y. Consider the thin-walled beam section shown in Fig. 16.38 and suppose that a temperature change $\Delta T\ (x, y)$ is applied.

The direct stress on an element δs in the wall of the section is then, from Eq. (16.45)

$$\sigma = E\alpha\, \Delta T(x, y) t\, \delta s$$

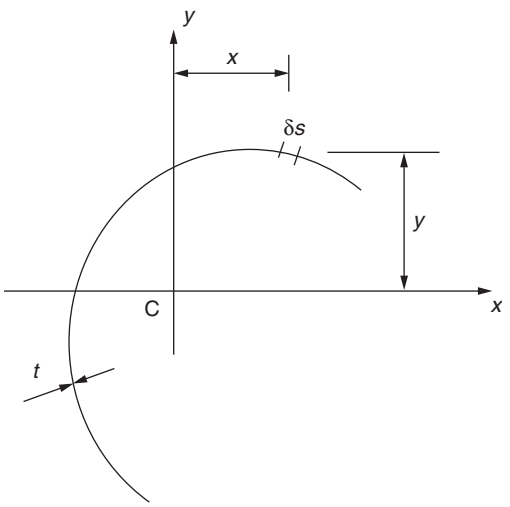

Fig. 16.38 Thin-walled beam section subjected to a varying temperature change.

Equations (16.46)–(16.48) then become

$$N_T = \int_A E\alpha\, \Delta T(x, y) t \, \mathrm{d}s \tag{16.52}$$

$$M_{xT} = \int_A E\alpha\, \Delta T(x, y) t y \, \mathrm{d}s \tag{16.53}$$

$$M_{yT} = \int_A E\alpha\, \Delta T(x, y) t x \, \mathrm{d}s \tag{16.54}$$

Example 16.16

If, in the beam section of Example 16.15, the temperature change in the upper flange is $2T_0$ but in the web varies linearly from $2T_0$ at its junction with the upper flange to zero at its junction with the lower flange determine the values of the stress resultants; the temperature change in the lower flange remains zero.

The temperature change at any point in the web is given by

$$T_\mathrm{w} = 2T_0(a + y)/2a = \frac{T_0}{a}(a + y)$$

Then, from Eqs (16.49) and (16.52)

$$N_T = E\alpha\, 2T_0\, at + \int_{-a}^{a} E\alpha \frac{T_0}{a}(a + y) t \, \mathrm{d}s$$

$$\text{i.e.} \quad N_T = E\alpha\, T_0 \left\{ 2at + \frac{1}{a}\left[ay + \frac{y^2}{2} \right]_{-a}^{a} \right\}$$

which gives

$$N_T = 4E\alpha\, T_0\, at$$

Note that, in this case, the answer is identical to that in Example 16.15 which is to be expected since the average temperature change in the web is $(2T_0 + 0)/2 = T_0$ which is equal to the constant temperature change in the web in Example 16.15.

From Eqs (16.50) and (16.53)

$$M_{xT} = E\alpha\, 2T_0 at(a) + \int_{-a}^{a} E\alpha \frac{T_0}{a}(a + y)yt\, \mathrm{d}s$$

i.e.

$$M_{xT} = E\alpha\, T_0 \left\{ 2a^2 t + \frac{1}{a}\left[\frac{ay^2}{2} + \frac{y^3}{3} \right]_{-a}^{a} \right\}$$

from which

$$M_{xT} = \frac{8E\alpha a^2 t T_0}{3}$$

Alternatively, the average temperature change T_0 in the web may be considered to act at the centroid of the temperature change distribution. Then

$$M_{xT} = E\alpha\, 2T_0 at(a) + E\alpha T_0 2at\left(\frac{a}{3}\right)$$

i.e.

$$M_{xT} = \frac{8E\alpha a^2 t T_0}{3} \quad \text{as before}$$

The contribution of the temperature change in the web to M_{yT} remains zero since the section centroid is in the web; the value of M_{yT} is therefore $-E\alpha a^2 t T_0$ as in Example 16.14.

References

1 Megson, T. H. G., *Structures and Stress Analysis*, 2nd edition, Elsevier, Oxford, 2005.

Problems

P.16.1 Figure P.16.1 shows the section of an angle purlin. A bending moment of 3000 N m is applied to the purlin in a plane at an angle of 30° to the vertical y axis. If the sense of the bending moment is such that its components M_x and M_y both produce tension in the positive xy quadrant, calculate the maximum direct stress in the purlin stating clearly the point at which it acts.

Ans. $\sigma_{z,\max} = -63.3\ \mathrm{N/mm^2}$ at C.

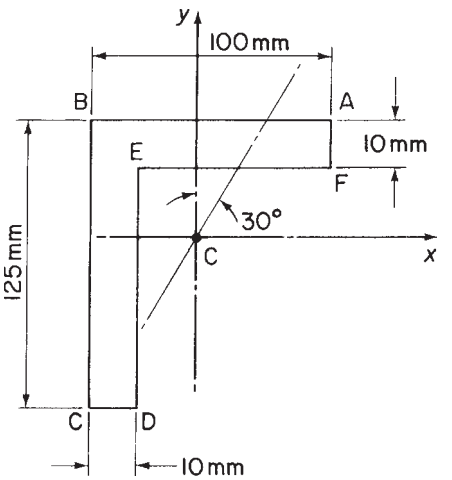

Fig. P.16.1

P.16.2 A thin-walled, cantilever beam of unsymmetrical cross-section supports shear loads at its free end as shown in Fig. P.16.2. Calculate the value of direct stress at the extremity of the lower flange (point A) at a section half-way along the beam if the position of the shear loads is such that no twisting of the beam occurs.

Ans. 194.7 N/mm^2 (tension).

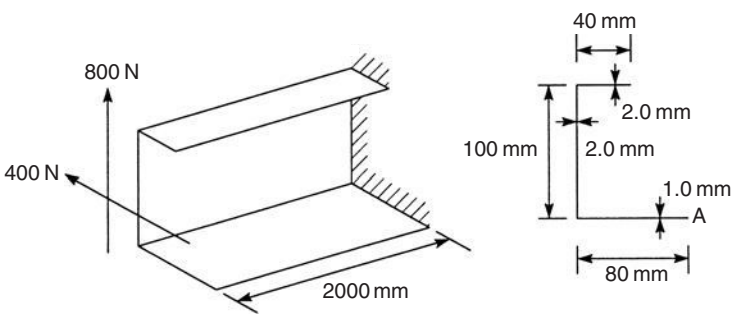

Fig. P.16.2

P.16.3 A beam, simply supported at each end, has a thin-walled cross-section shown in Fig. P.16.3. If a uniformly distributed loading of intensity w/unit length acts on the beam in the plane of the lower, horizontal flange, calculate the maximum direct stress due to bending of the beam and show diagrammatically the distribution of the stress at the section where the maximum occurs.

The thickness t is to be taken as small in comparison with the other cross-sectional dimensions in calculating the section properties I_{xx}, I_{yy} and I_{xy}.

Ans. $\sigma_{z,\max} = \sigma_{z,3} = 13wl^2/384a^2t,\ \sigma_{z,1} = wl^2/96a^2t,\ \sigma_{z,2} = -wl^2/48a^2t.$

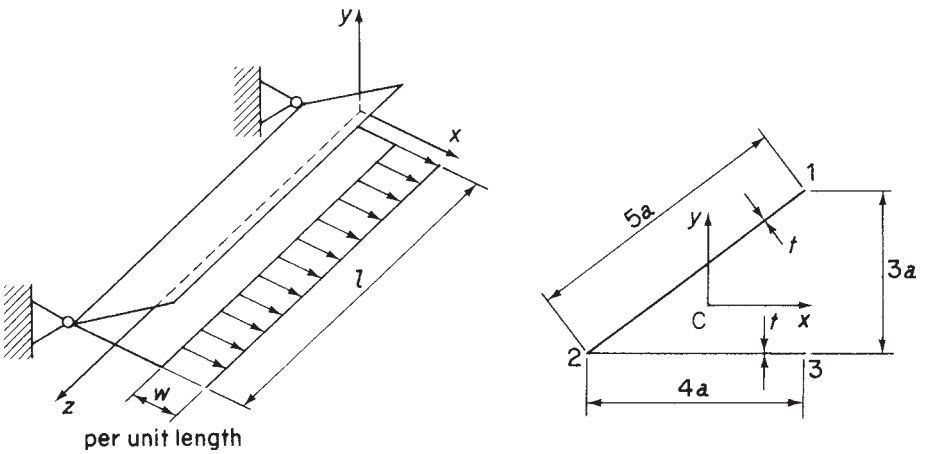

Fig. P.16.3

P.16.4 A thin-walled cantilever with walls of constant thickness t has the cross-section shown in Fig. P.16.4. It is loaded by a vertical force W at the tip and a horizontal force $2W$ at the mid-section, both forces acting through the shear centre. Determine and sketch the distribution of direct stress, according to the basic theory of bending, along the length of the beam for the points 1 and 2 of the cross-section.

The wall thickness t can be taken as very small in comparison with d in calculating the sectional properties I_{xx}, I_{xy}, etc.

Ans. $\sigma_{z,1}$ (mid-point) $= -0.05\, Wl/td^2$, $\sigma_{z,1}$ (built-in end) $= -1.85\, Wl/td^2$
$\sigma_{z,2}$ (mid-point) $= -0.63\, Wl/td^2$, $\sigma_{z,2}$ (built-in end) $= 0.1\, Wl/td^2$.

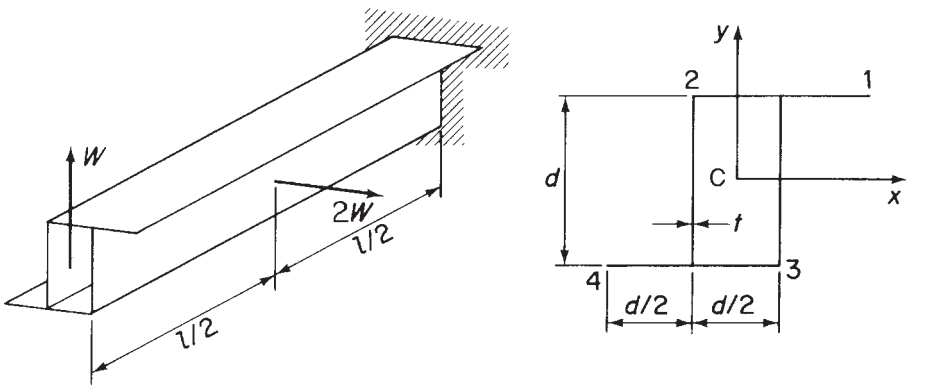

Fig. P.16.4

P. 16.5 A thin-walled beam has the cross-section shown in Fig. P.16.5. If the beam is subjected to a bending moment M_x in the plane of the web 23 calculate and sketch the distribution of direct stress in the beam cross-section.

Ans. At 1, $0.92M_x/th^2$; At 2, $-0.65M_x/th^2$; At 3, $0.65M_x/th^2$;
At 4, $-0.135M_x/th^2$

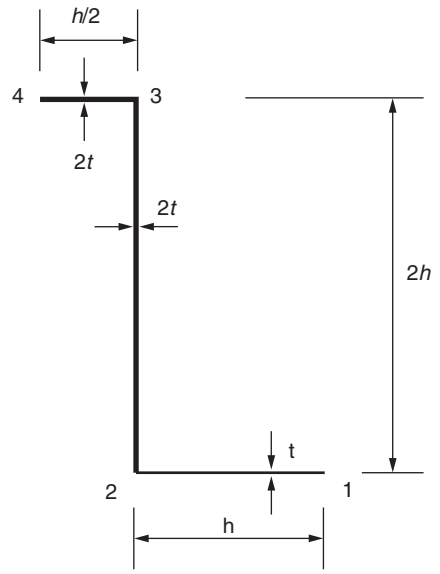

Fig. P.16.5

P.16.6 The thin-walled beam section shown in Fig. P.16.6 is subjected to a bending moment M_x applied in a negative sense. Find the position of the neutral axis and the maximum direct stress in the section.

Ans. NA inclined at 40.9° to Cx. $\pm 0.74\, M_x/ta^2$ at 1 and 2, respectively.

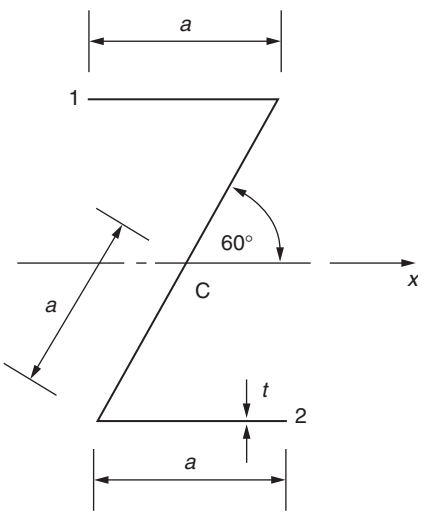

Fig. P.16.6

P.16.7 A thin-walled cantilever has a constant cross-section of uniform thickness with the dimensions shown in Fig. P.16.7. It is subjected to a system of point loads acting in the planes of the walls of the section in the directions shown.

Calculate the direct stresses according to the basic theory of bending at the points 1, 2 and 3 of the cross-section at the built-in end and half-way along the beam. Illustrate your answer by means of a suitable sketch.

The thickness is to be taken as small in comparison with the other cross-sectional dimensions in calculating the section properties I_{xx}, I_{xy}, etc.

Ans. At built-in end, $\sigma_{z,1} = -11.4\ \text{N/mm}^2$, $\sigma_{z,2} = -18.9\ \text{N/mm}^2$, $\sigma_{z,3} = 39.1\ \text{N/mm}^2$
Half-way, $\sigma_{z,1} = -20.3\ \text{N/mm}^2$, $\sigma_{z,2} = -1.1\ \text{N/mm}^2$, $\sigma_{z,3} = 15.4\ \text{N/mm}^2$.

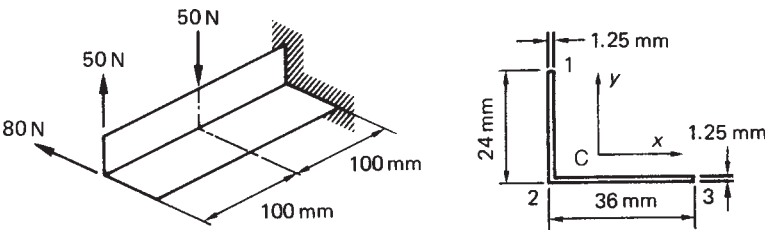

Fig. P.16.7

P.16.8 A uniform thin-walled beam has the open cross-section shown in Fig. P.16.8. The wall thickness t is constant. Calculate the position of the neutral axis and the maximum direct stress for a bending moment $M_x = 3.5\ \text{N m}$ applied about the horizontal axis Cx. Take $r = 5\ \text{mm}$, $t = 0.64\ \text{mm}$.

Ans. $\alpha = 51.9°$, $\sigma_{z,\max} = 101\ \text{N/mm}^2$.

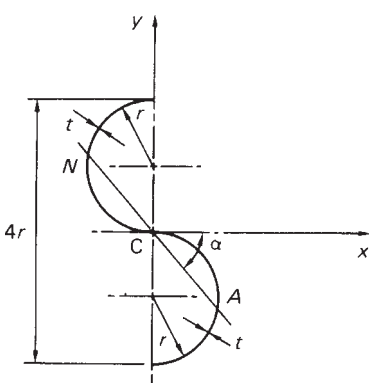

Fig. P.16.8

P.16.9 A uniform beam is simply supported over a span of 6 m. It carries a trapezoidally distributed load with intensity varying from 30 kN/m at the left-hand support to 90 kN/m at the right-hand support. Find the equation of the deflection curve and hence the deflection at the mid-span point. The second moment of area of the cross-section of the beam is $120 \times 10^6\ \text{mm}^4$ and Young's modulus $E = 206\,000\ \text{N/mm}^2$.

Ans. 41 mm (downwards).

P.16.10 A cantilever of length L and having a flexural rigidity EI carries a distributed load that varies in intensity from w/unit length at the built-in end to zero at the free end. Find the deflection of the free end.

Ans. $wL^4/30EI$ (downwards).

P.16.11 Determine the position and magnitude of the maximum deflection of the simply supported beam shown in Fig. P.16.11 in terms of its flexural rigidity EI.

Ans. $38.8/EI$ m downwards at 2.9 m from left-hand support.

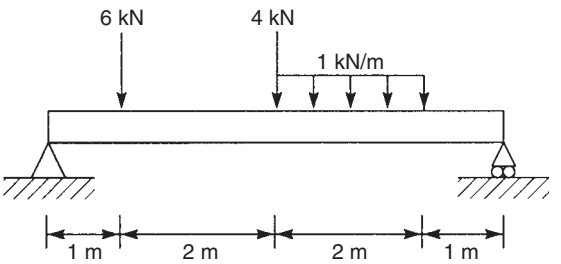

Fig. P.16.11

P.16.12 Determine the equation of the deflection curve of the beam shown in Fig. P.16.12. The flexural rigidity of the beam is EI.

Ans. $$v = -\frac{1}{EI}\left(\frac{125}{6}z^3 - 50[z-1]^2 + \frac{50}{12}[z-2]^4 - \frac{50}{12}[z-4]^4 - \frac{525}{6}[z-4]^3 + 237.5z\right)$$

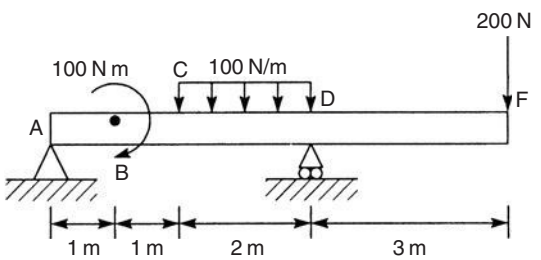

Fig. P.16.12

P.16.13 A uniform thin-walled beam ABD of open cross-section (Fig. P.16.13) is simply supported at points B and D with its web vertical. It carries a downward vertical force W at the end A in the plane of the web.

Derive expressions for the vertical and horizontal components of the deflection of the beam midway between the supports B and D. The wall thickness t and Young's modulus E are constant throughout.

Ans. $u = 0.186Wl^3/Ea^3t$, $v = 0.177Wl^3/Ea^3t$.

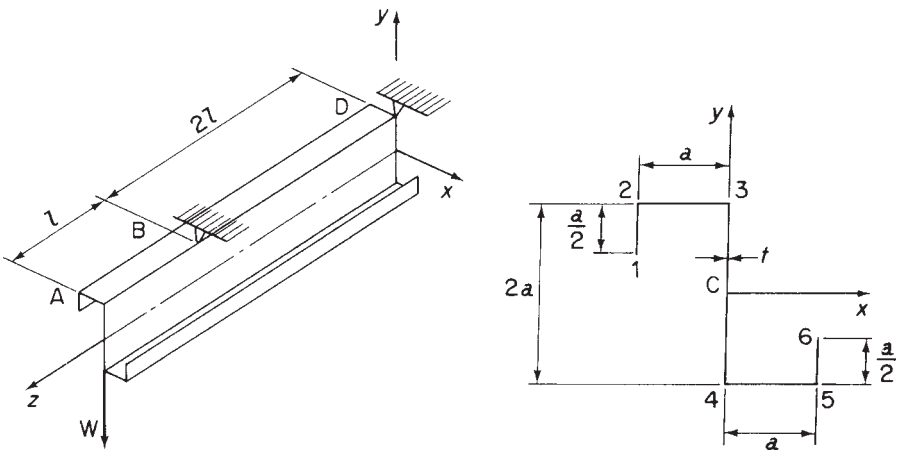

Fig. P.16.13

P.16.14 A uniform cantilever of arbitrary cross-section and length l has section properties I_{xx}, I_{yy} and I_{xy} with respect to the centroidal axes shown in Fig. P.16.14. It is loaded in the vertical (yz) plane with a uniformly distributed load of intensity w/unit length. The tip of the beam is hinged to a horizontal link which constrains it to move in the vertical direction only (provided that the actual deflections are small). Assuming that the link is rigid, and that there are no twisting effects, calculate:

(a) the force in the link;
(b) the deflection of the tip of the beam.

Ans. (a) $3wlI_{xy}/8I_{xx}$; (b) $wl^4/8EI_{xx}$.

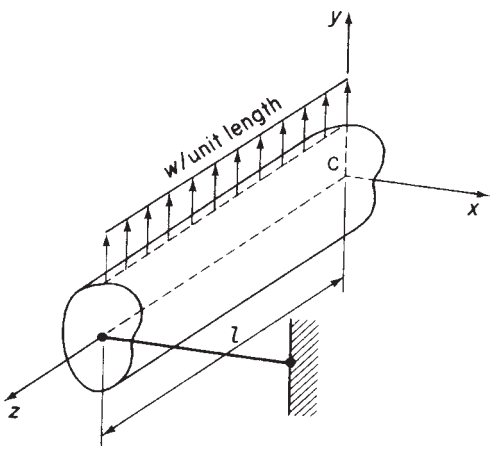

Fig. P.16.14

P.16.15 A uniform beam of arbitrary, unsymmetrical cross-section and length $2l$ is built-in at one end and simply supported in the vertical direction at a point half-way along its length. This support, however, allows the beam to deflect freely in the horizontal x direction (Fig. P.16.15).

For a vertical load W applied at the free end of the beam, calculate and draw the bending moment diagram, putting in the principal values.

Ans. $M_C = 0,\ M_B = Wl,\ M_A = -Wl/2$. Linear distribution.

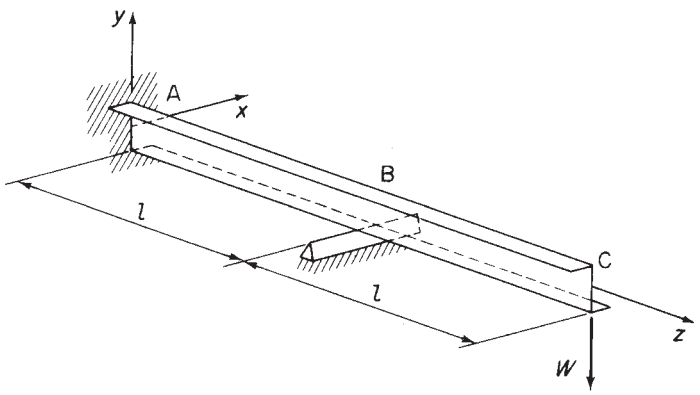

Fig. P.16.15

P.16.16 The beam section of P.16.4 is subjected to a temperature rise of $4T_0$ in its upper flange 12, a temperature rise of $2T_0$ in both vertical webs and a temperature rise of T_0 in its lower flange 34. Determine the changes in axial force and in the bending moments about the x and y axes. Young's modulus for the material of the beam is E and its coefficient of linear expansion is α.

Ans. $N_T = 9E\alpha\ \mathrm{d}tT_0,\ M_{xT} = 3E\alpha\ \mathrm{d}^2t\ T_0/2,\ M_{yT} = 3E\alpha\ \mathrm{d}^2t\ T_0/4$.

P.16.17 The beam section shown in Fig. P.16.17 is subjected to a temperature change which varies with y such that $T = T_0 y/2a$. Determine the corresponding changes in the stress resultants. Young's modulus for the material of the beam is E while its coefficient of linear expansion is α.

Ans. $N_T = 0, M_{xT} = 5E\alpha\ a^2t\ \ T_0/3,\ M_{yT} = E\alpha\ a^2t\ T_0/6$.

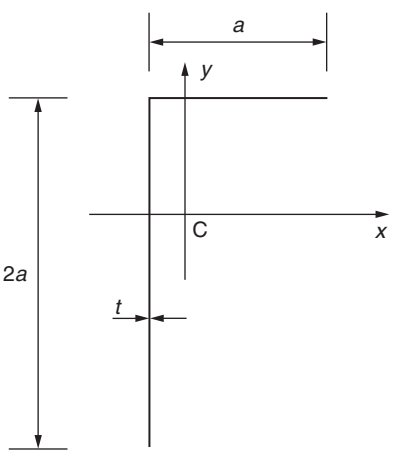

Fig. P.16.17

17

Shear of beams

In Chapter 16 we developed the theory for the bending of beams by considering solid or thick beam sections and then extended the theory to the thin-walled beam sections typical of aircraft structural components. In fact it is only in the calculation of section properties that thin-walled sections subjected to bending are distinguished from solid and thick sections. However, for thin-walled beams subjected to shear, the theory is based on assumptions applicable only to thin-walled sections so that we shall not consider solid and thick sections; the relevant theory for such sections may be found in any text on structural and stress analysis.[1] The relationships between bending moments, shear forces and load intensities derived in Section 16.2.5 still apply.

17.1 General stress, strain and displacement relationships for open and single cell closed section thin-walled beams

We shall establish in this section the equations of equilibrium and expressions for strain which are necessary for the analysis of open section beams supporting shear loads and closed section beams carrying shear and torsional loads. The analysis of open section beams subjected to torsion requires a different approach and is discussed separately in Chapter 18. The relationships are established from first principles for the particular case of thin-walled sections in preference to the adaption of Eqs (1.6), (1.27) and (1.28) which refer to different coordinate axes; the form, however, will be seen to be the same. Generally, in the analysis we assume that axial constraint effects are negligible, that the shear stresses normal to the beam surface may be neglected since they are zero at each surface and the wall is thin, that direct and shear stresses on planes normal to the beam surface are constant across the thickness, and finally that the beam is of uniform section so that the thickness may vary with distance around each section but is constant along the beam. In addition, we ignore squares and higher powers of the thickness t in the calculation of section properties (see Section 16.4.5).

The parameter s in the analysis is distance measured around the cross-section from some convenient origin.

An element $\delta s \times \delta z \times t$ of the beam wall is maintained in equilibrium by a system of direct and shear stresses as shown in Fig. 17.1(a). The direct stress σ_z is produced by bending moments or by the bending action of shear loads while the shear stresses are due

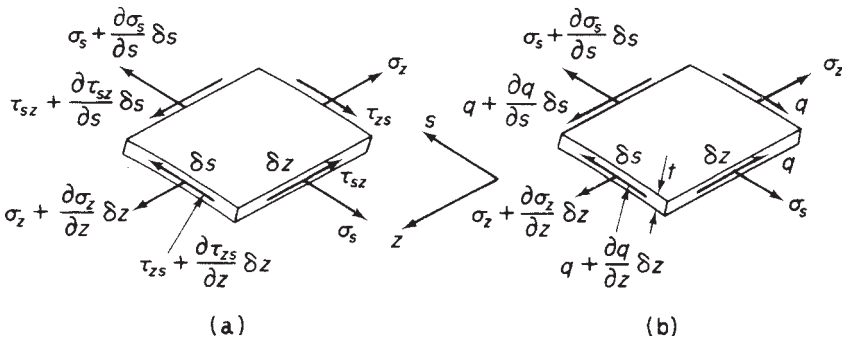

Fig. 17.1 (a) General stress system on element of a closed or open section beam; (b) direct stress and shear flow system on the element.

to shear and/or torsion of a closed section beam or shear of an open section beam. The hoop stress σ_s is usually zero but may be caused, in closed section beams, by internal pressure. Although we have specified that t may vary with s, this variation is small for most thin-walled structures so that we may reasonably make the approximation that t is constant over the length δs. Also, from Eq. (1.4), we deduce that $\tau_{zs} = \tau_{sz} = \tau$ say. However, we shall find it convenient to work in terms of *shear flow* q, i.e. shear force per unit length rather than in terms of shear stress. Hence, in Fig. 17.1(b)

$$q = \tau t \tag{17.1}$$

and is regarded as being positive in the direction of increasing s.

For equilibrium of the element in the z direction and neglecting body forces (see Section 1.2)

$$\left(\sigma_z + \frac{\partial \sigma_z}{\partial z}\delta z\right) t\delta s - \sigma_z t\delta s + \left(q + \frac{\partial q}{\partial s}\delta s\right)\delta_z - q\delta z = 0$$

which reduces to

$$\frac{\partial q}{\partial s} + t\frac{\partial \sigma_z}{\partial z} = 0 \tag{17.2}$$

Similarly for equilibrium in the s direction

$$\frac{\partial q}{\partial z} + t\frac{\partial \sigma_s}{\partial s} = 0 \tag{17.3}$$

The direct stresses σ_z and σ_s produce direct strains ε_z and ε_s, while the shear stress τ induces a shear strain $\gamma (= \gamma_{zs} = \gamma_{sz})$. We shall now proceed to express these strains in terms of the three components of the displacement of a point in the section wall (see Fig. 17.2). Of these components v_t is a tangential displacement in the xy plane and is taken to be positive in the direction of increasing s; v_n is a normal displacement in the xy plane and is positive outwards; and w is an axial displacement which has been defined previously in Section 16.2.1. Immediately, from the third of Eqs (1.18), we have

$$\varepsilon_z = \frac{\partial w}{\partial z} \tag{17.4}$$

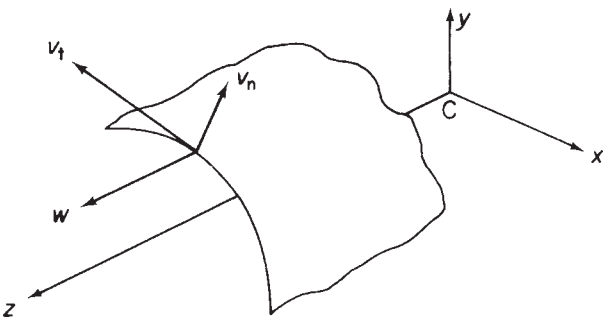

Fig. 17.2 Axial, tangential and normal components of displacement of a point in the beam wall.

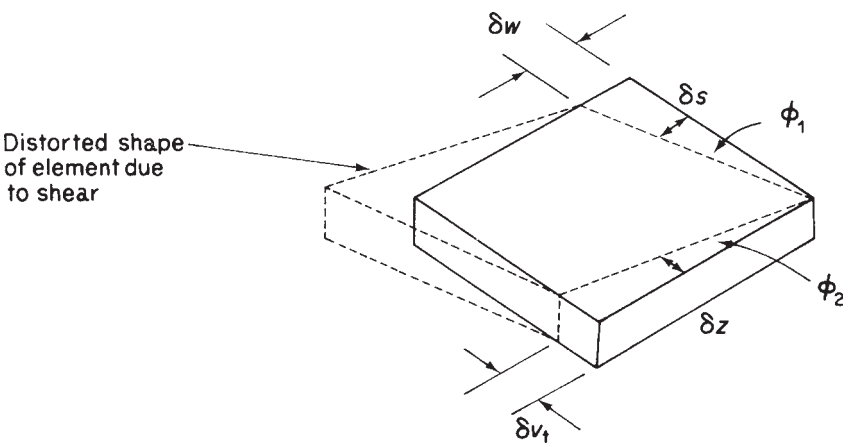

Fig. 17.3 Determination of shear strain γ in terms of tangential and axial components of displacement.

It is possible to derive a simple expression for the direct strain ε_s in terms of v_t, v_n, s and the curvature $1/r$ in the xy plane of the beam wall. However, as we do not require ε_s in the subsequent analysis we shall, for brevity, merely quote the expression

$$\varepsilon_s = \frac{\partial v_t}{\partial s} + \frac{v_n}{r} \tag{17.5}$$

The shear strain γ is found in terms of the displacements w and v_t by considering the shear distortion of an element $\delta s \times \delta z$ of the beam wall. From Fig. 17.3 we see that the shear strain is given by

$$\gamma = \phi_1 + \phi_2$$

or, in the limit as both δs and δz tend to zero

$$\gamma = \frac{\partial w}{\partial s} + \frac{\partial v_t}{\partial z} \tag{17.6}$$

In addition to the assumptions specified in the earlier part of this section, we further assume that during any displacement the shape of the beam cross-section is maintained

by a system of closely spaced diaphragms which are rigid in their own plane but are perfectly flexible normal to their own plane (CSRD assumption). There is, therefore, no resistance to axial displacement w and the cross-section moves as a rigid body in its own plane, the displacement of any point being completely specified by translations u and v and a rotation θ (see Fig. 17.4).

At first sight this appears to be a rather sweeping assumption but, for aircraft structures of the thin shell type described in Chapter 12 whose cross-sections are stiffened by ribs or frames positioned at frequent intervals along their lengths, it is a reasonable approximation for the actual behaviour of such sections. The tangential displacement v_t of any point N in the wall of either an open or closed section beam is seen from Fig. 17.4 to be

$$v_t = p\theta + u\cos\psi + v\sin\psi \tag{17.7}$$

where clearly u, v and θ are functions of z only (w may be a function of z and s).

The origin O of the axes in Fig. 17.4 has been chosen arbitrarily and the axes suffer displacements u, v and θ. These displacements, in a loading case such as pure torsion, are equivalent to a pure rotation about some point R(x_R,y_R) in the cross-section where R is the *centre of twist.* Therefore, in Fig. 17.4

$$v_t = p_R\theta \tag{17.8}$$

and

$$p_R = p - x_R\sin\psi + y_R\cos\psi$$

which gives

$$v_t = p\theta - x_R\theta\sin\psi + y_R\theta\cos\psi$$

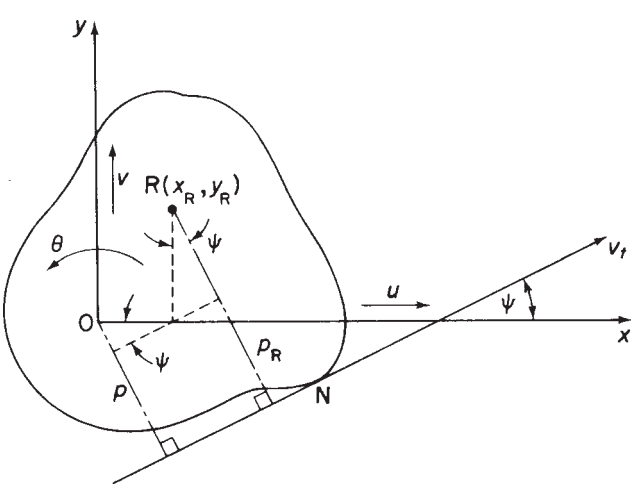

Fig. 17.4 Establishment of displacement relationships and position of centre of twist of beam (open or closed).

and

$$\frac{\partial v_t}{\partial z} = p\frac{d\theta}{dz} - x_R \sin\psi\frac{d\theta}{dz} + y_R \cos\psi\frac{d\theta}{dz} \tag{17.9}$$

Also from Eq. (17.7)

$$\frac{\partial v_t}{\partial z} = p\frac{d\theta}{dz} + \frac{du}{dz}\cos\psi + \frac{dv}{dz}\sin\psi \tag{17.10}$$

Comparing the coefficients of Eqs (17.9) and (17.10) we see that

$$x_R = -\frac{dv/dz}{d\theta/dz} \quad y_R = \frac{du/dz}{d\theta/dz} \tag{17.11}$$

17.2 Shear of open section beams

The open section beam of arbitrary section shown in Fig. 17.5 supports shear loads S_x and S_y such that there is no twisting of the beam cross-section. For this condition to be valid the shear loads must both pass through a particular point in the cross-section known as the *shear centre.*

Since there are no hoop stresses in the beam the shear flows and direct stresses acting on an element of the beam wall are related by Eq. (17.2), i.e.

$$\frac{\partial q}{\partial s} + t\frac{\partial \sigma_z}{\partial z} = 0$$

We assume that the direct stresses are obtained with sufficient accuracy from basic bending theory so that from Eq. (16.18)

$$\frac{\partial \sigma_z}{\partial z} = \frac{[(\partial M_y/\partial z)I_{xx} - (\partial M_x/\partial z)I_{xy}]}{I_{xx}I_{yy} - I_{xy}^2}x + \frac{[(\partial M_x/\partial z)I_{yy} - (\partial M_y/\partial z)I_{xy}]}{I_{xx}I_{yy} - I_{xy}^2}y$$

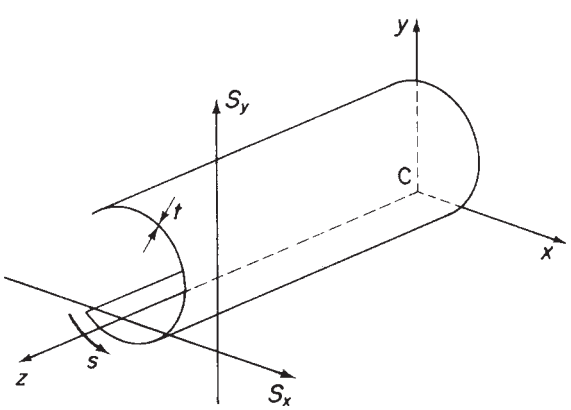

Fig. 17.5 Shear loading of open section beam.

Using the relationships of Eqs (16.23) and (16.24), i.e. $\partial M_y/\partial z = S_x$, etc., this expression becomes

$$\frac{\partial \sigma_z}{\partial z} = \frac{(S_x I_{xx} - S_y I_{xy})}{I_{xx} I_{yy} - I_{xy}^2} x + \frac{(S_y I_{yy} - S_x I_{xy})}{I_{xx} I_{yy} - I_{xy}^2} y$$

Substituting for $\partial \sigma_z/\partial z$ in Eq. (17.2) gives

$$\frac{\partial q}{\partial s} = -\frac{(S_x I_{xx} - S_y I_{xy})}{I_{xx} I_{yy} - I_{xy}^2} tx - \frac{(S_y I_{yy} - S_x I_{xy})}{I_{xx} I_{yy} - I_{xy}^2} ty \tag{17.12}$$

Integrating Eq. (17.12) with respect to s from some origin for s to any point around the cross-section, we obtain

$$\int_0^s \frac{\partial q}{\partial s} \mathrm{d}s = -\left(\frac{S_x I_{xx} - S_y I_{xy}}{I_{xx} I_{yy} - I_{xy}^2}\right) \int_0^s tx \, \mathrm{d}s - \left(\frac{S_y I_{yy} - S_x I_{xy}}{I_{xx} I_{yy} - I_{xy}^2}\right) \int_0^s ty \, \mathrm{d}s \tag{17.13}$$

If the origin for s is taken at the open edge of the cross-section, then $q = 0$ when $s = 0$ and Eq. (17.13) becomes

$$q_s = -\left(\frac{S_x I_{xx} - S_y I_{xy}}{I_{xx} I_{yy} - I_{xy}^2}\right) \int_0^s tx \, \mathrm{d}s - \left(\frac{S_y I_{yy} - S_x I_{xy}}{I_{xx} I_{yy} - I_{xy}^2}\right) \int_0^s ty \, \mathrm{d}s \tag{17.14}$$

For a section having either Cx or Cy as an axis of symmetry $I_{xy} = 0$ and Eq. (17.14) reduces to

$$q_s = -\frac{S_x}{I_{yy}} \int_0^s tx \, \mathrm{d}s - \frac{S_y}{I_{xx}} \int_0^s ty \, \mathrm{d}s$$

Example 17.1

Determine the shear flow distribution in the thin-walled Z-section shown in Fig. 17.6 due to a shear load S_y applied through the shear centre of the section.

The origin for our system of reference axes coincides with the centroid of the section at the mid-point of the web. From antisymmetry we also deduce by inspection that the shear centre occupies the same position. Since S_y is applied through the shear centre then no torsion exists and the shear flow distribution is given by Eq. (17.14) in which $S_x = 0$, i.e.

$$q_s = \frac{S_y I_{xy}}{I_{xx} I_{yy} - I_{xy}^2} \int_0^s tx \, \mathrm{d}s - \frac{S_y I_{yy}}{I_{xx} I_{yy} - I_{xy}^2} \int_0^s ty \, \mathrm{d}s$$

or

$$q_s = \frac{S_y}{I_{xx} I_{yy} - I_{xy}^2} \left(I_{xy} \int_0^s tx \, \mathrm{d}s - I_{yy} \int_0^s ty \, \mathrm{d}s\right) \tag{i}$$

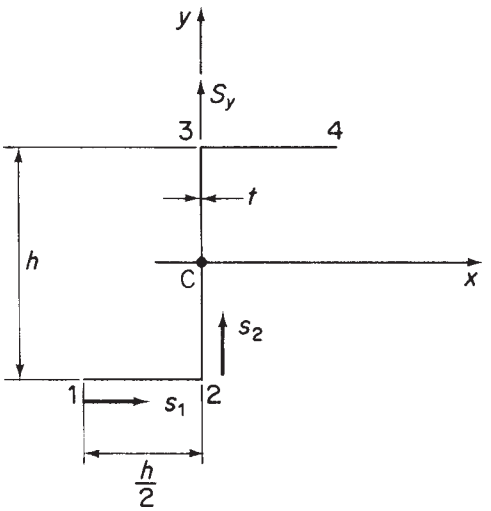

Fig. 17.6 Shear loaded Z-section of Example 17.1.

The second moments of area of the section have previously been determined in Example 16.14 and are

$$I_{xx} = \frac{h^3 t}{3}, \quad I_{yy} = \frac{h^3 t}{12}, \quad I_{xy} = \frac{h^3 t}{8}$$

Substituting these values in Eq. (i) we obtain

$$q_s = \frac{S_y}{h^3} \int_0^s (10.32x - 6.84y)\mathrm{d}s \tag{ii}$$

On the bottom flange 12, $y = -h/2$ and $x = -h/2 + s_1$, where $0 \le s_1 \le h/2$. Therefore

$$q_{12} = \frac{S_y}{h^3} \int_0^{s_1} (10.32s_1 - 1.74h)\mathrm{d}s_1$$

giving

$$q_{12} = \frac{S_y}{h^3}(5.16s_1^2 - 1.74hs_1) \tag{iii}$$

Hence at 1 ($s_1 = 0$), $q_1 = 0$ and at 2 ($s_1 = h/2$), $q_2 = 0.42S_y/h$. Further examination of Eq. (iii) shows that the shear flow distribution on the bottom flange is parabolic with a change of sign (i.e. direction) at $s_1 = 0.336h$. For values of $s_1 < 0.336h$, q_{12} is negative and therefore in the opposite direction to s_1.

In the web 23, $y = -h/2 + s_2$, where $0 \le s_2 \le h$ and $x = 0$. Then

$$q_{23} = \frac{S_y}{h^3} \int_0^{s_2} (3.42h - 6.84s_2)\mathrm{d}s_2 + q_2 \tag{iv}$$

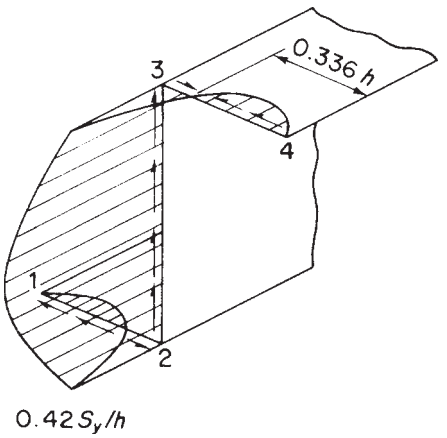

Fig. 17.7 Shear flow distribution in Z-section of Example 17.1.

We note in Eq. (iv) that the shear flow is not zero when $s_2 = 0$ but equal to the value obtained by inserting $s_1 = h/2$ in Eq. (iii), i.e. $q_2 = 0.42S_y/h$. Integration of Eq. (iv) yields

$$q_{23} = \frac{S_y}{h^3}(0.42h^2 + 3.42hs_2 - 3.42s_2^2) \qquad \text{(v)}$$

This distribution is symmetrical about Cx with a maximum value at $s_2 = h/2 (y = 0)$ and the shear flow is positive at all points in the web.

The shear flow distribution in the upper flange may be deduced from antisymmetry so that the complete distribution is of the form shown in Fig. 17.7.

17.2.1 Shear centre

We have defined the position of the shear centre as that point in the cross-section through which shear loads produce no twisting. It may be shown by use of the reciprocal theorem that this point is also the centre of twist of sections subjected to torsion. There are, however, some important exceptions to this general rule as we shall observe in Section 26.1. Clearly, in the majority of practical cases it is impossible to guarantee that a shear load will act through the shear centre of a section. Equally apparent is the fact that any shear load may be represented by the combination of the shear load applied through the shear centre and a torque. The stresses produced by the separate actions of torsion and shear may then be added by superposition. It is therefore necessary to know the location of the shear centre in all types of section or to calculate its position. Where a cross-section has an axis of symmetry the shear centre must, of course, lie on this axis. For cruciform or angle sections of the type shown in Fig. 17.8 the shear centre is located at the intersection of the sides since the resultant internal shear loads all pass through these points.

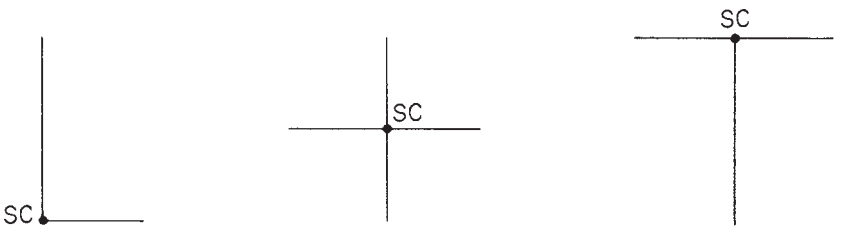

Fig. 17.8 Shear centre position for type of open section beam shown.

Example 17.2

Calculate the position of the shear centre of the thin-walled channel section shown in Fig. 17.9. The thickness t of the walls is constant.

The shear centre S lies on the horizontal axis of symmetry at some distance ξ_S, say, from the web. If we apply an arbitrary shear load S_y through the shear centre then the shear flow distribution is given by Eq. (17.14) and the moment about any point in the cross-section produced by these shear flows is *equivalent* to the moment of the applied shear load. S_y appears on both sides of the resulting equation and may therefore be eliminated to leave ξ_S.

For the channel section, Cx is an axis of symmetry so that $I_{xy} = 0$. Also $S_x = 0$ and therefore Eq. (17.14) simplifies to

$$q_s = -\frac{S_y}{I_{xx}} \int_0^s ty \, \mathrm{d}s \tag{i}$$

where

$$I_{xx} = 2bt\left(\frac{h}{2}\right)^2 + \frac{th^3}{12} = \frac{h^3 t}{12}\left(1 + \frac{6b}{h}\right)$$

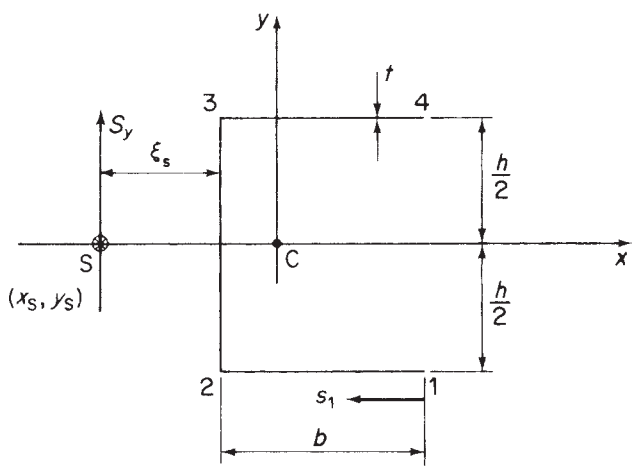

Fig. 17.9 Determination of shear centre position of channel section of Example 17.2.

Substituting for I_{xx} in Eq. (i) we have

$$q_s = \frac{-12S_y}{h^3(1+6b/h)} \int_0^s y \, \mathrm{d}s \tag{ii}$$

The amount of computation involved may be reduced by giving some thought to the requirements of the problem. In this case we are asked to find the position of the shear centre only, not a complete shear flow distribution. From symmetry it is clear that the moments of the resultant shears on the top and bottom flanges about the mid-point of the web are numerically equal and act in the same rotational sense. Furthermore, the moment of the web shear about the same point is zero. We deduce that it is only necessary to obtain the shear flow distribution on either the top or bottom flange for a solution. Alternatively, choosing a web/flange junction as a moment centre leads to the same conclusion.

On the bottom flange, $y = -h/2$ so that from Eq. (ii) we have

$$q_{12} = \frac{6S_y}{h^2(1+6b/h)} s_1 \tag{iii}$$

Equating the clockwise moments of the internal shears about the mid-point of the web to the clockwise moment of the applied shear load about the same point gives

$$S_y \xi_\mathrm{s} = 2 \int_0^b q_{12} \frac{h}{2} \mathrm{d}s_1$$

or, by substitution from Eq. (iii)

$$S_y \xi_\mathrm{s} = 2 \int_0^b \frac{6S_y}{h^2(1+6b/h)} \frac{h}{2} s_1 \mathrm{d}s_1$$

from which

$$\xi_\mathrm{s} = \frac{3b^2}{h(1+6b/h)} \tag{iv}$$

In the case of an unsymmetrical section, the coordinates (ξ_S, η_S) of the shear centre referred to some convenient point in the cross-section would be obtained by first determining ξ_S in a similar manner to that of Example 17.2 and then finding η_S by applying a shear load S_x through the shear centre. In both cases the choice of a web/flange junction as a moment centre reduces the amount of computation.

17.3 Shear of closed section beams

The solution for a shear loaded closed section beam follows a similar pattern to that described in Section 17.2 for an open section beam but with two important differences. First, the shear loads may be applied through points in the cross-section other than the shear centre so that torsional as well as shear effects are included. This is possible since, as we shall see, shear stresses produced by torsion in closed section beams have exactly the same form as shear stresses produced by shear, unlike shear stresses due to

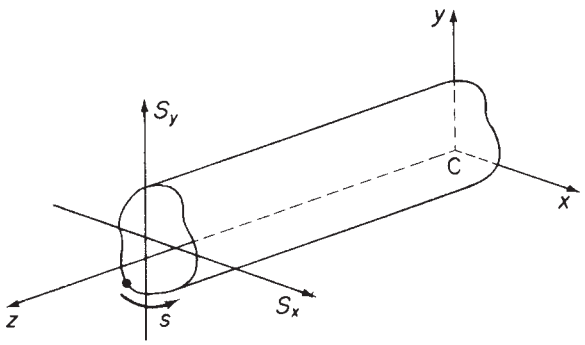

Fig. 17.10 Shear of closed section beams.

shear and torsion in open section beams. Secondly, it is generally not possible to choose an origin for s at which the value of shear flow is known. Consider the closed section beam of arbitrary section shown in Fig. 17.10. The shear loads S_x and S_y are applied through any point in the cross-section and, in general, cause direct bending stresses and shear flows which are related by the equilibrium equation (17.2). We assume that hoop stresses and body forces are absent. Therefore

$$\frac{\partial q}{\partial s} + t\frac{\partial \sigma_z}{\partial z} = 0$$

From this point the analysis is identical to that for a shear loaded open section beam until we reach the stage of integrating Eq. (17.13), namely

$$\int_0^s \frac{\partial q}{\partial s}\mathrm{d}s = -\left(\frac{S_x I_{xx} - S_y I_{xy}}{I_{xx}I_{yy} - I_{xy}^2}\right)\int_0^s tx\,\mathrm{d}s - \left(\frac{S_y I_{yy} - S_x I_{xy}}{I_{xx}I_{yy} - I_{xy}^2}\right)\int_0^s ty\,\mathrm{d}s$$

Let us suppose that we choose an origin for s where the shear flow has the unknown value $q_{s,0}$. Integration of Eq. (17.13) then gives

$$q_s - q_{s,0} = -\left(\frac{S_x I_{xx} - S_y I_{xy}}{I_{xx}I_{yy} - I_{xy}^2}\right)\int_0^s tx\,\mathrm{d}s - \left(\frac{S_y I_{yy} - S_x I_{xy}}{I_{xx}I_{yy} - I_{xy}^2}\right)\int_0^s ty\,\mathrm{d}s$$

or

$$q_s = -\left(\frac{S_x I_{xx} - S_y I_{xy}}{I_{xx}I_{yy} - I_{xy}^2}\right)\int_0^s tx\,\mathrm{d}s - \left(\frac{S_y I_{yy} - S_x I_{xy}}{I_{xx}I_{yy} - I_{xy}^2}\right)\int_0^s ty\,\mathrm{d}s + q_{s,0} \qquad (17.15)$$

We observe by comparison of Eqs (17.15) and (17.14) that the first two terms on the right-hand side of Eq. (17.15) represent the shear flow distribution in an open section beam loaded through its shear centre. This fact indicates a method of solution for a shear loaded closed section beam. Representing this 'open' section or 'basic' shear flow by q_b, we may write Eq. (17.15) in the form

$$q_s = q_\mathrm{b} + q_{s,0} \qquad (17.16)$$

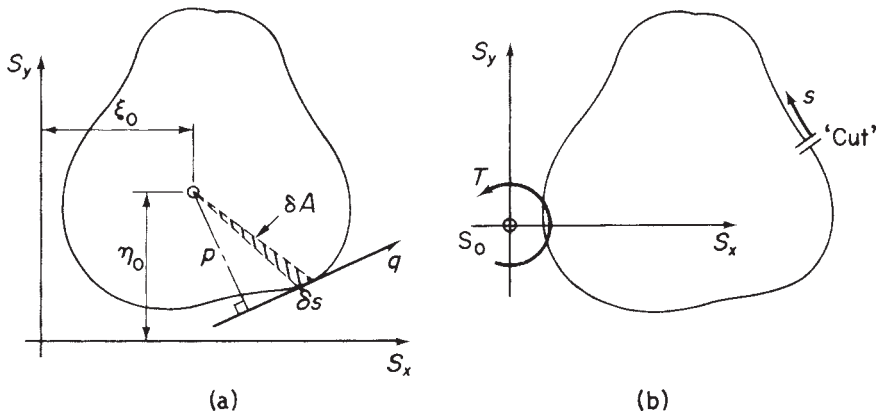

Fig. 17.11 (a) Determination of $q_{s,0}$; (b) equivalent loading on 'open' section beam.

We obtain q_b by supposing that the closed beam section is 'cut' at some convenient point thereby producing an 'open' section (see Fig. 17.11(b)). The shear flow distribution (q_b) around this 'open' section is given by

$$q_b = -\left(\frac{S_x I_{xx} - S_y I_{xy}}{I_{xx} I_{yy} - I_{xy}^2}\right)\int_0^s tx\,\mathrm{d}s - \left(\frac{S_y I_{yy} - S_x I_{xy}}{I_{xx} I_{xy} - I_{xy}^2}\right)\int_0^s ty\,\mathrm{d}s$$

as in Section 17.2. The value of shear flow at the cut ($s = 0$) is then found by equating applied and internal moments taken about some convenient moment centre. Then, from Fig. 17.11(a)

$$S_x\eta_0 - S_y\xi_0 = \oint pq\,\mathrm{d}s = \oint pq_b\,\mathrm{d}s + q_{s,0}\oint p\,\mathrm{d}s$$

where $\oint$ denotes integration completely around the cross-section. In Fig. 17.11 (a)

$$\delta A = \frac{1}{2}\delta s p$$

so that

$$\oint \mathrm{d}A = \frac{1}{2}\oint p\,\mathrm{d}s$$

Hence

$$\oint p\mathrm{d}s = 2A$$

where A is the area enclosed by the mid-line of the beam section wall. Hence

$$S_x\eta_0 - S_y\xi_0 = \oint pq_b\mathrm{d}s + 2Aq_{s,0} \tag{17.17}$$

If the moment centre is chosen to coincide with the lines of action of S_x and S_y then Eq. (17.17) reduces to

$$0 = \oint pq_b \, ds + 2Aq_{s,0} \tag{17.18}$$

The unknown shear flow $q_{s,0}$ follows from either of Eqs (17.17) or (17.18).

It is worthwhile to consider some of the implications of the above process. Equation (17.14) represents the shear flow distribution in an open section beam for the condition of zero twist. Therefore, by 'cutting' the closed section beam of Fig. 17.11(a) to determine q_b, we are, in effect, replacing the shear loads of Fig. 17.11(a) by shear loads S_x and S_y acting through the shear centre of the resulting 'open' section beam together with a torque T as shown in Fig. 17.11(b). We shall show in Section 18.1 that the application of a torque to a closed section beam results in a constant shear flow. In this case the constant shear flow $q_{s,0}$ corresponds to the torque but will have different values for different positions of the 'cut' since the corresponding various 'open' section beams will have different locations for their shear centres. An additional effect of 'cutting' the beam is to produce a statically determinate structure since the q_b shear flows are obtained from statical equilibrium considerations. It follows that a single cell closed section beam supporting shear loads is singly redundant.

17.3.1 Twist and warping of shear loaded closed section beams

Shear loads which are not applied through the shear centre of a closed section beam cause cross-sections to twist and warp; i.e., in addition to rotation, they suffer out of plane axial displacements. Expressions for these quantities may be derived in terms of the shear flow distribution q_s as follows. Since $q = \tau t$ and $\tau = G\gamma$ (see Chapter 1) then we can express q_s in terms of the warping and tangential displacements w and v_t of a point in the beam wall by using Eq. (17.6). Thus

$$q_s = Gt\left(\frac{\partial w}{\partial s} + \frac{\partial v_t}{\partial z}\right) \tag{17.19}$$

Substituting for $\partial v_t/\partial z$ from Eq. (17.10) we have

$$\frac{q_s}{Gt} = \frac{\partial w}{\partial s} + p\frac{d\theta}{dz} + \frac{du}{dz}\cos\psi + \frac{dv}{dz}\sin\psi \tag{17.20}$$

Integrating Eq. (17.20) with respect to s from the chosen origin for s and noting that G may also be a function of s, we obtain

$$\int_0^s \frac{q_s}{Gt} ds = \int_0^s \frac{\partial w}{\partial s} ds + \frac{d\theta}{dz}\int_0^s p \, ds + \frac{du}{dz}\int_0^s \cos\psi \, ds + \frac{dv}{dz}\int_0^s \sin\psi \, ds$$

or

$$\int_0^s \frac{q_s}{Gt} ds = \int_0^s \frac{\partial w}{\partial s} ds + \frac{d\theta}{dz}\int_0^s p \, ds + \frac{du}{dz}\int_0^s dx + \frac{dv}{dz}\int_0^s dy$$

which gives

$$\int_0^s \frac{q_s}{Gt}\mathrm{d}s = (w_s - w_0) + 2A_{\mathrm{O}s}\frac{\mathrm{d}\theta}{\mathrm{d}z} + \frac{\mathrm{d}u}{\mathrm{d}z}(x_s - x_0) + \frac{\mathrm{d}v}{\mathrm{d}z}(y_s - y_0) \tag{17.21}$$

where $A_{\mathrm{O}s}$ is the area swept out by a generator, centre at the origin of axes, O, from the origin for s to any point s around the cross-section. Continuing the integration completely around the cross-section yields, from Eq. (17.21)

$$\oint \frac{q_s}{Gt}\mathrm{d}s = 2A\frac{\mathrm{d}\theta}{\mathrm{d}z}$$

from which

$$\frac{\mathrm{d}\theta}{\mathrm{d}z} = \frac{1}{2A}\oint \frac{q_s}{Gt}\mathrm{d}s \tag{17.22}$$

Substituting for the rate of twist in Eq. (17.21) from Eq. (17.22) and rearranging, we obtain the warping distribution around the cross-section

$$w_s - w_0 = \int_0^s \frac{q_s}{Gt}\mathrm{d}s - \frac{A_{\mathrm{O}s}}{A}\oint \frac{q_s}{Gt}\mathrm{d}s - \frac{\mathrm{d}u}{\mathrm{d}z}(x_s - x_0) - \frac{\mathrm{d}v}{\mathrm{d}z}(y_s - y_0) \tag{17.23}$$

Using Eqs (17.11) to replace $\mathrm{d}u/\mathrm{d}z$ and $\mathrm{d}v/\mathrm{d}z$ in Eq. (17.23) we have

$$w_s - w_0 = \int_0^s \frac{q_s}{Gt}\mathrm{d}s - \frac{A_{\mathrm{O}s}}{A}\oint \frac{q_s}{Gt}\mathrm{d}s - y_{\mathrm{R}}\frac{\mathrm{d}\theta}{\mathrm{d}z}(x_s - x_0) + x_{\mathrm{R}}\frac{\mathrm{d}\theta}{\mathrm{d}z}(y_s - y_0) \tag{17.24}$$

The last two terms in Eq. (17.24) represent the effect of relating the warping displacement to an arbitrary origin which itself suffers axial displacement due to warping. In the case where the origin coincides with the centre of twist R of the section then Eq. (17.24) simplifies to

$$w_s - w_0 = \int_0^s \frac{q_s}{Gt}\mathrm{d}s - \frac{A_{\mathrm{O}s}}{A}\oint \frac{q_s}{Gt}\mathrm{d}s \tag{17.25}$$

In problems involving singly or doubly symmetrical sections, the origin for s may be taken to coincide with a point of zero warping which will occur where an axis of symmetry and the wall of the section intersect. For unsymmetrical sections the origin for s may be chosen arbitrarily. The resulting warping distribution will have exactly the same form as the actual distribution but will be displaced axially by the unknown warping displacement at the origin for s. This value may be found by referring to the torsion of closed section beams subject to axial constraint (see Section 26.3). In the analysis of such beams it is assumed that the direct stress distribution set up by the constraint is directly proportional to the free warping of the section, i.e.

$$\sigma = \text{constant} \times w$$

Also, since a pure torque is applied the resultant of any internal direct stress system must be zero, in other words it is self-equilibrating. Thus

$$\text{Resultant axial load} = \oint \sigma t\,\mathrm{d}s$$

where σ is the direct stress at any point in the cross-section. Then, from the above assumption

$$0 = \oint wt \, \mathrm{d}s$$

or

$$0 = \oint (w_s - w_0)t \, \mathrm{d}s$$

so that

$$w_0 = \frac{\oint w_s t \, \mathrm{d}s}{\oint t \, \mathrm{d}s} \tag{17.26}$$

17.3.2 Shear centre

The shear centre of a closed section beam is located in a similar manner to that described in Section 17.2.1 for open section beams. Therefore, to determine the coordinate ξ_S (referred to any convenient point in the cross-section) of the shear centre S of the closed section beam shown in Fig. 17.12, we apply an arbitrary shear load S_y through S, calculate the distribution of shear flow q_s due to S_y and then equate internal and external moments. However, a difficulty arises in obtaining $q_{s,0}$ since, at this stage, it is impossible to equate internal and external moments to produce an equation similar to Eq. (17.17) as the position of S_y is unknown. We therefore use the condition that a shear load acting through the shear centre of a section produces zero twist. It follows that $\mathrm{d}\theta/\mathrm{d}z$ in Eq. (17.22) is zero so that

$$0 = \oint \frac{q_s}{Gt} \mathrm{d}s$$

or

$$0 = \oint \frac{1}{Gt}(q_\mathrm{b} + q_{s,0})\mathrm{d}s$$

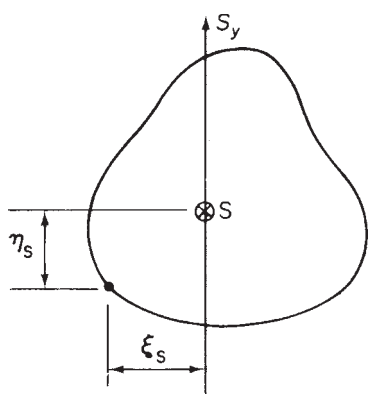

Fig. 17.12 Shear centre of a closed section beam.

which gives

$$q_{s,0} = -\frac{\oint (q_b/Gt)\mathrm{d}s}{\oint \mathrm{d}s/Gt} \tag{17.27}$$

If $Gt =$ constant then Eq. (17.27) simplifies to

$$q_{s,0} = -\frac{\oint q_b\,\mathrm{d}s}{\oint \mathrm{d}s} \tag{17.28}$$

The coordinate η_S is found in a similar manner by applying S_x through S.

Example 17.3

A thin-walled closed section beam has the singly symmetrical cross-section shown in Fig. 17.13. Each wall of the section is flat and has the same thickness t and shear modulus G. Calculate the distance of the shear centre from point 4.

The shear centre clearly lies on the horizontal axis of symmetry so that it is only necessary to apply a shear load S_y through S and to determine ξ_S. If we take the x reference axis to coincide with the axis of symmetry then $I_{xy} = 0$, and since $S_x = 0$ Eq. (17.15) simplifies to

$$q_s = -\frac{S_y}{I_{xx}} \int_0^s ty\,\mathrm{d}s + q_{s,0} \tag{i}$$

in which

$$I_{xx} = 2\left[\int_0^{10a} t\left(\frac{8}{10}s_1\right)^2 \mathrm{d}s_1 + \int_0^{17a} t\left(\frac{8}{17}s_2\right)^2 \mathrm{d}s_2\right]$$

Evaluating this expression gives $I_{xx} = 1152a^3t$.

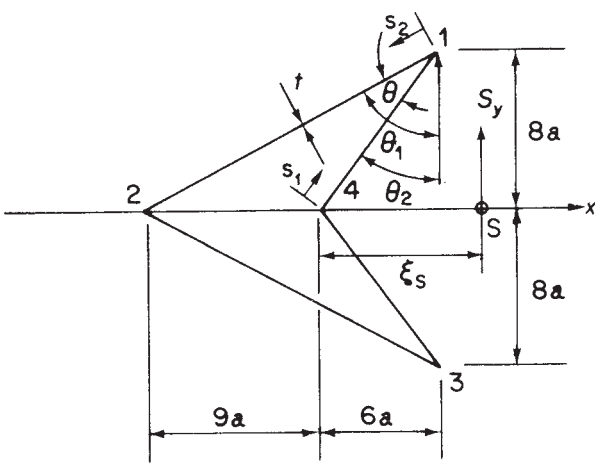

Fig. 17.13 Closed section beam of Example 17.3.

The basic shear flow distribution q_b is obtained from the first term in Eq. (i). Then, for the wall 41

$$q_{\mathrm{b},41} = \frac{-S_y}{1152a^3 t}\int_0^{s_1} t\left(\frac{8}{10}s_1\right)\mathrm{d}s_1 = \frac{-S_y}{1152a^3}\left(\frac{2}{5}s_1^2\right) \tag{ii}$$

In the wall 12

$$q_{\mathrm{b},12} = \frac{-S_y}{1152a^3}\left[\int_0^{s_2}(17a - s_2)\frac{8}{17}\mathrm{d}s_2 + 40a^2\right] \tag{ii}$$

which gives

$$q_{\mathrm{b},12} = \frac{-S_y}{1152a^3}\left(-\frac{4}{17}s_2^2 + 8as_2 + 40a^2\right) \tag{iii}$$

The q_{b} distributions in the walls 23 and 34 follow from symmetry. Hence from Eq. (17.28)

$$q_{s,0} = \frac{2S_y}{54a \times 1152a^3}\left[\int_0^{10a}\frac{2}{5}s_1^2\,\mathrm{d}s_1 + \int_0^{17a}\left(-\frac{4}{17}s_2^2 + 8as_2 + 40a^2\right)ds_2\right]$$

giving

$$q_{s,0} = \frac{S_y}{1152a^3}(58.7a^2) \tag{iv}$$

Taking moments about the point 2 we have

$$S_y(\xi_{\mathrm{S}} + 9a) = 2\int_0^{10a} q_{41}\,17a\sin\theta\,\mathrm{d}s_1$$

or

$$S_y(\xi_{\mathrm{S}} + 9a) = \frac{S_y 34a\sin\theta}{1152a^3}\int_0^{10a}\left(-\frac{2}{5}s_1^2 + 58.7a^2\right)\mathrm{d}s_1 \tag{v}$$

We may replace $\sin\theta$ by $\sin(\theta_1 - \theta_2) = \sin\theta_1\cos\theta_2 - \cos\theta_1\sin\theta_2$ where $\sin\theta_1 =$, $15/17$, $\cos\theta_2 = 8/10$, $\cos\theta_1 = 8/17$ and $\sin\theta_2 = 6/10$. Substituting these values and integrating Eq. (v) gives

$$\xi_{\mathrm{S}} = -3.35a$$

which means that the shear centre is inside the beam section.

Reference

1 Megson, T. H. G., *Structural and Stress Analysis,* 2nd edition, Elsevier, Oxford, 2005.

Problems

P.17.1 A beam has the singly symmetrical, thin-walled cross-section shown in Fig. P.17.1. The thickness t of the walls is constant throughout. Show that the distance of the shear centre from the web is given by

$$\xi_S = -d\frac{\rho^2 \sin\alpha\cos\alpha}{1 + 6\rho + 2\rho^3 \sin^2\alpha}$$

where

$$\rho = d/h$$

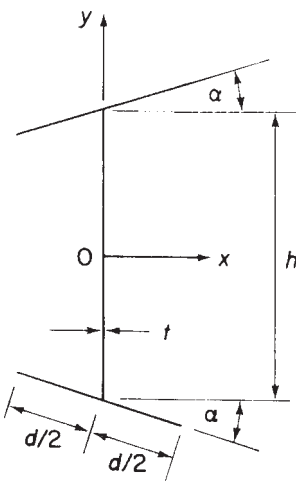

Fig. P.17.1

P.17.2 A beam has the singly symmetrical, thin-walled cross-section shown in Fig. P.17.2. Each wall of the section is flat and has the same length a and thickness t. Calculate the distance of the shear centre from the point 3.

Ans. $5a\cos\alpha/8$

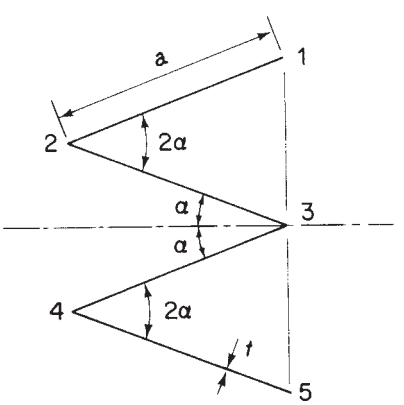

Fig. P.17.2

P.17.3 Determine the position of the shear centre S for the thin-walled, open cross-section shown in Fig. P.17.3. The thickness t is constant.

Ans. $\pi r/3$

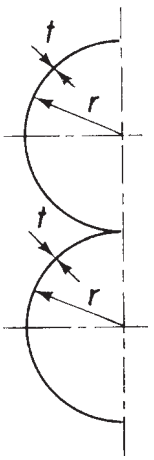

Fig. P.17.3

P.17.4 Figure P.17.4 shows the cross-section of a thin, singly symmetrical I-section. Show that the distance ξ_S of the shear centre from the vertical web is given by

$$\frac{\xi_S}{d} = \frac{3\rho(1-\beta)}{(1+12\rho)}$$

where $\rho = d/h$. The thickness t is taken to be negligibly small in comparison with the other dimensions.

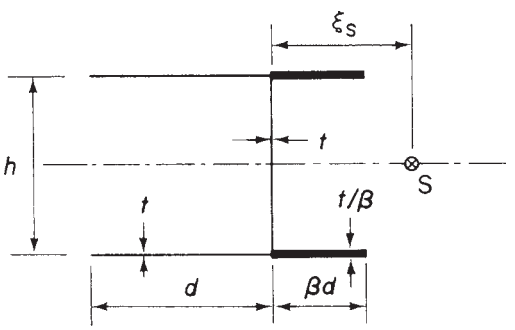

Fig. P.17.4

P.17.5 A thin-walled beam has the cross-section shown in Fig. P.17.5. The thickness of each flange varies linearly from t_1 at the tip to t_2 at the junction with the web. The

web itself has a constant thickness t_3. Calculate the distance ξ_S from the web to the shear centre S.

Ans. $d^2(2t_1 + t_2)/[3d(t_1 + t_2) + ht_3]$.

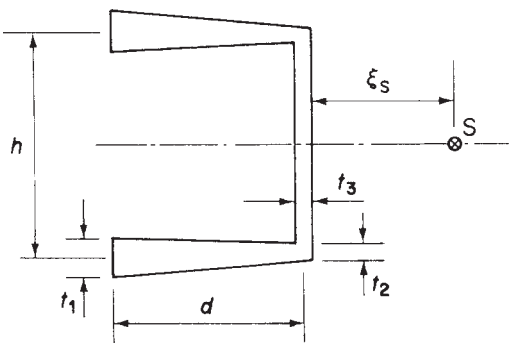

Fig. P.17.5

P.17.6 Figure P.17.6 shows the singly symmetrical cross-section of a thin-walled open section beam of constant wall thickness t, which has a narrow longitudinal slit at the corner 15.

Calculate and sketch the distribution of shear flow due to a vertical shear force S_y acting through the shear centre S and note the principal values. Show also that the distance ξ_S of the shear centre from the nose of the section is $\xi_S = l/2(1 + a/b)$.

Ans. $q_2 = q_4 = 3bS_y/2h(b + a)$, $q_3 = 3S_y/2h$. Parabolic distributions.

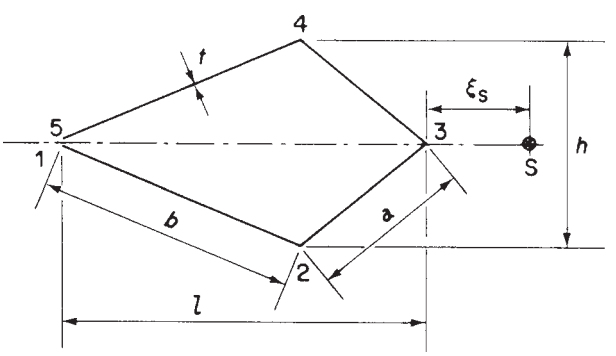

Fig. P.17.6

P.17.7 Show that the position of the shear centre S with respect to the intersection of the web and lower flange of the thin-walled section shown in Fig. P.17.7, is given by

$$\xi_S = -45a/97, \quad \eta_S = 46a/97$$

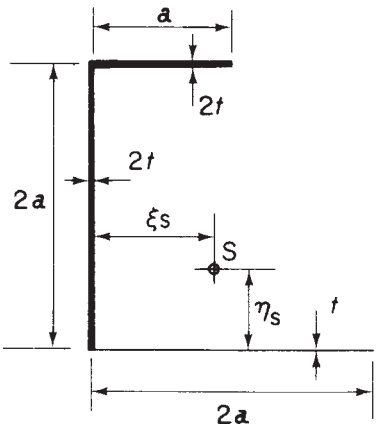

Fig. P.17.7

P.17.8 Define the term 'shear centre' of a thin-walled open section and determine the position of the shear centre of the thin-walled open section shown in Fig. P.17.8.

Ans. 2.66*r* from centre of semicircular wall.

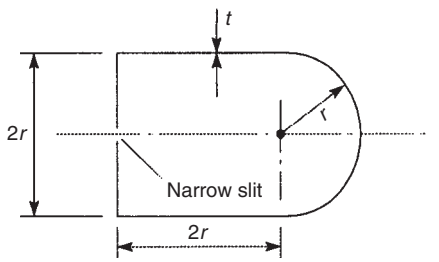

Fig. P.17.8

P.17.9 Determine the position of the shear centre of the cold-formed, thin-walled section shown in Fig. P.17.9. The thickness of the section is constant throughout.

Ans. 87.5 mm above centre of semicircular wall.

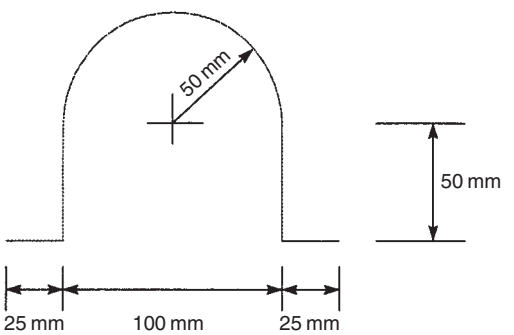

Fig. P.17.9

P.17.10 Find the position of the shear centre of the thin-walled beam section shown in Fig. P.17.10.

Ans. 1.2r on axis of symmetry to the left of the section.

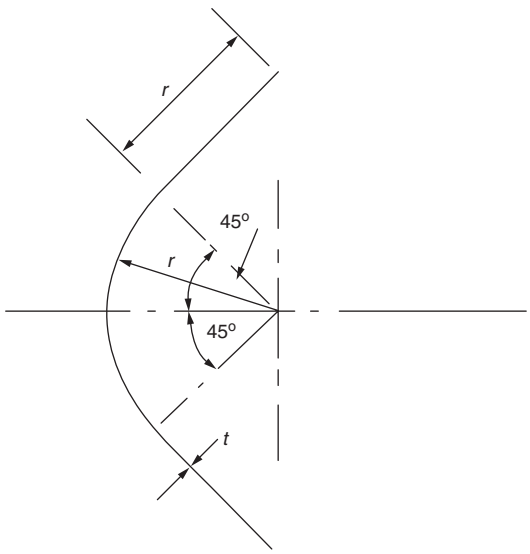

Fig. P.17.10

P.17.11 Calculate the position of the shear centre of the thin-walled section shown in Fig. P.17.11.

Ans. 20.2 mm to the left of the vertical web on axis of symmetry.

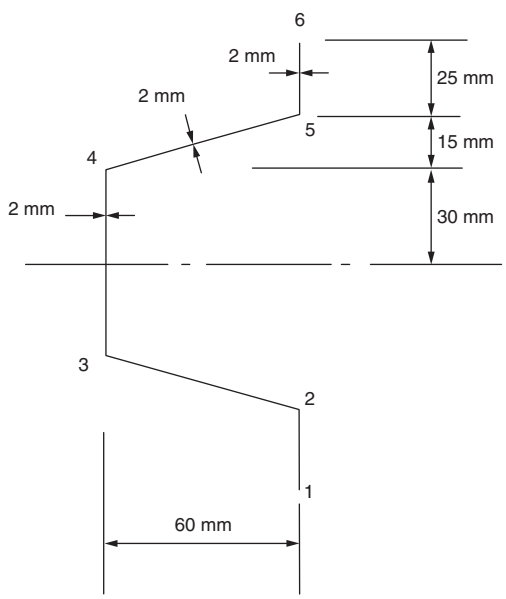

Fig. P.17.11

P.17.12 A thin-walled closed section beam of constant wall thickness t has the cross-section shown in Fig. P.17.12.

Assuming that the direct stresses are distributed according to the basic theory of bending, calculate and sketch the shear flow distribution for a vertical shear force S_y applied tangentially to the curved part of the beam.

Ans. $q_{O1} = S_y(1.61\cos\theta - 0.80)/r$

$$q_{12} = \frac{S_y}{r^3}(0.57s^2 - 1.14rs + 0.33r^2).$$

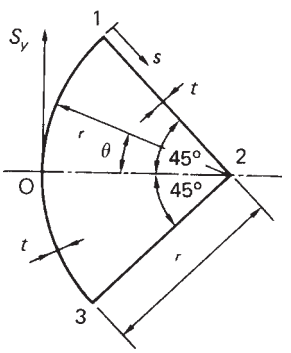

Fig. P.17.12

P.17.13 A uniform thin-walled beam of constant wall thickness t has a cross-section in the shape of an isosceles triangle and is loaded with a vertical shear force S_y applied at the apex. Assuming that the distribution of shear stress is according to the basic theory of bending, calculate the distribution of shear flow over the cross-section.

Illustrate your answer with a suitable sketch, marking in carefully with arrows the direction of the shear flows and noting the principal values.

Ans. $q_{12} = S_y(3s_1^2/d - h - 3d)/h(h + 2d)$

$q_{23} = S_y(-6s_2^2 + 6hs_2 - h^2)/h^2(h + 2d)$

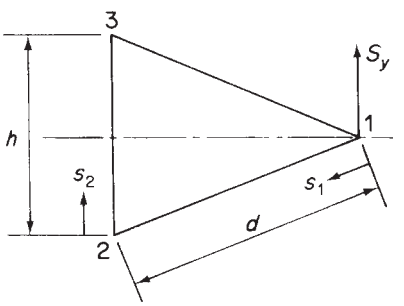

Fig. P.17.13

P.17.14 Figure P.17.14 shows the regular hexagonal cross-section of a thin-walled beam of sides a and constant wall thickness t. The beam is subjected to a transverse shear force S, its line of action being along a side of the hexagon, as shown.

Plot the shear flow distribution around the section, with values in terms of S and a.

Ans. $q_1 = -0.52S/a,\ q_2 = q_8 = -0.47S/a,\ q_3 = q_7 = -0.17S/\text{a},$
$q_4 = q_6 = 0.13S/a,\ q_5 = 0.18S/a$
Parabolic distributions, q positive clockwise.

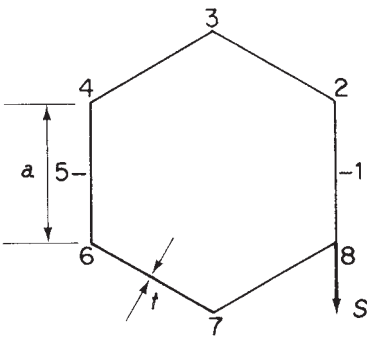

Fig. P.17.14

P.17.15 A box girder has the singly symmetrical trapezoidal cross-section shown in Fig. P.17.15. It supports a vertical shear load of 500 kN applied through its shear centre and in a direction perpendicular to its parallel sides. Calculate the shear flow distribution and the maximum shear stress in the section.

Ans. $q_{\text{OA}} = 0.25s_A$

$q_{\text{AB}} = 0.21s_B - 2.14 \times 10^{-4}s_{\text{B}}^2 + 250$

$q_{\text{BC}} = -0.17s_{\text{C}} + 246$

$\tau_{\max} = 30.2\,\text{N/mm}^2$

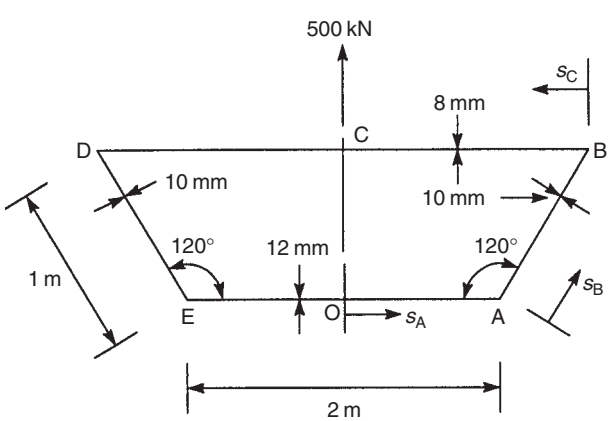

Fig. P.17.15

18

Torsion of beams

In Chapter 3 we developed the theory for the torsion of solid sections using both the Prandtl stress function approach and the St. Venant warping function solution. From that point we looked, via the membrane analogy, at the torsion of a narrow rectangular strip. We shall use the results of this analysis to investigate the torsion of thin-walled open section beams but first we shall examine the torsion of thin-walled closed section beams since the theory for this relies on the general stress, strain and displacement relationships which we established in Chapter 17.

18.1 Torsion of closed section beams

A closed section beam subjected to a pure torque T as shown in Fig. 18.1 does not, in the absence of an axial constraint, develop a direct stress system. It follows that the equilibrium conditions of Eqs (17.2) and (17.3) reduce to $\partial q/\partial s = 0$ and $\partial q/\partial z = 0$, respectively. These relationships may only be satisfied simultaneously by a constant value of q. We deduce, therefore, that the application of a pure torque to a closed section beam results in the development of a constant shear flow in the beam wall. However, the shear stress τ may vary around the cross-section since we allow the wall thickness t to be a function of s. The relationship between the applied torque and this constant shear flow is simply derived by considering the torsional equilibrium of the section shown in Fig. 18.2. The torque produced by the shear flow acting on an element δs of

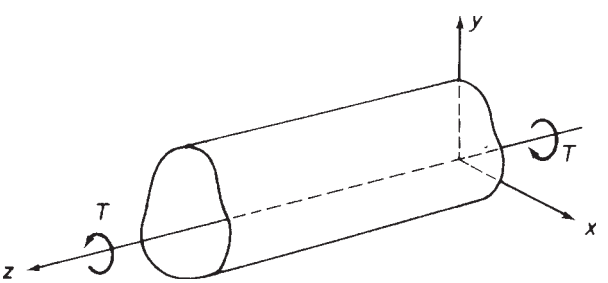

Fig. 18.1 Torsion of a closed section beam.

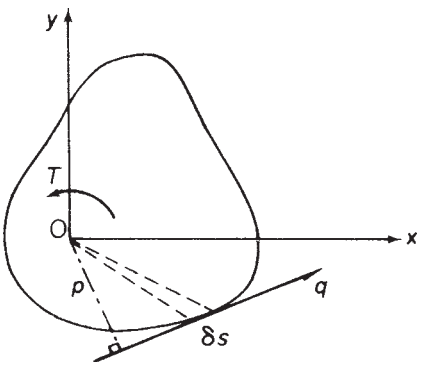

Fig. 18.2 Determination of the shear flow distribution in a closed section beam subjected to torsion.

the beam wall is $pq\delta s$. Hence

$$T = \oint pq \, \mathrm{d}s$$

or, since q is constant and $\oint p \, \mathrm{d}s = 2A$ (see Section 17.3)

$$T = 2Aq \tag{18.1}$$

Note that the origin O of the axes in Fig. 18.2 may be positioned in or outside the cross-section of the beam since the moment of the internal shear flows (whose resultant is a pure torque) is the same about any point in their plane. For an origin outside the cross-section the term $\oint p \, \mathrm{d}s$ will involve the summation of positive and negative areas. The sign of an area is determined by the sign of p which itself is associated with the sign convention for torque as follows. If the movement of the foot of p along the tangent at any point in the positive direction of s leads to an anticlockwise rotation of p about the origin of axes, p is positive. The positive direction of s is in the positive direction of q which is anticlockwise (corresponding to a positive torque). Thus, in Fig. 18.3 a generator OA, rotating about O, will initially sweep out a negative area since p_A is negative. At B, however, p_B is positive so that the area swept out by the generator has changed sign (at the point where the tangent passes through O and $p = 0$). Positive and negative areas cancel each other out as they overlap so that as the generator moves completely around the section, starting and returning to A say, the resultant area is that enclosed by the profile of the beam.

The theory of the torsion of closed section beams is known as the *Bredt–Batho theory* and Eq. (18.1) is often referred to as the *Bredt–Batho formula*.

18.1.1 Displacements associated with the Bredt–Batho shear flow

The relationship between q and shear strain γ established in Eq. (17.19), namely

$$q = Gt\left(\frac{\partial w}{\partial s} + \frac{\partial v_\mathrm{t}}{\partial z}\right)$$

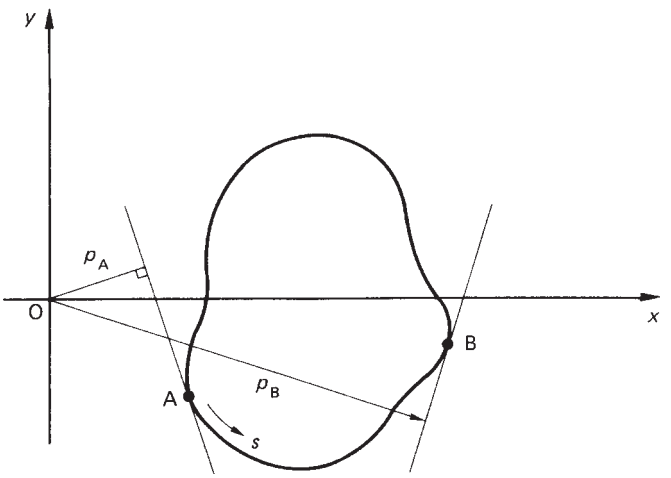

Fig. 18.3 Sign convention for swept areas.

is valid for the pure torsion case where q is constant. Differentiating this expression with respect to z we have

$$\frac{\partial q}{\partial z} = Gt\left(\frac{\partial^2 w}{\partial z\,\partial s} + \frac{\partial^2 v_t}{\partial z^2}\right) = 0$$

or

$$\frac{\partial}{\partial s}\left(\frac{\partial w}{\partial z}\right) + \frac{\partial^2 v_t}{\partial z^2} = 0 \tag{18.2}$$

In the absence of direct stresses the longitudinal strain $\partial w/\partial z(=\varepsilon_z)$ is zero so that

$$\frac{\partial^2 v_t}{\partial z^2} = 0$$

Hence from Eq. (17.7)

$$p\frac{\mathrm{d}^2\theta}{\mathrm{d}z^2} + \frac{\mathrm{d}^2 u}{\mathrm{d}z^2}\cos\psi + \frac{\mathrm{d}^2 v}{\mathrm{d}z^2}\sin\psi = 0 \tag{18.3}$$

For Eq. (18.3) to hold for all points around the section wall, in other words for all values of ψ

$$\frac{\mathrm{d}^2\theta}{\mathrm{d}z^2} = 0, \quad \frac{\mathrm{d}^2 u}{\mathrm{d}z^2} = 0, \quad \frac{\mathrm{d}^2 v}{\mathrm{d}z^2} = 0$$

It follows that $\theta = Az + B$, $u = Cz + D$, $v = Ez + F$, where A, B, C, D, E and F are unknown constants. Thus θ, u and v are all linear functions of z.

Equation (17.22), relating the rate of twist to the variable shear flow q_s developed in a shear loaded closed section beam, is also valid for the case $q_s = q =$ constant. Hence

$$\frac{\mathrm{d}\theta}{\mathrm{d}z} = \frac{q}{2A}\oint\frac{\mathrm{d}s}{Gt}$$

which becomes, on substituting for q from Eq. (18.1)

$$\frac{\mathrm{d}\theta}{\mathrm{d}z} = \frac{T}{4A^2}\oint \frac{\mathrm{d}s}{Gt} \tag{18.4}$$

The warping distribution produced by a varying shear flow, as defined by Eq. (17.25) for axes having their origin at the centre of twist, is also applicable to the case of a constant shear flow. Thus

$$w_s - w_0 = q\int_0^s \frac{\mathrm{d}s}{Gt} - \frac{A_{Os}}{A}q\oint \frac{\mathrm{d}s}{Gt}$$

Replacing q from Eq. (18.1) we have

$$w_s - w_0 = \frac{T\delta}{2A}\left(\frac{\delta_{Os}}{\delta} - \frac{A_{Os}}{A}\right) \tag{18.5}$$

where

$$\delta = \oint \frac{\mathrm{d}s}{Gt} \quad \text{and} \quad \delta_{Os} = \int_0^s \frac{\mathrm{d}s}{Gt}$$

The sign of the warping displacement in Eq. (18.5) is governed by the sign of the applied torque T and the signs of the parameters δ_{Os} and A_{Os}. Having specified initially that a positive torque is anticlockwise, the signs of δ_{Os} and A_{Os} are fixed in that δ_{Os} is positive when s is positive, i.e. s is taken as positive in an anticlockwise sense, and A_{Os} is positive when, as before, p (see Fig. 18.3) is positive.

We have noted that the longitudinal strain ε_z is zero in a closed section beam subjected to a pure torque. This means that all sections of the beam must possess identical warping distributions. In other words longitudinal generators of the beam surface remain unchanged in length although subjected to axial displacement.

Example 18.1

A thin-walled circular section beam has a diameter of 200 mm and is 2 m long; it is firmly restrained against rotation at each end. A concentrated torque of 30 kN m is applied to the beam at its mid-span point. If the maximum shear stress in the beam is limited to 200 N/mm^2 and the maximum angle of twist to 2°, calculate the minimum thickness of the beam walls. Take $G = 25\,000$ N/mm^2.

The minimum thickness of the beam corresponding to the maximum allowable shear stress of 200 N/mm^2 is obtained directly using Eq. (18.1) in which $T_{\max} = 15$ kN m.

Then

$$t_{\min} = \frac{15 \times 10^6 \times 4}{2 \times \pi \times 200^2 \times 200} = 1.2\,\text{mm}$$

The rate of twist along the beam is given by Eq. (18.4) in which

$$\oint \frac{\mathrm{d}s}{t} = \frac{\pi \times 200}{t_{\min}}$$

Hence

$$\frac{d\theta}{dz} = \frac{T}{4A^2G} \times \frac{\pi \times 200}{t_{min}} \tag{i}$$

Taking the origin for z at one of the fixed ends and integrating Eq. (i) for half the length of the beam we obtain

$$\theta = \frac{T}{4A^2G} \times \frac{200\pi}{t_{min}} z + C_1$$

where C_1 is a constant of integration. At the fixed end where $z = 0$, $\theta = 0$ so that $C_1 = 0$.

Hence

$$\theta = \frac{T}{4A^2G} \times \frac{200\pi}{t_{min}} z$$

The maximum angle of twist occurs at the mid-span of the beam where $z = 1$ m. Hence

$$t_{min} = \frac{15 \times 10^6 \times 200 \times \pi \times 1 \times 10^3 \times 180}{4 \times (\pi \times 200^2/4)^2 \times 25\,000 \times 2 \times \pi} = 2.7 \text{ mm}$$

The minimum allowable thickness that satisfies both conditions is therefore 2.7 mm.

Example 18.2

Determine the warping distribution in the doubly symmetrical rectangular, closed section beam, shown in Fig. 18.4, when subjected to an anticlockwise torque T.

From symmetry the centre of twist R will coincide with the mid-point of the cross-section and points of zero warping will lie on the axes of symmetry at the mid-points of the sides. We shall therefore take the origin for s at the mid-point of side 14 and measure s in the positive, anticlockwise, sense around the section. Assuming the shear modulus G to be constant we rewrite Eq. (18.5) in the form

$$w_s - w_0 = \frac{T\delta}{2AG}\left(\frac{\delta_{Os}}{\delta} - \frac{A_{Os}}{A}\right) \tag{i}$$

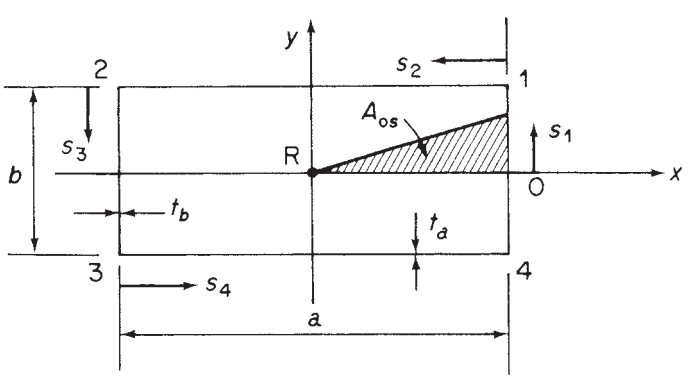

Fig. 18.4 Torsion of a rectangular section beam.

where

$$\delta = \oint \frac{\mathrm{d}s}{t} \quad \text{and} \quad \delta_{Os} = \int_0^s \frac{\mathrm{d}s}{t}$$

In Eq. (i)

$$w_0 = 0, \quad \delta = 2\left(\frac{b}{t_b} + \frac{a}{t_a}\right) \quad \text{and} \quad A = ab$$

From 0 to 1, $0 \leq s_1 \leq b/2$ and

$$\delta_{Os} = \int_0^{s_1} \frac{\mathrm{d}s_1}{t_b} = \frac{s_1}{t_b} \quad A_{Os} = \frac{as_1}{4} \tag{ii}$$

Note that δ_{Os} and A_{Os} are both positive.

Substitution for δ_{Os} and A_{Os} from Eq. (ii) in (i) shows that the warping distribution in the wall 01, w_{01}, is linear. Also

$$w_1 = \frac{T}{2abG} 2\left(\frac{b}{t_b} + \frac{a}{t_a}\right)\left[\frac{b/2t_b}{2(b/t_b + a/t_a)} - \frac{ab/8}{ab}\right]$$

which gives

$$w_1 = \frac{T}{8abG}\left(\frac{b}{t_b} - \frac{a}{t_a}\right) \tag{iii}$$

The remainder of the warping distribution may be deduced from symmetry and the fact that the warping must be zero at points where the axes of symmetry and the walls of the cross-section intersect. It follows that

$$w_2 = -w_1 = -w_3 = w_4$$

giving the distribution shown in Fig. 18.5. Note that the warping distribution will take the form shown in Fig. 18.5 as long as T is positive and $b/t_b > a/t_a$. If *either* of these conditions is reversed w_1 and w_3 will become negative and w_2 and w_4 positive. In the case when $b/t_b = a/t_a$ the warping is zero at all points in the cross-section.

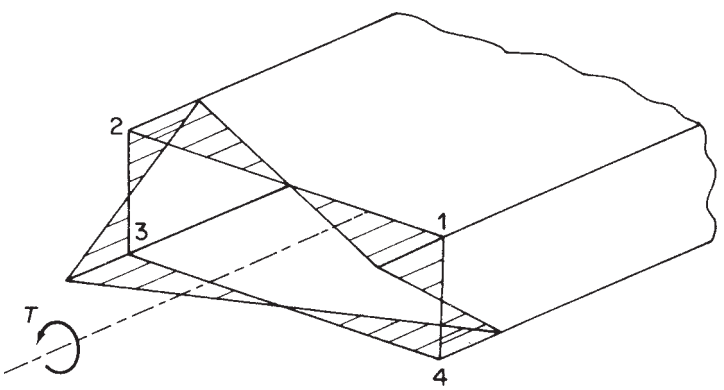

Fig. 18.5 Warping distribution in the rectangular section beam of Example 18.2.

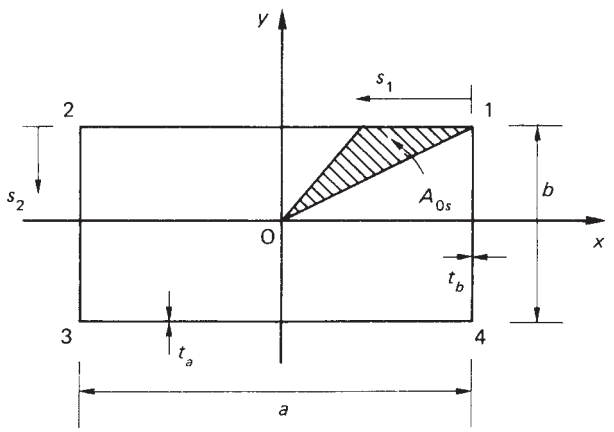

Fig. 18.6 Arbitrary origin for *s*.

Suppose now that the origin for s is chosen arbitrarily at, say, point 1. Then, from Fig. 18.6, δ_{Os} in the wall $12 = s_1/t_a$ and $A_{Os} = \frac{1}{2}s_1 b/2 = s_1 b/4$ and both are positive.

Substituting in Eq. (i) and setting $w_0 = 0$

$$w'_{12} = \frac{T\delta}{2abG}\left(\frac{s_1}{\delta t_a} - \frac{s_1}{4a}\right) \tag{iv}$$

so that w'_{12} varies linearly from zero at 1 to

$$w'_2 = \frac{T}{2abG}2\left(\frac{b}{t_b} + \frac{a}{t_a}\right)\left[\frac{a}{2(b/t_b + a/t_a)t_a} - \frac{1}{4}\right]$$

at 2. Thus

$$w'_2 = \frac{T}{4abG}\left(\frac{a}{t_a} - \frac{b}{t_b}\right)$$

or

$$w'_2 = -\frac{T}{4abG}\left(\frac{b}{t_b} - \frac{a}{t_a}\right) \tag{v}$$

Similarly

$$w'_{23} = \frac{T\delta}{2abG}\left[\frac{1}{\delta}\left(\frac{a}{t_a} + \frac{s_2}{t_b}\right) - \frac{1}{4b}(b + s_2)\right] \tag{vi}$$

The warping distribution therefore varies linearly from a value $-T(b/t_b - a/t_a)/4abG$ at 2 to zero at 3. The remaining distribution follows from symmetry so that the complete distribution takes the form shown in Fig. 18.7.

Comparing Figs 18.5 and 18.7 it can be seen that the form of the warping distribution is the same but that in the latter case the complete distribution has been displaced axially. The actual value of the warping at the origin for s is found using Eq. (17.26).

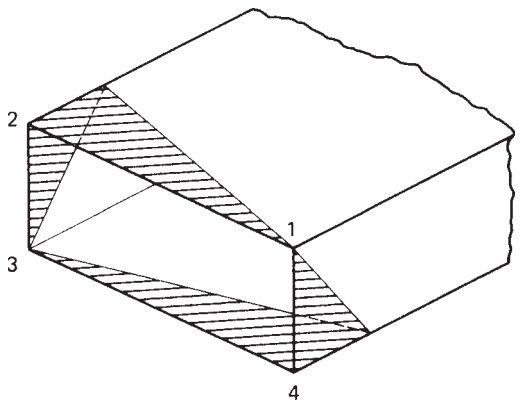

Fig. 18.7 Warping distribution produced by selecting an arbitrary origin for *s*.

Thus

$$w_0 = \frac{2}{2(at_a + bt_b)} \left(\int_0^a w'_{12} t_a \, \mathrm{d}s_1 + \int_0^b w'_{23} t_b \, \mathrm{d}s_2 \right) \tag{vii}$$

Substituting in Eq. (vii) for w'_{12} and w'_{23} from Eqs (iv) and (vi), respectively, and evaluating gives

$$w_0 = -\frac{T}{8abG} \left(\frac{b}{t_b} - \frac{a}{t_a} \right) \tag{viii}$$

Subtracting this value from the values of $w'_1 (= 0)$ and $w'_2 (= -T(b/t_b - a/t_a)/4abG)$ we have

$$w_1 = \frac{T}{8abG} \left(\frac{b}{t_b} - \frac{a}{t_a} \right), \quad w_2 = -\frac{T}{8abG} \left(\frac{b}{t_b} - \frac{a}{t_a} \right)$$

as before. Note that setting $w_0 = 0$ in Eq. (i) implies that w_0, the actual value of warping at the origin for s, has been added to all warping displacements. This value must therefore be *subtracted* from the calculated warping displacements (i.e. those based on an arbitrary choice of origin) to obtain true values.

It is instructive at this stage to examine the mechanics of warping to see how it arises. Suppose that each end of the rectangular section beam of Example 18.2 rotates through opposite angles θ giving a total angle of twist 2θ along its length L. The corner 1 at one end of the beam is displaced by amounts $a\theta/2$ vertically and $b\theta/2$ horizontally as shown in Fig. 18.8. Consider now the displacements of the web and cover of the beam due to rotation. From Figs 18.8 and 18.9 (a) and (b) it can be seen that the angles of rotation of the web and the cover are, respectively

$$\phi_b = (a\theta/2)/(L/2) = a\theta/L$$

and

$$\phi_a = (b\theta/2)/(L/2) = b\theta/L$$

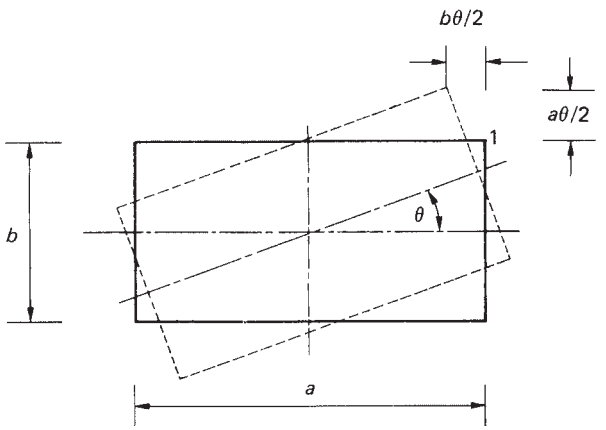

Fig. 18.8 Twisting of a rectangular section beam.

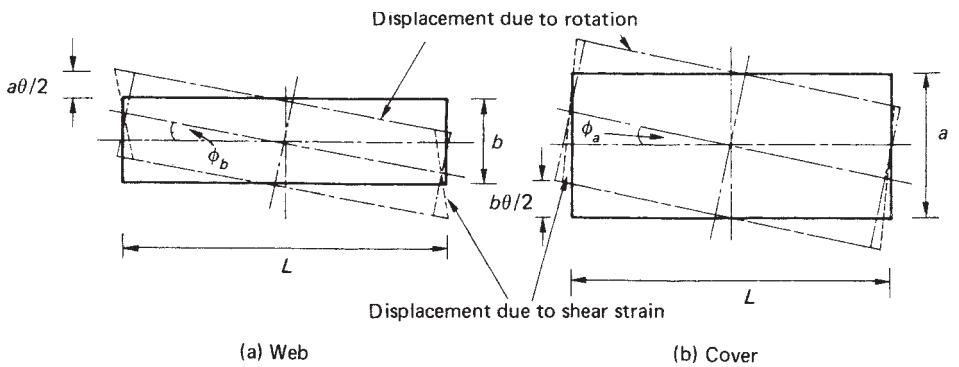

Fig. 18.9 Displacements due to twist and shear strain.

The axial displacements of the corner 1 in the web and cover are then

$$\frac{b}{2}\frac{a\theta}{L}, \quad \frac{a}{2}\frac{b\theta}{L}$$

respectively, as shown in Fig. 18.9(a) and (b). In addition to displacements produced by twisting, the webs and covers are subjected to shear strains γ_b and γ_a corresponding to the shear stress system given by Eq. (18.1). Due to γ_b the axial displacement of corner 1 in the web is $\gamma_b b/2$ in the positive z direction while in the cover the displacement is $\gamma_a a/2$ in the negative z direction. Note that the shear strains γ_b and γ_a correspond to the shear stress system produced by a positive anticlockwise torque. Clearly, the total axial displacement of the point 1 in the web and cover must be the same so that

$$-\frac{b}{2}\frac{a\theta}{L} + \gamma_b\frac{b}{2} = \frac{a}{2}\frac{b\theta}{L} - \gamma_a\frac{a}{2}$$

from which

$$\theta = \frac{L}{2ab}(\gamma_a a + \gamma_b b)$$

The shear strains are obtained from Eq. (18.1) and are

$$\gamma_a = \frac{T}{2abGt_a}, \quad \gamma_b = \frac{T}{2abGt_b}$$

whence

$$\theta = \frac{TL}{4a^2b^2G}\left(\frac{a}{t_a} + \frac{b}{t_b}\right)$$

The total angle of twist from end to end of the beam is 2θ, therefore

$$\frac{2\theta}{L} = \frac{TL}{4a^2b^2G}\left(\frac{2a}{t_a} + \frac{2b}{t_b}\right)$$

or

$$\frac{\mathrm{d}\theta}{\mathrm{d}z} = \frac{T}{4A^2G}\oint \frac{\mathrm{d}s}{t}$$

as in Eq. (18.4).

Substituting for θ in either of the expressions for the axial displacement of the corner 1 gives the warping w_1 at 1. Thus

$$w_1 = \frac{a}{2}\frac{b}{L}\frac{TL}{4a^2b^2G}\left(\frac{a}{t_a} + \frac{b}{t_b}\right) - \frac{T}{2abGt_a}\frac{a}{2}$$

i.e.

$$w_1 = \frac{T}{8abG}\left(\frac{b}{t_b} - \frac{a}{t_a}\right)$$

as before. It can be seen that the warping of the cross-section is produced by a combination of the displacements caused by twisting and the displacements due to the shear strains; these shear strains correspond to the shear stresses whose values are fixed by statics. The angle of twist must therefore be such as to ensure compatibility of displacement between the webs and covers.

18.1.2 Condition for zero warping at a section

The geometry of the cross-section of a closed section beam subjected to torsion may be such that no warping of the cross-section occurs. From Eq. (18.5) we see that this condition arises when

$$\frac{\delta_{Os}}{\delta} = \frac{A_{Os}}{A}$$

or

$$\frac{1}{\delta}\int_0^s \frac{\mathrm{d}s}{Gt} = \frac{1}{2A}\int_0^s p_\mathrm{R}\,\mathrm{d}s \tag{18.6}$$

Differentiating Eq. (18.6) with respect to s gives

$$\frac{1}{\delta G t} = \frac{p_R}{2A}$$

or

$$p_R G t = \frac{2A}{\delta} = \text{constant} \tag{18.7}$$

A closed section beam for which $p_R G t = \text{constant}$ does not warp and is known as a *Neuber beam*. For closed section beams having a constant shear modulus the condition becomes

$$p_R t = \text{constant} \tag{18.8}$$

Examples of such beams are: a circular section beam of constant thickness; a rectangular section beam for which $at_b = bt_a$ (see Example 18.2); and a triangular section beam of constant thickness. In the last case the shear centre and hence the centre of twist may be shown to coincide with the centre of the inscribed circle so that p_R for each side is the radius of the inscribed circle.

18.2 Torsion of open section beams

An approximate solution for the torsion of a thin-walled open section beam may be found by applying the results obtained in Section 3.4 for the torsion of a thin rectangular strip. If such a strip is bent to form an open section beam, as shown in Fig. 18.10(a), and if the distance s measured around the cross-section is large compared with its thickness t then

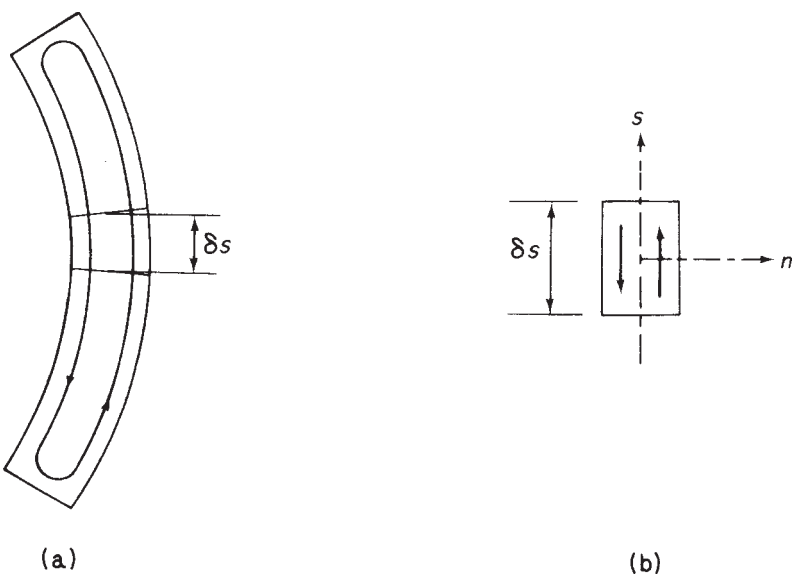

Fig. 18.10 (a) Shear lines in a thin-walled open section beam subjected to torsion; (b) approximation of elemental shear lines to those in a thin rectangular strip.

the contours of the membrane, i.e. lines of shear stress, are still approximately parallel to the inner and outer boundaries. It follows that the shear lines in an element δs of the open section must be nearly the same as those in an element δy of a rectangular strip as demonstrated in Fig. 18.10(b). Equations (3.27)–(3.29) may therefore be applied to the open beam but with reduced accuracy. Referring to Fig. 18.10(b) we observe that Eq. (3.27) becomes

$$\tau_{zs} = 2Gn\frac{\mathrm{d}\theta}{\mathrm{d}z}, \quad \tau_{zn} = 0 \tag{18.9}$$

Equation (3.28) becomes

$$\tau_{zs,\max} = \pm Gt\frac{\mathrm{d}\theta}{\mathrm{d}z} \tag{18.10}$$

and Eq. (3.29) is

$$J = \sum \frac{st^3}{3} \quad \text{or} \quad J = \frac{1}{3}\int_{\text{sect}} t^3\,\mathrm{d}s \tag{18.11}$$

In Eq. (18.11) the second expression for the torsion constant is used if the cross-section has a variable wall thickness. Finally, the rate of twist is expressed in terms of the applied torque by Eq. (3.12), viz.

$$T = GJ\frac{\mathrm{d}\theta}{\mathrm{d}z} \tag{18.12}$$

The shear stress distribution and the maximum shear stress are sometimes more conveniently expressed in terms of the applied torque. Therefore, substituting for $\mathrm{d}\theta/\mathrm{d}z$ in Eqs (18.9) and (18.10) gives

$$\tau_{zs} = \frac{2n}{J}T, \quad \tau_{zs,\max} = \pm\frac{tT}{J} \tag{18.13}$$

We assume in open beam torsion analysis that the cross-section is maintained by the system of closely spaced diaphragms described in Section 17.1 and that the beam is of uniform section. Clearly, in this problem the shear stresses vary across the thickness of the beam wall whereas other stresses such as axial constraint stresses which we shall discuss in Chapter 27 are assumed constant across the thickness.

18.2.1 Warping of the cross-section

We saw in Section 3.4 that a thin rectangular strip suffers warping across its thickness when subjected to torsion. In the same way a thin-walled open section beam will warp across its thickness. This warping, w_{t}, may be deduced by comparing Fig. 18.10(b) with Fig. 3.10 and using Eq. (3.32), thus

$$w_{\mathrm{t}} = ns\frac{\mathrm{d}\theta}{\mathrm{d}z} \tag{18.14}$$

In addition to warping across the thickness, the cross-section of the beam will warp in a similar manner to that of a closed section beam. From Fig. 17.3

$$\gamma_{zs} = \frac{\partial w}{\partial s} + \frac{\partial v_t}{\partial z} \tag{18.15}$$

Referring the tangential displacement v_t to the centre of twist R of the cross-section we have, from Eq. (17.8)

$$\frac{\partial v_t}{\partial z} = p_R \frac{d\theta}{dz} \tag{18.16}$$

Substituting for $\partial v_t/\partial z$ in Eq. (18.15) gives

$$\gamma_{zs} = \frac{\partial w}{\partial s} + p_R \frac{d\theta}{dz}$$

from which

$$\tau_{zs} = G\left(\frac{\partial w}{\partial s} + p_R \frac{d\theta}{dz}\right) \tag{18.17}$$

On the mid-line of the section wall $\tau_{zs} = 0$ (see Eq. (18.9)) so that, from Eq. (18.17)

$$\frac{\partial w}{\partial s} = -p_R \frac{d\theta}{dz}$$

Integrating this expression with respect to s and taking the lower limit of integration to coincide with the point of zero warping, we obtain

$$w_s = -\frac{d\theta}{dz}\int_0^s p_R \, ds \tag{18.18}$$

From Eqs (18.14) and (18.18) it can be seen that two types of warping exist in an open section beam. Equation (18.18) gives the warping of the mid-line of the beam; this is known as *primary warping* and is assumed to be constant across the wall thickness. Equation (18.14) gives the warping of the beam across its wall thickness. This is called *secondary warping*, is very much less than primary warping and is usually ignored in the thin-walled sections common to aircraft structures.

Equation (18.18) may be rewritten in the form

$$w_s = -2A_R \frac{d\theta}{dz} \tag{18.19}$$

or, in terms of the applied torque

$$w_s = -2A_R \frac{T}{GJ} \quad \text{(see Eq. (18.12))} \tag{18.20}$$

in which $A_R = \frac{1}{2}\int_0^s p_R \, ds$ is the area swept out by a generator, rotating about the centre of twist, from the point of zero warping, as shown in Fig. 18.11. The sign of w_s, for a given direction of torque, depends upon the sign of A_R which in turn depends upon the sign of

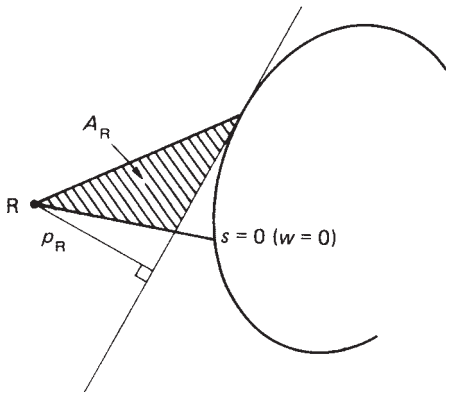

Fig. 18.11 Warping of an open section beam.

p_R, the perpendicular distance from the centre of twist to the tangent at any point. Again, as for closed section beams, the sign of p_R depends upon the assumed direction of a positive torque, in this case anticlockwise. Therefore, p_R (and therefore A_R) is positive if movement of the foot of p_R along the tangent in the assumed direction of s leads to an anticlockwise rotation of p_R about the centre of twist. Note that for open section beams the positive direction of s may be chosen arbitrarily since, for a given torque, the sign of the warping displacement depends only on the sign of the swept area A_R.

Example 18.3

Determine the maximum shear stress and the warping distribution in the channel section shown in Fig. 18.12 when it is subjected to an anticlockwise torque of 10 N m. $G = 25\,000\,\text{N/mm}^2$.

From the second of Eqs (18.13) it can be seen that the maximum shear stress occurs in the web of the section where the thickness is greatest. Also, from the first of Eqs (18.11)

$$J = \tfrac{1}{3}(2 \times 25 \times 1.5^3 + 50 \times 2.5^3) = 316.7\,\text{mm}^4$$

so that

$$\tau_{\max} = \pm\frac{2.5 \times 10 \times 10^3}{316.7} = \pm 78.9\,\text{N/mm}^2$$

The warping distribution is obtained using Eq. (18.20) in which the origin for s (and hence A_R) is taken at the intersection of the web and the axis of symmetry where the warping is zero. Further, the centre of twist R of the section coincides with its shear centre S whose position is found using the method described in Section 17.2.1, this gives $\xi_S = 8.04$ mm. In the wall O2

$$A_R = \tfrac{1}{2} \times 8.04 s_1 \quad (p_R \text{ is positive})$$

so that

$$w_{O2} = -2 \times \tfrac{1}{2} \times 8.04 s_1 \times \frac{10 \times 10^3}{25\,000 \times 316.7} = -0.01 s_1 \qquad \text{(i)}$$

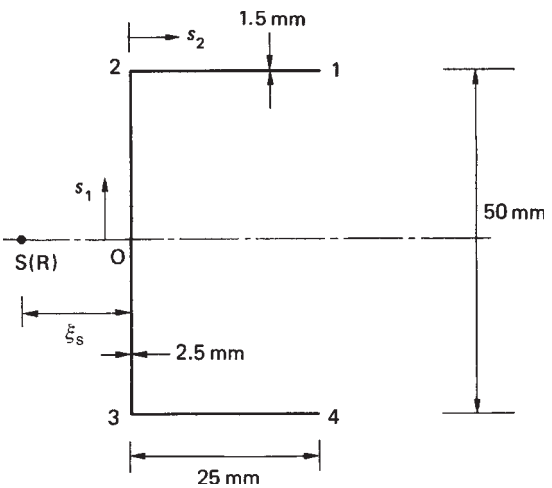

Fig. 18.12 Channel section of Example 18.3.

i.e. the warping distribution is linear in O2 and

$$w_2 = -0.01 \times 25 = -0.25\,\text{mm}$$

In the wall 21

$$A_R = \tfrac{1}{2} \times 8.04 \times 25 - \tfrac{1}{2} \times 25 s_2$$

in which the area swept out by the generator in the wall 21 provides a negative contribution to the total swept area A_R. Thus

$$w_{21} = -25(8.04 - s_2)\frac{10 \times 10^3}{25\,000 \times 316.7}$$

or

$$w_{21} = -0.03(8.04 - s_2) \tag{ii}$$

Again the warping distribution is linear and varies from -0.25 mm at 2 to $+0.54$ mm at 1. Examination of Eq. (ii) shows that w_{21} changes sign at $s_2 = 8.04$ mm. The remaining warping distribution follows from symmetry and the complete distribution is shown in Fig. 18.13. In unsymmetrical section beams the position of the point of zero warping is not known but may be found using the method described in Section 27.2 for the restrained warping of an open section beam. From the derivation of Eq. (27.3) we see that

$$2A'_R = \frac{\int_{\text{sect}} 2A_{R,O} t\,\mathrm{d}s}{\int_{\text{sect}} t\,\mathrm{d}s} \tag{18.21}$$

in which $A_{R,O}$ is the area swept out by a generator rotating about the centre of twist from some convenient origin and A'_R is the value of $A_{R,O}$ at the point of zero warping. As an illustration we shall apply the method to the beam section of Example 18.3.

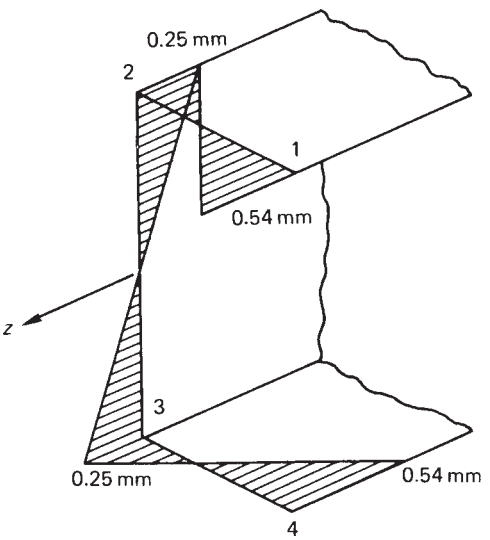

Fig. 18.13 Warping distribution in channel section of Example 18.3.

Suppose that the position of the centre of twist (i.e. the shear centre) has already been calculated and suppose also that we choose the origin for s to be at the point 1. Then, in Fig. 18.14

$$\int_{\text{sect}} t\,\mathrm{d}s = 2 \times 1.5 \times 25 + 2.5 \times 50 = 200\,\text{mm}^2$$

In the wall 12

$$A_{12} = \tfrac{1}{2} \times 25 s_1 \quad (A_{\text{R,O}} \text{ for the wall 12}) \tag{i}$$

from which

$$A_2 = \tfrac{1}{2} \times 25 \times 25 = 312.5\,\text{mm}^2$$

Also

$$A_{23} = 312.5 - \tfrac{1}{2} \times 8.04 s_2 \tag{ii}$$

and

$$A_3 = 312.5 - \tfrac{1}{2} \times 8.04 \times 50 = 111.5\,\text{mm}^2$$

Finally

$$A_{34} = 111.5 + \tfrac{1}{2} \times 25 s_3 \tag{iii}$$

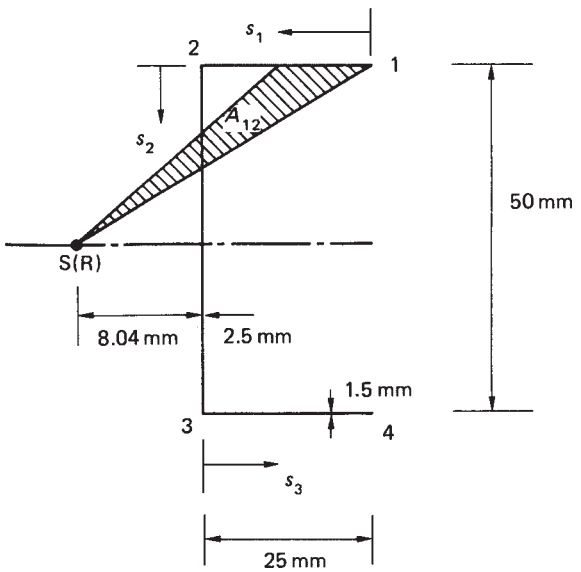

Fig. 18.14 Determination of points of zero warping.

Substituting for A_{12}, A_{23} and A_{34} from Eqs (i)–(iii) in Eq. (18.21) we have

$$2A'_{\mathrm{R}} = \frac{1}{200}\left[\int_0^{25} 25 \times 1.15 s_1 \, \mathrm{d}s_1 + \int_0^{50} 2(312.5 - 4.02 s_2) 2.5 \, \mathrm{d}s_2 + \int_0^{25} 2(111.5 + 12.5 s_3) 1.5 \, \mathrm{d}s_3\right] \quad \text{(iv)}$$

Evaluation of Eq. (iv) gives

$$2A'_{\mathrm{R}} = 424 \, \mathrm{mm}^2$$

We now examine each wall of the section in turn to determine points of zero warping. Suppose that in the wall 12 a point of zero warping occurs at a value of s_1 equal to $s_{1,0}$. Then

$$2 \times \tfrac{1}{2} \times 25 s_{1,0} = 424$$

from which

$$s_{1,0} = 16.96 \, \mathrm{mm}$$

so that a point of zero warping occurs in the wall 12 at a distance of 8.04 mm from the point 2 as before. In the web 23 let the point of zero warping occur at $s_2 = s_{2,0}$. Then

$$2 \times \tfrac{1}{2} \times 25 \times 25 - 2 \times \tfrac{1}{2} \times 8.04 s_{2,0} = 424$$

which gives $s_{2,0} = 25 \, \mathrm{mm}$ (i.e. on the axis of symmetry). Clearly, from symmetry, a further point of zero warping occurs in the flange 34 at a distance of 8.04 mm from the

point 3. The warping distribution is then obtained directly using Eq. (18.20) in which

$$A_{\mathrm{R}} = A_{\mathrm{R,O}} - A'_{\mathrm{R}}$$

Problems

P.18.1 A uniform, thin-walled, cantilever beam of closed rectangular cross-section has the dimensions shown in Fig. P.18.1. The shear modulus G of the top and bottom covers of the beam is 18 000 N/mm^2 while that of the vertical webs is 26 000 N/mm^2.

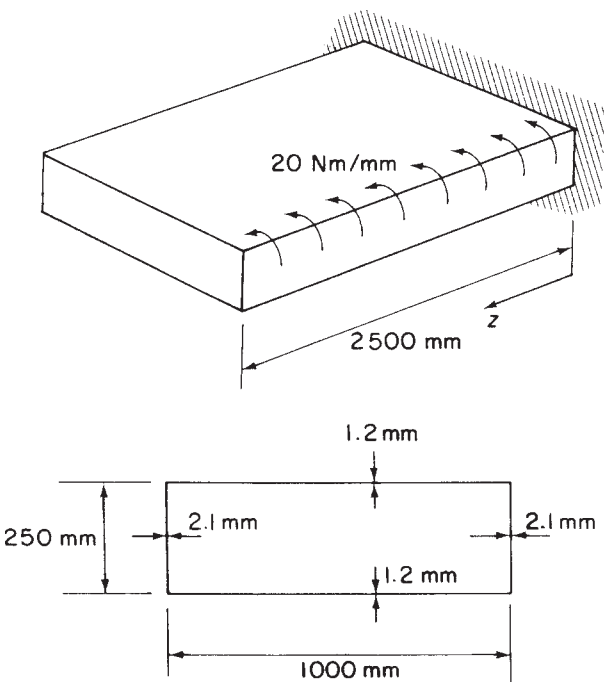

Fig. P.18.1

The beam is subjected to a uniformly distributed torque of 20 N m/mm along its length. Calculate the maximum shear stress according to the Bred–Batho theory of torsion. Calculate also, and sketch, the distribution of twist along the length of the cantilever assuming that axial constraint effects are negligible.

Ans. $\tau_{\max} = 83.3\,\mathrm{N/mm^2},\ \theta = 8.14 \times 10^{-9}\left(2500z - \dfrac{z^2}{2}\right)$ rad.

P.18.2 A single cell, thin-walled beam with the double trapezoidal cross-section shown in Fig. P.18.2, is subjected to a constant torque $T = 90\,500$ N m and is constrained to twist about an axis through the point R. Assuming that the shear stresses are distributed according to the Bredt–Batho theory of torsion, calculate the distribution of warping around the cross-section.

Illustrate your answer clearly by means of a sketch and insert the principal values of the warping displacements.

The shear modulus $G = 27\,500\,\text{N/mm}^2$ and is constant throughout.

Ans. $w_1 = -w_6 = -0.53\,\text{mm},\ w_2 = -w_5 = 0.05\,\text{mm},\ w_3 = -w_4 = 0.38\,\text{mm}.$

Linear distribution.

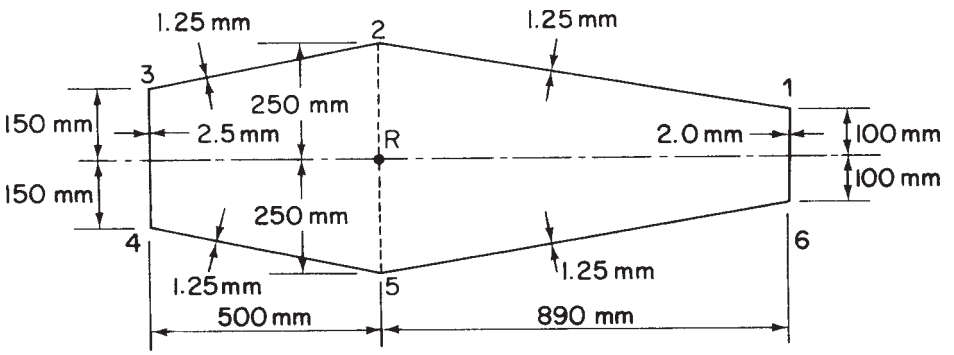

Fig. P.18.2

P.18.3 A uniform thin-walled beam is circular in cross-section and has a constant thickness of 2.5 mm. The beam is 2000 mm long, carrying end torques of 450 N m and, in the same sense, a distributed torque loading of 1.0 N m/mm. The loads are reacted by equal couples R at sections 500 mm distant from each end (Fig. P.18.3).

Calculate the maximum shear stress in the beam and sketch the distribution of twist along its length. Take $G = 30\,000\,\text{N/mm}^2$ and neglect axial constraint effects.

Ans. $\tau_{\max} = 24.2\,\text{N/mm}^2,\ \theta = -0.85 \times 10^{-8} z^2\ \text{rad},\ 0 \le z \le 500\,\text{mm},$
$\theta = 1.7 \times 10^{-8}(1450z - z^2/2) - 12.33 \times 10^{-3}\ \text{rad},\ 500 \le z \le 1000\,\text{mm}.$

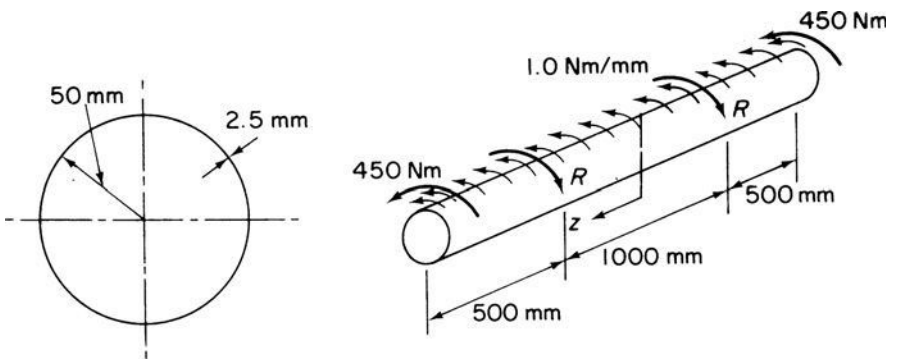

Fig. P.18.3

P.18.4 The thin-walled box section beam ABCD shown in Fig. P.18.4 is attached at each end to supports which allow rotation of the ends of the beam in the longitudinal vertical plane of symmetry but prevent rotation of the ends in vertical planes perpendicular to the longitudinal axis of the beam. The beam is subjected to a uniform torque

loading of 20 N m/mm over the portion BC of its span. Calculate the maximum shear stress in the cross-section of the beam and the distribution of angle of twist along its length, $G = 70\,000\,\text{N/mm}^2$.

Ans. $71.4\,\text{N/mm}^2$, $\theta_B = \theta_C = 0.36°$, θ at mid-span $= 0.72°$.

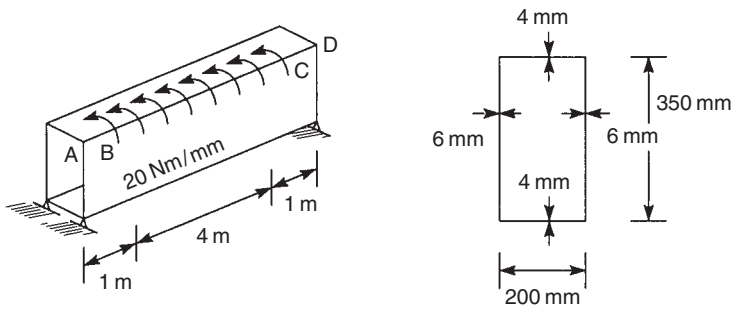

Fig. P.18.4

P.18.5 Figure P.18.5 shows a thin-walled cantilever box beam having a constant width of 50 mm and a depth which decreases linearly from 200 mm at the built-in end to 150 mm at the free end. If the beam is subjected to a torque of 1 kN m at its free end, plot the angle of twist of the beam at 500 mm intervals along its length and determine the maximum shear stress in the beam section. Take $G = 25\,000\,\text{N/mm}^2$.

Ans. $\tau_{max} = 33.3\,\text{N/mm}^2$.

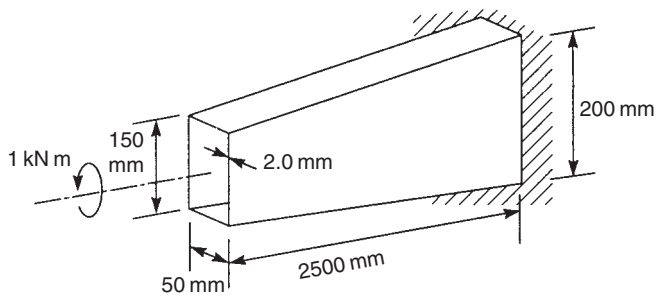

Fig. P.18.5

P.18.6 A uniform closed section beam, of the thin-walled section shown in Fig. P.18.6, is subjected to a twisting couple of 4500 N m. The beam is constrained to twist about a longitudinal axis through the centre C of the semicircular arc 12. For the curved wall 12 the thickness is 2 mm and the shear modulus is $22\,000\,\text{N/mm}^2$. For the plane walls 23, 34 and 41, the corresponding figures are 1.6 mm and $27\,500\,\text{N/mm}^2$. (*Note*: Gt = constant.)

Calculate the rate of twist in rad/mm. Give a sketch illustrating the distribution of warping displacement in the cross-section and quote values at points 1 and 4.

Ans. $d\theta/dz = 29.3 \times 10^{-6}$ rad/mm, $w_3 = -w_4 = -0.19$ mm, $w_2 = -w_1 = -0.056$ mm.

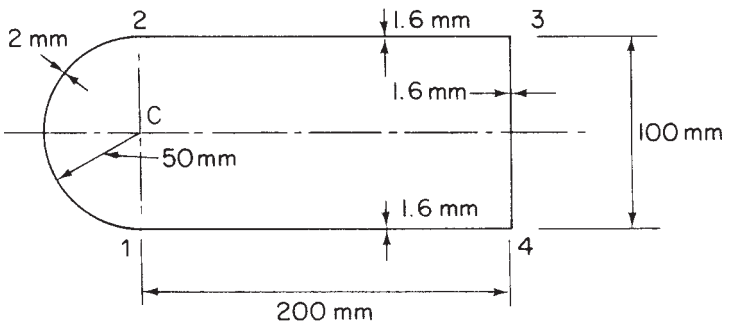

Fig. P.18.6

P.18.7 A uniform beam with the doubly symmetrical cross-section shown in Fig. P.18.7, has horizontal and vertical walls made of different materials which have shear moduli G_a and G_b, respectively. If for any material the ratio mass density/shear modulus is constant find the ratio of the wall thicknesses t_a and t_b, so that for a given torsional stiffness and given dimensions a, b the beam has minimum weight per unit span. Assume the Bredt–Batho theory of torsion is valid.

If this thickness requirement is satisfied find the a/b ratio (previously regarded as fixed), which gives minimum weight for given torsional stiffness.

Ans. $t_b/t_a = G_a/G_b$, $b/a = 1$.

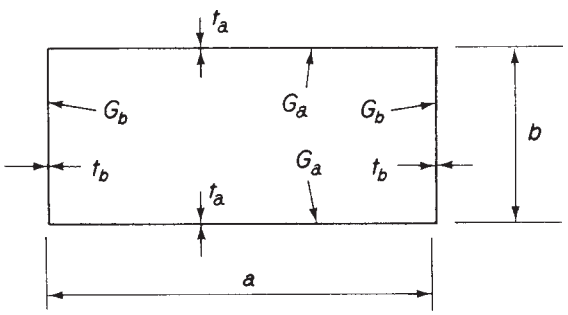

Fig. P.18.7

P.18.8 The cold-formed section shown in Fig. P.18.8 is subjected to a torque of 50 N m. Calculate the maximum shear stress in the section and its rate of twist. $G = 25\,000$ N/mm^2.

Ans. $\tau_{max} = 220.6$ N/mm^2, $d\theta/dz = 0.0044$ rad/mm.

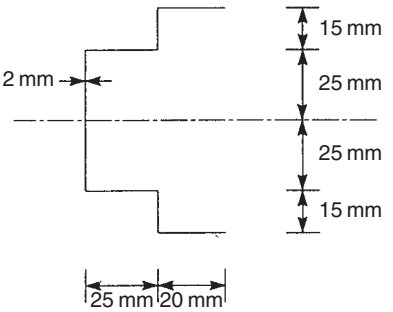

Fig. P.18.8

P.18.9 Determine the rate of twist per unit torque of the beam section shown in Fig. P.17.11 if the shear modulus G is 25 000 N/mm^2. (Note that the shear centre position has been calculated in P.17.11.)

Ans. 6.42×10^{-8} rad/mm.

P.18.10 Figure P.18.10 shows the cross-section of a thin-walled beam in the form of a channel with lipped flanges. The lips are of constant thickness 1.27 mm while the flanges increase linearly in thickness from 1.27 mm where they meet the lips to

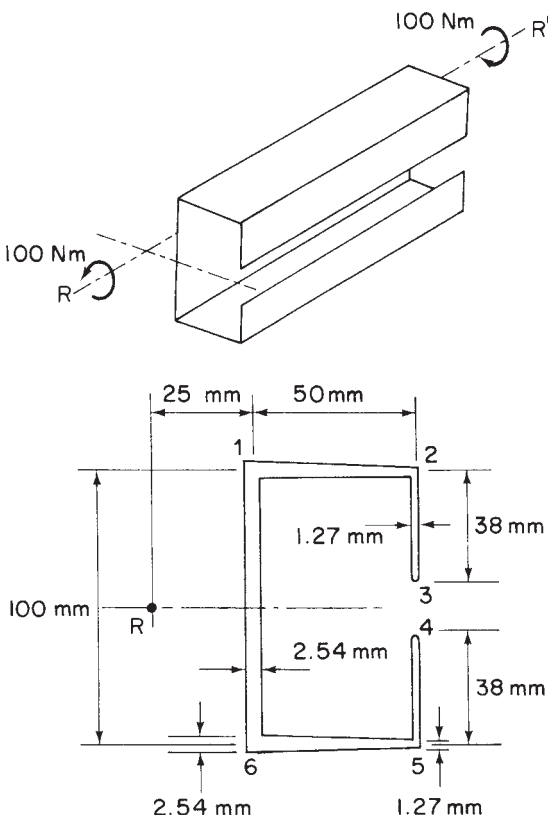

Fig. P.18.10

2.54 mm at their junctions with the web. The web has a constant thickness of 2.54 mm. The shear modulus G is 26 700 N/mm^2 throughout.

The beam has an enforced axis of twist RR′ and is supported in such a way that warping occurs freely but is zero at the mid-point of the web. If the beam carries a torque of 100 N m, calculate the maximum shear stress according to the St. Venant theory of torsion for thin-walled sections. Ignore any effects of stress concentration at the corners. Find also the distribution of warping along the middle line of the section, illustrating your results by means of a sketch.

Ans. $\tau_{\max} = \pm 297.4\ \text{N/mm}^2,\ w_1 = -5.48\ \text{mm} = -w_6.$
$w_2 = 5.48\ \text{mm} = -w_5,\ w_3 = 17.98\ \text{mm} = -w_4.$

P.18.11 The thin-walled section shown in Fig. P.18.11 is symmetrical about the x axis. The thickness t_0 of the centre web 34 is constant, while the thickness of the other walls varies linearly from t_0 at points 3 and 4 to zero at the open ends 1, 6, 7 and 8.

Determine the St. Venant torsion constant J for the section and also the maximum value of the shear stress due to a torque T. If the section is constrained to twist about an axis through the origin O, plot the relative warping displacements of the section per unit rate of twist.

Ans. $J = 4at_0^3/3,\ \tau_{\max} = \pm 3T/4at_0^2,\ w_1 = +a^2(1 + 2\sqrt{2}).$
$w_2 = +\sqrt{2}a^2,\ w_7 = -a^2,\ w_3 = 0.$

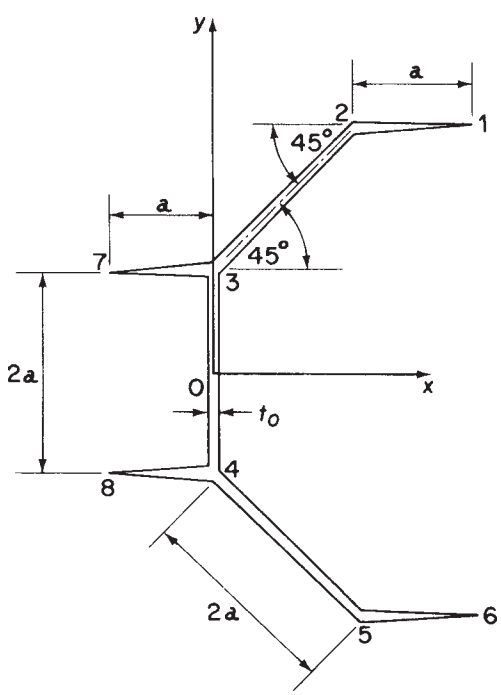

Fig. P.18.11

P.18.12 The thin walled section shown in Fig. P.18.12 is constrained to twist about an axis through R, the centre of the semicircular wall 34. Calculate the maximum shear

stress in the section per unit torque and the warping distribution per unit rate of twist. Also compare the value of warping displacement at the point 1 with that corresponding to the section being constrained to twist about an axis through the point O and state what effect this movement has on the maximum shear stress and the torsional stiffness of the section.

Ans. Maximum shear stress is $\pm 0.42/rt^2$ per unit torque.

$$w_{03} = +r^2\theta, \quad w_{32} = +\frac{r}{2}(\pi r + 2s_1), \quad w_{21} = -\frac{r}{2}(2s_2 - 5.142r).$$

With centre of twist at O_1 $w_1 = -0.43r^2$. Maximum shear stress is unchanged, torsional stiffness increased since warping reduced.

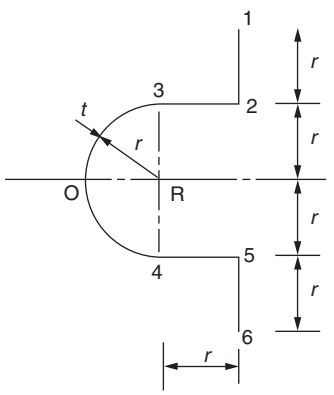

Fig. P.18.12

P.18.13 Determine the maximum shear stress in the beam section shown in Fig. P.18.13 stating clearly the point at which it occurs. Determine also the rate of twist of the beam section if the shear modulus G is $25\,000\,\text{N/mm}^2$.

Ans. $70.2\,\text{N/mm}^2$ on underside of 24 at 2 or on upper surface of 32 at 2.
9.0×10^{-4} rad/mm.

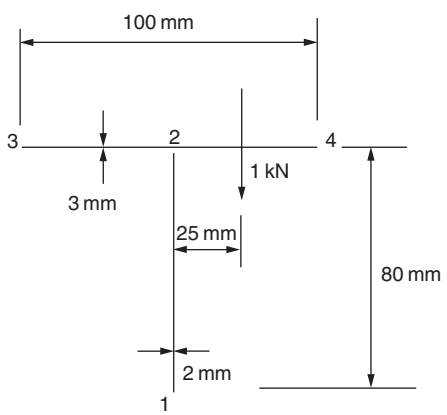

Fig. P.18.13

19

Combined open and closed section beams

So far, in Chapters 16–18, we have analysed thin-walled beams which consist of either completely closed cross-sections or completely open cross-sections. Frequently aircraft components comprise combinations of open and closed section beams. For example the section of a wing in the region of an undercarriage bay could take the form shown in Fig. 19.1. Clearly part of the section is an open channel section while the nose portion is a single cell closed section. We shall now examine the methods of analysis of such sections when subjected to bending, shear and torsional loads.

19.1 Bending

It is immaterial what form the cross-section of a beam takes; the direct stresses due to bending are given by either of Eq. (16.18) or (16.19).

19.2 Shear

The methods described in Sections 17.2 and 17.3 are used to determine the shear stress distribution although, unlike the completely closed section case, shear loads must be applied through the shear centre of the combined section, otherwise shear stresses of the type described in Section 18.2 due to torsion will arise. Where shear loads do not act through the shear centre its position must be found and the loading system replaced

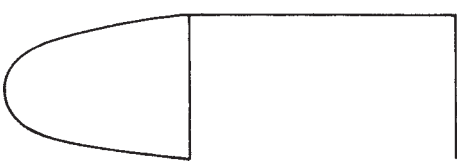

Fig. 19.1 Wing section comprising open and closed components.

by shear loads acting through the shear centre together with a torque; the two loading cases are then analysed separately. Again we assume that the cross-section of the beam remains undistorted by the loading.

Example 19.1

Determine the shear flow distribution in the beam section shown in Fig. 19.2, when it is subjected to a shear load in its vertical plane of symmetry. The thickness of the walls of the section is 2 mm throughout.

The centroid of area C lies on the axis of symmetry at some distance $\bar{y}$ from the upper surface of the beam section. Taking moments of area about this upper surface

$$(4 \times 100 \times 2 + 4 \times 200 \times 2)\bar{y} = 2 \times 100 \times 2 \times 50 + 2 \times 200 \times 2 \times 100 + 200 \times 2 \times 200$$

which gives $\bar{y} = 75$ mm.

The second moment of area of the section about Cx is given by

$$I_{xx} = 2\left(\frac{2 \times 100^3}{12} + 2 \times 100 \times 25^2\right) + 400 \times 2 \times 75^2 + 200 \times 2 \times 125^2 + 2\left(\frac{2 \times 200^3}{12} + 2 \times 200 \times 25^2\right)$$

i.e.

$$I_{xx} = 14.5 \times 10^6 \text{ mm}^4$$

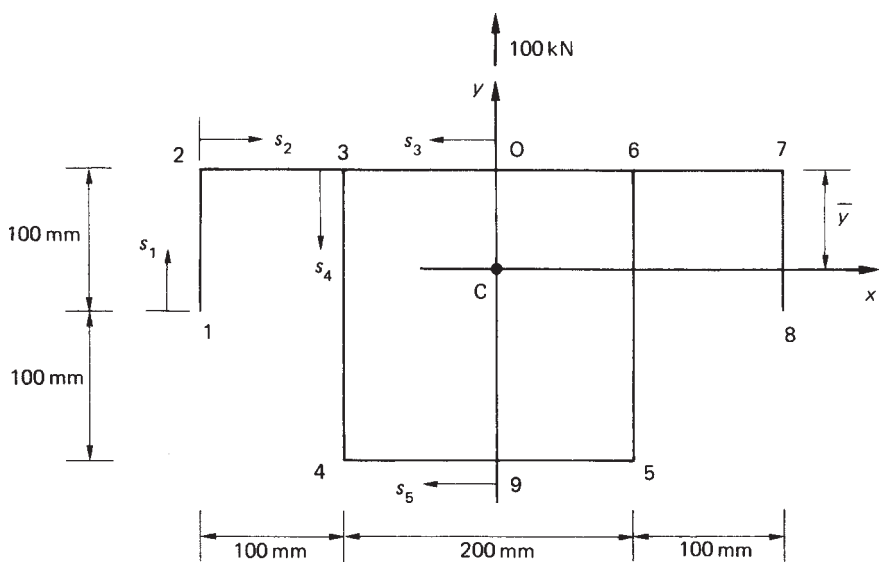

Fig. 19.2 Beam section of Example 19.1.

The section is symmetrical about Cy so that $I_{xy} = 0$ and since $S_x = 0$ the shear flow distribution in the closed section 3456 is, from Eq. (17.15)

$$q_s = -\frac{S_y}{I_{xx}} \int_0^s ty \, \mathrm{d}s + q_{s,0} \tag{i}$$

Also the shear load is applied through the shear centre of the complete section, i.e. along the axis of symmetry, so that in the open portions 123 and 678 the shear flow distribution is, from Eq. (17.14)

$$q_s = -\frac{S_y}{I_{xx}} \int_0^s ty \, \mathrm{d}s \tag{ii}$$

We note that the shear flow is zero at the points 1 and 8 and therefore the analysis may conveniently, though not necessarily, begin at either of these points. Thus, referring to Fig. 19.2

$$q_{12} = -\frac{100 \times 10^3}{14.5 \times 10^6} \int_0^{s_1} 2(-25 + s_1) \, \mathrm{d}s_1$$

i.e.

$$q_{12} = -69.0 \times 10^{-4}(-50s_1 + s_1^2) \tag{iii}$$

whence $q_2 = -34.5$ N/mm.

Examination of Eq. (iii) shows that q_{12} is initially positive and changes sign when $s_1 = 50$ mm. Further, q_{12} has a turning value ($\mathrm{d}q_{12}/\mathrm{d}s_1 = 0$) at $s_1 = 25$ mm of 4.3 N/mm. In the wall 23

$$q_{23} = -69.0 \times 10^{-4} \int_0^{s_2} 2 \times 75 \, \mathrm{d}s_2 - 34.5$$

i.e.

$$q_{23} = -1.04s_2 - 34.5 \tag{iv}$$

Hence q_{23} varies linearly from a value of -34.5 N/mm at 2 to -138.5 N/mm at 3 in the wall 23.

The analysis of the open part of the beam section is now complete since the shear flow distribution in the walls 67 and 78 follows from symmetry. To determine the shear flow distribution in the closed part of the section we must use the method described in Section 17.3 in which the line of action of the shear load is known. Thus we 'cut' the closed part of the section at some convenient point, obtain the q_b or 'open section' shear flows for the complete section and then take moments as in Eqs (17.17) or (17.18). However, in this case, we may use the symmetry of the section and loading to deduce that the final value of shear flow must be zero at the mid-points of the walls 36 and 45, i.e. $q_s = q_{s,0} = 0$ at these points. Hence

$$q_{03} = -69.0 \times 10^{-4} \int_0^{s_3} 2 \times 75 \, \mathrm{d}s_3$$

so that

$$q_{03} = -1.04s_3 \tag{v}$$

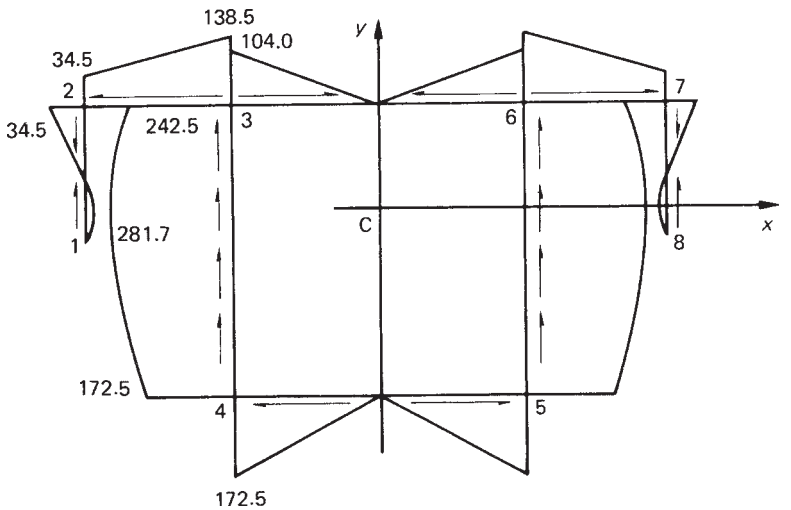

Fig. 19.3 Shear flow distribution in beam of Example 19.1 (all shear flows in N/mm).

and $q_3 = -104$ N/mm in the wall 03. It follows that for equilibrium of shear flows at 3, q_3, in the wall 34, must be equal to $-138.5 - 104 = -242.5$ N/mm. Hence

$$q_{34} = -69.0 \times 10^{-4} \int_0^{s_4} 2(75 - s_4)\,\mathrm{d}s_4 - 242.5$$

which gives

$$q_{34} = -1.04 s_4 + 69.0 \times 10^{-4} s_4^2 - 242.5 \qquad \text{(vi)}$$

Examination of Eq. (vi) shows that q_{34} has a maximum value of -281.7 N/mm at $s_4 = 75$ mm; also $q_4 = -172.5$ N/mm. Finally, the distribution of shear flow in the wall 94 is given by

$$q_{94} = -69.0 \times 10^{-4} \int_0^{s_5} 2(-125)\,\mathrm{d}s_5$$

i.e.

$$q_{94} = 1.73 s_5 \qquad \text{(vii)}$$

The complete distribution is shown in Fig. 19.3.

19.3 Torsion

Generally, in the torsion of composite sections, the closed portion is dominant since its torsional stiffness is far greater than that of the attached open section portion which may

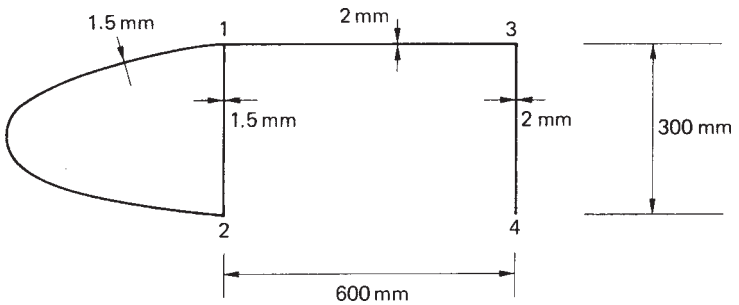

Fig. 19.4 Wing section of Example 19.2.

therefore be frequently ignored in the calculation of torsional stiffness; shear stresses should, however, be checked in this part of the section.

Example 19.2

Find the angle of twist per unit length in the wing whose cross-section is shown in Fig. 19.4 when it is subjected to a torque of 10 kN m. Find also the maximum shear stress in the section. $G = 25\,000\,\text{N/mm}^2$.

Wall 12 (outer) = 900 mm. Nose cell area = $20\,000\,\text{mm}^2$.

It may be assumed, in a simplified approach, that the torsional rigidity GJ of the complete section is the sum of the torsional rigidities of the open and closed portions. For the closed portion the torsional rigidity is, from Eq. (18.4)

$$(GJ)_{\text{cl}} = \frac{4A^2G}{\oint \mathrm{d}s/t} = \frac{4 \times 20\,000^2 \times 25\,000}{(900 + 300)/1.5}$$

which gives

$$(GJ)_{\text{cl}} = 5000 \times 10^7\,\text{N mm}^2$$

The torsional rigidity of the open portion is found using Eq. (18.11), thus

$$(GJ)_{\text{op}} = G\sum \frac{st^3}{3} = \frac{25\,000 \times 900 \times 2^3}{3}$$

i.e.

$$(GJ)_{\text{op}} = 6 \times 10^7\,\text{N mm}^2$$

The torsional rigidity of the complete section is then

$$GJ = 5000 \times 10^7 + 6 \times 10^7 = 5006 \times 10^7\,\text{N mm}^2$$

In all unrestrained torsion problems the torque is related to the rate of twist by the expression

$$T = GJ\frac{\mathrm{d}\theta}{\mathrm{d}z}$$

The angle of twist per unit length is therefore given by

$$\frac{\mathrm{d}\theta}{\mathrm{d}z} = \frac{T}{GJ} = \frac{10 \times 10^6}{5006 \times 10^7} = 0.0002\,\text{rad/mm}$$

Substituting for T in Eq. (18.1) from Eq. (18.4), we obtain the shear flow in the closed section. Thus

$$q_{\text{cl}} = \frac{(GJ)_{\text{cl}}}{2A}\frac{\mathrm{d}\theta}{\mathrm{d}z} = \frac{5000 \times 10^7}{2 \times 20\,000} \times 0.0002$$

from which

$$q_{\text{cl}} = 250\,\text{N/mm}$$

The maximum shear stress in the closed section is then $250/1.5 = 166.7\,\text{N/mm}^2$.

In the open portion of the section the maximum shear stress is obtained directly from Eq. (18.10) and is

$$\tau_{\text{max,op}} = 25\,000 \times 2 \times 0.0002 = 10\,\text{N/mm}^2$$

It can be seen from the above that in terms of strength and stiffness the closed portion of the wing section dominates. This dominance may be used to determine the warping distribution. Having first found the position of the centre of twist (the shear centre) the warping of the closed portion is calculated using the method described in Section 18.1. The warping in the walls 13 and 34 is then determined using Eq. (18.19), in which the origin for the swept area A_{R} is taken at the point 1 and the value of warping is that previously calculated for the closed portion at 1.

Problems

P.19.1 The beam section of Example 19.1 (see Fig. 19.2) is subjected to a bending moment in a vertical plane of 20 kN m. Calculate the maximum direct stress in the cross-section of the beam.

Ans. $172.5\,\text{N/mm}^2$.

P.19.2 A wing box has the cross-section shown diagrammatically in Fig. P.19.2 and supports a shear load of 100 kN in its vertical plane of symmetry. Calculate the shear stress at the mid-point of the web 36 if the thickness of all walls is 2 mm.

Ans. $89.7\,\text{N/mm}^2$.

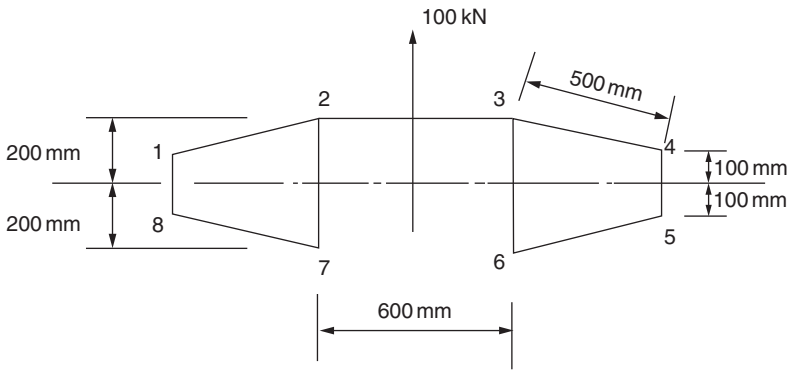

Fig. P.19.2

P.19.3 If the wing box of P.19.2 is subjected to a torque of 100 kN m, calculate the rate of twist of the section and the maximum shear stress. The shear modulus G is 25000 N/mm^2.

Ans. 18.5×10^{-6} rad/mm, 170 N/mm^2.

20

Structural idealization

So far we have been concerned with relatively uncomplicated structural sections which in practice would be formed from thin plate or by the extrusion process. While these sections exist as structural members in their own right they are frequently used, as we saw in Chapter 12, to stiffen more complex structural shapes such as fuselages, wings and tail surfaces. Thus a two spar wing section could take the form shown in Fig. 20.1 in which Z-section stringers are used to stiffen the thin skin while angle sections form the spar flanges. Clearly, the analysis of a section of this type would be complicated and tedious unless some simplifying assumptions are made. Generally, the number and nature of these simplifying assumptions determine the accuracy and the degree of complexity of the analysis; the more complex the analysis the greater the accuracy obtained. The degree of simplification introduced is governed by the particular situation surrounding the problem. For a preliminary investigation, speed and simplicity are often of greater importance than extreme accuracy; on the other hand a final solution must be as exact as circumstances allow.

Complex structural sections may be idealized into simpler 'mechanical model' forms which behave, under given loading conditions, in the same, or very nearly the same, way as the actual structure. We shall see, however, that different models of the same structure are required to simulate actual behaviour under different systems of loading.

20.1 Principle

In the wing section of Fig. 20.1 the stringers and spar flanges have small cross-sectional dimensions compared with the complete section. Therefore, the variation in stress

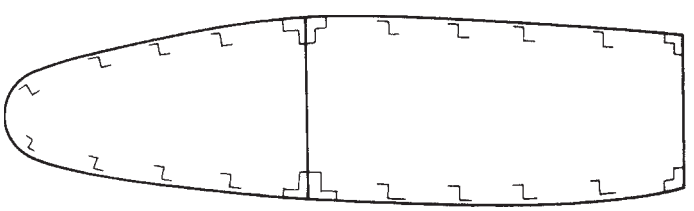

Fig. 20.1 Typical wing section.

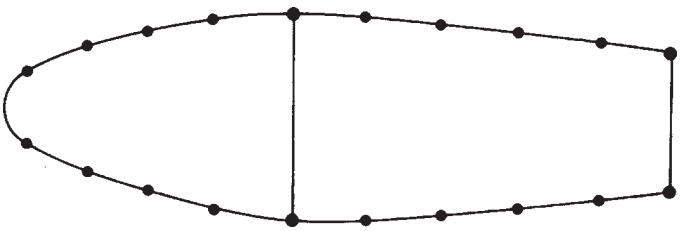

Fig. 20.2 Idealization of a wing section.

over the cross-section of a stringer due to, say, bending of the wing would be small. Furthermore, the difference between the distances of the stringer centroids and the adjacent skin from the wing section axis is small. It would be reasonable to assume therefore that the direct stress is constant over the stringer cross-sections. We could therefore replace the stringers and spar flanges by concentrations of area, known as *booms*, over which the direct stress is constant and which are located along the mid-line of the skin, as shown in Fig. 20.2. In wing and fuselage sections of the type shown in Fig. 20.1, the stringers and spar flanges carry most of the direct stresses while the skin is mainly effective in resisting shear stresses although it also carries some of the direct stresses. The idealization shown in Fig. 20.2 may therefore be taken a stage further by assuming that all direct stresses are carried by the booms while the skin is effective only in shear. The direct stress carrying capacity of the skin may be allowed for by increasing each boom area by an area equivalent to the direct stress carrying capacity of the adjacent skin panels. The calculation of these equivalent areas will generally depend upon an initial assumption as to the form of the distribution of direct stress in a boom/skin panel.

20.2 Idealization of a panel

Suppose that we wish to idealize the panel of Fig. 20.3(a) into a combination of direct stress carrying booms and shear stress only carrying skin as shown in Fig. 20.3(b). In Fig. 20.3(a) the direct stress carrying thickness t_D of the skin is equal to its actual thickness t while in Fig. 20.3(b) $t_D = 0$. Suppose also that the direct stress distribution in the actual panel varies linearly from an unknown value σ_1 to an unknown value σ_2. Clearly the analysis should predict the extremes of stress σ_1 and σ_2 although the distribution of direct stress is obviously lost. Since the loading producing the direct stresses in the actual and idealized panels must be the same we can equate moments to obtain expressions for the boom areas B_1 and B_2. Thus, taking moments about the right-hand edge of each panel

$$\sigma_2 t_D \frac{b^2}{2} + \frac{1}{2}(\sigma_1 - \sigma_2) t_D b \frac{2}{3} b = \sigma_1 B_1 b$$

whence

$$B_1 = \frac{t_D b}{6}\left(2 + \frac{\sigma_2}{\sigma_1}\right) \tag{20.1}$$

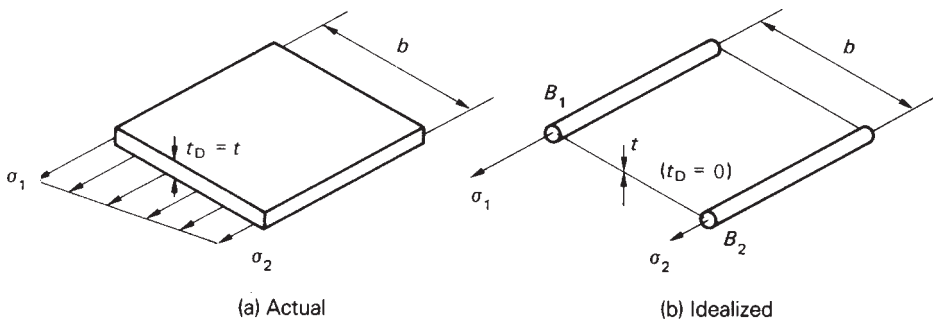

Fig. 20.3 Idealization of a panel.

Similarly

$$B_2 = \frac{t_D b}{6}\left(2 + \frac{\sigma_1}{\sigma_2}\right) \tag{20.2}$$

In Eqs (20.1) and (20.2) the ratio of σ_1 to σ_2, if not known, may frequently be assumed.

The direct stress distribution in Fig. 20.3(a) is caused by a combination of axial load and bending moment. For axial load only $\sigma_1/\sigma_2 = 1$ and $B_1 = B_2 = t_D b/2$; for a pure bending moment $\sigma_1/\sigma_2 = -1$ and $B_1 = B_2 = t_D b/6$. Thus, different idealizations of the same structure are required for different loading conditions.

Example 20.1

Part of a wing section is in the form of the two-cell box shown in Fig. 20.4(a) in which the vertical spars are connected to the wing skin through angle sections all having a cross-sectional area of 300 mm^2. Idealize the section into an arrangement of direct stress carrying booms and shear stress only carrying panels suitable for resisting bending moments in a vertical plane. Position the booms at the spar/skin junctions.

The idealized section is shown in Fig. 20.4(b) in which, from symmetry, $B_1 = B_6$, $B_2 = B_5$, $B_3 = B_4$. Since the section is required to resist bending moments in a vertical plane the direct stress at any point in the actual wing section is directly proportional to its distance from the horizontal axis of symmetry. Further, the distribution of direct stress in all the panels will be linear so that either of Eqs (20.1) or (20.2) may be used. We note that, in addition to contributions from adjacent panels, the boom areas include

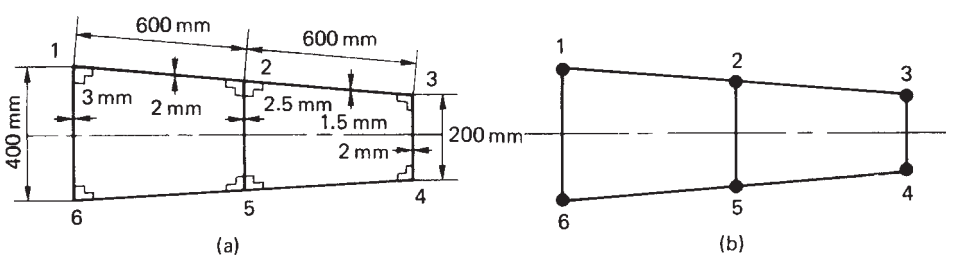

Fig. 20.4 Idealization of a wing section.

the existing spar flanges. Hence

$$B_1 = 300 + \frac{3.0 \times 400}{6}\left(2 + \frac{\sigma_6}{\sigma_1}\right) + \frac{2.0 \times 600}{6}\left(2 + \frac{\sigma_2}{\sigma_1}\right)$$

or

$$B_1 = 300 + \frac{3.0 \times 400}{6}(2 - 1) + \frac{2.0 \times 600}{6}\left(2 + \frac{150}{200}\right)$$

which gives

$$B_1 (= B_6) = 1050\,\text{mm}^2$$

Also

$$B_2 = 2 \times 300 + \frac{2.0 \times 600}{6}\left(2 + \frac{\sigma_1}{\sigma_2}\right) + \frac{2.5 \times 300}{6}\left(2 + \frac{\sigma_5}{\sigma_2}\right) + \frac{1.5 \times 600}{6}\left(2 + \frac{\sigma_3}{\sigma_2}\right)$$

i.e.

$$B_2 = 2 \times 300 + \frac{2.0 \times 600}{6}\left(2 + \frac{200}{150}\right) + \frac{2.5 \times 300}{6}(2 - 1) + \frac{1.5 \times 600}{6}\left(2 + \frac{100}{150}\right)$$

from which

$$B_2 (= B_5) = 1791.7\,\text{mm}^2$$

Finally

$$B_3 = 300 + \frac{1.5 \times 600}{6}\left(2 + \frac{\sigma_2}{\sigma_3}\right) + \frac{2.0 \times 200}{6}\left(2 + \frac{\sigma_4}{\sigma_3}\right)$$

i.e.

$$B_3 = 300 + \frac{1.5 \times 600}{6}\left(2 + \frac{150}{100}\right) + \frac{2.0 \times 200}{6}(2 - 1)$$

so that

$$B_3 (= B_4) = 891.7\,\text{mm}^2$$

20.3 Effect of idealization on the analysis of open and closed section beams

The addition of direct stress carrying booms to open and closed section beams will clearly modify the analyses presented in Chapters 16–18. Before considering individual cases we shall discuss the implications of structural idealization. Generally, in any idealization, different loading conditions require different idealizations of the same structure. In Example 20.1, the loading is applied in a vertical plane. If, however, the loading had been applied in a horizontal plane the assumed stress distribution in

the panels of the section would have been different, resulting in different values of boom area.

Suppose that an open or closed section beam is subjected to given bending or shear loads and that the required idealization has been completed. The analysis of such sections usually involves the determination of the neutral axis position and the calculation of sectional properties. The position of the neutral axis is derived from the condition that the resultant load on the beam cross-section is zero, i.e.

$$\int_A \sigma_z \, \mathrm{d}A = 0 \quad \text{(see Eq. (16.3))}$$

The area A in this expression is clearly the direct stress carrying area. It follows that the centroid of the cross-section is the centroid of the direct stress carrying area of the section, depending on the degree and method of idealization. The sectional properties, I_{xx}, etc., must also refer to the direct stress carrying area.

20.3.1 Bending of open and closed section beams

The analysis presented in Sections 16.1 and 16.2 applies and the direct stress distribution is given by any of Eqs (16.9), (16.18) or (16.19), depending on the beam section being investigated. In these equations the coordinates (x, y) of points in the cross-section are referred to axes having their origin at the centroid of the direct stress carrying area. Furthermore, the section properties I_{xx}, I_{yy} and I_{xy} are calculated for the direct stress carrying area only.

In the case where the beam cross-section has been completely idealized into direct stress carrying booms and shear stress only carrying panels, the direct stress distribution consists of a series of direct stresses concentrated at the centroids of the booms.

Example 20.2

The fuselage section shown in Fig. 20.5 is subjected to a bending moment of 100 kN m applied in the vertical plane of symmetry. If the section has been completely idealized into a combination of direct stress carrying booms and shear stress only carrying panels, determine the direct stress in each boom.

The section has Cy as an axis of symmetry and resists a bending moment $M_x = 100\,\text{kN m}$. Equation (16.18) therefore reduces to

$$\sigma_z = \frac{M_x}{I_{xx}} y \tag{i}$$

The origin of axes Cxy coincides with the position of the centroid of the direct stress carrying area which, in this case, is the centroid of the boom areas. Thus, taking moments of area about boom 9

$$\begin{aligned}(6 \times 640 + 6 \times 600 + 2 \times 620 + 2 \times 850)\bar{y} \\ = 640 \times 1200 + 2 \times 600 \times 1140 + 2 \times 600 \times 960 + 2 \times 600 \times 768 \\ + 2 \times 620 \times 565 + 2 \times 640 \times 336 + 2 \times 640 \times 144 + 2 \times 850 \times 38\end{aligned}$$

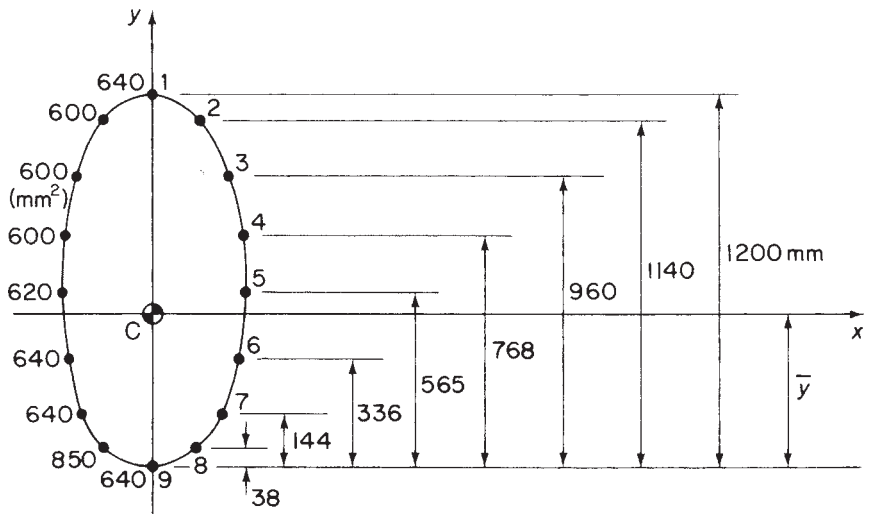

Fig. 20.5 Idealized fuselage section of Example 20.2.

Table 20.1

① Boom	② y (mm)	③ B (mm^2)	④ $\Delta I_{xx} = By^2$ (mm^4)	⑤ σ_z (N/mm^2)
1	+660	640	278×10^6	35.6
2	+600	600	216×10^6	32.3
3	+420	600	106×10^6	22.6
4	+228	600	31×10^6	12.3
5	+25	620	0.4×10^6	1.3
6	−204	640	27×10^6	−11.0
7	−396	640	100×10^6	−21.4
8	−502	850	214×10^6	−27.0
9	−540	640	187×10^6	−29.0

which gives

$$\bar{y} = 540\,\text{mm}$$

The solution is now completed in Table 20.1

From column ④

$$I_{xx} = 1854 \times 10^6\,\text{mm}^4$$

and column ⑤ is completed using Eq. (i).

20.3.2 Shear of open section beams

The derivation of Eq. (17.14) for the shear flow distribution in the cross-section of an open section beam is based on the equilibrium equation (17.2). The thickness t in this

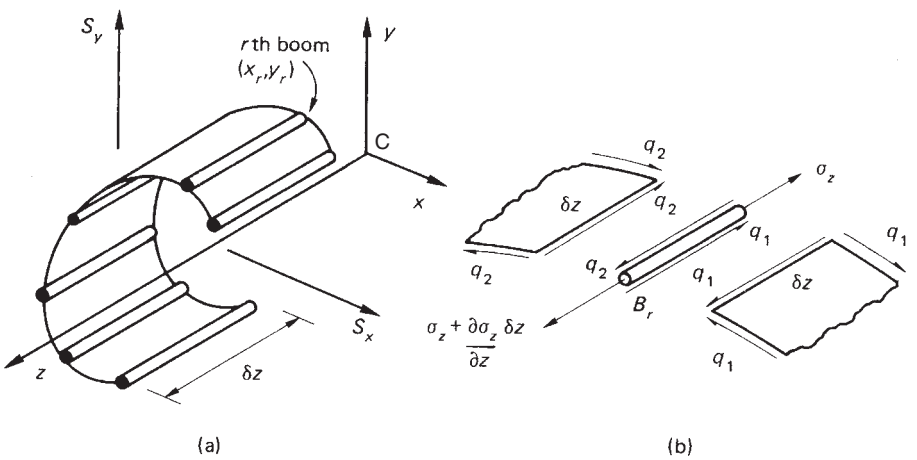

Fig. 20.6 (a) Elemental length of shear loaded open section beam with booms; (b) equilibrium of boom element.

equation refers to the direct stress carrying thickness t_D of the skin. Equation (17.14) may therefore be rewritten

$$q_s = -\left(\frac{S_x I_{xx} - S_y I_{xy}}{I_{xx} I_{yy} - I_{xy}^2}\right) \int_0^s t_D x \, ds - \left(\frac{S_y I_{yy} - S_x I_{xy}}{I_{xx} I_{yy} - I_{xy}^2}\right) \int_0^s t_D y \, ds \tag{20.3}$$

in which $t_D = t$ if the skin is fully effective in carrying direct stress or $t_D = 0$ if the skin is assumed to carry only shear stresses. Again the section properties in Eq. (20.3) refer to the direct stress carrying area of the section since they are those which feature in Eqs (16.18) and (16.19).

Equation (20.3) makes no provision for the effects of booms which cause discontinuities in the skin and therefore interrupt the shear flow. Consider the equilibrium of the rth boom in the elemental length of beam shown in Fig. 20.6(a) which carries shear loads S_x and S_y acting through its shear centre S. These shear loads produce direct stresses due to bending in the booms and skin and shear stresses in the skin. Suppose that the shear flows in the skin adjacent to the rth boom of cross-sectional area B_r are q_1 and q_2. Then, from Fig. 20.6(b)

$$\left(\sigma_z + \frac{\partial \sigma_z}{\partial z} \delta z\right) B_r - \sigma_z B_r + q_2 \delta z - q_1 \delta z = 0$$

which simplifies to

$$q_2 - q_1 = -\frac{\partial \sigma_z}{\partial z} B_r \tag{20.4}$$

Substituting for σ_z in Eq. (20.4) from (16.18) we have

$$q_2 - q_1 = -\left[\frac{(\partial M_y/\partial z)I_{xx} - (\partial M_x/\partial z)I_{xy}}{I_{xx}I_{yy} - I_{xy}^2}\right]B_r x_r - \left[\frac{(\partial M_x/\partial z)I_{yy} - (\partial M_y/\partial z)I_{xy}}{I_{xx}I_{yy} - I_{xy}^2}\right]B_r y_r$$

or, using the relationships of Eqs (16.23) and (16.24)

$$q_2 - q_1 = -\left(\frac{S_x I_{xx} - S_y I_{xy}}{I_{xx}I_{yy} - I_{xy}^2}\right)B_r x_r - \left(\frac{S_y I_{yy} - S_x I_{xy}}{I_{xx}I_{yy} - I_{xy}^2}\right)B_r y_r \tag{20.5}$$

Equation (20.5) gives the change in shear flow induced by a boom which itself is subjected to a direct load ($\sigma_z B_r$). Each time a boom is encountered the shear flow is incremented by this amount so that if, at any distance s around the profile of the section, n booms have been passed, the shear flow at the point is given by

$$q_s = -\left(\frac{S_x I_{xx} - S_y I_{xy}}{I_{xx}I_{yy} - I_{xy}^2}\right)\left(\int_0^s t_D x\,\mathrm{d}s + \sum_{r=1}^{n} B_r x_r\right) - \left(\frac{S_y I_{yy} - S_x I_{xy}}{I_{xx}I_{yy} - I_{xy}^2}\right)\left(\int_0^s t_D y\,\mathrm{d}s + \sum_{r=1}^{n} B_r y_r\right) \tag{20.6}$$

Example 20.3

Calculate the shear flow distribution in the channel section shown in Fig. 20.7 produced by a vertical shear load of 4.8 kN acting through its shear centre. Assume that the walls of the section are only effective in resisting shear stresses while the booms, each of area 300 mm^2, carry all the direct stresses.

The effective direct stress carrying thickness t_D of the walls of the section is zero so that the centroid of area and the section properties refer to the boom areas only. Since Cx (and Cy as far as the boom areas are concerned) is an axis of symmetry $I_{xy} = 0$; also $S_x = 0$ and Eq. (20.6) thereby reduces to

$$q_s = -\frac{S_y}{I_{xx}}\sum_{r=1}^{n} B_r y_r \tag{i}$$

in which $I_{xx} = 4 \times 300 \times 200^2 = 48 \times 10^6$ mm^4. Substituting the values of S_y and I_{xx} in Eq. (i) gives

$$q_s = -\frac{4.8 \times 10^3}{48 \times 10^6}\sum_{r=1}^{n} B_r y_r = -10^{-4}\sum_{r=1}^{n} B_r y_r \tag{ii}$$

At the outside of boom 1, $q_s = 0$. As boom 1 is crossed the shear flow changes by an amount given by

$$\Delta q_1 = -10^{-4} \times 300 \times 200 = -6\,\mathrm{N/mm}$$

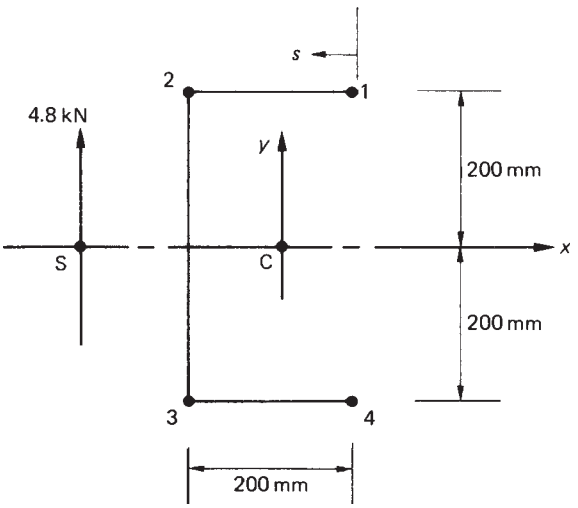

Fig. 20.7 Idealized channel section of Example 20.3.

Hence $q_{12} = -6\,\text{N/mm}$ since, from Eq. (i), it can be seen that no further changes in shear flow occur until the next boom (2) is crossed. Hence

$$q_{23} = -6 - 10^{-4} \times 300 \times 200 = -12\,\text{N/mm}$$

Similarly

$$q_{34} = -12 - 10^{-4} \times 300 \times (-200) = -6\,\text{N/mm}$$

while, finally, at the outside of boom 4 the shear flow is

$$-6 - 10^{-4} \times 300 \times (-200) = 0$$

as expected. The complete shear flow distribution is shown in Fig. 20.8.

It can be seen from Eq. (i) in Example 20.3 that the analysis of a beam section which has been idealized into a combination of direct stress carrying booms and shear

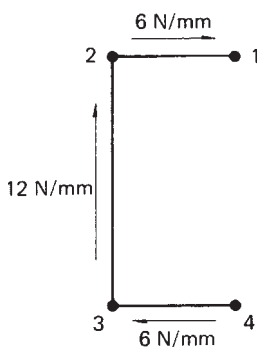

Fig. 20.8 Shear flow in channel section of Example 20.3.

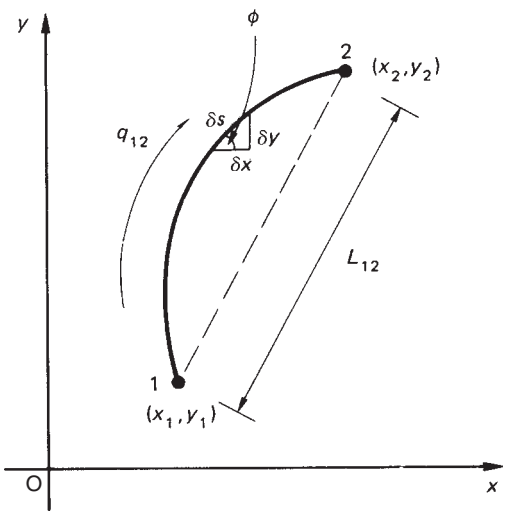

Fig. 20.9 Curved web with constant shear flow.

stress only carrying skin gives constant values of the shear flow in the skin between the booms; the actual distribution of shear flows is therefore lost. What remains is in fact the average of the shear flow, as can be seen by referring to Example 20.3. Analysis of the unidealized channel section would result in a parabolic distribution of shear flow in the web 23 whose resultant is statically equivalent to the externally applied shear load of 4.8 kN. In Fig. 20.8 the resultant of the constant shear flow in the web 23 is $12 \times 400 = 4800\,\text{N} = 4.8\,\text{kN}$. It follows that this constant value of shear flow is the average of the parabolically distributed shear flows in the unidealized section.

The result, from the idealization of a beam section, of a constant shear flow between booms may be used to advantage in parts of the analysis. Suppose that the curved web 12 in Fig. 20.9 has booms at its extremities and that the shear flow q_{12} in the web is constant. The shear force on an element δs of the web is $q_{12}\delta s$, whose components horizontally and vertically are $q_{12}\delta s \cos\phi$ and $q_{12}\delta s \sin\phi$. The resultant, parallel to the x axis, S_x, of q_{12} is therefore given by

$$S_x = \int_1^2 q_{12} \cos\phi \, \mathrm{d}s$$

or

$$S_x = q_{12} \int_1^2 \cos\phi \, \mathrm{d}s$$

which, from Fig. 20.9, may be written

$$S_x = q_{12} \int_1^2 \mathrm{d}x = q_{12}(x_2 - x_1) \tag{20.7}$$

Similarly the resultant of q_{12} parallel to the y axis is

$$S_y = q_{12}(y_2 - y_1) \tag{20.8}$$

Thus the resultant, in a given direction, of a constant shear flow acting on a web is the value of the shear flow multiplied by the projection on that direction of the web.

The resultant shear force S on the web of Fig. 20.9 is

$$S = \sqrt{S_x^2 + S_y^2} = q_{12}\sqrt{(x_2 - x_1)^2 + (y_2 - y_1)^2}$$

i.e.

$$S = q_{12}L_{12} \tag{20.9}$$

Therefore, the resultant shear force acting on the web is the product of the shear flow and the length of the straight line joining the ends of the web; clearly the direction of the resultant is parallel to this line.

The moment M_q produced by the shear flow q_{12} about any point O in the plane of the web is, from Fig. 20.10

$$M_q = \int_1^2 q_{12} p \, \mathrm{d}s = q_{12} \int_1^2 2 \, \mathrm{d}A$$

or

$$M_q = 2Aq_{12} \tag{20.10}$$

in which A is the area enclosed by the web and the lines joining the ends of the web to the point O. This result may be used to determine the distance of the line of action of the resultant shear force from any point. From Fig. 20.10

$$Se = 2Aq_{12}$$

from which

$$e = \frac{2A}{S} q_{12}$$

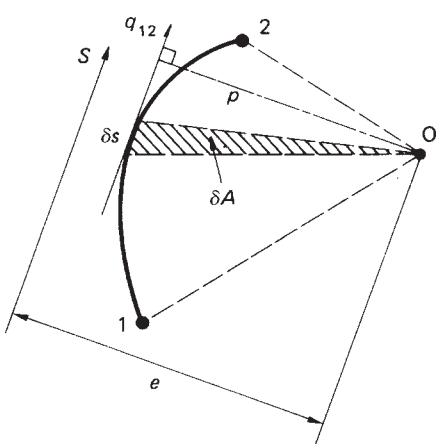

Fig. 20.10 Moment produced by a constant shear flow.

Substituting for q_{12} from Eq. (20.9) gives

$$e = \frac{2A}{L_{12}}$$

20.3.3 Shear loading of closed section beams

Arguments identical to those in the shear of open section beams apply in this case. Thus, the shear flow at any point around the cross-section of a closed section beam comprising booms and skin of direct stress carrying thickness t_D is, by a comparison of Eqs (20.6) and (17.15)

$$q_s = -\left(\frac{S_x I_{xx} - S_y I_{xy}}{I_{xx} I_{yy} - I_{xy}^2}\right)\left(\int_0^s t_D x \, ds + \sum_{r=1}^{n} B_r x_r\right) - \left(\frac{S_y I_{yy} - S_x I_{xy}}{I_{xx} I_{yy} - I_{xy}^2}\right)\left(\int_0^s t_D y \, ds + \sum_{r=1}^{n} B_r y_r\right) + q_{s,0} \tag{20.11}$$

Note that the zero value of the 'basic' or 'open section' shear flow at the 'cut' in a skin for which $t_D = 0$ extends from the 'cut' to the adjacent booms.

Example 20.4

The thin-walled single cell beam shown in Fig. 20.11 has been idealized into a combination of direct stress carrying booms and shear stress only carrying walls. If the section supports a vertical shear load of 10 kN acting in a vertical plane through booms 3 and 6, calculate the distribution of shear flow around the section.

Boom areas: $B_1 = B_8 = 200\,\text{mm}^2$, $B_2 = B_7 = 250\,\text{mm}^2$, $B_3 = B_6 = 400\,\text{mm}^2$, $B_4 = B_5 = 100\,\text{mm}^2$.

The centroid of the direct stress carrying area lies on the horizontal axis of symmetry so that $I_{xy} = 0$. Also, since $t_D = 0$ and only a vertical shear load is applied,

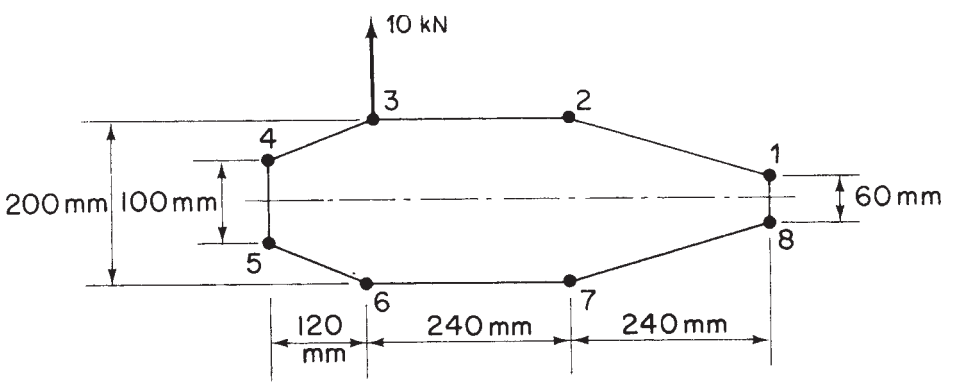

Fig. 20.11 Closed section of beam of Example 20.4.

Eq. (20.11) reduces to

$$q_s = -\frac{S_y}{I_{xx}} \sum_{r=1}^{n} B_r y_r + q_{s,0} \tag{i}$$

in which

$$I_{xx} = 2(200 \times 30^2 + 250 \times 100^2 + 400 \times 100^2 + 100 \times 50^2) = 13.86 \times 10^6 \,\text{mm}^4$$

Equation (i) then becomes

$$q_s = -\frac{10 \times 10^3}{13.86 \times 10^6} \sum_{r=1}^{n} B_r y_r + q_{s,0}$$

i.e.

$$q_s = -7.22 \times 10^{-4} \sum_{r=1}^{n} B_r y_r + q_{s,0} \tag{ii}$$

'Cutting' the beam section in the wall 23 (any wall may be chosen) and calculating the 'basic' shear flow distribution q_b from the first term on the right-hand side of Eq. (ii) we have

$$q_{b,23} = 0$$

$$q_{b,34} = -7.22 \times 10^{-4}(400 \times 100) = -28.9\,\text{N/mm}$$

$$q_{b,45} = -28.9 - 7.22 \times 10^{-4}(100 \times 50) = -32.5\,\text{N/mm}$$

$$q_{b,56} = q_{b,34} = -28.9\,\text{N/mm} \text{ (by symmetry)}$$

$$q_{b,67} = q_{b,23} = 0 \text{ (by symmetry)}$$

$$q_{b,21} = -7.22 \times 10^{-4}(250 \times 100) = -18.1\,\text{N/mm}$$

$$q_{b,18} = -18.1 - 7.22 \times 10^{-4}(200 \times 30) = -22.4\,\text{N/mm}$$

$$q_{b,87} = q_{b,21} = -18.1\,\text{N/mm} \text{ (by symmetry)}$$

Taking moments about the intersection of the line of action of the shear load and the horizontal axis of symmetry and referring to the results of Eqs (20.7) and (20.8) we have, from Eq. (17.18)

$$0 = [q_{b,81} \times 60 \times 480 + 2q_{b,12}(240 \times 100 + 70 \times 240) + 2q_{b,23} \times 240 \times 100 - 2q_{b,43} \times 120 \times 100 - q_{b,54} \times 100 \times 120] + 2 \times 97\,200 q_{s,0}$$

Substituting the above values of q_b in this equation gives

$$q_{s,0} = -5.4\,\text{N/mm}$$

the negative sign indicating that $q_{s,0}$ acts in a clockwise sense.

In any wall the final shear flow is given by $q_s = q_b + q_{s,0}$ so that

$$q_{21} = -18.1 + 5.4 = -12.7\,\text{N/mm} = q_{87}$$

$$q_{23} = -5.4\,\text{N/mm} = q_{67}$$

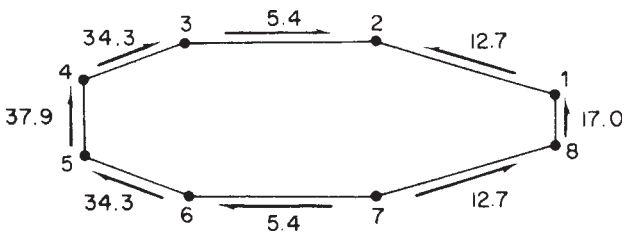

Fig. 20.12 Shear flow distribution N/mm in walls of the beam section of Example 20.4.

$$q_{34} = -34.3\,\text{N/mm} = q_{56}$$
$$q_{45} = -37.9\,\text{N/mm}$$

and

$$q_{81} = 17.0\,\text{N/mm}$$

giving the shear flow distribution shown in Fig. 20.12.

20.3.4 Alternative method for the calculation of shear flow distribution

Equation (20.4) may be rewritten in the form

$$q_2 - q_1 = \frac{\partial P_r}{\partial z} \tag{20.12}$$

in which P_r is the direct load in the rth boom. This form of the equation suggests an alternative approach to the determination of the effect of booms on the calculation of shear flow distributions in open and closed section beams.

Let us suppose that the boom load varies linearly with z. This will be the case for a length of beam over which the shear force is constant. Equation (20.12) then becomes

$$q_2 - q_1 = -\Delta P_r \tag{20.13}$$

in which ΔP_r is the *change* in boom load over unit length of the rth boom. ΔP_r may be calculated by first determining the *change* in bending moment between two sections of a beam a unit distance apart and then calculating the corresponding change in boom stress using either of Eq. (16.18) or (16.19); the change in boom load follows by multiplying the change in boom stress by the boom area B_r. Note that the section properties contained in Eqs (16.18) and (16.19) refer to the direct stress carrying area of the beam section. In cases where the shear force is not constant over the unit length of beam the method is approximate.

We shall illustrate the method by applying it to Example 20.3. In Fig. 20.7 the shear load of 4.8 kN is applied to the face of the section which is seen when a view is taken along the z axis towards the origin. Thus, when considering unit length of the beam, we must ensure that this situation is unchanged. Figure 20.13 shows a unit (1 mm say) length of beam. The change in bending moment between the front and rear faces of the

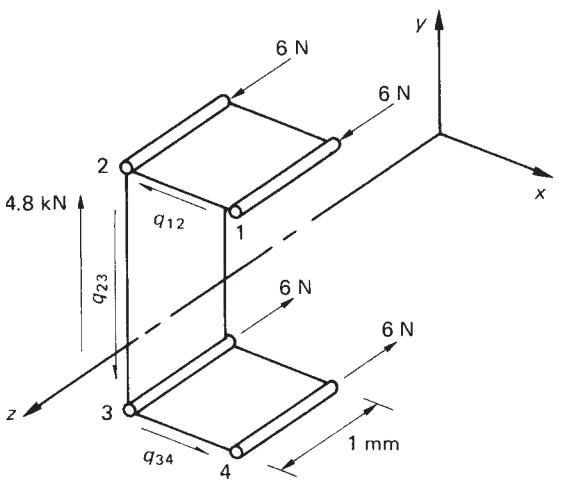

Fig. 20.13 Alternative solution to Example 20.3.

length of beam is 4.8×1 kN mm which produces a change in boom load given by (see Eq. (16.18))

$$\Delta P_r = \frac{4.8 \times 10^3 \times 200}{48 \times 10^6} \times 300 = 6\,\text{N}$$

The change in boom load is compressive in booms 1 and 2 and tensile in booms 3 and 4.

Equation (20.12), and hence Eq. (20.13), is based on the tensile load in a boom increasing with increasing z. If the tensile load had increased with decreasing z the right-hand side of these equations would have been positive. It follows that in the case where a compressive load increases with decreasing z, as for booms 1 and 2 in Fig. 20.13, the right-hand side is negative; similarly for booms 3 and 4 the right-hand side is positive. Thus

$$q_{12} = -6\,\text{N/mm}$$
$$q_{23} = -6 + q_{12} = -12\,\text{N/mm}$$

and

$$q_{34} = +6 + q_{23} = -6\,\text{N/mm}$$

giving the same solution as before. Note that if the unit length of beam had been taken to be 1 m the solution would have been $q_{12} = -6000$ N/m, $q_{23} = -12\,000$ N/m, $q_{34} = -6000$ N/m.

20.3.5 Torsion of open and closed section beams

No direct stresses are developed in either open or closed section beams subjected to a pure torque unless axial constraints are present. The shear stress distribution is therefore unaffected by the presence of booms and the analyses presented in Chapter 18 apply.

20.4 Deflection of open and closed section beams

Bending, shear and torsional deflections of thin-walled beams are readily obtained by application of the unit load method described in Section 5.5.

The displacement in a given direction due to torsion is given directly by the last of Eqs (5.21), thus

$$\Delta_T = \int_L \frac{T_0 T_1}{GJ} \mathrm{d}z \tag{20.14}$$

where J, the torsion constant, depends on the type of beam under consideration. For an open section beam J is given by either of Eqs (18.11) whereas in the case of a closed section beam $J = 4A^2/(\oint \mathrm{d}s/t)$ (Eq. (18.4)) for a constant shear modulus.

Expressions for the bending and shear displacements of unsymmetrical thin-walled beams may also be determined by the unit load method. They are complex for the general case and are most easily derived from first principles by considering the complementary energy of the elastic body in terms of stresses and strains rather than loads and displacements. In Chapter 5 we observed that the theorem of the principle of the stationary value of the total complementary energy of an elastic system is equivalent to the application of the principle of virtual work where virtual forces act through real displacements.We may therefore specify that in our expression for total complementary energy the displacements are the actual displacements produced by the applied loads while the virtual force system is the unit load.

Considering deflections due to bending, we see, from Eq. (5.6), that the increment in total complementary energy due to the application of a virtual unit load is

$$-\int_L \left(\int_A \sigma_{z,1} \varepsilon_{z,0} \, \mathrm{d}A \right) \mathrm{d}z + 1\Delta_M$$

where $\sigma_{z,1}$ is the direct bending stress at any point in the beam cross-section corresponding to the unit load and $\varepsilon_{z,0}$ is the strain at the point produced by the actual loading system. Further, Δ_M is the actual displacement due to bending at the point of application and in the direction of the unit load. Since the system is in equilibrium under the action of the unit load the above expression must equal zero (see Eq. (5.6)). Hence

$$\Delta_M = \int_L \left(\int_A \sigma_{z,1} \varepsilon_{z,0} \, \mathrm{d}A \right) \mathrm{d}z \tag{20.15}$$

From Eq. (16.18) and the third of Eqs (1.42)

$$\sigma_{z,1} = \left(\frac{M_{y,1} I_{xx} - M_{x,1} I_{xy}}{I_{xx} I_{yy} - I_{xy}^2} \right) x + \left(\frac{M_{x,1} I_{yy} - M_{y,1} I_{xy}}{I_{xx} I_{yy} - I_{xy}^2} \right) y$$

$$\varepsilon_{z,0} = \frac{1}{E} \left[\left(\frac{M_{y,0} I_{xx} - M_{x,0} I_{xy}}{I_{xx} I_{yy} - I_{xy}^2} \right) x + \left(\frac{M_{x,0} I_{yy} - M_{y,0} I_{xy}}{I_{xx} I_{yy} - I_{xy}^2} \right) y \right]$$

where the suffixes 1 and 0 refer to the unit and actual loading systems and x, y are the coordinates of any point in the cross-section referred to a centroidal system of

axes. Substituting for $\sigma_{z,1}$ and $\varepsilon_{z,0}$ in Eq. (20.15) and remembering that $\int_A x^2\,\mathrm{d}A = I_{yy}$, $\int_A y^2\,\mathrm{d}A = I_{xx}$, and $\int_A xy\,\mathrm{d}A = I_{xy}$, we have

$$\begin{aligned}\Delta_M = \frac{1}{E(I_{xx}I_{yy} - I_{xy}^2)^2}\int_L \{&(M_{y,1}I_{xx} - M_{x,1}I_{xy})(M_{y,0}I_{xx} - M_{x,0}I_{xy})I_{yy}\\ &+ (M_{x,1}I_{yy} - M_{y,1}I_{xy})(M_{x,0}I_{yy} - M_{y,0}I_{xy})I_{xx}\\ &+ [(M_{y,1}I_{xx} - M_{x,1}I_{xy})(M_{x,0}I_{yy} - M_{y,0}I_{xy})\\ &+ (M_{x,1}I_{yy} - M_{y,1}I_{xy})(M_{y,0}I_{xx} - M_{x,0}I_{xy})]I_{xy}\}\mathrm{d}z\end{aligned} \tag{20.16}$$

For a section having either the x or y axis as an axis of symmetry, $I_{xy} = 0$ and Eq. (20.16) reduces to

$$\Delta_M = \frac{1}{E}\int_L \left(\frac{M_{y,1}M_{y,0}}{I_{yy}} + \frac{M_{x,1}M_{x,0}}{I_{xx}}\right)\mathrm{d}z \tag{20.17}$$

The derivation of an expression for the shear deflection of thin-walled sections by the unit load method is achieved in a similar manner. By comparison with Eq. (20.15) we deduce that the deflection Δ_S, due to shear of a thin-walled open or closed section beam of thickness t, is given by

$$\Delta_S = \int_L \left(\int_{\text{sect}} \tau_1 \gamma_0 t\,\mathrm{d}s\right)\mathrm{d}z \tag{20.18}$$

where τ_1 is the shear stress at an arbitrary point s around the section produced by a unit load applied at the point and in the direction Δ_S, and γ_0 is the shear strain at the arbitrary point corresponding to the actual loading system. The integral in parentheses is taken over all the walls of the beam. In fact, both the applied and unit shear loads must act through the shear centre of the cross-section, otherwise additional torsional displacements occur. Where shear loads act at other points these must be replaced by shear loads at the shear centre plus a torque. The thickness t is the actual skin thickness and may vary around the cross-section but is assumed to be constant along the length of the beam. Rewriting Eq. (20.18) in terms of shear flows q_1 and q_0, we obtain

$$\Delta_S = \int_L \left(\int_{\text{sect}} \frac{q_0 q_1}{Gt}\mathrm{d}s\right)\mathrm{d}z \tag{20.19}$$

where again the suffixes refer to the actual and unit loading systems. In the cases of both open and closed section beams the general expressions for shear flow are long and are best evaluated before substituting in Eq. (20.19). For an open section beam comprising booms and walls of direct stress carrying thickness t_D we have, from Eq. (20.6)

$$\begin{aligned}q_0 = &-\left(\frac{S_{x,0}I_{xx} - S_{y,0}I_{xy}}{I_{xx}I_{yy} - I_{xy}^2}\right)\left(\int_0^s t_\mathrm{D}x\,\mathrm{d}s + \sum_{r=1}^{n} B_r x_r\right)\\ &-\left(\frac{S_{y,0}I_{yy} - S_{x,0}I_{xy}}{I_{xx}I_{yy} - I_{xy}^2}\right)\left(\int_0^s t_\mathrm{D}y\,\mathrm{d}s + \sum_{r=1}^{n} B_r y_r\right)\end{aligned} \tag{20.20}$$

and

$$q_1 = -\left(\frac{S_{x,1}I_{xx} - S_{y,1}I_{xy}}{I_{xx}I_{yy} - I_{xy}^2}\right)\left(\int_0^s t_D x\,\mathrm{d}s + \sum_{r=1}^{n} B_r x_r\right) - \left(\frac{S_{y,1}I_{yy} - S_{x,1}I_{xy}}{I_{xx}I_{yy} - I_{xy}^2}\right)\left(\int_0^s t_D y\,\mathrm{d}s + \sum_{r=1}^{n} B_r y_r\right) \tag{20.21}$$

Similar expressions are obtained for a closed section beam from Eq. (20.11).

Example 20.5

Calculate the deflection of the free end of a cantilever 2000 mm long having a channel section identical to that in Example 20.3 and supporting a vertical, upward load of 4.8 kN acting through the shear centre of the section. The effective direct stress carrying thickness of the skin is zero while its actual thickness is 1 mm. Young's modulus E and the shear modulus G are 70 000 and 30 000 N/mm^2, respectively.

The section is doubly symmetrical (i.e. the direct stress carrying area) and supports a vertical load producing a vertical deflection. Thus we apply a unit load through the shear centre of the section at the tip of the cantilever and in the same direction as the applied load. Since the load is applied through the shear centre there is no twisting of the section and the total deflection is given, from Eqs (20.17), (20.19), (20.20) and (20.21), by

$$\Delta = \int_0^L \frac{M_{x,0}M_{x,1}}{EI_{xx}}\mathrm{d}z + \int_0^L \left(\int_{\text{sect}} \frac{q_0 q_1}{Gt}\mathrm{d}s\right)\mathrm{d}z \tag{i}$$

where $M_{x,0} = -4.8 \times 10^3(2000 - z)$, $M_{x,1} = -1(2000 - z)$

$$q_0 = -\frac{4.8 \times 10^3}{I_{xx}}\sum_{r=1}^{n} B_r y_r \quad q_1 = -\frac{1}{I_{xx}}\sum_{r=1}^{n} B_r y_r$$

and z is measured from the built-in end of the cantilever. The actual shear flow distribution has been calculated in Example 20.3. In this case the q_1 shear flows may be deduced from the actual distribution shown in Fig. 20.8, i.e.

$$q_1 = q_0/4.8 \times 10^3$$

Evaluating the bending deflection, we have

$$\Delta_M = \int_0^{2000} \frac{4.8 \times 10^3(2000 - z)^2\mathrm{d}z}{70\,000 \times 48 \times 10^6} = 3.81\,\text{mm}$$

The shear deflection Δ_S is given by

$$\Delta_S = \int_0^{2000} \frac{1}{30\,000 \times 1}\left[\frac{1}{4.8 \times 10^3}(6^2 \times 200 + 12^2 \times 400 + 6^2 \times 200)\right]\mathrm{d}z = 1.0\,\text{mm}$$

The total deflection Δ is then $\Delta_M + \Delta_S = 4.81$ mm in a vertical upward direction.

Problems

P.20.1 Idealize the box section shown in Fig. P.20.1 into an arrangement of direct stress carrying booms positioned at the four corners and panels which are assumed to carry only shear stresses. Hence determine the distance of the shear centre from the left-hand web.

Ans. 225 mm.

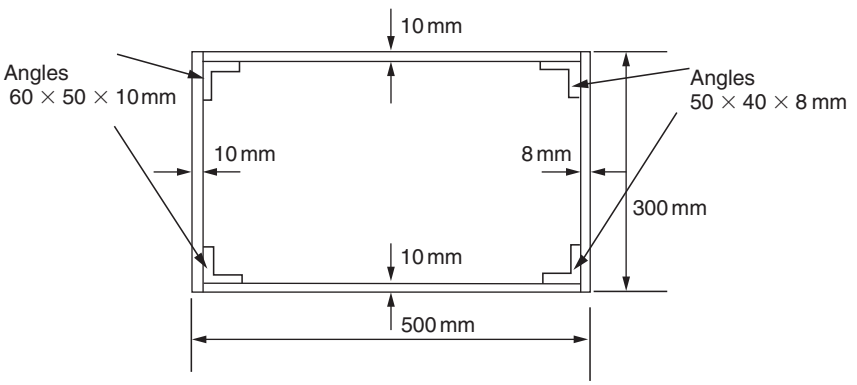

Fig. P.20.1

P.20.2 The beam section shown in Fig. P.20.2 has been idealized into an arrangement of direct stress carrying booms and shear stress only carrying panels. If the beam section is subjected to a vertical shear load of 1495 N through its shear centre, booms 1, 4, 5 and 8 each have an area of 200 mm^2 and booms 2, 3, 6 and 7 each have an area of 250 mm^2 determine the shear flow distribution and the position of the shear centre.

Ans. Wall 12, 1.86 N/mm; 43, 1.49 N/mm; 32, 5.21 N/mm; 27, 10.79 N/mm; remaining distribution follows from symmetry. 122 mm to the left of the web 27.

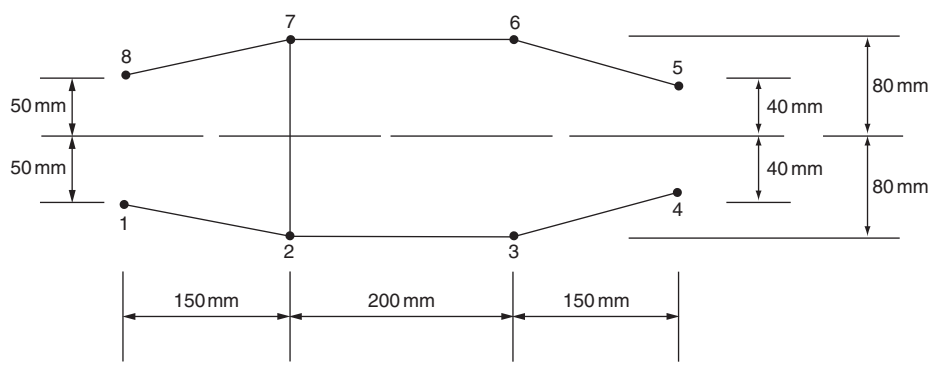

Fig. P.20.2

P.20.3 Figure P.20.3 shows the cross-section of a single cell, thin-walled beam with a horizontal axis of symmetry. The direct stresses are carried by the booms B_1 to B_4, while the walls are effective only in carrying shear stresses. Assuming that the basic theory of bending is applicable, calculate the position of the shear centre S. The shear modulus G is the same for all walls.

Cell area = 135 000 mm^2. Boom areas: $B_1 = B_4 = 450\,\text{mm}^2$, $B_2 = B_3 = 550\,\text{mm}^2$.

Ans. 197.2 mm from vertical through booms 2 and 3.

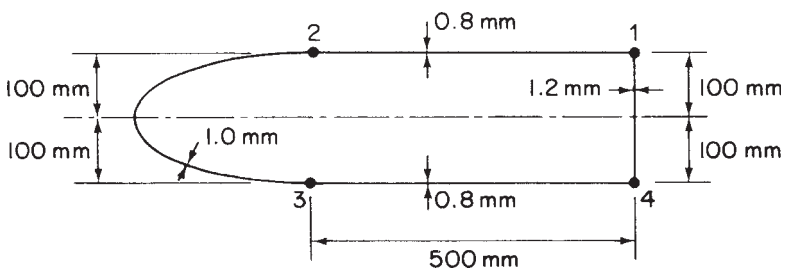

Fig. P.20.3

Wall	Length (mm)	Thickness (mm)
12, 34	500	0.8
23	580	1.0
41	200	1.2

P.20.4 Find the position of the shear centre of the rectangular four boom beam section shown in Fig. P.20.4. The booms carry only direct stresses but the skin is fully effective in carrying both shear and direct stress. The area of each boom is 100 mm^2.

Ans. 142.5 mm from side 23.

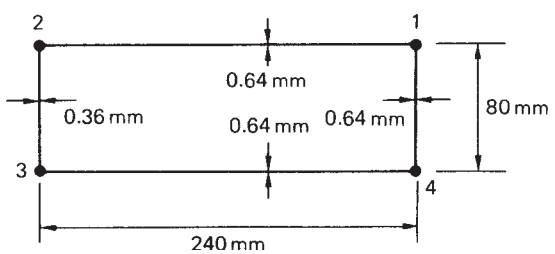

Fig. P.20.4

P.20.5 A uniform beam with the cross-section shown in Fig. P.20.5(a) is supported and loaded as shown in Fig. P.20.5(b). If the direct and shear stresses are given by the basic theory of bending, the direct stresses being carried by the booms and the shear stresses by the walls, calculate the vertical deflection at the ends of the beam when the loads act through the shear centres of the end cross-sections, allowing for the effect of shear strains.

Take $E = 69\,000\,\text{N/mm}^2$ and $G = 26\,700\,\text{N/mm}^2$. Boom areas: 1, 3, 4, 6 = 650 mm^2, 2, 5 = 1300 mm^2.

Ans. 3.4 mm.

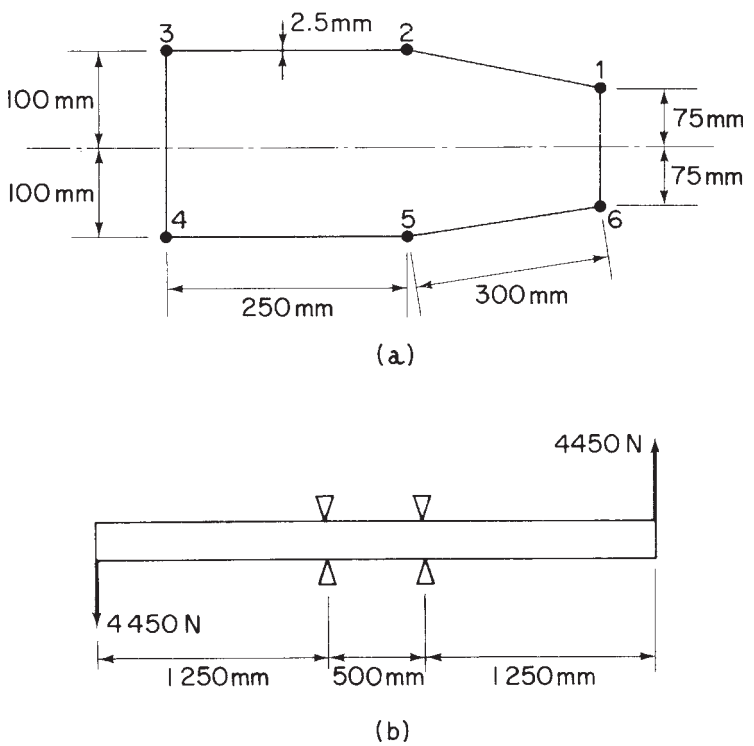

Fig. P.20.5

P.20.6 A cantilever, length L, has a hollow cross-section in the form of a doubly symmetric wedge as shown in Fig. P.20.6. The chord line is of length c, wedge thickness is t, the length of a sloping side is $a/2$ and the wall thickness is constant and equal to t_0. Uniform pressure distributions of magnitudes shown act on the faces of the wedge. Find the vertical deflection of point A due to this given loading. If $G = 0.4E$, $t/c = 0.05$ and $L = 2c$ show that this deflection is approximately $5600 p_0 c^2/Et_0$.

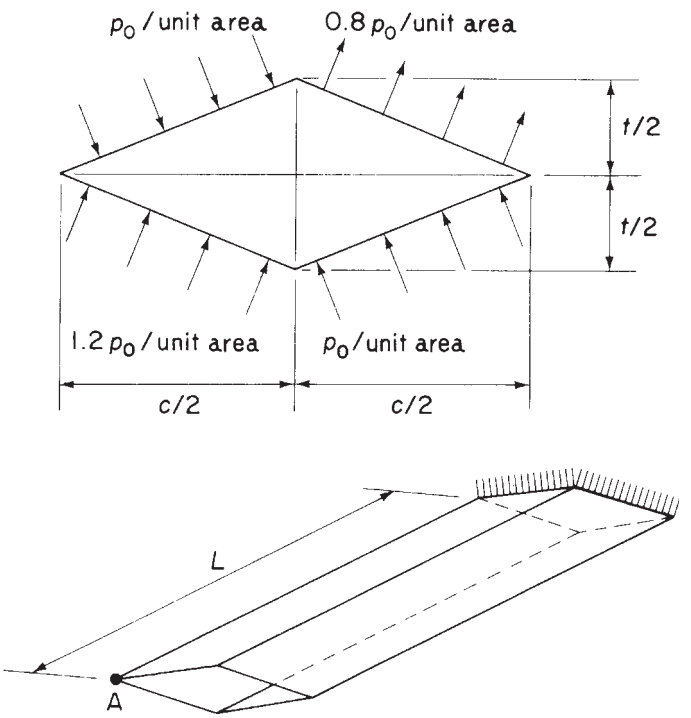

Fig. P.20.6

P.20.7 A rectangular section thin-walled beam of length L and breadth $3b$, depth b and wall thickness t is built in at one end (Fig. P.20.7). The upper surface of the beam is subjected to a pressure which varies linearly across the breadth from a value p_0 at edge AB to zero at edge CD. Thus, at any given value of x the pressure is constant in the z direction. Find the vertical deflection of point A.

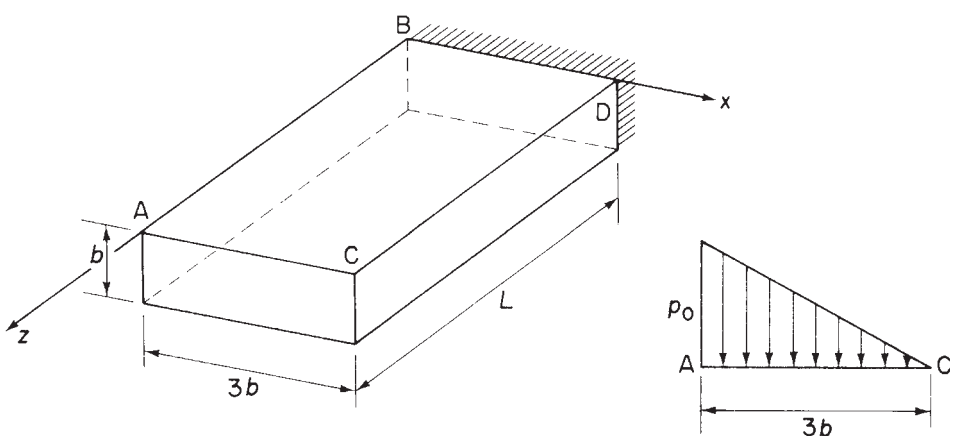

Fig. P.20.7

Ans. $p_0L^2(9L^2/80Eb^2 + 1609/2000G)/t$.

26

Closed section beams

The analysis presented in Chapters 16–20 relies on elementary theory for the determination of stresses and displacements produced by axial loads, shear forces and bending moments and torsion. No allowance is made for the effects of restrained warping produced by structural or loading discontinuities in the torsion of open or closed section beams, or for the effects of shear strains on the calculation of direct and shear stresses in beams subjected to bending and shear.

In this chapter we shall examine some relatively simple examples of the above effects; more complex cases require analysis by computer-based techniques such as the finite element method.

26.1 General aspects

Structural constraint stresses in either closed or open beams result from a restriction on the freedom of any section of the beam to assume its normal displaced shape under load. Such a restriction arises when one end of the beam is built-in although the same effect may be produced practically, in a variety of ways. For example, the root section of a beam subjected to torsion is completely restrained from warping into the displaced shape indicated by Eq. (18.5) and a longitudinal stress system is induced which, in a special case discussed later, is proportional to the free warping of the beam.

A slightly different situation arises when the beam supports shear loads. The stress system predicted by elementary bending theory relies on the basic assumption of plane sections remaining plane after bending. However, for a box beam comprising thin skins and booms, the shear strains in the skins are of sufficient magnitude to cause a measurable redistribution of direct load in the booms and hence previously plane sections warp. We shall discuss the phenomenon of load redistribution resulting from shear, known as *shear lag*, in detail later in the chapter. The prevention of this warping by some form of axial constraint modifies the stress system still further.

The most comprehensive analysis yet published of multi-cell and single cell beams under arbitrary loading and support conditions is that by Argyris and Dunne.[1] Their work concentrates in the main on beams of idealized cross-section and while the theory they present is in advance of that required here, it is beneficial to examine some of the results of their analysis. We shall limit the present discussion to closed beams of idealized cross-section.

The problem of axial constraint may be conveniently divided into two parts. In the first, the shear stress distribution due to an arbitrary loading is calculated exclusively at the built-in end of the beam. In the second, the stress (and/or load) distributions are calculated along the length of the beam for the separate loading cases of torsion and shear. Obviously the shear stress systems predicted by each portion of theory must be compatible at the built-in end.

Argyris and Dunne showed that the calculation of the shear stress distribution at a built-in end is a relatively simple problem, the solution being obtained for any loading and beam cross-section by statics. More complex is the determination of the stress distributions at sections along the beam. These stresses, for the torsion case, are shown to be the sum of the stresses predicted by elementary theory and stresses caused by systems of self-equilibrating end loads. For a beam supporting shear loads the total stresses are again the sum of those corresponding to elementary bending theory and stresses due to systems of self-equilibrating end loads.

For an n-boom, idealized beam, Argyris and Dunne found that there are $n-3$ self-equilibrating end load, or *eigenload*, systems required to nullify $n-3$ possible modes of warping displacement. These eigenloads are analogous to, say, the buckling loads corresponding to the different buckled shapes of an elastic strut. The fact that, generally, there are a number of warping displacements possible in an idealized beam invalidates the use of the shear centre or flexural axis as a means of separating torsion and shear loads. For, associated with each warping displacement is an axis of twist that is different for each warping mode. In practice, a good approximation is obtained if the torsion loads are referred to the axis of twist corresponding to the lowest eigenload. Transverse loads through this axis, the *zero warping axis* produce no warping due to twist, although axial constraint stresses due to shear will still be present.

In the special case of a doubly symmetrical section the problem of separating the torsion and bending loads does not arise since it is obvious that the torsion loads may be referred to the axis of symmetry. Double symmetry has the further effect of dividing the eigenloads into four separate groups corresponding to $(n/4)-1$ pure flexural modes in each of the xz and yz planes, $(n/4)$ pure twisting modes about the centre of symmetry and $(n/4)-1$ pure warping modes which involve neither flexure nor twisting. A doubly symmetrical six boom beam supporting a single shear load has therefore just one eigenload system if the centre boom in the top and bottom panels is regarded as being divided equally on either side of the axis of symmetry thereby converting it, in effect, into an eight boom beam.

It will be obvious from the above that, generally, the self-equilibrating stress systems cannot be proportional to the free warping of the beam unless the free warping can be nullified by just one eigenload system. This is true only for the four boom beam which, from the above, has one possible warping displacement. If, in addition, the beam is doubly symmetrical then its axis of twist will pass through the centre of symmetry. We note that only in cases of doubly symmetrical beams do the zero warping and flexural axes coincide.

A further special case arises when the beam possesses the properties of a Neuber beam (Section 18.1.2) which does not warp under torsion. The stresses in this case are the elementary torsion theory stresses since no constraint effects are present. When bending loads predominate, however, it is generally impossible to design an efficient structure which does not warp.

In this chapter the calculation of spanwise stress distributions in closed section beams is limited to simple cases of beams having doubly symmetrical cross-sections. It should be noted that simplifications of this type can be misleading in that some of the essential characteristics of beam analysis, for example the existence of the $n-3$ self-equilibrating end load systems, vanish.

26.2 Shear stress distribution at a built-in end of a closed section beam

This special case of structural constraint is of interest due to the fact that the shear stress distribution at the built-in end of a closed section beam is statically determinate. Figure 26.1 represents the cross-section of a thin-walled closed section beam at its built-in end. It is immaterial for this analysis whether or not the section is idealized since the expression for shear flow in Eq. (17.19), on which the solution is based, is applicable to either case. The beam supports shear loads S_x and S_y which generally will produce torsion in addition to shear. We again assume that the cross-section of the beam remains undistorted by the applied loads so that the displacement of the beam cross-section is completely defined by the displacements u, v, w and the rotation θ referred to an arbitrary system of axes Oxy. The shear flow q at any section of the beam is then given by Eq. (17.20), that is

$$q = Gt\left(p\frac{\mathrm{d}\theta}{\mathrm{d}z} + \frac{\mathrm{d}u}{\mathrm{d}z}\cos\psi + \frac{\mathrm{d}v}{\mathrm{d}z}\sin\psi + \frac{\partial w}{\partial s}\right)$$

At the built-in end, $\partial w/\partial s$ is zero and hence

$$q = Gt\left(p\frac{\mathrm{d}\theta}{\mathrm{d}z} + \frac{\mathrm{d}u}{\mathrm{d}z}\cos\psi + \frac{\mathrm{d}v}{\mathrm{d}z}\sin\psi\right) \tag{26.1}$$

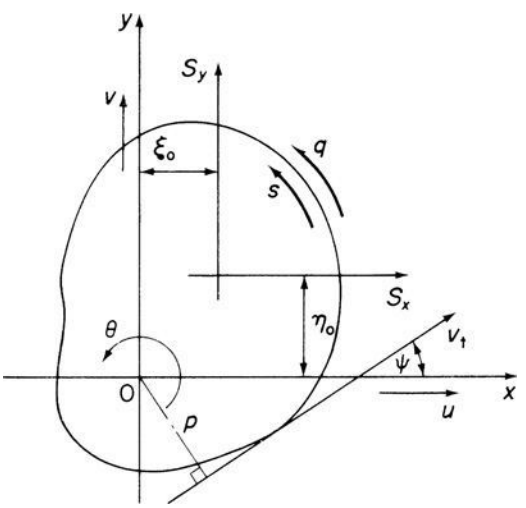

Fig. 26.1 Cross-section of a thin-walled beam at the built-in end.

in which $\mathrm{d}\theta/\mathrm{d}z$, $\mathrm{d}u/\mathrm{d}z$ and $\mathrm{d}v/\mathrm{d}z$ are the unknowns, the remaining terms being functions of the section geometry.

The resultants of the internal shear flows q must be statically equivalent to the applied loading, so that

$$\left.\begin{aligned} \oint q\cos\psi\,\mathrm{d}s &= S_x \\ \oint q\sin\psi\,\mathrm{d}s &= S_y \\ \oint qp\,\mathrm{d}s &= S_y\xi_0 - S_x\eta_0 \end{aligned}\right\} \tag{26.2}$$

Substitution for q from Eq. (26.1) in Eqs (26.2) yields

$$\left.\begin{aligned} \frac{\mathrm{d}\theta}{\mathrm{d}z}\oint tp\cos\psi\,\mathrm{d}s + \frac{\mathrm{d}u}{\mathrm{d}z}\oint t\cos^2\psi\,\mathrm{d}s + \frac{\mathrm{d}v}{\mathrm{d}z}\oint t\cos\psi\sin\psi\,\mathrm{d}s &= \frac{S_x}{G} \\ \frac{\mathrm{d}\theta}{\mathrm{d}z}\oint tp\sin\psi\,\mathrm{d}s + \frac{\mathrm{d}u}{\mathrm{d}z}\oint t\sin\psi\cos\psi\,\mathrm{d}s + \frac{\mathrm{d}v}{\mathrm{d}z}\oint t\sin^2\psi\,\mathrm{d}s &= \frac{S_y}{G} \\ \frac{\mathrm{d}\theta}{\mathrm{d}z}\oint tp^2\,\mathrm{d}s + \frac{\mathrm{d}u}{\mathrm{d}z}\oint tp\cos\psi\,\mathrm{d}s + \frac{\mathrm{d}v}{\mathrm{d}z}\oint tp\sin\psi\,\mathrm{d}s &= \frac{(S_y\xi_0 - S_x\eta_0)}{G} \end{aligned}\right\} \tag{26.3}$$

Equations (26.3) are solved simultaneously for $\mathrm{d}\theta/\mathrm{d}z$, $\mathrm{d}u/\mathrm{d}z$ and $\mathrm{d}v/\mathrm{d}z$. These values are then substituted in Eq. (26.1) to obtain the shear flow, and hence the shear stress distribution.

Attention must be paid to the signs of ψ, p and q in Eqs (26.3). Positive directions for each parameter are suggested in Fig. 26.1 although alternative conventions may be adopted. In general, however, there are rules which must be obeyed, these having special importance in the solution of multicell beams. Briefly, these are as follows. The positive directions of q and s are the same but may be assigned arbitrarily in each wall. Then p is positive if movement of the foot of the perpendicular along the positive direction of the tangent leads to an anticlockwise rotation of p about O. ψ is the clockwise rotation of the tangent vector necessary to bring it into coincidence with the positive direction of the x axis.

Example 26.1

Calculate the shear stress distribution at the built-in end of the beam shown in Fig. 26.2(a) when, at this section, it carries a shear load of 22 000 N acting at a distance of 100 mm from and parallel to side 12. The modulus of rigidity G is constant throughout the section:

Wall	12	34	23
Length (mm)	375	125	500

It is helpful at the start of the problem to sketch the notation and sign convention as shown in Fig. 26.2(b). The walls of the beam are flat and therefore p and ψ are constant along each wall. Also the thickness of each wall is constant so that the shear flow q is independent of s in each wall. Let point 1 be the origin of the axes, then, writing

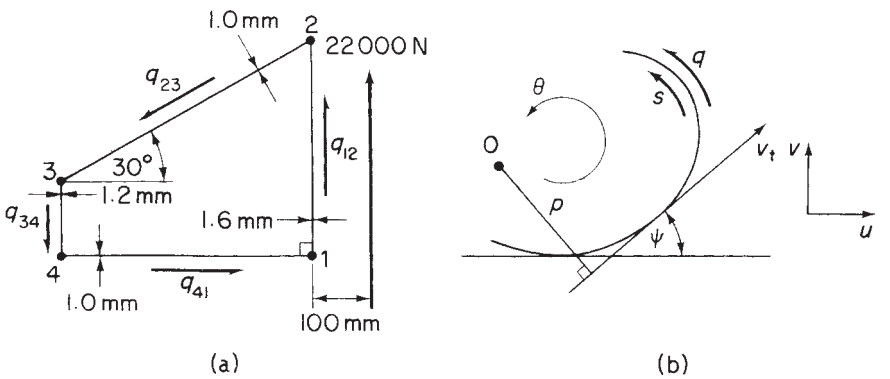

Fig. 26.2 (a) Beam cross-section at built-in end; (b) notation and sign convention.

$\theta' = \mathrm{d}\theta/\mathrm{d}z$, $u' = \mathrm{d}u/\mathrm{d}z$ and $v' = \mathrm{d}v/\mathrm{d}z$, we obtain from Eq. (26.1)

$$q_{12} = 1.6Gv' \tag{i}$$

$$q_{23} = 1.0G(375 \times 0.886\theta' - 0.886u' - 0.5v') \tag{ii}$$

$$q_{34} = 1.2G(500 \times 0.866\theta' - v') \tag{iii}$$

$$q_{41} = 1.0Gu' \tag{iv}$$

For horizontal equilibrium

$$500 \times 0.886q_{41} - 500 \times 0.886q_{23} = 0$$

giving

$$q_{41} = q_{23} \tag{v}$$

For vertical equilibrium

$$375q_{12} - 125q_{34} - 250q_{23} = 22\,000 \tag{vi}$$

For moment equilibrium about point 1

$$500 \times 375 \times 0.886q_{23} + 125 \times 500 \times 0.886q_{34} = 22\,000 \times 100$$

or

$$3q_{23} + q_{34} = 40.6 \tag{vii}$$

Substituting for q_{12}, etc. from Eqs (i), (ii), (iii) and (iv) into Eqs (v), (vi) and (vii), and solving for θ', u' and v', gives $\theta' = 0.122/G$, $u\prime = 9.71/G$, $v' = 42.9/G$. The values of θ', u' and v' are now inserted in Eqs (i), (ii), (iii) and (iv), giving $q_{12} = 68.5$ N/mm, $q_{23} = 9.8$ N/mm, $q_{34} = 11.9$ N/mm, $q_{41} = 9.8$ N/mm from which

$$\tau_{12} = 42.8\,\mathrm{N/mm^2} \quad \tau_{23} = \tau_{41} = 9.8\,\mathrm{N/mm^2} \quad \tau_{34} = 9.9\,\mathrm{N/mm^2}$$

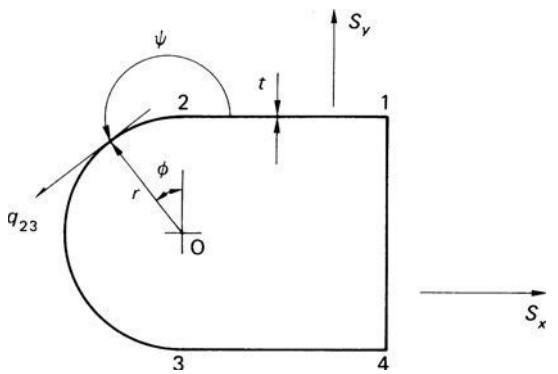

Fig. 26.3 Built-in end of a beam section having a curved wall.

We note in Example 26.1 that there is a discontinuity of shear flow at each of the corners of the beam. This implies the existence of axial loads at the corners which would, in practice, be resisted by booms, if stress concentrations are to be avoided. We see also that in a beam having straight walls the shear flows are constant along each wall so that, from Eq. (17.2), the direct stress gradient $\partial\sigma_z/\partial z = 0$ in the walls at the built-in end although not necessarily in the booms. Finally, the centre of twist of the beam section at the built-in end may be found using Eq. (17.11), i.e.

$$x_R = -\frac{v'}{\theta'} \quad y_R = \frac{u'}{\theta'}$$

which, from the results of Example 26.1, give $x_R = -351.6$ mm, $y_R = 79.6$ mm. Thus, the centre of twist is 351.6 mm to the left of and 79.6 mm above corner 1 of the section and will not, as we noted in Section 26.1, coincide with the shear centre of the section.

The method of analysis of beam sections having curved walls is similar to that of Example 26.1 except that in the curved walls the shear flow will not be constant since both p and ψ in Eq. (26.1) will generally vary. Consider the beam section shown in Fig. 26.3 in which the curved wall 23 is semicircular and of radius r. In the wall 23, $p = r$ and $\psi = 180 + \phi$, so that Eq. (26.1) gives

$$q_{23} = Gt(r\theta' - u'\cos\phi - v'\sin\phi)$$

The resultants of q_{23} are then

$$\text{Horizontally} : \int_0^\pi q_{23}\cos\phi r\,\mathrm{d}\phi$$

$$\text{Vertically} : \int_0^\pi q_{23}\sin\phi r\,\mathrm{d}\phi$$

$$\text{Moment (about 0)} : \int_0^\pi q_{23}r^2\,\mathrm{d}\phi$$

The shear flows in the remaining walls are constant and the solution proceeds as before.

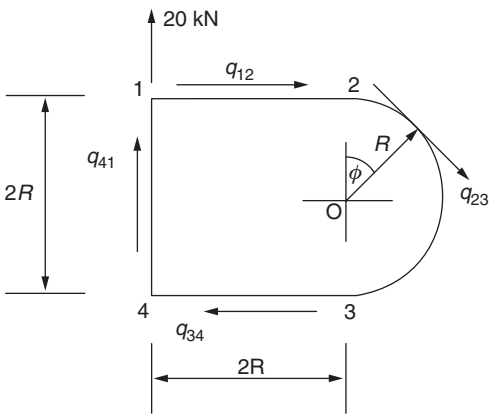

Fig. 26.4 Beam section of Example 26.2.

Example 26.2

Determine the shear flow distribution at the built-in end of a beam whose cross-section is shown in Fig. 26.4. All walls have the same thickness t and shear modulus G; $R = 200\,\text{mm}$.

In general at a built-in end (see Eq (26.1))

$$q = Gt\left(p\frac{\mathrm{d}\theta}{\mathrm{d}z} + \frac{\mathrm{d}u}{\mathrm{d}z}\cos\psi + \frac{\mathrm{d}v}{\mathrm{d}z}\sin\psi\right)$$

Therefore, taking O as the origin and writing $\theta' = \mathrm{d}\theta/\mathrm{d}z$, $u' = \mathrm{d}u/\mathrm{d}z$ and $v' = \mathrm{d}v/\mathrm{d}z$

$$q_{41} = Gt(-2R\theta' + v') \tag{i}$$

$$q_{12} = Gt(-R\theta' + u') \tag{ii}$$

$$q_{34} = Gt(-R\theta' - u') \tag{iii}$$

$$q_{23} = Gt(-R\theta' + u'\cos\phi - v'\sin\phi) \tag{iv}$$

From symmetry

$$q_{12} = q_{34}$$

i.e.

$$Gt(-R\theta' + u') = Gt(-R\theta' - u')$$

Therefore

$$u' = 0$$

Resolving vertically

$$q_{41}2R - \int_0^{\pi} q_{23}\sin\phi\, R\,\mathrm{d}\phi = 20 \times 10^3$$

i.e.

$$q_{41} - \frac{1}{2}\int_0^{\pi} q_{23} \sin\phi \, \mathrm{d}\phi = \frac{10\,000}{R}$$

Substituting from Eqs (i) and (iv) gives

$$-R\theta' + 1.79v' = \frac{10\,000}{GtR} \tag{v}$$

Now taking moments about O

$$q_{41}\, 2R\, 2R + q_{12}\, 2R\, R + q_{34}\, 2R\, R + \int_0^{\pi} q_{23}\, R^2 \mathrm{d}\phi = 20\,000 \times 2R$$

which gives

$$2q_{41} + q_{12} + q_{34} + \frac{1}{2}\int_0^{\pi} q_{23}\, \mathrm{d}\phi = \frac{20\,000}{R}$$

Substituting from Eqs (i), (ii), (iii) and (iv)

$$2Gt(-2R\theta' + v') - 2GtR\theta' + \frac{Gt}{2}\int_0^{\pi} (-R\theta' - v'\sin\phi)\, \mathrm{d}\phi = \frac{20\,000}{R}$$

from which

$$R\theta' - 0.13v' = -\frac{2641.7}{GtR} \tag{vi}$$

Solving Eqs (v) and (vi)

$$v' = \frac{4432.7}{GtR}, \quad R\theta' = -\frac{2065.4}{GtR}$$

Therefore

$$q_{41} = Gt\left(\frac{2 \times 2065.4}{200Gt} + \frac{4432.7}{200Gt}\right) = 42.8\,\mathrm{N/mm}$$

Similarly

$$q_{12} = q_{34} = 10.3\,\mathrm{N/mm}$$

Finally

$$q_{23} = 10.3 - 22.2 \sin\phi\,\mathrm{N/mm}$$

26.3 Thin-walled rectangular section beam subjected to torsion

In Example 18.2 we determined the warping distribution in a thin-walled rectangular section beam which was not subjected to structural constraint. This free warping distribution (w_0) was found to be linear around a cross-section and uniform along the length of the beam having values at the corners of

$$w_0 = \pm \frac{T}{8abG}\left(\frac{b}{t_b} - \frac{a}{t_a}\right)$$

The effect of structural constraint, such as building one end of the beam in, is to reduce this free warping to zero at the built-in section so that direct stresses are induced which subsequently modify the shear stresses predicted by elementary torsion theory. These direct stresses must be self-equilibrating since the applied load is a pure torque.

The analysis of a rectangular section beam built-in at one end and subjected to a pure torque at the other is simplified if the section is idealized into one comprising four corner booms which are assumed to carry all the direct stresses together with shear–stress-only carrying walls. The assumption on which the idealization is based is that the direct stress distribution at any cross-section is directly proportional to the warping which has been suppressed. Therefore, the distribution of direct stress is linear around any cross-section and has values equal in magnitude but opposite in sign at opposite corners of a wall. This applies at all cross-sections since the free warping will be suppressed to some extent along the complete length of the beam. In Fig. 26.5(b) all the booms will have the same cross-sectional area from anti-symmetry and, from Eq. (20.1) or (20.2)

$$B = \frac{at_a}{6}(2-1) + \frac{bt_b}{6}(2-1) = \frac{1}{6}(at_a + bt_b)$$

To the boom area B will be added existing concentrations of area such as connecting angle sections at the corners. The contributions of stringers may be included by allowing for their direct stress carrying capacity by increasing the actual wall thickness by an amount equal to the total stringer area on one wall before idealizing the section.

We have seen in Chapter 20 that the effect of structural idealization is to reduce the shear flow in the walls of a beam to a constant value between adjacent booms.

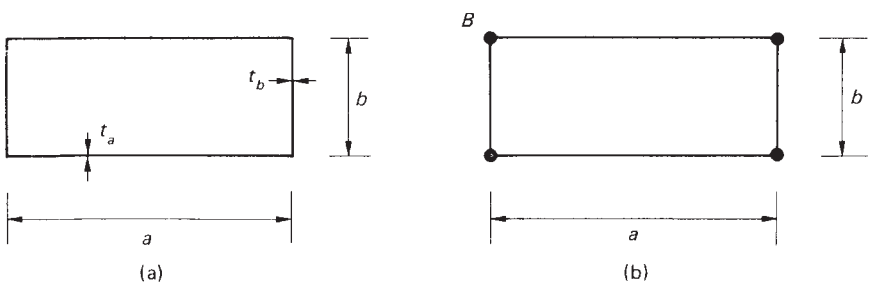

Fig. 26.5 Idealization of a rectangular section beam subjected to torsion: (a) actual; (b) idealized.

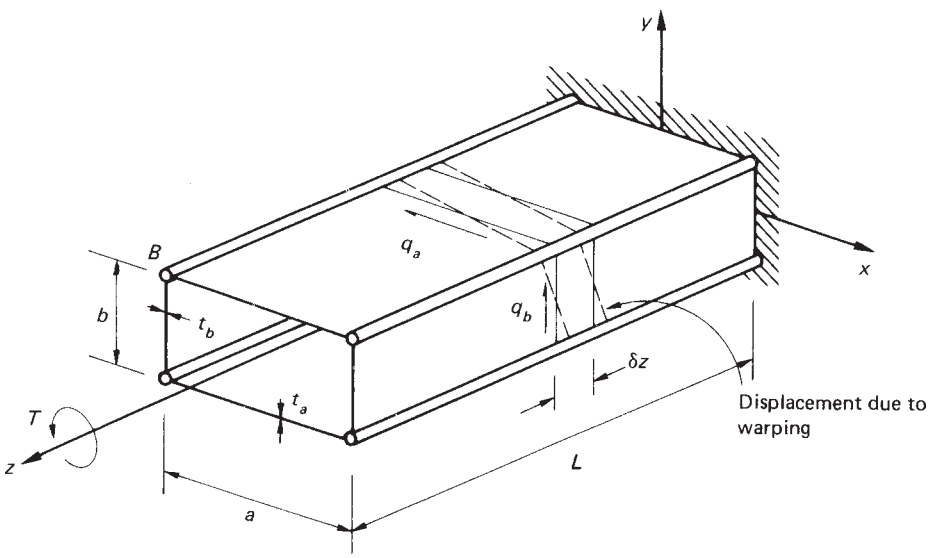

Fig. 26.6 Idealized rectangular section beam built-in at one end and subjected to a torque at the other.

In Fig. 26.6 suppose that the shear flows in the covers and webs at any section are q_a and q_b, respectively; from antisymmetry the shear flows in both covers will be q_a and in both webs q_b. The resultant of these shear flows is equivalent to the applied torque so that

$$T = \oint qp \, \mathrm{d}s = 2q_a a\frac{b}{2} + 2q_b b\frac{a}{2}$$

or

$$T = ab(q_a + q_b) \tag{26.4}$$

We now use Eq. (17.19), i.e.

$$q = Gt\left(\frac{\partial w}{\partial s} + \frac{\partial v}{\partial z}\right)$$

to determine q_a and q_b. Since the beam cross-section is doubly symmetrical the axis of twist passes through the centre of symmetry at any section so that, from Eq. (17.8)

$$\frac{\partial v_\mathrm{t}}{\partial z} = p_\mathrm{R}\frac{\mathrm{d}\theta}{\mathrm{d}z} \tag{26.5}$$

Therefore for the covers of the beam

$$\frac{\partial v_\mathrm{t}}{\partial z} = \frac{b}{2}\frac{\mathrm{d}\theta}{\mathrm{d}z} \tag{26.6}$$

and for the webs

$$\frac{\partial v_\mathrm{t}}{\partial z} = \frac{a}{2}\frac{\mathrm{d}\theta}{\mathrm{d}z} \tag{26.7}$$

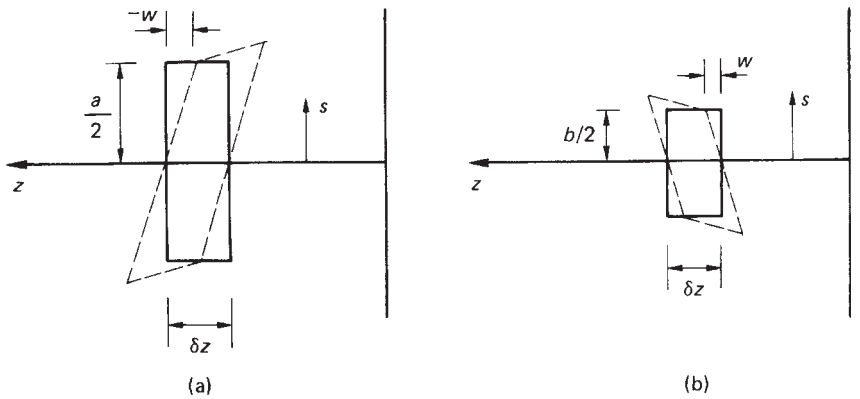

Fig. 26.7 Shear distortion of (a) an element of the top cover; (b) an element of the right hand web.

The elements of length δz of the covers and webs of the beam will warp into the shapes shown in Fig. 26.6 if T is positive (anticlockwise) and $b/t_b > a/t_a$. Clearly there must be compatibility of displacement at adjacent edges of the elements. From Fig. 26.7(a)

$$\frac{\partial w}{\partial s} = \frac{-w}{a/2} \tag{26.8}$$

and from Fig. 26.7(b)

$$\frac{\partial w}{\partial s} = \frac{w}{b/2} \tag{26.9}$$

Substituting for $\partial w/\partial s$ and $\partial v_t/\partial z$ in Eq. (17.19) separately for the covers and webs, we obtain

$$q_a = Gt_a\left(\frac{-2w}{a} + \frac{b}{2}\frac{\mathrm{d}\theta}{\mathrm{d}z}\right) \quad q_b = Gt_b\left(\frac{2w}{b} + \frac{a}{2}\frac{\mathrm{d}\theta}{\mathrm{d}z}\right) \tag{26.10}$$

Now substituting for q_a and q_b in Eq. (26.4) we have

$$T = abG\left[t_a\left(\frac{-2w}{a} + \frac{b}{2}\frac{\mathrm{d}\theta}{\mathrm{d}z}\right) + t_b\left(\frac{2w}{b} + \frac{a}{2}\frac{\mathrm{d}\theta}{\mathrm{d}z}\right)\right]$$

Rearranging

$$\frac{\mathrm{d}\theta}{\mathrm{d}z} = \frac{4w(bt_a - at_b)}{ab(bt_a + at_b)} + \frac{2T}{abG(bt_a + at_b)} \tag{26.11}$$

If we now substitute for $\mathrm{d}\theta/\mathrm{d}z$ from Eq. (26.11) into Eqs (26.10) we have

$$q_a = \frac{-4wGt_bt_a}{bt_a + at_b} + \frac{Tt_a}{a(bt_a + at_b)} \quad q_b = \frac{4wGt_bt_a}{bt_a + at_b} + \frac{Tt_b}{b(bt_a + at_b)} \tag{26.12}$$

Equations (26.11) and (26.12) give the rate of twist and the shear flows (and hence shear stresses) in the beam in terms of the warping w and the applied torque T. Their derivation is based on the compatibility of displacement which exists at the cover/boom/web

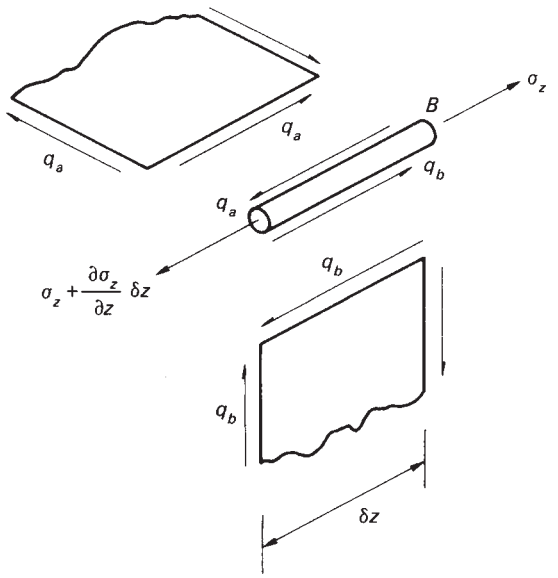

Fig. 26.8 Equilibrium of boom element.

junctions. We shall now use the further condition of equilibrium between the shears in the covers and webs and the direct load in the booms to obtain expressions for the warping displacement and the distributions of boom stress and load. Thus, for the equilibrium of an element of the top right-hand boom shown in Fig. 26.8

$$\left(\sigma_z + \frac{\partial \sigma_z}{\partial z}\delta z\right) B - \sigma_z B + q_a \delta z - q_b \delta z = 0$$

i.e.

$$B\frac{\partial \sigma_z}{\partial z} + q_a - q_b = 0 \tag{26.13}$$

Now

$$\sigma_z = E\frac{\partial w}{\partial z} \quad \text{(see Chapter 1)}$$

Substituting for σ_z in Eq. (26.13) we obtain

$$BE\frac{\partial^2 w}{\partial z^2} + q_a - q_b = 0 \tag{26.14}$$

Replacing q_a and q_b from Eqs (26.12) gives

$$BE\frac{\partial^2 w}{\partial z^2} - \frac{8Gt_b t_a}{bt_a + at_b}w = -\frac{T}{ab}\frac{(bt_a - at_b)}{(bt_a + at_b)}$$

or

$$\frac{\partial^2 w}{\partial z^2} - \mu^2 w = -\frac{T}{abBE}\frac{(bt_a - at_b)}{(bt_a + at_b)} \tag{26.15}$$

where

$$\mu^2 = \frac{8Gt_bt_a}{BE(bt_a + at_b)}$$

The differential equation (26.15) is of standard form and its solution is

$$w = C\cosh \mu z + D\sinh \mu z + \frac{T}{8abG}\left(\frac{b}{t_b} - \frac{a}{t_a}\right) \tag{26.16}$$

in which the last term is seen to be the free warping displacement w_0 of the top right-hand corner boom. The constants C and D in Eq. (26.16) are found from the boundary conditions of the beam. In this particular case the warping $w = 0$ at the built-in end and the direct strain $\partial w/\partial z = 0$ at the free end where there is no direct load. From the first of these

$$C = -\frac{T}{8abG}\left(\frac{b}{t_b} - \frac{a}{t_a}\right) = -w_0$$

and from the second

$$D = w_0 \tanh \mu L$$

Then

$$w = w_0(1 - \cosh \mu z + \tanh \mu L \sinh \mu z) \tag{26.17}$$

or rearranging

$$w = w_0\left[1 - \frac{\cosh \mu(L - z)}{\cosh \mu L}\right] \tag{26.18}$$

The variation of direct stress in the boom is obtained from $\sigma_z = E\partial w/\partial z$ and Eq. (26.18), i.e.

$$\sigma_z = \mu E w_0 \frac{\sinh \mu(L - z)}{\cosh \mu L} \tag{26.19}$$

and the variation of boom load P is then

$$P = B\sigma_z = B\mu E w_o \frac{\sinh \mu(L - z)}{\cosh \mu L} \tag{26.20}$$

Substituting for w in Eqs (26.12) and rearranging, we obtain the shear stress distribution in the covers and webs. Thus

$$\tau_a = \frac{q_a}{t_a} = \frac{T}{2abt_a}\left[1 + \frac{(bt_a - at_b)}{(bt_a + at_b)}\frac{\cosh \mu(L - z)}{\cosh \mu L}\right] \tag{26.21}$$

$$\tau_b = \frac{q_b}{t_b} = \frac{T}{2abt_b}\left[1 - \frac{(bt_a - at_b)}{(bt_a + at_b)}\frac{\cosh \mu(L - z)}{\cosh \mu L}\right] \tag{26.22}$$

Inspection of Eqs (26.21) and (26.22) shows that the shear stress distributions each comprise two parts. The first terms, $T/2abt_a$ and $T/2abt_b$, are the shear stresses predicted by elementary theory (see Section 18.1), while the hyperbolic second terms

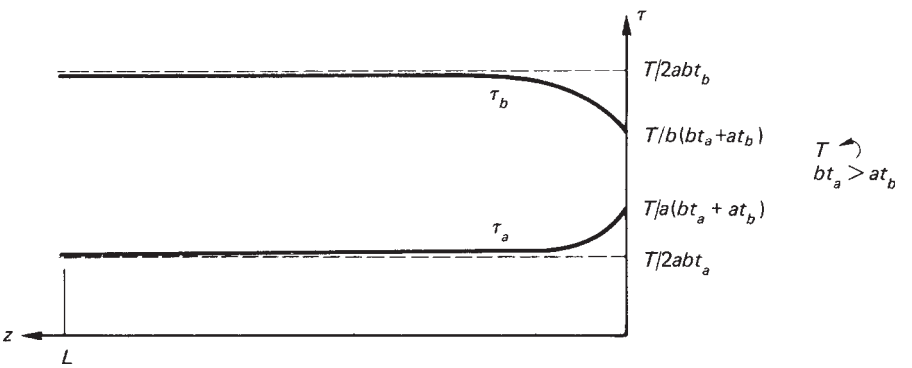

Fig. 26.9 Shear stress distributions along the beam of Fig. 11.5.

represent the effects of the warping restraint. Clearly, for an anticlockwise torque and $bt_a > at_b$, the effect of this constraint is to increase the shear stress in the covers over that predicted by elementary theory and decrease the shear stress in the webs. It may also be noted that for bt_a to be greater than at_b for the beam of Fig. 26.6, in which $a > b$, then t_a must be appreciably greater than t_b so that $T/2abt_a < T/2abt_b$. Also at the built-in end ($z = 0$), Eqs (26.21) and (26.22) reduce to $\tau_a = T/a(bt_a + at_b)$ and $\tau_b = T/b(bt_a + at_b)$ so that even though τ_b is reduced by the axial constraint and τ_a increased, τ_b is still greater than τ_a. It should also be noted that these values of τ_a and τ_b at the built-in end may be obtained using the method of Section 26.2 and that these are the values of shear stress irrespective of whether the section has been idealized or not. In other words, the presence of intermediate stringers and/or direct stress carrying walls does not affect the shear flows at the built-in end since the direct stress gradient at this section is zero (see Section 26.2 and Eq. (17.2)) except in the corner booms. Finally, when both z and L become large, i.e. at the free end of a long, slender beam

$$\tau_a \to \frac{T}{2abt_a} \quad \text{and} \quad \tau_b \to \frac{T}{2abt_b}$$

The above situation is shown in Fig. 26.9.

In the particular case when $bt_a = at_b$ we see that the second terms on the right-hand side of Eqs (26.21) and (26.22) disappear and no constraint effects are present; the direct stress of Eqs (26.19) is also zero since $w_0 = 0$ (see Example 18.2).

The rate of twist is obtained by substituting for w from Eq. (26.18) in Eq. (26.11). Thus

$$\frac{\mathrm{d}\theta}{\mathrm{d}z} = \frac{T}{2a^2b^2G}\left(\frac{b}{t_b} + \frac{a}{t_a}\right)\left[1 - \left(\frac{bt_a - at_b}{bt_a + at_b}\right)^2 \frac{\cosh \mu(L - z)}{\cosh \mu L}\right] \tag{26.23}$$

in which we see that again the expression on the right-hand side comprises the rate of twist given by elementary theory, $T(b/t_b + a/t_a)/2a^2b^2G$ (see Section 18.1), together with a correction due to the warping restraint. Clearly the rate of twist is always reduced by the constraint since $(bt_a - at_b)^2$ is always positive. Integration of Eq. (26.23) gives the distribution of angle of twist along the length of the beam, the boundary condition in this case being $\theta = 0$ at $z = 0$.

Example 26.3

A uniform four boom box of span 5 m is 500 mm wide by 20 mm deep and has four corner booms each of cross-sectional area 800 mm^2, its wall thickness is 1.0 mm. If the box is subjected to a uniformly distributed torque loading of 20 Nm/mm along its length and it is supported at each end such that complete freedom of warping exists at the end cross-sections calculate the angle of twist at the mid-span section. Take $G = 20\,000$ N/mm^2 and $G/E = 0.36$.

The reactive torques at each support are $= 20 \times 5000/2 = 50\,000$ Nm

Taking the origin for z at the mid-span of the beam the torque at any section is given by

$$T(z) = 20(2500 - z) - 50\,000 = -20z \text{ Nm}$$

Substituting in Eq. (26.16) we obtain

$$w = C\cosh \mu z + D\sinh \mu z - \frac{20z \times 10^3(b-a)}{8abGt}$$

The boundary conditions are:

$w = 0$ when $z = 0$ from symmetry and $\partial w/\partial z = 0$ when $z = L$ ($L = 2500$ mm)

From the first of these $C = 0$ while from the second

$$D = \frac{20 \times 10^3(b-a)}{8\mu abGt \cosh \mu L}$$

Therefore

$$w = \frac{20(b-a) \times 10^3}{8abGt}\left(\frac{\sinh \mu z}{\mu \cosh \mu L} - z\right) \tag{i}$$

Further

$$\mu^2 = \frac{8Gt}{AE(b+a)} = \frac{8 \times 0.36 \times 1.0}{800(200+500)} = 5.14 \times 10^{-6}$$

so that Eq. (i) becomes

$$w = -3.75 \times 10^{-4}(3.04 \sinh \mu z - z) \tag{ii}$$

Substituting for w, etc. in Eq. (26.11)

$$\frac{\mathrm{d}\theta}{\mathrm{d}z} = 10^{-8}(1.95 \sinh \mu z - 3.49z)$$

Hence

$$\theta = 10^{-8}\left(\frac{1.95}{\mu}\cosh \mu z - 1.75z^2 + F\right) \tag{iii}$$

When $z = L$ (2500 mm) $\quad \theta = 0$. Then, from Eq. (iii)

$$F = 10.8 \times 10^6$$

so that

$$\theta = 10^{-8}(859\cosh \mu z - 1.75z^2 + 10.8 \times 10^6) \qquad \text{(iv)}$$

At mid-span where $z = 0$, from Eq. (iv)

$$\theta = 0.108\,\text{rad} \quad \text{or} \quad \theta = 6.2^\circ$$

26.4 Shear lag

A problem closely related to the restrained torsion of rectangular section beams is that generally known as *shear lag*. We have seen in Chapter 18 that torsion induces shear stresses in the walls of beams and these cause shear strains which produce warping of the cross-section. When this warping is restrained, direct stresses are set up which modify the shear stresses. In a similar manner the shear strains in the thin walls of beams subjected to shear loads cause cross-sections to distort or warp so that the basic assumption of elementary bending theory of plane sections remaining plane is no longer valid. The direct and shear stress distributions predicted by elementary theory therefore become significantly inaccurate. Further modifications arise when any form of structural constraint prevents the free displacement of the cross-sections of a beam. Generally, shear lag becomes a problem in wide, relatively shallow, thin-walled beams such as wings in which the shear distortion of the thin upper and lower surface skins causes redistribution of stress in the stringers and spar caps while the thicker and shallower spar webs experience little effect.

Consider the box beam shown in Fig. 26.10. Elementary bending theory predicts that the direct stress at any section AA would be uniform across the width of the covers so that the stringers and web flanges would all be subjected to the same stress. However, the shear strains at the section cause the distortion shown so that the intermediate stringers carry lower stresses than the web flanges. Since the resultant of the direct stresses must

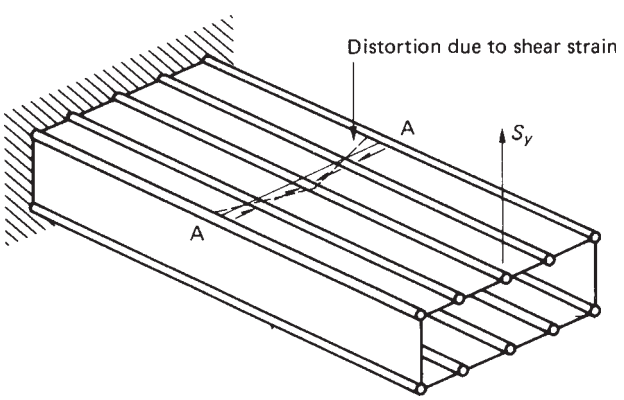

Fig. 26.10 Shear distortion in the covers of a box beam.

be equivalent to the applied bending moment this means that the direct stresses in the web flanges must be greater than those predicted by elementary bending theory. Our investigation of the shear lag problem will be restricted to idealized six- and eight-boom doubly symmetrical rectangular section beams subjected to shear loads acting in the plane of symmetry and in which the axis of twist, the flexural axis and the zero warping axis coincide; the shear loads therefore produce no twist and hence no warping due to twist. In the analysis we shall assume that the cross-sections of beams remain undistorted in their own plane.

Figure 26.11 shows an idealized six-boom beam built-in at one end and carrying a shear load at the other; the corner booms have a cross-sectional area B while the central booms have a cross-sectional area A. At any section the vertical shear load is shared equally by the two webs. Also, since the beam has been idealized, the shear flow at any section will be constant between the booms so that, for a web, the situation is that shown in the free body diagram of Fig. 26.12, in addition, the corner booms are subjected to equal and opposite loads P_B. The complementary shear flows $S_y/2h$ are applied to the corner booms as shown so that the top cover, say, is subjected to loads as shown in Fig. 26.13. We assume that suitable edge members are present at the free end of the cover to equilibrate the shear flows; we also assume that strains in the transverse direction are negligible.

It is advantageous to adopt a methodical approach in the analysis. Thus, use may be made of the symmetry of the cover so that only one edge boom, one panel and the central boom need to be considered as long as the symmetry is allowed for in the assumed directions of the panel shear flows q, as shown in Fig. 26.13. Further, the origin for z may be taken to be at either the free or built-in end. A marginally simpler solution is obtained if the origin is taken to be at the free end, in which case the solution represents that for an infinitely long panel. Considering the equilibrium of an element of an edge boom (Fig. 26.14), in which we assume that the boom load is positive (tension)

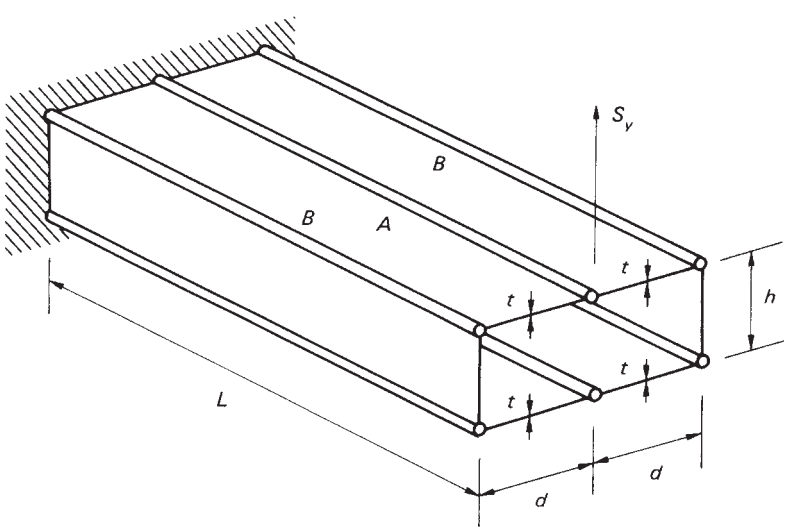

Fig. 26.11 Six-boom beam subjected to a shear load.

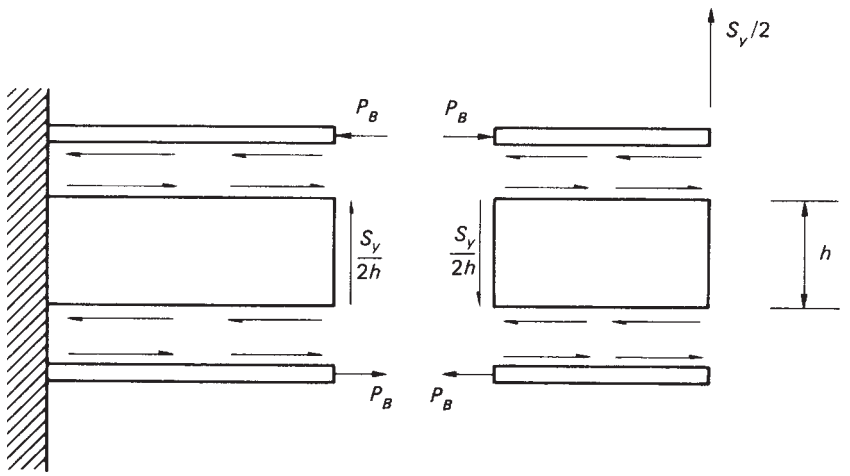

Fig. 26.12 Loads on webs and corner booms of the beam of Fig. 26.11.

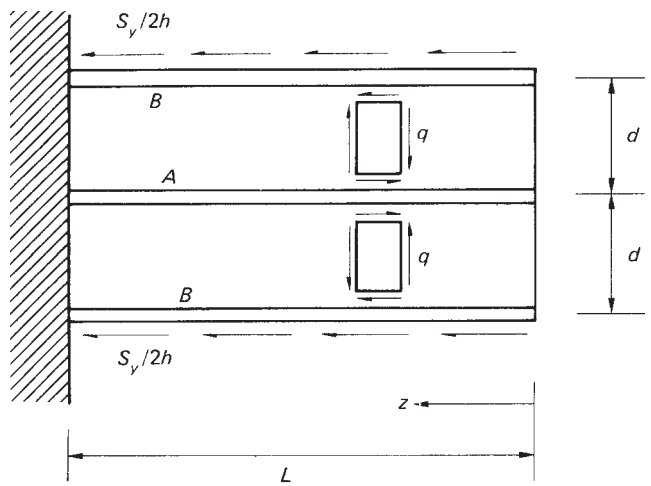

Fig. 26.13 Top cover of the beam of Fig. 26.11.

and increases with increasing z, we have

$$P_B + \frac{\partial P_B}{\partial z}\delta z - P_B - q\delta z + \frac{S_y}{2h}\delta z = 0$$

or

$$\frac{\partial P_B}{\partial z} - q + \frac{S_y}{2h} = 0 \tag{26.24}$$

Similarly, for an element of the central boom (Fig. 26.15)

$$\frac{\partial P_A}{\partial z} + 2q = 0 \tag{26.25}$$

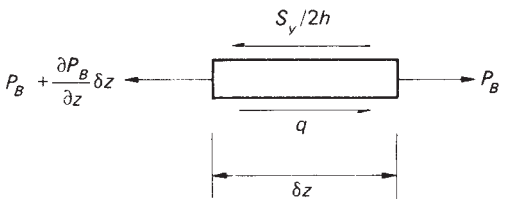

Fig. 26.14 Equilibrium of boom element.

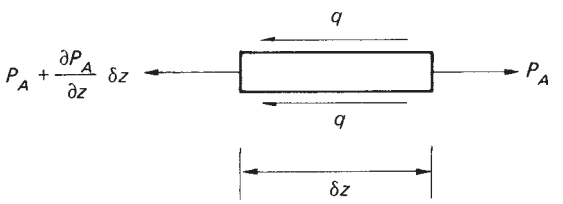

Fig. 26.15 Equilibrium of element of central boom.

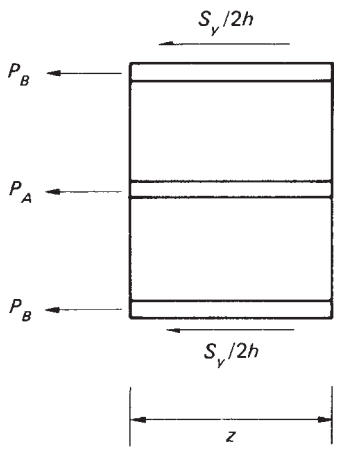

Fig. 26.16 Equilibrium of a length z of cover.

Now considering the overall equilibrium of a length z of the cover (Fig. 26.16), we have

$$2P_B + P_A + \frac{S_y}{h}z = 0 \tag{26.26}$$

We now consider the compatibility condition which exists in the displacements of elements of the booms and adjacent elements of the panels. Figure 26.17(a) shows the displacements of the cover and an element of a panel and the adjacent elements of the boom. Note that the element of the panel is distorted in a manner which agrees with the assumed directions of the shear flows in Fig. 26.13 and that the shear strain increases with z. From Fig. 26.17(b)

$$(1 + \varepsilon_B)\delta z = (1 + \varepsilon_A)\delta z + d\frac{\partial \gamma}{\partial z}\partial z$$

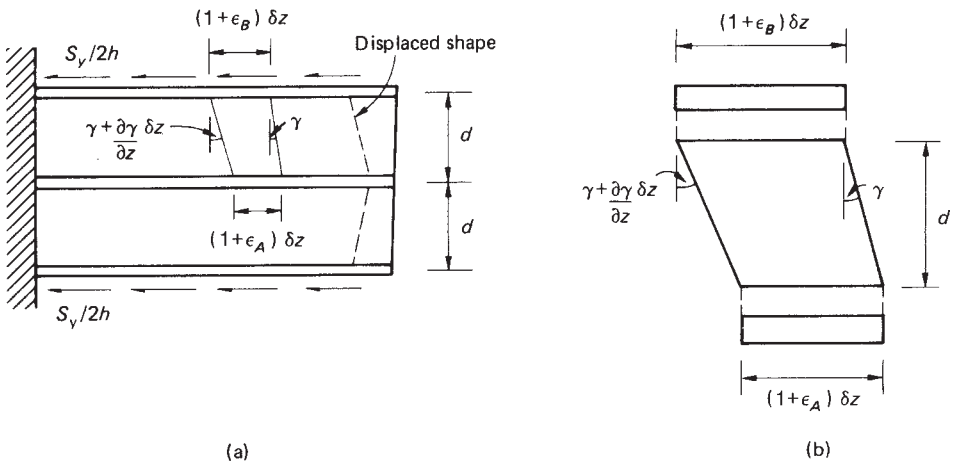

Fig. 26.17 Compatibility condition.

in which ε_B and ε_A are the direct strains in the elements of boom. Then, rearranging and noting that γ is a function of z only when the section is completely idealized, we have

$$\frac{\mathrm{d}\gamma}{\mathrm{d}z} = \frac{1}{d}(\varepsilon_B - \varepsilon_A) \tag{26.27}$$

Now

$$\varepsilon_B = \frac{P_B}{BE} \quad \varepsilon_A = \frac{P_A}{AE} \quad \gamma = \frac{q}{Gt}$$

so that Eq. (26.27) becomes

$$\frac{\mathrm{d}q}{\mathrm{d}z} = \frac{Gt}{dE}\left(\frac{P_B}{B} - \frac{P_A}{A}\right) \tag{26.28}$$

We now select the unknown to be determined initially. Generally, it is simpler mathematically to determine either of the boom load distributions, P_B or P_A, rather than the shear flow q. Thus, choosing P_A, say, as the unknown, we substitute in Eq. (26.28) for q from Eq. (11.25) and for P_B from Eq. (26.26). Hence

$$-\frac{1}{2}\frac{\partial^2 P_A}{\partial z^2} = \frac{Gt}{dE}\left(-\frac{P_A}{2B} - \frac{S_y z}{2Bh} - \frac{P_A}{A}\right)$$

Rearranging, we obtain

$$\frac{\partial^2 P_A}{\partial z^2} - \frac{Gt(2B+A)}{dEAB}P_A = \frac{GtS_y z}{dEBh}$$

or

$$\frac{\partial^2 P_A}{\partial z^2} - \lambda^2 P_A = \frac{GtS_y z}{dEBh} \tag{26.29}$$

in which $\lambda^2 = Gt(2B+A)/dEAB$. The solution of Eq. (26.29) is of standard form and is

$$P_A = C\cosh\lambda z + D\sinh\lambda z - \frac{S_y A}{h(2B+A)}z$$

The constants C and D are determined from the boundary conditions of the cover of the beam namely, $P_A = 0$ when $z = 0$ and $\gamma = q/Gt = -(\partial P_A/\partial z)/2Gt = 0$ when $z = L$ (see Eq. (26.25)). From the first of these $C = 0$ and from the second

$$D = \frac{S_y A}{\lambda h(2B+A)\cosh\lambda L}$$

Thus

$$P_A = -\frac{S_y A}{h(2B+A)}\left(z - \frac{\sinh\lambda z}{\lambda\cosh\lambda L}\right) \tag{26.30}$$

The direct stress distribution $\sigma_A (= P_A/A)$ follows, i.e.

$$\sigma_A = -\frac{S_y}{h(2B+A)}\left(z - \frac{\sinh\lambda z}{\lambda\cosh\lambda L}\right) \tag{26.31}$$

The distribution of load in the edge booms is obtained by substituting for P_A from Eq. (26.30) in Eq. (26.26), thus

$$P_B = -\frac{S_y B}{h(2B+A)}\left(z + \frac{A}{2B\lambda}\frac{\sinh\lambda z}{\cosh\lambda L}\right) \tag{26.32}$$

whence

$$\sigma_B = -\frac{S_y}{h(2B+A)}\left(z + \frac{A}{2B\lambda}\frac{\sinh\lambda z}{\cosh\lambda L}\right) \tag{26.33}$$

Finally, from either pairs of Eqs (26.25) and (26.30) or (26.24) and (26.32)

$$q = \frac{S_y A}{2h(2B+A)}\left(1 - \frac{\cosh\lambda z}{\cosh\lambda L}\right) \tag{26.34}$$

so that the shear stress distribution $\tau (= q/t)$ is

$$\tau = \frac{S_y A}{2ht(2B+A)}\left(1 - \frac{\cosh\lambda z}{\cosh\lambda L}\right) \tag{26.35}$$

Elementary theory gives

$$\sigma_A = \sigma_B = -\frac{S_y z}{h(2B+A)}$$

and

$$q = \frac{S_y A}{2h(2B+A)}$$

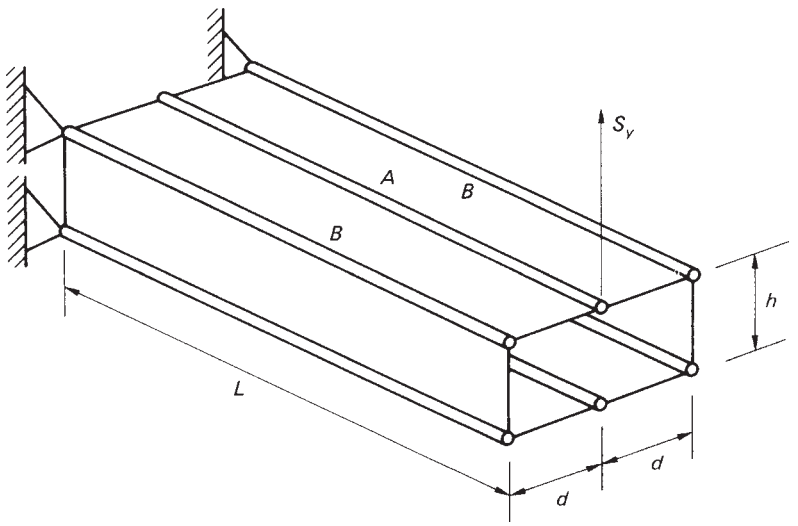

Fig. 26.18 Rectangular section beam supported at corner booms only.

so that, as in the case of the torsion of a four boom rectangular section beam, the solution comprises terms corresponding to elementary theory together with terms representing the effects of shear lag and structural constraint.

Many wing structures are spliced only at the spars so that the intermediate stringers are not subjected to bending stresses at the splice. The situation for a six boom rectangular section beam is then as shown in Fig. 26.18. The analysis is carried out in an identical manner to that in the previous case except that the boundary conditions for the central stringer are $P_A = 0$ when $z = 0$ and $z = L$. The solution is

$$P_A = -\frac{S_y A}{h(2B + A)}\left(z - L\frac{\sinh \lambda z}{\sinh \lambda L}\right) \tag{26.36}$$

$$P_B = -\frac{S_y B}{h(2B + A)}\left(z + \frac{AL}{2B}\frac{\sinh \lambda z}{\sinh \lambda L}\right) \tag{26.37}$$

$$q = \frac{S_y A}{2h(2B + A)}\left(1 - \lambda L\frac{\cosh \lambda z}{\sinh \lambda L}\right) \tag{26.38}$$

where $\lambda^2 = Gt(2B + A)/dEAB$. Examination of Eq. (26.38) shows that q changes sign when $\cosh \lambda z = (\sinh \lambda L)/\lambda L$, the solution of which gives a value of z less than L, i.e. q changes sign at some point along the length of the beam. The displaced shape of the top cover is therefore as shown in Fig. 26.19. Clearly, the final length of the central stringer is greater than in the previous case and appreciably greater than the final length of the spar flanges. The shear lag effect is therefore greater than before. In some instances this may be beneficial since a larger portion of the applied bending moment is resisted by the heavier section spar flanges. These are also restrained against buckling in two directions by the webs and covers while the lighter section stringers are restrained in one direction only. The beam is therefore able to withstand higher bending moments than those calculated from elementary theory.

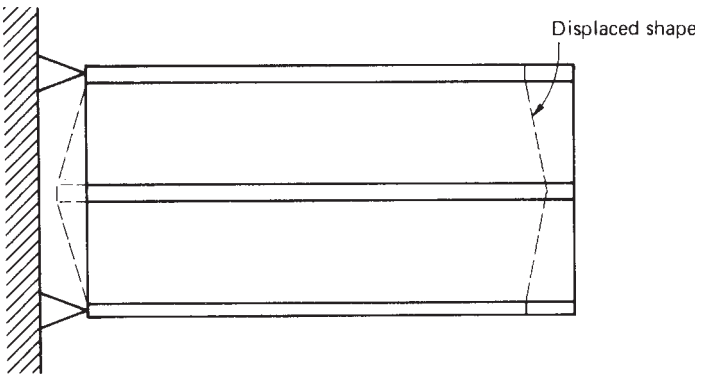

Fig. 26.19 Displaced shape of top cover of box team of Fig. 26.18.

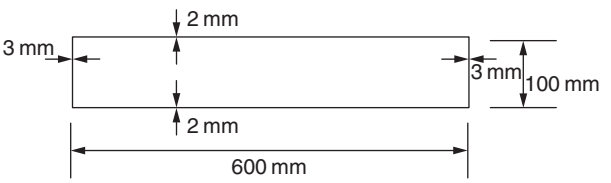

Fig. 26.20 Beam section of Example 26.4.

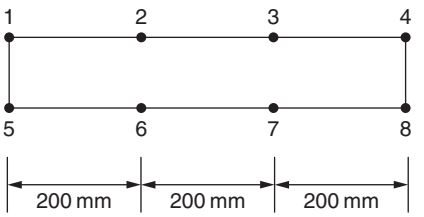

Fig. 26.21 Idealized beam section of Example 26.4.

Example 26.4

A shallow box section beam whose cross-section is shown in Fig. 26.20 is simply supported over a span of 2 m and carries a vertically downward load of 20 kN at mid-span. Idealise the section into one suitable for shear lag analysis, comprising eight booms, and hence determine the distribution of direct stress along the top right-hand corner of the beam. Take $G/E = 0.36$.

The idealized section is shown in Fig. 26.21.
Using either Eqs (20.1) or (20.2)

$$B_1 = B_4 = B_8 = B_5 = \frac{100 \times 3}{6}(2-1) + \frac{200 \times 2}{6}(2+1) = 250\,\text{mm}^2$$

$$B_2 = B_3 = B_6 = B_7 = \frac{200 \times 2}{6}(2+1) \times 2 = 400\,\text{mm}^2$$

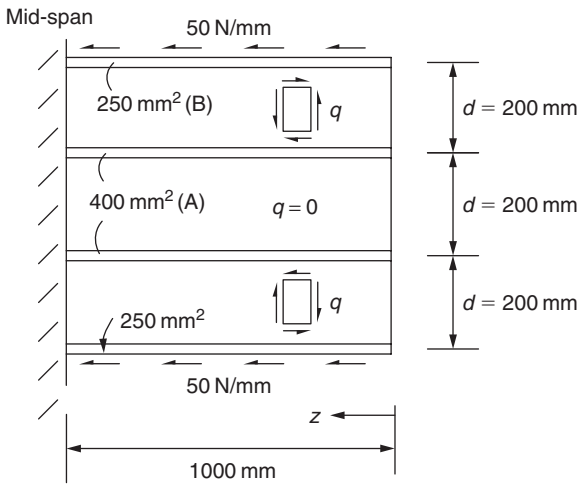

Fig. 26.22 Shear flows acting on top cover of idealized beam section of Example 26.4.

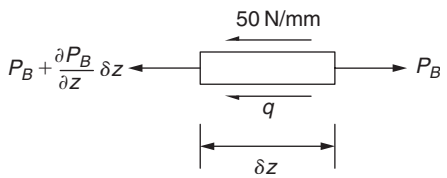

Fig. 26.23 Element of boom B.

The support reactions of 10 kN produce loads of 5 kN on each vertical web. These, in turn, produce shear flows of 50 N/mm along each corner boom as shown in Fig. 26.22 for the top cover of the beam.

Considering the equilibrium of elements of the booms we have, for the top boom, Fig. 26.23

$$P_B + \frac{\partial P_B}{\partial z}\delta z - P_B + q\delta z + 50\delta z = 0$$

which gives

$$\frac{\partial P_B}{\partial z} = -q - 50 \tag{i}$$

Similarly for an element of boom A

$$\frac{\partial P_A}{\partial z} = q \tag{ii}$$

Overall equilibrium of a length z of the panel gives

$$2P_B + 2P_A + 2 \times 50z = 0$$

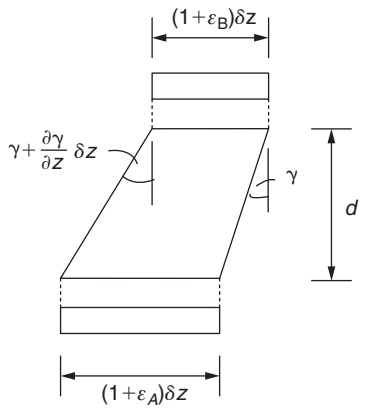

Fig. 26.24 Compatibility condition for top cover of beam of Example 26.4.

i.e

$$P_B + P_A + 50z = 0 \tag{iii}$$

The compatibility of displacement between elements of boom and adjacent panel, Fig. 26.24 gives

$$\frac{\partial \gamma}{\partial z} = \frac{1}{d}(\varepsilon_A - \varepsilon_B) \tag{iv}$$

But

$$\varepsilon_A = P_A/E_A \quad \varepsilon_B = P_B/E_B \quad \gamma = q/Gt$$

Substituting in Eq. (iv) we obtain

$$\frac{\partial q}{\partial z} = \frac{Gt}{dE}\left(\frac{P_A}{A} - \frac{P_B}{B}\right) \tag{v}$$

From Eq. (iii)

$$P_A = -P_B - 50z$$

From Eq. (i)

$$\frac{\partial q}{\partial z} = -\frac{\partial^2 P_B}{\partial z^2}$$

Substituting in Eq. (v)

$$\frac{\partial^2 P_B}{\partial z^2} - \mu^2 P_B = \frac{50Gt}{dEA} z \tag{vi}$$

in which

$$\mu^2 = \frac{Gt}{dE}\left(\frac{A+B}{AB}\right)$$

The solution of Eq. (vi) is

$$P_B = C\cosh\mu z + D\sinh\mu z - \frac{50B}{A+B}z$$

The boundary conditions are;

$$\text{when } z = 0,\ P_B = 0$$

$$\text{and when } z = 100\,\text{mm} \quad \frac{\partial P_B}{\partial z} = -50 \text{ (from Eq (i) since } q = 0 \text{ at } z = 1000\,\text{mm)}$$

From the first of these $C = 0$ while from the second

$$D = \frac{-50A}{(A+B)\mu\cosh 1000\mu}$$

Therefore

$$\sigma_B = \frac{P_B}{B} = \frac{-50A}{B(A+B)\mu\cosh 1000\mu} = \sinh\mu z - \frac{50}{A+B}z$$

Substituting the boom areas, etc. gives

$$\sigma_B = -0.4\sinh\mu z - 0.08z$$

In certain situations beams, or parts of beams, carry loads which cause in-plane bending of the covers. An example is shown in Fig. 26.25 where the loads P cause bending in addition to axial effects. Shear lag modifies the stresses predicted by elementary theory in a similar manner to the previous cases. From symmetry we can consider either the

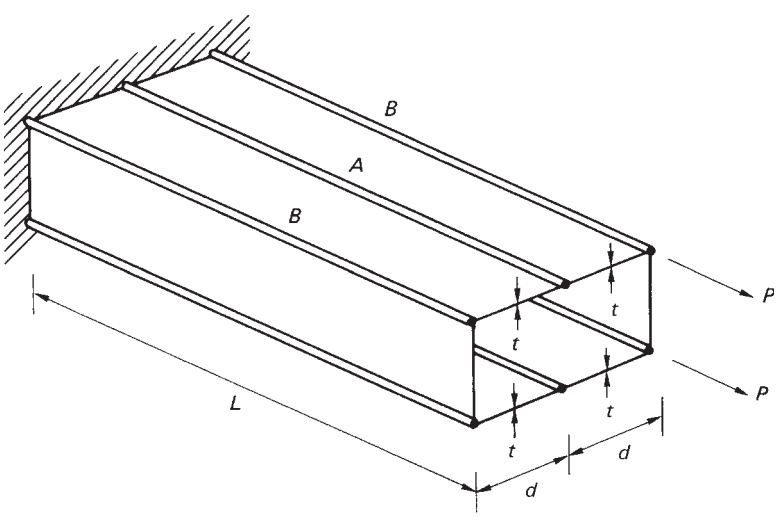

Fig. 26.25 Beam subjected to combined bending and axial load.

top or bottom cover in isolation as shown in Fig. 26.26(a). In this case the load P causes bending as well as extension of the cover so that at any section z the beam has a slope $\partial v/\partial z$ (Fig. 26.26(b)). We shall again assume that transverse strains are negligible and that the booms carry all the direct load.

Initially, as before, we choose directions for the shear flows in the top and bottom panels. Any directions may be chosen since the question of symmetry does not arise. The equilibrium of an element δz of each boom is first considered giving

$$\frac{\partial P_{B1}}{\partial z} = -q_1 \quad \frac{\partial P_A}{\partial z} = q_1 - q_2 \quad \frac{\partial P_{B2}}{\partial z} = q_2 \tag{26.39}$$

where P_{B1} is the load in boom 1 and P_{B2} is the load in boom 2. Longitudinal and moment equilibrium about boom 2 of a length z of the cover give, respectively

$$P_{B1} + P_{B2} + P_A = P \quad P_{B1}2d + P_A d = P2d \tag{26.40}$$

The compatibility condition now includes the effect of bending in addition to extension, as shown in Fig. 26.27. Note that the panel is distorted in a manner which agrees with the assumed direction of shear flow and that γ_1 and $\partial v/\partial z$ increase with z. Thus

$$(1 + \varepsilon_A)\delta z = (1 + \varepsilon_{B1})\delta z + d\left(\frac{\mathrm{d}\gamma_1}{\mathrm{d}z} + \frac{\mathrm{d}^2 v}{\mathrm{d}z^2}\right)\delta z$$

where γ_1 and v are functions of z only. Thus

$$\frac{\mathrm{d}\gamma_1}{\mathrm{d}z} = \frac{1}{d}(\varepsilon_A - \varepsilon_{B1}) - \frac{\mathrm{d}^2 v}{\mathrm{d}z^2} \tag{26.41}$$

Similarly, for an element of the lower panel

$$\frac{\mathrm{d}\gamma_2}{\mathrm{d}z} = \frac{1}{d}(\varepsilon_{B2} - \varepsilon_A) - \frac{\mathrm{d}^2 v}{\mathrm{d}z^2} \tag{26.42}$$

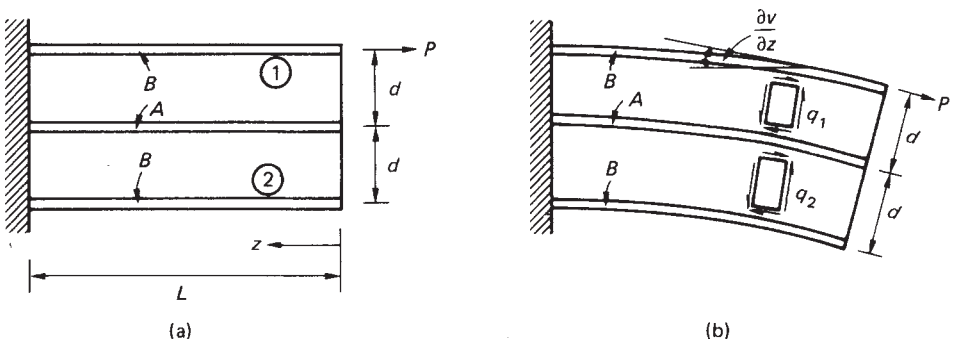

Fig. 26.26 Cover of beam of Fig. 11.19.

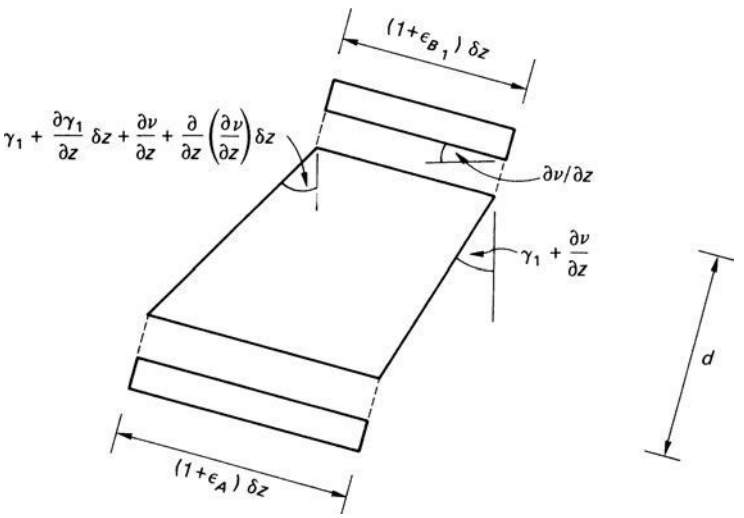

Fig. 26.27 Compatibility condition for combined bending and axial load.

Subtraction of Eq. (26.42) from Eq. (26.41) eliminates $\mathrm{d}^2v/\mathrm{d}z^2$, i.e.

$$\frac{\mathrm{d}\gamma_1}{\mathrm{d}z} - \frac{\mathrm{d}\gamma_2}{\mathrm{d}z} = \frac{1}{d}(2\varepsilon_A - \varepsilon_{B1} - \varepsilon_{B2})$$

or, as before

$$\frac{\mathrm{d}q_1}{\mathrm{d}z} - \frac{\mathrm{d}q_2}{\mathrm{d}z} = \frac{Gt}{dE}\left(\frac{2P_A}{A} - \frac{P_{B1}}{B} - \frac{P_{B2}}{B}\right) \tag{26.43}$$

In this particular problem the simplest method of solution is to choose P_A as the unknown since, from Eqs (26.39)

$$\frac{\mathrm{d}q_1}{\mathrm{d}z} - \frac{\mathrm{d}q_2}{\mathrm{d}z} = \frac{\partial^2 P_A}{\partial z^2}$$

Also substituting for P_{B1} and P_{B2} from Eq. (26.40), we obtain

$$\frac{\partial^2 P_A}{\partial z^2} - \frac{Gt}{dE}\left(\frac{2B+A}{AB}\right)P_A = -\frac{PGt}{dEB}$$

or

$$\frac{\partial^2 P_A}{\partial z^2} - \lambda^2 P_A = -\frac{PGt}{dEB} \tag{26.44}$$

where $\lambda^2 = Gt(2B+A)/dEAB$. The solution of Eq. (26.44) is of standard form and is

$$P_A = C\cosh\lambda z + D\sinh\lambda z + \frac{PA}{2B+A} \tag{26.45}$$

The boundary conditions are $P_A = 0$ when $z = 0$ and $q_1 = q_2 = 0 = \partial P_A/\partial z$ at the built-in end (no shear loads are applied). Hence

$$P_A = \frac{PA}{2B + A}(1 - \cosh \lambda z + \tanh \lambda L \sinh \lambda z)$$

or, rearranging

$$P_A = \frac{PA}{2B + A}\left[1 - \frac{\cosh \lambda(L - z)}{\cosh \lambda L}\right] \tag{26.46}$$

Hence

$$\sigma_A = \frac{P}{2B + A}\left[1 - \frac{\cosh \lambda(L - z)}{\cosh \lambda L}\right] \tag{26.47}$$

Substituting for P_A in the second of Eqs (26.40), we have

$$P_{B1} = \frac{PA}{2(2B + A)}\left[\frac{4B + A}{A} + \frac{\cosh \lambda(L - z)}{\cosh \lambda L}\right] \tag{26.48}$$

whence

$$\sigma_{B1} = \frac{PA}{2B(2B + A)}\left[\frac{4B + A}{A} + \frac{\cosh \lambda(L - z)}{\cosh \lambda L}\right] \tag{26.49}$$

Also from Eqs (26.40)

$$P_{B2} = -\frac{P_A}{2}$$

so that

$$P_{B2} = \frac{-PA}{2(2B + A)}\left[1 - \frac{\cosh \lambda(L - z)}{\cosh \lambda L}\right] \tag{26.50}$$

and

$$\sigma_{B2} = \frac{-PA}{2B(2B + A)}\left[1 - \frac{\cosh \lambda(L - z)}{\cosh \lambda L}\right] \tag{26.51}$$

Finally, the shear flow distributions are obtained from Eqs (16.39), thus

$$q_1 = \frac{-\partial P_{B1}}{\partial z} = \frac{PA\lambda}{2(2B + A)}\frac{\sinh \lambda(L - z)}{\cosh \lambda L} \tag{26.52}$$

$$q_2 = \frac{\partial P_{B2}}{\partial z} = \frac{-PA\lambda}{2(2B + A)}\frac{\sinh \lambda(L - z)}{\cosh \lambda L} \tag{26.53}$$

Again we see that each expression for direct stress, Eqs (26.47), (26.49) and (26.51), comprises a term which gives the solution from elementary theory together with a correction for the shear lag effect. The shear flows q_1 and q_2 are self-equilibrating, as can be seen from Eqs (26.52) and (26.53), and are entirely produced by the shear lag effect (q_1 and q_2 must be self-equilibrating since no shear loads are applied).

Example 26.5

The unsymmetrical panel shown in Fig. 26.28 comprises three direct stress carrying booms and two shear stress carrying panels. If the panel supports a load P at its free end and is pinned to supports at the ends of its outer booms determine the distribution of direct load in the central boom. Determine also the load in the central boom when $A = B = C$ and shear lag effects are absent.

As before we consider the equilibrium of elements of the booms, say A and B. This gives

$$\frac{\partial P_A}{\partial z} = -q_1 \tag{i}$$

and

$$\frac{\partial P_B}{\partial z} = q_1 - q_2 \tag{ii}$$

For overall equilibrium of a length z of the panel

$$P_A + P_B + P_C = P \tag{iii}$$

and taking moments about boom C

$$2P_A + P_B = P \tag{iv}$$

The compatibility condition is shown in Fig. 26.29 and gives

$$\frac{\partial \gamma_1}{\partial z} = \frac{1}{d}(\varepsilon_A - \varepsilon_A) - \frac{\partial^2 v}{\partial z^2} \tag{v}$$

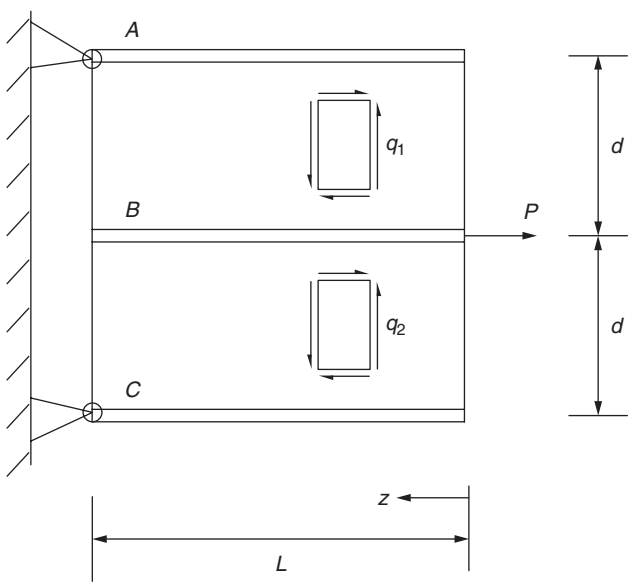

Fig. 26.28 Panel of Example 26.5.

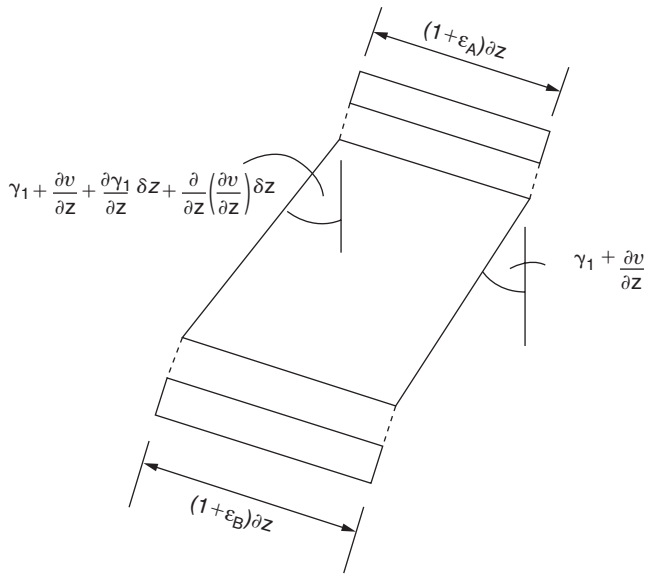

Fig. 26.29 Compatibility condition for the panel of Example 26.5.

Similarly, for elements of the booms B and C

$$\frac{\partial \gamma_2}{\partial z}=\frac{1}{d}(\varepsilon_C-\varepsilon_B)-\frac{\partial^2 v}{\partial z^2} \tag{vi}$$

Subtracting Eq. (vi) from (v) gives

$$\frac{\partial \gamma_1}{\partial z}-\frac{\partial \gamma_2}{\partial z}=\frac{1}{d}(2\varepsilon_B-\varepsilon_A-\varepsilon_C) \tag{vii}$$

Also

$$\gamma_1=\frac{q_1}{Gt}\quad \gamma_2=\frac{q_2}{Gt}\quad \varepsilon_A=\frac{P_A}{AE}\quad \varepsilon_B=\frac{P_B}{BE}\quad \text{and}\quad \varepsilon_C=\frac{P_C}{CE}$$

Substituting these expressions in Eq. (vii) gives

$$\frac{\partial q_1}{\partial z}-\frac{\partial q_2}{\partial z}=\frac{Gt}{dE}\left(\frac{2P_B}{B}-\frac{P_A}{A}-\frac{P_C}{C}\right) \tag{viii}$$

From Eqs (iv) and (iii)

$$P_A=\frac{1}{2}(P-P_B),\quad P_C=\frac{1}{2}(P-P_B)$$

Substituting in Eq. (viii), using Eq. (ii) and rearranging we have

$$\frac{\partial^2 P_B}{\partial z^2}-\frac{Gt}{dE}\left(\frac{4AC+BC+AB}{2ABC}\right)P_B=-\frac{GtP}{2dE}\left(\frac{A+C}{AC}\right)$$

the solution of which is

$$P_B = D\cosh \mu z + F \sinh \mu z + \frac{B(A + C)P}{(4AC + BC + AB)}$$

where

$$\mu^2 = \frac{Gt}{dE}\left(\frac{4AC + BC + AB}{2ABC}\right)$$

The boundary conditions are: when $z = 0$, $P_B = P$ and when $z = L$, $P_B = 0$. From the first of these

$$D = \frac{4AC}{4AC + BC + AB}P$$

while from the second

$$F = -\frac{P}{\sinh \mu L}\left[\frac{4AC}{4AC + BC + AB}\cosh \mu L + \frac{B(A + C)}{4AC + BC + AB}\right]$$

The expression for the load in the central boom is then

$$P_B = \frac{P}{4AC + BC + AB}\left[4AC\cosh \mu z - \left(\frac{4AC\cosh \mu L + AB + BC}{\sinh \mu L}\right) \times \sinh \mu z + B(A + C)\right]$$

If there is no shear lag the hyperbolic terms disappear and when $A = B = C$

$$P_B = P/3$$

Reference

1 Argyris, J. H. and Dunne, P. C., The general theory of cylindrical and conical tubes under torsion and bending loads, *J. Roy. Aero. Soc.*, Parts I–IV, February 1947; Part V, September and November 1947; Part VI, May and June 1949.

Problems

P.26.1 A thin-walled beam with the singly symmetrical cross-section shown in Fig. P.26.1, is built-in at one end where the shear force $S_y = 111\,250\,\text{N}$ is applied through the web 25. Assuming the cross-section remains undistorted by the loading, determine the shear flow and the position of the centre of twist at the built-in end. The shear modulus G is the same for all walls.

Ans: $q_{12} = q_{56} = 46.6\,\text{N/mm}$, $q_{52} = 180.8\,\text{N/mm}$,
$q_{32} = q_{54} = 1.4\,\text{N/mm}$, $q_{43} = 74.6\,\text{N/mm}$,
$x_R = -630.1\,\text{mm}$, $y_R = 0$ (relative to mid-point of 52).

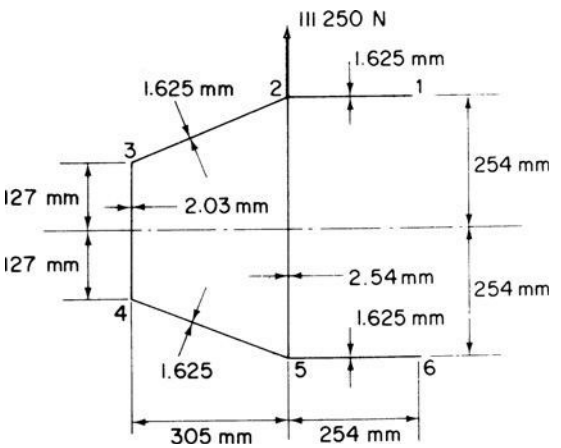

Fig. P.26.1

P.26.2 A thin-walled two-cell beam with the singly symmetrical cross-section shown in Fig. P.26.2 is built-in at one end where the torque is 11 000 Nm. Assuming the cross-section remains undistorted by the loading, determine the distribution of shear flow and the position of the centre of twist at the built-in end. The shear modulus G is the same for all walls.

Ans: $q_{12} = q_{45} = 44.1\,\text{N/mm}$, $q_{23} = q_{34} = 42.9\,\text{N/mm}$,
$q_{51} = 80.2\,\text{N/mm}$, $q_{24} = 37.4\,\text{N/mm}$,
$x_R = -79.5\,\text{mm}$, $y_R = 0$ (referred to mid-point of web 24).

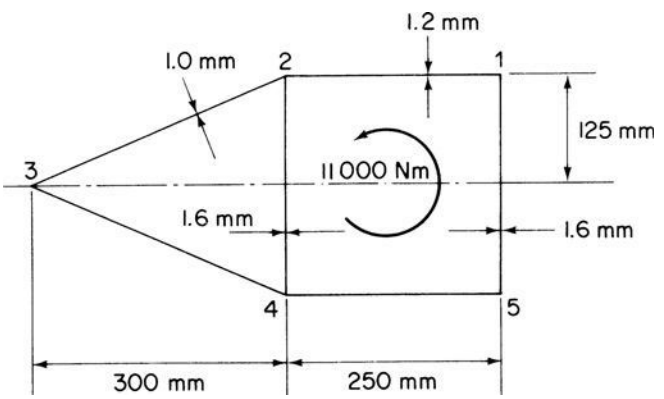

Fig. P.26.2

P.26.3 A singly symmetrical, thin-walled, closed section beam is built-in at one end where a shear load of 10 000 N is applied as shown in Fig. P.26.3. Calculate the resulting shear flow distribution at the built-in end if the cross-section of the beam

remains undistorted by the loading and the shear modulus G and wall thickness t are each constant throughout the section.

Ans: $q_{12} = 3992.9/R$ N/mm, $q_{23} = 711.3/R$ N/mm,
$q_{31} = (1502.4 - 1894.7\cos\phi - 2102.1\sin\phi)/R$ N/mm.

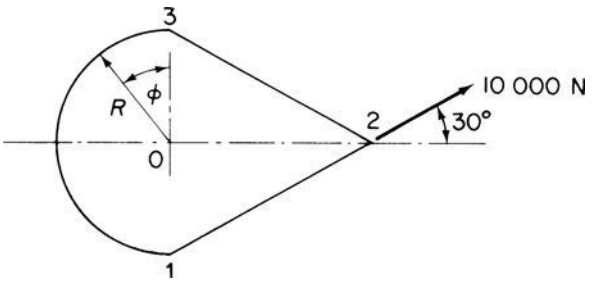

Fig. P.26.3

P.26.4 A uniform, four-boom beam, built-in at one end, has the rectangular cross-section shown in Fig. P.26.4. The walls are assumed to be effective only in shear, the thickness and shear modulus being the same for all walls while the booms, which are of equal area, carry only direct stresses. Assuming that the cross-section remains undistorted by the loading, calculate the twist at the free end due to a uniformly distributed torque loading $T = 20$ N m/mm along its entire length. Take $G = 20\,000$ N/mm^2 and $G/E = 0.36$.

Ans: 5.9° anticlockwise.

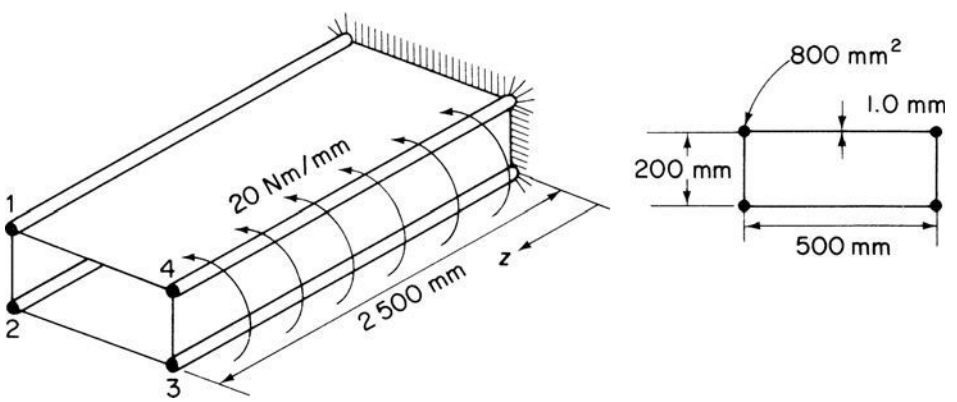

Fig. P.26.4

P.26.5 Figure P.26.5 shows the doubly symmetrical idealized cross-section of a uniform box beam of length l. Each of the four corner booms has area B and Young's modulus E, and they constitute the entire direct stress carrying area. The thin walls all have the same shear modulus G. The beam transmits a torque T from one end to the other, and at each end warping is completely suppressed. Between the ends, the shape of the cross-section is maintained without further restriction of warping.

Obtain an expression for the distribution of the end load along the length of one of the corner booms. Assuming $bt_1 > at_2$, indicate graphically the relation between torque direction and tension and compression in the boom end loads.

Ans. $$P = \frac{\mu BET}{8abGt_1t_2}(bt_1 - at_2)\left[-\sinh \mu z + \frac{(\cosh \mu l - 1)}{\sinh \mu l}\cosh \mu z\right]$$

where

$$\mu^2 = 8Gt_1t_2/BE(at_2 + bt_1).$$

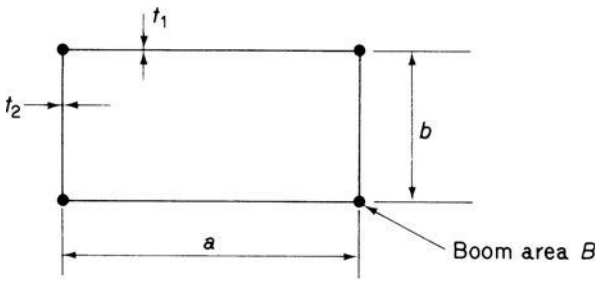

Fig. P.26.5

P.26.6 The idealized cross-section of a beam is shown in Fig. P.26.6. The beam is of length L and is attached to a flexible support at one end which only partially prevents warping of the cross-section; at its free end the beam carries a concentrated torque T.

Assuming that the warping at the built-in end is directly proportional to the free warping, ie $w = kw_o$, derive an expression for the distribution of direct stress along the top right-hand corner boom. State the conditions corresponding to the values $k = 0$ and $k = 1$.

Ans. $$\sigma = -\mu E w_0(k-1)\frac{\sinh \mu(L-z)}{\cosh \mu L}, \quad \mu^2 = \frac{8Gt_bt_a}{BE(bt_a + at_b)}$$

when $k = 0$, $\sigma = \mu E w_0 \dfrac{\sinh \mu(L-z)}{\cosh \mu L}$ (i.e a rigid foundation)

when $k = 1$, $\sigma = 0$ (i.e free warping)

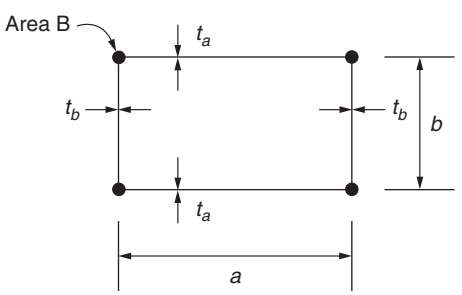

Fig. P.26.6

P.26.7 In the panel shown in Fig. P.26.7 the area, A_s, of the central stringer is to be designed so that the stress in it is 80% of the constant stress, σ_e, in the edge members, each of area B.

Assuming that the sheet, which is of constant thickness, t, carries only shear stress and that transverse strains are prevented, derive expressions for A_s and B in terms of the applied loads and the appropriate elastic moduli, E for the longitudinal members and G for the sheet.

Evaluate these expressions in the case where $P = 450\,000$ N; $P_s = 145\,000$ N; $S = 350$ N/mm; $\sigma_e = 275$ N/mm^2; $l = 1250$ mm; $b = 250$ mm; $t = 2.5$ mm and $G = 0.38E$. Find the fraction of the total tension at the abutment which is carried by the stringer.

Ans. $A_s = \dfrac{Gt}{2Eb}\left(lz - \frac{z^2}{2}\right) + \dfrac{1.25P_s}{\sigma_e}$,

$$B = \frac{0.1Gt}{Eb}z^2 + \frac{1}{\sigma_c}\left[\left(S - \frac{0.2Gt\sigma_e l}{bE}\right)z + P\right],\quad 0.25.$$

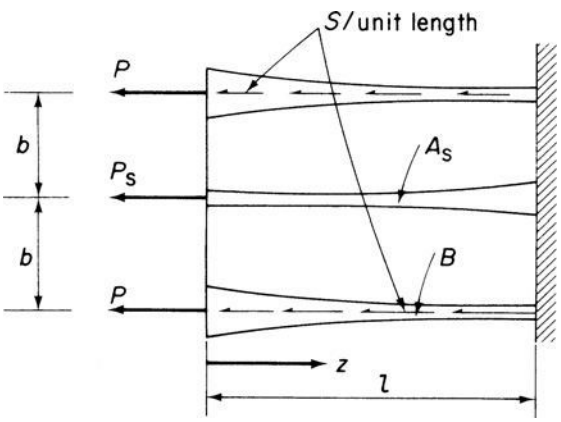

Fig. P.26.7

P.26.8 A symmetrical panel has the form shown in Fig. P.26.8. The longerons are of constant area, B_1 for the edge members and B_2 for the central member, and the sheet is of uniform thickness t. The panel is assembled without stress.

Obtain an expression for the distribution of end load in the central longeron if it is then raised to a temperature T (constant along its length) above the edge members. Also give the longitudinal displacement, at one end of the panel, of the central longeron relative to the edge members.

Assume that end loads are carried only by the longerons, that the sheet carries only shear, and that transverse members are provided to prevent transverse straining and to ensure shear effectiveness of the sheet at the ends of the panel.

Ans. $$P_2 = E\alpha T\left(\cosh \mu z - \tanh\frac{\mu l}{2}\sinh \mu z - 1\right) \Big/ \left(\frac{1}{2B_1} + \frac{1}{B_2}\right)$$

$$\text{Disp.} = \frac{\alpha T}{\mu} \tanh \mu \frac{l}{2}$$

where

$$u^2 = \frac{2Gt}{dE}\left(\frac{1}{2B_1} + \frac{1}{B_2}\right).$$

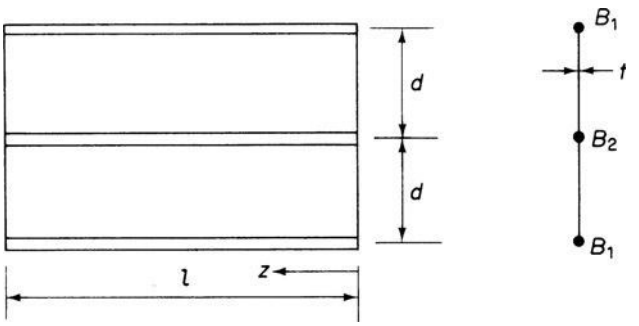

Fig. P.26.8

P.26.9 The flat panel shown in Fig. P.26.9 comprises a sheet of uniform thickness t, a central stringer of constant area A and edge members of varying area. The panel is supported on pinned supports and is subjected to externally applied shear flows S_1 and S_2, together with end loads $P_{1,0}$ and $P_{2,0}$ as shown. The areas of the edge members vary such that the direct stresses σ_1 and σ_2 in the edge members are constant.

Assuming that transverse strains are prevented, that the sheet transmits shear stress only and that each part has suitable end members to take the complementary shear stresses, derive expressions for the variation of direct stress σ_3 in the stringer and for the variation of shear flow in the upper panel in terms of the dimensions given and the elastic moduli E and G for the material.

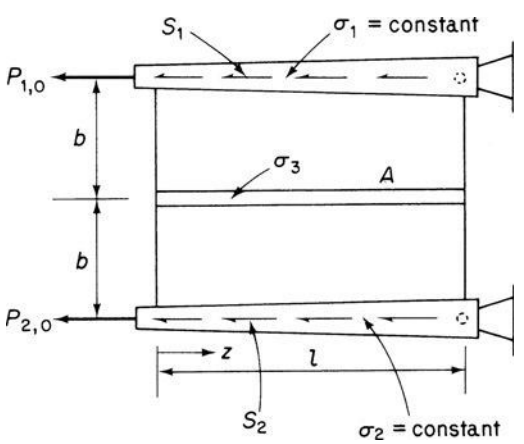

Fig. P.26.9

$$\textit{Ans.}\quad \sigma_3 = \left(\frac{\sigma_1+\sigma_2}{2}\right)\left[1-\cosh\mu z-\frac{\sinh\mu z}{\sinh\mu l}(1-\cosh\mu l)\right]$$

$$q_1 = A\left(\frac{\sigma_1+\sigma_2}{4}\right)\mu\left[\sinh\mu z+\frac{\cosh\mu z}{\sinh\mu l}(1-\cosh\mu l)\right]$$

where

$$\mu^2 = 2Gt/bAE$$

P.26.10 The panel shown in Fig. P.26.10 has been idealized into a combination of direct stress carrying booms and shear stress carrying plates; the boom areas are shown and the plate thickness is t. Derive expressions for the distribution of direct load in each boom and state how the load distributions are affected when $A = B$.

$$\textit{Ans.}\quad P_1 = \frac{6P}{2A+B}\left[-\left(\frac{B+8A}{6}\right)-\left(\frac{B-A}{3}\right)\frac{\cosh\mu(L-z)}{\cosh\mu L}\right]$$

$$P_2 = \frac{6P}{2A+B}\left[-B+\frac{2}{3}(B-A)\frac{\cosh\mu(L-z)}{\cosh\mu L}\right]$$

$$P_3 = \frac{6P}{2A+B}\left[-\left(\frac{4A-B}{6}\right)-\left(\frac{B-A}{3}\right)\frac{\cosh\mu(L-z)}{\cosh\mu L}\right]$$

When $A = B$, $P_1 = -3P$, $P_2 = -2P$, $P_3 = -P$, i.e no shear lag.

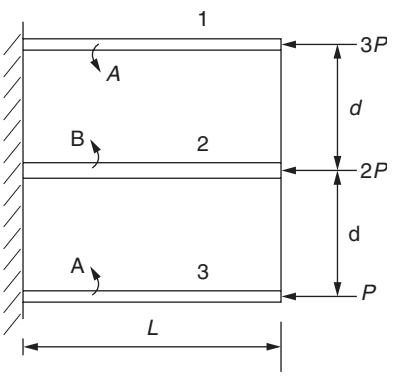

Fig. P.26.10

P.26.11 A uniform cantilever of length l has the doubly symmetrical cross-section shown in Fig. P.26.11. The section shape remains undistorted in its own plane after loading. Direct stresses on the cross-section are carried only in the concentrated longeron areas shown, and the wall thickness dimensions given relate only to shearing effects. All longerons have the same Young's modulus E and all walls the same effective shear modulus G.

The root of the cantilever is built-in, warping being completely suppressed there, and a shearing force S is applied at the tip in the position indicated.

Derive an expression for the resultant end load in a corner longeron. Also calculate the resultant deflection of the tip, including the effects of both direct and shear strains.

Ans. $P = -\dfrac{S}{8h}\left(\dfrac{\sinh \mu z}{\mu \cosh \mu l} + 3z\right)$

where $\mu^2 = 4Gt/3dBE$ (top right hand) (origin for z at free end)

$$\text{Def.} = \frac{Sl}{12h}\left(\frac{11}{4Gt} + \frac{l^2}{EBh}\right).$$

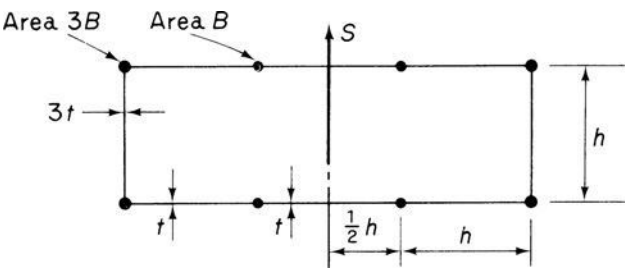

Fig. P.26.11

P.26.12 The idealized cantilever beam shown in Fig. P.26.12 carries a uniformly distributed load of intensity w. Assuming that all direct stresses are carried by the booms while the panels are effective only in shear determine the distribution of direct stress in the central boom in the top cover. Young's modulus for the booms is E and the shear modulus of the walls is G.

Ans. $P_A = -\dfrac{wA}{h(2B+A)}\left[\dfrac{\cosh \mu z}{\mu^2} + \left(\dfrac{\mu L - \sinh \mu L}{\mu^2 \cosh \mu L}\right)\sinh \mu z - \dfrac{1}{\mu^2} - \dfrac{z^2}{2}\right]$

where

$$\mu^2 = \frac{Gt(2B+A)}{dEAB}$$

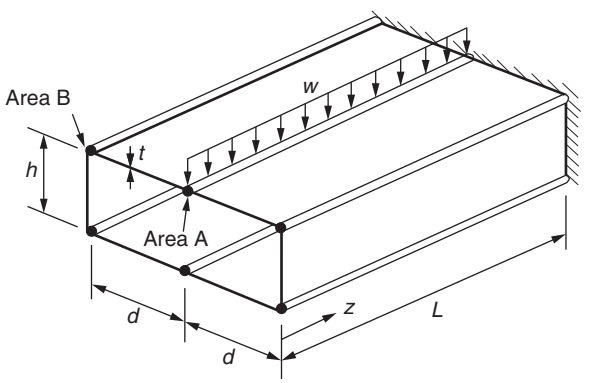

Fig. P.26.12

27

Open section beams

Instances of open section beams occurring in isolation are infrequent in aircraft structures. The majority of wing structures do, however, contain cut-outs for undercarriages, inspection panels and the like, so that at these sections the wing is virtually an open section beam. We saw in Chapter 23 that one method of analysis for such cases is to regard the applied torque as being resisted by the differential bending of the front and rear spars in the cut-out bay. An alternative approach is to consider the cut-out bay as an open section beam built-in at each end and subjected to a torque. We shall now investigate the method of analysis of such beams.

27.1 I-section beam subjected to torsion

If such a beam is axially unconstrained and loaded by a pure torque T the rate of twist is constant along the beam and is given by

$$T = GJ\frac{\mathrm{d}\theta}{\mathrm{d}z} \quad \text{(from Eq. (18.12))}$$

We also showed in Section 18.2 that the shear stress varies linearly across the thickness of the beam wall and is zero at the middle plane (Fig. 27.1). It follows that although the beam and the middle plane warp (we are concerned here with primary warping), there is no shear distortion of the middle plane. The mechanics of this warping are more easily understood by reference to the thin-walled I-section beam of Fig. 27.2(a). A plan view of the beam (Fig. 27.2(b)) reveals that the middle plane of each flange remains rectangular, although twisted, after torsion. We now observe the effect of applying a restraint to one end of the beam. The flanges are no longer free to warp and will

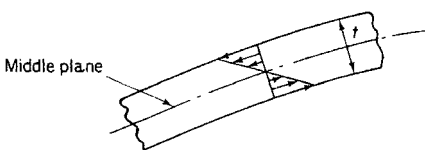

Fig. 27.1 Shear stress distribution across the wall of an open section beam subjected to torsion.

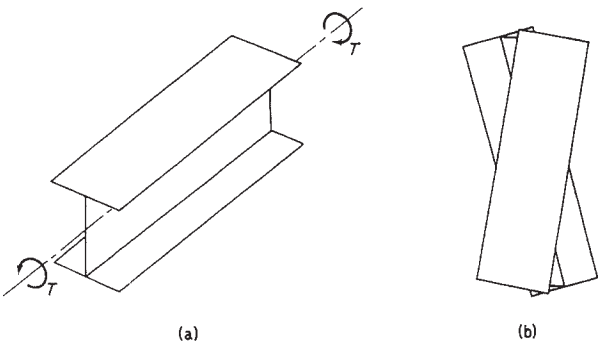

Fig. 27.2 (a) Torsion of I-section beam; (b) plan view of beam showing undistorted shape of flanges.

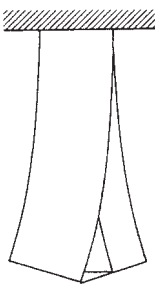

Fig. 27.3 Bending effect of axial constraint on flanges of I-section beam subjected to torsion.

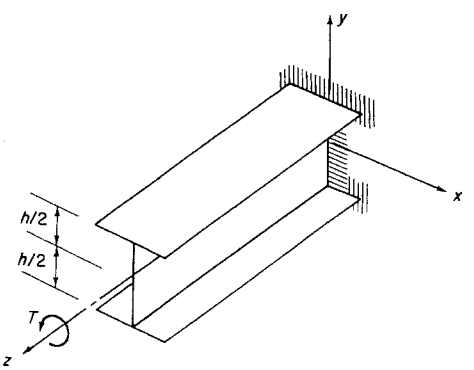

Fig. 27.4 Torsion of I-section beam fully built-in at one end.

bend in their own planes into the shape shown in plan in Fig. 27.3. Obviously the beam still twists along its length but the rate of twist is no longer constant and the resistance to torsion is provided by the St. Venant shear stresses (unrestrained warping) plus the resistance of the flanges to bending. The total torque may therefore be written $T = T_J + T_\Gamma$, where $T_J = GJ\ \mathrm{d}\theta/\mathrm{d}z$ from the unconstrained torsion of open sections but in which $\mathrm{d}\theta/\mathrm{d}z$ is not constant, and T_Γ is obtained from a consideration of the bending of the flanges. It will be instructive to derive an expression for T_Γ for the I-section beam of Fig. 27.4 before we turn our attention to the case of a beam of arbitrary section.

Suppose that at any section z the angle of twist of the I-beam is θ. Then the lateral displacement u of the lower flange is

$$u = \theta \frac{h}{2}$$

and the bending moment M_F in the plane of the flange is given by

$$M_F = -EI_F \frac{d^2u}{dz^2}$$

where I_F is the second moment of area of the *flange* cross-section about the y axis. It is assumed here that displacements produced by shear are negligible so that the lateral deflection of the flange is completely due to the self-equilibrating direct stress system σ_Γ set up by the bending of the flange. We shall not, however, assume that the shear stresses in the flange are negligible. The shear S_F in the flange is then

$$S_F = \frac{dM_F}{dz} = -EI_F \frac{d^3u}{dz^3}$$

or substituting for u in terms of θ and h

$$S_F = -EI_F \frac{h}{2} \frac{d^3\theta}{dz^3}$$

Similarly, there is a shear force in the top flange of the same magnitude but opposite in direction. Together they form a couple which represents the second part T_Γ of the total torque, thus

$$T_\Gamma = S_F h = -EI_F \frac{h^2}{2} \frac{d^3\theta}{dz^3}$$

and the expression for the total torque may be written

$$T = GJ \frac{d\theta}{dz} - EI_F \frac{h^2}{2} \frac{d^3\theta}{dz^3}$$

27.2 Torsion of an arbitrary section beam

The insight into the physical aspects of the problem gained in the above will be found helpful in the development of the general theory for the arbitrary section beam shown in Fig. 27.5.

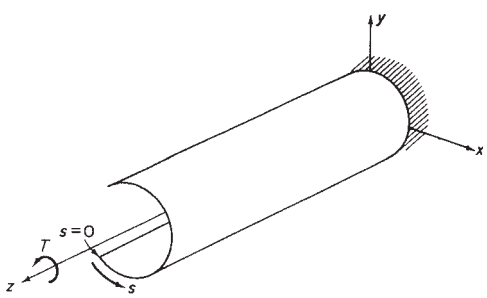

Fig. 27.5 Torsion of an open section beam fully built-in at one end.

The theory, originally developed by Wagner and Kappus, is most generally known as the Wagner torsion bending theory. It assumes that the beam is long compared with its cross-sectional dimensions, that the cross-section remains undistorted by the loading and that the shear strain γ_{zs} of the middle plane of the beam is negligible although the stresses producing the shear strain are not. From similar assumptions is derived, in Section 18.2.1, an expression for the primary warping w of the beam, viz.

$$w = -2A_{\mathrm{R}}\frac{\mathrm{d}\theta}{\mathrm{d}z} \qquad \text{(Eq. (18.19))}$$

In the presence of axial constraint, $\mathrm{d}\theta/\mathrm{d}z$ is no longer constant so that the longitudinal strain $\partial w/\partial z$ is not zero and direct (also shear) stresses are induced. Then

$$\sigma_\Gamma = E\frac{\partial w}{\partial z} = -2A_{\mathrm{R}}E\frac{\mathrm{d}^2\theta}{\mathrm{d}z^2} \tag{27.1}$$

The σ_Γ stress system must be self-equilibrating since the applied load is a pure torque. Therefore, at any section the resultant end load is zero and

$$\int_c \sigma_\Gamma t\,\mathrm{d}s = 0 \quad \left(\int_c \text{denotes integration around the beam section}\right)$$

or, from Eq. (27.1) and observing that $\mathrm{d}^2\theta/\mathrm{d}z^2$ is a function of z only

$$\int_c 2A_{\mathrm{R}}t\,\mathrm{d}s = 0 \tag{27.2}$$

The limits of integration of Eq. (27.2) present some difficulty in that A_{R} is zero when w is zero at an unknown value of s. Let

$$2A_{\mathrm{R}} = 2A_{\mathrm{R},0} - 2A'_{\mathrm{R}}$$

where $A_{\mathrm{R},0}$ is the area swept out from $s=0$ and A'_{R} is the value of $A_{\mathrm{R},0}$ at $w=0$ (see Fig. 27.6). Then in Eq. (27.2)

$$\int_c 2A_{\mathrm{R},0}t\,\mathrm{d}s - 2A'_R\int_c t\,\mathrm{d}s = 0$$

and

$$2A'_{\mathrm{R}} = \frac{\int_c 2A_{\mathrm{R},0}t\,\mathrm{d}s}{\int_c t\,\mathrm{d}s}$$

giving

$$2A_{\mathrm{R}} = 2A_{\mathrm{R},0} - \frac{\int_c 2A_{\mathrm{R},0}t\,\mathrm{d}s}{\int_c t\,\mathrm{d}s} \tag{27.3}$$

The axial constraint shear flow system, q_Γ, is in equilibrium with the self-equilibrating direct stress system. Thus, from Eq. (17.2)

$$\frac{\partial q_\Gamma}{\partial s} + t\frac{\partial \sigma_\Gamma}{\partial z} = 0$$

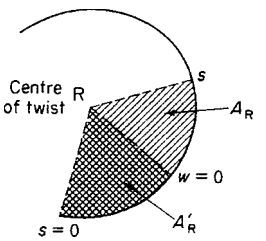

Fig. 27.6 Computation of swept area A_R.

Hence

$$\frac{\partial q_\Gamma}{\partial s} = -t\frac{\partial \sigma_\Gamma}{\partial z}$$

Substituting for σ_Γ from Eq. (27.1) and noting that $q_\Gamma = 0$ when $s = 0$, we have

$$q_\Gamma = \int_0^s 2A_R Et\frac{\mathrm{d}^3\theta}{\mathrm{d}z^3}\mathrm{d}s$$

or

$$q_\Gamma = E\frac{\mathrm{d}^3\theta}{\mathrm{d}z^3}\int_0^s 2A_R t\,\mathrm{d}s \tag{27.4}$$

Now

$$T_\Gamma = \int_c p_R q_\Gamma\,\mathrm{d}s$$

or, from Eq. (27.4)

$$T_\Gamma = E\frac{\mathrm{d}^3\theta}{\mathrm{d}z^3}\int_c p_R\left(\int_0^s 2A_R t\,\mathrm{d}s\right)\mathrm{d}s$$

The integral in this equation is evaluated by substituting $p_R = (\mathrm{d}/\mathrm{d}s)(2A_R)$ and integrating by parts. Thus

$$\int_c \frac{\mathrm{d}}{\mathrm{d}s}(2A_R)\left(\int_0^s 2A_R t\,\mathrm{d}s\right)\mathrm{d}s = \left[2A_R\int_0^s 2A_R t\,\mathrm{d}s\right]_c - \int_c 4A_R^2 t\,\mathrm{d}s$$

At each open edge of the beam q_Γ, and therefore $\int_0^s 2A_R t\,\mathrm{d}s$, is zero so that the integral reduces to $-\int_c 4A_R^2 t\,\mathrm{d}s$, giving

$$T_\Gamma = -E\Gamma_R\frac{\mathrm{d}^3\theta}{\mathrm{d}z^3} \tag{27.5}$$

where $\Gamma_R = \int_c 4A_R^2 t\,\mathrm{d}s$, the *torsion-bending constant*, and is purely a function of the geometry of the cross-section. The total torque T, which is the sum of the St. Venant torque and the Wagner torsion bending torque, is then written

$$T = GJ\frac{\mathrm{d}\theta}{\mathrm{d}z} - E\Gamma_R\frac{\mathrm{d}^3\theta}{\mathrm{d}z^3} \tag{27.6}$$

(*Note*: Compare Eq. (27.6) with the expression derived for the I-section beam.)

In the expression for Γ_R the thickness t is actually the direct stress carrying thickness t_D of the beam wall so that Γ_R, for a beam with n booms, may be generally written

$$\Gamma_R = \int_c 4A_R^2 t_D \, ds + \sum_{r=1}^{n} (2A_{R,r})^2 B_r$$

where B_r is the cross-sectional area of the rth boom. The calculation of Γ_R enables the second order differential equation in $d\theta/dz$ (Eq. (27.6)) to be solved. The constraint shear flows, q_Γ, follow from Eqs (27.4) and (27.3) and the longitudinal constraint stresses from Eq. (27.1). However, before illustrating the complete method of solution with examples we shall examine the calculation of Γ_R.

So far we have referred the swept area A_R, and hence Γ_R, to the centre of twist of the beam without locating its position. This may be accomplished as follows. At any section of the beam the resultant of the q_Γ shear flows is a pure torque (as is the resultant of the St. Venant shear stresses) so that in Fig. 27.7

$$\int_c q_\Gamma \sin\psi \, ds = S_y = 0$$

Therefore, from Eq. (27.4)

$$E\frac{d^3\theta}{dz^3}\int_c \left(\int_0^s 2A_R t \, ds\right) \sin\psi \, ds = 0$$

Now

$$\sin\psi = \frac{dy}{ds} \qquad \frac{d}{ds}(2A_R) = p_R$$

and the above expression may be integrated by parts, thus

$$\int_c \frac{dy}{ds}\left(\int_0^s 2A_R t \, ds\right) ds = \left[y\int_0^s 2A_R t \, ds\right]_c - \int_c y 2A_R t \, ds = 0$$

The first term on the right-hand side vanishes as $\int_0^s 2A_R t \, ds$ is zero at each open edge of the beam, leaving

$$\int_c y 2A_R t \, ds = 0$$

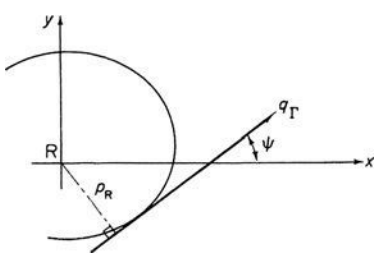

Fig. 27.7 Determination of the position of the centre of twist.

Again integrating by parts

$$\int_c y2A_R t\,\mathrm{d}s = \left[2A_R \int_0^s yt\,\mathrm{d}s\right]_c - \int_c p_R \left(\int_0^s yt\,\mathrm{d}s\right)\mathrm{d}s = 0$$

The integral in the first term on the right-hand side of the above equation may be recognized, from Chapter 17, as being directly proportional to the shear flow produced in a singly symmetrical open section beam supporting a shear load S_y. Its value is therefore zero at each open edge of the beam. Hence

$$\int_c p_R \left(\int_0^s yt\,\mathrm{d}s\right)\mathrm{d}s = 0 \tag{27.7}$$

Similarly, for the horizontal component S_x to be zero

$$\int_c p_R \left(\int_0^s xt\,\mathrm{d}s\right)\mathrm{d}s = 0 \tag{27.8}$$

Equations (27.7) and (27.8) hold if the centre of twist coincides with the shear centre of the cross-section. To summarize, the centre of twist of a section of an open section beam carrying a pure torque is the shear centre of the section.

We are now in a position to calculate Γ_R. This may be done by evaluating $\int_c 4A_R^2 t\,\mathrm{d}s$ in which $2A_R$ is given by Eq. (27.3). In general, the calculation may be lengthy unless the section has flat sides in which case a convenient analogy shortens the work considerably. For the flat-sided section in Fig. 27.8(a) we first plot the area $2A_{R,0}$ swept out from the point 1 where we choose $s = 0$ (Fig. 27.8(b)). The swept area $A_{R,0}$ increases linearly from zero at 1 to $(1/2)p_{12}d_{12}$ at 2 and so on. Note that movement along side 23 produces no increment of $2A_{R,0}$ as $p_{23} = 0$. Further, we adopt a sign convention for p such that p is positive if movement in the positive s direction of the foot of p along the tangent causes anticlockwise rotation about R. The increment of $2A_{R,0}$ from side 34 is therefore negative.

In the derivation of Eq. (27.3) we showed that

$$2A'_R = \frac{\int_c 2A_{R,0} t\,\mathrm{d}s}{\int_c t\,\mathrm{d}s}$$

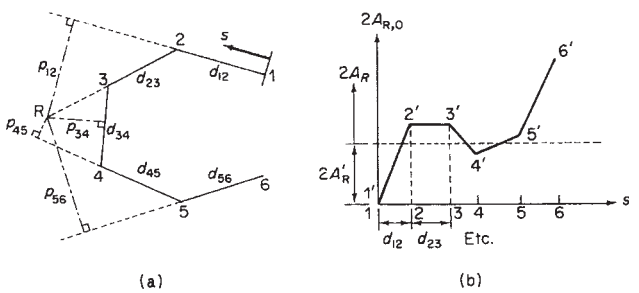

Fig. 27.8 Computation of torsion bending constant Γ_R: (a) dimensions of flat-sided open section beam; (b) variation of $2A_{R,0}$ around beam section.

Suppose now that the line $1'2'3' \ldots 6'$ is a wire of varying density such that the weight of each element $\delta s'$ is $t\delta s$. Thus the weight of length $1'2'$ is td_{12}, etc. The y coordinate of the centre of gravity of the 'wire' is then

$$\bar{y} = \frac{\int yt \, \mathrm{d}s}{\int t \, \mathrm{d}s}$$

Comparing this expression with the previous one for $2A'_{\mathrm{R}}$, y and $\bar{y}$ are clearly analogous to $2A_{\mathrm{R},0}$ and $2A'_{\mathrm{R}}$, respectively. Further

$$\Gamma_{\mathrm{R}} = \int_c (2A_{\mathrm{R}})^2 t \, \mathrm{d}s = \int_c (2A_{\mathrm{R},0} - 2A'_{\mathrm{R}})^2 t \, \mathrm{d}s$$

Expanding and substituting

$$2A'_{\mathrm{R}} \int_c t \, \mathrm{d}s \quad \text{for} \quad \int_c 2A_{R,0} t \, \mathrm{d}s$$

gives

$$\Gamma_{\mathrm{R}} = \int_c (2A_{\mathrm{R},0})^2 t \, \mathrm{d}s - (2A'_{\mathrm{R}})^2 \int_c t \, \mathrm{d}s \tag{27.9}$$

Therefore, in Eq. (27.9), Γ_{R} is analogous to the moment of inertia of the 'wire' about an axis through its centre of gravity parallel to the s axis.

Example 27.1

An open section beam of length L has the section shown in Fig. 27.9. The beam is firmly built-in at one end and carries a pure torque T. Derive expressions for the direct stress and shear flow distributions produced by the axial constraint (the σ_Γ and q_Γ systems) and the rate of twist of the beam.

The beam is loaded by a pure torque so that the axis of twist passes through the shear centre S(R) of each section. We shall take the origin for s at the point 1 and initially plot $2A_{\mathrm{R},0}$ against s to determine Γ_{R} (see Fig. 27.10). The position of the centre of gravity, $(2A'_{\mathrm{R}})$, of the wire $1'2'3'4'$ is found by taking moments about the s axis. Then

$$t(2d + h)2A'_{\mathrm{R}} = td\left(\frac{hd}{4}\right) + th\left(\frac{hd}{2}\right) + td\left(\frac{hd}{4}\right)$$

from which

$$2A'_{\mathrm{R}} = \frac{hd(h + d)}{2(h + 2d)} \tag{i}$$

Γ_{R} follows from the moment of inertia of the 'wire' about an axis through its centre of gravity. Hence

$$\Gamma_{\mathrm{R}} = 2td\frac{1}{3}\left(\frac{hd}{2}\right)^2 + th\left(\frac{hd}{2}\right)^2 - \left[\frac{hd(h + d)}{2(h + 2d)}\right]^2 t(h + 2d)$$

which simplifies to

$$\Gamma_{\mathrm{R}} = \frac{t \, \mathrm{d}^3 h^2}{12}\left(\frac{2h + d}{h + 2d}\right) \tag{ii}$$

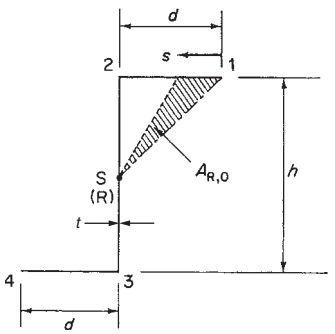

Fig. 27.9 Section of axially constrained open section beam under torsion.

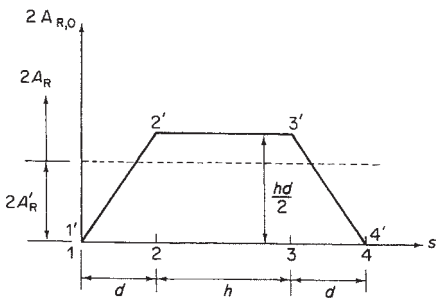

Fig. 27.10 Calculation of Γ_R for the section of Example 27.1.

Equation (27.6), i.e.

$$T = GJ\frac{\mathrm{d}\theta}{\mathrm{d}z} - E\Gamma_{\mathrm{R}}\frac{\mathrm{d}^3\theta}{\mathrm{d}z^3}$$

may now be solved for $\mathrm{d}\theta/\mathrm{d}z$. Rearranging and writing $\mu^2 = GJ/E\Gamma_{\mathrm{R}}$ we have

$$\frac{\mathrm{d}^3\theta}{\mathrm{d}z^3} - \mu^2\frac{\mathrm{d}\theta}{\mathrm{d}z} = -\mu^2\frac{T}{GJ} \tag{iii}$$

The solution of Eq. (iii) is of standard form, i.e.

$$\frac{\mathrm{d}\theta}{\mathrm{d}z} = \frac{T}{GJ} + A\cosh\mu z + B\sinh\mu z$$

The constants A and B are found from the boundary conditions:

(1) At the built-in end the warping $w = 0$ and since $w = -2A_{\mathrm{R}}\mathrm{d}\theta/\mathrm{d}z$ then $\mathrm{d}\theta/\mathrm{d}z = 0$ at the built-in end.

(2) At the free end $\sigma_\Gamma = 0$, as there is no constraint and no externally applied direct load. Therefore, from Eq. (27.1), $\mathrm{d}^2\theta/\mathrm{d}z^2 = 0$ at the free end.

From (1)

$$A = -T/GJ$$

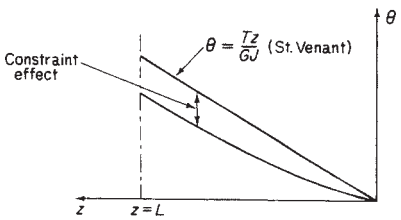

Fig. 27.11 Stiffening effect of axial constraint.

From (2)

$$B = (T/GJ)\tanh \mu L$$

so that

$$\frac{\mathrm{d}\theta}{\mathrm{d}z} = \frac{T}{GJ}(1 - \cosh \mu z + \tanh \mu L \sinh \mu z)$$

or

$$\frac{\mathrm{d}\theta}{\mathrm{d}z} = \frac{T}{GJ}\left[1 - \frac{\cosh \mu(L - z)}{\cosh \mu L}\right] \tag{iv}$$

The first term in Eq. (iv) is seen to be the rate of twist derived from the St. Venant torsion theory. The hyperbolic second term is therefore the modification introduced by the axial constraint. Equation (iv) may be integrated to find the distribution of angle of twist θ, the appropriate boundary condition being $\theta = 0$ at the built-in end, i.e.

$$\theta = \frac{T}{GJ}\left[z + \frac{\sinh \mu(L - z)}{\mu \cosh \mu L} - \frac{\sinh \mu L}{\mu \cosh \mu L}\right] \tag{v}$$

and the angle of twist, $\theta_{\mathrm{F,E}}$, at the free end of the beam is

$$\theta_{\mathrm{F,E}} = \frac{TL}{GJ}\left(1 - \frac{\tanh \mu L}{\mu L}\right) \tag{vi}$$

Plotting θ against z (Fig. 27.11) illustrates the stiffening effect of axial constraint on the beam.

The decrease in the effect of axial constraint towards the free end of the beam is shown by an examination of the variation of the St. Venant (T_J) and Wagner (T_Γ) torques along the beam. From Eq. (iv)

$$T_J = GJ\frac{\mathrm{d}\theta}{\mathrm{d}z} = T\left[1 - \frac{\cosh \mu(L - z)}{\cosh \mu L}\right] \tag{vii}$$

and

$$T_\Gamma = -E\Gamma_{\mathrm{R}}\frac{\mathrm{d}^3\theta}{\mathrm{d}z^3} = T\frac{\cosh \mu(L - z)}{\cosh \mu L} \tag{viii}$$

T_J and T_Γ are now plotted against z as fractions of the total torque T (Fig. 27.12). At the built-in end the entire torque is carried by the Wagner stresses, but although the

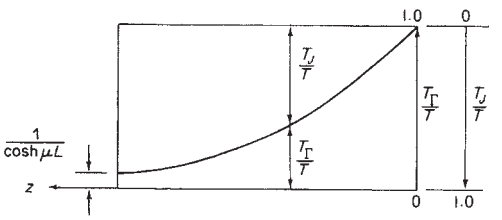

Fig. 27.12 Distribution of St. Venant and torsion-bending torques along the length of the open section beam shown in Fig. 27.9.

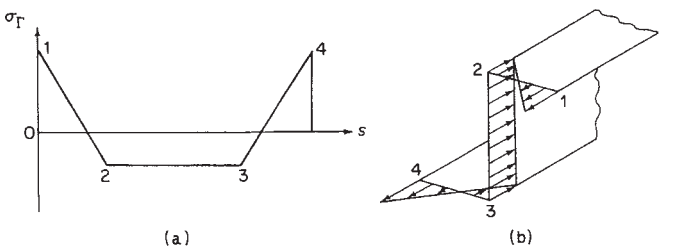

Fig. 27.13 Distribution of axial constraint direct stress around the section.

constraint effect diminishes towards the free end it does not disappear entirely. This is due to the fact that the axial constraint shear flow, q_Γ, does not vanish at $z = L$, for at this section (and all other sections) $\mathrm{d}^3\theta/\mathrm{d}z^3$ is not zero.

Equations (iii)–(viii) are, of course, valid for open section beams of any cross-section. Their application in a particular case is governed by the value of the torsion bending constant Γ_R and the St. Venant torsion constant $J[= (h + 2\mathrm{d})t^3/3$ for this example]. With this in mind we can proceed, as required by the example, to derive the direct stress and shear flow distributions. The former is obtained from Eqs (27.1) and (iv), i.e.

$$\sigma_\Gamma = -2A_\mathrm{R}E\frac{T}{GJ}\mu\frac{\sinh \mu(L-z)}{\cosh \mu L}$$

or writing $\mu^2 = GJ/E\Gamma_\mathrm{R}$ and rearranging

$$\sigma_\Gamma = -\sqrt{\frac{E}{GJ\Gamma_\mathrm{R}}}T2A_\mathrm{R}\frac{\sinh \mu(L-z)}{\cosh \mu L} \qquad \text{(ix)}$$

In Eq. (ix) E, G, J and Γ_R are constants for a particular beam, T is the applied torque, A_R is a function of s and the hyperbolic term is a function of z. It follows that at a given section of the beam the direct stress is proportional to $-2A_\mathrm{R}$, and for the beam of this example the direct stress distribution has, from Fig. 27.10, the form shown in Figs 27.13(a) and (b). In addition, the value of σ_Γ at a particular value of s varies along the beam in the manner shown in Fig. 27.14.

Finally, the axial constraint shear flow, q_Γ, is obtained from Eq. (27.4), namely

$$q_\Gamma = E\frac{\mathrm{d}^3\theta}{\mathrm{d}z^3}\int_0^s 2A_\mathrm{R}t\,\mathrm{d}s$$

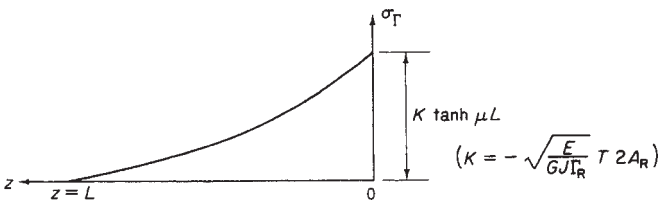

Fig. 27.14 Spanwise distribution of axial constraint direct stress.

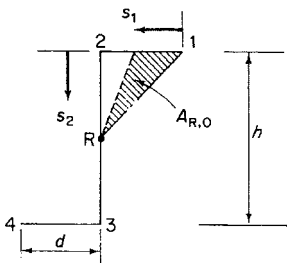

Fig. 27.15 Calculation of axial constraint shear flows.

At any section z, q_Γ is proportional to $\int_0^s 2A_R t\,\mathrm{d}s$ and is computed as follows. Referring to Fig. 27.15, $2A_R = 2A_{R,0} - 2A'_R$ so that in flange 12

$$2A_R = \frac{hs_1}{2} - \frac{hd}{2}\left(\frac{h+d}{h+2d}\right)$$

Hence

$$\int_0^s 2A_R t\,\mathrm{d}s = t\left[\frac{hs_1^2}{4} - \frac{hd}{2}\left(\frac{h+d}{h+2d}\right)s_1\right]$$

so that

$$q_{\Gamma,1} = 0 \quad \text{and} \quad q_{\Gamma,2} = -E\frac{\mathrm{d}^3\theta}{\mathrm{d}z^3}\frac{h^2d^2t}{4(h+2d)}$$

Similarly

$$q_{\Gamma,23} = E\frac{\mathrm{d}^3\theta}{\mathrm{d}z^3}\left[\frac{hd^2t}{2(h+2d)}s_2 - \frac{h^2d^2t}{4(h+2d)}\right]$$

whence

$$q_{\Gamma,2} = -E\frac{\mathrm{d}^3\theta}{\mathrm{d}z^3}\frac{h^2d^2t}{4(h+2d)} \qquad q_{\Gamma,3} = E\frac{\mathrm{d}^3\theta}{\mathrm{d}z^3}\frac{h^2d^2t}{4(h+2d)}$$

Note that in the above $\mathrm{d}^3\theta/\mathrm{d}z^3$ is negative (Eq. (viii)). Also at the mid-point of the web where $s_2 = h/2$, $q_\Gamma = 0$. The distribution on the lower flange follows from antisymmetry and the distribution of q_Γ around the section is of the form shown in Fig. 27.16.

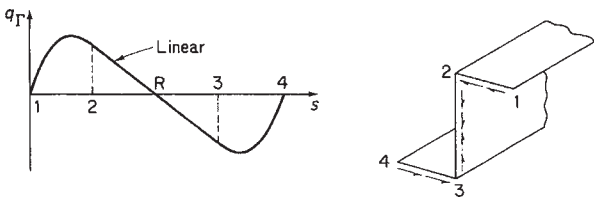

Fig. 27.16 Distribution of axial constraint shear flows.

The spanwise variation of q_Γ has the same form as the variation of T_Γ since

$$T_\Gamma = -E\Gamma_R \frac{d^3\theta}{dz^3}$$

giving

$$q_\Gamma = -\frac{T_\Gamma}{\Gamma_R}\int_0^s 2A_R t\, ds \quad \text{from Eq. (27.4)}$$

Hence for a given value of s, ($\int_0^s 2A_R t\, ds$), q_Γ is proportional to T_Γ (see Fig. 27.12).

27.3 Distributed torque loading

We now consider the more general case of a beam carrying a distributed torque loading. In Fig. 27.17 an element of a beam is subjected to a distributed torque of intensity $T_i(z)$, i.e. a torque per unit length. At the section z the torque comprises the St. Venant torque T_J plus the torque due to axial constraint T_Γ. At the section $z + \delta z$ the torque increases to $T + \delta T (= T_J + \delta T_J + T_\Gamma + \delta T_\Gamma)$ so that for equilibrium of the beam element

$$T_J + \delta T_J + T_\Gamma + \delta T_\Gamma + T_i(z)\delta z - T_J - T_\Gamma = 0$$

or

$$-T_i(z)\delta z = \delta T_J + \delta T_\Gamma = \delta T$$

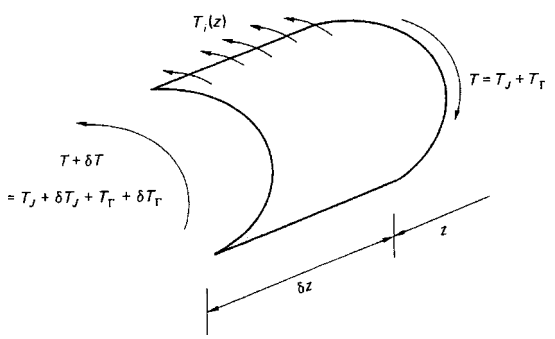

Fig. 27.17 Beam carrying a distributed torque loading.

Hence

$$\frac{\mathrm{d}T}{\mathrm{d}z} = -T_i(z) = \frac{\mathrm{d}T_J}{\mathrm{d}z} + \frac{\mathrm{d}T_\Gamma}{\mathrm{d}z} \tag{27.10}$$

Now

$$T_J = GJ\frac{\mathrm{d}\theta}{\mathrm{d}z} \quad \text{(Eq. (18.12))}$$

and

$$T_\Gamma = -E\Gamma\frac{\mathrm{d}^3\theta}{\mathrm{d}z^3} \quad \text{(Eq. (27.5))}$$

so that Eq. (27.10) becomes

$$E\Gamma\frac{\mathrm{d}^4\theta}{\mathrm{d}z^4} - GJ\frac{\mathrm{d}^2\theta}{\mathrm{d}z^2} = T_i(z) \tag{27.11}$$

The solution of Eq. (27.11) is again of standard form in which the constants of integration are found from the boundary conditions of the particular beam under consideration. For example, for a cantilever beam of length L in which the origin for z is at the built-in end and which is subjected to a uniform torque loading, the boundary conditions are:

when $z = L$, $\mathrm{d}^2\theta/\mathrm{d}z^2 = 0$ (from Eq. (27.1))
when $z = 0$, $\mathrm{d}\theta/\mathrm{d}z = 0$ (since the warping is zero at the built-in end, see Eq. (18.19))
when $z = L$, $\mathrm{d}^3\theta/\mathrm{d}z^3 = 0$ (since $T_\Gamma = T_J = T = 0$ at the free end, see Eq. (27.5))
when $z = 0$, $\theta = 0$ (there is no rotation at the built-in end).

27.4 Extension of the theory to allow for general systems of loading

So far we have been concerned with open section beams subjected to torsion in which, due to constraint effects, axial stresses are induced. Since pure torsion can generate axial stresses it is logical to suppose that certain distributions of axial stress applied as external loads will cause twisting. The problem is to determine that component of an applied direct stress system which causes twisting.

Figure 27.18 shows the profile of a thin-walled open section beam subjected to a general system of loads which produce longitudinal, transverse and rotational displacements of its cross-section. In the analysis we assume that the cross-section of the beam is undistorted by the loading and that displacements corresponding to the shear strains are negligible. In Fig. 27.18 the tangential displacement v_t is given by Eq. (17.7), i.e.

$$v_\mathrm{t} = p_\mathrm{R}\theta + u\cos\psi + v\sin\psi \tag{27.12}$$

Also, since shear strains are assumed to be negligible, Eq. (17.6) becomes

$$\gamma = \frac{\partial w}{\partial s} + \frac{\partial v_\mathrm{t}}{\partial z} = 0 \tag{27.13}$$

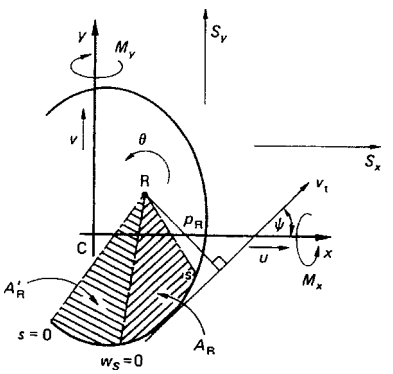

Fig. 27.18 Cross-section of an open section beam subjected to a general system of loads.

Substituting for v_t in Eq. (27.13) from (27.12) and integrating from the origin for s to any point s around the cross-section, we have

$$w_s - w_0 = -\frac{\mathrm{d}\theta}{\mathrm{d}z}2A_{\mathrm{R},0} - \frac{\mathrm{d}u}{\mathrm{d}z}(x - x_0) - \frac{\mathrm{d}v}{\mathrm{d}z}(y - y_0) \tag{27.14}$$

where $2A_{\mathrm{R},0} = \int_0^s p_{\mathrm{R}}\,\mathrm{d}s$. The direct stress at any point in the wall of the beam is given by

$$\sigma_z = E\frac{\partial w_s}{\partial z}$$

Therefore, from Eq. (27.14)

$$\sigma_z = E\left[\frac{\partial w_0}{\partial z} - \frac{\mathrm{d}^2\theta}{\mathrm{d}z^2}2A_{\mathrm{R},0} - \frac{\mathrm{d}^2u}{\mathrm{d}z^2}(x - x_0) - \frac{\mathrm{d}^2v}{\mathrm{d}z^2}(y - y_0)\right] \tag{27.15}$$

Now $A_{\mathrm{R},0} = A'_{\mathrm{R}} + A_{\mathrm{R}}$ (Fig. 27.18) so that Eq. (27.15) may be rewritten

$$\sigma_z = f_1(z) - E\frac{\mathrm{d}^2\theta}{\mathrm{d}z^2}2A_{\mathrm{R}} - E\frac{\mathrm{d}^2u}{\mathrm{d}z^2}x - E\frac{\mathrm{d}^2v}{\mathrm{d}z^2}y \tag{27.16}$$

in which

$$f_1(z) = E\left(\frac{\partial w_0}{\partial z} - \frac{\mathrm{d}^2\theta}{\mathrm{d}z^2}2A'_{\mathrm{R}} + \frac{\mathrm{d}^2u}{\mathrm{d}z^2}x_0 + \frac{\mathrm{d}^2v}{\mathrm{d}z^2}y_0\right)$$

The axial load P on the section is given by

$$P = \int_c \sigma_z t\,\mathrm{d}s = f_1(z)\int_c t\,\mathrm{d}s - E\frac{\mathrm{d}^2\theta}{\mathrm{d}z^2}\int_c 2A_{\mathrm{R}}t\,\mathrm{d}s - E\frac{\mathrm{d}^2u}{\mathrm{d}z^2}\int_c tx\,\mathrm{d}s - E\frac{\mathrm{d}^2v}{\mathrm{d}z^2}\int_c ty\,\mathrm{d}s$$

where $\int_c$ denotes integration taken completely around the section. From Eq. (27.2) we see that $\int_c 2A_{\mathrm{R}}t\,\mathrm{d}s = 0$. Also, if the origin of axes coincides with the centroid of the section $\int_c tx\,\mathrm{d}s = \int_c ty\,\mathrm{d}s = 0$ and $\int ty\,\mathrm{d}s = 0$ so that

$$P = \int_c \sigma_z t\,\mathrm{d}s = f_1(z)A \tag{27.17}$$

in which A is the cross-sectional area of the material in the wall of the beam.

The component of bending moment, M_x, about the x axis is given by

$$M_x = \int_c \sigma_z t y \, \mathrm{d}s$$

Substituting for σ_z from Eq. (27.16) we have

$$M_x = f_1(z) \int_c t y \, \mathrm{d}s - E \frac{\mathrm{d}^2\theta}{\mathrm{d}z^2} \int_c 2A_\mathrm{R} t y \, \mathrm{d}s - E \frac{\mathrm{d}^2 u}{\mathrm{d}z^2} \int_c t x y \, \mathrm{d}s - E \frac{\mathrm{d}^2 v}{\mathrm{d}z^2} \int_c t y^2 \, \mathrm{d}s$$

We have seen in the derivation of Eqs (27.7) and (27.8) that $\int_c 2A_\mathrm{R} t y \, \mathrm{d}s = 0$. Also since

$$\int_c t y \, \mathrm{d}s = 0 \quad \int_c t x y \, \mathrm{d}s = I_{xy} \quad \int_c t y^2 \, \mathrm{d}s = I_{xx}$$

$$M_x = -E \frac{\mathrm{d}^2 u}{\mathrm{d}z^2} I_{xy} - E \frac{\mathrm{d}^2 v}{\mathrm{d}z^2} I_{xx} \tag{27.18}$$

Similarly

$$M_y = \int_c \sigma_z t x \, \mathrm{d}s = -E \frac{\mathrm{d}^2 u}{\mathrm{d}z^2} I_{yy} - E \frac{\mathrm{d}^2 v}{\mathrm{d}z^2} I_{xy} \tag{27.19}$$

Equations (27.18) and (27.19) are identical to Eqs (16.31) so that from Eqs (16.29)

$$E \frac{\mathrm{d}^2 u}{\mathrm{d}z^2} = \frac{M_x I_{xy} - M_y I_{xx}}{I_{xx} I_{yy} - I_{xy}^2} \quad E \frac{\mathrm{d}^2 v}{\mathrm{d}z^2} = \frac{-M_x I_{yy} + M_y I_{xy}}{I_{xx} I_{yy} - I_{xy}^2} \tag{27.20}$$

The first differential, $\mathrm{d}^2\theta/\mathrm{d}z^2$, of the rate of twist in Eq. (27.16) may be isolated by multiplying throughout by $2A_\mathrm{R} t$ and integrating around the section. Thus

$$\int_c \sigma_z 2A_\mathrm{R} t \, \mathrm{d}s = f_1(z) \int_c 2A_\mathrm{R} t \, \mathrm{d}s - E \frac{\mathrm{d}^2\theta}{\mathrm{d}z^2} \int_c (2A_\mathrm{R})^2 t \, \mathrm{d}s - E \frac{\mathrm{d}^2 u}{\mathrm{d}z^2} \int_c 2A_\mathrm{R} t x \, \mathrm{d}s - E \frac{\mathrm{d}^2 v}{\mathrm{d}z^2} \int_c 2A_\mathrm{R} t y \, \mathrm{d}s$$

As before

$$\int_c 2A_\mathrm{R} t \, \mathrm{d}s = 0 \quad \int_c 2A_\mathrm{R} t x \, \mathrm{d}s = \int_c 2A_\mathrm{R} t y \, \mathrm{d}s = 0$$

and

$$\int_c (2A_\mathrm{R})^2 t \, \mathrm{d}s = \Gamma_\mathrm{R}$$

so that

$$\int_c \sigma_z 2A_\mathrm{R} t \, \mathrm{d}s = -E\Gamma_\mathrm{R} \frac{\mathrm{d}^2\theta}{\mathrm{d}z^2}$$

or

$$\frac{\mathrm{d}^2\theta}{\mathrm{d}z^2} = -\int_c \frac{\sigma_z 2A_\mathrm{R} t\,\mathrm{d}s}{E\Gamma_\mathrm{R}} \tag{27.21}$$

Substituting in Eq. (27.16) from Eqs (27.17), (27.20) and (27.21), we obtain

$$\sigma_z = \frac{P}{A} + \left(\frac{M_y I_{xx} - M_x I_{xy}}{I_{xx}I_{yy} - I_{xy}^2}\right)x + \left(\frac{M_x I_{yy} - M_y I_{xy}}{I_{xx}I_{yy} - I_{xy}^2}\right)y + \frac{2A_\mathrm{R}\int_c \sigma_z 2A_\mathrm{R} t\,\mathrm{d}s}{\Gamma_\mathrm{R}} \tag{27.22}$$

The second two terms on the right-hand side of Eq. (27.22) give the direct stress due to bending as predicted by elementary beam theory; note that the above approach provides an alternative method of derivation of Eq. (16.18).

Comparing the last term on the right-hand side of Eq. (27.22) with Eq. (27.1), we see that

$$\frac{2A_\mathrm{R}\int_c \sigma_z 2A_\mathrm{R} t\,\mathrm{d}s}{\Gamma_\mathrm{R}} = \sigma_\Gamma$$

It follows therefore that the external application of a direct stress system σ_z induces a self-equilibrating direct stress system σ_Γ. Also, the first differential of the rate of twist ($\mathrm{d}^2\theta/\mathrm{d}z^2$) is related to the applied σ_z stress system through the term $\int_c \sigma_z 2A_\mathrm{R} t\,\mathrm{d}s$. Therefore, if $\int_c \sigma_z 2A_\mathrm{R} t\,\mathrm{d}s$ is interpreted in terms of the applied loads at a particular section then a boundary condition exists (for $\mathrm{d}^2\theta/\mathrm{d}z^2$) which determines one of the constants in the solution of either Eq. (27.6) or (27.11).

27.5 Moment couple (bimoment)

The units of $\int_c \sigma_z 2A_\mathrm{R} t\,\mathrm{d}s$ are *force* × (*distance*)^2 or *moment* × *distance*. A simple physical representation of this expression would thus consist of two equal and opposite moments applied in parallel planes some distance apart. This combination has been termed a *moment couple*[1] or a *bimoment*[2] and is given the symbol M_Γ or B_ω. Equation (27.22) is then written

$$\sigma_z = \frac{P}{A} + \left(\frac{M_y I_{xx} - M_x I_{xy}}{I_{xx}I_{yy} - I_{xy}^2}\right)x + \left(\frac{M_x I_{yy} - M_y I_{xy}}{I_{xx}I_{yy} - I_{xy}^2}\right)y + \frac{M_\Gamma 2A_\mathrm{R}}{\Gamma_\mathrm{R}} \tag{27.23}$$

As a simple example of the determination of M_Γ consider the open section beam shown in Fig. 27.19 which is subjected to a series of concentrated loads $P_1, P_2, \ldots, P_k, \ldots, P_n$ parallel to its longitudinal axis. The term $\sigma_z t\,\mathrm{d}s$ in $\int_c \sigma_z 2A_\mathrm{R} t\mathrm{d}s$ may be regarded as a concentrated load acting at a point in the wall of the beam. Thus, $\int_c \sigma_z 2A_\mathrm{R} t\,\mathrm{d}s$ becomes $\sum_{k=1}^{n} P_k 2A_{\mathrm{R}k}$ and hence

$$M_\Gamma = \sum_{k=1}^{n} P_\mathrm{R} 2A_{\mathrm{R}k} \tag{27.24}$$

M_Γ is determined for a range of other loading systems in Ref. [2].

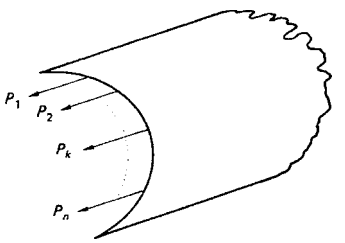

Fig. 27.19 Open section beam subjected to concentrated loads parallel to its longitudinal axis.

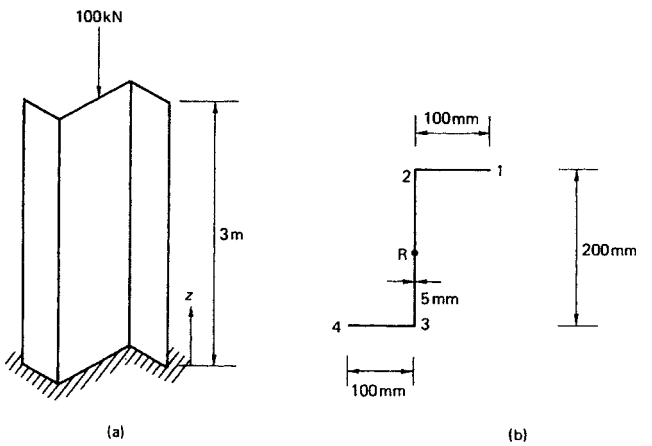

Fig. 27.20 Column of Example 27.2.

Example 27.2

The column shown in Fig. 27.20(a) carries a vertical load of 100 kN. Calculate the angle of twist at the top of the column and the distribution of direct stress at its base. $E = 200\,000\,\text{N/mm}^2$ and $G/E = 0.36$.

The centre of twist R of the column cross-section coincides with its shear centre at the mid-point of the web 23. The distribution of $2A_\text{R}$ is obtained by the method detailed in Example 27.1 and is shown in Fig. 27.21. The torsion bending constant Γ_R is given by Eq. (ii) of Example 27.1 and has the value $2.08 \times 10^{10}\,\text{mm}^6$. The St. Venant torsion constant $J = \Sigma st^3/3 = 0.17 \times 10^5\,\text{mm}^4$ so that $\sqrt{GJ/E\Gamma_\text{R}}$ ($=\mu$ in Eq. (iii) of Example 27.1) $= 0.54 \times 10^{-3}$. Since no torque is applied to the column the solution of Eq. (iii) in Example 27.1 is

$$\frac{\text{d}\theta}{\text{d}z} = C\cosh\mu z + D\sinh\mu z \qquad \text{(i)}$$

At the base of the column warping of the cross-section is suppressed so that, from Eq. (18.19), $\text{d}\theta/\text{d}z = 0$ when $z = 0$. Substituting in Eq. (i) gives $C = 0$. The moment couple at the top of the column is obtained from Eq. (27.24) and is

$$M_\Gamma = P2A_\text{R} = -100 \times 2.5 \times 10^3 = -25 \times 10^5\,\text{kN mm}^2$$

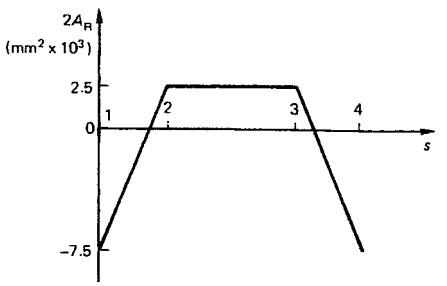

Fig. 27.21 Distribution of area $2A_R$ in the column of Example 27.2.

Therefore, from Eq. (27.21) and noting that $\int_c \sigma_z 2A_R t\,\mathrm{d}s = M_\Gamma$, we have

$$\frac{\mathrm{d}^2\theta}{\mathrm{d}z^2} = \frac{2.5 \times 10^5 \times 10^3}{200\,000 \times 2.08 \times 10^{10}} = 0.06 \times 10^{-6}/\mathrm{mm}^2$$

at $z = 3000$ mm. Substitution in the differential of Eq. (i) gives $D = 0.04 \times 10^{-3}$ so that Eq. (i) becomes

$$\frac{\mathrm{d}\theta}{\mathrm{d}z} = 0.04 \times 10^{-3} \sinh 0.54 \times 10^{-3}\, z \tag{ii}$$

Integration of Eq. (ii) gives

$$\theta = 0.08 \cosh 0.54 \times 10^{-3}\, z + F$$

At the built-in end ($z = 0$) $\theta = 0$ so that $F = -0.08$. Hence

$$\theta = 0.08(\cosh 0.54 \times 10^{-3} z - 1) \tag{iii}$$

At the top of the column ($z = 3000$ mm) the angle of twist is then

$$\theta(\text{top}) = 0.08 \cosh 0.54 \times 10^{-3} \times 3000 = 0.21\,\text{rad}(12.01^\circ)$$

The axial load is applied through the centroid of the cross-section so that no bending occurs and Eq. (27.23) reduces to

$$\sigma_z = \frac{P}{A} + \frac{M_\Gamma 2A_R}{\Gamma_R} \tag{iv}$$

At the base of the column

$$(M_\Gamma)_{z=0} = -E\Gamma_R \left(\frac{\mathrm{d}^2\theta}{\mathrm{d}z^2}\right)_{z=0} \qquad \text{(see Eq. (27.21))}$$

Therefore, from Eq. (ii)

$$(M_\Gamma)_{z=0} = -200\,000 \times 2.08 \times 10^{10} \times 0.02 \times 10^{-6} = -83.2 \times 10^6\,\mathrm{N\,mm}^2$$

The direct stress distribution at the base of the column is then, from Eq. (iv)

$$\sigma_z = -\frac{100 \times 10^3}{400 \times 5} - \frac{83.2 \times 10^6}{2.08 \times 10^{10}} 2A_{\mathrm{R}}$$

or

$$\sigma_z = -50 - 4.0 \times 10^{-3}\, 2A_{\mathrm{R}}$$

The direct stress distribution is therefore linear around the base of the column (see Fig. 27.21) with

$$\sigma_{z_1} = \sigma_{z_4} = 20.0\,\mathrm{N/mm^2}$$
$$\sigma_{z_2} = \sigma_{z_3} = -68.0\,\mathrm{N/mm^2}$$

27.5.1 Shear flow due to M_Γ

The self-equilibrating shear flow distribution, q_Γ, produced by axial constraint is given by

$$\frac{\partial q_\Gamma}{\partial s} = -t\frac{\partial \sigma_\Gamma}{\partial z} \qquad \text{(see derivation of Eq. (27.4))}$$

From the last term on the right-hand side of Eqs (27.23)

$$\frac{\partial \sigma_\Gamma}{\partial z} = \frac{\partial M_\Gamma}{\partial z}\frac{2A_{\mathrm{R}}}{\Gamma_{\mathrm{R}}}$$

From Eq. (27.21)

$$M_\Gamma = -E\Gamma_{\mathrm{R}}\frac{\mathrm{d}^2\theta}{\mathrm{d}z^2}$$

so that

$$\frac{\partial M_\Gamma}{\partial z} = -E\Gamma_{\mathrm{R}}\frac{\mathrm{d}^2\theta}{\mathrm{d}z^3} = T_\Gamma \qquad \text{(see Eq. (27.5))}$$

Hence

$$\frac{\partial q_\Gamma}{\partial s} = -T_\Gamma\frac{2A_{\mathrm{R}}t}{\Gamma_{\mathrm{R}}}$$

and

$$q_\Gamma = -\frac{T_\Gamma}{\Gamma_{\mathrm{R}}}\int_0^s 2A_{\mathrm{R}}t\,\mathrm{d}s \qquad \text{(as before)}$$

References

1 Megson, T. H. G., Extension of the Wagner torsion bending theory to allow for general systems of loading, *The Aeronautical Quarterly*, Vol. XXVI, August 1975.

2 Vlasov, V. Z., Thin-walled elastic beams, *Israel Program for Scientific Translations*, Jerusalem, 1961.

Problems

P.27.1 An axially symmetric beam has the thin-walled cross-section shown in Fig. P.27.1. If the thickness t is constant throughout and making the usual assumptions for a thin-walled cross-section, show that the torsion bending constant Γ_R calculated about the shear centre S is

$$\Gamma_R = \frac{13}{12} d^5 t$$

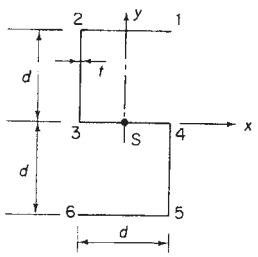

Fig. P.27.1

P.27.2 A uniform beam has the point-symmetric cross-section shown in Fig. P.27.2. Making the usual assumptions for a thin-walled cross-section, show that the torsion-bending constant Γ calculated about the shear centre S is $\Gamma = \frac{8}{3} a^5 t \sin^2 2\alpha$. The thickness t is constant throughout.

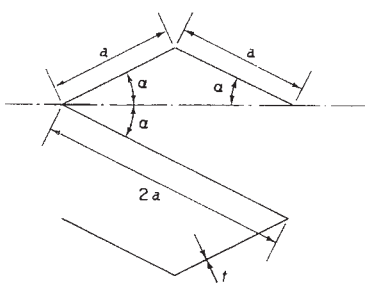

Fig. P.27.2

P.27.3 The thin-walled section shown in Fig. P.27.3 consists of two semicircular arcs of constant thickness t. Show that the torsion bending constant about the shear centre S is

$$\Gamma = \pi^2 r^5 t \left(\frac{\pi}{3} - \frac{3}{\pi} \right)$$

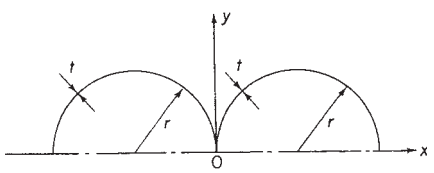

Fig. P.27.3

P.27.4 A thin-walled, I-section beam, of constant wall thickness t, is mounted as a cantilever with its web horizontal. At the tip, a downward force is applied in the plane of one of the flanges, as shown in Fig. P.27.4. Assuming the necessary results of the elementary theory of bending, the St. Venant theory of torsion and the Wagner torsion-bending theory, determine the distribution of direct stress over the cross-section at the supported end.

Take

$$E/G = 2.6 \qquad P = 200\,\text{N}$$
$$h = 75\,\text{mm} \qquad d = 37.5\,\text{mm}$$
$$t = 2.5\,\text{mm} \qquad l = 375\,\text{mm}$$

Ans. $-\sigma_1 = \sigma_3 = 108.9\,\text{N/mm}^2,\ \sigma_6 = -\sigma_5 = 18.9\,\text{N/mm}^2,\ \sigma_2 = \sigma_4 = \sigma_{24} = 0.$

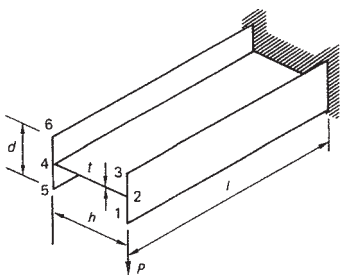

Fig. P.27.4

P.27.5 An open section beam of length $2l$, whose ends are free to warp, consists of two uniform portions of equal length l, as shown in Fig. P.27.5. The cross-sections of the two halves are identical except that the thickness in one half is t and in the other $2t$. If the St. Venant torsion constant and the torsion-bending constant for the portion of thickness t are J and Γ, respectively, show that when the beam is loaded by a constant torque T the relative twist between the free ends is given by

$$\theta = \frac{Tl}{8GJ}\left[9 - \frac{49\sinh 2\mu l}{2\mu l(10\cosh^2 \mu l - 1)}\right]$$

where

$$\mu^2 = GJ/E\Gamma \text{ and } G = \text{shear modulus (constant throughout)}$$

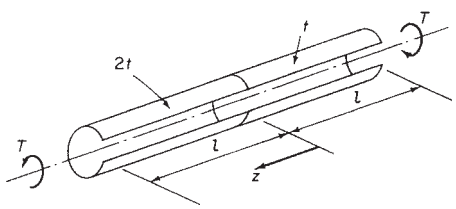

Fig. P.27.5

P.27.6 A thin-walled cantilever beam of length L has the cross-section shown in Fig. P.27.6 and carries a load P positioned as shown at its free end. Determine the

torsion bending constant for the beam section and derive an expression for the angle of twist θ_T at the free end of the beam. Calculate the value of this angle for $P = 100\,\text{N}$, $a = 30\,\text{mm}$, $L = 1000\,\text{mm}$, $t = 2.0\,\text{mm}$, $E = 70\,000\,\text{N/mm}^2$ and $G = 25\,000\,\text{N/mm}^2$

Ans. $\Gamma = 1.25a^5t \quad \theta_T = 6.93°$.

$$\theta_\Gamma = \frac{TL}{GJ}\left[1 - \frac{\tanh \mu L}{\mu L}\right]$$

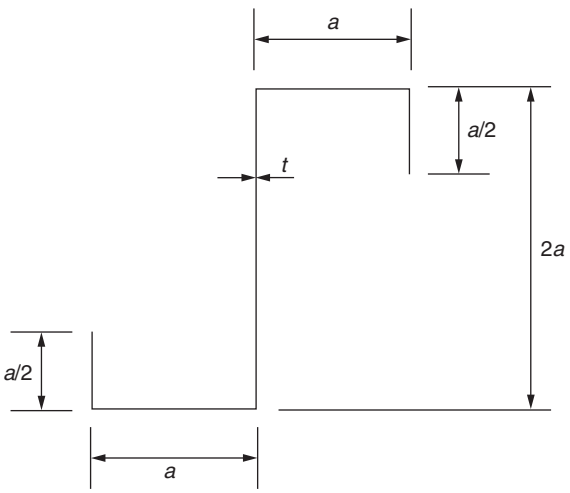

Fig. P.27.6

P.27.7 Determine the torsion bending constant for the thin-walled beam shown in Fig. P.27.7 and also derive an expression for the angle of twist at its free end.

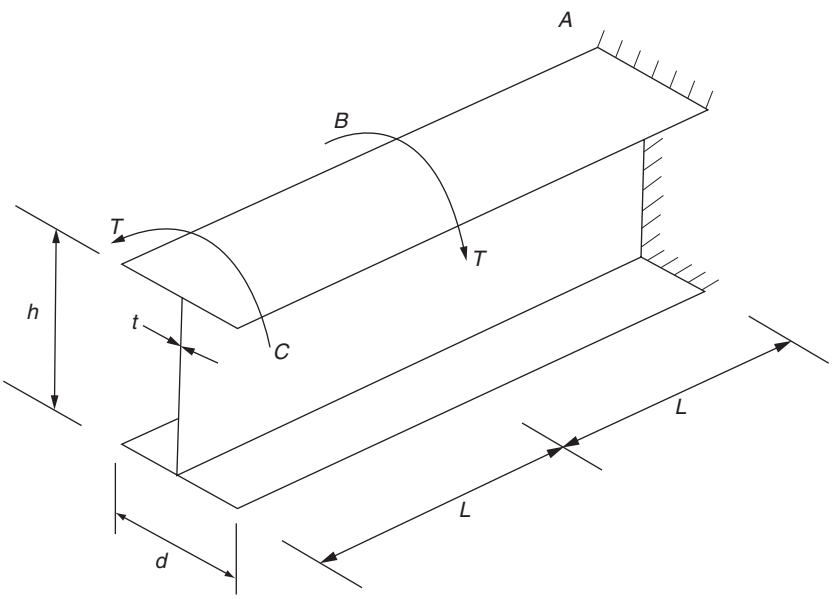

Fig. P.27.7

Ans. $\Gamma = th^2d^3/24 \quad \theta_T = \dfrac{T}{GJ}\left(L - \dfrac{\sinh \mu L}{\mu L \cosh 2\mu L}\right)$

P.27.8 A thin-walled cantilever beam of length L has the cross-section shown in Fig. P.27.8 and carries an anticlockwise torque T at its free end. Determine the torsion bending constant for the beam section and derive an expression for the rate of twist along the length of the beam.

In a practical case the beam supports a shear load of 150 N at its free end applied vertically upwards in the plane of the web. If $L = 500\,\text{mm}$, $a = 20\,\text{mm}$, $t = 1.0\,\text{mm}$ and $G/E = 0.3$ calculate the value of direct stress at the point 2 including both axial constraint and elementary bending stresses.

Ans. $\Gamma = 7a^5t/24 \quad \dfrac{\mathrm{d}\theta}{\mathrm{d}z} = \dfrac{T}{GJ}\left(1 - \dfrac{\cosh \mu(L-z)}{\cosh \mu L}\right)$

$125.7\,\text{N/mm}^2$ (compression).

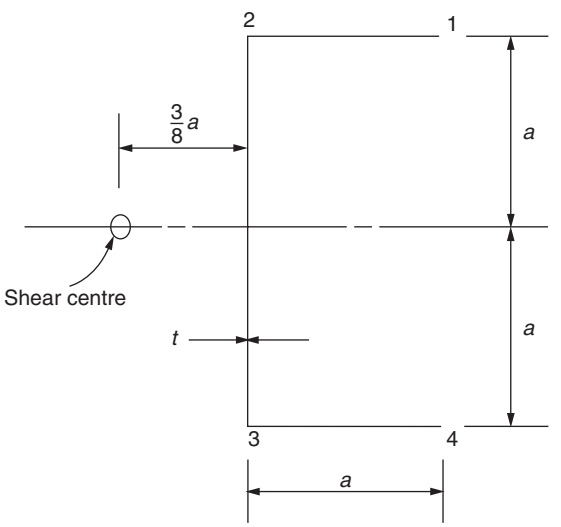

Fig. P.27.8

P.27.9 Calculate the direct stress distribution (including both axial constraint and elementary bending stresses) at the built-in end of the cantilever beam shown in

Fig. P.27.9 for the case when $w = 0.5$ N/mm, $L = 1500$ mm, $h = 200$ mm, $d = 50$ mm, $t = 5$ mm and $E/G = 3.0$.

Ans. $\sigma_1 = -\sigma_3 = 197.5\ \text{N/mm}^2 \quad \sigma_2 = \sigma_5 = 0 \quad \sigma_4 = -\sigma_6 = -72.5\ \text{N/mm}^2$.

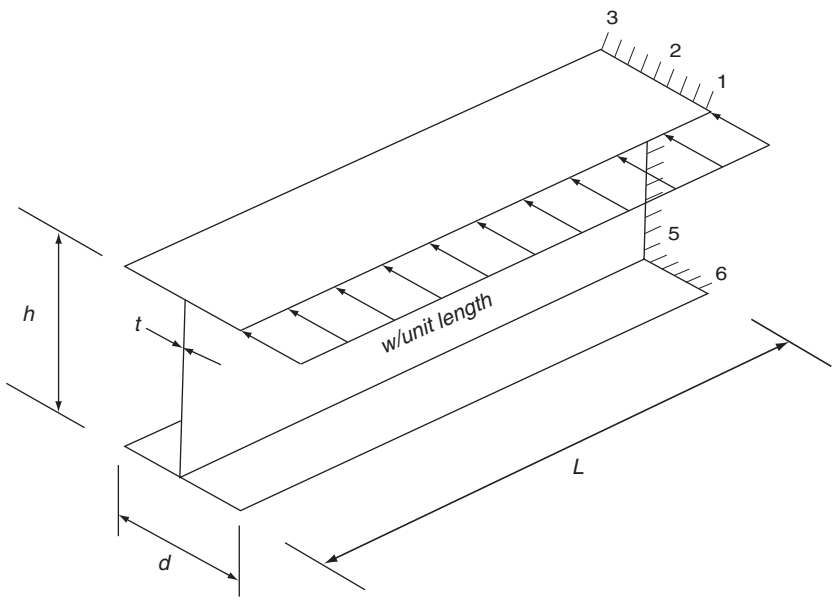

Fig. P.27.9

21

Wing spars and box beams

In Chapters 16–18 we established the basic theory for the analysis of open and closed section thin-walled beams subjected to bending, shear and torsional loads. In addition, in Chapter 20, we saw how complex stringer stiffened sections could be idealized into sections more amenable to analysis. We shall now extend this analysis to actual aircraft components including, in this chapter, wing spars and box beams. In subsequent chapters we shall investigate the analysis of fuselages, wings, frames and ribs, and consider the effects of cut-outs in wings and fuselages. Finally, in Chapter 25, an introduction is given to the analysis of components fabricated from composite materials.

Aircraft structural components are, as we saw in Chapter 12, complex, consisting usually of thin sheets of metal stiffened by arrangements of stringers. These structures are highly redundant and require some degree of simplification or idealization before they can be analysed. The analysis presented here is therefore approximate and the degree of accuracy obtained depends on the number of simplifying assumptions made. A further complication arises in that factors such as warping restraint, structural and loading discontinuities and shear lag significantly affect the analysis; we shall investigate these effects in some simple structural components in Chapters 26 and 27. Generally, a high degree of accuracy can only be obtained by using computer-based techniques such as the finite element method (see Chapter 6). However, the simpler, quicker and cheaper approximate methods can be used to advantage in the preliminary stages of design when several possible structural alternatives are being investigated; they also provide an insight into the physical behaviour of structures which computer-based techniques do not.

Major aircraft structural components such as wings and fuselages are usually tapered along their lengths for greater structural efficiency. Thus, wing sections are reduced both chordwise and in depth along the wing span towards the tip and fuselage sections aft of the passenger cabin taper to provide a more efficient aerodynamic and structural shape.

The analysis of open and closed section beams presented in Chapters 16–18 assumes that the beam sections are uniform. The effect of taper on the prediction of direct stresses produced by bending is minimal if the taper is small and the section properties are calculated at the particular section being considered; Eqs (16.18)–(16.22) may therefore be used with reasonable accuracy. On the other hand, the calculation of shear stresses in beam webs can be significantly affected by taper.

21.1 Tapered wing spar

Consider first the simple case of a beam, for example a wing spar, positioned in the yz plane and comprising two flanges and a web: an elemental length δz of the beam is shown in Fig. 21.1. At the section z the beam is subjected to a positive bending moment M_x and a positive shear force S_y. The bending moment resultants $P_{z,1}$ and $P_{z,2}$ are parallel to the z axis of the beam. For a beam in which the flanges are assumed to resist all the direct stresses, $P_{z,1} = M_x/h$ and $P_{z,2} = -M_x/h$. In the case where the web is assumed to be fully effective in resisting direct stress, $P_{z,1}$ and $P_{z,2}$ are determined by multiplying the direct stresses $\sigma_{z,1}$ and $\sigma_{z,2}$ found using Eq. (16.18) or (16.19) by the flange areas B_1 and B_2. $P_{z,1}$ and $P_{z,2}$ are the components in the z direction of the axial loads P_1 and P_2 in the flanges. These have components $P_{y,1}$ and $P_{y,2}$ parallel to the y axis given by

$$P_{y,1} = P_{z,1}\frac{\delta y_1}{\delta z} \quad P_{y,2} = -P_{z,2}\frac{\delta y_2}{\delta z} \tag{21.1}$$

in which, for the direction of taper shown, δy_2 is negative. The axial load in flange ① is given by

$$P_1 = (P_{z,1}^2 + P_{y,1}^2)^{1/2}$$

Substituting for $P_{y,1}$ from Eq. (21.1) we have

$$P_1 = P_{z,1}\frac{(\delta z^2 + \delta y_1^2)^{1/2}}{\delta z} = \frac{P_{z,1}}{\cos\alpha_1} \tag{21.2}$$

Similarly

$$P_2 = \frac{P_{z,2}}{\cos\alpha_2} \tag{21.3}$$

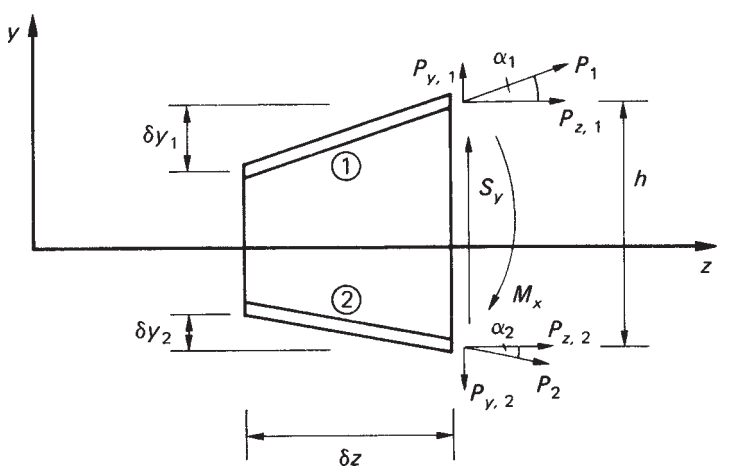

Fig. 21.1 Effect of taper on beam analysis.

The internal shear force S_y comprises the resultant $S_{y,w}$ of the web shear flows together with the vertical components of P_1 and P_2. Thus

$$S_y = S_{y,w} + P_{y,1} - P_{y,2}$$

or

$$S_y = S_{y,w} + P_{z,1}\frac{\delta y_1}{\delta z} + P_{z,2}\frac{\delta y_2}{\delta z} \tag{21.4}$$

so that

$$S_{y,w} = S_y - P_{z,1}\frac{\delta y_1}{\delta z} - P_{z,2}\frac{\delta y_2}{\delta z} \tag{21.5}$$

Again we note that δy_2 in Eqs (21.4) and (21.5) is negative. Equation (21.5) may be used to determine the shear flow distribution in the web. For a completely idealized beam the web shear flow is constant through the depth and is given by $S_{y,w}/h$. For a beam in which the web is fully effective in resisting direct stresses the web shear flow distribution is found using Eq. (20.6) in which S_y is replaced by $S_{y,w}$ and which, for the beam of Fig. 21.1, would simplify to

$$q_s = -\frac{S_{y,w}}{I_{xx}}\left(\int_0^s t_D y\,\mathrm{d}s + B_1 y_1\right) \tag{21.6}$$

or

$$q_s = -\frac{S_{y,w}}{I_{xx}}\left(\int_0^s t_D y\,\mathrm{d}s + B_2 y_2\right) \tag{21.7}$$

Example 21.1

Determine the shear flow distribution in the web of the tapered beam shown in Fig. 21.2, at a section midway along its length. The web of the beam has a thickness of 2 mm

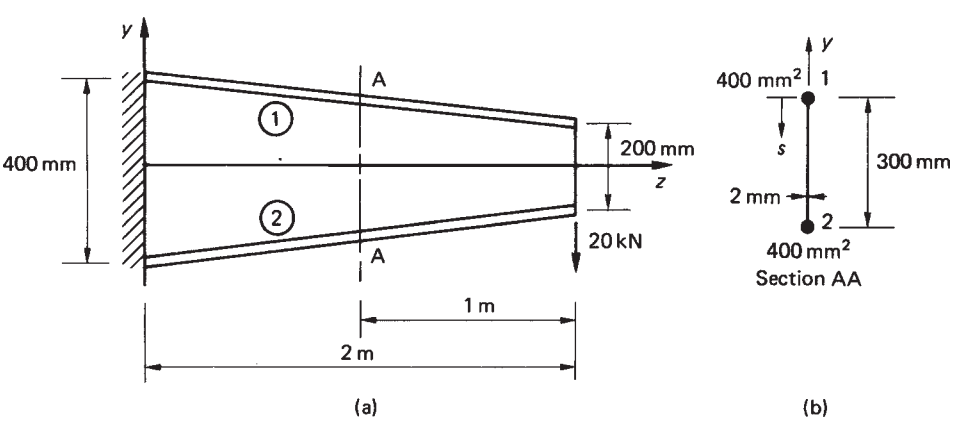

Fig. 21.2 Tapered beam of Example 21.1.

and is fully effective in resisting direct stress. The beam tapers symmetrically about its horizontal centroidal axis and the cross-sectional area of each flange is 400 mm^2.

The internal bending moment and shear load at the section AA produced by the externally applied load are, respectively

$$M_x = 20 \times 1 = 20\,\text{kN m} \quad S_y = -20\,\text{kN}$$

The direct stresses parallel to the z axis in the flanges at this section are obtained either from Eqs (16.18) or (16.19) in which $M_y = 0$ and $I_{xy} = 0$. Thus, from Eq. (16.18)

$$\sigma_z = \frac{M_x y}{I_{xx}} \tag{i}$$

in which

$$I_{xx} = 2 \times 400 \times 150^2 + 2 \times 300^3/12$$

i.e.

$$I_{xx} = 22.5 \times 10^6\,\text{mm}^4$$

Hence

$$\sigma_{z,1} = -\sigma_{z,2} = \frac{20 \times 10^6 \times 150}{22.5 \times 10^6} = 133.3\,\text{N/mm}^2$$

The components parallel to the z axis of the axial loads in the flanges are therefore

$$P_{z,1} = -P_{z,2} = 133.3 \times 400 = 53\,320\,\text{N}$$

The shear load resisted by the beam web is then, from Eq. (21.5)

$$S_{y,w} = -20 \times 10^3 - 53\,320\frac{\delta y_1}{\delta z} + 53\,320\frac{\delta y_2}{\delta z}$$

in which, from Figs 21.1 and 21.2, we see that

$$\frac{\delta y_1}{\delta z} = \frac{-100}{2 \times 10^3} = -0.05 \quad \frac{\delta y_2}{\delta z} = \frac{100}{2 \times 10^3} = 0.05$$

Hence

$$S_{y,w} = -20 \times 10^3 + 53\,320 \times 0.05 + 53\,320 \times 0.05 = -14\,668\,\text{N}$$

The shear flow distribution in the web follows either from Eq. (21.6) or Eq. (21.7) and is (see Fig. 21.2(b))

$$q_{12} = \frac{14\,668}{22.5 \times 10^6}\left(\int_0^s 2(150 - s)\,\text{d}s + 400 \times 150\right)$$

i.e.

$$q_{12} = 6.52 \times 10^{-4}(-s^2 + 300s + 60\,000) \tag{ii}$$

The maximum value of q_{12} occurs when $s = 150$ mm and q_{12} (max) = 53.8 N/mm. The values of shear flow at points 1 ($s = 0$) and 2 ($s = 300$ mm) are $q_1 = 39.1$ N/mm and $q_2 = 39.1$ N/mm; the complete distribution is shown in Fig. 21.3.

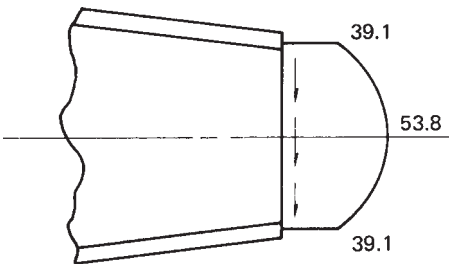

Fig. 21.3 Shear flow (N/mm) distribution at Section AA in Example 21.1.

21.2 Open and closed section beams

We shall now consider the more general case of a beam tapered in two directions along its length and comprising an arrangement of booms and skin. Practical examples of such a beam are complete wings and fuselages. The beam may be of open or closed section; the effects of taper are determined in an identical manner in either case.

Figure 21.4(a) shows a short length δz of a beam carrying shear loads S_x and S_y at the section z; S_x and S_y are positive when acting in the directions shown. Note that if the beam were of open cross-section the shear loads would be applied through its shear centre so that no twisting of the beam occurred. In addition to shear loads the beam is subjected to bending moments M_x and M_y which produce direct stresses σ_z in the booms and skin. Suppose that in the rth boom the direct stress in a direction parallel to the z axis is $\sigma_{z,r}$, which may be found using either Eq. (16.18) or Eq. (16.19). The component $P_{z,r}$ of the axial load P_r in the rth boom is then given by

$$P_{z,r} = \sigma_{z,r} B_r \tag{21.8}$$

where B_r is the cross-sectional area of the rth boom.

From Fig. 21.4(b)

$$P_{y,r} = P_{z,r} \frac{\delta y_r}{\delta z} \tag{21.9}$$

Further, from Fig. 21.4(c)

$$P_{x,r} = P_{y,r} \frac{\delta x_r}{\delta y_r}$$

or, substituting for $P_{y,r}$ from Eq. (21.9)

$$P_{x,r} = P_{z,r} \frac{\delta x_r}{\delta z} \tag{21.10}$$

The axial load P_r is then given by

$$P_r = (P_{x,r}^2 + P_{y,r}^2 + P_{z,r}^2)^{1/2} \tag{21.11}$$

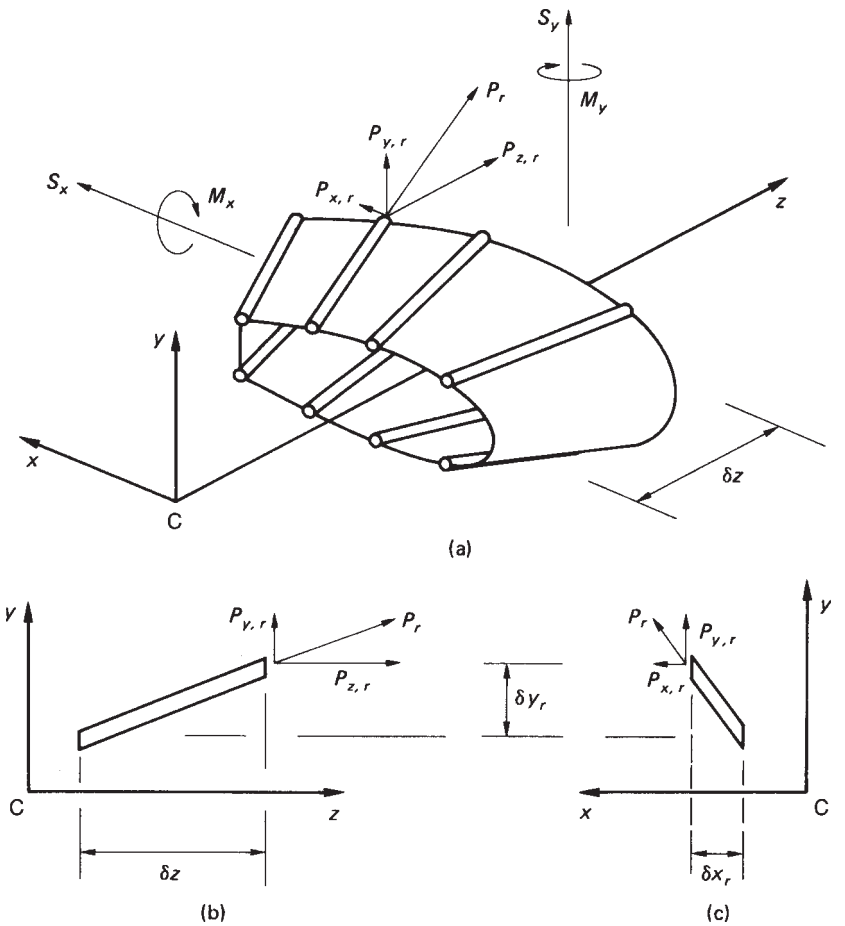

Fig. 21.4 Effect of taper on the analysis of open and closed section beams.

or, alternatively

$$P_r = P_{z,r}\frac{(\delta x_r^2 + \delta y_r^2 + \delta z^2)^{1/2}}{\delta z} \tag{21.12}$$

The applied shear loads S_x and S_y are reacted by the resultants of the shear flows in the skin panels and webs, together with the components $P_{x,r}$ and $P_{y,r}$ of the axial loads in the booms. Therefore, if $S_{x,w}$ and $S_{y,w}$ are the resultants of the skin and web shear flows and there is a total of m booms in the section

$$S_x = S_{x,w} + \sum_{r=1}^{m} P_{x,r} \quad S_y = S_{y,w} + \sum_{r=1}^{m} P_{y,r} \tag{21.13}$$

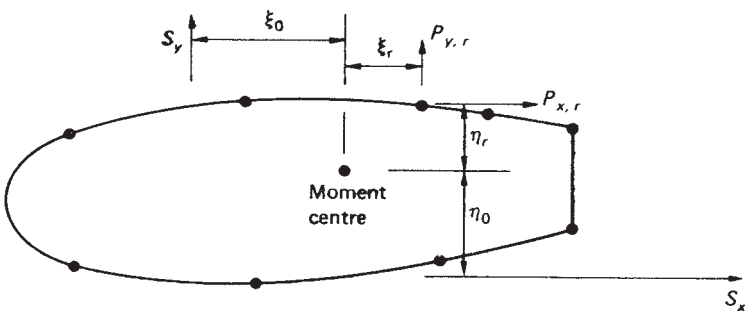

Fig. 21.5 Modification of moment equation in shear of closed section beams due to boom load.

Substituting in Eq. (21.13) for $P_{x,r}$ and $P_{y,r}$ from Eqs (21.10) and (21.9) we have

$$S_x = S_{x,w} + \sum_{r=1}^{m} P_{z,r}\frac{\delta x_r}{\delta z} \quad S_y = S_{y,w} + \sum_{r=1}^{m} P_{z,r}\frac{\delta y_r}{\delta z} \tag{21.14}$$

Hence

$$S_{x,w} = S_x - \sum_{r=1}^{m} P_{z,r}\frac{\delta x_r}{\delta z} \quad S_{y,w} = S_y - \sum_{r=1}^{m} P_{z,r}\frac{\delta y_r}{\delta z} \tag{21.15}$$

The shear flow distribution in an open section beam is now obtained using Eq. (20.6) in which S_x is replaced by $S_{x,w}$ and S_y by $S_{y,w}$ from Eq. (21.15). Similarly for a closed section beam, S_x and S_y in Eq. (20.11) are replaced by $S_{x,w}$ and $S_{y,w}$. In the latter case the moment equation (Eq. (17.17)) requires modification due to the presence of the boom load components $P_{x,r}$ and $P_{y,r}$. Thus from Fig. 21.5 we see that Eq. (17.17) becomes

$$S_x\eta_0 - S_y\xi_0 = \oint q_b p \, \mathrm{d}s + 2Aq_{s,0} - \sum_{r=1}^{m} P_{x,r}\eta_r + \sum_{r=1}^{m} P_{y,r}\xi_r \tag{21.16}$$

Equation (21.16) is directly applicable to a tapered beam subjected to forces positioned in relation to the moment centre as shown. Care must be taken in a particular problem to ensure that the moments of the forces are given the correct sign.

Example 21.2

The cantilever beam shown in Fig. 21.6 is uniformly tapered along its length in both x and y directions and carries a load of 100 kN at its free end. Calculate the forces in the booms and the shear flow distribution in the walls at a section 2 m from the built-in end if the booms resist all the direct stresses while the walls are effective only in shear. Each corner boom has a cross-sectional area of 900 mm^2 while both central booms have cross-sectional areas of 1200 mm^2.

The internal force system at a section 2 m from the built-in end of the beam is

$$S_y = 100\,\text{kN} \quad S_x = 0 \quad M_x = -100 \times 2 = -200\,\text{kN m} \quad M_y = 0$$

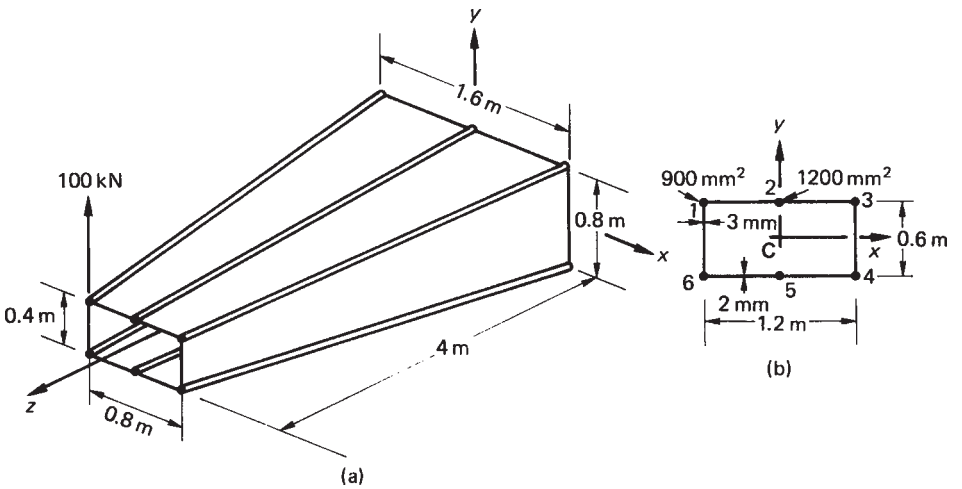

Fig. 21.6 (a) Beam of Example 21.2; (b) section 2 m from built-in end.

The beam has a doubly symmetrical cross-section so that $I_{xy} = 0$ and Eq. (16.18) reduces to

$$\sigma_z = \frac{M_x y}{I_{xx}} \tag{i}$$

in which, for the beam section shown in Fig. 21.6(b)

$$I_{xx} = 4 \times 900 \times 300^2 + 2 \times 1200 \times 300^2 = 5.4 \times 10^8 \,\text{mm}^4$$

Then

$$\sigma_{z,r} = \frac{-200 \times 10^6}{5.4 \times 10^8} y_r$$

or

$$\sigma_{z,r} = -0.37 y_r \tag{ii}$$

Hence

$$P_{z,r} = -0.37 y_r B_r \tag{iii}$$

The value of $P_{z,r}$ is calculated from Eq. (iii) in column ② in Table 21.1; $P_{x,r}$ and $P_{y,r}$ follow from Eqs (21.10) and (21.9), respectively in columns ⑤ and ⑥. The axial load P_r, column ⑦, is given by $[②^2 + ⑤^2 + ⑥^2]^{1/2}$ and has the same sign as $P_{z,r}$ (see Eq. (21.12)). The moments of $P_{x,r}$ and $P_{y,r}$ are calculated for a moment centre at the centre of symmetry with anticlockwise moments taken as positive. Note that in Table 21.1, $P_{x,r}$ and $P_{y,r}$ are positive when they act in the positive directions of the section x and y axes, respectively; the distances η_r and ξ_r of the lines of action of $P_{x,r}$ and

Table 21.1

① Boom	② $P_{z,r}$ (kN)	③ $\delta x_r/\delta z$	④ $\delta y_r/\delta z$	⑤ $P_{x,r}$ (kN)	⑥ $P_{y,r}$ (kN)	⑦ P_r (kN)	⑧ ξ_r (m)	⑨ η_r (m)	⑩ $P_{x,r}\eta_r$ (kN m)	⑪ $P_{y,r}\xi_r$ (kN m)
1	−100	0.1	−0.05	−10	5	−101.3	0.6	0.3	3	−3
2	−133	0	−0.05	0	6.7	−177.3	0	0.3	0	0
3	−100	−0.1	−0.05	10	5	−101.3	0.6	0.3	−3	3
4	100	−0.1	0.05	−10	5	101.3	0.6	0.3	−3	3
5	133	0	0.05	0	6.7	177.3	0	0.3	0	0
6	100	0.1	0.05	10	5	101.3	0.6	0.3	3	−3

$P_{y,r}$ from the moment centre are not given signs since it is simpler to determine the sign of each moment, $P_{x,r}\eta_r$ and $P_{y,r}\xi_r$, by referring to the directions of $P_{x,r}$ and $P_{y,r}$ individually.
From column ⑥

$$\sum_{r=1}^{6} P_{y,r} = 33.4\,\text{kN}$$

From column ⑩

$$\sum_{r=1}^{6} P_{x,r}\eta_r = 0$$

From column ⑪

$$\sum_{r=1}^{6} P_{y,r}\xi_r = 0$$

From Eq. (21.15)

$$S_{x,w} = 0 \quad S_{y,w} = 100 - 33.4 = 66.6\,\text{kN}$$

The shear flow distribution in the walls of the beam is now found using the method described in Section 20.3. Since, for this beam, $I_{xy} = 0$ and $S_x = S_{x,w} = 0$, Eq. (20.11) reduces to

$$q_s = \frac{-S_{y,w}}{I_{xx}} \sum_{r=1}^{n} B_r y_r + q_{s,0} \tag{iv}$$

We now 'cut' one of the walls, say 16. The resulting 'open section' shear flow is given by

$$q_\text{b} = -\frac{66.6 \times 10^3}{5.4 \times 10^8} \sum_{r=1}^{n} B_r y_r$$

or

$$q_{\mathrm{b}} = -1.23 \times 10^{-4} \sum_{r=1}^{n} B_r y_r \qquad \text{(v)}$$

Thus

$$\begin{aligned}
q_{\mathrm{b},16} &= 0 \\
q_{\mathrm{b},12} &= 0 - 1.23 \times 10^{-4} \times 900 \times 300 = -33.2\,\mathrm{N/mm} \\
q_{\mathrm{b},23} &= -33.2 - 1.23 \times 10^{-4} \times 1200 \times 300 = -77.5\,\mathrm{N/mm} \\
q_{\mathrm{b},34} &= -77.5 - 1.23 \times 10^{-4} \times 900 \times 300 = -110.7\,\mathrm{N/mm} \\
q_{\mathrm{b},45} &= -77.5\,\mathrm{N/mm}\ \text{(from symmetry)} \\
q_{\mathrm{b},56} &= -33.2\,\mathrm{N/mm}\ \text{(from symmetry)}
\end{aligned}$$

giving the distribution shown in Fig. 21.7. Taking moments about the centre of symmetry we have, from Eq. (21.16)

$$\begin{aligned}
-100 \times 10^3 \times 600 = {} & 2 \times 33.2 \times 600 \times 300 + 2 \times 77.5 \times 600 \times 300 \\
& + 110.7 \times 600 \times 600 + 2 \times 1200 \times 600 q_{s,0}
\end{aligned}$$

from which $q_{s,0} = -97.0\,\mathrm{N/mm}$ (i.e. clockwise). The complete shear flow distribution is found by adding the value of $q_{s,0}$ to the q_{b} shear flow distribution of Fig. 21.7 and is shown in Fig. 21.8.

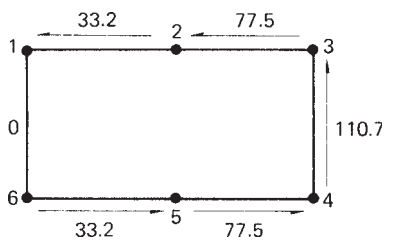

Fig. 21.7 'Open section' shear flow (N/mm) distribution in beam section of Example 21.2.

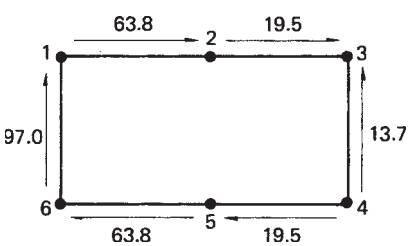

Fig. 21.8 Shear flow (N/mm) distribution in beam section of Example 21.2.

21.3 Beams having variable stringer areas

In many aircraft, structural beams, such as wings, have stringers whose cross-sectional areas vary in the spanwise direction. The effects of this variation on the determination of shear flow distribution cannot therefore be found by the methods described in Section 20.3 which assume constant boom areas. In fact, as we noted in Section 20.3, if the stringer stress is made constant by varying the area of cross-section there is no change in shear flow as the stringer/boom is crossed.

The calculation of shear flow distributions in beams having variable stringer areas is based on the alternative method for the calculation of shear flow distributions described in Section 20.3 and illustrated in the alternative solution of Example 20.3. The stringer loads $P_{z,1}$ and $P_{z,2}$ are calculated at two sections z_1 and z_2 of the beam a convenient distance apart. We assume that the stringer load varies linearly along its length so that the change in stringer load per unit length of beam is given by

$$\Delta P = \frac{P_{z,1} - P_{z,2}}{z_1 - z_2}$$

The shear flow distribution follows as previously described.

Example 21.3

Solve Example 21.2 by considering the differences in boom load at sections of the beam either side of the specified section.

In this example the stringer areas do not vary along the length of the beam but the method of solution is identical.

We are required to find the shear flow distribution at a section 2 m from the built-in end of the beam. We therefore calculate the boom loads at sections, say 0.1 m either side of this section. Thus, at a distance 2.1 m from the built-in end

$$M_x = -100 \times 1.9 = -190\,\text{kN m}$$

The dimensions of this section are easily found by proportion and are width = 1.18 m, depth = 0.59 m. Thus the second moment of area is

$$I_{xx} = 4 \times 900 \times 295^2 + 2 \times 1200 \times 295^2 = 5.22 \times 10^8\,\text{mm}^4$$

and

$$\sigma_{z,r} = \frac{-190 \times 10^6}{5.22 \times 10^8} y_r = -0.364 y_r$$

Hence

$$P_1 = P_3 = -P_4 = -P_6 = -0.364 \times 295 \times 900 = -96\,642\,\text{N}$$

and

$$P_2 = -P_5 = -0.364 \times 295 \times 1200 = -128\,856\,\text{N}$$

At a section 1.9 m from the built-in end

$$M_x = -100 \times 2.1 = -210\,\text{kN m}$$

and the section dimensions are width = 1.22 m, depth = 0.61 m so that

$$I_{xx} = 4 \times 900 \times 305^2 + 2 \times 1200 \times 305^2 = 5.58 \times 10^8\,\text{mm}^4$$

and

$$\sigma_{z,r} = \frac{-210 \times 10^6}{5.58 \times 10^8} y_r = -0.376 y_r$$

Hence

$$P_1 = P_3 = -P_4 = -P_6 = -0.376 \times 305 \times 900 = -103\,212\,\text{N}$$

and

$$P_2 = -P_5 = -0.376 \times 305 \times 1200 = -137\,616\,\text{N}$$

Thus, there is an increase in compressive load of $103\,212 - 96\,642 = 6570$ N in booms 1 and 3 and an increase in tensile load of 6570 N in booms 4 and 6 between the two sections. Also, the compressive load in boom 2 increases by $137\,616 - 128\,856 = 8760$ N while the tensile load in boom 5 increases by 8760 N. Therefore, the change in boom load per unit length is given by

$$\Delta P_1 = \Delta P_3 = -\Delta P_4 = -\Delta P_6 = \frac{6570}{200} = 32.85\,\text{N}$$

and

$$\Delta P_2 = -\Delta P_5 = \frac{8760}{200} = 43.8\,\text{N}$$

The situation is illustrated in Fig. 21.9. Suppose now that the shear flows in the panels 12, 23, 34, etc. are q_{12}, q_{23}, q_{34}, etc. and consider the equilibrium of boom 2, as shown in Fig. 21.10, with adjacent portions of the panels 12 and 23. Thus

$$q_{23} + 43.8 - q_{12} = 0$$

or

$$q_{23} = q_{12} - 43.8$$

Similarly

$$\begin{aligned} q_{34} &= q_{23} - 32.85 = q_{12} - 76.65 \\ q_{45} &= q_{34} + 32.85 = q_{12} - 43.8 \\ q_{56} &= q_{45} + 43.8 = q_{12} \\ q_{61} &= q_{45} + 32.85 = q_{12} + 32.85 \end{aligned}$$

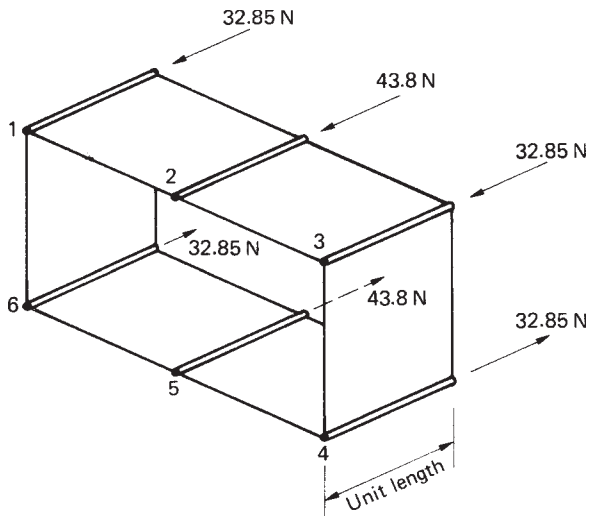

Fig. 21.9 Change in boom loads/unit length of beam.

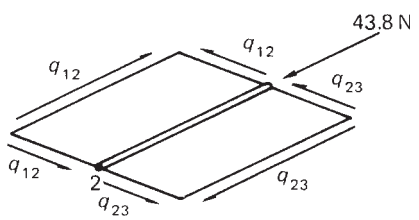

Fig. 21.10 Equilibrium of boom.

The moment resultant of the internal shear flows, together with the moments of the components $P_{y,r}$ of the boom loads about any point in the cross-section, is equivalent to the moment of the externally applied load about the same point. We note from Example 21.2 that for moments about the centre of symmetry

$$\sum_{r=1}^{6} P_{x,r}\eta_r = 0 \quad \sum_{r=1}^{6} P_{y,r}\xi_r = 0$$

Therefore, taking moments about the centre of symmetry

$$\begin{aligned} 100 \times 10^3 \times 600 = {} & 2q_{12} \times 600 \times 300 + 2(q_{12} - 43.8)600 \times 300 \\ & + (q_{12} - 76.65)600 \times 600 + (q_{12} + 32.85)600 \times 600 \end{aligned}$$

from which

$$q_{12} = 62.5\,\text{N/mm}$$

whence

$$q_{23} = 19.7\,\text{N/mm} \quad q_{34} = -13.2\,\text{N/mm} \quad q_{45} = 19.7\,\text{N/mm},$$
$$q_{56} = 63.5\,\text{N/mm} \quad q_{61} = 96.4\,\text{N/mm}$$

so that the solution is almost identical to the longer exact solution of Example 21.2.

The shear flows q_{12}, q_{23}, etc. induce complementary shear flows q_{12}, q_{23}, etc. in the panels in the longitudinal direction of the beam; these are, in fact, the average shear flows between the two sections considered. For a complete beam analysis the above procedure is applied to a series of sections along the span. The distance between adjacent sections may be taken to be any convenient value; for actual wings distances of the order of 350–700 mm are usually chosen. However, for very small values small percentage errors in $P_{z,1}$ and $P_{z,2}$ result in large percentage errors in ΔP. On the other hand, if the distance is too large the average shear flow between two adjacent sections may not be quite equal to the shear flow midway between the sections.

Problems

P.21.1 A wing spar has the dimensions shown in Fig. P.21.1 and carries a uniformly distributed load of 15 kN/m along its complete length. Each flange has a cross-sectional area of 500 mm^2 with the top flange being horizontal. If the flanges are assumed to resist all direct loads while the spar web is effective only in shear, determine the flange loads and the shear flows in the web at sections 1 and 2 m from the free end.

Ans. 1 m from free end: $P_U = 25\,\text{kN}$ (tension), $P_L = 25.1\,\text{kN}$ (compression), $q = 41.7\,\text{N/mm}$.

2 m from free end: $P_U = 75\,\text{kN}$ (tension), $P_L = 75.4\,\text{kN}$ (compression), $q = 56.3\,\text{N/mm}$.

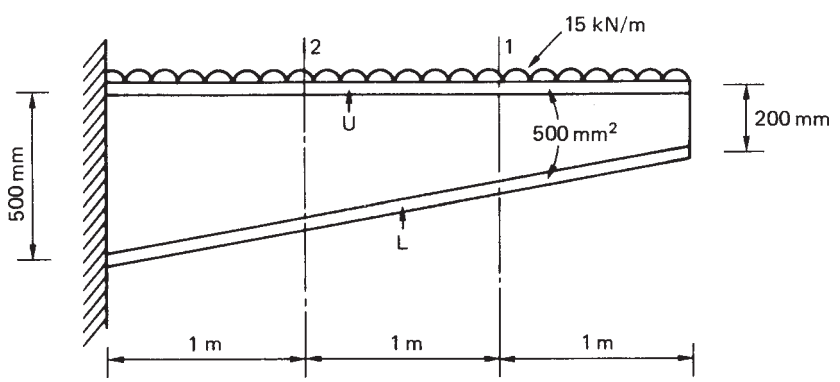

Fig. P.21.1

P.21.2 If the web in the wing spar of P.21.1 has a thickness of 2 mm and is fully effective in resisting direct stresses, calculate the maximum value of shear flow in the web at a section 1 m from the free end of the beam.

Ans. 46.8 N/mm.

P.21.3 Calculate the shear flow distribution and the stringer and flange loads in the beam shown in Fig. P.21.3 at a section 1.5 m from the built-in end. Assume that the skin and web panels are effective in resisting shear stress only; the beam tapers symmetrically in a vertical direction about its longitudinal axis.

Ans. $q_{13} = q_{42} = 36.9\,\text{N/mm}$, $q_{35} = q_{64} = 7.3\text{N/mm}$, $q_{21} = 96.2\,\text{N/mm}$, $q_{65} = 22.3\,\text{N/mm}$.

$$P_2 = -P_1 = 133.3\,\text{kN},\ P_4 = P_6 = -P_3 = -P_5 = 66.7\,\text{kN}.$$

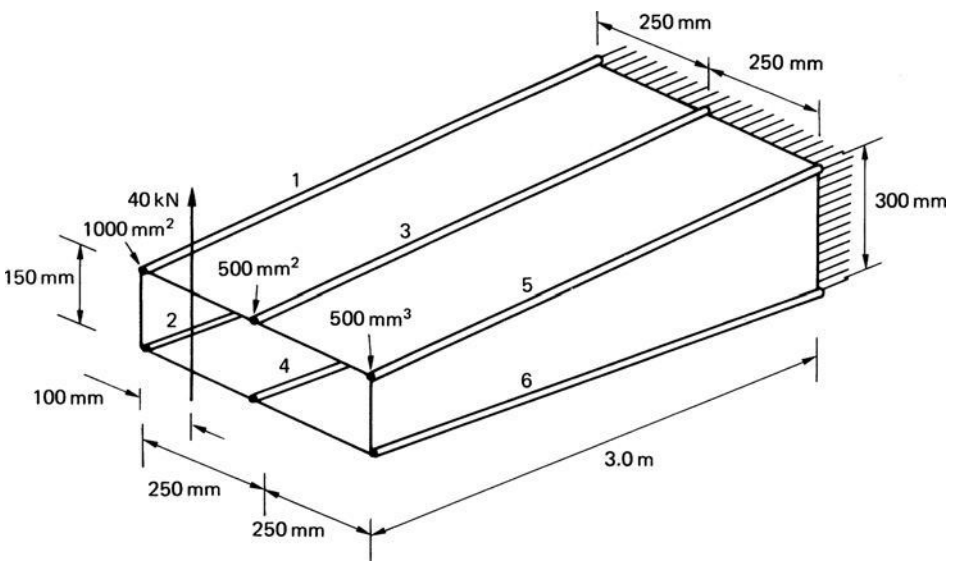

Fig. P.21.3

22

Fuselages

Aircraft fuselages consist, as we saw in Chapter 12, of thin sheets of material stiffened by large numbers of longitudinal stringers together with transverse frames. Generally, they carry bending moments, shear forces and torsional loads which induce axial stresses in the stringers and skin together with shear stresses in the skin; the resistance of the stringers to shear forces is generally ignored. Also, the distance between adjacent stringers is usually small so that the variation in shear flow in the connecting panel will be small. It is therefore reasonable to assume that the shear flow is constant between adjacent stringers so that the analysis simplifies to the analysis of an idealized section in which the stringers/booms carry all the direct stresses while the skin is effective only in shear. The direct stress carrying capacity of the skin may be allowed for by increasing the stringer/boom areas as described in Section 20.3. The analysis of fuselages therefore involves the calculation of direct stresses in the stringers and the shear stress distributions in the skin; the latter are also required in the analysis of transverse frames, as we shall see in Chapter 24.

22.1 Bending

The skin/stringer arrangement is idealized into one comprising booms and skin as described in Section 20.3. The direct stress in each boom is then calculated using either Eqs (16.18) or (16.19) in which the reference axes and the section properties refer to the direct stress carrying areas of the cross-section.

Example 22.1

The fuselage of a light passenger carrying aircraft has the circular cross-section shown in Fig. 22.1(a). The cross-sectional area of each stringer is 100 mm^2 and the vertical distances given in Fig. 22.1(a) are to the mid-line of the section wall at the corresponding stringer position. If the fuselage is subjected to a bending moment of 200 kN m applied in the vertical plane of symmetry, at this section, calculate the direct stress distribution.

The section is first idealized using the method described in Section 20.3. As an approximation we shall assume that the skin between adjacent stringers is flat so that

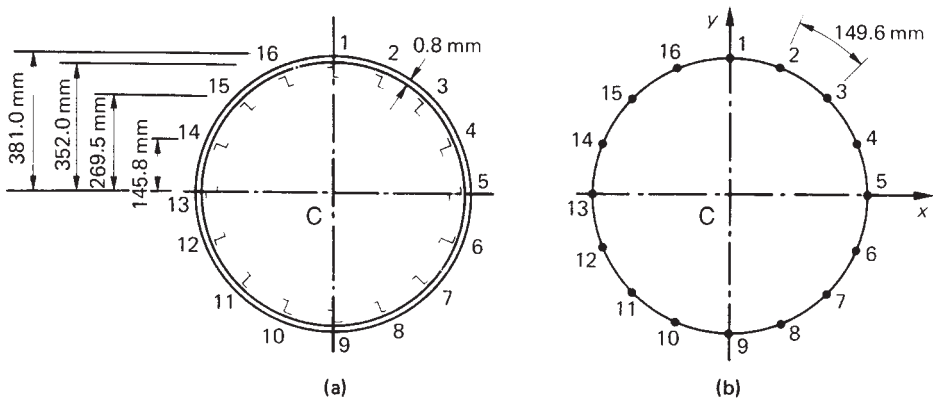

Fig. 22.1 (a) Actual fuselage section; (b) idealized fuselage section.

we may use either Eq. (20.1) or Eq. (20.2) to determine the boom areas. From symmetry $B_1 = B_9$, $B_2 = B_8 = B_{10} = B_{16}$, $B_3 = B_7 = B_{11} = B_{15}$, $B_4 = B_6 = B_{12} = B_{14}$ and $B_5 = B_{13}$. From Eq. (20.1)

$$B_1 = 100 + \frac{0.8 \times 149.6}{6}\left(2 + \frac{\sigma_2}{\sigma_1}\right) + \frac{0.8 \times 149.6}{6}\left(2 + \frac{\sigma_{16}}{\sigma_1}\right)$$

i.e.

$$B_1 = 100 + \frac{0.8 \times 149.6}{6}\left(2 + \frac{352.0}{381.0}\right) \times 2 = 216.6\,\text{mm}^2$$

Similarly $B_2 = 216.6\,\text{mm}^2$, $B_3 = 216.6\,\text{mm}^2$, $B_4 = 216.7\,\text{mm}^2$. We note that stringers 5 and 13 lie on the neutral axis of the section and are therefore unstressed; the calculation of boom areas B_5 and B_{13} does not then arise. For this particular section $I_{xy} = 0$ since Cx (and Cy) is an axis of symmetry. Further, $M_y = 0$ so that Eq. (16.18) reduces to

$$\sigma_z = \frac{M_x y}{I_{xx}}$$

in which

$$I_{xx} = 2 \times 216.6 \times 381.0^2 + 4 \times 216.6 \times 352.0^2 + 4 \times 216.6 \times 2695^2 + 4 \times 216.7 \times 145.8^2 = 2.52 \times 10^8\,\text{mm}^4$$

The solution is completed in Table 22.1.

Table 22.1

Stringer/boom	y (mm)	σ_z (N/mm^2)
1	381.0	302.4
2, 16	352.0	279.4
3, 15	269.5	213.9
4, 14	145.8	115.7
5, 13	0	0
6, 12	−145.8	−115.7
7, 11	−269.5	−213.9
8, 10	−352.0	−279.4
9	−381.0	−302.4

22.2 Shear

For a fuselage having a cross-section of the type shown in Fig. 22.1(a), the determination of the shear flow distribution in the skin produced by shear is basically the analysis of an idealized single cell closed section beam. The shear flow distribution is therefore given by Eq. (20.11) in which the direct stress carrying capacity of the skin is assumed to be zero, i.e. $t_D = 0$, thus

$$q_s = -\left(\frac{S_x I_{xx} - S_y I_{xy}}{I_{xx} I_{yy} - I_{xy}^2}\right) \sum_{r=1}^{n} B_r y_r - \left(\frac{S_y I_{yy} - S_x I_{xy}}{I_{xx} I_{yy} - I_{xy}^2}\right) \sum_{r=1}^{n} B_r x_r + q_{s,0} \qquad (22.1)$$

Equation (22.1) is applicable to loading cases in which the shear loads are not applied through the section shear centre so that the effects of shear and torsion are included simultaneously. Alternatively, if the position of the shear centre is known, the loading system may be replaced by shear loads acting through the shear centre together with a pure torque, and the corresponding shear flow distributions may be calculated separately and then superimposed to obtain the final distribution.

Example 22.2

The fuselage of Example 22.1 is subjected to a vertical shear load of 100 kN applied at a distance of 150 mm from the vertical axis of symmetry as shown, for the idealized section, in Fig. 22.2. Calculate the distribution of shear flow in the section.

As in Example 22.1, $I_{xy} = 0$ and, since $S_x = 0$, Eq. (22.1) reduces to

$$q_s = -\frac{S_y}{I_{xx}} \sum_{r=1}^{n} B_r y_r + q_{s,0} \qquad \text{(i)}$$

in which $I_{xx} = 2.52 \times 10^8$ mm^4 as before. Then

$$q_s = \frac{-100 \times 10^3}{2.52 \times 10^8} \sum_{r=1}^{n} B_r y_r + q_{s,0}$$

or

$$q_s = -3.97 \times 10^{-4} \sum_{r=1}^{n} B_r y_r + q_{s,0} \qquad \text{(ii)}$$

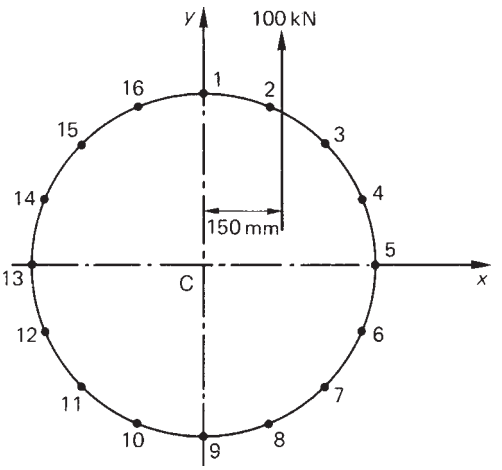

Fig. 22.2 Idealized fuselage section of Example 22.2.

Table 22.2

Skin panel	Boom	B_r (mm^2)	y_r (mm)	q_b (N/mm)
1 2	–	–	–	0
2 3	2	216.6	352.0	−30.3
3 4	3	216.6	269.5	−53.5
4 5	4	216.7	145.8	−66.0
5 6	5	–	0	−66.0
6 7	6	216.7	−145.8	−53.5
7 8	7	216.6	−269.5	−30.3
8 9	8	216.6	−352.0	0
1 16	1	216.6	381.0	−32.8
16 15	16	216.6	352.0	−63.1
15 14	15	216.6	269.5	−86.3
14 13	14	216.6	145.8	−98.8
13 12	13	–	0	−98.8
12 11	12	216.7	−145.8	−86.3
11 10	11	216.6	−269.5	−63.1
10 9	10	216.6	−352.0	−32.8

The first term on the right-hand side of Eq. (ii) is the 'open section' shear flow q_b. We therefore 'cut' one of the skin panels, say 12, and calculate q_b. The results are presented in Table 22.2.

Note that in Table 22.2, the column headed Boom indicates the boom that is crossed when the analysis moves from one panel to the next. Note also that, as would be expected, the q_b shear flow distribution is symmetrical about the Cx axis. The shear flow $q_{s,0}$ in the panel 12 is now found by taking moments about a convenient moment centre, say C. Therefore from Eq. (17.17)

$$100 \times 10^3 \times 150 = \oint q_b p \mathrm{d}s + 2Aq_{s,0} \qquad \text{(iii)}$$

in which $A = \pi \times 381.0^2 = 4.56 \times 10^5\,\text{mm}^2$. Since the q_b shear flows are constant between the booms, Eq. (iii) may be rewritten in the form (see Eq. (20.10))

$$100 \times 10^3 \times 150 = -2A_{12}q_{\text{b},12} - 2A_{23}q_{\text{b},23} - \cdots - 2A_{161}q_{\text{b},161} + 2Aq_{s,0} \qquad \text{(iv)}$$

in which A_{12}, A_{23}, ... , A_{161} are the areas subtended by the skin panels 12, 23, … , 161 at the centre C of the circular cross-section and anticlockwise moments are taken as positive. Clearly $A_{12} = A_{23} = \cdots = A_{161} = 4.56 \times 10^5/16 = 28\,500\,\text{mm}^2$. Equation (iv) then becomes

$$100 \times 10^3 \times 150 = 2 \times 28\,500(-q_{\text{b}_{12}} - q_{\text{b}_{23}} - \cdots - q_{\text{b}_{161}}) + 2 \times 4.56 \times 10^5 q_{s,0} \quad \text{(v)}$$

Substituting the values of q_b from Table 22.2 in Eq. (v), we obtain

$$100 \times 10^3 \times 150 = 2 \times 28\,500(-262.4) + 2 \times 4.56 \times 10^5 q_{s,0}$$

from which

$$q_{s,0} = 32.8\,\text{N/mm (acting in an anticlockwise sense)}$$

The complete shear flow distribution follows by adding the value of $q_{s,0}$ to the q_b shear flow distribution, giving the final distribution shown in Fig. 22.3. The solution may be checked by calculating the resultant of the shear flow distribution parallel to the Cy axis. Thus

$$2[(98.8 + 66.0)145.8 + (86.3 + 53.5)123.7 + (63.1 + 30.3)82.5 + (32.8 - 0)29.0] \times 10^{-3} = 99.96\,\text{kN}$$

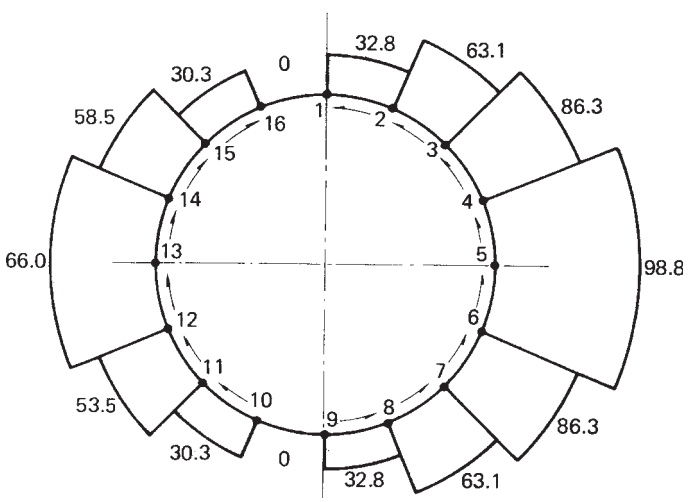

Fig. 22.3 Shear flow (N/mm) distribution in fuselage section of Example 22.2.

which agrees with the applied shear load of 100 kN. The analysis of a fuselage which is tapered along its length is carried out using the method described in Section 21.2 and illustrated in Example 21.2.

22.3 Torsion

A fuselage section is basically a single cell closed section beam. The shear flow distribution produced by a pure torque is therefore given by Eq. (18.1) and is

$$q = \frac{T}{2A} \tag{22.2}$$

It is immaterial whether or not the section has been idealized since, in both cases, the booms are assumed not to carry shear stresses.

Equation (22.2) provides an alternative approach to that illustrated in Example 22.2 for the solution of shear loaded sections in which the position of the shear centre is known. In Fig. 22.1 the shear centre coincides with the centre of symmetry so that the loading system may be replaced by the shear load of 100 kN acting through the shear centre together with a pure torque equal to $100 \times 10^3 \times 150 = 15 \times 10^6$ N mm as shown in Fig. 22.4. The shear flow distribution due to the shear load may be found using the method of Example 22.2 but with the left-hand side of the moment equation (iii) equal to zero for moments about the centre of symmetry. Alternatively, use may be made of the symmetry of the section and the fact that the shear flow is constant between adjacent booms. Suppose that the shear flow in the panel 21 is $q_{2\,1}$. Then from symmetry and using the results of Table 22.2

$$q_{9\,8} = q_{9\,10} = q_{16\,1} = q_{2\,1}$$
$$q_{3\,2} = q_{8\,7} = q_{10\,11} = q_{15\,16} = 30.3 + q_{2\,1}$$

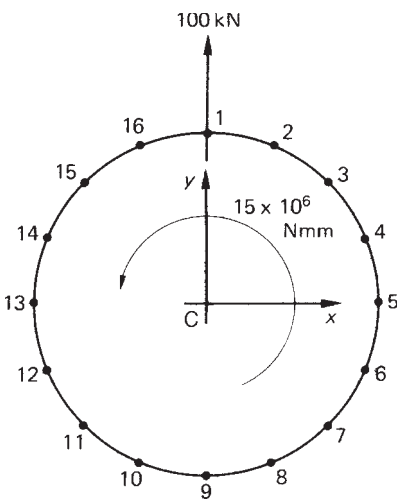

Fig. 22.4 Alternative solution of Example 22.2.

$$q_{4\,3} = q_{7\,6} = q_{11\,12} = q_{14\,15} = 53.5 + q_{2\,1}$$
$$q_{5\,4} = q_{6\,5} = q_{12\,13} = q_{13\,14} = 66.0 + q_{2\,1}$$

The resultant of these shear flows is statically equivalent to the applied shear load so that

$$4(29.0q_{2\,1} + 82.5q_{3\,2} + 123.7q_{4\,3} + 145.8q_{5\,4}) = 100 \times 10^3$$

Substituting for $q_{3\,2}$, $q_{4\,3}$ and $q_{5\,4}$ from the above we obtain

$$4(381q_{2\,1} + 18\,740.5) = 100 \times 10^3$$

whence

$$q_{2\,1} = 16.4\,\text{N/mm}$$

and

$$q_{3\,2} = 46.7\,\text{N/mm}, \quad q_{4\,3} = 69.9\,\text{N/mm}, \quad q_{5\,4} = 83.4\,\text{N/mm etc.}$$

The shear flow distribution due to the applied torque is, from Eq. (22.2)

$$q = \frac{15 \times 10^6}{2 \times 4.56 \times 10^5} = 16.4\,\text{N/mm}$$

acting in an anticlockwise sense completely around the section. This value of shear flow is now superimposed on the shear flows produced by the shear load; this gives the solution shown in Fig. 22.3, i.e.

$$q_{2\,1} = 16.4 + 16.4 = 32.8\,\text{N/mm}$$
$$q_{16\,1} = 16.4 - 16.4 = 0 \text{ etc.}$$

22.4 Cut-outs in fuselages

So far we have considered fuselages to be closed sections stiffened by transverse frames and longitudinal stringers. In practice it is necessary to provide openings in these closed stiffened shells for, for example, doors, cockpits, bomb bays, windows in passenger cabins, etc. These openings or 'cut-outs' produce discontinuities in the otherwise continuous shell structure so that loads are redistributed in the vicinity of the cut-out thereby affecting loads in the skin, stringers and frames. Frequently these regions must be heavily reinforced resulting in unavoidable weight increases. In some cases, for example door openings in passenger aircraft, it is not possible to provide rigid fuselage frames on each side of the opening because the cabin space must not be restricted. In such situations a rigid frame is placed around the opening to resist shear loads and to transmit loads from one side of the opening to the other.

The effects of smaller cut-outs, such as those required for rows of windows in passenger aircraft, may be found approximately as follows. Figure 22.5 shows a fuselage panel provided with cut-outs for windows which are spaced a distance l apart. The panel is subjected to an average shear flow q_{av} which would be the value of the shear

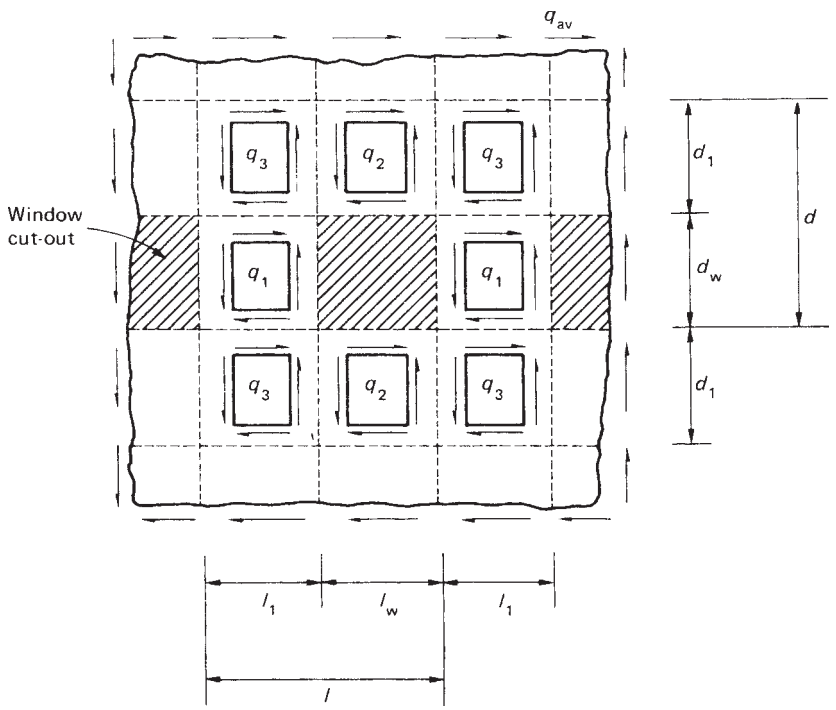

Fig. 22.5 Fuselage panel with windows.

flow in the panel without cut-outs. Considering a horizontal length of the panel through the cut-outs we see that

$$q_1 l_1 = q_{\text{av}} l$$

or

$$q_1 = \frac{l}{l_1} q_{\text{av}} \tag{22.3}$$

Now considering a vertical length of the panel through the cut-outs

$$q_2 d_1 = q_{\text{av}} d$$

or

$$q_2 = \frac{d}{d_1} q_{\text{av}} \tag{22.4}$$

The shear flows q_3 may be obtained by considering either vertical or horizontal sections not containing the cut-out. Thus

$$q_3 l_1 + q_2 l_{\text{w}} = q_{\text{av}} l$$

Substituting for q_2 from Eq. (22.3) and noting that $l = l_1 + l_w$ and $d = d_1 + d_w$, we obtain

$$q_3 = \left(1 - \frac{d_\mathrm{w}}{d_\mathrm{l}} \frac{l_\mathrm{w}}{l_\mathrm{l}}\right) q_\mathrm{av} \tag{22.5}$$

Problems

P.22.1 The doubly symmetrical fuselage section shown in Fig. P.22.1 has been idealized into an arrangement of direct stress carrying booms and shear stress carrying skin panels; the boom areas are all 150 mm^2. Calculate the direct stresses in the booms and the shear flows in the panels when the section is subjected to a shear load of 50 kN and a bending moment of 100 kN m.

Ans. $\sigma_{z,1} = -\sigma_{z,6} = 180\,\mathrm{N/mm^2}$, $\sigma_{z,2} = \sigma_{z,10} = -\sigma_{z,5} = -\sigma_{z,7} = 144.9\,\mathrm{N/mm^2}$, $\sigma_{z,3} = \sigma_{z,9} = -\sigma_{z,4} = -\sigma_{z,8} = 60\,\mathrm{N/mm^2}$.

$q_{2\,1} = q_{6\,5} = 1.9\,\mathrm{N/mm}$, $q_{3\,2} = q_{5\,4} = 12.8\,\mathrm{N/mm}$, $q_{4\,3} = 17.3\,\mathrm{N/mm}$, $q_{6\,7} = q_{10\,1} = 11.6\,\mathrm{N/mm}$, $q_{7\,8} = q_{9\,10} = 22.5\,\mathrm{N/mm}$, $q_{8\,9} = 27.0\,\mathrm{N/mm}$.

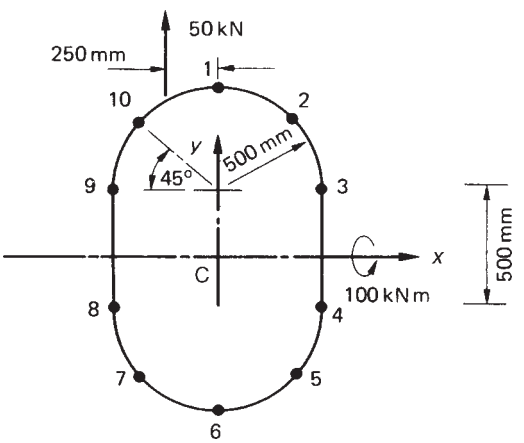

Fig. P.22.1

P.22.2 Determine the shear flow distribution in the fuselage section of P.22.1 by replacing the applied load by a shear load through the shear centre together with a pure torque.

23

Wings

We have seen in Chapters 12 and 20 that wing sections consist of thin skins stiffened by combinations of stringers, spar webs, and caps and ribs. The resulting structure frequently comprises one, two or more cells, and is highly redundant. However, as in the case of fuselage sections, the large number of closely spaced stringers allows the assumption of a constant shear flow in the skin between adjacent stringers so that a wing section may be analysed as though it were completely idealized as long as the direct stress carrying capacity of the skin is allowed for by additions to the existing stringer/boom areas. We shall investigate the analysis of multicellular wing sections subjected to bending, torsional and shear loads, although, initially, it will be instructive to examine the special case of an idealized three-boom shell.

23.1 Three-boom shell

The wing section shown in Fig. 23.1 has been idealized into an arrangement of direct stress carrying booms and shear–stress-only carrying skin panels. The part of the wing section aft of the vertical spar 31 performs an aerodynamic role only and is therefore

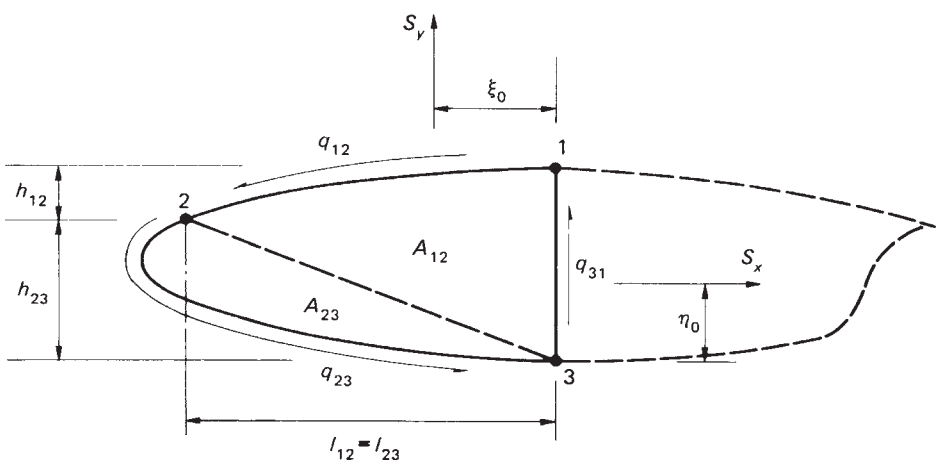

Fig. 23.1 Three-boom wing section.

unstressed. Lift and drag loads, S_y and S_x, induce shear flows in the skin panels which are constant between adjacent booms since the section has been completely idealized. Therefore, resolving horizontally and noting that the resultant of the internal shear flows is equivalent to the applied load, we have

$$S_x = -q_{12}l_{12} + q_{23}l_{23} \tag{23.1}$$

Now resolving vertically

$$S_y = q_{31}(h_{12} + h_{23}) - q_{12}h_{12} - q_{23}h_{23} \tag{23.2}$$

Finally, taking moments about, say, boom 3

$$S_x\eta_0 + S_y\xi_0 = -2A_{12}q_{12} - 2A_{23}q_{23} \tag{23.3}$$

(see Eqs (20.9) and (20.10)). In the above there are three unknown values of shear flow, q_{12}, q_{23}, q_{31} and three equations of statical equilibrium. We conclude therefore that a three-boom idealized shell is statically determinate.

We shall return to the simple case of a three-boom wing section when we examine the distributions of direct load and shear flows in wing ribs. Meanwhile, we shall consider the bending, torsion and shear of multicellular wing sections.

23.2 Bending

Bending moments at any section of a wing are usually produced by shear loads at other sections of the wing. The direct stress system for such a wing section (Fig. 23.2) is given by either Eqs (16.18) or (16.19) in which the coordinates (x, y) of any point in the cross-section and the sectional properties are referred to axes Cxy in which the origin C coincides with the centroid of the direct stress carrying area.

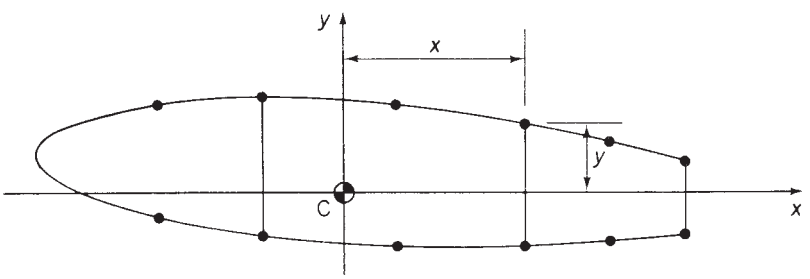

Fig. 23.2 Idealized section of a multicell wing.

Example 23.1

The wing section shown in Fig. 23.3 has been idealized such that the booms carry all the direct stresses. If the wing section is subjected to a bending moment of 300 kN m applied in a vertical plane, calculate the direct stresses in the booms.

Boom areas: $B_1 = B_6 = 2580\,\text{mm}^2 \quad B_2 = B_5 = 3880\,\text{mm}^2 \quad B_3 = B_4 = 3230\,\text{mm}^2$

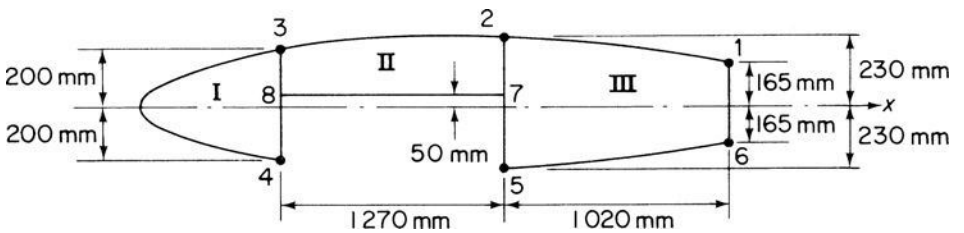

Fig. 23.3 Wing section of Example 23.1.

Table 23.1

Boom	y (mm)	σ_z (N/mm^2)
1	165	61.2
2	230	85.3
3	200	74.2
4	−200	−74.2
5	−230	−85.3
6	−165	−61.2

We note that the distribution of the boom areas is symmetrical about the horizontal x axis. Hence, in Eq. (16.18), $I_{xy} = 0$. Further, $M_x = 300\,\text{kN m}$ and $M_y = 0$ so that Eq. (16.18) reduces to

$$\sigma_z = \frac{M_x y}{I_{xx}} \tag{i}$$

in which

$$I_{xy} = 2(2580 \times 165^2 + 3880 \times 230^2 + 3230 \times 200^2) = 809 \times 10^6\,\text{mm}^4$$

Hence

$$\sigma_z = \frac{300 \times 10^6}{809 \times 10^6} y = 0.371y \tag{ii}$$

The solution is now completed in Table 23.1 in which positive direct stresses are tensile and negative direct stresses compressive.

23.3 Torsion

The chordwise pressure distribution on an aerodynamic surface may be represented by shear loads (lift and drag loads) acting through the aerodynamic centre together with a pitching moment M_0 (see Section 12.1). This system of shear loads may be transferred to the shear centre of the section in the form of shear loads S_x and S_y together with a torque T. It is the pure torsion case that is considered here. In the analysis we assume that no axial constraint effects are present and that the shape of the wing section remains unchanged by the load application. In the absence of axial constraint there is no development of direct stress in the wing section so that only shear

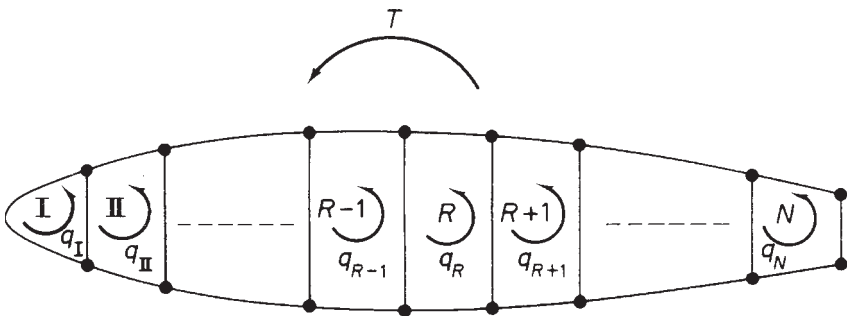

Fig. 23.4 Multicell wing section subjected to torsion.

stresses are present. It follows that the presence of booms does not affect the analysis in the pure torsion case.

The wing section shown in Fig. 23.4 comprises N cells and carries a torque T which generates individual but unknown torques in each of the N cells. Each cell therefore develops a constant shear flow $q_{\mathrm{I}}, q_{\mathrm{II}}, \ldots, q_R, \ldots, q_N$ given by Eq. (18.1).

The total is therefore

$$T = \sum_{R=1}^{N} 2A_R q_R \tag{23.4}$$

Although Eq. (23.4) is sufficient for the solution of the special case of a single cell section, which is therefore statically determinate, additional equations are required for an N-cell section. These are obtained by considering the rate of twist in each cell and the compatibility of displacement condition that all N cells possess the same rate of twist $\mathrm{d}\theta/\mathrm{d}z$; this arises directly from the assumption of an undistorted cross-section.

Consider the Rth cell of the wing section shown in Fig. 23.5. The rate of twist in the cell is, from Eq. (17.22)

$$\frac{\mathrm{d}\theta}{\mathrm{d}z} = \frac{1}{2A_R G} \oint_R q \frac{\mathrm{d}s}{t} \tag{23.5}$$

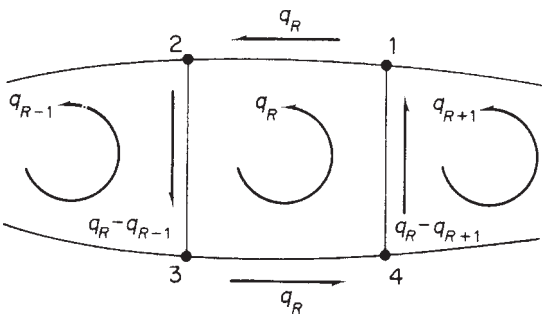

Fig. 23.5 Shear flow distribution in the Rth cell of an N-cell wing section.

The shear flow in Eq. (23.5) is constant along each wall of the cell and has the values shown in Fig. 23.5. Writing $\int \mathrm{d}s/t$ for each wall as δ, Eq. (23.5) becomes

$$\frac{\mathrm{d}\theta}{\mathrm{d}z} = \frac{1}{2A_R G}[q_R\delta_{12} + (q_R - q_{R-1})\delta_{23} + q_R\delta_{34} + (q_R - q_{R+1})\delta_{41}]$$

or, rearranging the terms in square brackets

$$\frac{\mathrm{d}\theta}{\mathrm{d}z} = \frac{1}{2A_R G}[-q_{R-1}\delta_{23} + q_R(\delta_{12} + \delta_{23} + \delta_{34} + \delta_{41}) - q_{R+1}\delta_{41}]$$

In general terms, this equation may be rewritten in the form

$$\frac{\mathrm{d}\theta}{\mathrm{d}z} = \frac{1}{2A_R G}(-q_{R-1}\delta_{R-1,R} + q_R\delta_R - q_{R+1}\delta_{R+1,R}) \tag{23.6}$$

in which $\delta_{R-1,R}$ is $\int \mathrm{d}s/t$ for the wall common to the Rth and $(R-1)$th cells, δ_R is $\int \mathrm{d}s/t$ for all the walls enclosing the Rth cell and $\delta_{R+1,R}$ is $\int \mathrm{d}s/t$ for the wall common to the Rth and $(R+1)$th cells.

The general form of Eq. (23.6) is applicable to multicell sections in which the cells are connected consecutively, i.e. cell I is connected to cell II, cell II to cells I and III and so on. In some cases, cell I may be connected to cells II and III, etc. (see problem P.23.4) so that Eq. (23.6) cannot be used in its general form. For this type of section the term $\oint q(\mathrm{d}s/t)$ should be computed by considering $\int q(\mathrm{d}s/t)$ for each wall of a particular cell in turn.

There are N equations of the type (23.6) which, with Eq. (23.4), comprise the $N+1$ equations required to solve for the N unknown values of shear flow and the one unknown value of $\mathrm{d}\theta/\mathrm{d}z$.

Frequently, in practice, the skin panels and spar webs are fabricated from materials possessing different properties such that the shear modulus G is not constant. The analysis of such sections is simplified if the actual thickness t of a wall is converted to a modulus-weighted thickness t^* as follows. For the Rth cell of an N-cell wing section in which G varies from wall to wall, Eq. (23.5) takes the form

$$\frac{\mathrm{d}\theta}{\mathrm{d}z} = \frac{1}{2A_R}\oint_R q\frac{\mathrm{d}s}{Gt}$$

This equation may be rewritten as

$$\frac{\mathrm{d}\theta}{\mathrm{d}z} = \frac{1}{2A_R G_{\mathrm{REF}}}\oint_R q\frac{\mathrm{d}s}{(G/G_{\mathrm{REF}})t} \tag{23.7}$$

in which G_{REF} is a convenient reference value of the shear modulus. Equation (23.7) is now rewritten as

$$\frac{\mathrm{d}\theta}{\mathrm{d}z} = \frac{1}{2A_R G_{\mathrm{REF}}}\oint_R q\frac{\mathrm{d}s}{t^*} \tag{23.8}$$

in which the modulus-weighted thickness t^* is given by

$$t^* = \frac{G}{G_{\mathrm{REF}}}t \tag{23.9}$$

Then, in Eq. (23.6), δ becomes $\int \mathrm{d}s/t^*$.

Example 23.2

Calculate the shear stress distribution in the walls of the three-cell wing section shown in Fig. 23.6, when it is subjected to an anticlockwise torque of 11.3 kN m.

Wall	Length (mm)	Thickness (mm)	G (N/mm^2)	Cell area (mm^2)
12^{o}	1650	1.22	24 200	$A_{\mathrm{I}} = 258\,000$
12^{i}	508	2.03	27 600	$A_{\mathrm{II}} = 355\,000$
13, 24	775	1.22	24 200	$A_{\mathrm{III}} = 161\,000$
34	380	1.63	27 600	
35, 46	508	0.92	20 700	
56	254	0.92	20 700	

Note: The superscript symbols o and i are used to distinguish between outer and inner walls connecting the same two booms.

Since the wing section is loaded by a pure torque the presence of the booms has no effect on the analysis.

Choosing $G_{\mathrm{REF}} = 27\,600\,\mathrm{N/mm^2}$ then, from Eq. (23.9)

$$t^*_{12^{o}} = \frac{24\,200}{27\,600} \times 1.22 = 1.07\,\mathrm{mm}$$

Similarly

$$t^*_{13} = t^*_{24} = 1.07\,\mathrm{mm} \quad t^*_{35} = t^*_{46} = t^*_{56} = 0.69\,\mathrm{mm}$$

Hence

$$\delta_{12^{o}} = \int_{12^{o}} \frac{\mathrm{d}s}{t^*} = \frac{1650}{1.07} = 1542$$

Similarly

$$\delta_{12^{i}} = 250 \quad \delta_{13} = \delta_{24} = 725 \quad \delta_{34} = 233 \quad \delta_{35} = \delta_{46} = 736 \quad \delta_{56} = 368$$

Substituting the appropriate values of δ in Eq. (23.6) for each cell in turn gives the following:

- For cell I

$$\frac{\mathrm{d}\theta}{\mathrm{d}z} = \frac{1}{2 \times 258\,000 G_{\mathrm{REF}}} [q_{\mathrm{I}}(1542 + 250) - 250 q_{\mathrm{II}}] \qquad \text{(i)}$$

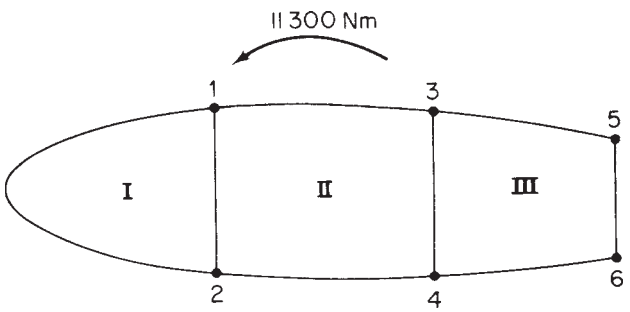

Fig. 23.6 Wing section of Example 23.2

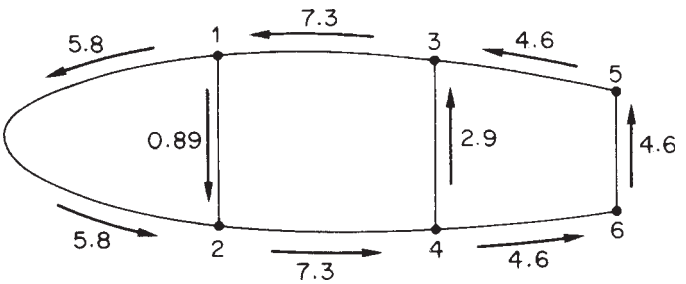

Fig. 23.7 Shear stress (N/mm^2) distribution in wing section of Example 23.2.

- For cell II

$$\frac{d\theta}{dz} = \frac{1}{2 \times 355\,000 G_{REF}}[-250q_I + q_{II}(250 + 725 + 233 + 725) - 233q_{III}] \quad \text{(ii)}$$

- For cell III

$$\frac{d\theta}{dz} = \frac{1}{2 \times 161\,000 G_{REF}}[-233q_{II} + q_{III}(736 + 233 + 736 + 368)] \quad \text{(iii)}$$

In addition, from Eq. (23.4)

$$11.3 \times 10^6 = 2(258\,000q_I + 355\,000q_{II} + 161\,000q_{III}) \quad \text{(iv)}$$

Solving Eqs (i)–(iv) simultaneously gives

$$q_I = 7.1\,\text{N/mm} \quad q_{II} = 8.9\,\text{N/mm} \quad q_{III} = 4.2\,\text{N/mm}$$

The shear stress in any wall is obtained by dividing the shear flow by the *actual* wall thickness. Hence the shear stress distribution is as shown in Fig. 23.7.

23.4 Shear

Initially we shall consider the general case of an N-cell wing section comprising booms and skin panels, the latter being capable of resisting both direct and shear stresses. The wing section is subjected to shear loads S_x and S_y whose lines of action do not necessarily pass through the shear centre S (see Fig. 23.8); the resulting shear flow distribution is therefore due to the combined effects of shear and torsion.

The method for determining the shear flow distribution and the rate of twist is based on a simple extension of the analysis of a single cell beam subjected to shear loads (Sections 17.3 and 20.3). Such a beam is statically indeterminate, the single redundancy being selected as the value of shear flow at an arbitrarily positioned 'cut'. Thus, the N-cell wing section of Fig. 23.8 may be made statically determinate by 'cutting' a skin panel in each cell as shown. While the actual position of these 'cuts' is theoretically immaterial there are advantages to be gained from a numerical point of view if the 'cuts' are made near the centre of the top or bottom skin panel in each cell. Generally,

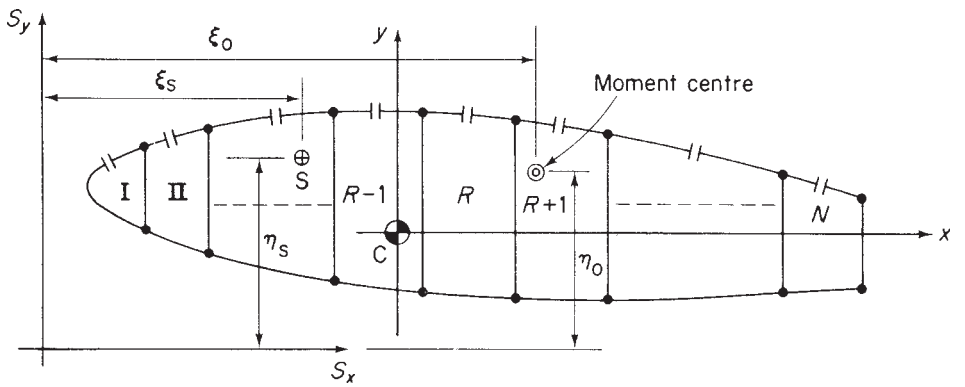

Fig. 23.8 *N*-cell wing section subjected to shear loads.

at these points, the redundant shear flows ($q_{s,0}$) are small so that the final shear flows differ only slightly from those of the determinate structure. The system of simultaneous equations from which the final shear flows are found will then be 'well conditioned' and will produce reliable results. The solution of an 'ill conditioned' system of equations would probably involve the subtraction of large numbers of a similar size which would therefore need to be expressed to a large number of significant figures for reasonable accuracy. Although this reasoning does not apply to a completely idealized wing section since the calculated values of shear flow are constant between the booms, it is again advantageous to 'cut' either the top or bottom skin panels for, in the special case of a wing section having a horizontal axis of symmetry, a 'cut' in, say, the top skin panels will result in the 'open section' shear flows (q_b) being zero in the bottom skin panels. This decreases the arithmetical labour and simplifies the derivation of the moment equation, as will become obvious in Example 23.4.

The 'open section' shear flow q_b in the wing section of Fig. 23.8 is given by Eq. (20.6), i.e.

$$q_b = -\left(\frac{S_x I_{xx} - S_y I_{xy}}{I_{xx} I_{yy} - I_{xy}^2}\right)\left(\int_0^s t_D x \, ds + \sum_{r=1}^{n} B_r x_r\right) - \left(\frac{S_y I_{yy} - S_x I_{xy}}{I_{xx} I_{yy} - I_{xy}^2}\right)\left(\int_0^s t_D y \, ds + \sum_{r=1}^{n} B_r y_r\right)$$

We are left with an unknown value of shear flow at each of the 'cuts', i.e. $q_{s,0,\mathrm{I}}$, $q_{s,0,\mathrm{II}}, \ldots, q_{s,0,N}$ plus the unknown rate of twist $d\theta/dz$ which, from the assumption of an undistorted cross-section, is the same for each cell. Therefore, as in the torsion case, there are $N + 1$ unknowns requiring $N + 1$ equations for a solution.

Consider the Rth cell shown in Fig. 23.9. The complete distribution of shear flow around the cell is given by the summation of the 'open section' shear flow q_b and the value of shear flow at the 'cut', $q_{s,0,R}$. We may therefore regard $q_{s,0,R}$ as a constant shear flow acting around the cell. The rate of twist is again given by Eq. (17.22); thus

$$\frac{d\theta}{dz} = \frac{1}{2A_R G} \oint_R q \frac{ds}{t} = \frac{1}{2A_R G} \oint_R (q_b + q_{s,0,R}) \frac{ds}{t}$$

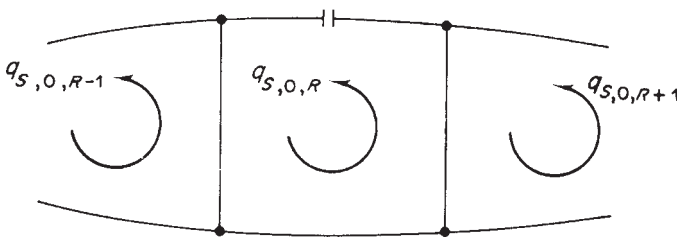

Fig. 23.9 Redundant shear flow in the *R*th cell of an *N*-cell wing section subjected to shear.

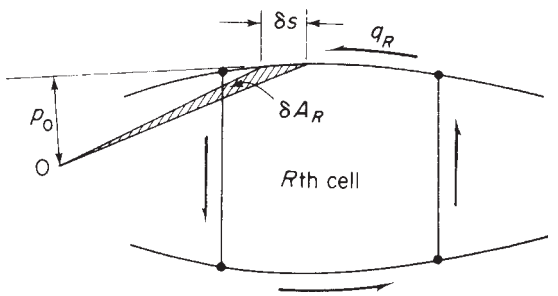

Fig. 23.10 Moment equilibrium of *R*th cell.

By comparison with the pure torsion case we deduce that

$$\frac{\mathrm{d}\theta}{\mathrm{d}z} = \frac{1}{2A_R G}\left(-q_{s,0,R-1}\delta_{R-1,R} + q_{s,0,R}\delta_R - q_{s,0,R+1}\delta_{R+1,R} + \oint_R q_\mathrm{b}\frac{\mathrm{d}s}{t}\right) \quad (23.10)$$

in which q_b has previously been determined. There are N equations of the type (23.10) so that a further equation is required to solve for the $N+1$ unknowns. This is obtained by considering the moment equilibrium of the Rth cell in Fig. 23.10.

The moment $M_{q,R}$ produced by the total shear flow about any convenient moment centre O is given by

$$M_{q,R} = \oint q_R p_0 \,\mathrm{d}s \quad \text{(see Section 18.1)}$$

Substituting for q_R in terms of the 'open section' shear flow q_b and the redundant shear flow $q_{s,0,R}$, we have

$$M_{q,R} = \oint_R q_\mathrm{b} p_0 \,\mathrm{d}s + q_{s,0,R}\oint_R p_0 \,\mathrm{d}s$$

or

$$M_{q,R} = \oint_R q_\mathrm{b} p_0 \,\mathrm{d}s + 2A_R q_{s,0,R}$$

The sum of the moments from the individual cells is equivalent to the moment of the externally applied loads about the same point. Thus, for the wing section of Fig. 23.8

$$S_x\eta_0 - S_y\xi_0 = \sum_{R=1}^{N} M_{q,R} = \sum_{R=1}^{N} \oint_R q_b p_0 \, \mathrm{d}s + \sum_{R=1}^{N} 2A_R q_{s,0,R} \tag{23.11}$$

If the moment centre is chosen to coincide with the point of intersection of the lines of action of S_x and S_y, Eq. (23.11) becomes

$$0 = \sum_{R=1}^{N} \oint_R q_b p_0 \, \mathrm{d}s + \sum_{R=1}^{N} 2A_R q_{s,0,R} \tag{23.12}$$

Example 23.3

The wing section of Example 23.1 (Fig. 23.3) carries a vertically upward shear load of 86.8 kN in the plane of the web 572. The section has been idealized such that the booms resist all the direct stresses while the walls are effective only in shear. If the shear modulus of all walls is 27 600 N/mm^2 except for the wall 78 for which it is three times this value, calculate the shear flow distribution in the section and the rate of twist. Additional data are given below.

Wall	Length (mm)	Thickness (mm)	Cell area (mm^2)
12, 56	1023	1.22	$A_{\mathrm{I}} = 265\,000$
23	1274	1.63	$A_{\mathrm{II}} = 213\,000$
34	2200	2.03	$A_{\mathrm{III}} = 413\,000$
483	400	2.64	
572	460	2.64	
61	330	1.63	
78	1270	1.22	

Choosing G_{REF} as 27 600 N/mm^2 then, from Eq. (23.9)

$$t_{78}^{*} = \frac{3 \times 27\,600}{27\,600} \times 1.22 = 3.66\,\mathrm{mm}$$

Hence

$$\delta_{78} = \frac{1270}{3.66} = 347$$

Also

$$\delta_{12} = \delta_{56} = 840 \quad \delta_{23} = 783 \quad \delta_{34} = 1083 \quad \delta_{38} = 57 \quad \delta_{84} = 95 \quad \delta_{87} = 347$$
$$\delta_{27} = 68 \quad \delta_{75} = 106 \quad \delta_{16} = 202$$

We now 'cut' the top skin panels in each cell and calculate the 'open section' shear flows using Eq. (20.6) which, since the wing section is idealized, singly symmetrical

(as far as the direct stress carrying area is concerned) and is subjected to a vertical shear load only, reduces to

$$q_{\mathrm{b}} = \frac{-S_y}{I_{xx}} \sum_{r=1}^{n} B_r y_r \tag{i}$$

where, from Example 23.1, $I_{xx} = 809 \times 10^6\ \mathrm{mm}^4$. Thus, from Eq. (i)

$$q_{\mathrm{b}} = -\frac{86.8 \times 10^3}{809 \times 10^6} \sum_{r=1}^{n} B_r y_r = -1.07 \times 10^{-4} \sum_{r=1}^{n} B_r y_r \tag{ii}$$

Since $q_{\mathrm{b}} = 0$ at each 'cut', then $q_{\mathrm{b}} = 0$ for the skin panels 12, 23 and 34. The remaining q_{b} shear flows are now calculated using Eq. (ii). Note that the order of the numerals in the subscript of q_{b} indicates the direction of movement from boom to boom.

$$q_{\mathrm{b},27} = -1.07 \times 10^{-4} \times 3880 \times 230 = -95.5\,\mathrm{N/mm}$$

$$q_{\mathrm{b},16} = -1.07 \times 10^{-4} \times 2580 \times 165 = -45.5\,\mathrm{N/mm}$$

$$q_{\mathrm{b},65} = -45.5 - 1.07 \times 10^{-4} \times 2580 \times (-165) = 0$$

$$q_{\mathrm{b},57} = -1.07 \times 10^{-4} \times 3880 \times (-230) = 95.5\,\mathrm{N/mm}$$

$$q_{\mathrm{b},38} = -1.07 \times 10^{-4} \times 3230 \times 200 = -69.0\,\mathrm{N/mm}$$

$$q_{\mathrm{b},48} = -1.07 \times 10^{-4} \times 3230 \times (-200) = 69.0\,\mathrm{N/mm}$$

Therefore, as $q_{\mathrm{b},83} = q_{\mathrm{b},48}$ (or $q_{\mathrm{b},72} = q_{\mathrm{b},57}$), $q_{\mathrm{b},78} = 0$. The distribution of the q_{b} shear flows is shown in Fig. 23.11. The values of δ and q_{b} are now substituted in Eq. (23.10) for each cell in turn.

- For cell I

$$\frac{\mathrm{d}\theta}{\mathrm{d}z} = \frac{1}{2 \times 265\,000 G_{\mathrm{REF}}} [q_{s,0,\mathrm{I}}(1083+95+57) - 57 q_{s,0,\mathrm{II}} + 69 \times 95 + 69 \times 57] \tag{iii}$$

- For cell II

$$\frac{\mathrm{d}\theta}{\mathrm{d}z} = \frac{1}{2 \times 213\,000 G_{\mathrm{REF}}} [-57 q_{s,0,\mathrm{I}} + q_{s,0,\mathrm{II}}(783 + 57 + 347 + 68) - 68 q_{s,0,\mathrm{III}} + 95.5 \times 68 - 69 \times 57] \tag{iv}$$

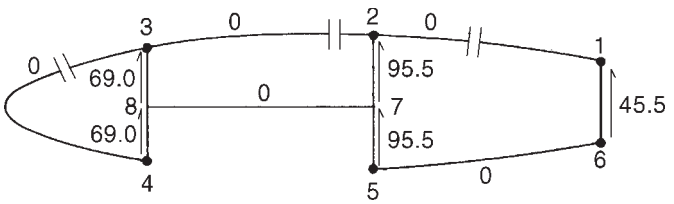

Fig. 23.11 q_{b} distribution (N/mm).

- For cell III

$$\frac{\mathrm{d}\theta}{\mathrm{d}z} = \frac{1}{2 \times 413\,000 G_{\mathrm{REF}}}[-68q_{s,0,\mathrm{II}} + q_{s,0,\mathrm{III}}(840 + 68 + 106 + 840 + 202) + 45.5 \times 202 - 95.5 \times 68 - 95.5 \times 106] \quad \text{(v)}$$

The solely numerical terms in Eqs (iii)–(v) represent $\oint_R q_{\mathrm{b}}(\mathrm{d}s/t)$ for each cell. Care must be taken to ensure that the contribution of each q_{b} value to this term is interpreted correctly. The path of the integration follows the positive direction of $q_{s,0}$ in each cell, i.e. anticlockwise. Thus, the positive contribution of $q_{\mathrm{b},83}$ to $\oint_{\mathrm{I}} q_{\mathrm{b}}(\mathrm{d}s/t)$ becomes a negative contribution to $\oint_{\mathrm{II}} q_{\mathrm{b}}(\mathrm{d}s/t)$ and so on.

The fourth equation required for a solution is obtained from Eq. (23.12) by taking moments about the intersection of the x axis and the web 572. Thus

$$0 = -69.0 \times 250 \times 1270 - 69.0 \times 150 \times 1270 + 45.5 \times 330 \times 1020 + 2 \times 265\,000 q_{s,0,\mathrm{I}} + 2 \times 213\,000 q_{s,0,\mathrm{II}} + 2 \times 413\,000 q_{s,0,\mathrm{III}} \quad \text{(vi)}$$

Simultaneous solution of Eqs (iii)–(vi) gives

$$q_{s,0,\mathrm{I}} = 5.5\,\mathrm{N/mm} \quad q_{s,0,\mathrm{II}} = 10.2\,\mathrm{N/mm} \quad q_{s,0,\mathrm{III}} = 16.5\,\mathrm{N/mm}$$

Superimposing these shear flows on the q_{b} distribution of Fig. 23.11, we obtain the final shear flow distribution. Thus

$$q_{34} = 5.5\,\mathrm{N/mm} \quad q_{23} = q_{87} = 10.2\,\mathrm{N/mm} \quad q_{12} = q_{56} = 16.5\,\mathrm{N/mm}$$
$$q_{61} = 62.0\,\mathrm{N/mm} \quad q_{57} = 79.0\,\mathrm{N/mm} \quad q_{72} = 89.2\,\mathrm{N/mm}$$
$$q_{48} = 74.5\,\mathrm{N/mm} \quad q_{83} = 64.3\,\mathrm{N/mm}$$

Finally, from any of Eqs (iii)–(v)

$$\frac{\mathrm{d}\theta}{\mathrm{d}z} = 1.16 \times 10^{-6}\,\mathrm{rad/mm}$$

23.5 Shear centre

The position of the shear centre of a wing section is found in an identical manner to that described in Section 17.3. Arbitrary shear loads S_x and S_y are applied in turn through the shear centre S, the corresponding shear flow distributions determined and moments taken about some convenient point. The shear flow distributions are obtained as described previously in the shear of multicell wing sections except that the N equations of the type (23.10) are sufficient for a solution since the rate of twist $\mathrm{d}\theta/\mathrm{d}z$ is zero for shear loads applied through the shear centre.

23.6 Tapered wings

Wings are generally tapered in both spanwise and chordwise directions. The effects on the analysis of taper in a single cell beam have been discussed in Section 21.2. In a multicell wing section the effects are dealt with in an identical manner except that the moment equation (21.16) becomes, for an N-cell wing section (see Figs 21.5 and 23.8)

$$S_x\eta_0 - S_y\xi_0 = \sum_{R=1}^{N} \oint_R q_b p_0 \, \mathrm{d}s + \sum_{R=1}^{N} 2A_R q_{s,0,R} - \sum_{r=1}^{m} P_{x,r}\eta_r + \sum_{r=1}^{m} P_{y,r}\xi_r \qquad (23.13)$$

Example 23.4

A two-cell beam has singly symmetrical cross-sections 1.2 m apart and tapers symmetrically in the y direction about a longitudinal axis (Fig. 23.12). The beam supports loads which produce a shear force $S_y = 10\,\mathrm{kN}$ and a bending moment $M_x = 1.65\,\mathrm{kN\,m}$ at the larger cross-section; the shear load is applied in the plane of the internal spar web. If booms 1 and 6 lie in a plane which is parallel to the yz plane calculate the forces in the booms and the shear flow distribution in the walls at the larger cross-section. The booms are assumed to resist all the direct stresses while the walls are effective only in shear. The shear modulus is constant throughout, the vertical webs are all 1.0 mm thick while the remaining walls are all 0.8 mm thick:

$$\text{Boom areas: } B_1 = B_3 = B_4 = B_6 = 600\,\mathrm{mm}^2 \quad B_2 = B_5 = 900\,\mathrm{mm}^2$$

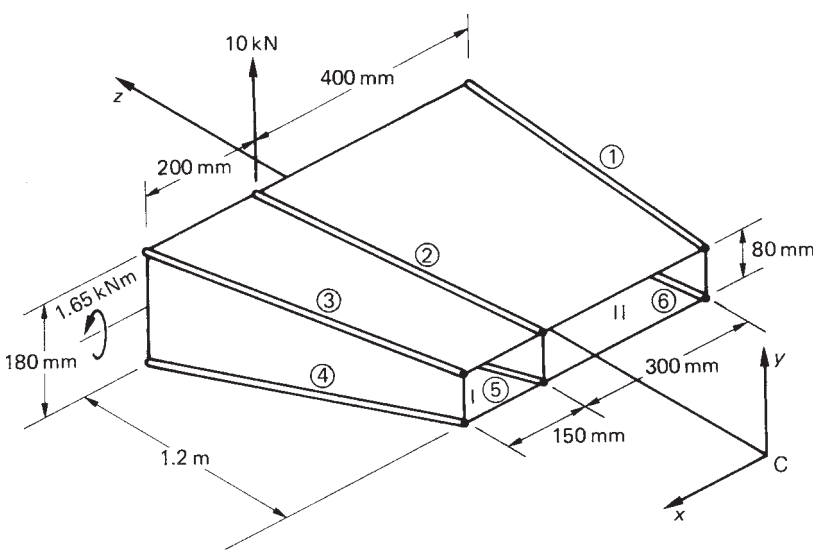

Fig. 23.12 Tapered beam of Example 23.4.

At the larger cross-section

$$I_{xx} = 4 \times 600 \times 90^2 + 2 \times 900 \times 90^2 = 34.02 \times 10^6 \text{ mm}^4$$

The direct stress in a boom is given by Eq. (16.18) in which $I_{xy} = 0$ and $M_y = 0$, i.e.

$$\sigma_{z,r} = \frac{M_x y_r}{I_{xx}}$$

whence

$$P_{z,r} = \frac{M_x y_r}{I_{xx}} B_r$$

or

$$P_{z,r} = \frac{1.65 \times 10^6 y_r B_r}{34.02 \times 10^6} = 0.08 y_r B_r \tag{i}$$

The value of $P_{z,r}$ is calculated from Eq. (i) in column ② of Table 23.2; $P_{x,r}$ and $P_{y,r}$ follow from Eqs (21.10) and (21.9), respectively in columns ⑤ and ⑥. The axial load P_r is given by $[②^2 + ⑤^2 + ⑥^2]^{1/2}$ in column ⑦ and has the same sign as $P_{z,r}$ (see Eq. (21.12)). The moments of $P_{x,r}$ and $P_{y,r}$, columns ⑩ and ⑪, are calculated for a moment centre at the mid-point of the internal web taking anticlockwise moments as positive.

From column ⑤

$$\sum_{r=1}^{6} P_{x,r} = 0$$

(as would be expected from symmetry).

From column ⑥

$$\sum_{r=1}^{6} P_{y,r} = 764.4 \text{ N}$$

From column ⑩

$$\sum_{r=1}^{6} P_{x,r} \eta_r = -117\,846 \text{ N mm}$$

Table 23.2

①	②	③	④	⑤	⑥	⑦	⑧	⑨	⑩	⑪
Boom	$P_{z,r}$ (N)	$\frac{\delta_{x_r}}{\delta_z}$	$\frac{\delta_{y_r}}{\delta_z}$	$P_{x,r}$ (N)	$P_{y,r}$ (N)	P_r (N)	ξ_r (mm)	η_r (mm)	$P_{x,r}\eta_r$ (N mm)	$P_{y,r}\xi_r$ (N mm)
1	2619.0	0	0.0417	0	109.2	2621.3	400	90	0	43 680
2	3928.6	0.0833	0.0417	327.3	163.8	3945.6	0	90	−29 457	0
3	2619.0	0.1250	0.0417	327.4	109.2	2641.6	200	90	−29 466	21 840
4	−2619.0	0.1250	−0.0417	−327.4	109.2	−2641.6	200	90	−29 466	21 840
5	−3928.6	0.0833	−0.0417	−327.3	163.8	−3945.6	0	90	−29 457	0
6	−2619.0	0	−0.0417	0	109.2	−2621.3	400	90	0	−43 680

From column ⑪

$$\sum_{r=1}^{6} P_{y,r}\xi_r = -43\,680\,\text{N mm}$$

From Eq. (21.15)

$$S_{x,w} = 0 \quad S_{y,w} = 10 \times 10^3 - 764.4 = 9235.6\,\text{N}$$

Also, since Cx is an axis of symmetry, $I_{xy} = 0$ and Eq. (20.6) for the 'open section' shear flow reduces to

$$q_\text{b} = -\frac{S_{y,w}}{I_{xx}} \sum_{r=1}^{n} B_r y_r$$

or

$$q_\text{b} = -\frac{9235.6}{34.02 \times 10^6} \sum_{r=1}^{n} B_r y_r = -2.715 \times 10^{-4} \sum_{r=1}^{n} B_r y_r \qquad \text{(ii)}$$

'Cutting' the top walls of each cell and using Eq. (ii), we obtain the q_b distribution shown in Fig. 23.13. Evaluating δ for each wall and substituting in Eq. (23.10) gives for cell I

$$\frac{\text{d}\theta}{\text{d}z} = \frac{1}{2 \times 36\,000G}(760q_{s,0,\text{I}} - 180q_{s,0,\text{II}} - 1314) \qquad \text{(iii)}$$

for cell II

$$\frac{\text{d}\theta}{\text{d}z} = \frac{1}{2 \times 72\,000G}(-180q_{s,0,\text{I}} + 1160q_{s,0,\text{II}} + 1314) \qquad \text{(iv)}$$

Taking moments about the mid-point of web 25 we have, using Eq. (23.13)

$$0 = -14.7 \times 180 \times 400 + 14.7 \times 180 \times 200 + 2 \times 36\,000q_{s,0,\text{I}} + 2 \times 72\,000q_{s,0,\text{II}} - 117\,846 - 43\,680$$

or

$$0 = -690\,726 + 72\,000q_{s,0,\text{I}} + 144\,000q_{s,0,\text{II}} \qquad \text{(v)}$$

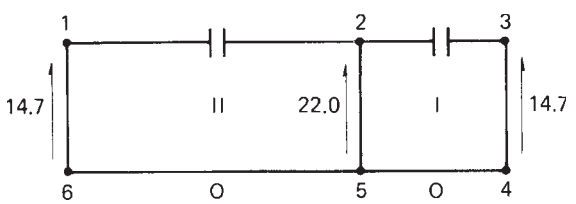

Fig. 23.13 q_b (N/mm) distribution in beam section of Example 23.4 (view along z axis towards C).

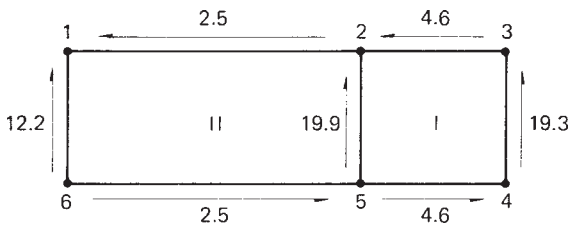

Fig. 23.14 Shear flow (N/mm) distribution in tapered beam of Example 23.4.

Solving Eqs (iii)–(v) gives

$$q_{s,0,\mathrm{I}} = 4.6\,\mathrm{N/mm} \quad q_{s,0,\mathrm{II}} = 2.5\,\mathrm{N/mm}$$

and the resulting shear flow distribution is shown in Fig. 23.14.

23.7 Deflections

Deflections of multicell wings may be calculated by the unit load method in an identical manner to that described in Section 20.4 for open and single cell beams.

Example 23.5

Calculate the deflection at the free end of the two-cell beam shown in Fig. 23.15 allowing for both bending and shear effects. The booms carry all the direct stresses while the skin panels, of constant thickness throughout, are effective only in shear.

Take $E = 69\,000\,\mathrm{N/mm^2}$ and $G = 25\,900\,\mathrm{N/mm^2}$

Boom areas: $B_1 = B_3 = B_4 = B_6 = 650\,\mathrm{mm^2}$ $B_2 = B_5 = 1300\,\mathrm{mm^2}$

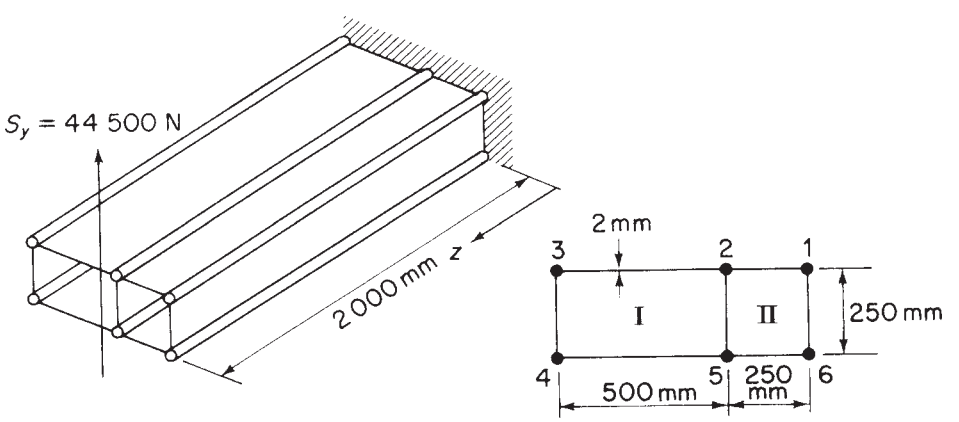

Fig. 23.15 Deflection of two-cell wing section.

The beam cross-section is symmetrical about a horizontal axis and carries a vertical load at its free end through the shear centre. The deflection Δ at the free end is then, from Eqs (20.17) and (20.19)

$$\Delta = \int_0^{2000} \frac{M_{x,0}M_{x,1}}{EI_{xx}}\mathrm{d}z + \int_0^{2000}\left(\int_{\text{section}} \frac{q_0 q_1}{Gt}\mathrm{d}s\right)\mathrm{d}z \qquad \text{(i)}$$

where

$$M_{x,0} = -44.5 \times 10^3(2000 - z) \quad M_{x,1} = -(2000 - z)$$

and

$$I_{xx} = 4 \times 650 \times 125^2 + 2 \times 1300 \times 125^2 = 81.3 \times 10^6\,\text{mm}^4$$

also

$$S_{y,0} = 44.5 \times 10^3\,\text{N} \quad S_{y,1} = 1$$

The q_0 and q_1 shear flow distributions are obtained as previously described (note $\mathrm{d}\theta/\mathrm{d}z = 0$ for a shear load through the shear centre) and are

$$q_{0,12} = 9.6\,\text{N/mm} \quad q_{0,23} = -5.8\,\text{N/mm} \quad q_{0,43} = 50.3\,\text{N/mm}$$
$$q_{0,45} = -5.8\,\text{N/mm} \quad q_{0,56} = 9.6\,\text{N/mm} \quad q_{0,61} = 54.1\,\text{N/mm}$$
$$q_{0,52} = 73.6\,\text{N/mm at all sections of the beam}$$

The q_1 shear flows in this case are given by $q_0/44.5 \times 10^3$. Thus

$$\begin{aligned}\int_{\text{section}} \frac{q_0 q_1}{Gt}\mathrm{d}s &= \frac{1}{25\,900 \times 2 \times 44.5 \times 10^3}(9.6^2 \times 250 \times 2 + 5.8^2 \times 500 \times 2 \\ &\quad + 50.3^2 \times 250 + 54.1^2 \times 250 + 73.6^2 \times 250) \\ &= 1.22 \times 10^{-3}\end{aligned}$$

Hence, from Eq. (i)

$$\Delta = \int_0^{2000} \frac{44.5 \times 10^3(2000 - z)^2}{69\,000 \times 81.3 \times 10^6}\mathrm{d}z + \int_0^{2000} 1.22 \times 10^{-3}\mathrm{d}z$$

giving

$$\Delta = 23.5\,\text{mm}$$

23.8 Cut-outs in wings

Wings, as well as fuselages, have openings in their surfaces to accommodate undercarriages, engine nacelles and weapons installations, etc. In addition inspection panels are required at specific positions so that, as for fuselages, the loads in adjacent portions of the wing structure are modified.

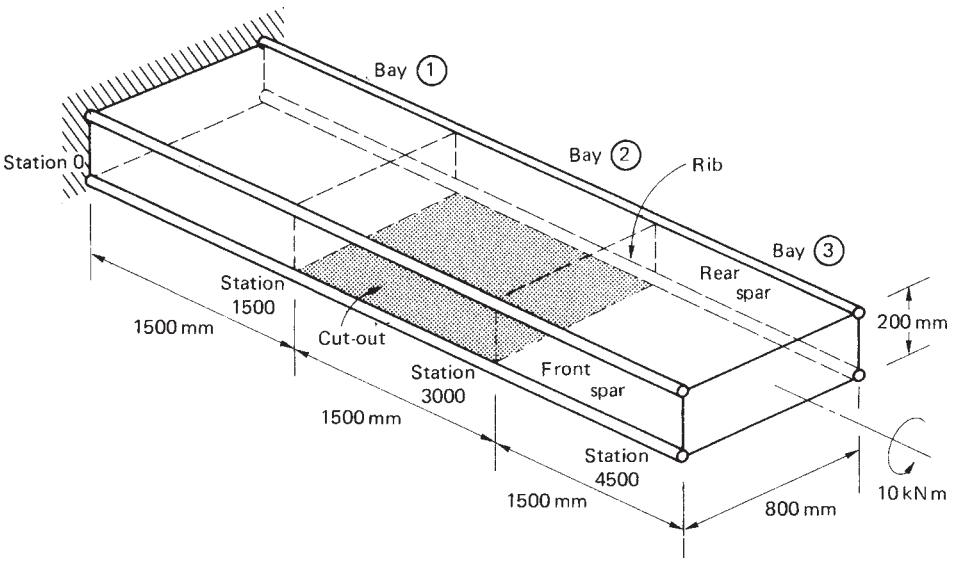

Fig. 23.16 Three-bay wing structure with cut-out of Example 23.6.

Initially we shall consider the case of a wing subjected to a pure torque in which one bay of the wing has the skin on its undersurface removed. The method is best illustrated by a numerical example.

Example 23.6

The structural portion of a wing consists of a three-bay rectangular section box which may be assumed to be firmly attached at all points around its periphery to the aircraft fuselage at its inboard end. The skin on the undersurface of the central bay has been removed and the wing is subjected to a torque of 10 kN m at its tip (Fig. 23.16). Calculate the shear flows in the skin panels and spar webs, the loads in the corner flanges and the forces in the ribs on each side of the cut-out assuming that the spar flanges carry all the direct loads while the skin panels and spar webs are effective only in shear.

If the wing structure were continuous and the effects of restrained warping at the built-in end ignored, the shear flows in the skin panels would be given by Eq. (18.1), i.e.

$$q = \frac{T}{2A} = \frac{10 \times 10^6}{2 \times 200 \times 800} = 31.3\,\text{N/mm}$$

and the flanges would be unloaded. However, the removal of the lower skin panel in bay ② results in a torsionally weak channel section for the length of bay ② which must in any case still transmit the applied torque to bay ① and subsequently to the wing support points. Although open section beams are inherently weak in torsion (see Section 18.2), the channel section in this case is attached at its inboard and outboard ends to torsionally stiff closed boxes so that, in effect, it is built-in at both ends. We shall examine the effect of axial constraint on open section beams subjected to torsion in Chapter 27. An alternative approach is to assume that the torque is transmitted

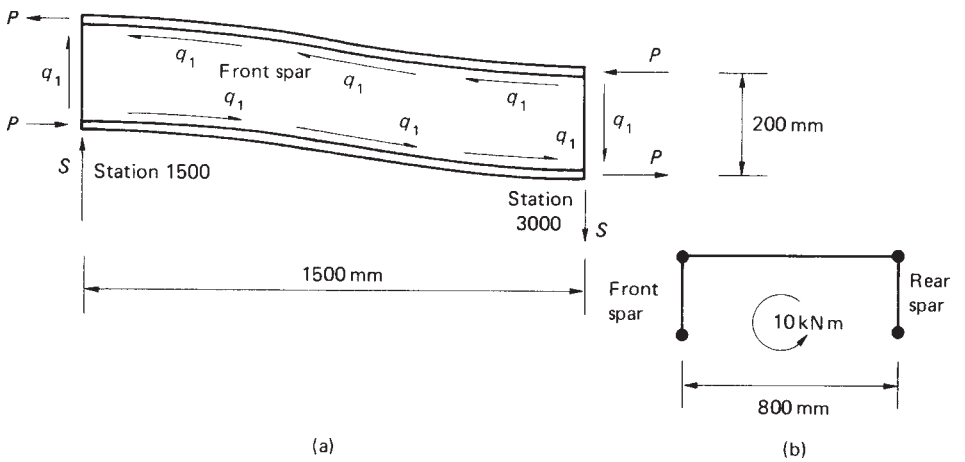

Fig. 23.17 Differential bending of front spar.

across bay ② by the differential bending of the front and rear spars. The bending moment in each spar is resisted by the flange loads P as shown, for the front spar, in Fig. 23.17(a). The shear loads in the front and rear spars form a couple at any station in bay ② which is equivalent to the applied torque. Thus, from Fig. 23.17(b)

$$800S = 10 \times 10^6 \text{ N mm}$$

i.e.

$$S = 12\,500 \text{ N}$$

The shear flow q_1 in Fig. 23.17(a) is given by

$$q_1 = \frac{12\,500}{200} = 62.5 \text{ N/mm}$$

Midway between stations 1500 and 3000 a point of contraflexure occurs in the front and rear spars so that at this point the bending moment is zero. Hence

$$200P = 12\,500 \times 750 \text{ N mm}$$

so that

$$P = 46\,875 \text{ N}$$

Alternatively, P may be found by considering the equilibrium of either of the spar flanges. Thus

$$2P = 1500q_1 = 1500 \times 62.5 \text{ N}$$

whence

$$P = 46\,875 \text{ N}$$

The flange loads P are reacted by loads in the flanges of bays ① and ③. These flange loads are transmitted to the adjacent spar webs and skin panels as shown

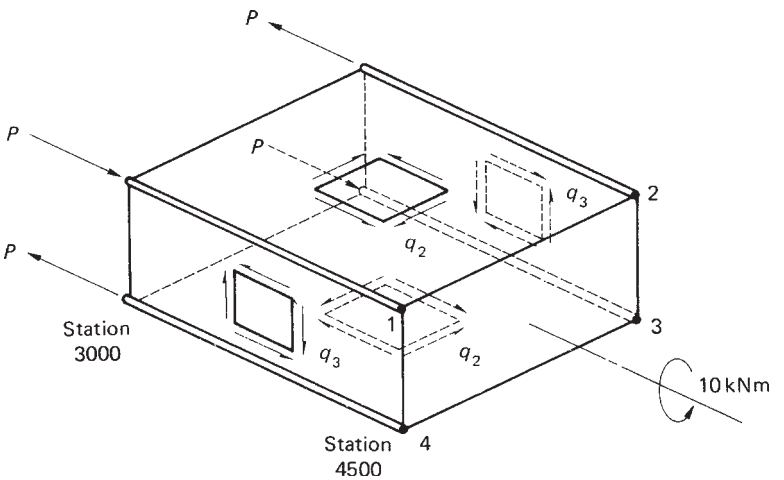

Fig. 23.18 Loads on bay ③ of the wing of Example 23.6.

in Fig. 23.18 for bay ③ and modify the shear flow distribution given by Eq. (18.1). For equilibrium of flange 1

$$1500q_2 - 1500q_3 = P = 46\,875\,\text{N}$$

or

$$q_2 - q_3 = 31.3 \tag{i}$$

The resultant of the shear flows q_2 and q_3 must be equivalent to the applied torque. Hence, for moments about the centre of symmetry at any section in bay ③ and using Eq. (20.10)

$$200 \times 800q_2 + 200 \times 800q_3 = 10 \times 10^6\,\text{N mm}$$

or

$$q_2 + q_3 = 62.5 \tag{ii}$$

Solving Eqs (i) and (ii) we obtain

$$q_2 = 46.9\,\text{N/mm} \quad q_3 = 15.6\,\text{N/mm}$$

Comparison with the results of Eq. (18.1) shows that the shear flows are increased by a factor of 1.5 in the upper and lower skin panels and decreased by a factor of 0.5 in the spar webs.

The flange loads are in equilibrium with the resultants of the shear flows in the adjacent skin panels and spar webs. Thus, for example, in the top flange of the front spar

$$P(\text{st.}4500) = 0$$
$$P(\text{st.}3000) = 1500q_2 - 1500q_3 = 46\,875\,\text{N (compression)}$$
$$P(\text{st.}2250) = 1500q_2 - 1500q_3 - 750q_1 = 0$$

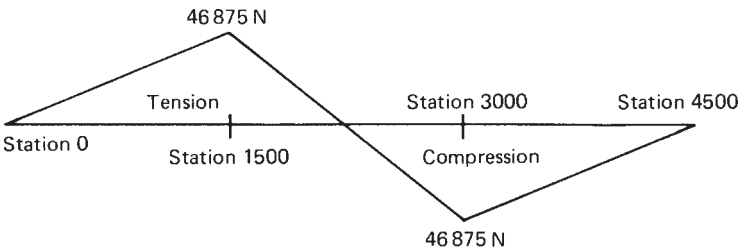

Fig. 23.19 Distribution of load in the top flange of the front spar of the wing of Example 23.6.

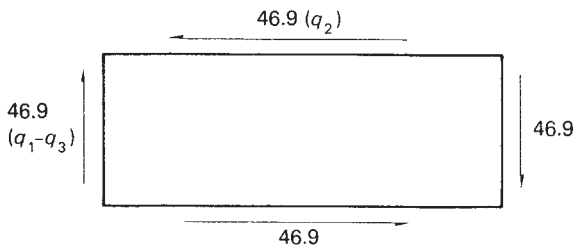

Fig. 23.20 Shear flows (N/mm) on wing rib at station 3000 in the wing of Example 23.6.

The loads along the remainder of the flange follow from antisymmetry giving the distribution shown in Fig. 23.19. The load distribution in the bottom flange of the rear spar will be identical to that shown in Fig. 23.19 while the distributions in the bottom flange of the front spar and the top flange of the rear spar will be reversed. We note that the flange loads are zero at the built-in end of the wing (station 0). Generally, however, additional stresses are induced by the warping restraint at the built-in end; these are investigated in Chapter 26. The loads on the wing ribs on either the inboard or outboard end of the cut-out are found by considering the shear flows in the skin panels and spar webs immediately inboard and outboard of the rib. Thus, for the rib at station 3000 we obtain the shear flow distribution shown in Fig. 23.20.

In Example 23.6 we implicitly assumed in the analysis that the local effects of the cut-out were completely dissipated within the length of the adjoining bays which were equal in length to the cut-out bay. The validity of this assumption relies on St. Venant's principle (Section 2.4). It may generally be assumed therefore that the effects of a cut-out are restricted to spanwise lengths of the wing equal to the length of the cut-out on both inboard and outboard ends of the cut-out bay.

We shall now consider the more complex case of a wing having a cut-out and subjected to shear loads which produce both bending and torsion. Again the method is illustrated by a numerical example.

Example 23.7

A wing box has the skin panel on its undersurface removed between stations 2000 and 3000 and carries lift and drag loads which are constant between stations 1000 and 4000 as shown in Fig. 23.21(a). Determine the shear flows in the skin panels and spar webs and also the loads in the wing ribs at the inboard and outboard ends of the cut-out bay.

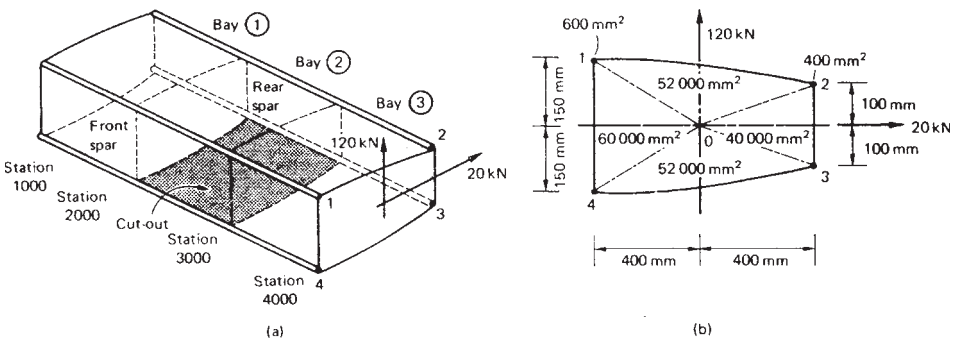

Fig. 23.21 Wing box of Example 23.7.

Assume that all bending moments are resisted by the spar flanges while the skin panels and spar webs are effective only in shear.

The simplest approach is first to determine the shear flows in the skin panels and spar webs as though the wing box were continuous and then to apply an equal and opposite shear flow to that calculated around the edges of the cut-out. The shear flows in the wing box without the cut-out will be the same in each bay and are calculated using the method described in Section 20.3 and illustrated in Example 20.4. This gives the shear flow distribution shown in Fig. 23.22.

We now consider bay ② and apply a shear flow of 75.9 N/mm in the wall 34 in the opposite sense to that shown in Fig. 23.22. This reduces the shear flow in the wall 34 to zero and, in effect, restores the cut-out to bay ②. The shear flows in the remaining walls of the cut-out bay will no longer be equivalent to the externally applied shear loads so that corrections are required. Consider the cut-out bay (Fig. 23.23) with the shear flow of 75.9 N/mm applied in the opposite sense to that shown in Fig. 23.22. The correction shear flows q'_{12}, q'_{32} and q'_{14} may be found using statics. Thus, resolving forces horizontally we have

$$800q'_{12} = 800 \times 75.9\,\text{N}$$

whence

$$q'_{12} = 75.9\,\text{N/mm}$$

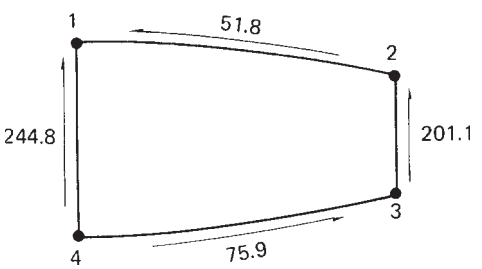

Fig. 23.22 Shear flow (N/mm) distribution at any station in the wing box of Example 23.7 without cut-out.

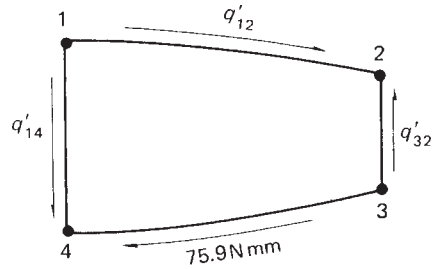

Fig. 23.23 Correction shear flows in the cut-out bay of the wing box of Example 23.7.

Resolving forces vertically

$$200q'_{32} = 50q'_{12} - 50 \times 75.9 - 300q'_{14} = 0 \qquad \text{(i)}$$

and taking moments about O in Fig. 23.21(b) we obtain

$$2 \times 52\,000q'_{12} - 2 \times 40\,000q'_{32} + 2 \times 52\,000 \times 75.9 - 2 \times 60\,000q'_{14} = 0 \qquad \text{(ii)}$$

Solving Eqs (i) and (ii) gives

$$q'_{32} = 117.6\,\text{N/mm} \quad q'_{14} = 53.1\,\text{N/mm}$$

The final shear flows in bay ② are found by superimposing q'_{12}, q'_{32} and q'_{14} on the shear flows in Fig. 23.22, giving the distribution shown in Fig. 23.24. Alternatively, these shear flows could have been found directly by considering the equilibrium of the cut-out bay under the action of the applied shear loads.

The correction shear flows in bay ② (Fig. 23.23) will also modify the shear flow distributions in bays ① and ③. The correction shear flows to be applied to those shown in Fig. 23.22 for bay ③ (those in bay ① will be identical) may be found by determining the flange loads corresponding to the correction shear flows in bay ②.

It can be seen from the magnitudes and directions of these correction shear flows (Fig. 23.23) that at any section in bay ② the loads in the upper and lower flanges of the front spar are equal in magnitude but opposite in direction; similarly for the rear spar. Thus, the correction shear flows in bay ② produce an identical system of flange loads to that shown in Fig. 23.17 for the cut-out bays in the wing structure of Example 23.6.

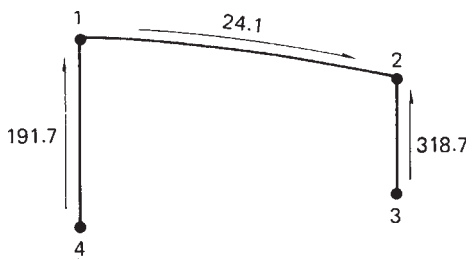

Fig. 23.24 Final shear flows (N/mm) in the cut-out bay of the wing box of Example 23.7.

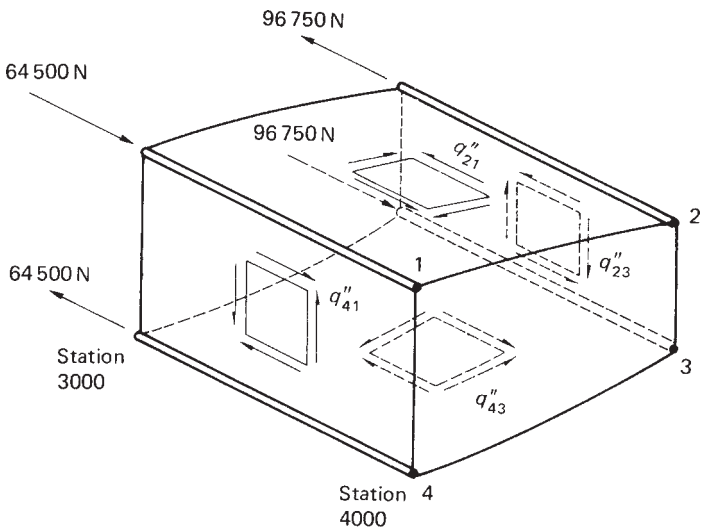

Fig. 23.25 Correction shear flows in bay ③ of the wing box of Example 23.7.

It follows that these correction shear flows produce differential bending of the front and rear spars in bay ② and that the spar bending moments and hence the flange loads are zero at the mid-bay points. Therefore, at station 3000 the flange loads are

$$P_1 = (75.9 + 53.1) \times 500 = 64\,500\,\text{N (compression)}$$
$$P_4 = 64\,500\,\text{N (tension)}$$
$$P_2 = (75.9 + 117.6) \times 500 = 96\,750\,\text{N (tension)}$$
$$P_3 = 96\,750\,\text{N (tension)}$$

These flange loads produce correction shear flows q''_{21}, q''_{43}, q''_{23} and q''_{41} in the skin panels and spar webs of bay ③ as shown in Fig. 23.25. Thus for equilibrium of flange 1

$$1000q''_{41} + 1000q''_{21} = 64\,500\,\text{N} \tag{iii}$$

and for equilibrium of flange 2

$$1000q''_{21} + 1000q''_{23} = 96\,750\,\text{N} \tag{iv}$$

For equilibrium in the chordwise direction at any section in bay ③

$$800q''_{21} = 800q''_{43}$$

or

$$q''_{21} = q''_{43} \tag{v}$$

Finally, for vertical equilibrium at any section in bay ③

$$300q''_{41} + 50q''_{43} + 50q''_{21} - 200q''_{23} = 0 \tag{vi}$$

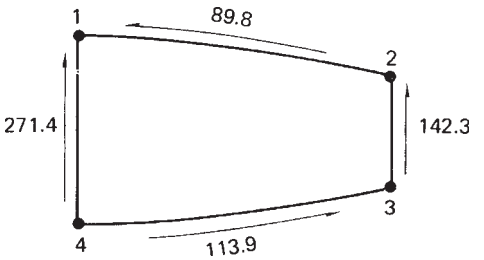

Fig. 23.26 Final shear flows in bay ③ (and bay ①) of the wing box of Example 23.7.

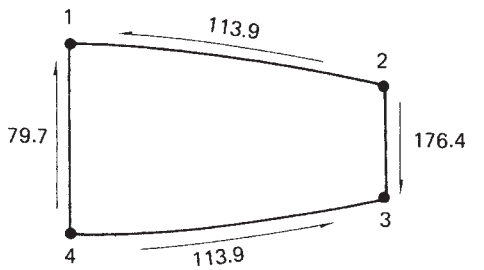

Fig. 23.27 Shear flows (N/mm) applied to the wing rib at station 3000 in the wing box of Example 23.7.

Simultaneous solution of Eqs (iii)–(vi) gives

$$q''_{21} = q''_{43} = 38.0\,\text{N/mm} \quad q''_{23} = 58.8\,\text{N/mm} \quad q''_{41} = 26.6\,\text{N/mm}$$

Superimposing these correction shear flows on those shown in Fig. 23.22 gives the final shear flow distribution in bay ③ as shown in Fig. 23.26. The rib loads at stations 2000 and 3000 are found as before by adding algebraically the shear flows in the skin panels and spar webs on each side of the rib. Thus, at station 3000 we obtain the shear flows acting around the periphery of the rib as shown in Fig. 23.27. The shear flows applied to the rib at the inboard end of the cut-out bay will be equal in magnitude but opposite in direction.

Note that in this example only the shear loads on the wing box between stations 1000 and 4000 are given. We cannot therefore determine the final values of the loads in the spar flanges since we do not know the values of the bending moments at these positions caused by loads acting on other parts of the wing.

Problems

P.23.1 The central cell of a wing has the idealized section shown in Fig. P.23.1. If the lift and drag loads on the wing produce bending moments of $-120\,000$ N m and $-30\,000$ N m, respectively at the section shown, calculate the direct stresses in the booms. Neglect axial constraint effects and assume that the lift and drag vectors are in vertical and horizontal planes.

$$\text{Boom areas: } B_1 = B_4 = B_5 = B_8 = 1000\,\text{mm}^2$$
$$B_2 = B_3 = B_6 = B_7 = 600\,\text{mm}^2$$

Ans. $\sigma_1 = -190.7\,\text{N/mm}^2$ $\sigma_2 = -181.7\,\text{N/mm}^2$ $\sigma_3 = -172.8\,\text{N/mm}^2$
$\sigma_4 = -163.8\,\text{N/mm}^2$ $\sigma_5 = 140\,\text{N/mm}^2$ $\sigma_6 = 164.8\,\text{N/mm}^2$
$\sigma_7 = 189.6\,\text{N/mm}^2$ $\sigma_8 = 214.4\,\text{N/mm}^2$.

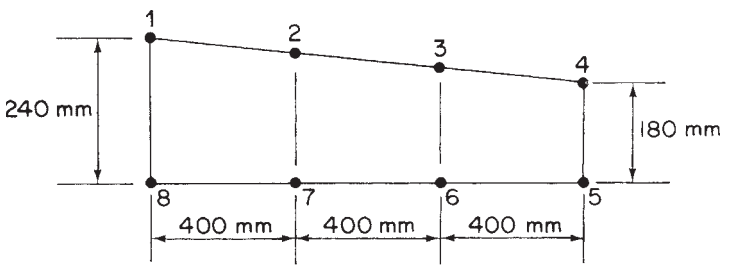

Fig. P.23.1

P.23.2 Figure P.23.2 shows the cross-section of a two-cell torque box. If the shear stress in any wall must not exceed $140\,\text{N/mm}^2$, find the maximum torque which can be applied to the box.

If this torque were applied at one end and resisted at the other end of such a box of span 2500 mm, find the twist in degrees of one end relative to the other and the torsional rigidity of the box. The shear modulus $G = 26\,600\,\text{N/mm}^2$ for all walls.

Data:

Shaded areas:	$A_{34} = 6450\,\text{mm}^2$, $A_{16} = 7750\,\text{mm}^2$
Wall lengths:	$s_{34} = 250\,\text{mm}$, $s_{16} = 300\,\text{mm}$
Wall thickness:	$t_{12} = 1.63\,\text{mm}$, $t_{34} = 0.56\,\text{mm}$
	$t_{23} = t_{45} = t_{56} = 0.92\,\text{mm}$
	$t_{61} = 2.03\,\text{mm}$
	$t_{25} = 2.54\,\text{mm}$

Ans. $T = 102\,417\,\text{N m}$, $\theta = 1.46°$, $GJ = 10 \times 10^{12}\,\text{N mm}^2/\text{rad}$.

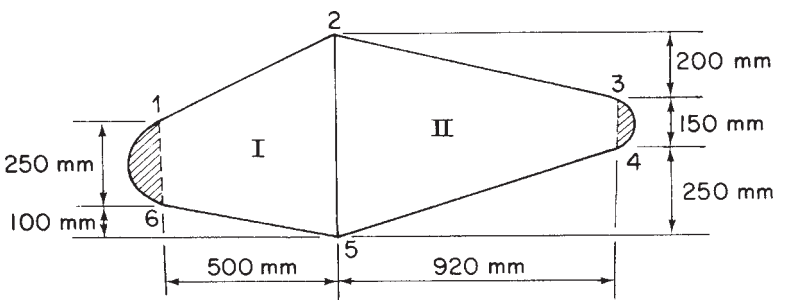

Fig. P.23.2

P.23.3 Determine the torsional stiffness of the four-cell wing section shown in Fig. P.23.3.

Data:

Wall	12	23	34					
	78	67	56	45^{o}	45^{i}	36	27	18
Peripheral length (mm)	762	812	812	1525	356	406	356	254
Thickness (mm)	0.915	0.915	0.915	0.711	1.220	1.625	1.220	0.915

Cell areas (mm^2) $A_{\mathrm{I}} = 161\,500$ $A_{\mathrm{II}} = 291\,000$
$A_{\mathrm{III}} = 291\,000$ $A_{\mathrm{IV}} = 226\,000$

Ans. $522.5 \times 10^6 G\,\mathrm{N\,mm^2/rad}$.

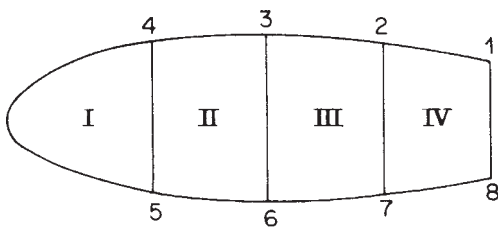

Fig. P.23.3

P.23.4 Determine the shear flow distribution for a torque of 56 500 N m for the three cell section shown in Fig. P.23.4. The section has a constant shear modulus throughout.

Wall	Length (mm)	Thickness (mm)	Cell	Area (mm^2)
12^{U}	1084	1.220	I	108 400
12^{L}	2160	1.625	II	202 500
14, 23	127	0.915	III	528 000
34^{U}	797	0.915		
34^{L}	797	0.915		

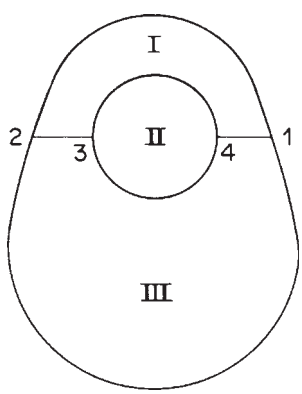

Fig. P.23.4

Ans. $q_{12^U} = 25.4\,\text{N/mm}$ $q_{21^L} = 33.5\,\text{N/mm}$ $q_{14} = q_{32} = 8.1\,\text{N/mm}$
$q_{43^U} = 13.4\,\text{N/mm}$ $q_{34^L} = 5.3\,\text{N/mm}$.

P.23.5 The idealized cross-section of a two-cell thin-walled wing box is shown in Fig. P.23.5. If the wing box supports a load of 44 500 N acting along the web 25, calculate the shear flow distribution. The shear modulus G is the same for all walls of the wing box.

Wall	Length (mm)	Thickness (mm)	Boom	Area (mm^2)
16	254	1.625	1, 6	1290
25	406	2.032	2, 5	1936
34	202	1.220	3, 4	645
12, 56	647	0.915		
23, 45	775	0.559		

Cell areas: $A_I = 232\,000\,mm^2$, $A_{II} = 258\,000\,mm^2$

Ans. $q_{16} = 33.9\,\text{N/mm}$ $q_{65} = q_{21} = 1.1\,\text{N/mm}$
$q_{45} = q_{23} = 7.2\,\text{N/mm}$ $q_{34} = 20.8\,\text{N/mm}$
$q_{25} = 73.4\,\text{N/mm}$.

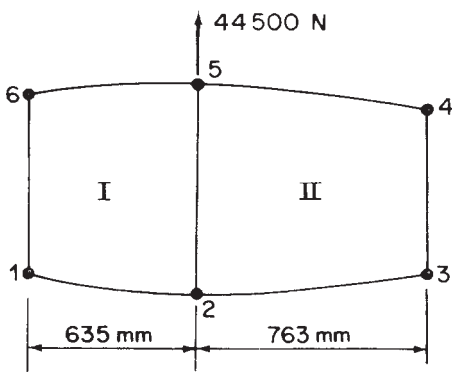

Fig. P.23.5

P.23.6 Figure P.23.6 shows a singly symmetric, two-cell wing section in which all direct stresses are carried by the booms, shear stresses alone being carried by the walls. All walls are flat with the exception of the nose portion 45. Find the position of the

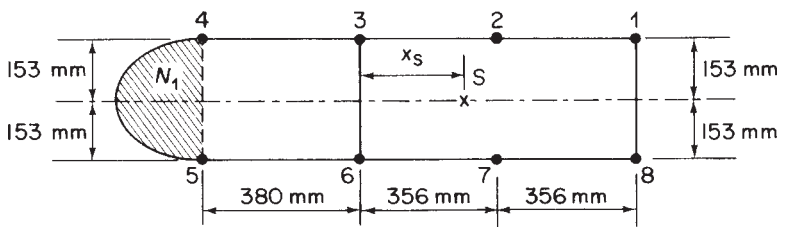

Fig. P.23.6

shear centre S and the shear flow distribution for a load of $S_y = 66\,750$ N through S. Tabulated below are lengths, thicknesses and shear moduli of the shear carrying walls. Note that dotted line 45 is not a wall.

Wall	Length (mm)	Thickness (mm)	G(N/mm^2)	Boom	Area (mm^2)
34, 56	380	0.915	20 700	1, 3, 6, 8	1290
12, 23, 67, 78	356	0.915	24 200	2, 4, 5, 7	645
36, 81	306	1.220	24 800		
45	610	1.220	24 800		
Nose area $N_1 = 51\,500$ mm^2					

Ans. $x_S = 160.1$ mm $q_{12} = q_{78} = 17.8$ N/mm $q_{32} = q_{76} = 18.5$ N/mm
$q_{63} = 88.2$ N/mm $q_{43} = q_{65} = 2.9$ N/mm $q_{54} = 39.2$ N/mm
$q_{81} = 90.4$ N/mm.

P.23.7 A singly symmetric wing section consists of two closed cells and one open cell (see Fig. P.23.7). The webs 25, 34 and the walls 12, 56 are straight, while all other walls are curved. All walls of the section are assumed to be effective in carrying shear stresses only, direct stresses being carried by booms 1–6. Calculate the distance x_S of the shear centre S aft of the web 34. The shear modulus G is the same for all walls.

Wall	Length (mm)	Thickness (mm)	Boom	Area (mm^2)	Cell	Area (mm^2)
12, 56	510	0.559	1, 6	645	I	93 000
23, 45	765	0.915	2, 5	1290	II	258 000
34^o	1015	0.559	3, 4	1935		
34^i	304	2.030				
25	304	1.625				

Ans. 241.4 mm.

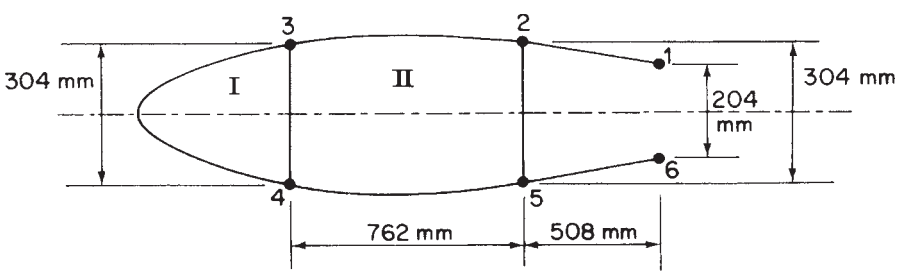

Fig. P.23.7

P.23.8 A portion of a tapered, three-cell wing has singly symmetrical idealized cross-sections 1000 mm apart as shown in Fig. P.23.8. A bending moment $M_x = 1800$ N m and a shear load $S_y = 12\,000$ N in the plane of the web 52 are applied at the larger cross-section. Calculate the forces in the booms and the shear flow distribution

at this cross-section. The modulus G is constant throughout. Section dimensions at the larger cross-section are given below.

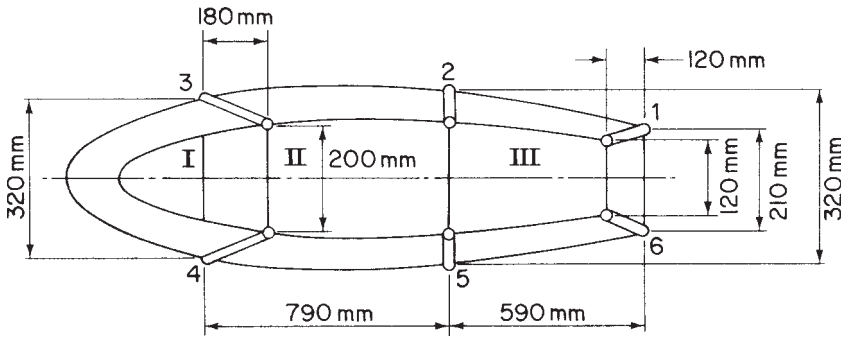

Fig. P.23.8

Wall	Length (mm)	Thickness (mm)	Boom	Area (mm^2)	Cell	Area (mm^2)
12, 56	600	1.0	1, 6	600	I	100 000
23, 45	800	1.0	2, 5	800	II	260 000
34^o	1200	0.6	3, 4	800	III	180 000
34^i	320	2.0				
25	320	2.0				
16	210	1.5				

Ans. $P_1 = -P_6 = 1200\,\text{N}$ $P_2 = -P_5 = 2424\,\text{N}$ $P_3 = -P_4 = 2462\,\text{N}$
$q_{12} = q_{56} = 3.74\,\text{N/mm}$ $q_{23} = q_{45} = 3.11\,\text{N/mm}$ $q_{34^o} = 0.06\,\text{N/mm}$
$q_{43^i} = 12.16\,\text{N/mm}$ $q_{52} = 14.58\,\text{N/mm}$ $q_{61} = 11.22\,\text{N/mm}$.

P.23.9 A portion of a wing box is built-in at one end and carries a shear load of 2000 N through its shear centre and a torque of 1000 N m as shown in Fig. P.23.9. If

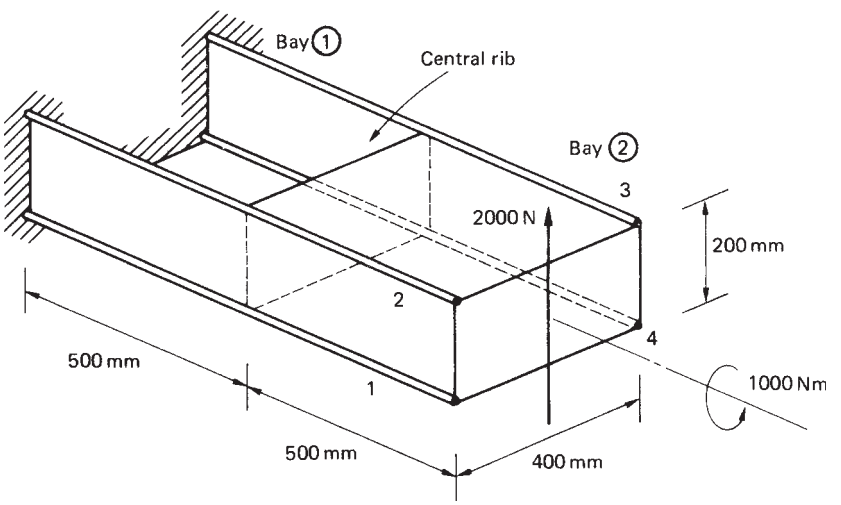

Fig. P.23.9

the skin panel in the upper surface of the inboard bay is removed, calculate the shear flows in the spar webs and remaining skin panels, the distribution of load in the spar flanges and the loading on the central rib. Assume that the spar webs and skin panels are effective in resisting shear stresses only.

Ans. Bay ①: q in spar webs = 7.5 N/mm
Bay ②: q in spar webs = 1.9 N/mm, in skin panels = 9.4 N/mm
Flange loads (2): at built-in end = 1875 N (compression)
at central rib = 5625 N (compression)
Rib loads: q (horizontal edges) = 9.4 N/mm
q (vertical edges) = 9.4 N/mm.

24

Fuselage frames and wing ribs

Aircraft are constructed primarily from thin metal skins which are capable of resisting in-plane tension and shear loads but buckle under comparatively low values of in-plane compressive loads. The skins are therefore stiffened by longitudinal stringers which resist the in-plane compressive loads and, at the same time, resist small distributed loads normal to the plane of the skin. The effective length in compression of the stringers is reduced, in the case of fuselages, by transverse frames or bulkheads or, in the case of wings, by ribs. In addition, the frames and ribs resist concentrated loads in transverse planes and transmit them to the stringers and the plane of the skin. Thus, cantilever wings may be bolted to fuselage frames at the spar caps while undercarriage loads are transmitted to the wing through spar and rib attachment points.

24.1 Principles of stiffener/web construction

Generally, frames and ribs are themselves fabricated from thin sheets of metal and therefore require stiffening members to distribute the concentrated loads to the thin webs. If the load is applied in the plane of a web the stiffeners must be aligned with the direction of the load. Alternatively, if this is not possible, the load should be applied at the intersection of two stiffeners so that each stiffener resists the component of load in its direction. The basic principles of stiffener/web construction are illustrated in Example 24.1.

Example 24.1

A cantilever beam (Fig. 24.1) carries concentrated loads as shown. Calculate the distribution of stiffener loads and the shear flow distribution in the web panels assuming that the latter are effective only in shear.

We note that stiffeners HKD and JK are required at the point of application of the 4000 N load to resist its vertical and horizontal components. A further transverse stiffener GJC is positioned at the unloaded end J of the stiffener JK since stress concentrations are produced if a stiffener ends in the centre of a web panel. We note also that the web panels are only effective in shear so that the shear flow is constant throughout a particular web panel; the assumed directions of the shear flows are shown in Fig. 24.1.

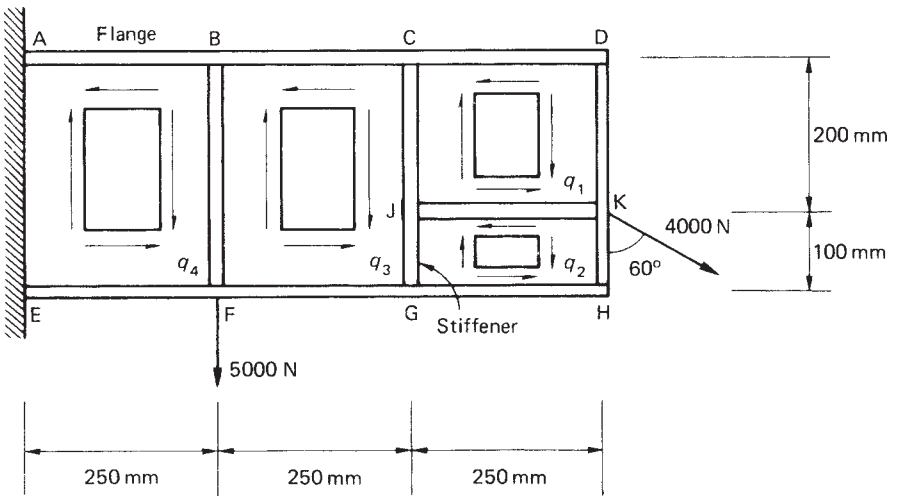

Fig. 24.1 Cantilever beam of Example 24.1.

It is instructive at this stage to examine the physical role of the different structural components in supporting the applied loads. Generally, stiffeners are assumed to withstand axial forces only so that the horizontal component of the load at K is equilibrated locally by the axial load in the stiffener JK and not by the bending of stiffener HKD. By the same argument the vertical component of the load at K is resisted by the axial load in the stiffener HKD. These axial stiffener loads are equilibrated in turn by the resultants of the shear flows q_1 and q_2 in the web panels CDKJ and JKHG. Thus we see that the web panels resist the shear component of the externally applied load and at the same time transmit the bending and axial load of the externally applied load to the beam flanges; subsequently, the flange loads are reacted at the support points A and E.

Consider the free body diagrams of the stiffeners JK and HKD shown in Figs. 24.2(a) and (b).

From the equilibrium of stiffener JK we have

$$(q_1 - q_2) \times 250 = 4000 \sin 60^\circ = 3464.1 \text{ N} \qquad \text{(i)}$$

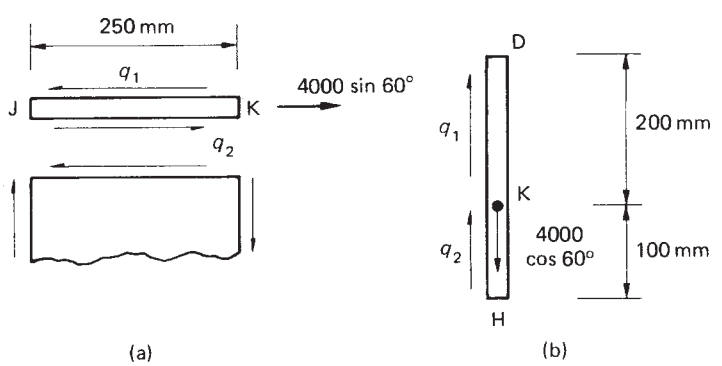

Fig. 24.2 Free body diagrams of stiffeners JK and HKD in the beam of Example 24.1.

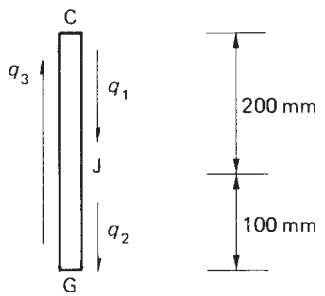

Fig. 24.3 Equilibrium of stiffener CJG in the beam of Example 24.1.

and from the equilibrium of stiffener HKD

$$200q_1 + 100q_2 = 4000\cos 60^\circ = 2000\,\text{N} \qquad \text{(ii)}$$

Solving Eqs (i) and (ii) we obtain

$$q_1 = 11.3\,\text{N/mm} \quad q_2 = -2.6\,\text{N/mm}$$

The vertical shear force in the panel BCGF is equilibrated by the vertical resultant of the shear flow q_3. Thus

$$300q_3 = 4000\cos 60^\circ = 2000\,\text{N}$$

whence

$$q_3 = 6.7\,\text{N/mm}$$

Alternatively, q_3 may be found by considering the equilibrium of the stiffener CJG. From Fig. 24.3

$$300q_3 = 200q_1 + 100q_2$$

or

$$300q_3 = 200 \times 11.3 - 100 \times 2.6$$

from which

$$q_3 = 6.7\,\text{N/mm}$$

The shear flow q_4 in the panel ABFE may be found using either of the above methods. Thus, considering the vertical shear force in the panel

$$300q_4 = 4000\cos 60^\circ + 5000 = 7000\,\text{N}$$

whence

$$q_4 = 23.3\,\text{N/mm}$$

Alternatively, from the equilibrium of stiffener BF

$$300q_4 - 300q_3 = 5000\,\text{N}$$

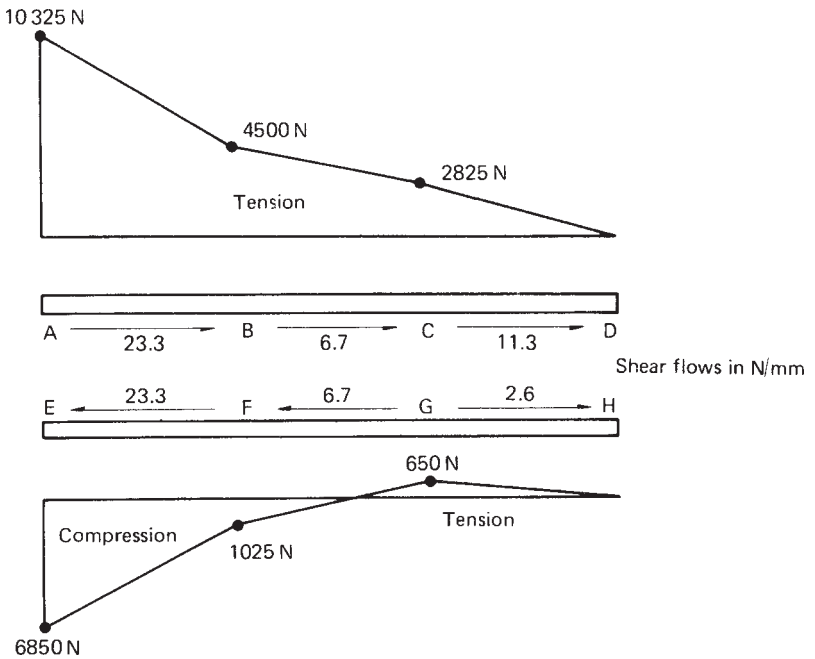

Fig. 24.4 Load distributions in flanges of the beam of Example 24.1.

whence

$$q_4 = 23.3\,\text{N/mm}$$

The flange and stiffener load distributions are calculated in the same way and are obtained from the algebraic summation of the shear flows along their lengths. For example, the axial load P_A at A in the flange ABCD is given by

$$P_\text{A} = 250q_1 + 250q_3 + 250q_4$$

or

$$P_\text{A} = 250 \times 11.3 + 250 \times 6.7 + 250 \times 23.3 = 10\,325\,\text{N (tension)}$$

Similarly

$$P_\text{E} = -250q_2 - 250q_3 - 250q_4$$

i.e.

$$P_\text{E} = 250 \times 2.6 - 250 \times 6.7 - 250 \times 23.3 = -6850\,\text{N (compression)}$$

The complete load distribution in each flange is shown in Fig. 24.4. The stiffener load distributions are calculated in the same way and are shown in Fig. 24.5.

The distribution of flange load in the bays ABFE and BCGF could have been obtained by considering the bending and axial loads on the beam at any section. For

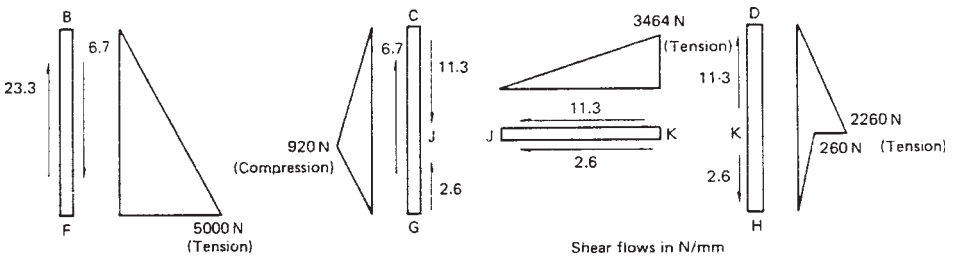

Fig. 24.5 Load distributions in stiffeners of the beam of Example 24.1.

example, at the section AE we can replace the actual loading system by a bending moment

$$M_{\mathrm{AE}} = 5000 \times 250 + 2000 \times 750 - 3464.1 \times 50 = 2\,576\,800\,\mathrm{N\,mm}$$

and an axial load acting midway between the flanges (irrespective of whether or not the flange areas are symmetrical about this point) of

$$P = 3464.1\,\mathrm{N}$$

Thus

$$P_A = \frac{2\,576\,800}{300} + \frac{3464.1}{2} = 10\,321\,\mathrm{N\ (tension)}$$

and

$$P_E = \frac{-2\,576\,800}{300} + \frac{3464.1}{2} = -6857\,\mathrm{N\ (compression)}$$

This approach cannot be used in the bay CDHG except at the section CJG since the axial load in the stiffener JK introduces an additional unknown.

The above analysis assumes that the web panels in beams of the type shown in Fig. 24.1 resist pure shear along their boundaries. In Chapter 9 we saw that thin webs may buckle under the action of such shear loads producing tension field stresses which, in turn, induce additional loads in the stiffeners and flanges of beams. The tension field stresses may be calculated separately by the methods described in Chapter 9 and then superimposed on the stresses determined as described above.

So far we have been concerned with web/stiffener arrangements in which the loads have been applied in the plane of the web so that two stiffeners are sufficient to resist the components of a concentrated load. Frequently, loads have an out-of-plane component in which case the structure should be arranged so that two webs meet at the point of load application with stiffeners aligned with the three component directions (Fig. 24.6). In some situations it is not practicable to have two webs meeting at the point of load application so that a component normal to a web exists. If this component is small it may be resisted in bending by an in-plane stiffener, otherwise an additional member must be provided spanning between adjacent frames or ribs, as shown in Fig. 24.7. In general, no normal loads should be applied to an unsupported web no matter how small their magnitude.

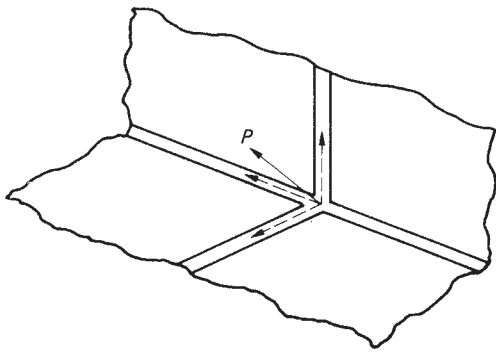

Fig. 24.6 Structural arrangement for an out of plane load.

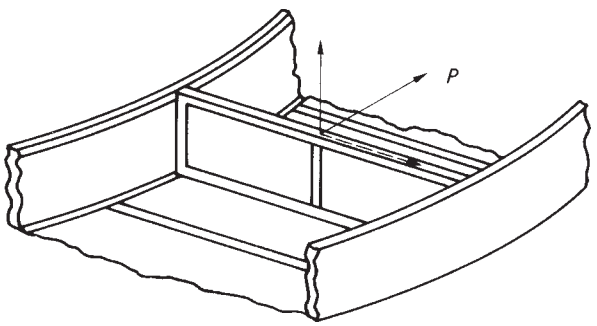

Fig. 24.7 Support of load having a component normal to a web.

24.2 Fuselage frames

We have noted that fuselage frames transfer loads to the fuselage shell and provide column support for the longitudinal stringers. The frames generally take the form of open rings so that the interior of the fuselage is not obstructed. They are connected continuously around their peripheries to the fuselage shell and are not necessarily circular in form but will usually be symmetrical about a vertical axis.

A fuselage frame is in equilibrium under the action of any external loads and the reaction shear flows from the fuselage shell. Suppose that a fuselage frame has a vertical axis of symmetry and carries a vertical external load W, as shown in Fig. 24.8(a) and (b). The fuselage shell/stringer section has been idealized such that the fuselage skin is effective only in shear. Suppose also that the shear force in the fuselage immediately to the left of the frame is $S_{y,1}$ and that the shear force in the fuselage immediately to the right of the frame is $S_{y,2}$; clearly, $S_{y,2} = S_{y,1} - W$. $S_{y,1}$ and $S_{y,2}$ generate shear flow distributions q_1 and q_2, respectively in the fuselage skin, each given by Eq. (22.1) in which $S_{x,1} = S_{x,2} = 0$ and $I_{xy} = 0$ (Cy is an axis of symmetry). The shear flow q_{f} transmitted to the periphery of the frame is equal to the algebraic sum of q_1 and q_2, i.e.

$$q_{\mathrm{f}} = q_1 - q_2$$

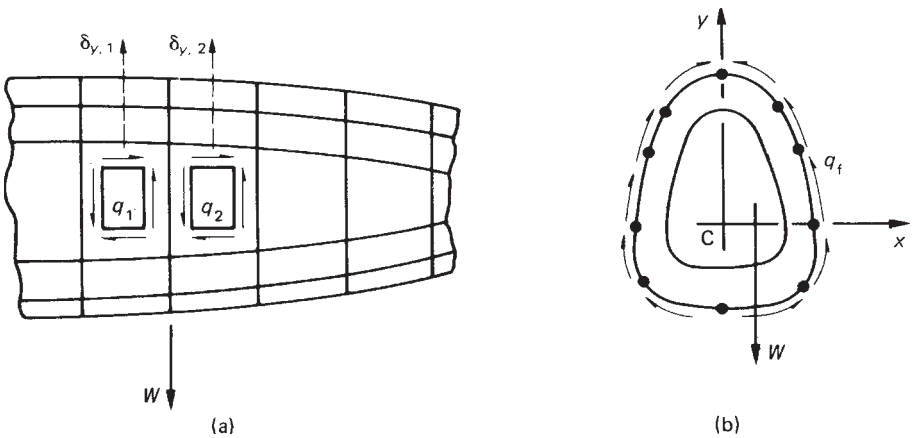

Fig. 24.8 Loads on a fuselage frame.

Thus, substituting for q_1 and q_2 obtained from Eq. (22.1) and noting that $S_{y,2} = S_{y,1} - W$, we have

$$q_{\mathrm{f}} = \frac{-W}{I_{xx}} \sum_{r=1}^{n} B_r y_r + q_{s,0}$$

in which $q_{s,0}$ is calculated using Eq. (17.17) where the shear load is W and

$$q_{\mathrm{b}} = \frac{-W}{I_{xx}} \sum_{r=1}^{n} B_r y_r$$

The method of determining the shear flow distribution applied to the periphery of a fuselage frame is identical to the method of solution (or the alternative method) of Example 22.2.

Having determined the shear flow distribution around the periphery of the frame, the frame itself may be analysed for distributions of bending moment, shear force and normal force, as described in Section 5.4.

24.3 Wing ribs

Wing ribs perform similar functions to those performed by fuselage frames. They maintain the shape of the wing section, assist in transmitting external loads to the wing skin and reduce the column length of the stringers. Their geometry, however, is usually different in that they are frequently of unsymmetrical shape and possess webs which are continuous except for lightness holes and openings for control runs.

Wing ribs are subjected to loading systems which are similar to those applied to fuselage frames. External loads applied in the plane of the rib produce a change in shear force in the wing across the rib; this induces reaction shear flows around its periphery. These are calculated using the methods described in Chapter 17 and in Chapter 23.

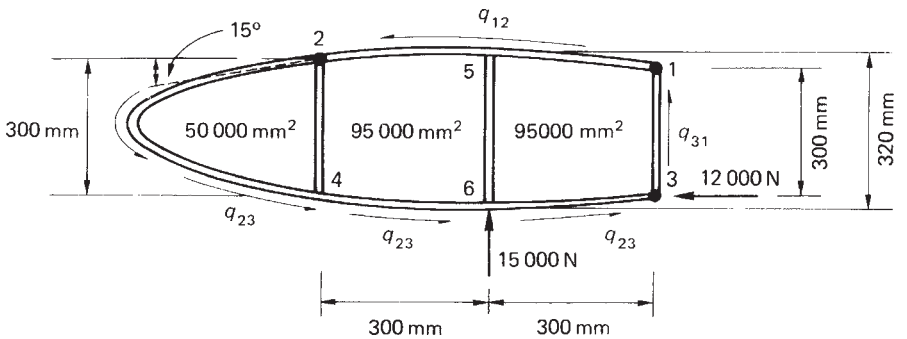

Fig. 24.9 Wing rib of Example 24.2.

To illustrate the method of rib analysis we shall use the example of a three-flange wing section in which, as we noted in Section 23.1, the shear flow distribution is statically determinate.

Example 24.2

Calculate the shear flows in the web panels and the axial loads in the flanges of the wing rib shown in Fig. 24.9. Assume that the web of the rib is effective only in shear while the resistance of the wing to bending moments is provided entirely by the three flanges 1, 2 and 3.

Since the wing bending moments are resisted entirely by the flanges 1, 2 and 3, the shear flows developed in the wing skin are constant between the flanges. Using the method described in Section 23.1 for a three-flange wing section we have, resolving forces horizontally

$$600q_{12} - 600q_{23} = 12\,000\,\text{N} \tag{i}$$

Resolving vertically

$$300q_{31} - 300q_{23} = 15\,000\,\text{N} \tag{ii}$$

Taking moments about flange 3

$$2(50\,000 + 95\,000)q_{23} + 2 \times 95\,000q_{12} = -15\,000 \times 300\,\text{N mm} \tag{iii}$$

Solution of Eqs (i)–(iii) gives

$$q_{12} = 13.0\,\text{N/mm} \quad q_{23} = -7.0\,\text{N/mm} \quad q_{31} = 43.0\,\text{N/mm}$$

Consider now the nose portion of the rib shown in Fig. 24.10 and suppose that the shear flow in the web immediately to the left of the stiffener 24 is q_1. The total vertical shear force $S_{y,1}$ at this section is given by

$$S_{y,1} = 7.0 \times 300 = 2100\,\text{N}$$

The horizontal components of the rib flange loads resist the bending moment at this section. Thus

$$P_{x,4} = P_{x,2} = \frac{2 \times 50\,000 \times 7.0}{300} = 2333.3\,\text{N}$$

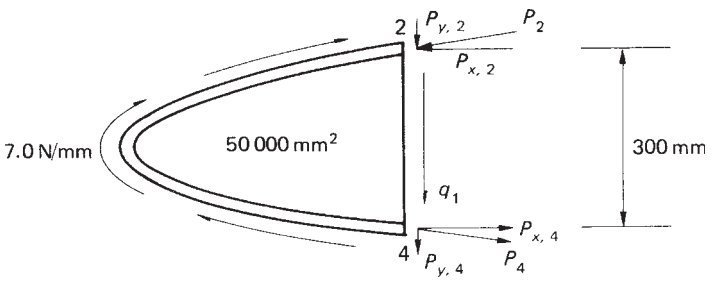

Fig. 24.10 Equilibrium of nose portion of the rib.

The corresponding vertical components are then

$$P_{y,2} = P_{y,4} = 2333.3 \tan 15^\circ = 625.2\,\text{N}$$

Thus the shear force carried by the web is $2100 - 2 \times 625.2 = 849.6\,\text{N}$. Hence

$$q_1 = \frac{849.6}{300} = 2.8\,\text{N/mm}$$

The axial loads in the rib flanges at this section are given by

$$P_2 = P_4 = (2333.3^2 + 625.2^2)^{1/2} = 2415.6\,\text{N}$$

The rib flange loads and web panel shear flows, at a vertical section immediately to the left of the intermediate web stiffener 56, are found by considering the free body diagram shown in Fig. 24.11. At this section the rib flanges have zero slope so that the flange loads P_5 and P_6 are obtained directly from the value of bending moment at this section. Thus

$$P_5 = P_6 = 2[(50\,000 + 46\,000) \times 7.0 - 49\,000 \times 13.0]/320 = 218.8\,\text{N}$$

The shear force at this section is resisted solely by the web. Hence

$$320q_2 = 7.0 \times 300 + 7.0 \times 10 - 13.0 \times 10 = 2040\,\text{N}$$

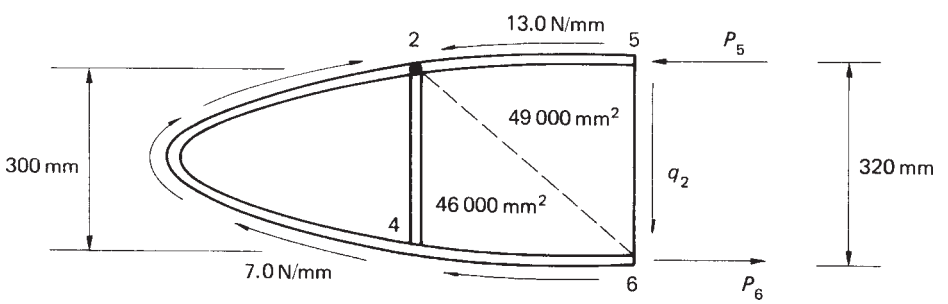

Fig. 24.11 Equilibrium of rib forward of intermediate stiffener 56.

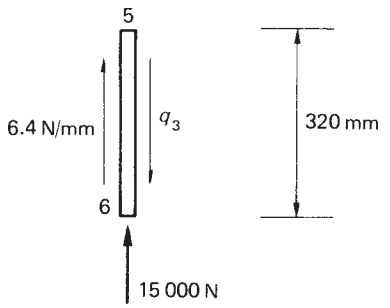

Fig. 24.12 Equilibrium of stiffener 56.

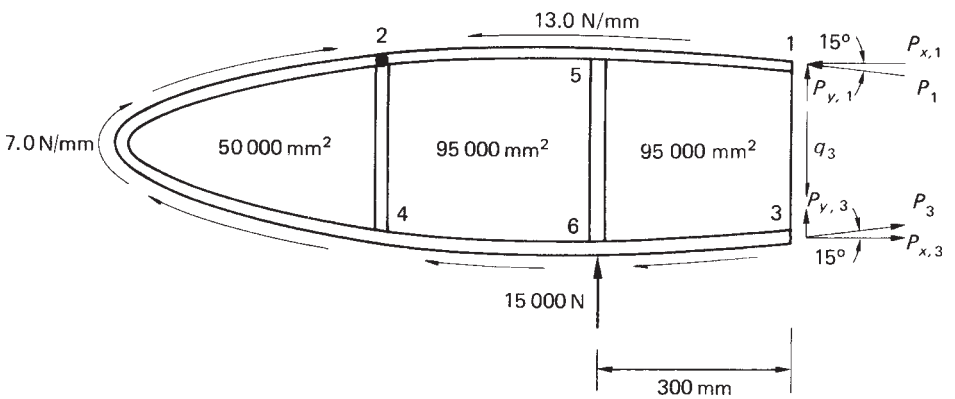

Fig. 24.13 Equilibrium of the rib forward of stiffener 31.

so that

$$q_2 = 6.4\,\text{N/mm}$$

The shear flow in the rib immediately to the right of stiffener 56 is found most simply by considering the vertical equilibrium of stiffener 56 as shown in Fig. 24.12. Thus

$$320q_3 = 6.4 \times 320 + 15\,000$$

which gives

$$q_3 = 53.3\,\text{N/mm}$$

Finally, we shall consider the rib flange loads and the web shear flow at a section immediately forward of stiffener 31. From Fig. 24.13, in which we take moments about the point 3

$$M_3 = 2[(50\,000 + 95\,000) \times 7.0 - 95\,000 \times 13.0] + 15\,000 \times 300 = 4.06 \times 10^6\,\text{N mm}$$

The horizontal components of the flange loads at this section are then

$$P_{x,1} = P_{x,3} = \frac{4.06 \times 10^6}{300} = 13\,533.3\,\text{N}$$

and the vertical components are

$$P_{y,1} = P_{y,3} = 3626.2\,\text{N}$$

Hence

$$P_1 = P_3 = \sqrt{13\,533.3^2 + 3626.2^2} = 14\,010.7\,\text{N}$$

The total shear force at this section is $15\,000 + 300 \times 7.0 = 17\,100$ N. Therefore, the shear force resisted by the web is $17\,100 - 2 \times 3626.2 = 9847.6$ N so that the shear flow q_3 in the web at this section is

$$q_3 = \frac{9847.6}{300} = 32.8\,\text{N/mm}$$

Problems

P.24.1 The beam shown in Fig. P.24.1 is simply supported at each end and carries a load of 6000 N. If all direct stresses are resisted by the flanges and stiffeners and the web panels are effective only in shear, calculate the distribution of axial load in the flange ABC and the stiffener BE and the shear flows in the panels.

Ans: $q(\text{ABEF}) = 4$ N/mm, $q(\text{BCDE}) = 2$ N/mm
P_{BE} increases linearly from zero at B to 6000 N (tension) at E
P_{AB} and P_{CB} increase linearly from zero at A and C to 4000 N (compression) at B.

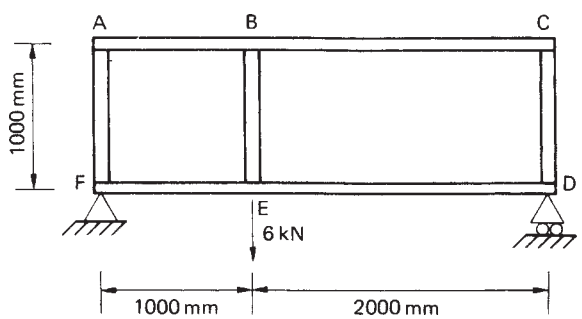

Fig. P.24.1

P.24.2 Calculate the shear flows in the web panels and direct load in the flanges and stiffeners of the beam shown in Fig. P.24.2 if the web panels resist shear stresses only.

Ans. $q_1 = 21.6$ N/mm $q_2 = -1.6$ N/mm $q_3 = 10$ N/mm
$P_{\text{C}} = 0$ $P_{\text{B}} = 6480$ N (tension) $P_{\text{A}} = 9480$ N (tension)
$P_{\text{F}} = 0$ $P_{\text{G}} = 480$ N (tension) $P_{\text{H}} = 2520$ N (compression)
P_{E} in BEG $= 2320$ N (compression) P_{D} in ED $= 6928$ N (tension)
P_{D} in CD $= 4320$ N (tension) P_{D} in DF $= 320$ N (tension).

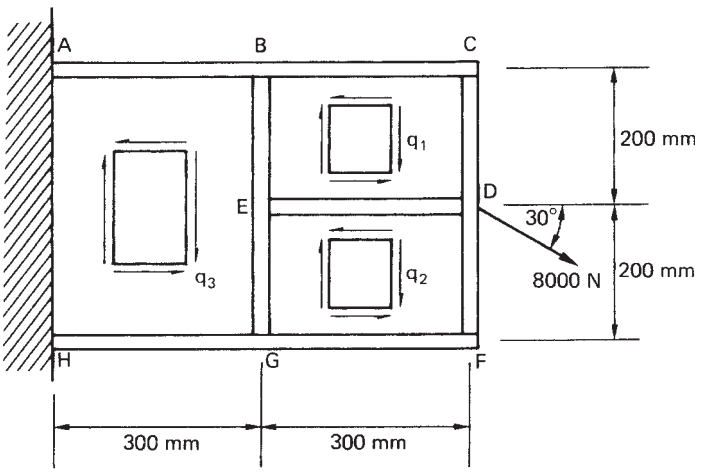

Fig. P.24.2

P.24.3 A three-flange wing section is stiffened by the wing rib shown in Fig. P.24.3. If the rib flanges and stiffeners carry all the direct loads while the rib panels are effective only in shear, calculate the shear flows in the panels and the direct loads in the rib flanges and stiffeners.

Ans. $q_1 = 4.0\,\text{N/mm}$ $q_2 = 26.0\,\text{N/mm}$ $q_3 = 6.0\,\text{N/mm}$

P_2 in $12 = -P_3$ in $43 = 1200\,\text{N}$ (tension) P_5 in $154 = 2000\,\text{N}$ (tension)

P_3 in $263 = 8000\,\text{N}$ (compression) P_5 in $56 = 12\,000\,\text{N}$ (tension)

P_6 in $263 = 6000\,\text{N}$ (compression).

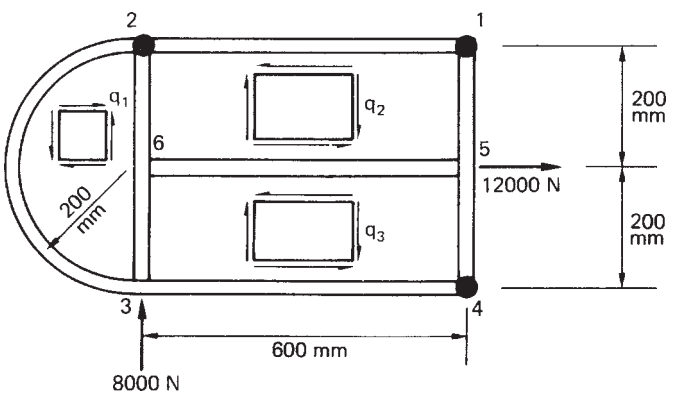

Fig. P.24.3